A QUILT AFTER FIBONACCI, PART 2 OF 3: COHORTS, FREE MONOIDS, AND NUMERATION

J. PARKER SHECTMAN

Dedicated to my parents, Norton and Mikki

Date: 5 April 2021.

2010 *Mathematics Subject Classification.* 52C20 (Primary), 05A17, 11A63, 11B37, 11B39, 11P81, 52C23, 68R15, 97F30 (Secondary).

Key words and phrases. Quilt Tiling, Cohort Sequence, Fibonacci Numbers, Pell Numbers, Wythoff Array, Numeration System, Maximal Fibonacci Expansion, Binary Tree, Complementary Equations, Interspersion, Dispersion, I–D array, p-adic, Sieve, Palindrome.

Abstract. Part 1 of the paper began an investigation of the quilt, a tiling whose black squares and white rectangles are each described by a quartet of integer arrays. The "black quartet" contains the "quilt interspersion," one such array. To study columns of the arrays and similar sequences, this second part of the paper considers *cohorts* of the sequences, a cohort being a block of consecutive elements that depends on earlier cohort(s) through an affine catenative recurrence. The affine term of the recurrence need not take a constant value throughout the sequence. Rather, the affine term, while constant across an individual (sub)cohort, may depend on the cohort index and thus change from one cohort to the next. The paper provides a table of cohort sequences encountered along the course of the investigation.

Cohorts provide a framework to enumerate *complementary equations*, recurrences such as those studied by Kimberling between Wythoff compositions, or those between inverse Wythoff compositions. Cohorts also yield convenient formulas to describe many types of integer sequences, in particular, those that describe the quilt geometry and columns of the Wythoff array.

The paper classifies eight interspersions into two more quartets, the *branch quartet* and the *clade quartet*. The latter includes both the quilt interspersion and the Wythoff array. To generate the quartets of interspersions, the paper offers four (4) equivalent approaches. The "cohort approaches" employ cohort-based formulas or tabular manipulations of *cohort tableaux* to produce the quartets. These tableaux are "tetrangles" or "irregular triangle arrays," which are also planar-graph isomorphic to infinite, regular, single-rooted binary trees. Such is the case with the *Fibonacci cohort tableaux* and *successor tableaux*.

The paper generalizes cohort sequences of integers to cohort sequences of integer-valued tuples, with the catenative recurrence using a (highest-) digit increment and / or (suffix-) concatenation, instead of scalar addition of an affine term. This generalization allows cohorts to describe numeration systems, providing constructive, enumerative proofs of known results on compositions of integers. These results relate back to the quilt, with a role played by the *maximal Fibonacci expansion*, a variant of the lazy Fibonacci representation. Restriction on the prefix or suffix of the Fibonacco expansion also generates columns of the interspersions ("numeration approach").

Further extending the definition of cohort, the paper considers cohort sequences of functions in a free monoid, where instead of adding an affine term, the catenative recurrence employs inner or outer composition with a generator of the monoid ("cohort calculus"). Placing functions into cohort sequences provides a total order for free monoids generated by pairs of functions under composition, or equivalence classes thereof.

For free monoids on the Wythoff or inverse Wythoff pairs, this calculus enumerates functions in the free monoid. Restrictions on the prefix or suffix of the compositions form equivalence classes, and the image of 1 under each class yields columns of interspersions in the two quartets (the "free-monoid approach"), though the paper also extends the procedure to other Beatty and inverse Beatty pairs, and "shifted branching functions" using Beatty pairs that also arrange the positive integers into binary trees.

Indeed, the eight interspersions are also "harvested" from four distinct binary trees of the positive integers in multiple ways: gathering rows or columns in branches or clades of the trees, from the left or right (the "tree approach"). The pair of branching functions for each tree generates a free monoid. Taking a prefix or suffix as a modulus forms equivalence classes on this free monoid which totally order as a cohort sequence. Cohort sequences of class representatives then yield columns of the interspersions — an algebraic procedure (cohort sequencing) equivalent to the geometric procedure of gathering and straightening tree clades.

The treatment of extensions offers a glimpse of additional devices that include *diatomic tableaux* and *floor-powerfree numbers* — positive integers not expressible as a (non-trivially) nested floor function.

Contents

List of Figures

List of Tables

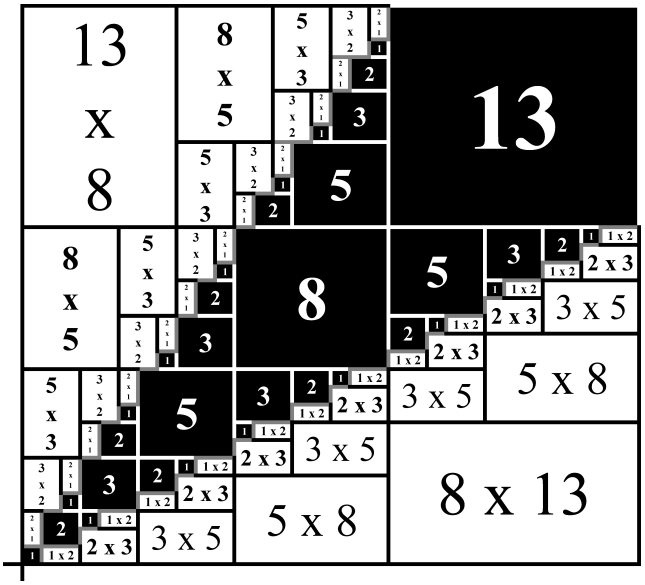

FIGURE 1. A Corner Patch of the Quilt Tiling

1. INTRODUCTION

This paper examines the integer sequences that describe the geometry of the quilt (Figure 1) — a tiling composed of black squares and white rectangles. As described in Part 1 of the paper [38], each new phase of construction replicates an existing existing portion of the quilt, imparting to the quilt its self-similar quality. To describe this self-similarity, Part 1 defined a *cohort* as a collection of squares or rectangles reproduced at an individual phase of construction.

Extending this definition, the present part of the paper will use cohorts to analyze sequences, such as the two quartets of coordinate arrays for corners of the quilt's squares (Table 1) and rectangles (Table 2). To facilitate the analysis, this part of the paper gives an algebraic definition of "cohort" as a block of consecutive elements in a sequence that depends on (an) earlier cohort(s) through an affine catenative recurrence, that is, a concatenation of earlier cohorts plus an affine term, the latter said to "cohortize" the sequence. This affine term (the "cohortizer"), while not depending on individual elements, may depend on the cohort index.

The paper will use results of Fraenkel, Mushkin, and Tassa [17] and Bunder and Tognetti [7], to derive convenient formulas for cohort sequences (Proposition 4.2). In particular, cohort-based formulas produce the columns of the eight arrays that describe the quilt geometry (Proposition 3.2). The application of cohort-based formulas (Section 4.1.4), and the formulation of "cohortizers" (Table 17) allow convenient calculation for columns of related interspersion-dispersion arrays (I–D arrays), such as those of the *branch quartet* and *clade quartet* (Tables 3 and 4).

Cohort-based formulas simplify the enumeration of complementary equations for Wythoff sequences studied by Kimberling [22], thus reproducing and extending

known results (see Example 4.7 and Proposition 4.14 for the general case; Corollary 4.9 and Remark 4.8 for a restricted class of homogeneous complementary equations studied by Kimberling [22]; Example 4.15, Example 4.4 and Remark 4.10 for a result due to Fraenkel [16]; and Remark 4.30 for the Wythoff array).

Table 6 depicts Fibonacci cohorts C_t of the positive integers $n \in \mathbb{Z}_+$. The cohort index $t(n)$ of n is the row of the *cohort tableau* in which n appears, for Fibonacci cohort tableaux, given by $t(n) = F^{-1}(n) - 1 = \underline{\texttt{072649}}(n) = \left\lfloor \log_\phi(\sqrt{5}n+1) \right\rfloor - 1$. These tableaux can be manipulated (Sections 8.2.2 and 8.2.4), and by means of such manipulations (as summarized in Figure 24(b)), the tableaux (Tables 6 and 19) generate columns of the branch quartet (see Table 28) and clade quartet arrays, respectively. The paper calls this the "cohort-tableau approach" or "cohort-tableau description" of these arrays.

The cohort property is a recursive structure which often appears in sequences that interest researchers, both 0-1–sequences (more generally those on finite alphabets), as well as integer sequences. However, other than a handful of 0-1–sequences, the current discussion targets non-decreasing sequences of positive integers, and treats each sequence directly, rather than reducing it to a 0-1–sequence through successive differences or using its characteristic sequence. Thus, the paper focuses on the cohort property itself rather than underlying properties of the sequence (automatic, morphic, regular, balanced, uniform), that may give rise to such a property. Also, the treatment here does not reference the theory of difference equations, though its methods may apply to some of the examples. Table 8 provides a list of some cohort sequences encountered along the course of the investigation, of known interest to researchers.

Cohort sequencing induces total order on free monoids under composition generated by the pair of Wythoff functions $\{\kappa, \lambda\}$ or Wythoff^{-1} functions $\{\eta, \theta\}$ (Propositions 5.2, respectively, 5.4). Though these both use the golden ratio, the paper will also apply the cohort calculus to totally order free monoids generated by Beatty pairs of spectrum sequences on other slopes (Section 9), and "shifted" tree branching functions that use Beatty pairs (Proposition 4.12 and Corollary 9.2).

More generally, for free monoids with two generators, such as any lexicon $\{l, r\}^\star$ on a two-symbol alphabet, *Fibonacci cohort sequencing* induces four distinct total orders (Tables 7). (Remark 8.1 suggests a generalization). Abusing the word "cohort," the paper adopts the verb *cohortize* to refer to the recursive evolution of a total order in the specific way Section 5 describes: To cohortize the sequences of functions, inner or outer composition of prior cohorts with a generating element of the monoid (the "cohort calculus"), plays a role analogous to the addition of an affine term (cohortizer) to cohorts of integers.

Inner and outer composition provide two distinct ways to arrange the functions in any free monoid $\{l, r\}^\star$ on two generators l and r into binary trees. As examples, two distinct binary trees (Figures 2 and 4, respectively, Figures 7 and 9) arrange each of the free monoids $\{\kappa, \lambda\}^\star$ and $\{\eta, \theta\}^\star$.

In bijective correspondence with these four binary trees of Wythoff and Wythoff^{-1} compositions, four corresponding trees that each arrange $\mathbb{Z}_+$ (Together in Table 5, individually in Figures 3, 5, 8, and 10) provide a combinatorial means to generate rows or columns of the branch quartet and clade quartet by "harvesting" from the trees, that is, by gathering branches or clades.

Ultimately, the "branch quartet" and "clade quartet" of interspersions take their names from this harvesting of branches, respectively, clades from the *Fibonacci trees*, to form their rows and columns, respectively (see Figure 24(a)). The paper takes these two trees (Figures 5 and 8) as the canonical reference, owing to the ease of their recursive calculation in a numeration system (Figures 14, respectively, 13).

Despite their names, however, the branch quartet can also be harvested from clades and the clade quartet can also be harvested from branches, by considering the two *successor trees* (Figures 3 and 10), rather than the Fibonacci trees. Branches of the successor trees are merely the "straightened" clades of the Fibonacci trees, and vice versa. This, together with the fact that the quartets consider only interspersions and *not* transposed interspersions, explains the total of eight arrays, that is, {4 trees} × {from tree branches, from tree clades} × {on left, on right} × {to array rows, to array columns} ÷ {2 alternatives for each tree} ÷ {I–D array, transposed I–D array} = $\frac{4\times2\times2\times2}{2\times2}$ = 8 arrays. Each of Tables 3 and 4 indicates how to generate the arrays on the left from the *minimal trees* (Figures 3 and 5) and those on the right from the *maximal trees* (Figures 8 and 10). As a mnemonic, "**c**lades are **c**olumns," while branches are rows.

Besides harvesting the two quartets from the trees of integers as just described (the "tree approach," Figure 24(a)), a second, equivalent approach defines columns of the arrays by restricting the prefix or suffix of compositions in $\{\kappa, \lambda\}^\star$ and $\{\eta, \theta\}^\star$, as Tables 3 and 4 also indicate, and then using the aforementioned bijections between these free monoids and $\mathbb{Z}_+$ (the "free-monoid approach," Figure 25(a)). Proposition 4.16(b) and Corollary 4.26 provide these bijections. Thus, these restrictions configure the map between each interspersion and one of these two free monoids. Implicitly, harvesting any individual branch or clade from Figures 2, 4, 7, or 9 involves such a restriction, since all nodes of a given branch or clade share either the same prefix or the same suffix.

Whether working with a tree of integers or a tree of compositions in a free monoid, any array at the top of Tables 3 or 4 and the array below it obtain from one another by swapping the roles of left and right in gathering branches or clades from the underlying tree. The paper refers to this swapping of left and right as *mirror duality*. For an interspersion–dispersion array with infinitely many rows, the mirror dual is what Kimberling termed the "inverse I–D array," with the present naming convention intended to avoid confusion with several other types of duality discussed herein (cohort dual, blade dual). Thus, Kimberling's "inversion" is equivalent to constructing a binary tree of the positive integers rooted at 1 by grafting together rows from one of the arrays, then harvesting the other array by gathering tree branches from the opposite side (Remark 9.3).

The paper designates another type of duality between arrays as *cohort duality* and describes how pairs of interspersions, including Tables 12 and 15, are *cohort duals* of one another. Specifically, the paper defines cohort duality between pairs of arrays, as swapping the 1–2- and 2–1-Fibonacci recursive structures in the same capacity for generating the array. This swap is easy to visualize when applying the cohort-tableau approach (Figure 24(b)). Equivalently when using the tree approach, cohort duality obtains by swapping the minimal and maximal trees in the same capacity for generating the array, whether formulated in terms of Wythoff and Wythoff^{-1} functions (Figure 25(a)), or in terms of the branching functions,

when harvesting branches (Figures 25(b)(i) and (b)(ii)) or when harvesting clades (Figure 25(c)(i) and (c)(ii)).

Thus, in each of Tables 3 and 4, the array at the top left and the array at the top right are cohort duals, while the array at the bottom left and the array at the bottom right are also cohort duals. A third approach, the cohort-tableau approach manipulates the pair of Fibonacci tableaux (Tables 6) into each cohort-dual pair of arrays in the branch quartet (Section 8.2.2, Table 28), whilst for each cohort-dual pair of the clade quartet, the cohort-tableau approach manipulates the pair of successor tableaux (Tables 19) into each cohort-dual pair of arrays (Section 8.2.4).

For each cohort-dual pair, an equivalent approach via cohort recursion formulates columns of one array as 1–2-Fibonacci cohort sequences and columns of the other array as 2–1-Fibonacci cohort sequences, cohortizers of corresponding columns having identical degree. For instance, the Wythoff array $w_{n,k}$ and the quilt interspersion $a_{n,k}$ (Table 4 at top left, respectively, top right), are cohort duals, whereas the k^{th} column of w is a 1–2-Fibonacci cohort sequence under cohortizer $\langle F_{t+k}, F_{t+k+2}\rangle$, while the k^{th} column of a is a 2–1-Fibonacci cohort sequence under cohortizer F_{t+k+1}, cohortizers of the same overall *rate* $p = k + 1$. Similarly, columns k of $\mathfrak{w}$ and $\mathfrak{a}$ are 1–2- and 2–1-Fibonacci cohort sequences, respectively, under cohortizers $\langle F_{t+2k-2}, F_{t+2k}\rangle$ and F_{t+2k-1}, of the same overall rate $p = 2k - 1$. Table 17 summarizes the cohortizers for columns of the branch and clade quartet arrays.

Trading Fibonacci cohorts for Pell cohorts, and binary trees for ternary trees, the notion of cohort "duality" changes from the dual to the triple (Remark 8.1); more generally, it extends from the dual to the multiple (Section 9.5). Remaining in the realm of binary trees, Definition 9.2 attempts to formalize the idea of cohort duality while remaining anchored to the notion of cohort. However, once the scope extends beyond the golden ratio to encompass other irrational slopes in floor functions (Sections 9.5, 9.6, and 9.7), the notion of cohort can become illusive as the structure of the resulting sequences succumb to the irrationality of the underlying slope: Cohorts lengths cease to follow simple recurrences (Conjecture 9.5) or powers of the right branching function fail to intersperse in a regular fashion with those of the left branching function (Conjecture 9.8), resulting in irregular cohort lengths.

The regularity of cohorts emerges once again as the slope approaches two, generating the "Positions tree" (Figure 18) in the limit. It arranges the positive integers with consecutive integers as left and right sibling nodes, thus minimizing an aggregate measure of distance over binary trees that arrange $\mathbb{Z}_+$. Its "Blade-dual" tree (Figure 21) likewise arranges the positive integers, but with 2-adic distance between left and right sibling nodes decreasing with each level of the tree, such that the arrangement minimizes a measure of central tendency of the 2-adic distance between neighboring nodes over the space of binary-tree arrangements of the positive integers (Remark 6.18).

As a further approach to the taxonomy of these trees, Section 9.9 gives preliminary computational results on generating the trees systematically, while also presenting sieves — a device for relating the trees to slopes by identifying *floor-powerfree* (Table 48), capping off the smörgåsbord of extensions presented in Section 9. Floor-powerfree numbers are those positive integers not expressible as a (non-trivially) nested floor function using the same slope throughout the nesting.

Beyond cohort sequences of integers and functions, Section 7 of the paper will extend the notion of "cohort" to sequences of integer-valued tuples, using the operations of increment and concatenation to cohortize sequences of tuples / words. For example, the method of constructing the quilt described in Part 1 of the paper associates to each quilt square a unique *genealogy* — an integer tuple / word that records the sequence of generations u at which that square and each of its ancestors first appeared. Genealogy allows a lexicographic ordering of all squares in the quilt. As the quilt evolves, the population of squares of ordinal size k lags the population of squares of (ordinal) size $k-1$ by one generation, as Part 1 showed. Proposition 7.5 will present a more general result: that the genealogy for the n^{th} quilt square of ordinal size $k = 2, 3, 4, \ldots$ equals one plus the genealogy for the n^{th} quilt square of (ordinal) size $k-1$. Moreover, the genealogy for the n^{th} quilt square of size 1 equals a certain *maximal Fibonacci expansion* of n, introduced in Section 6, and related to, albeit distinct from, the lazy Fibonacci representation.

As each action of the quilt construction method adds new squares to the quilt, new integers — the coordinates of these new squares — are *composed*. The wording "composed" is deliberate, because the aforementioned Fibonacci expansions relate quilt squares to *restricted compositions*, that is, ordered partitions of a positive integer. For example, the paper will consider, for the n^{th} quilt square of ordinal size k in Figure 1, the coordinate $a_{n,k}$ (Table 1(a)) of its southernmost row. The paper will show that while $a_{n,k}$ encodes within its *maximal Fibonacci gaps* a composition using only ones and twos of integer $F^{-1}(n) + k - 1$, coordinate $a_{n,k+1}$ encodes a related composition of $F^{-1}(n) + k$ obtained by prepending a "1" to the former composition (Corollary 7.4). Thus the quilt also illustrates a constructive proof for known combinatorial results on the number of restricted compositions of a given integer, with spinal quilt square $S_{0,h+1}$ and all squares directly south of it visually representing all compositions of integer h that use only ones and twos (Figure 22).

In this context of Fibonacci expansions, restricted composition of integers provides a fourth, equivalent approach to generate the branch quartet and the clade quartet. As Tables 3 and 4 indicate, restrictions on the minimal Fibonacci gaps describe the columns of arrays on the left side of each table, whereas restrictions on the maximal Fibonacci gaps describe the columns of arrays on the right side. Figure 24(c) summarizes this "numeration approach" to generating the octet, showing that cohort duality in the numeration approach entails swapping the minimal Fibonacci representation and maximal Fibonacci expansion in the same capacity for generating the array.

Evidently, an array in Table 4 relates to the array in the same position of Table 3, by a reversal of the Fibonacci gaps of (entries in) the respective columns vis-à-vis the same underlying system of Fibonacci numeration (minimal Fibonacci representation for arrays on the left of the tables, and maximal Fibonacci expansion for the arrays on the right of the tables). In particular, the column-wise restriction moves between the suffix (branch quartet) and prefix (clade quartet) of the gaps.

This transformation of gaps with respect to a given Fibonacci expansion produces what the paper calls *blade duality* (a contraction of "**b**ranch–c**lade**") between arrays. (Proposition 9.9 gives sufficient conditions for the blade dual of an I–D array to also be an I–D array). The same action transforms between blade-dual pairs of trees, Figures 3 and 5 being one such pair and Figures 8 and 10 being another.

For whole columns, blade duality corresponds to swapping an "inner" restriction for an "outer" one in the free-monoid approach, and thus blade duality also applies directly to the compositions in $\{\kappa, \lambda\}^\star$ and $\{\eta, \theta\}^\star$, again by moving the restriction on the compositions between prefix and suffix (Figure 25(a)).

The equivalence of the "tree description" and "cohort description" of the two quartets of I–D arrays figures prominently in the planar-graph isomorphism (Proposition 6.21) between the successor trees (Figures 3 and 10) and the Fibonacci cohort tableaux (Tables 6). In this restricted topological sense, therefore, the Fibonacci cohort tableaux *are* the successor trees. Meanwhile the Fibonacci trees (Figures 5 and 8) are planar-graph isomorphic to the successor cohort tableaux (Tables 19). (These latter tableaux can also be written as *diatomic tableaux* (Tables 40).)

Overall, the paper begins with a more concrete approach, restricting the discussion to examples of cohort sequences of integers, before treating more abstractly the space of compositions (or equivalence classes thereof) in a free monoid under inner or outer composition. In contrast to outer composition, inner composition cannot be calculated iteratively. One advantage of the more abstract approach is that it facilitates counting arguments that produce closed formulas, such as that of Proposition 4.16(a), where the inner composition along rows of Table 9 would otherwise preclude the recursive calculation of Table 12.

This more abstract approach also introduces tree-branching forms $\{\boldsymbol{l}, \boldsymbol{r}\}$, $\{\boldsymbol{L}, \boldsymbol{R}\}$, $\{\bar{\boldsymbol{l}}, \bar{\boldsymbol{r}}\}$, and $\{\bar{\boldsymbol{L}}, \bar{\boldsymbol{R}}\}$, which replace suffix forms involving $\{\kappa, \lambda\}$ and $\{\theta, \eta\}$ in Figures 25(a) and (b), respectively, with all-prefix forms using $\{\boldsymbol{l}, \boldsymbol{r}\}$ and $\{\bar{\boldsymbol{L}}, \bar{\boldsymbol{R}}\}$ in Figures 25(b)(i) and (b)(ii), respectively; or alternatively, those which replace prefix forms involving $\{\theta, \eta\}$ and $\{\kappa, \lambda\}$ in Figures 25(a) and (b), respectively, with all-suffix forms using $\{\bar{\boldsymbol{L}}, \bar{\boldsymbol{R}}\}$ and $\{\boldsymbol{l}, \boldsymbol{r}\}$ in Figures 25(c)(i) and (c)(ii), respectively. In effect, the all-prefix forms correspond to tree branches, while the all-suffix forms correspond to tree clades.

Thus, the free monoids on pairs of tree branching functions under composition, $\{\boldsymbol{l}, \boldsymbol{r}\}^\star$, $\{\boldsymbol{L}, \boldsymbol{R}\}^\star$, $\{\bar{\boldsymbol{l}}, \bar{\boldsymbol{r}}\}^\star$, and $\{\bar{\boldsymbol{L}}, \bar{\boldsymbol{R}}\}^\star$, provide a more unified approach than the free monoids on Wythoff and Wythoff^{-1} pairs, $\{\kappa, \lambda\}^\star$ and $\{\theta, \eta\}^\star$, in the following sense. Firstly, arrays can be described using free-monoids on pairs of branching functions in such a way that their cohort duality (Figures 25(c)(i) and (b)(ii)) more closely parallels that of their numeration description (Figure 24(c)), which uses all-suffix forms for the branch quartet and all-prefix forms for the clade quartet.

Secondly, the tree branching functions standardize the procedure whereby an ordered tableau of $\{\kappa, \lambda\}^\star$, Table 10, or equivalences classes thereof, Table 11, is used to calculate columns of F, $\exists$, and $\vDash$ (Remark 8.6). Once the cohort calculus totally orders the (equivalence classes of) free monoids of tree branching functions into the Fibonacci cohort tableaux in Tables 32 and 33, these tableaux allow calculation of all eight arrays of the branch and clade quartets, column by column, using the same procedure. Moreover, each tableau also "straightens" the entirety of the corresponding tree into the entire sequence of positive integers in its natural order, in the same way that it "straightens" individual clades of the tree into the individual ordered columns of the interspersion arrays.

This clade–tree order isomorphism is a self-symmetry of binary-tree arrangements of the positive integers (Figures 3, 5, 8, 10, 18, 21) that figures prominently in the investigation. Section 9.9.1 presents preliminary results of computational experiments that aim to discover and understand other trees of $\mathbb{Z}_+$ that exhibit

complete clade–tree order isomorphism, in which all left and right clades are ordered the same way as the tree itself. A much less restrictive single-clade–tree order isomorphism proves to provide a sufficient condition to preserve the I–D properties of arrays under blade duality.

As a further self-symmetry, the successor trees exhibit a half-clade–tree order isomorphism. (This symmetry is incomplete in the Fibonacci trees.) Compositions S in the free monoids $\{\bar{\boldsymbol{l}}, \bar{\boldsymbol{r}}\}^\star$, and $\{\bar{\boldsymbol{L}}, \bar{\boldsymbol{R}}\}^\star$ have a defined zero–one *Wythoff signature*, meaning that either $SK \to K$ or $SK \to \Lambda$ injectively (Lemma 8.19, where K and Λ are the collection of lower, respectively, upper Wythoff numbers). The cohort tableaux (Table 33) totally order these compositions into sequences, for which the sequence of Wythoff signatures gives the Fibonacci word (Proposition 8.20).

Thirdly, the tree branching formulation for the Fibonacci and successor trees (Figure 15) inspires the various generalizations that appear in Section 9.

Finally, returning to the quilt, the rich self-similarity of its coordinate interspersion array $a_{n,k}$ (Proposition 8.7 through Corollary 8.13) shows that the sequences of integers that describe the quilt geometry share the self-similar quality apparent when viewing the quilt — a theme continued in Part 3 [40].

2. Notation

$\phi \equiv (\sqrt{5}+1)/2$,	The Golden Ratio;
$\chi \equiv \sqrt{2}+1$,	The Silver Ratio;
$F_{k+1} = F_k + F_{k-1}$, $k \geq 1$, with $F_0 = 0$ and $F_1 = 1$	The Fibonacci numbers;
$\underline{123456}$,	An integer sequence from Sloane's OEIS [41];
$\underline{123456}_n$,	The sequence reindexed (relative to the "list" in the OEIS);
$F^{-1}(n) \equiv \underline{130233}(n)$,	Greatest Fibonacci number $\leq n$;

The quilt (Figure 1):

$(i,j) \in \mathbb{Z}_+ \times \mathbb{Z}_+$,	Coordinate pair for cell in row i and column j;
$A(z)$,	Westernmost (southernmost) black cell in row (column) z;
$\Omega(z)$,	Easternmost (northernmost) black cell in row (column) z;
$[a,b] \times [c,d]$,	An interval of rows $\times$ columns;
$[a,b] \times [c,d] + r \times s \equiv [a+r, b+r] \times [c+s, d+s]$,	Typical interval arithmetic (scalar addition);

Black quilt squares (Table 1) and White quilt rectangles (Table 2):

$S_{0,k} = [a_{0,k}, b_{0,k}] \times [c_{0,k}, d_{0,k}] \subset \mathbb{Z}_+ \times \mathbb{Z}_+$	Quilt square lying on the main diagonal;
$S_{n,k} \subset \mathbb{Z}_+ \times \mathbb{Z}_+$,	A pair of equivalent squares: $[a_{n,k}, b_{n,k}] \times [c_{n,k}, d_{n,k}]$ below the diagonal, and $[c_{n,k}, d_{n,k}] \times [a_{n,k}, b_{n,k}]$ above the diagonal;
$R_{n,k} \subset \mathbb{Z}_+ \times \mathbb{Z}_+$,	A pair of equivalent rectangles: $[\alpha_{n,k}, \beta_{n,k}] \times [\gamma_{n,k}, \delta_{n,k}]$ below the diagonal, and $[\gamma_{n,k}, \delta_{n,k}] \times [\alpha_{n,k}, \beta_{n,k}]$ above the diagonal;
$v_{n,k}$,	Genealogy of a quilt square;

Cohort sequences:

$S_1, S_2, \ldots$,	A sequence of integers;
$S_1 S_2 \cdots$,	The equivalent integer word;
$f(t)$, $g(t)$, $h(t)$,	Cohortizers for cohort t;
$f(t) = \langle f_L, f_R \rangle(t)$,	Cohortizer with left and right subcohort distinction for cohort t;
p,	Growth rate parameter of a cohort sequence;
$C_1, C_2, \ldots, C_t, \ldots$,	A sequence of Cohorts;
$C \oplus D = (C_1, \ldots, C_n, D_1, \ldots, D_m)$,	Tuples $C = (C_1, \ldots, C_n)$ and

	$D = (D_1, \ldots, D_m)$ concatenated;
$CD = C_1 \cdots C_n D_1 \cdots D_m$,	Words $C = C_1 \cdots C_n$ and $D = D_1 \cdots D_m$ juxtaposed;
$C \ominus (C_t) \equiv (C_1, \ldots, C_{t-1}, C_{t+1}, \ldots, C_n)$	Tuple C with element C_t removed;
$C \setminus C_n \equiv C_1 \cdots C_{n-1}$,	Word C with last letter C_n removed;
$\texttt{++}C \equiv (C_1 + 1, \ldots, C_{n-1}, C_n)$,	Tuple C with first element incremented;
$C\texttt{++} \equiv (C_1, \ldots, C_{n-1}, C_n + 1)$,	Tuple C with last element incremented;
$T_1, T_2 \cdots$,	A sequence of tuples;
$\prec, \succ$,	Lexicographic order (on tuples or words);
$()$,ε,	Empty tuple, empty word;
Beatty Sequences:	
$(\kappa, \lambda)(n) \equiv \left(\lfloor n\phi \rfloor, \lfloor n\phi^2 \rfloor\right)$,	Pair of Wythoff sequences;
$(\theta, \eta)(n) \equiv \left(\lfloor n/\phi \rfloor, \lfloor n/\phi^2 \rfloor\right)$,	Pair of Wythoff^{-1} sequences;
$K = \kappa(\mathbb{Z}_+)$, $\Lambda = \lambda(\mathbb{Z}_+)$, $\Theta = \theta(\mathbb{Z}_+)$, $H = \eta(\mathbb{Z}_+)$,	Ranges of Wythoff and Wythoff^{-1} sequences on $\mathbb{Z}_+$;
$K_{-1} = \kappa(\mathbb{Z}_-)$, $\Lambda_{-1} = \lambda(\mathbb{Z}_-)$,	Ranges of Wythoff sequences on $\mathbb{Z}_-$;
$\kappa^\star(n) = \lfloor \cdots \lfloor n\phi \rfloor \cdots \phi \rfloor$,	Arbitrarily many nested applications of κ to n;
$\theta^\star(n) = \left\lfloor .^{\cdot^{\lfloor n/\phi \rfloor}} \cdot_{\cdot} / \phi \right\rfloor$,	Arbitrarily many nested applications of θ to n;
$M = \lambda\kappa^\star$,	Suffix of equivalent compositions $S'\lambda \overset{\circ\kappa^\star}{\sim} S'\lambda\kappa \overset{\circ\kappa^\star}{\sim} S'\lambda\kappa^2 \overset{\circ\kappa^\star}{\sim} \cdots \overset{\circ\kappa^\star}{\sim} S'M \in \{\kappa, \lambda\}^\star \setminus \{\kappa\}^\star$;
$L = \theta^\star\eta$,	Prefix of equivalent compositions $\eta S' \overset{\theta^\star\circ}{\sim} \theta\eta S' \overset{\theta^\star\circ}{\sim} \theta^2\eta S' \overset{\theta^\star\circ}{\sim} \cdots \overset{\theta^\star\circ}{\sim} LS' \in \{\theta, \eta\}^\star \setminus \{\theta\}^\star$;
$N_0(S)$,	Number of leading zeros on $\mathbb{Z}_+$ of an element S in the free monoid $\{\theta, \eta\}^\star$ of compositions on $\{\theta, \eta\}$;
$N_{-1}(S)$,	Number of leading -1s on $\mathbb{Z}_-$ of an element S in the free monoid $\{\theta, \eta\}^\star$ of compositions on $\{\theta, \eta\}$;
μ, ν,	Conjugate irrational slopes for use in complementary floor functions (spectrum sequences on Beatty pairs);
$\mathsf{BeattyInvert}(S)$,	Composition S in a free monoid on a Beatty pair mapped to the corresponding composition on the Beatty^{-1} pair;

$\overleftrightarrow{T}$,	Reverse of T (a tuple, word, or composition);
$(\kappa_b, \lambda_b)\,(n)$,	Pair of Bergman-b sequences;
$(\theta_b, \eta_b)\,(n)$,	Pair of Bergman^{-1}-b sequences;

Fibonacci Numeration and Binary Trees:

$\mathbf{f}(n)$, $\mathbf{F}(n)$, $\mathbf{F}_\star(n)$,	Fibonacci indices in minimal, lazy representation, and *maximal expansion*, respectively, of n;
$(\partial_1, \ldots, \partial_r)$	Gaps between Fibonacci indices as a tuple ("del" chosen to avoid confusion with sequence $\delta_{n,k}$), and
$\partial_1 \cdots \partial_r$	written as a word;
$\boldsymbol{\partial}(n)$, $\boldsymbol{\nabla}(n)$, $\boldsymbol{\nabla}_\star(n)$	Gaps for minimal & lazy representation, and maximal expansion, respectively, of n ("del" chosen to avoid confusion with quilt sequence $\delta_{n,k}$);
$\sigma(n)$, $\sigma_\star(n)$,	Fibonacci successor of n in Zeckendorf representation, in maximal expansion, respectively;
$\sigma^{-1}(n)$, $\sigma_\star^{-1}(n)$,	Fibonacci predecessor of n in Zeckendorf representation, in maximal expansion, respectively;
$\mathbf{p}(n)$, $\mathbf{P}(n)$,	Position of integer n in the minimal, respectively, maximal Fibonacci trees, Figures 5 and 8;
$\boldsymbol{l}(n)$, $\boldsymbol{r}(n)$,	Left and right children of n in the minimal Fibonacci tree, Figure 5;
$\boldsymbol{L}(n)$, $\boldsymbol{R}(n)$,	Left and right children of n in the maximal Fibonacci tree, Figure 8;
$\bar{\mathbf{p}}(n)$, $\bar{\mathbf{P}}(n)$,	Position of integer n in the minimal, respectively, maximal successor trees, Figure 3 and 10;
$\bar{\boldsymbol{l}}(n)$, $\bar{\boldsymbol{r}}(n)$,	Left and right children of n in the minimal successor tree, Figure 3;
$\bar{\boldsymbol{L}}(n)$, $\bar{\boldsymbol{R}}(n)$,	Left and right children of n in the maximal successor tree, Figure 10;
$W_1, A_1, F_1, \Bumpeq_1$,	Suffixes that form equivalence classes on the free monoids of branching functions $\{\boldsymbol{l}, \boldsymbol{r}\}^\star$, $\{\boldsymbol{L}, \boldsymbol{R}\}^\star$, $\{\bar{\boldsymbol{l}}, \bar{\boldsymbol{r}}\}^\star$, $\{\bar{\boldsymbol{L}}, \bar{\boldsymbol{R}}\}^\star$, respectively;

Branch and Clade Quartets:

$\mathsf{F}, \mathsf{L}, \mathsf{\exists}, \mathsf{\perp}$,	Branch quartet of interspersion arrays (Table 3);
$\mathsf{F}^{(2)}, \mathsf{L}^{(2)}, \mathsf{F}^{(3)}, \mathsf{L}^{(3)}$,	Extrapolation of branch quartet (Tables 37 and 38);
$w, a, \mathfrak{w}, \mathfrak{a}$,	Clade quartet of interspersion arrays (Table 4).

(a)

1	2	4	7	12	20	33	
3	5	9	15	25	41	67	
6	10	17	28	46	75	122	
8	13	22	36	59	96	156	
11	18	30	49	80	130	211	
14	23	38	62	101	164	266	
16	26	43	70	114	185	300	
$a_{n,k},\ n = 0, \ldots, 6,\ k = 1, \ldots, 7;$							

(b)

1	3	6	11	19	32	53	
3	6	11	19	32	53	87	
6	11	19	32	53	87	142	
8	14	24	40	66	108	176	
11	19	32	53	87	142	231	
14	24	40	66	108	176	286	
16	27	45	74	121	197	320	
$b_{n,k},\ n = 0, \ldots, 6,\ k = 1, \ldots, 7;$							

(c)

1	2	4	7	12	20	33	
4	7	12	20	33	54	88	
9	15	25	41	67	109	177	
12	20	33	54	88	143	232	
17	28	46	75	122	198	321	
22	36	59	96	156	253	410	
25	41	67	109	177	287	465	
$c_{n,k},\ n = 0, \ldots, 6,\ k = 1, \ldots, 7;$							

(d)

1	3	6	11	19	32	53	
4	8	14	24	40	66	108	
9	16	27	45	74	121	197	
12	21	35	58	95	155	252	
17	29	48	79	129	210	341	
22	37	61	100	163	265	430	
25	42	69	113	184	299	485	
$d_{n,k},\ n = 0, \ldots, 6,\ k = 1, \ldots, 7.$							

TABLE 1. Quilt black quartet, describing squares $S_{n,k} = [a_{n,k}, b_{n,k}] \times [c_{n,k}, d_{n,k}]$ in Figure 1

3. Panorama of Results

3.1. **Quilt results.** Each part of the paper treats one the following three results:

Proposition 3.1. *For Figure 1, consider the underlying grid of unit square cells. Then for $n = 1, 2, \ldots$, blackening in row (column) n of Figure 1 begins in column (row) $A(n) = \lceil n/\phi \rceil$ and ends in column (row) $\Omega(n) = \lfloor n\phi \rfloor$.*

Proof. In Part 1 of this paper [38], where it is shown for the stair-cone figure. □

Proposition 3.2 (Cohort-based formulas)**.** *For the black squares in Figure 1, $n = 0, 1, 2, \ldots$, $k = 1, 2, 3 \ldots$, the coordinate arrays (Table 1) satisfy*

$$a_{n,k} = F_{k+2} + \lfloor n\phi \rfloor F_{k+1} + nF_k \quad -1; \tag{1}$$

$$b_{n,k} = F_{k+3} + \lfloor n\phi \rfloor F_{k+1} + nF_k \quad -2; \tag{2}$$

$$c_{n,k} = F_{k+2} + \lfloor n\phi \rfloor F_{k+2} + nF_{k+1} - 1; \tag{3}$$

$$d_{n,k} = F_{k+3} + \lfloor n\phi \rfloor F_{k+2} + nF_{k+1} - 2; \tag{4}$$

	1	1	1	1	1	1	1	1	2	3	5	8	13	21	
	3	4	6	9	14	22	35	3	5	8	13	21	34	55	
	4	6	9	14	22	35	56	4	7	11	18	29	47	176	
(α)	6	9	14	22	35	56	90	6	10	16	26	42	68	110	(β)
	8	12	19	30	48	77	124	8	13	21	34	55	89	144	
	9	14	22	35	56	90	145	9	15	24	39	63	102	165	
	11	17	27	43	69	111	179	11	18	29	47	76	123	199	
	$\alpha_{n,k},\ n=1,\ldots,7,\ k=1,\ldots,7;$							$\beta_{n,k},\ n=1,\ldots,7,\ k=1,\ldots,7;$							
	2	4	7	12	20	33	54	3	6	11	19	32	53	87	
	5	9	15	25	41	67	109	6	11	19	32	53	87	142	
	7	12	20	33	54	88	143	8	14	24	40	66	108	176	
(γ)	10	17	28	46	75	122	198	11	19	32	53	87	142	231	(δ)
	13	22	36	59	96	156	253	14	24	40	66	108	176	286	
	15	25	41	67	109	177	287	16	27	45	74	121	197	320	
	18	30	49	80	130	211	342	19	32	53	87	142	231	375	
	$\gamma_{n,k},\ n=1,\ldots,7,\ k=1,\ldots,7;$							$\delta_{n,k},\ n=1,\ldots,7,\ k=1,\ldots,7.$							

TABLE 2. Quilt white quartet, describing rectangles $R_{n,k} = [\alpha_{n,k}, \beta_{n,k}] \times [\gamma_{n,k}, \delta_{n,k}]$ in Figure 1

Whereas for the white rectangles in Figure 1, $n = 1, 2, 3 \ldots$, $k = 1, 2, 3 \ldots$, the coordinate arrays (Table 2) satisfy.

$$\alpha_{n,k} = -F_{k+1} + \lfloor n\phi \rfloor F_k \quad + nF_{k-1} + 1; \tag{5}$$

$$\beta_{n,k} = \qquad \lfloor n\phi \rfloor F_k \quad + nF_{k-1}; \tag{6}$$

$$\gamma_{n,k} = \quad F_{k+1} + \lfloor n\phi \rfloor F_{k+1} + nF_k \quad - 1; \tag{7}$$

$$\delta_{n,k} = \quad F_{k+3} + \lfloor n\phi \rfloor F_{k+1} + nF_k \quad - 2. \tag{8}$$

Proof. Detailed in Section 4.1.4, the proof follows from Corollary 4.4 on cohort sequences. □

Corollary 3.3 (of Proposition 3.2, Fibonacci word in the quilt)**.** $\forall n, k \in \mathbb{Z}^+, n \geq 2$

$$\begin{aligned}
\underline{005614}(n-2) &= \quad A_n - A_{n-1}, \\
&= \quad \Omega_n - \Omega_{n-1} - 1, \\
&= (\alpha_{n,k} - \alpha_{n-1,k} - F_{k+1})/F_k, \\
&= (\beta_{n,k} - \beta_{n-1,k} - F_{k+1})/F_k, \\
&= (a_{n,k} - a_{n-1,k} - F_{k+2})/F_{k+1}, \\
&= (b_{n,k} - b_{n-1,k} - F_{k+2})/F_{k+1}, \\
&= (\gamma_{n,k} - \gamma_{n-1,k} - F_{k+2})/F_{k+1}, \\
&= (\delta_{n,k} - \delta_{n-1,k} - F_{k+2})/F_{k+1}, \\
&= (c_{n,k} - c_{n-1,k} - F_{k+3})/F_{k+2}, \\
&= (d_{n,k} - d_{n-1,k} - F_{k+3})/F_{k+2}.
\end{aligned}$$

Proof. Direct calculation from Propositions 3.1 and 3.2. □

Part 3 of this paper [40] will treat the following result:

Proposition 3.4 (Spectrum relationship between a and d)**.**

$$d_{n,k} = \lfloor a_{n,k}\phi \rfloor, n = 0, 1, 2, \ldots, k = 1, 2, 3 \ldots. \tag{9}$$

Proof. In Part 3 of this paper [40]. □

3.2. **Cohort results — a by-product of the investigation of the quilt.** This part of the paper emphasizes cohort sequences, a device introduced in Part 1 [38] and further developed here to prove properties of the quilt, such as Proposition 3.2. Designations of cohort sequences as "2–1-" or "1–2-" follow the convention of *formula* in Definition 10 of Rozenberg and Lindenmayer [30] for a catenative recurrence.

The paper displays sequences in *cohort tableaux* such as Tables 6 and 7. To distinguish a 1–2-structure from a 2–1-structure, the dense tableaux use left, respectively, right, alignment of what has been called various a "tetrangle" or "irregular triangle array." Thus, the tableau format makes the specific cohort structure of the sequence easier to visualize. Each of the *Fibonacci cohort tableau* is planar graph isomorphic to an infinite, regular, single-rooted binary tree of the positive integers.

Definition 9.2 extends the notion of tableau beyond dense tableaux to diatomic tableaux (Table 40). Tableaux with a less-decidedly left or right structure also appear (Table 26), as ultimately, the above duality of cohort structures may expand to a multiplicity (Corollary 9.2). (It may also collapse to a unity (Section 9.4).) The results obtained using cohorts include:

- For various sequences of integers, tuples, and functions, classification under the rubric of "cohort sequence" (Table 8);
- Unified treatment of the free monoids $\{\kappa, \lambda\}^\star$ and $\{\theta, \eta\}^\star$, comprising:
  - For the free monoid $\{\kappa, \lambda\}^\star$ generated by the Wythoff pair $\{\kappa, \lambda\}$ under composition, three canonical forms (Corollary 4.4 — a form similar to that given by Kimberling [22], Proposition 4.6 — the homogeneous form, and Corollary 4.15 — the "pure-κ" form), and total order of its individual members, via Propositions 4.16(b) or 5.2. The paper also arranges the free monoid in an array, Table 9, and in a *1–2-Fibonacci cohort tableau*, Table 10.
  - For equivalence classes $S/\circ\kappa^\star \in \{\kappa, \lambda\}^\star/\circ\kappa^\star$ on the same free monoid $\{\kappa, \lambda\}^\star$, total order via Corollary 4.11 or Corollary 5.3. The paper arranges the classes in a *1–2-Fibonacci cohort tableau*, Table 11 and in an "outside inward" tree, Figure 4.
  - For the free monoid $\{\theta, \eta\}^\star$ generated by the Wythoff^{-1} pair $\{\theta, \eta\}$ under composition, two canonical forms (Proposition 4.19 — the homogeneous form, and Corollary 4.29 — the "pure-θ" form), and total order of its individual members, via Propositions 4.30 or 5.4, shown in an array, Table 14, in a *2–1-Fibonacci cohort tableau*, Table 13, and in an "inside outward" tree, Figure 7.
  - Also for the free monoid $\{\theta, \eta\}^\star$, a total order of equivalence classes $S/\theta^\star\circ \in \{\theta, \eta\}^\star/\theta^\star\circ$, via Corollary 4.39 or Corollary 5.5, arranged in a *1–2-Fibonacci cohort tableau*, Table 16.

⟸ Cohort Duality ⟹

Right clades of min successor tree | Right clades of max successor tree

$\circ I$	$\circ\kappa$	$\circ\kappa^2$	$\circ\kappa^3$	$\circ\kappa^4$	$\circ\kappa^5$	$I\circ$	$\theta\circ$	$\theta^2\circ$	$\theta^3\circ$	$\theta^4\circ$	$\theta^5\circ$
	$\bullet 2$	$\bullet 3$	$\bullet 4$	$\bullet 5$	$\bullet 6$	$\bullet 7$		$\bullet 1$	$\bullet 1^2$	$\bullet 1^3$	$\bullet 1^4$	$\bullet 1^5$
1	2	3	5	8	13		1	2	4	7	12	20
4	6	9	14	22	35		3	6	11	19	32	53
7	10	15	23	36	57		5	10	18	31	52	86
11	16	24	37	58	92		8	16	29	50	84	139
12	17	25	38	59	93		9	17	30	51	85	140
18	26	39	60	94	149		13	26	47	81	136	225
19	27	40	61	95	150		14	27	48	82	137	226
20	28	41	62	96	151		15	28	49	83	138	227
29	42	63	97	152	241		21	42	76	131	220	364
30	43	64	98	153	242		22	43	77	132	221	365

1–2-Fibonacci Array(𝖥) — $n + F_{F^{-1}(n)+k+1}$ (194030)

2–1-Fibonacci Array(𝖤) — $n + F_{F^{-1}(n)+k+2} - F_{F^{-1}(n)+2}$

All-left branchings in min Fib tree / Columns of 1–2 Fib cohort tableau

All-left branchings in max Fib tree / Columns of 2–1 Fib cohort tableau

⟸ Mirror Duality ⟹

$\circ I$	$\circ\lambda$	$\circ\lambda^2$	$\circ\lambda^3$	$\circ\lambda^4$	$\circ\lambda^5$	$I\circ$	$\eta\circ$	$\eta^2\circ$	$\eta^3\circ$	$\eta^4\circ$	$\eta^5\circ$
	$\bullet 2$	$\bullet 2^2$	$\bullet 2^3$	$\bullet 2^4$	$\bullet 2^5$		$\bullet 2$	$\bullet 2^2$	$\bullet 2^3$	$\bullet 2^4$	$\bullet 2^5$
1	4	12	33	88	232	1	3	8	21	55	144
2	7	20	54	143	376	2	5	13	34	89	233
3	11	32	87	231	608	4	9	22	56	145	378
5	18	52	141	374	984	6	14	35	90	234	611
6	19	53	142	375	985	7	15	36	91	235	612
8	29	84	228	605	1592	10	23	57	146	379	989
9	30	85	229	606	1593	11	24	58	147	380	990
10	31	86	230	607	1594	12	25	59	148	381	991
13	47	136	369	979	2576	16	37	92	236	613	1600
14	48	137	370	980	2577	17	38	93	237	614	1601

1–2-mirror Array(𝖧) — $F_{2k+1} - 1$, $n=0$; $n+F_{F^{-1}(n)+2k}-2F_{F^{-1}(n)}, n\geq 1$

2–1-mirror Array(𝖩) — F_{2k}, $n=0$; $n+F_{F^{-1}(n)+2k-1}-F_{F^{-1}(n)-1}$, $n\geq 1$

All-right branchings in min Fib tree / Split cols of 2–1 Fib cohort tableau

All-right branchings in max Fib tree / Split cols of 1–2 Fib cohort tableau

Left clades of min successor tree | Left clades of max successor tree

TABLE 3. Branch Quartet of interspersion arrays: At left, array rows equal straight paths in minimal Fibonacci tree (Figure 5), columns equal $S(2)-1$ for compositions $S \in \{\kappa, \lambda\}^\star$ restricted in suffix, as shown, or integers with minimal Fibonacci gaps restricted in suffix, as shown (Proposition 8.5). At right, array rows equal straight paths in the maximal Fibonacci tree (Figure 8), columns equal $N_0(S)+1$ for compositions $S \in \{\theta, \eta\}^\star$ restricted in prefix, as shown, or integers with maximal Fibonacci gaps restricted in suffix, as shown. Blade dual of Clade Quartet, Table 4.

$\Longleftarrow$ Cohort Duality $\Longrightarrow$

	Right clades of min Fib tree						Right clades of max Fib tree					
	$I\circ$	$\kappa\circ$	$\kappa^2\circ$	$\kappa^3\circ$	$\kappa^4\circ$	$\kappa^5\circ$	$\circ I$	$\circ\theta$	$\circ\theta^2$	$\circ\theta^3$	$\circ\theta^4$	$\circ\theta^5$
	$2\bullet$	$3\bullet$	$4\bullet$	$5\bullet$	$6\bullet$	$7\bullet$		$1\bullet$	$1^2\bullet$	$1^3\bullet$	$1^4\bullet$	$1^5\bullet$
All-left paths in min successor tree / Columns of 1–2 successor tableau	1	2	3	5	8	13	1	2	4	7	12	20
	4	7	11	18	29	47	3	5	9	15	25	41
	6	10	16	26	42	68	6	10	17	28	46	75
	9	15	24	39	63	102	8	13	22	36	59	96
	12	20	32	52	84	136	11	18	30	49	80	130
	14	23	37	60	97	157	14	23	38	62	101	164
	17	28	45	73	118	191	16	26	43	70	114	185
	19	31	50	81	131	212	19	31	51	83	135	219
	22	36	58	94	152	246	21	34	56	91	148	240
	25	41	66	107	173	280	24	39	64	104	169	274
	Wythoff Array, (w) (035513)						**Quilt Array,** (a) (083047)					
	$F_{k+1}\kappa(n+1)+F_kn, n\geq 0$						$F_{k+1}\kappa(n)+F_kn+F_{k+2}-1, n\geq 0$					
$\Longleftarrow$ Mirror Duality $\Longrightarrow$												
	$I\circ$	$\lambda\circ$	$\lambda^2\circ$	$\lambda^3\circ$	$\lambda^4\circ$	$\lambda^5\circ$	$\circ I$	$\circ\eta$	$\circ\eta^2$	$\circ\eta^3$	$\circ\eta^4$	$\circ\eta^5$
		$2\bullet$	$2^2\bullet$	$2^3\bullet$	$2^4\bullet$	$2^5\bullet$		$2\bullet$	$2^2\bullet$	$2^3\bullet$	$2^4\bullet$	$2^5\bullet$
All-right paths in min successor tree / Split cols of left-justified 2–1 tableau	1	4	12	33	88	232	1	3	8	21	55	144
	2	6	17	46	122	321	2	6	16	42	110	288
	3	9	25	67	177	465	4	11	29	76	199	521
	5	14	38	101	266	698	5	14	37	97	254	665
	7	19	51	135	355	931	7	19	50	131	343	898
	8	22	59	156	410	1075	9	24	63	165	432	1131
	10	27	72	190	499	1308	10	27	71	186	487	1275
	11	30	80	211	554	1452	12	32	84	220	576	1508
	13	35	93	245	643	1685	13	35	92	241	631	1652
	15	40	106	279	732	1918	15	40	105	275	720	1885
	Wythoff Mirror Array, $(\mathfrak{w})$						**Quilt Mirror Array,** $(\mathfrak{a})$					
	$F_{2k+1}-1,\ n=0;$ (191436)						(132827)					
	$F_{2k-1}\kappa(n+1)+F_{2k-2}n-1, n\geq 1$						$F_{2k-1}\kappa(n)+F_{2k-2}n+F_{2k}, n\geq 0$					
	Left clades of min Fib tree						Left clades of max Fib tree					

All-left paths in max successor tree / Columns of 2–1 successor tableau

All-right paths in max successor tree / Split cols of right-justified 1–2 tableau

TABLE 4. Clade Quartet of interspersion arrays: At left, array columns equal clades of minimal Fibonacci tree (Figure 5); columns also equal $S(2)-1$ for compositions $S \in \{\kappa,\lambda\}^\star$ restricted in prefix, as shown, or integers with minimal Fibonacci gaps restricted in prefix, as shown (Proposition 8.6). At right, array columns equal clades of maximal Fibonacci tree (Figure 8); columns also equal $N_0(S)+1$ for compositions $S \in \{\theta,\eta\}^\star$ restricted in suffix, as shown, or integers with maximal Fibonacci gaps restricted in prefix, as shown. Blade dual of Branch Quartet, Table 3.

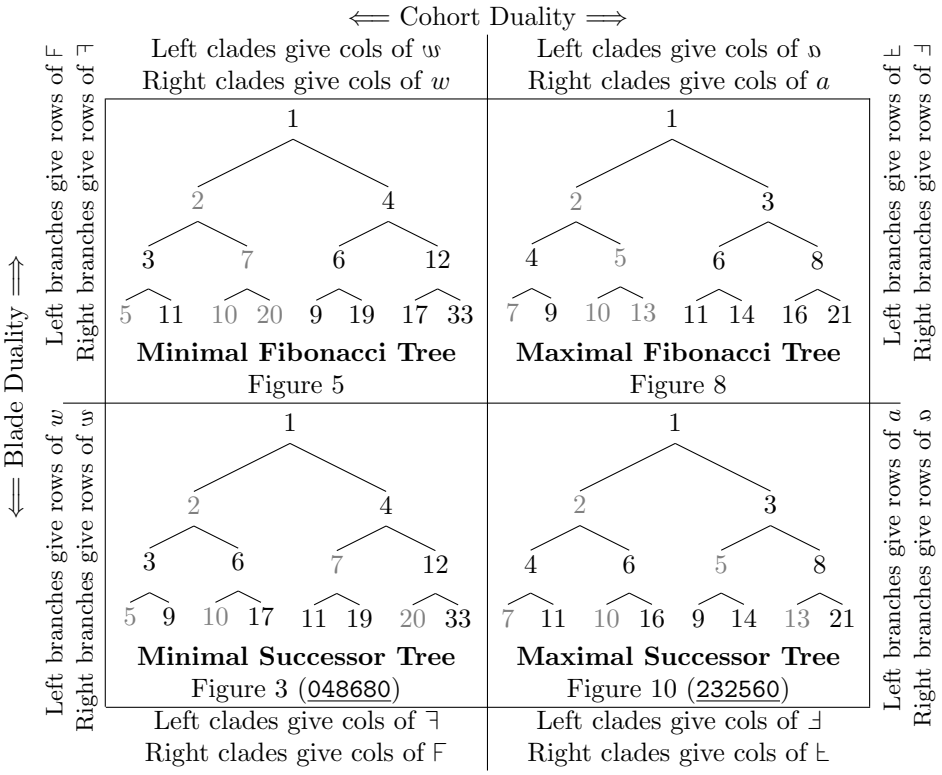

TABLE 5. Quartet of binary trees (see Figure 20 for commutative diagram).

- Fibonacci Numeration
  - For the maximal Fibonacci expansion, characterization by *2–1-Fibonacci cohort tableaux* (Tables 20–22) and an "outer" tree (equivalent Figures 8 and 13), positions in the tree given by a 2–1-Fibonacci cohort tableau (Table 18(ii)); and correspondence of the expansion to compositions of integers using 1's and 2's (Proposition 7.1). Study of the structure of the free monoid $\{\boldsymbol{L}, \boldsymbol{R}\}^\star$ on its branching functions $\boldsymbol{L}$ and $\boldsymbol{R}$ (Section 8.6).
  - For the minimal Fibonacci representation, a characterization by *1–2-Fibonacci cohort tableaux* (Tables 23–25) and an "outer" tree (equivalent Figures 5 and 14), positions in the tree given by a 1–2-Fibonacci cohort tableau (Table 18(i)); and correspondence of the representation to compositions of integers without 1's (Proposition 7.6). Study of the structure of the free monoid $\{\boldsymbol{l}, \boldsymbol{r}\}^\star$ on its branching functions $\boldsymbol{l}$ and $\boldsymbol{r}$ (Section 8.6).
- The eight interspersion arrays, comprising the branch quartet (Table 3) and the clade quartet (Table 4), and four equivalent ways of generating them:
  - 1. The "tree approach": Gathering branches or clades, from the minimal and maximal Fibonacci trees (Remarks 4.15 and 4.24) to form array rows

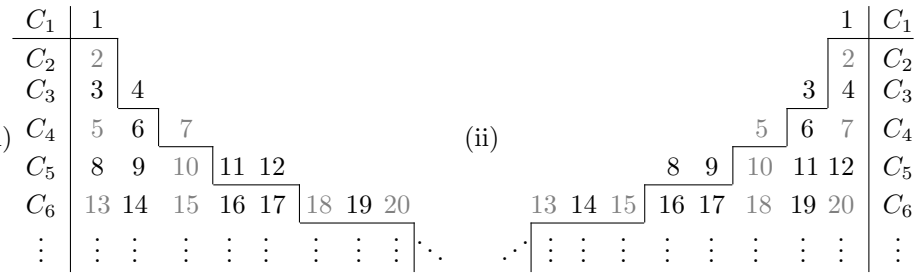

TABLE 6. The positive integers in 1–2-, respectively, 2–1-Fibonacci cohort tableau, (i) and (ii). Both tableaux place $(F_{t+1}, \ldots, F_{t+2} - 1)$ in *cohort* C_t. Whereas columns from left to right give successive rows of F (Table 12), tableau (i) corresponds bijectively to Tables 10, 11, and 16, as well as Table 28(i). Whereas columns give rows of L (Table 15), tableau (ii) corresponds bijectively to Table 13, as well as Table 28(ii). Taking "split columns" — which alternate cohorts of the tableau — of (i) and (ii) gives rows of J and P (Figure 3 at bottom right and left), respectively, (see Tables 28(iii) and (iv)). Blade duals of Tables 40(i) and (ii), respectively. Planar graph isomorphs of the minimal, respectively, maximal successor trees, Figures 3 and 10.

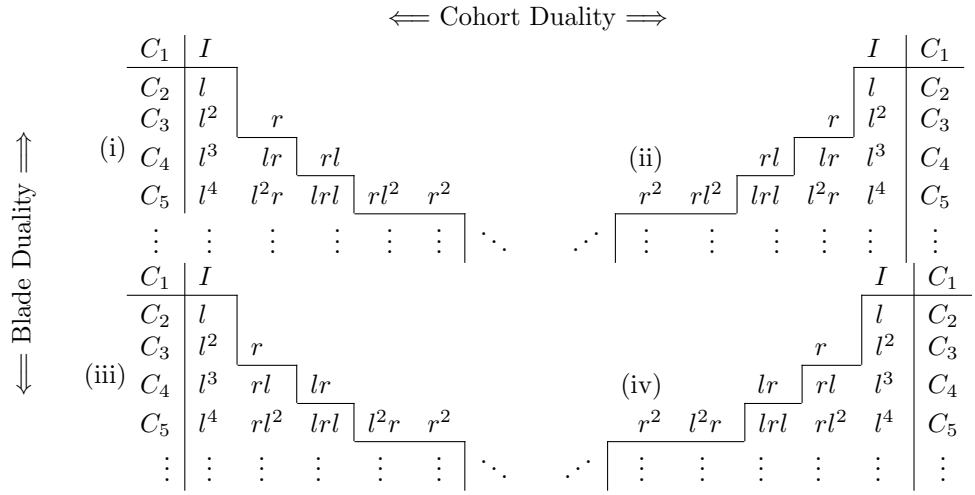

TABLE 7. Four orderings of words on two letters as Fibonacci cohort tableaux: (i) 1–2-Fibonacci outer cohort tableau and (ii) 2–1-Fibonacci outer cohort tableau (Example: Table 13), both isomorphic to an infinite, regular, single-rooted "outer" binary tree. (iii) 1–2-Fibonacci inner cohort tableau (Example: Table 10) and (iv) 2–1-Fibonacci inner cohort tableau, both isomorphic to an infinite, regular, single-rooted "inner" binary tree. Sequences $\underline{\texttt{102364}}$ and $\underline{\texttt{112310}}_0$ give number of symbols l, r in (i) and (iii), respectively, (ii) and (iv).

of the branch quartet, respectively, array columns of the clade quartet — See Figure 24(a); alternatively, Figure 25(b) for all-branches, Figure 25(c) for all-clades.

- 2. The "free-monoid approach": Restricting the order of compositions in $S \in \{\kappa, \lambda\}^\star$ and $S \in \{\theta, \eta\}^\star$, then using the maps of Propositions 4.16 and 4.30, to generate columns of arrays on the left, respectively, right, of Tables 3 and 4 (Figure 25(a)); alternatively, restricting compositions in $\{\boldsymbol{l}, \boldsymbol{r}\}^\star$, $\{\boldsymbol{L}, \boldsymbol{R}\}^\star$, $\{\bar{\boldsymbol{l}}, \bar{\boldsymbol{r}}\}^\star$, and $\{\bar{\boldsymbol{L}}, \bar{\boldsymbol{R}}\}^\star$ (Figures 25(b) and (c)).
- 3. The "numeration approach": Restricting gaps in minimal or maximal Fibonacci numeration (restricted composition of integers) to form columns — See Figure 24(c).
- 4. The "cohort-tableau approach": Manipulation of (columns of) cohort tableaux to form rows — See Figure 24(b).

- Three types of duality (Section 9.8)
  - *Cohort duality*
    - between 1–2- and 2–1-Fibonacci cohort tableaux, Tables 6(i),(ii);
    - between other pairs of dense cohort tableaux, such as Tables 34, 39, and 42(i) and (iii);
    - between 1–2 and 2–1-diatomic tableaux, Figures 40;
    - between other pairs of diatomic tableaux, Tables 42(ii) and (iv);
    - between arrays *within* the branch quartet: $\mathsf{F}_{n,k}$ to $\mathsf{L}_{n,k}$, respectively, $\mathsf{H}_{n,k}$ to $\mathsf{J}_{n,k}$, (left to right of Table 3), inherited from duality between tableaux (Section 8.2.2) or by swapping min and max trees (Remark 8.10);
    - between arrays *within* the clade quartet: $w_{n,k}$ to $a_{n,k}$ and $\mathfrak{w}_{n,k}$ to $\mathfrak{a}_{n,k}$, (left to right of Table 4)), by swapping minimal and maximal trees (Remark 8.8).
    - between other pairs of I–D arrays in Tables 35–38, 41, and 45;
    - Mutual dispersion of cohort duals (Proposition 8.22) by analogy to that of mirror duals.
    - between trees Figures 3 and 10 and between trees Figures 5 and 8.
    - between other pairs of trees, Left to right of Figure 29, Figures 30 and 31, Figures 32 and 33;
  - *Mirror duality* between individual arrays *within* the branch (clade) quartet by swapping left and right in the gathering of tree branches (clades)
    - Top to bottom of Table 3 (4).
    - Mutual dispersion of mirror duals (Proposition 8.21).
  - *Blade duality*
    - between the branch and clade quartets, swapping the gathering of tree branches with the gathering of tree clades in respective arrays;

    - between other pairs of I–D arrays (Table 41), where blade duality equals mirror duality;
    - between trees Figures 3 and 5 and between trees Figures 8 and 10, under the *tree blade permutation*, 059893;
    - between other pairs of trees Figures 18 and 21;
    - sufficient conditions for the blade dual of an I–D array to be an I–D array, Proposition 9.9.

- Tableau–tree planar graph isomorphism (Section 6.7)
  - between Fibonacci cohort tableaux (Table 6) and successor trees (Figures 3 and 10).
  - between successor tableaux (Table 19) and Fibonacci trees (Figures 5 and 8).
- Clade–tree order isomorphism (Sections 8.6.1 and 8.6.3).
  - with associated complete clade–column order isomorphism for the clade quartet and branch quartet, Corollaries 8.11 and 8.18;
  - with associated half-clade–column order isomorphism, and clade / column / cohort splitting for the branch mirror arrays (Proposition 8.20);
  - for the Positions tree and Blade tree (Figures 18 and 21).
- Extrapolations
  - "Shifting" branching functions to produce multiple trees arranging $\mathbb{Z}_+$ for each slope, Section 9.5;
  - The "Positions tree" (Figure 18) resulting from the limit of such slopes (Section 9.4). Together with its blade dual, the "Blade tree" (Figure 21), the pair minimize aggregate measures of distance between (the values of) neighboring nodes in the usual metric and in 2-adic distance, respectively (Remark 6.18);
  - A computational search for binary-tree arrangements of $\mathbb{Z}_+$ with a single clade–tree order isomorphism (necessary condition) for blade duality, as well as for those trees with complete clade–tree order isomorphism;
  - "Shifting" dense tableaux and Fibonacci numeration (Sections 9.1, 9.2);
  - A sieve (Figure 48) for the "floor-powerfree" integers, which cannot appear at outside nodes of trees, also extended to that shifted branching functions that use floor functions on Beatty pairs.

2–1-Fibonacci Cohort Sequences of Integers				
OEIS$_n$	Name	Notation	Form	Cohortizer
060145		$\lceil n/\phi \rceil - \left\lceil \frac{n}{1+\phi} \right\rceil$	2–1	F_{t-3}
189663$_2$ 060144		$\left\lceil n/\phi^2 \right\rceil$ $\left\lfloor n/\phi^2 \right\rfloor \equiv \eta(n)$	2–1	F_{t-2}
060143 019446		$\lfloor n/\phi \rfloor \equiv\ \theta(n)$ $\lceil n/\phi \rceil$	2–1	F_{t-1}
000027$_n$ 256958$_n$	Naturals Integers	n	2–1	F_t
003622 035336 035337 035338 035339 035340	Column j of Wythoff Array	$F_j(n-1)$ $+F_{j+1}\kappa(n)$	2–1	F_jF_t $+F_{j+1}F_{t+1}$
000201 022342 004956 026351 099267$_2$ 026355$_2$	Lower Wythoff, $\bar{\boldsymbol{L}}(n)-1$	$\lfloor n\phi \rfloor \equiv \kappa(n)$ $\kappa(n)-1$ $\lceil n\phi \rceil$ $\kappa(n)+1$ $\kappa(n-1)+2$	2–1	F_{t+1}
001950 003622	Upper Wythoff, $\bar{\boldsymbol{R}}(n)-1$	$\lfloor n\phi^2 \rfloor \equiv \lambda(n)$ $\lambda(n)-1$	2–1	F_{t+2}
134859 003623	Wythoff AAA Wythoff AB	$\kappa^3(n)$ $\kappa\lambda(n)$	2–1	F_{t+3}
151915 134860 101864	Wythoff AAAA Wythoff AAB Wythoff BB	$\kappa^4(n)$ $\kappa^2\lambda(n)$ $\lambda^2(n)$	2–1	F_{t+4}
134862	Wythoff ABB	$\kappa\lambda^2(n)$	2–1	F_{t+5}
134864	Wythoff BBB	$\lambda^3(n)$	2–1	F_{t+6}
003754 247648	Lazy Fibbinary Max Fibbinary		2–1 2–1	2^{t-2} 2^{t-1}
016789 060747		$3n+2$ $2n-1$	2–1	$3F_t$ $2F_t$
249115 195121	$1 \in$ max base-ϕ or κ_2 $1 \notin$ min base-ϕ	$3n-\kappa(n)-1$ $3n-\kappa(n)$	2–1	L_{t-1}
050140 054770		$2\kappa(n)-n$ $\kappa(n)+2n-1$	2–1	L_t
003231 214971	$1 \notin$ max base-ϕ or λ_2 $1 \in$ min base-ϕ	$\kappa(n)+2n$ $\kappa(n)+2n+1$	2–1	L_{t+1}
—	Column k of $\vdash$		2–1	$\langle F_{t+k+2}-F_{t+1},$ $F_{t+k+1}-F_{t-1}\rangle$
—	Column k of $\dashv$			$\langle F_{t+2k-1}+F_{t-2},$ $F_{t+2k-2}+F_{t-1}\rangle$
083047	Column k of a		2–1	F_{t+k+1}

—	Column k of $\mathfrak{s}$			F_{t+2k-1}
066628	Row indices of $\mathbb{Z}_+$ in F			$\langle 0, F_{t-2}\rangle$
130312	F_t F_t times	$\bar{\boldsymbol{R}}(n)-\bar{\boldsymbol{L}}(n)$		$\langle F_{t-1}, F_{t-2}\rangle$
—	F_t F_{t+1} times	$\bar{\boldsymbol{r}}(n)-\bar{\boldsymbol{l}}(n)$	2–1	$\langle 2F_t, 2F_{t-1}\rangle$
087172	F_{t+1} F_t times	$F_{F^{-1}(n)}$		$\langle F_t, F_{t-1}\rangle$
—	F_{t+p} F_t times			$\langle F_{t+p-1}, F_{t+p-2}\rangle$
	Left min Fib branch	$\boldsymbol{l}(n)$	2–1	$\langle F_{t+1}, F_{t+1}-F_{t-3}\rangle$
183544$_2$	Left branch, 1st tab shift	$\boldsymbol{l}(n)-1$		
	Right min Fib branch	$\boldsymbol{r}(n)$	2–1	$\langle F_{t+3}-F_{t-1}, F_{t+2}\rangle$
183545	Right branch, 1st tab shift	$\boldsymbol{r}(n)-1$		
	Left max Fib branch	$\boldsymbol{L}(n)$	2–1	$\langle F_{t+2}-F_{t-1}, F_{t+1}\rangle$
133512		$\boldsymbol{L}(n)-1$		
	Right max Fib branch	$\boldsymbol{R}(n)$		$\langle F_{t+2}, F_{t+2}-F_{t-1}\rangle$
096270$_0$	∞-Fib Word	$0,1,\ldots$	2–1	0
189661$_2$		$1,0,\ldots$		
112310$_0$	Lazy Terms Wythoff^{-1} Symbols		2–1	1
200648$_2$	Max Terms			
200650$_2$	Max Non Terms		2–1	$\langle 1, 0\rangle$
256660	Min Alt Terms			
130233$_1$	$F^{-1}(n)$	$\lfloor \log_\phi(\sqrt{5}n+1)\rfloor$	2–1	$\langle 2, 1\rangle$
072649	$F^{-1}(n)-1 \equiv t(n)$	$\lfloor \log_\phi(\sqrt{5}n+1)\rfloor-1$		
243571‡	**P**ositions in max fib tree	‡corrected $=\mathbf{P}$	2–1	$\mathbf{P}\mapsto\langle 2\mathbf{P}+1, 2\mathbf{P}\rangle$
167198-1	Rows in a		2–1	$\langle \boldsymbol{R}, \boldsymbol{L}\rangle$
—	Rows in $\mathfrak{s}$			
083368	Cols in a		2–1	$\langle I, \texttt{++}\rangle$

1–2-Fibonacci Cohort Sequences of Integers

060145		$\lceil n/\phi\rceil-\left\lceil \frac{n}{1+\phi}\right\rceil$	1–2	$\langle F_{t-4}, F_{t-2}\rangle$
060144		$\eta(n)$		$\langle F_{t-3}, F_{t-1}\rangle$
060143		$\theta(n)$		$\langle F_{t-2}, F_t\rangle$
000027$_\mathrm{n}$	Naturals	n	1–2	$\langle F_{t-1}, F_{t+1}\rangle$
256958$_\mathrm{n}$	Integers			
026273$_1$	$\bar{\boldsymbol{l}}(n)-1$	$\lfloor (n-1)\phi+\sqrt{5}\rfloor-1$	1–2	$\langle F_t, F_{t+2}\rangle$
058065$_0$		$\lfloor n\phi+\sqrt{5}\rfloor-2$		
026274$_1$	$\bar{\boldsymbol{r}}(n)-1$		1–2	$\langle F_{t+1}, F_{t+3}\rangle$
003714$_1$	Min Fibbinary		1–2	$\langle 2^{t-2}, 2^{t-1}\rangle$
194030	Column k of F		1–2	$\langle F_{t+k}+F_{t-1}, F_{t+k+1}+F_{t+1}\rangle$
—	Column k of $\mathsf{\exists}$			$\langle F_{t+2k-1}-F_{t-1}, F_{t+2k}-F_{t-2}\rangle$
035513	Column k of w			$\langle F_{t+k}, F_{t+k+2}\rangle$
—	Column k of $\mathfrak{w}$		1–2	$\langle F_{t+2k-2}, F_{t+2k}\rangle$
080164	Column k of w difference			
066628	Row indices of $\mathbb{Z}_+$ in F			$\langle 0, F_{t-1}\rangle$
130312	F_t F_t times	$\bar{\boldsymbol{R}}(n)-\bar{\boldsymbol{L}}(n)$		$\langle F_{t-2}, F_{t-1}\rangle$
			1–2	

—	F_t F_{t+1} times	$\bar{\boldsymbol{r}}(n) - \bar{\boldsymbol{l}}(n)$		$\langle 2F_{t-1}, 2F_t\rangle$
087172	F_{t+1} F_t times			$\langle F_{t-1}, F_t\rangle$
—	F_{t+p} F_t times			$\langle F_{t+p-2}, F_{t+p-1}\rangle$
005614_1	∞-Fib Word	$0, 1, \ldots$	1–2	$\langle 0, 0\rangle$
003849_1		$1, 0, \ldots$		
007895_1	Wythoff 1 Terms			$\langle 0, 1\rangle$
135818_2	Min Terms		1–2	$\langle 1, 0\rangle$
102364	Wythoff Symbols			$\langle 1, 1\rangle$
135817	Wythoff Terms			
130233_1	$F^{-1}(n)$	$\lfloor \log_\phi(\sqrt{5}n+1)\rfloor$	1–2	$\langle 1, 2\rangle$
072649	$F^{-1}(n) - 1 \equiv t(n)$	$\lfloor \log_\phi(\sqrt{5}n+1)\rfloor - 1$		
—	**p**ositions in min fib tree	$\mathbf{p}$	1–2	$\mathbf{p} \mapsto \langle 2\mathbf{p}, 2\mathbf{p}+1\rangle$
019586	Rows in w			
—	Rows in $\mathfrak{w}$		1–2	$\langle \boldsymbol{l}, \boldsymbol{r}\rangle$
026272				
035612	Cols in w		1–2	$\langle \mathtt{++}, I\rangle$

Fibonacci Cohort Sequences of Tuples

Max Indices	$\mathbf{F}_\star(n)$	2–1	$\oplus(t)$
Max Gaps	$\boldsymbol{\nabla}_\star(n)$	2–1	$\langle \oplus(2), \oplus(1)\rangle$
Min Indices	$\mathbf{f}(n)$	1–2	$\langle \mathtt{++}, \oplus(t+1)\rangle$
Min Gaps	$\boldsymbol{\partial}(n)$	1–2	$\langle \mathtt{++}, \oplus(2)\rangle$

Fibonacci Cohort Sequences of Functions

Compositions in free monoid	$S \in \{\kappa, \lambda\}^\star$	1–2	$\langle \circ\kappa, \circ\lambda\rangle$
S_1-classes of compositions	$S \in \{\kappa, \lambda\}^\star / \circ\kappa^\star$		
Compositions in free monoid	$S \in \{\theta, \eta\}^\star$	2–1	$\langle \eta\circ, \theta\circ\rangle$
$N_{-1}(S)$ classes of compositions	$S \in \{\theta, \eta\}^\star / \theta^\star\circ$	1–2	$\langle \theta\circ, \eta\circ\rangle$

Pell Cohort Sequences

256958	Integers	n	2-1-1	$\langle P_{t-2}+P_{t-1}, P_{t-2}+P_{t-1}, P_t\rangle$
064437		$\lfloor n\chi - {}^3\!/_2\sqrt{2}\rfloor + 1$	2-1-1	$\langle P_{t-1}+P_t, P_{t-1}+P_t, P_{t+1}\rangle$
080652		$\lfloor n\chi - {}^1\!/_2\sqrt{2}\rfloor + 1$		
081841		$\lfloor n\chi - {}^3\!/_2\sqrt{2}\rfloor + 2$		
086377		$\lfloor n\chi - {}^1\!/_2\sqrt{2}\rfloor$		
328987		$\lfloor \lfloor n\chi - {}^1\!/_2\sqrt{2}\rfloor \chi - {}^1\!/_2\sqrt{2}\rfloor + 2$	2-1-1	$\langle P_t + P_{t+1}, P_t + P_{t+1}, P_{t+2}\rangle$
256958	Integers	n	1-2-1	$\langle P_{t-1}, P_t, P_t\rangle$
003151	Silver Beatty	$\lfloor n\chi\rfloor$	1-2-1	$\langle P_t, P_{t+1}, P_{t+1}\rangle$
080754		$\lceil n\chi\rceil$		
082845		$\lfloor n\chi + \sqrt{2}\rfloor - 1$		
285075		$\lfloor n\chi - \sqrt{2}\rfloor + 1$		
098021		$\lfloor \lfloor n\chi\rfloor \chi\rfloor + 1$	1-2-1	$\langle P_{t+1}, P_{t+2}, P_{t+2}\rangle$
140868		$\lfloor \lfloor n\chi\rfloor \chi\rfloor$		

188039 276879		$\lfloor \lfloor n\chi - \sqrt{2} \rfloor \chi \rfloor$ $\lfloor \lfloor n\chi - \sqrt{2} \rfloor \chi \rfloor - 1$		
187975		$\lfloor \lfloor \lfloor n\chi \rfloor \chi \rfloor \chi \rfloor + 3$	1-2-1	$\langle P_{t+2}, P_{t+3}, P_{t+3} \rangle$
256958	Integers	n	1-1-2	$\langle P_{t-1}, 2P_{t-2}, P_{t-1} + P_t \rangle$

TABLE 8. Table of Fibonacci & Pell cohort sequences of integers, tuples, and functions.

4. Cohort Sequences of Integers

Remark 4.1. "Cohort" provides a convenient name for a generic property of sequences studied in this paper, though in the context of integer sequences it is similar to structures that have been discussed for decades by researchers including Cobham [10], Rozenberg and Lindenmayer [30], Shallit [33] and Stolarsky [43]). For integer sequences, *cohorts* refers to consecutive blocks (factors) of elements (letters), that decompose a sequence (word), each of which relates to preceding ones(s) through an affine catenative recurrence. Part 1 of the paper [38] used the term "cohort" to refer to specific collections of squares or rectangles in the quilt (Figure 1), which gave rise to the integer sequences to be investigated in this part of the paper. Later, the paper will extend this definition to cohort sequences of functions and cohort sequences of tuples.

In the context of binary words, the *Fibonacci word* provides an example of a cohort sequence. For the version 096270, each of the cohorts $0, 1, 01, 101, 01101$, 10101101 is merely the concatenation of the previous two, thus the recurrence is *purely catenative*, with the affine term of the *cohortizer* being zero.

Example 4.1. In the quilt (Figure 1), the formation of cohorts can be seen most prominently by examining the spacings between same-sized squares. For example, the 1×1 squares appear to be spaced *almost linearly* in the sense of [4], but furthermore, the spacings form self-similar clusters. Considering the 1×1 squares strictly below the diagonal, the third and fourth such squares, with southeast corners at $(a_{3,1}, d_{3,1}) = (8,12)$ and $(a_{4,1}, d_{4,1}) = (11,17)$, are spaced similarly to the first and second, at $(a_{1,1}, d_{1,1}) = (3,4)$ and $(a_{2,1}, d_{2,1}) = (6,9)$. The fifth, sixth, and seventh squares, at (14,22), (16,25) and (19,30), are spaced similarly to the second, third, and fourth, etc.

Referring to a sequential method for constructing the quilt [38], these clusters of squares are precisely the set of squares placed *simultaneously*, by the same action of the method. Further to this observation, Part 1 of the paper introduced the term *cohort* and the notation $C_{t,k}$ for the set of quilt squares of ordinal size k (cardinal dimensions $F_{k+1} \times F_{k+1}$) placed by action t of the method. In fact, the sequences of spacings between like-sized squares or rectangles of the quilt are scaled and shifted versions of the Fibonacci word 096270 (Corollary 3.3). In contrast to "block" which evokes a specific concept about 0–1-characteristic words or indicator sequences, "cohort" serves as a catchword for a structure present in the quilt geometry, as well as in related sequences of integers, functions, and tuples.

The quilt and the methods of constructing it reveal numerous occurrences of the Fibonacci word, as well as other cohort sequences. This motivates the remainder

of Section 4, which introduces several classes of cohort sequences of integers, giving examples along the way.

4.1. **Affine Fibonacci cohort sequences.**

Definition 4.1 (Fibonacci Cohort Sequence)**.** Decompose a sequence $S_1, S_2, \ldots, S_n, \ldots$ into finite blocks of consecutive elements, called *cohorts*, $C_1, C_2, \ldots, C_t, \ldots$, of increasing length $|C_t| = F_t$, such that

$$\begin{aligned} C_1 &\equiv (S_1), \\ C_2 &\equiv (S_2), \\ C_3 &\equiv (S_3, S_4), \\ C_4 &\equiv (S_5, S_6, S_7), \\ C_5 &\equiv (S_8, S_9, S_{10}, S_{11}, S_{12}), \\ &\vdots \\ C_t &\equiv (S_{F_{t+1}}, \ldots, S_{F_{t+2}-1}). \end{aligned}$$

If, for a function $f(t)$ depending only on t, elements in cohort C_t satisfy the t relations

$$\begin{aligned} S_{F_{t+1}} &= S_{F_{t-1}} + f(t), \\ &\vdots \\ S_{F_{t+2}-1} &= S_{F_{t+1}-1} + f(t), \end{aligned} \tag{10}$$

for each cohort C_t, $t = 3, 4, \ldots$, then designate $(S_n)_{n\geq 1}$ a *Fibonacci cohort sequence under* f. Equivalently, designate $S_1S_2S_3\cdots$ a *Fibonacci cohort word*. Also designate $f(t)$ a *Fibonacci cohortizer* of $(S_n)_{n\geq 1}$. Equivalently, let it be said that $f(t)$ *cohortizes* the sequence $(S_n)_{n\geq 1}$, or that it furnishes the sequence with a *Fibonacci cohort structure*, which will mean only that the sequence comes to satisfy the above relations via $f(t)$ (This is not an abstract-algebraic or model-theoretic use of "structure").

Remark 4.2. The relations (10) can be written using cohorts rather than elements, giving $C_t = C_{t-2}C_{t-1} + f(t)$, where the juxtaposition $C_{t-2}C_{t-1} = (S_{F_{t-1}}, \ldots, S_{F_{t+1}-1})$ represents the concatenation of C_{t-2} and C_{t-1}, over which, the addition of $f(t)$ distributes to each to element S_n. Thus, when $f(t) \equiv 0$, the sequence of cohorts is *locally catenative* in the language of Rozenberg and Lindenmayer [30], and purely so. Extending the definitions in [30], the present section defines a Fibonacci sequence of cohorts to be "locally affinely catenative," with a *width* of 2, a *cut* of 3, and a *locally catenative formula* of $\langle 2, 1\rangle$ plus an affine term $f(t)$ (Section 4.2 treats the $\langle 1, 2\rangle$ formula and gives examples. Section 4.3 treats the $\langle 2, 1, 1\rangle$, $\langle 1, 2, 1\rangle$, and $\langle 1, 1, 2\rangle$ formulas for a Pell sequence of cohorts and gives examples). Depending on context, the present paper uses "Fibonacci cohort sequence" interchangeably — to refer either to the sequence of cohorts, or to the sequence of elements provided with a Fibonacci cohort structure having the specified parameters.

Definition 4.2 (Fibonacci Cohort Sequence from the u^{th} cohort, $u \geq 0$)**.** If a sequence satisfies relations (10) only for cohorts indexed $t = u + 1, u + 2, \ldots$, then designate the sequence a *Fibonacci cohort sequence from the* u^{th} *cohort*. In this case, the F_{u+1} elements $S_{F_u}, \ldots, S_{F_{u+2}-1}$ (of cohorts C_{u-1} and C_u) constitute the "seed"

that must be known in order to continue the sequence, or in the language of [30], $u + 1$ equals the cut. Hence, to be precise, Definition 4.1 describes a *Fibonacci cohort sequence from the* 2^{nd} *cohort*.

If the sequence satisfies $S_2 = S_1 + f(2)$, in addition to the relations (10), then the sequence is a *Fibonacci cohort sequence from the* 1^{st} *cohort*. In this case, since $F_{1+1} = 1$, the first element, S_1, alone suffices to continue the sequence, with the remaining elements $S_2, S_3, \ldots$ obtained from the singleton "seed," recursively, using the relations (10) and the additional relation just given.

If the sequence also has a zeroth "seed" element S_0, permitting the convention $|C_0| = 1$, and the sequence satisfies $S_1 = S_0 + f(1)$ and $S_2 = S_1 + f(2)$, in addition to (10), then designate the sequence a *Fibonacci cohort sequence from the* 0^{th} *cohort*. In this case, since $F_{0+1} = 1$, the zeroth element, S_0, alone suffices to continue the sequence, with the remaining elements $S_1, S_2, \ldots$ obtained recursively using the relations (10) and the two additional relations just given.

Though not immediately obvious, the relations for a Fibonacci cohort sequence from the 1^{st} cohort, (namely (10) and $S_2 = S_1 + f(2)$), provide a graph isomorphism between the sequence S and a binary tree with a single root at S_1, since for positive integer $n \in [F_{t+1}, F_{t+2})$ each element $S_n \in C_t$, of the sequence generates two subsequent elements $S_n + f(t+1) = S_{n+F_{t+1}} \in C_{t+1}$ and $S_n + f(t+2) = S_{n+F_{t+2}} \in C_{t+2}$. Hence, the text will refer to these as *children* of S_n, and, conversely, S_n as their *parent*.

Remark 4.3. A sequence can also begin to satisfy the Fibonacci cohort relations (10) mid-cohort. See Section 4.1.10 for an example.

Initially, the paper will address Fibonacci cohort sequences of integers, with the "+" operation of Definitions 4.1 and 4.2 indicating ordinary scalar addition.

4.1.1. *Constant Cohortizer.* As previously noted, the constant 0 cohortizes a version of the Fibonnaci word, Sloane's $\underline{\texttt{096270}}_0$, (equivalent to $\underline{\texttt{005614}}_0$ with a 0 prepended). Thus, for this *purely catenative* sequence, $S = 0,\ 1,\ 0, 1,\ 1, 0, 1,\ 0, 1, 1, 0, 1, \ldots$, we have $S_n = S_{n-F_t}$. The same is true of its binary complement, $\underline{\texttt{189661}}_2$, (that is, $\underline{\texttt{189661}}$ with the initial 0 omitted, equivalent to $\underline{\texttt{003849}}_0$ with a 1 prepended). Proposition 4.43, to come, illustrates additional properties of these sequences.

The constant 1 cohortizes the number of terms in the lazy Fibonacci representation of nonnegative integers $n = 0, 1, 2, \ldots$ (Sloane's $\underline{\texttt{112310}}_0$). That is, for this sequence $S = 0,\ 1,\ 1, 2,\ 2, 2, 3,\ 2, 3, 3, 3, 4, \ldots$, we have $S_n - S_{n-F_t} = 1$. Adding one to each value, the resulting sequence $\underline{\texttt{112310}}_0{+}1{=}\underline{\texttt{200648}}_2$ plays the corresponding role for the *maximal Fibonacci expansion* (Definition 6.1) of positive integers $n = 1, 2, 3, \ldots$, counting the number of terms in the expansion depicted in Figure 13. Example 4.19, to come, illustrates this and others properties of the latter sequence. Now, the sequence $\underline{\texttt{112310}}_0$ also gives the number of symbols appearing in 2–1-Fibonacci cohort tableaux, Tables 7(ii) and (iv).

Example 4.19 describes a Fibonacci cohort sequence from the 0^{th} cohort under cohortizer 1 giving the level of the trees, Figures 8 or 10, on which appear successive elements of the first columns $\vdash_{n,1}$, $\dashv_{n,1}$, $a_{n,1}$ and $\wr_{n,1}$ of arrays: 1, 2, 3, 3, 4, 4, 4, 5, 4, 5, 5, 5, 6, 5, 5, 6, 5, 6, 6, 6, 7, ... The sequence does not appear in [41] as of this writing, though it resembles $\underline{\texttt{200648}}{+}1$ (except for the first element).

4.1.2. *The Cohortizer* 2^{t+p}. Allouche, Shallit, and Skordev [3] show that a sequence $0,\ 1,\ 2, 3,\ 5, 6, 7,\ 10, 11, 13, 14, 15,\ 21, 22, 23, 26, 27, 29, 30, 31, \ldots$ (003754), studied by Kimberling [21], comprises integers that do not contain the block 00 in their binary expansions. Consequently, they denote this sequence the 'lazy fibbinary transform' of the nonnegative integers ([3], Proposition 6). In other words, these numbers result from taking the Fibonacci indices of their lazy Fibonacci expansions, and convolving these coefficients with a basis of powers of two, substituted for the basis of Fibonacci numbers $(F_2, F_3, F_4, \ldots)$. Beginning with $S_1 = 0$, it is a Fibonacci cohort sequence under cohortizer $f(t) = 2^{t-2}$.

By contrast, starting with $S_1 = 1$ and applying the cohortizer $f(t) = 2^{t-1}$, yields the Fibonacci cohort sequence $1,\ 3,\ 5, 7,\ 11, 13, 15,\ 21, 23, 27, 29, 31,\ 43, 45, 47, 53,$ $55, 59, 61, 63, \ldots$ (247648), comprising integers whose binary expansions end in a 1 *and* do not contain the block 00. This sequence results from taking Fibonacci indices of the *maximal Fibonacci expansion* (Definition 6.1), for the positive integers, and convolving these coefficients with a basis of powers of two, substituted for the Fibonacci numbers $(F_1, F_2, F_3, \ldots)$. The lazy fibbinary numbers and 'maximal fibbinary numbers' are both cohort sequences, a result which follows from the recursive expansions (63) and (64), of the respective Fibonacci indices.

4.1.3. *Generalized Fibonacci cohortizer.* For many cohort sequences investigated herein, the cohortizer $g(t)$ obeys the generalized Fibonacci property. That is, $g(t) = g(t-2) + g(t-1)$ for $t = 3, 4, 5, \ldots$. The following lemma concerns itself with this more general type of Fibonacci cohort sequence.

Lemma 4.1 (Fibonacci cohort sequence with generalized Fibonacci cohortizer)**.** *Let $S = S_0, S_1, S_2, \ldots$ be a Fibonacci cohort sequence from the 0^{th} cohort under cohortizer $g(t)$, where $g(t)$ satisfies the generalized Fibonacci property $g(t) = g(t-2) + g(t-1)$ for $t = 3, 4, 5, \ldots$. Let $g(0) = g(2) - g(1)$, if otherwise undefined. By Definition 4.2, $C_1 = C_0 + g(1)$, $C_2 = C_1 + g(2)$, and $C_t = C_{t-2}C_{t-1} + g(t)$ for $t = 3, 4, 5 \ldots$. In addition,*

(a): *For $t \geq 2$ even, $C_t = C_0 C_1 \cdots C_{t-3} C_{t-2} + g(t+1)$.*
(b): *For $t \geq 1$ odd, $C_t = [C_0 - g(0)] C_1 \cdots C_{t-3} C_{t-2} + g(t+1)$.*
(c): *For $t \geq 0$, the last element in each cohort satisfies $S_{F_{t+2}-1} = S_0 + g(t+2) - g(2)$.*

Proof of Lemma 4.1. Prove all three statements by induction. First calculate the first few cohorts to confirm the base cases from which to induce the claims:

$$
\begin{aligned}
C_0 &= (S_0), \\
C_1 &= (S_0 + g(1)), \\
C_2 &= (S_0 + g(1) + g(2)) \\
&= (S_0 + g(3)), \\
C_3 &= (S_0 + g(1) + g(3), S_0 + g(1) + g(2) + g(3)) \\
&= (S_0 + g(4) - g(0), S_0 + g(5) - g(2)), \\
C_4 &= (S_0 + g(1) + g(2) + g(4), S_0 + g(1) + g(3) + g(4), S_0 + g(1) + g(2) + g(3) + g(4)) \\
&= (S_0 + g(5), S_0 + g(1) + g(5), S_0 + g(6) - g(2)).
\end{aligned}
$$

Next, show the induction step for each of the three claims **(a)**, **(b)**, and **(c)**.

(a): By definition of Fibonacci cohort sequence, $C_{t-1} = C_{t-3}C_{t-2} + g(t-1)$ and $C_t = C_{t-2}C_{t-1} + g(t)$. By the generalized Fibonacci property of

the cohortizer $g(t-1)+g(t)=g(t+1)$. By the induction hypothesis, $C_{t-2}=C_0C_1\cdots C_{t-5}C_{t-4}+g(t-1)$, since $t-2$ is also even. Thus,

$$\begin{aligned} C_t &= C_{t-2}C_{t-1}+g(t)\\ &= [C_0C_1\cdots C_{t-5}C_{t-4}+g(t-1)][C_{t-3}C_{t-2}+g(t-1)]+g(t)\\ &= C_0C_1\cdots C_{t-3}C_{t-2}+g(t+1). \end{aligned}$$

(b): By definition of Fibonacci cohort sequence, $C_{t-1}=C_{t-3}C_{t-2}+g(t-1)$ and $C_t=C_{t-2}C_{t-1}+g(t)$. By the generalized Fibonacci property of the cohortizer $g(t-1)+g(t)=g(t+1)$. By the induction hypothesis, $C_{t-2}=[C_0-g(0)]C_1\cdots C_{t-5}C_{t-4}+g(t-1)$, since $t-2$ is also odd. Thus,

$$\begin{aligned} C_t &= C_{t-2}C_{t-1}+g(t)\\ &= [[C_0-g(0)]C_1\cdots C_{t-5}C_{t-4}+g(t-1)][C_{t-3}C_{t-2}+g(t-1)]+g(t)\\ &= [C_0-g(0)]C_1\cdots C_{t-3}C_{t-2}+g(t+1). \end{aligned}$$

(c): By (10), $S_{F_{t+2}-1}=S_{F_{t+1}-1}+g(t)$. By the generalized Fibonacci property of the cohortizer $g(t)+g(t+1)=g(t+2)$. By the induction hypothesis, $S_{F_{t+1}-1}=S_0+g(t+1)-g(2)$. Thus, $S_{F_{t+2}-1}=S_{F_{t+1}-1}+g(t)=S_0+g(t+2)-g(2)$, as desired.

□

4.1.4. *The Cohortizer F_{t+p}.* The following discussion concerns cohortizers of the form $f(t)=F_{t+p}$, where constant $p\in\mathbb{Z}$ regulates the *rate* of increase of a cohort sequence of integers. For example, if the initial "seeds" are consecutive integers, then for $p=0$, the sequence will continue with consecutive integers, thus each successive element will increase strictly by 1. For $p>0$ it will increase more quickly, and for $p<1$ and $f(t)=F_{(t+p)^+}$, it will increase more slowly, yet remain nondecreasing.

Proposition 4.2. *For integers S_1, S_2 and $p\geq -2$, take $f(t)=F_{t+p}$ in (10) to obtain relations that define a Fibonacci cohort sequence from the 2^{nd} cohort as:*

$$S_n \equiv \begin{cases} S_1, & n=1;\\ S_2, & n=2;\\ S_{n-F_t}+F_{t+p}, & F_{t+1}\leqslant n<F_{t+2},\ t=3,4,\ldots \end{cases} \tag{11}$$

Then (11) holds if and only if

$$\begin{aligned} S_n = &-(F_{p+1}+S_1-S_2)\lfloor n/\phi\rfloor\\ &+(F_{p+2}+S_1-S_2)\lfloor (n-1)/\phi\rfloor\\ &+F_{p+1}(n-1)\\ &+S_1. \end{aligned} \tag{12}$$

Proof. Substituting $n=1$ and $n=2$ into (12) yields S_1 and S_2, respectively. To verify the formula for $n\geq 3$, take $S_n-S_{n-F_t}$ and make the substitution $n=j+F_t$ to obtain:

$$\begin{aligned} S_n-S_{n-F_t} = &-(S_1-S_2+F_{p+1})(\lfloor (j+F_t)/\phi\rfloor-\lfloor j/\phi\rfloor)\\ &+(S_1-S_2+F_{p+2})(\lfloor (j-1+F_t)/\phi\rfloor-\lfloor (j-1)/\phi\rfloor)\\ &+F_tF_{p+1} \end{aligned} \tag{13}$$

Now $F_{t+1} \leq n < F_{t+2}$ implies that $F_{t-1} \leqslant j < F_{t+1}$, and Lemma 2 of Fraenkel, Mushkin, and Tassa [17] (see also Lemma 1 of Bunder & Tognetti [7]) gives $\lfloor (j+F_t)/\phi \rfloor - \lfloor j/\phi \rfloor = F_{t-1}$ for $1 \leq j < F_{t+1}$. It also gives $\lfloor (j-1+F_t)/\phi \rfloor - \lfloor (j-1)/\phi \rfloor = F_{t-1}$, since $F_{t-1} - 1 \leq j - 1 < F_{t+1} - 1$. Thus (13) reduces to $S_n - S_{n-F_t} = F_{p+2}F_{t-1} + F_{p+1}F_{t-2} = F_{t+p}$, where the last equality obtains using Binet's Formula or by Lemma 8 of Bunder & Tognetti [7]. □

Remark 4.4. Compared to (11), formula (12) simplifies the calculation of S_n, since the cohort index t does *not* appear. If it did, one might need to calculate t from n, using $t = F^{-1}(n) - 1 = \left\lfloor \log_\phi(\sqrt{5}n + 1) \right\rfloor - 1$ to relate t to n by logarithm.

The reader familiar with the continued fraction expansion of irrational numbers may recognize the mechanism of the proof and the resulting formula as belonging to this area. The formula (12) employs terms in $\lfloor (n-1)/\phi \rfloor$ and $\lfloor n/\phi \rfloor$. These are spectrum sequences with irrational base $1/\phi$. Whereas convergents to $1/\phi$ have numerator and denominator F_{t-1} and F_t, respectively, the proof decomposes the cohortizer F_{t+p} into terms in factor F_{t-1}, while the recurrence holds between elements of the sequence that lag one another by the cohort lengths $|C_t| = F_{t+2} - F_{t+1} = F_t$.

Proposition 4.49 will show relations for Bergman cohort sequences analogous to those of (11) and Corollary 4.50 will show formulas similar to those of Proposition 4.2 and Corollary 4.3.

Corollary 4.3. *Whereas $x = \phi$ uniquely solves the system $\lfloor nx \rfloor - \lfloor n/x \rfloor = n$, $\forall n \in \mathbb{Z}$, the following form is equivalent to (12):*

$$\begin{aligned} S_n = &- (F_{p+1} + S_1 - S_2) \lfloor n\phi \rfloor \\ &+ (F_{p+2} + S_1 - S_2) \lfloor (n-1)\phi \rfloor \\ &+ F_{p-1} n \\ &+ F_p + 2S_1 - S_2 \end{aligned} \tag{14}$$

Corollary 4.4. *For sequences that are Fibonacci cohort from the 1^{st} cohort (Definition 4.2), meeting the condition*

$$S_2 = S_1 + F_{p+2}, \tag{15}$$

in addition to (11), the formulas of Proposition 4.2 and Corollary 4.3 reduce to

$$S_n = F_p \lfloor n/\phi \rfloor + F_{p+1}(n-1) + S_1, \tag{16}$$

and, respectively,

$$S_n = F_p \lfloor n\phi \rfloor + F_{p-1} n - F_{p+1} + S_1. \tag{17}$$

Proof. Include the condition (15) in (11), then simplify (12) and (14) to obtain (16) and (17), respectively. □

Proof. (of Proposition 3.2) Consider black squares on or below the diagonal in the quilt. For each $k = 1, 2, \ldots$, Part 1 of the paper [38] describes the sequence $(S_{n,k})_{n=1}$ of quilt squares $S_{n,k}$ having size $F_{k+1} \times F_{k+1}$ (in unit cells) as a Fibonacci cohort sequence satisfying the recurrence

$$S_{n,k} = S_{n-F_t,k} + F_{t+k+1} \times F_{t+k+2}, F_{t+1} \leq n < F_{t+2}, t = 1, 2, \ldots. \tag{18}$$

Whereas this recurrence satisfies Definition 4.2 of a Fibonacci cohort sequence from the 0^{th} cohort, use Corollary 4.4, substituting the following into (17):

$$\begin{aligned}
&\text{For } a_{n,k}, \text{ take } S_1 = a_{1,k} = 2F_{k+2} - 1 \text{ and } p = k+1;\\
&\text{For } b_{n,k}, \text{ take } S_1 = b_{1,k} = \ F_{k+4} - 2 \text{ and } p = k+1;\\
&\text{For } c_{n,k}, \text{ take } S_1 = c_{1,k} = \ F_{k+4} - 1 \text{ and } p = k+2;\\
&\text{For } d_{n,k}, \text{ take } S_1 = d_{1,k} = 2F_{k+3} - 2 \text{ and } p = k+2.\\
&\text{Moreover,}\\
&\text{For } \mathfrak{s}_{n,k}, \text{ take } S_1 = \mathfrak{s}_{1,k} = 2F_{2k} \qquad \text{and } p = 2k-1.
\end{aligned}$$

Consider white rectangles below the diagonal in the quilt. For $k = 1, 2, \ldots$, Part 1 of the paper [38] describes the sequence of rectangles comprising $F_{k+1} \times F_{k+2}$ cells, as a Fibonacci cohort sequence satisfying the recurrence

$$R_{n,k} = R_{n-F_t,k} + F_{t+k} \times F_{t+k+1}, F_{t+1} \le n < F_{t+2}, t = 2, 3, \ldots. \tag{19}$$

Whereas this recurrence satisfies Definition 4.2 of a Fibonacci cohort sequence from the 1^{st} cohort, use Corollary 4.4, substituting the following into (17):

$$\begin{aligned}
&\text{For } \alpha_{n,k}, \quad \text{take } S_1 = \alpha_{1,k} = 1 \qquad\quad \text{and } p = \ k;\\
&\text{For } \beta_{n,k}, \quad \text{take } S_1 = \beta_{1,k} = F_{k+1} \qquad \text{and } p = \ k;\\
&\text{For } \gamma_{n,k}, \quad \text{take } S_1 = \gamma_{1,k} = F_{k+3} - 1 \ \text{ and } p = \ k+1;\\
&\text{For } \delta_{n,k}, \quad \text{take } S_1 = \delta_{1,k} = F_{k+4} - 2 \ \text{ and } p = \ k+1.\\
&\text{Moreover,}\\
&\text{For } w_{n-1,k}, \text{ take } S_1 = w_{0,k} = F_{k+1} \qquad \text{and } p = \ k+1;\\
&\text{For } \hat{\mathfrak{w}}_{n-1,k}, \text{ take } S_1 \qquad\quad = F_{2k-1} - 1 \text{ and } p = 2k-1;
\end{aligned}$$

where $\hat{\mathfrak{w}}_{n-1,k} = \begin{cases} F_{2k-1} - 1, & n = 1; \\ \mathfrak{w}_{n-1,k}, & n \ge 2. \end{cases}$ Section 4.1.10 and Examples 4.15 and 4.23 treat w and $\mathfrak{w}$ in greater detail. □

Note that the choice to count squares from zero, rather than one, assigning labels $S_{0,k}$ to the spinal squares in Figure 1, yields a formula in terms of $\lfloor n\phi \rfloor$ rather than $\lfloor (n-1)\phi \rfloor$. By contrast, the alternate choice $S_1 = a_{0,k} = F_{k+2} - 1$, $S_2 = a_{1,k} = 2F_{k+2} - 1$ also gives a valid formula, $a_{n,k} = F_{k+1} + \lfloor (n-1)\phi \rfloor F_{k+1} + nF_k - 1$, $n \ge 1$, albeit a formula stated in a form less reduced than (1), in terms of $\lfloor (n-1)\phi \rfloor$, rather than $\lfloor n\phi \rfloor$. For an interspersion-dispersion array such as $a_{n,k}$ here, designating the top row "row zero" simplifies the formulation of Kimberling's dispersion property (D4) [20], further motivating this convention.

Visually, the self-similar pattern of the quilt squares only becomes apparent from the first square $S_{1,k}$, since the squares $S_{3,k}$ and $S_{4,k}$ appear in an identical context to $S_{1,k}$ and $S_{2,k}$, respectively (Example 4.1), whereas the pair $S_{2,k}$, $S_{3,k}$ appear in different surroundings from $S_{0,k}$, $S_{1,k}$. Hence, the visual self-similarity of the quilt also motivates the choice to make the first cohort $C_{1,k} = (S_{1,k})$ rather than $(S_{0,k})$.

By contrast, for the quilt rectangle recurrence (19), the first cohort $C_{1,k} = R_{1,k}$ comprises the very first quilt rectangle, involved in the very first recurrence $R_{2,k} = R_{1,k} + F_{k+2} \times F_{k+3}$.

Lemma 4.5 (Bounds on S_n, a Fibonacci cohort sequence under cohortizer F_{t+p})**.**

Lower Bounds *Let $p \geq -3$ and $F_{t+1} \leqslant n < F_{t+2}$, $t = 3, 4, \ldots$. For a Fibonacci cohort sequence from the 2^{nd} cohort under $f(t) = F_{t+p}$,*

$$S_n \geq F_{t+p+1} + \begin{cases} S_1 - F_{p+2}, & t \text{ odd}; \\ S_2 - F_{p+3}, & t \text{ even}. \end{cases} \tag{20}$$

Let $p \geq -2$ and $F_{t+1} \leqslant n < F_{t+2}$, $t = 2, 3, \ldots$. For a Fibonacci cohort sequence from the 1^{st} cohort under $f(t) = F_{t+p}$,

$$S_n \geq S_1 + F_{t+p+1} - \begin{cases} F_{p+1}, & t \text{ even}; \\ F_{p+2}, & t \text{ odd}. \end{cases} \tag{21}$$

Upper Bounds *Let $p \geq -3$ and $F_{t+1} \leqslant n < F_{t+2}$, $t = 3, 4, \ldots$. For a Fibonacci cohort sequence from the 2^{nd} cohort under $f(t) = F_{t+p}$,*

$$S_n \leq S_2 + F_{t+p+2} - F_{p+4}. \tag{22}$$

Let $p \geq -2$ and $F_{t+1} \leqslant n < F_{t+2}$, $t = 2, 3, \ldots$. For a Fibonacci cohort sequence from the 1^{st} cohort under $f(t) = F_{t+p}$,

$$S_n \leq S_1 + F_{t+p+2} - F_{p+3}. \tag{23}$$

Proof of Lemma 4.5: In Section 11 □

4.1.5. *Free monoid on $\{\lfloor n\phi \rfloor, \lfloor n\phi^2 \rfloor\}$ under composition, and total ordering by 1–2-Fibonacci inner cohort tableau.*

Example 4.2. Examine the effect of increasing values of p in Proposition 4.2. For $p = 0$, any sequence of consecutive integers, *e.g.*, $\underline{256958}_z$ or $\underline{000027}_n$, is a Fibonacci cohort sequence under cohortizer F_t, being the case of consecutive integer seeds noted in the preamble to Section 4.1.4. For $p > 0$, however, the sequences increase more quickly.

For instance, with $p = 1$ and $p = 2$, the Wythoff sequences $\kappa \equiv \lfloor n\phi \rfloor$ (000201) and $\lambda \equiv \lfloor n\phi^2 \rfloor$ (001950) for $n = 1, 2, \ldots$, are Fibonacci cohort sequences with respect to cohortizers F_{t+1} and F_{t+2}, respectively.

Additional examples are 022342, 004956 = 026351, $099267_2 = 026355_2$ under cohortizer F_{t+1}, and 003622 under cohortizer F_{t+2}.

For larger values of p, examples include Sloane's 134859 (Wythoff AAA numbers) and 003623 (Wythoff AB numbers) under cohortizer F_{t+3}; 151915 (Wythoff AAAA numbers), 134860 (Wythoff AAB numbers), and 101864 (Wythoff BB numbers) under cohortizer F_{t+4}; 134862 (Wythoff ABB numbers) under cohortizer F_{t+5}; and 134864 (Wythoff BBB numbers) under cohortizer F_{t+6}. These examples, which employ repeated composition of κ and λ, motivate the following proposition.

Proposition 4.6 (Cohortizers for compositions of κ and λ)**.** *Let $\kappa(n) = \lfloor n\phi \rfloor$, $\lambda(n) = \lfloor n\phi^2 \rfloor$. Then for a composition S of k κ's and l λ's (in any order), the sequence $S_1, S_2, S_3, \ldots \equiv S(1), S(2), S(3), \ldots$ forms a Fibonacci Cohort sequence from the 1^{st} cohort, under cohortizer F_{t+p}, where $p = k + 2l$.*

Proof. Induction. Consider (17), and note that $p = 1$ and $S_1 = 1$ are the unique values that give $S_n = \kappa(n)$, and that $p = 2$ and $S_1 = 2$ are the unique values that give $S_n = \kappa(n) + n = \lambda(n)$.

For the induction step, first consider the composition, $T = \kappa \circ S$, of κ with an existing composition, S, of κ's and λ's. Let F_{t+p} cohortize S_n and let $F_{t+1} \leq n <$

F_{t+2}. This gives

$$\begin{aligned} T_n &= \kappa(S_n) \\ &= \lfloor (S_{n-F_t} + F_{t+p})\phi \rfloor \\ &= S_{n-F_t} + F_{t+p} + \lfloor (S_{n-F_t} + F_{t+p})/\phi \rfloor \quad (24) \\ &= S_{n-F_t} + F_{t+p} + F_{t+p-1} + \lfloor S_{n-F_t}/\phi \rfloor \quad (25) \\ &= S_{n-F_t} + \lfloor S_{n-F_t}/\phi \rfloor + F_{t+p+1} \\ &= \lfloor S_{n-F_t}\phi \rfloor + F_{t+p+1} \\ &= T_{n-F_t} + F_{t+p+1}, \end{aligned}$$

as desired.

Now, the step from (24) to (25) follows from Lemma 2 of Fraenkel, Mushkin, and Tassa [17] (see also Lemma 1 of Bunder & Tognetti [7]), which requires the bounds $1 \leq S_{n-F_t} \leq F_{t+p+1} - 1$. The lower bound is trivial, whereas the two initial cases $S_n = \kappa(n)$ and $S_n = \lambda(n)$ satisfy $S_1 = 1$, respectively $S_1 = 2$, and S_1 can only increase further for higher-order compositions of κ's and λ's, and the S_n increase with n. For the upper bound, rewrite (11) as $S_{n-F_t} = S_n - F_{t+p}$ and use the upper bound from Lemma 4.5 to obtain $S_{n-F_t} = S_n - F_{t+p} \leq F_{t+p+2} - F_{t+p} + S_1 - F_{p+3} = F_{t+p+1} + S_1 - F_{p+3} \leq F_{t+p+1} - 2 < F_{t+p+1} - 1$.

On the other hand, consider the composition, $T = \lambda \circ S$, of λ with the existing composition S. Let $F_{t+1} \leq n < F_{t+2}$. This gives

$$\begin{aligned} T_n &= \lambda(S_n) \\ &= \left\lfloor (S_{n-F_t} + F_{t+p})\phi^2 \right\rfloor \\ &= S_{n-F_t} + F_{t+p} + \lfloor (S_{n-F_t} + F_{t+p})\phi \rfloor \\ &= 2(S_{n-F_t} + F_{t+p}) + \lfloor (S_{n-F_t} + F_{t+p})/\phi \rfloor \\ &= 2(S_{n-F_t} + F_{t+p}) + F_{t+p-1} + \lfloor S_{n-F_t}/\phi \rfloor \\ &= 2S_{n-F_t} + \lfloor S_{n-F_t}/\phi \rfloor + F_{t+p+2} \\ &= S_{n-F_t} + \lfloor S_{n-F_t}\phi \rfloor + F_{t+p+2} \\ &= \left\lfloor S_{n-F_t}\phi^2 \right\rfloor + F_{t+p+2} \\ &= T_{n-F_t} + F_{t+p+2}. \end{aligned}$$

□

Remark 4.5. In particular, Proposition 4.6, combined with the cohort formula (17), reproduces a version of Theorem 5 of Kimberling [22], using affine combinations of n and $\kappa(n)$, rather than $\kappa(n)$ and $\lambda(n)$. For the constant term S_1 of the affine expression (17), Corollary 4.8 and Proposition 4.10, to come, will provide algorithms to complement Theorems 8 and 9 of [22].

Proposition 4.7 (Elements S_1, S_2, S_3, and S_5 for Compositions S of κ and λ)**.** *As in Proposition 4.6, consider a composition S of k κ's and l λ's in any order. Let $p = k + 2l$, and refer to p as the* degree *of S. From the integer argument n of $S(n)$ outward, consider the first λ applied. Then, starting with that λ, let the count of κ's be $k_\star$. In other words, $k_\star$ counts only the κ's applied after the first λ has been applied. Let $p_\star = k_\star + 2l$ and refer to $p_\star$ as the* reduced degree *of S. Then, for the integer sequence $S_1, S_2, S_3, \ldots \equiv S(1), S(2), S(3), \ldots$,*

(a): *The first element S_1 satisfies $F_{p_\star} < S_1 \leq F_{p_\star+1}$. That is, $p_\star = F^{-1}(S_1 - 1)$.*

(b): *For the second, third, and fifth elements:* $S_2 = n+1$, $S_3 = n+1+F_t$, *and* $S_5 = n+1+F_{t+3}$, *where* $F_{t+1} \le n < F_{t+2}$ *and* $t = p+1$.

Proof of **(a)**. *Induction.* Let $\kappa^\star$ denote arbitrarily many applications of κ. For $S = \kappa^\star$, observe that $F_0 < S_1 = 1 \le F_1$, and $S(1) - 1 = 1 - 1 = 0$, consistent with $p_\star = F^{-1}(0) = 0$, as claimed. A subsequent application of λ increases the degree p by 2. Thus, $1 = F_1 < \lambda\kappa^\star(1) = \lambda(1) \equiv \lfloor \phi^2 \rfloor = 2 \le F_{2+1} = 2$, proving the statement for a composition $\lambda\kappa^\star$ with a single application of λ.

Now, Lemma 2 of Fraenkel, Mushkin, and Tassa [17] (see also Lemma 1 of Bunder & Tognetti [7]) gives

$$\lfloor (F_{p_\star} + j)\phi \rfloor - (F_{p_\star+1} + \lfloor j\phi \rfloor) = \begin{cases} 0, & 1 \le j < F_{p_\star+1} + 1; \\ 1, & j = F_{p_\star+1} + 1; \end{cases}$$

and consequently,

$$\lfloor (F_{p_\star} + 1)\phi \rfloor - (F_{p_\star+1} + 1) = \begin{cases} 1, & p_\star = 1; \\ 0, & p_\star \ge 2. \end{cases} \tag{26}$$

Thus, for induction from S to $T = \kappa(S)$ with $p_\star(S) \ge 2$, use (26) to get from the hypothesis $F_{p_\star} < S_1 \le F_{p_\star+1}$ to the lower bound $T_1 = \kappa(S_1) \ge \lfloor (F_{p_\star} + 1)\phi \rfloor = F_{p_\star+1} + 1 > F_{p_\star+1}$. Using the identity $F_{p_\star+1} = \left\lfloor F_{p_\star}\phi + \frac{1}{2} \right\rfloor$, observe that the hypothesis also gives the upper bound $T_1 = \kappa(S_1) \le \lfloor F_{p_\star+1}\phi \rfloor \le \left\lfloor F_{p_\star+1}\phi + \frac{1}{2} \right\rfloor = F_{p_\star+2}$. Thus, $F_{p_\star+1} < \kappa(S_1) \le F_{p_\star+2}$, as claimed, given that $p_\star(\kappa(S)) = p_\star(S) + 1$.

Similarly, for induction from S to $T = \lambda(S)$ with $p_\star(S) \ge 2$, use (26) to get from the induction hypothesis to the lower bound $T_1 = \lambda(S_1) = \left\lfloor (F_{p_\star} + 1)\phi^2 \right\rfloor = \lfloor (F_{p_\star} + 1)\phi \rfloor + F_{p_\star} + 1 = F_{p_\star+1} + F_{p_\star} + 2 = F_{p_\star+2} + 2 > F_{p_\star+2}$. For the upper bound, $T_1 = \lambda(S_1) \le \left\lfloor F_{p_\star+1}\phi^2 \right\rfloor = \lfloor F_{p_\star+1}\phi \rfloor + F_{p_\star+1} \le \left\lfloor F_{p_\star+1}\phi + \frac{1}{2} \right\rfloor + F_{p_\star+1} = F_{p_\star+1} + F_{p_\star+2} = F_{p_\star+3}$. Thus, $F_{p_\star+2} < \lambda(S_1) \le F_{p_\star+3}$, as claimed, given that $p_\star(\lambda(S)) = p_\star(S) + 2$. □

Proof of **(b)**. Use $F_{p_\star} < S_1 \le F_{p_\star+1}$ from Part **(a)** to obtain $F_{p_\star} + F_{p+2} < S_1 + F_{p+2} \le F_{p_\star+1} + F_{p+2}$. Now, since Proposition 4.6 showed S_n to be a Fibonacci cohort sequence from the 1st cohort, by the cohort expression (17), $S_2 = S_1 + F_{p+2}$, so that $F_{p_\star} + F_{p+2} < S_2 \le F_{p_\star+1} + F_{p+2}$. Since $0 \le p_\star \le p$, write $F_{p+2} \le F_{p_\star} + F_{p+2} \le S_2 - 1 < F_{p_\star+1} + F_{p+2} \le F_{p+3}$. Substituting $t = p+1$ gives $F_{t+1} \le S_2 - 1 < F_{t+2}$. Thus, $S_2 = n+1$ for some n satisfying $F_{t+1} \le n < F_{t+2}$.

Use the cohort formula (17) again to obtain $S_2 - S_1 = F_{p+2}$, $S_3 - S_1 = F_{p+3}$, and $S_5 - S_2 = F_{p+4}$, and combining the first two, $S_3 - S_2 = F_{p+1}$. The claims $S_3 = n+1+F_t$ and $S_5 = n+1+F_{t+3}$ follow, respectively, from $S_3 - S_2 = F_{p+1}$ and $S_5 - S_2 = F_{p+4}$. □

Remark 4.6. Table 9 shows one consequence of Proposition 4.7(a). Compositions S of κ and λ can be arranged in rows of constant $S(1)$. From the top down, successive rows shown evaluate to $S(1) = 1, 2, 3, \ldots$ throughout the row. The rows also have constant values of the reduced degree $p_\star = F^{-1}(S(1)-1) = 0, 2, 3, 4, 4, 5, 5, 5, \ldots =$ 130233. Within each row, the compositions are arranged according to increasing p. Proposition 4.16 constructs a bijection between Table 9 and $\mathbb{Z}_+$.

The preamble to Section 4.1.4 quantified the speed of an integer sequence by the *rate* parameter p of its cohortizer. Examples included the two complementary spectrum sequences generated by Wythoff's two floor functions. In Proposition 4.7, the degree p continues to describe the speed of integer sequences — those generated

I	κ	κ^2	κ^3	κ^4	κ^5	$\kappa^6\cdots$
λ	$\lambda\kappa$	$\lambda\kappa^2$	$\lambda\kappa^3$	$\lambda\kappa^4$	$\lambda\kappa^5$	$\lambda\kappa^6\cdots$
$\kappa\lambda$	$\kappa\lambda\kappa$	$\kappa\lambda\kappa^2$	$\kappa\lambda\kappa^3$	$\kappa\lambda\kappa^4$	$\kappa\lambda\kappa^5$	$\kappa\lambda\kappa^6\cdots$
$\kappa^2\lambda$	$\kappa^2\lambda\kappa$	$\kappa^2\lambda\kappa^2$	$\kappa^2\lambda\kappa^3$	$\kappa^2\lambda\kappa^4$	$\kappa^2\lambda\kappa^5$	$\kappa^2\lambda\kappa^6\cdots$
λ^2	$\lambda^2\kappa$	$\lambda^2\kappa^2$	$\lambda^2\kappa^3$	$\lambda^2\kappa^4$	$\lambda^2\kappa^5$	$\lambda^2\kappa^6\cdots$
$\kappa^3\lambda$	$\kappa^3\lambda\kappa$	$\kappa^3\lambda\kappa^2$	$\kappa^3\lambda\kappa^3$	$\kappa^3\lambda\kappa^4$	$\kappa^3\lambda\kappa^5$	$\kappa^3\lambda\kappa^6\cdots$
$\lambda\kappa\lambda$	$\lambda\kappa\lambda\kappa$	$\lambda\kappa\lambda\kappa^2$	$\lambda\kappa\lambda\kappa^3$	$\lambda\kappa\lambda\kappa^4$	$\lambda\kappa\lambda\kappa^5$	$\lambda\kappa\lambda\kappa^6\cdots$
$\kappa\lambda^2$	$\kappa\lambda^2\kappa$	$\kappa\lambda^2\kappa^2$	$\kappa\lambda^2\kappa^3$	$\kappa\lambda^2\kappa^4$	$\kappa\lambda^2\kappa^5$	$\kappa\lambda^2\kappa^6\cdots$
$\kappa^4\lambda$	$\kappa^4\lambda\kappa$	$\kappa^4\lambda\kappa^2$	$\kappa^4\lambda\kappa^3$	$\kappa^4\lambda\kappa^4$	$\kappa^4\lambda\kappa^5$	$\kappa^4\lambda\kappa^6\cdots$
$\lambda\kappa^2\lambda$	$\lambda\kappa^2\lambda\kappa$	$\lambda\kappa^2\lambda\kappa^2$	$\lambda\kappa^2\lambda\kappa^3$	$\lambda\kappa^2\lambda\kappa^4$	$\lambda\kappa^2\lambda\kappa^5$	$\lambda\kappa^2\lambda\kappa^6\cdots$
$\kappa\lambda\kappa\lambda$	$\kappa\lambda\kappa\lambda\kappa$	$\kappa\lambda\kappa\lambda\kappa^2$	$\kappa\lambda\kappa\lambda\kappa^3$	$\kappa\lambda\kappa\lambda\kappa^4$	$\kappa\lambda\kappa\lambda\kappa^5$	$\kappa\lambda\kappa\lambda\kappa^6\cdots$
$\kappa^2\lambda^2$	$\kappa^2\lambda^2\kappa$	$\kappa^2\lambda^2\kappa^2$	$\kappa^2\lambda^2\kappa^3$	$\kappa^2\lambda^2\kappa^4$	$\kappa^2\lambda^2\kappa^5$	$\kappa^2\lambda^2\kappa^6\cdots$
λ^3	$\lambda^3\kappa$	$\lambda^3\kappa^2$	$\lambda^3\kappa^3$	$\lambda^3\kappa^4$	$\lambda^3\kappa^5$	$\lambda^3\kappa^6\cdots$
$\kappa^5\lambda$	$\kappa^5\lambda\kappa$	$\kappa^5\lambda\kappa^2$	$\kappa^5\lambda\kappa^3$	$\kappa^5\lambda\kappa^4$	$\kappa^5\lambda\kappa^5$	$\kappa^5\lambda\kappa^6\cdots$
$\vdots$	$\vdots$	$\vdots$	$\vdots$	$\vdots$	$\vdots$	$\vdots\ \ddots$

TABLE 9. Array of elements $S \in \{\kappa, \lambda\}^\star$ of the free monoid on $\{\kappa, \lambda\}$, arranged with degree p increasing along rows, and $S(1)$ and reduced degree $p_\star$ constant along rows, with $S(1)$ increasing and $p_\star$ nondecreasing down columns. Rows reproduce columns of Table 10 in order. Column 1 concatenates right subcohorts of Table 10, column 2 concatenates right subcohorts of left subcohorts, and so forth (see Section 8.2.2). For rows $n = 0, 1, 2, \ldots$ and columns $k = 1, 2, 3, \ldots$, the entry in position (n, k) of the table is the k^{th} representative of the n^{th} S_1-equivalence class in Table 11. Each row is a sequence of left branchings in the inner binary tree, Figure 4. Column k comprises the k^{th} right clade in the outer binary tree, Figure 2. $S(2) - 1$ provides a bijection to Table 12.

by compositions of the Wythoff pair previously considered. Parameter p will now be used for initial classification of these Wythoff compositions into cohorts. The image of 2 under each composition will then be used to order the compositions within the cohort for final classification.

Proposition 4.7(b) allows a rearrangement of Table 9 into a *1–2-Fibonacci inner cohort tableau*, Table 10, similar to Table 7(iii). Here, the elements S of Table 9 are sorted by increasing values of $S(2) = 2, 3, 4, \ldots$, beginning with $I(2) = 2$, and subsequently, $\kappa(2) = 3$, $\kappa^2(2) = 4$, $\lambda(2) = 5$, $\kappa^3(2) = 6$, $\lambda\kappa(2) = 7$, $\kappa\lambda(2) = 8$, and so forth. The tableau gathers the elements into cohorts C_{p+1} according to increasing value of the degree $p = 0, 1, 2, 2, 3, 3, 3 \ldots = \underline{\texttt{072649}} - 1 = \underline{\texttt{130233}}_1 - 2$, with one cohort per level $p + 1$.

C_1	I							
C_2	κ							
C_3	κ^2	λ						
C_4	κ^3	$\lambda\kappa$	$\kappa\lambda$					
C_5	κ^4	$\lambda\kappa^2$	$\kappa\lambda\kappa$	$\kappa^2\lambda$	λ^2			
C_6	κ^5	$\lambda\kappa^3$	$\kappa\lambda\kappa^2$	$\kappa^2\lambda\kappa$	$\lambda^2\kappa$	$\kappa^3\lambda$	$\lambda\kappa\lambda$	$\kappa\lambda^2$
$\vdots$	$\vdots$	$\vdots$	$\vdots$	$\vdots$	$\vdots$	$\vdots$	$\vdots$	$\vdots$

TABLE 10. 1–2-Fibonacci (inner) cohort sequence of functions $S \in \{\kappa, \lambda\}^\star$, ordered by strictly increasing $S(2)-1 = 1, 2, 3, \ldots$, which provides a bijection to Table 6(i), and gathered into cohorts C_{p+1} by degree $p(S) = \underline{\texttt{072649}} - 1 = \underline{\texttt{130233}}_1 - 2 = 0, 1, 2, 2, 3, 3, 3, \ldots$. Sequence $\underline{\texttt{102364}} = \underline{\texttt{135817}}_2 - 1 = 0, 1, 2, 1, 3, 2, 2, \ldots$ gives the number of symbols. Isomorph of Tables 11 and 33(i). Planar graph isomorph of Figure 2.

C_0	$\kappa^\star$							
C_1	M							
C_2	κM							
C_3	$\kappa^2 M$	λM						
C_4	$\kappa^3 M$	$\lambda\kappa M$	$\kappa\lambda M$					
C_5	$\kappa^4 M$	$\lambda\kappa^2 M$	$\kappa\lambda\kappa M$	$\kappa^2\lambda M$	$\lambda^2 M$			
C_6	$\kappa^5 M$	$\lambda\kappa^3 M$	$\kappa\lambda\kappa^2 M$	$\kappa^2\lambda\kappa M$	$\lambda^2\kappa M$	$\kappa^3\lambda M$	$\lambda\kappa\lambda M$	$\kappa\lambda^2 M$
$\vdots$	$\vdots$	$\vdots$	$\vdots$	$\vdots$	$\vdots$	$\vdots$	$\vdots$	$\vdots$

TABLE 11. 1–2-Fibonacci (inner) cohort tableau of equivalence classes $S/\!\circ\kappa^\star \in \{\kappa, \lambda\}^\star/\!\circ\kappa^\star$ (by right infix) from the 0^{th} cohort, ordered by strictly increasing $S(1)-1 = 0, 1, 2, 3, \ldots$, which provides a bijection to Table 6(i), and gathered into cohorts $C_{p_\star - 1}$ by reduced degree $p_\star = \underline{\texttt{130233}} = 0, 2, 3, 4, 4, 5, 5, 5, \ldots$. Counting $M = \lambda\kappa^\star$ as one symbol, $\underline{\texttt{135817}}_{n+1}$ gives the number of symbols in the n^{th} element. Isomorph of Tables 10 and 33(i). With $C_0 = (\kappa^\star)$ and suffix M omitted, planar graph isomorph of Figure 2.

Throughout the tableau, the value of $S(2)$ increases by 1 between consecutive elements S, providing a bijection between this tableau and Table 6(i) (Proposition 5.2). In particular, $S(2)$ takes the range $\{F_{p+2}+1, \ldots, F_{p+3}\}$ over cohort C_{p+1}, which illustrates Proposition 4.7(b), that $F_{p+2} \le S(2) - 1 < F_{p+3}$.

Further, Proposition 4.7(a) allows entire rows of Table 9 to be condensed to S_1–*equivalence classes* $S/\!\circ\kappa^\star$ of $\{\kappa, \lambda\}^\star/\!\circ\kappa^\star$, also placed into a 1–2-Fibonacci cohort tableau (Table 11). The 0^{th} cohort $C_0 = (\kappa^\star)$ comprises the 0^{th} equivalence class $\kappa^\star$, corresponding to the zeroth (top) row of Table 9. Likewise, the 1^{st}, 2^{nd}, and 3^{rd} cohorts, respectively $C_1 = (M)$, $C_2 = (\kappa M)$, $C_3 = (\kappa^2 M, \lambda M)$ comprise the equivalence classes $\lambda\kappa^\star$, $\kappa\lambda\kappa^\star$, $\kappa^2\lambda\kappa^\star$, and $\lambda^2\kappa^\star$, whose members appear in rows one through four, respectively, of Table 9.

Take $\kappa^0 = I$ as the standard representative of the 0^{th} equivalence class. Then beginning with the 1^{st} class, replace M in the tableau by λ to obtain the standard representatives having $p = p_\star$ found in the first column of Table 9: $I, \lambda, \kappa\lambda, \kappa^2\lambda, \ldots$. For subsequent columns $2, 3, 4, \ldots, k, \ldots$ of the table, replace M by $\lambda\kappa$, $\lambda\kappa^2$, $\lambda\kappa^3, \ldots, \lambda\kappa^{k-1}, \ldots$ to obtain class representatives having $p = p_\star + 1$, $p_\star + 2$, $p_\star + 3, \ldots, p_\star + k - 1$, respectively, (also taking κ^{k-1} as the k^{th} representative of the 0^{th} class).

Thus, Table 11 enumerates S_1-classes, that is, equivalence classes of compositions S having the same first element $S(1)$. The tableau sorts the equivalence classes by increasing values of $S(1)$, beginning with the 0^{th} equivalence class $\kappa^\star$, for which $\kappa^\star(1) = 1$, the 1^{st} equivalence class $M = \lambda\kappa^\star$, for which $M(1) = \lambda\kappa^\star(1) = 2$, and subsequently, $\kappa\lambda\kappa^\star(1) = 3$, $\kappa^2\lambda\kappa^\star(1) = 4$, $\lambda^2\kappa^\star(1) = 5$, $\kappa^3\lambda\kappa^\star(1) = 6$, $\lambda\kappa\lambda\kappa^\star(1) = 7$, $\kappa\lambda^2\kappa^\star(1) = 8$, and so forth.

Observe that the tableau gathers the classes into cohorts according to increasing value of the reduced degree $p_\star = \underline{130233} = 0, 2, 3, 4, 4, 5, 5, 5, \ldots$. The tableau displays one cohort per level. While the 0^{th} cohort has length 1 by convention, for $p_\star \geq 2$, cohort $C_{p_\star - 1}$ appearing on level $p_\star - 1$ of the tableau has length $F_{p_\star - 1}$. The value of $S(1)$ strictly increases throughout the tableau, with range $\{F_{p_\star} + 1, \ldots, F_{p_\star + 1}\}$ over each cohort $C_{p_\star - 1}$, providing a bijection to Table 6(i). In particular, this illustrates Proposition 4.7(a), that $F_{p_\star} < S_1 \leq F_{p_\star + 1}$.

Proposition 4.7 described the structure shown in Table 11. Now, the algorithm of Corollary 4.8 will exploit this structure.

Corollary 4.8 (Inside–outward algorithm for S_1 of compositions of κ and λ)**.** *For compositions S of k κ's and l λ's (in any order),* the following algorithm gives $S_1 \equiv S(1)$*:*

Initialization: *Starting from the inside with the integer argument n of $S(n)$ and moving outward, ignore any κ's that apply to the integer argument first (since $\kappa(1) = \lfloor \phi \rfloor = 1$ is a fixed point of κ), and beginning with the first λ applied, let l count this and subsequent applications of λ's, and let and $k_\star$ count subsequent applications of κ's. Let $p_\star = k_\star + 2l$ be the reduced degree, as in Proposition 4.7.*

If the first λ is the last, that is, if $S_n = \lambda\kappa^\star$, then $S_1 = 2$. Otherwise, initialize t to $p_\star - 1$ and initialize S_1 to 2, accounting for the initial application of $\lambda\kappa^\star(1) = 2$.

Main Step: *Then, starting with the next function applied after the initial $\lambda\kappa^\star$ and until the last function is applied, iterate as follows:*

$$t \longleftarrow \begin{cases} t - 1, & \text{if } \kappa \text{ is applied;} \\ t - 2, & \text{if } \lambda \text{ is applied;} \end{cases}$$

and

$$S_1 \leftarrow S_1 + \begin{cases} F_t, & \text{if } \kappa \text{ is applied;} \\ F_{t+3}, & \text{if } \lambda \text{ is applied;} \end{cases}$$

Proof. First, prove the values used to initialize the algorithm: By Proposition 4.7(a), $F_{p_\star} < S_1 \leq F_{p_\star + 1}$, placing S in cohort $C_{p_\star - 1}$ of Table 11. Now, write $S = S'\lambda\kappa^\star$ and use the fact that $\lambda\kappa^\star(1) = 2$ to obtain $S_1 = S'\lambda\kappa^\star(1) = S'_2$. Thus, the algorithm assigns to S_1 the initial value of 2. Moreover, this implies $F_{p_\star} < S'_2 \leq F_{p_\star + 1}$. By Proposition 4.7(b), there exists an integer t_1 such that $F_{t_1 + 1} < S'_2 \leq F_{t_1 + 2}$.

Thus, $F_{p_\star} < S'_2 \leq F_{p_\star+1}$ necessarily implies that $t_1 = p_\star - 1$, the initial value of t assigned by the algorithm.

Secondly, prove the main step of the algorithm. At a given iteration t of the main step, let S' be the incumbent, partial composition of κ's and λ's, where either $S' = R'\kappa$ or $S' = R'\lambda$. Let the current iteration of the algorithm treat the removal from the inside of the suffix, either κ or λ, leaving the composition R'.

In the case $S' = R'\kappa$, use the fact that $\kappa(2) = 3$, and thus $S'_2 = R'_3$. By Proposition 4.7(b), there exists an integer t_2 for which $F_{t_2+2} < R'_3 \leq F_{t_2+2} + F_{t_2}$. Thus, $F_{p_\star} < R'_3 \leq F_{p_\star+1}$ necessarily implies that $t_2 = p_\star - 2 = t_1 - 1$, the increment of t used in the algorithm when applying a κ. Thus, it remains to reduce the argument of R' from 3 back to 2. Now, by Proposition 4.6, R' is a Fibonacci cohort sequence under F_{t+t_2-1}. Thus by (17) (also see proof of Proposition 4.7(b)), $R'_2 = R'_3 - F_{t_2}$, precisely the increment of S_1 used in the algorithm when applying a κ. Application of these increments gives $F_{t_2+1} = F_{t_2+2} - F_{t_2} < R'_2 \leq F_{t_2+2} + F_{t_2} - F_{t_2} = F_{t_2+2}$, placing $R = R'M$ in cohort $C_{t_2} = C_{p_\star-2}$ of Table 11.

In the case $S' = R'\lambda$, use the fact that $\lambda(2) = 5$, and thus $S'_2 = R'_5$. By Proposition 4.7(b), there exists an integer t_2 for which $F_{t_2+3} + F_{t_2+1} < R'_5 \leq F_{t_2+4}$. Thus, $F_{p_\star} < R'_5 \leq F_{p_\star+1}$ necessarily implies that $t_2 = p_\star - 3 = t_1 - 2$, the increment of t used in the algorithm when applying a λ. Thus, it remains to reduce the argument of R' from 5 back to 2. Now, by Proposition 4.6, R' is a Fibonacci cohort sequence under F_{t+t_2-1}. Thus by (17) (also see proof of Proposition 4.7(b)), $R'_2 = R'_5 - F_{t_2+3}$, precisely the increment of S_1 used in the algorithm when applying a λ. Application of these increments gives $F_{t_2+1} = F_{t_2+3} + F_{t_2+1} - F_{t_2+3} < R'_2 \leq F_{t_2+4} - F_{t_2+3} = F_{t_2+2}$, placing $R = R'M$ in cohort $C_{t_2} = C_{p_\star-3}$ of Table 11. □

Remark 4.7. The proof of Corollary 4.8 also shows the algorithm to be a journey upwards through Table 11, or equivalently, Figure 4. The algorithm always terminates with the counter t having the value 1, the value of $p_\star - 1$ (and cohort index) for the 1st equivalence class M.

Example 4.3. Consider $S = \kappa^2\lambda\kappa\lambda\kappa^\star$. Then $p_\star = 7$ and successive steps of the algorithm give $(t, S_1) = (6, 2), (5, F_5+2), (3, F_5+F_6+2), (2, F_5+F_6+F_2+2), (1, F_5+F_6+F_2+F_1+2) = (1, 17)$.

For any positive integer n, the cohort formula (17), now allows calculation of element $S(n)$ of the sequence as $\kappa^2\lambda\kappa\lambda\kappa^k(n) = F_{k+7}\kappa(n) + F_{k+6}n - F_{k+8} + 17$.

Corollary 4.9 (A sequence whose cohort expression (17) has no constant term)**.**

$$\left.\begin{array}{ll} \lambda^{(i-1)/2}(n), & i \text{ odd;} \\ \kappa\lambda^{(i-2)/2}(n), & i \text{ even.} \end{array}\right\} = F_{i-1}\kappa(n) + F_{i-2}n \tag{27}$$

Proof. By Proposition 4.6, the left-hand side of (27) is a Fibonacci Cohort sequence from the 1st cohort, under cohortizer F_{t+i-1}. By (17), therefore, it equals

$$F_{i-1}\kappa(n) + F_{i-2}n - F_i + \left\{\begin{array}{ll} \lambda^{(i-1)/2}(1), & i \text{ odd;} \\ \kappa\lambda^{(i-2)/2}(1), & i \text{ even.} \end{array}\right. \tag{28}$$

For the expression to be homogeneous, it suffices to show the last term equal to F_i. In both the odd and even cases, $p_\star = p = i - 1$ as defined in the preamble of Corollary 4.8. Thus, when applied to the last term of (28), the algorithm can be initialized to $(i - 2, 2)$. In the odd case, the algorithm iterates through the last application of λ, terminating with $(t, S_1) = (1, 2 + F_{i-1} + F_{i-3} + \cdots + F_6 + F_4) = (1, 2 + F_i - 1 - F_2) = (1, F_i)$.

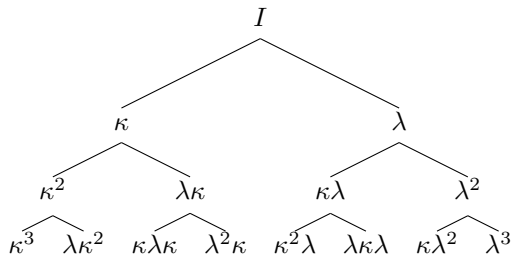

FIGURE 2. "Outer" binary tree of functions $S \in \{\kappa, \lambda\}^\star$ in the free monoid on $\{\kappa, \lambda\}$. $S(2) - 1$ provides a bijection to Figure 3. Also, for suffix $M = \lambda\kappa^\star$, outer binary tree of prefix S' of each equivalence class $\{S'M \in \{\kappa, \lambda\}^\star \setminus \{\kappa\}^\star | S'M(1) = S'\lambda(1)\} \in \{\kappa, \lambda\}^\star / \circ\kappa^\star$. The algorithm of Corollary 4.8 follows this tree *downward* to calculate $S'M(1)$, which provides the bijection $S'M(1) - 1$ to Figure 3. Planar graph isomorph of Table 10 and of (prefixes in) Table 11 with $C_0 = (\kappa^\star)$ omitted. Blade dual of Figure 4.

In the even case, the algorithm iterates through the last application of λ, returning $(t, S_1) = (2, 2 + F_{i-1} + F_{i-3} + \cdots + F_7 + F_5) = (2, 2 + F_i - F_3 - F_1)$, which, after the application of κ returns $(t, S_1) = (1, 2 + F_i - F_3) = (1, F_i)$. □

Remark 4.8. The odd case of Corollary 4.9 resembles Example 7 of Kimberling [22], expressed in $\kappa(n)$ and n, rather than $\kappa(n)$ and $\lambda(n)$.

Remark 4.9. The left-hand side of (27) reappears in Proposition 7.5(v) as $V_{n,k}$, a quantity evaluated from the genealogy $v_{n,k}$ of quilt square $S_{n,k}$ (there, k indexes the ordinal size of quilt squares, different from the notation of the present section).

Consider the last element in each cohort of the tableaux, Tables 10 and 11. To express the former as well as the prefix of the latter, the same quantity (27) can be used.

Thus the last composition in each cohort $C_1, C_2, \ldots, C_{p+1}, \ldots$ of Table 10 is $V_{n,p+1}$, and the last class in each cohort $C_1, C_2, \ldots, C_{p_\star - 1}, \ldots$ of Table 11 is $V_{M,p_\star - 1}$ (considering 0 to be even, (27) also gives a valid identity $V_{M,0} = \kappa\lambda^{(0-2)/2}(M) = \kappa\lambda^{-1}\lambda\kappa^\star = \kappa^\star$ for cohort C_0 of the latter).

Example 4.4. Consider the sequence $S = (\kappa\lambda)^r$, having degree $p = p_\star = 3r$. The algorithm of Corollary 4.8 gives $(t, S_1) = (3r - 1, 2), (3r - 2, 2 + F_{3r-2}), (3r - 4, 2 + F_{3r-2} + F_{3r-1}), (3r - 5, 2 + F_{3r-2} + F_{3r-1} + F_{3r-5}), \ldots, (2, 2 + F_{3r-2} + F_{3r-1} + F_{3r-5} + \cdots + F_5), (1, 2 + F_{3r-2} + F_{3r-1} + F_{3r-5} + \cdots + F_5 + F_1) = (1, 1 + \sum_{i=1}^{r} F_{3i})$.

Using the cohort formula (17), allows us to write the sequence as $(\kappa\lambda)^r(n) = F_{3r}\kappa(n) + F_{3r-1}n - F_{3r+1} + 1 + \sum_{i=1}^{r} F_{3i} = F_{3r}\kappa(n) + F_{3r-1}n - \frac{1}{2}(F_{3r-1} - 1)$.

Remark 4.10. Example 4.4 gives the first result in Theorem 5 of Fraenkel [16], expressed in $\kappa(n)$ and n, rather than $\kappa(n)$ and $\lambda(n)$.

Remark 4.11. The algorithm of Corollary 4.8 operates on compositions of κ's and λ's from the inside outward, traversing a path downward through an "outer" binary tree of equivalence classes $S/\circ\kappa^\star$ of the free monoid $\{\kappa, \lambda\}^\star$ (Figure 2). The nodes of the tree correspond to (the prefixes of) the same classes as those in the tableau, Table 11 (for $p_\star > 1$), arranged according to the branching of the algorithm, with

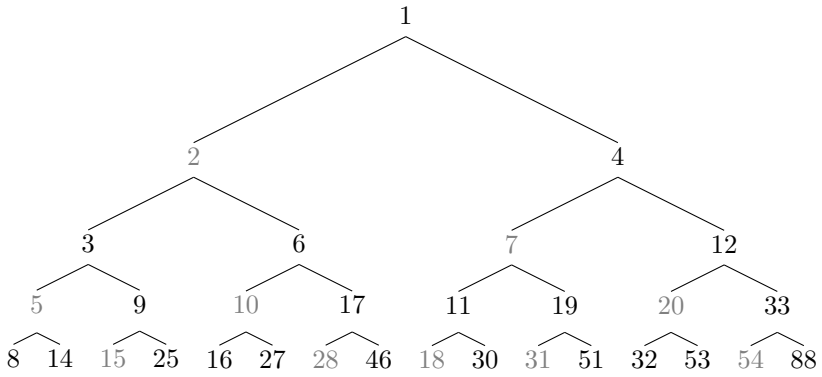

FIGURE 3. *Minimal Successor Tree* (048680). Corresponds bijectively to Figures 2 and 9 via $S(2)-1$ and $N_{-1}(LS)-1$, respectively, for compositions S shown therein. Blade dual of Figure 5 and 059893 permutes the two. Cohort dual of Figure 10. Sequences of left branchings and right branchings are rows of Wythoff array $w_{n,k}$, respectively, Wythoff mirror array $\mathfrak{w}_{n,k}$ (Table 4). k^{th} right clade and k^{th} left clade give column k of 1–2-Fibonacci array, respectively, 1–2-mirror array (Table 3). 048679 gives positions $\bar{\mathbf{p}}$ of the positive integers in the tree. Planar graph isomorph of the tableaux in Table 6.

left, respectively, right branching corresponding to successive applications of κ, respectively, λ, on the outside, the root node being the prefix I of $IM = I\lambda\kappa^\star$, the 1^{st} equivalence class. (The tree omits the 0^{th} equivalence class $\kappa^\star$, kernel of the equivalence defined by compositions $S, R \in \{\kappa, \lambda\}^\star$ having the same value $S(1) = R(1)$ at 1.) For example, the branching left–right–right descending from the root node of Figure 2 corresponds to $\lambda^2\kappa$, the prefix of equivalence class $\lambda^2\kappa M$.

Figure 3 shows the respective values of $S(1) - 1$ for these compositions. The algorithm accumulates the value of $S(1)$ as a Fibonacci expansion, and, since t decreases with each step of the algorithm, the "most significant digits" of this expansion arise from the functions κ, λ applied earliest. Writing the values themselves going from left to right on each successive level of the tree, $1,\ 2, 4,\ 3, 6, 7, 12,\ 5, 9, 10, 17, 11, 19, 20, 33, \ldots$, gives 048680, a permutation of the positive integers. This suggests that Figure 3 arranges $\mathbb{Z}_+$ and whereas the value $S(1) - 1$ maps between Figures 2 and 3, $S(1)$ provides a bijection between $\{\kappa, \lambda\}^\star/\circ\kappa^\star$ and $\mathbb{Z}_+$.

Correlating the two figures, observe that in Figure 3 the left child of n must equal $\kappa(n + 1) - 1$ and the right child of n must equal $\lambda(n + 1) - 1$ (see Figure 15(i)).

Indeed, *the entry for* 048680 *in Sloane [41], indicates that the algorithm of Corollary 4.8 produces a Zeckendorf representation of* $S(1) - 1$. Moreover, any node in the minimal successor tree, Figure 3, produces its left, respectively, right, child by prepending 0, respectively, 10 to the Zeckendorf binary notation (Figure 16(i)), where bit significance increases from left to right (Remark 6.2 explains this choice of notational convention). For example, $6 = F_2 + F_5 = 1001$ begets $10 = F_3 + F_6 = 01001$ and $17 = F_2 + F_4 + F_7 = 101001$, respectively, in minimal Fibonacci representation. Lazy Fibonacci representation gives the same result, $6 = F_2 + F_3 + F_4 = 111$ begets $10 = F_3 + F_4 + F_5 = 0111$ and

$17 = F_2 + F_4 + F_5 + F_6 = 10111$. Section 6.7.1 further investigates the branching of the minimal successor tree.

The foregoing discussion foreshadows the following algorithm, equivalent to that of Corollary 4.8.

Proposition 4.10 (Radix algorithm for $S(1)$ of compositions $S \in \{\kappa, \lambda\}^\star$ [27])**.** *Consider S, a composition of κ's and λ's having at least one λ. From the outside inward, write a 0 for each κ applied and 10 for each λ applied.*

Treat the resulting word as Zeckendorf binary notation and apply its bits, as coefficients, to a basis of Fibonacci numbers $(F_2, F_3, F_4, \ldots)$ to obtain $S(1) - 1$.

Example 4.5 (Radix algorithm of Proposition 4.10)**.** Encode $S = \kappa\lambda\kappa\lambda\kappa^\star$ as $0100100\ldots0 = 01001$. Evaluate the latter to $F_3 + F_6 = 2 + 8 = 10$. Thus, $\kappa\lambda\kappa\lambda\kappa^\star(1) - 1 = 10$.

Example 4.6 (Radix algorithm for Example 4.3)**.** Consider $S = \kappa^2\lambda\kappa\lambda\kappa^\star$. Then S encodes as $00100100\ldots0 = 001001$,

which subsequently evaluates to $F_4 + F_7 = 3 + 13 = 16$. Thus, the radix algorithm gives $S_1 = 16 + 1 = 17$, agreeing with the inside–outward algorithm used in Example 4.3.

Corollary 4.11 (Bijection between equivalence classes on free monoid of Wythoff compositions and positive integers)**.** *The map*

$$\begin{array}{rcl} \{\kappa, \lambda\}^\star / \circ\kappa^\star & \to & \mathbb{Z}_+ \\ S / \circ\kappa^\star & \mapsto & S(1). \end{array}$$

is a bijection.

Proof. The algorithm of Proposition 4.10 gives the value of $S(1)$ for functions S in the free monoid $\{\kappa, \lambda\}^\star$ under composition. Moreover, the algorithm produces the value $S(1)$ in minimal Fibonacci representation, since the map $\{\kappa, \lambda\} \mapsto \{0, 10\}$ ensures that the representation does not use any two consecutive Fibonacci numbers. Further, zeroes at the "most significant" end of the word do not affect the evaluation of $S(1)$. Thus, the value of $S(1)$ is distinct up to final zeroes, which correspond to inner κs of S, and thus two representatives of the same equivalence class have the same value of $S(1)$.

With reference to Table 9, the algorithm produces a distinct value of $S(1)$ for each row and the same value for all entries in the same row. That is, compositions $S, R \in \{\kappa, \lambda\}^\star$ representing two distinct equivalence classes $S / \circ\kappa^\star, R / \circ\kappa^\star \in \{\kappa, \lambda\}^\star / \circ\kappa^\star$, respectively, have $S(1) \neq R(1)$. Thus, the algorithm produces a distinct minimal Fibonacci representation for each distinct class of compositions in $\{\kappa, \lambda\}^\star$. It follows from the uniqueness of the minimal Fibonacci representation that each distinct $S / \circ\kappa^\star \in \{\theta, \eta\}^\star / \circ\kappa^\star$ has a distinct value of $S(1)$, which thus provides a bijection between $\{\kappa, \lambda\}^\star / \circ\kappa^\star$ and $\mathbb{Z}_+$. □

Rearranging the elements on each level of Figures 2 and 3, yields, respectively, Figures 4 and 5. Each node of Figure 4 also gives the prefix of an equivalence classe $S / \circ\kappa^\star \in \{\kappa, \lambda\}^\star / \circ\, \kappa^\star$ of compositions $S \in \{\kappa, \lambda\}^\star \setminus \{\kappa\}^\star$, while the corresponding node of Figure 5 also gives the value $S'M(1) - 1$ common to all compositions in the class with prefix S'. However, Figure 4 arranges its nodes according to the application, from the *outside inward*, of κ's and λ's, corresponding to left, respectively, right branching in a path downward through the tree. For example,

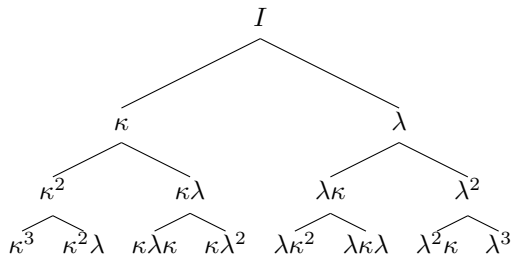

FIGURE 4. "Inner" binary tree of functions $S \in \{\kappa, \lambda\}^\star$ in the free monoid on $\{\kappa, \lambda\}$. $S(2) - 1$ provides a bijection to Figure 5. Also, for suffix $M = \lambda\kappa^\star$, inner binary tree of prefix S' of each equivalence class $\{S'M \in \{\kappa, \lambda\}^\star \setminus \{\kappa\}^\star | S'M(1) = S'\lambda(1)\} \in \{\kappa, \lambda\}^\star / \circ \kappa^\star$. The algorithm of Corollary 4.8 follows this tree *upward* to calculate $S'M(1)$, which provides the value $S'M(1) - 1$ in the corresponding position of Figure 5. Blade dual of Figure 2.

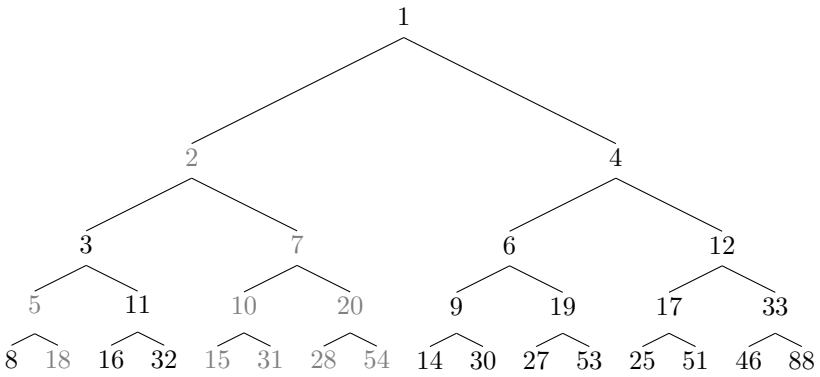

FIGURE 5. *Minimal Fibonacci Tree*. Corresponds bijectively to Figures 4 and 7 via $S(2) - 1$ and $N_{-1}(LS) - 1$, respectively, for compositions S shown therein. Expanded in Figure 14. Blade dual of Figure 3 and 059893 permutes the two. Cohort dual of Figures 8 and 13. Sequences of left branchings and right branchings are rows of 1–2-Fibonacci array $\digamma_{n,k}$, respectively, 1–2-mirror array $\rotatebox{180}{$\digamma$}_{n,k}$ (Table 3). k^{th} right clade and k^{th} left clade give column k of Wythoff array $w_{n,k}$, respectively, Wythoff mirror array $\text{ɯ}_{n,k}$ (Table 4).

the path left–right–left–right descending from the root node in (the continuation of) Figure 4 corresponds to $\kappa\lambda\kappa\lambda$, the prefix of equivalence class $\kappa\lambda\kappa\lambda^2\kappa^\star = \kappa\lambda\kappa\lambda M$. The same branching sequence in Figure 5 determines the corresponding value $31 = \kappa\lambda\kappa\lambda^2\kappa^\star(1) - 1$ common to all compositions in the class. Lemma 4.13 further investigates this branching.

Writing the values going from left to right on each successive level of Figure 5 yields the sequence 1, 2, 4, 3, 7, 6, 12, 5, 11, 10, 20, 9, 19, 17, 33,..., not found in the OEIS [41] as of this writing. Evidently, the sequence rearranges 048680, if each level of Figure 5 merely rearranges the corresponding level of Figure 3. The paper refers to this permutation, 059893, as the *tree blade permutation*, as it plays the role of swapping **b**ranches of one tree for c**lade**s of the other. Both Figures 2

and 4 exemplify Corollary 4.11 in as much as both generate all compositions $S \in \{\kappa, \lambda\}^\star$, or equivalently the prefix S' of all equivalence classes of $\{\kappa, \lambda\}^\star \setminus \{\kappa\}^\star$. Thus, by the map $S'M(1) - 1$, both Figures 3 and 5 arrange the positive integers. Section 6.3 will formalize the relation between the branching of Figure 5 and the *minimal Fibonacci representation*. First, however, Proposition 4.12 uses the fact that Figure 5 rearranges each level of Figure 3 to directly prove that the trees arrange $\mathbb{Z}_{\geq 1}$.

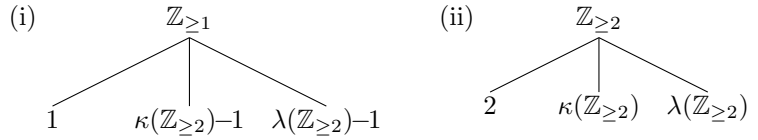

FIGURE 6. (i) A partition of the positive integers into three non-intersecting subsequences: $\mathbb{Z}_{\geq 1} = \{1\} \cup [\kappa(\mathbb{Z}_{\geq 2})–1] \cup [\lambda(\mathbb{Z}_{\geq 2})–1]$ (ii) A partition of the integers ≥ 2 into three non-intersecting subsequences: $\mathbb{Z}_{\geq 2} = \{2\} \cup \kappa(\mathbb{Z}_{\geq 1}) \cup \lambda(\mathbb{Z}_{\geq 1})$

Proposition 4.12 (Figures 3 and 5 arrange the positive integers)**.** *As previously noted, in Figure 3 the left child of n is $\kappa(n+1) - 1$ and the right child of n is $\lambda(n+1) - 1$ (Remark 4.11), and each level of Figure 5 merely rearranges the corresponding level of Figure 3. Consequently, these binary trees both arrange $\mathbb{Z}_{\geq 1}$.*

Proof. Consider the partition of the positive integers shown in Figure 6(i). The first two levels of Figure 3 (comprising its first three nodes) contain the first element of each subsequence in the partition. That is, 1 at the root node, and $(\kappa(2), \lambda(2)) - 1 = (\min \kappa(\mathbb{Z}_{\geq 2}), \min \lambda(\mathbb{Z}_{\geq 2})) - 1 = (2, 4)$ at its (left, right) children. Note that considering the second level alone, the nodes contain the first elements of two subsequences that partition $\mathbb{Z}_{\geq 2}$.

Now consider the third level, $(\kappa^2(2), \lambda(\kappa(2)), \kappa(\lambda(2)), \lambda^2(2)) - 1 = (3, 6, 7, 12)$ of Figure 3, and rearrange this level to give $(\kappa^2(2), \kappa(\lambda(2)), \lambda(\kappa(2)), \lambda^2(2)) - 1 = (\min \kappa(\kappa(\mathbb{Z}_{\geq 2})), \min \kappa(\lambda(\mathbb{Z}_{\geq 2})), \min \lambda(\kappa(\mathbb{Z}_{\geq 2})), \min \lambda(\lambda(\mathbb{Z}_{\geq 2}))) - 1 = (3, 7, 6, 12)$.

Gathering the nodes of levels 2 and 3 into two sets $\{\kappa(2), \kappa^2(2), \kappa(\lambda(2))\} - 1 = \{\kappa(2), \min \kappa(\kappa(\mathbb{Z}_{\geq 2})), \min \kappa(\lambda(\mathbb{Z}_{\geq 2}))\} - 1$ and $\{\lambda(2), \lambda(\kappa(2)), \lambda^2(2)\} - 1 = \{\lambda(2), \min \lambda(\kappa(\mathbb{Z}_{\geq 2})), \min \lambda(\lambda(\mathbb{Z}_{\geq 2}))\} - 1$ shows that the partition of $\mathbb{Z}_{\geq 2}$ in Figure 6(ii) was substituted for "2" in each node of the second level and the first element then taken, to form the third level.

The trees then repeat this process *ad infinitum*, at each level effectively substituting the "2" at the inside of each expression with the partition of $\mathbb{Z}_{\geq 2}$ shown in Figure 6(ii), and taking its smallest element to produce the next level. □

Remark 4.12. Observe from Figure 6 that, without loss of generality, the spectrum sequences $\kappa(n) = \lfloor n\phi \rfloor$ and $\lambda(n) = \lfloor n\phi^2 \rfloor$ in Proposition 4.12 can be substituted by any pair of complementary spectrum sequences $\lfloor n\mu \rfloor$ and $\lfloor n\nu \rfloor$ with irrational slopes μ and ν that satisfy $3/2 < \mu < 2 < \nu \equiv \frac{1}{1-1/\mu} < 3$.

Corollary 9.2 provides a more general result.

Remark 4.13. By Proposition 4.10, the encoding (in Zeckendorf binary notation) of $S'\kappa M$ is that of $S'M$ with a 0 inserted before the final 1, so that $S'\kappa M(1) - S'M(1) = F_{t+1} - F_t = F_{t-1}$, where F_t is the largest Fibonacci number in $S'M(1) - 1$.

The encoding of $S'\lambda M$ is that of $S'M$ with a 10 inserted before the final 1 — or equivalently, a 01 appended after the final 1 — so that $S'\lambda M(1) - S'M(1) = F_{t+2}$, where F_t is the largest Fibonacci number in $S'M(1) - 1$. Figures 15(iii) (in a Fibonacci inverse formulation) and 16(iii) (in Zeckendorf binary notation) illustrate this branching of the minimal Fibonacci tree (Figure 5).

This description of branching in the minimal Fibonacci tree applies only to the minimal Fibonacci representation of the parent node, in contrast to the branching in the minimal successor tree (Figure 3), which applied in any Zeckendorf representation (Remark 4.11). Specifically, the minimal Fibonacci tree produces the left, respectively, right, children of a node by substituting 01 for the last 1, respectively, appending 01 to the Fibonacci representation (Figure 16(iii)). However, the substitution *only* works in minimal Fibonacci representation. For example, $6 = F_2 + F_5 = 1001$ begets $9 = F_2 + F_6 = 10001$ and $19 = F_2 + F_5 + F_7 = 100101$, respectively, in minimal Fibonacci representation. However, in lazy Fibonacci representation, the algorithm applied to $6 = F_2+F_3+F_4 = 111$ would beget a different pair of children, $8 = F_2 + F_3 + F_5 = 1101$ and $14 = F_2 + F_3 + F_4 + F_6 = 11101$.

The algorithm of Corollary 4.8 effectively follows the tree of Figure 4 *upward* as each iteration removes symbols from the incumbent composition from the inside outward. By contrast to the radix algorithm of Proposition 4.10, the inside–outward algorithm of Corollary 4.8 expands integers in a series far from a standard Zeckendorf representation. The same Fibonacci numbers can appear multiple times in the expansion. For example, the algorithm uses F_4 twice to produce $15 = 2 + F_4 + F_3 + F_4 + F_5 = \lambda\kappa^3\lambda\kappa^\star(1)$. Not surprisingly, for Figure 5, a formula for left and right children in terms of the parent node proves to be more elusive than for Figure 3, which follows from the formula given in Remark 4.11 and Proposition 4.12.

However, considering the compositions from the outside inward provides a way to reformulate the algorithm. In fact, every path downward through Figure 5 corresponds to a path backward through the algorithm of Corollary 4.8, and, correspondingly, a calculation starting from the last iterate and reconstructing S from the outside inward. Since the algorithm always terminates with $t = 1$, the last addend to S_1 is either F_1 or F_4. On the other hand, by the initialization, the first addend is "2".

Thus, if the inside–outward algorithm terminates without iterating, it gives $S_1 - 1 = 1$, the root node of Figure 5. If the algorithm terminates after a single iteration, then it gives $S_1 - 1 \in \{1 + F_1, 1 + F_4\} = \{2, 4\}$, the second level of the tree. Continuing to move through the algorithm backwards, if it terminates after two iterations, and the last addend were F_1, then the penultimate addend is either $F_{1+1} = F_2$ or $F_{1+4} = F_5$, whereas, if the last addend were F_4, then the penultimate addend is either $F_{4-1} = F_3$ or $F_{4+2} = F_6$. This gives $S_1 - 1 \in \{1 + F_1 + F_2, 1 + F_1 + F_5, 1 + F_4 + F_3, 1 + F_4 + F_6\} = \{3, 7, 6, 12\}$, the third level of the tree. This shows that, for the recurrence implied by Corollary 4.8, a node effectively depends on its grandparent.

To simplify this recurrence, recall that for parent node n satisfying $F_t \leq n < F_{t+1}$, the tree of Figure 5 forms the left child and right child by adding F_{t-1} and F_{t+2}, respectively (Remark 4.13). For example, take $\kappa\lambda\kappa\lambda M(1)-1 = 31 = 1+F_1+F_5+F_4+F_8$ (Example 4.5). The partial sums backwards through the algorithm of Corollary 4.8 correspond to the paths I, κ, $\kappa\lambda$, $\kappa\lambda\kappa$, $\kappa\lambda\kappa\lambda$ and $1, 2, 7, 10, 31$

through Figures 4, respectively, 5. Partial sums of the latter satisfy, respectively, $F_2 \leq 1 < F_{2+1}$, $F_3 \leq 1 + F_{2-1} < F_{3+1}$, $F_5 \leq 1 + F_1 + F_{3+2} < F_{5+1}$, $F_6 \leq 1 + F_1 + F_5 + F_{5-1} < F_{6+1}$, and $F_8 \leq 1 + F_1 + F_5 + F_4 + F_{6+2} < F_{8+1}$. Moreover, substituting F_1 or F_2 for 1, as required, and simplifying, allows us to rewrite the expansions as $1 = F_2$, $1 + F_1 = F_3$, $1 + F_1 + F_{3+2} = F_3 + F_5$, $1 + F_1 + F_5 + F_{5-1} = F_3 + F_6$, and $1 + F_1 + F_5 + F_4 + F_{6+2} = F_3 + F_6 + F_8$, exactly as they will appear in Figure 14.

Lemma 4.13 will now generalize this example of branching.

Lemma 4.13 (Nodes and branches of the "inner" and "minimal Fibonacci" trees)**.** *Let $n \in \mathbb{Z}_+$ be a node in Figure 5. Then, there exists $t \geq 2$ such that $F_t \leq n < F_{t+1}$, and*

(a): *Either* **(i)** *n is a Fibonacci number and the position of $n = F_t = \kappa^{t-2}(2) - 1$ in Figure 5 corresponds to that of κ^{t-2} in Figure 4, or* **(ii)** *there exists an ancestor $m = R(2) - 1$ of n in Figure 5, with $m = n - F_t$, and the positions of m and n in Figure 5 corresponding to those of R, respectively, $T = R\lambda\kappa^{t-u-2}$ in Figure 4, where $F_u \leq m < F_{u+1}$.*

(b): *For $n = S(2) - 1$ in Figure 5 corresponding to S in Figure 4, the left and right children of n equal $n + F_{t-1} = S\kappa(2) - 1$ and $n + F_{t+2} = S\lambda(2) - 1$, respectively, corresponding to $S\kappa$, and $S\lambda$, respectively.*

Proof of Lemma 4.13: In Section 11 □

Remark 4.14. Observing the form of T in Lemma 4.13(a)(ii) shows that if and only if n is not a Fibonacci number, then T and n descend (in Figures 4 and 5, respectively), from ancestors R, respectively, m by a single right branching possibly followed by one or more left branchings ($t - u - 2$ left branchings, to be precise). Thus, the ancestor m of n can be read from Figure 5 as the node on any previous level to the left of n and horizontally closest to it.

On the other hand, if and only if $n = F_t$ is a Fibonacci number, then it is the left child of $m = F_t - F_{t-2} = F_{t-1}$ in Figure 5, its position corresponding to that of κ^{t-2}, the left child of κ^{t-1}, in Figure 4.

For example, the fourth level of the tree contains, from left to right, $5 = F_5$, corresponding to κ^3 in Figure 4; $11 = 3 + F_6$, corresponding to $\kappa^2\lambda = \kappa^2 \circ \lambda$; $10 = 2 + F_6$, corresponding to $\kappa\lambda\kappa = \kappa \circ \lambda\kappa$; $20 = 7 + F_7$, corresponding to $\kappa\lambda^2 = \kappa\lambda \circ \lambda$; $9 = 1 + F_6$, corresponding to $\lambda\kappa^2 = I \circ \lambda\kappa^2$; $19 = 6 + F_7$, corresponding to $\lambda\kappa\lambda = \lambda\kappa \circ \lambda$; $17 = 4 + F_7$, corresponding to $\lambda^2\kappa = \lambda \circ \lambda\kappa$; and $33 = 12 + F_8$, corresponding to $\lambda^3 = \lambda^2 \circ \lambda$.

Similarly, the fifth level of the tree contains, from left to right, $8 = F_6$, $18 = 5 + F_7$, $16 = 3 + F_7$, $32 = 11 + F_8$, $15 = 2 + F_7$, $31 = 10 + F_8$, $28 = 7 + F_8$, $54 = 20 + F_9$, $14 = 1 + F_7$, $30 = 9 + F_8$, $27 = 6 + F_8$, $53 = 19 + F_9$, $25 = 4 + F_8$, $51 = 17 + F_9$, $46 = 12 + F_9$, and $88 = 33 + F_{10}$.

Using Lemma 4.13(b), Remark 6.8 will discuss the recursive definition (67) of the *minimal Fibonacci representation*, and show for values in Figure 5 the equivalent series expansion in Figure 14, formalizing the connection between the minimal Fibonacci tree, and minimal Fibonacci representation. Section 8.6.1 will use Lemma 4.13(b) to show an order isomorphism between the tree and individual clades thereof.

Remark 4.15 (Sequences of all-left branchings or all-right branchings in Figures 4, 5). Take the sequence of left branchings $S = (\lambda,\ \lambda\kappa,\ \lambda\kappa^2,\ \lambda\kappa^3, \ldots)$ in Figure 4, corresponding to $S(2) - 1 = (4, 6, 9, 14, \ldots)$ in Figure 5. The radix algorithm (Proposition 4.10) encodes SM as $(10100^\star,\ 100100^\star,\ 1000100^\star,\ 10000100^\star, \ldots) = (101,\ 1001,\ 10001,\ 100001, \ldots) = (F_2 + F_4,\ F_2 + F_5,\ F_2 + F_6,\ F_2 + F_7, \ldots)$ in Figure 14. By Lemma 4.13(b), a left branching in Figure 5 replaces F_t with F_{t+1} in the minimal Fibonacci representation, where F_t is the largest Fibonacci number in the minimal Fibonacci representation of the parent, equivalent to an increment (by one) of its most significant Fibonacci index (see Definition 6.2 and Figure 16(iii)), or equivalently, an increment (by one) of its last Fibonacci gap (see Definition 6.3 and Figure 17(iii)). Indeed, each row $S_{n,1}, S_{n,2}, S_{n,3}, \ldots$ of Table 9 appears as a sequence of left branchings in Figure 4, and conversely. For corresponding values $S(2) - 1$, all sequences of left branchings in Figure 5 appear as rows of ⅁, the 1–2-Fibonacci Array (Table 3, top left, reproduced in Table 12), and conversely.

By contrast, consider the sequence of right branchings $S = (\kappa,\ \kappa\lambda,\ \kappa\lambda^2,\ \kappa\lambda^3, \ldots)$ in Figure 4, corresponding to $S(2) - 1 = (2, 7, 20, 54, \ldots)$ in Figure 5. The radix algorithm encodes SM as $(010^\star,\ 01010^\star,\ 0101010^\star,\ 010101010^\star, \ldots) = (01,\ 0101,\ 010101,\ 01010101, \ldots) = (F_3,\ F_3 + F_5,\ F_3 + F_5 + F_7,\ F_3 + F_5 + F_7 + F_9, \ldots)$. By Lemma 4.13(b), a right branching in Figure 5 appends F_{t+2} to the Fibonacci expansion, where F_t is the largest Fibonacci number in the minimal Fibonacci representation of the parent, equivalent to appending $t + 2$ to its Fibonacci indices (Figure 16(iii)), or equivalently, appending 2 to its Fibonacci gaps (Figure 17(iii)). Here, sequences of right branchings in Figure 5 appear as rows of ⅂, the 1–2-mirror Array (Table 3, bottom left), and conversely.

Section 8.3.1 will expound on how to generate rows of the branch quartet arrays using tree branches, summarized in Figures 24(a)(i) and 25(b)(i). Proposition 8.5 will formalize the statements about gaps of the branch quartet arrays, with a summary in Remark 8.4.

Corollary 4.11 shows the equivalence classes on the free monoid $\{\kappa, \lambda\}^\star$ to be in bijective correspondence with $\mathbb{Z}_+$. It follows that any positive integer is the value $S(1) - 1$ for a unique class of compositions $S'M$ of κ's and λ's having at least one λ (Table 11), (while zero is the value $S(1) - 1$ for the class $\kappa^\star$). The total order of the classes S by $S(1)$ allows a systematic listing of the complementary equations studied by Kimberling [22], as Proposition 4.14 demonstrates.

Proposition 4.14 (Complementary equations for Compositions of κ and λ)**.** *For compositions S of κ's and λ's with degree p and reduced degree $p_\star$ as defined in Proposition 4.7:*

(a): *There exists an S for which $S(1) \geq 1$ and having degree $p \geq 1$, if and only if $p \geq F^{-1}(S(1)-1)$. Moreover, if $p = p_\star$, then S is unique.*

(b): *For two compositions S, R of κ's and λ's having the same degree p, the equation $S(n) - S(1) = R(n) - R(1)$ holds for integers $n \geq 1$.*

Proof of **(a)**. The "only if" follows from part (a) of Proposition 4.7 and the fact that $p \geq p_\star$. For the "if", in the case of $p = 1$, S cannot include any λ's, so $S = \kappa^\star$, uniquely. In the case of $p \geq 2$, Corollary 4.11 assures the existence and uniqueness of the standard class representatives having $p = p_\star$, by showing the bijection between the equivalence classes (Table 11) and the positive integers (Table 6(i)). For $p > p_\star$,

it suffices to match $S(1)$ with $S^\star(1)$, where $S^\star$ is the standard class representative for $p_\star$, and then set $S(n) = S^\star(\kappa^{p-p_\star}(n))$ to match p. □

Proof of **(b)**. For integers $n \geq 1$, Proposition 4.6 allows us to write S and $S^\star$ in the form (17). The coefficients of n and $\lfloor n\phi \rfloor$ in $S(n)$ must equal those for $R(n)$, since these coefficients depend only on p. Thus, to match the left-hand and right-hand sides of the equation, it suffices to subtract out the constant terms, S_1 and R_1. □

Example 4.7 (Complementary equations)**.** Over the positive integers, Proposition 4.14 generates pairwise equalities between compositions of Wythoff functions κ and λ by (i) repeatedly applying initial κ's to the integer argument ("inside") to match p, and (ii) adding constants ("outside") to match $S(1)$. Thus, following Table 11 and generating all complementary equations possible by Proposition 4.14 gives, up to the addition of a constant,

$$\begin{aligned}
&\text{For } p = 2,\\
&\quad \kappa^2 + 1 = \lambda;\\
&\text{For } p = 3,\\
&\quad \kappa^3 + 2 = \lambda\kappa + 1 = \kappa\lambda;\\
&\text{For } p = 4,\\
&\quad \kappa^4 + 4 = \lambda\kappa^2 + 3 = \kappa\lambda\kappa + 2 = \kappa^2\lambda + 1 = \lambda^2;\\
&\text{For } p = 5,\\
&\quad \kappa^5 + 7 = \lambda\kappa^3 + 6 = \kappa\lambda\kappa^2 + 5 = \kappa^2\lambda\kappa + 4\\
&\qquad\quad = \lambda^2\kappa + 3 = \kappa^3\lambda + 2 = \lambda\kappa\lambda + 1 = \kappa\lambda^2;\\
&\qquad\quad \vdots
\end{aligned}$$

Corollary 4.15 ("Pure-κ" form of Fibonacci cohort sequence from 1st cohort)**.** *As in (17), let S_n be a Fibonacci cohort sequence from 1st cohort under cohortizer F_{t+p} and initial element S_1. Then, in particular, $S_n = \kappa^p(n) + S_1 - 1$, for $n = 1, 2, 3, \ldots$. Proposition 6.3 gives another derivation of the result, using maximal Fibonacci successors.*

Remark 4.16. Per Remark 4.15, consider that each row of Table 9 corresponds to a succession of left branchings in Figure 4, such that if $\epsilon_{n,k}$ is an entry of Table 9 with $k \geq 1$, then $\epsilon_{n,k+1} = \epsilon_{n,k} \circ \kappa$. Row $n = 0$ of Table 9 begins at the root node of Figure 4. For subsequent rows $n \geq 1$ of Table 9, the first entry $\epsilon_{n,1}$ ends in λ and therefore corresponds to a node of Figure 4 that is the right child of an entry in some previous row $m < n$ of Table 9 (by construction of the table with $p_\star$ non-decreasing down columns). Thus the remainder of row n in the table follows from $\epsilon_{n,1}$ by a succession of left branchings (See Remark 4.14). With the functions built up in this manner, no two functions $\epsilon_{n,k} \in \{\kappa, \lambda\}^\star$ of Table 9 can appear at the same node of Figure 4, and, therefore, cannot have the same value of $\epsilon_{n,k}(2) - 1$ in the corresponding tree, Figure 5. Proposition 4.16 formalizes this observation.

For the functions S in Table 9, tabulating the values $S(2) - 1$ gives the *1–2-Fibonacci array*, Table 12, which turns out to be the interspersion 194030. Proposition 4.16 considers the two tables and expresses the bijection between individual

1	2	3	5	8	13	21 $\cdots$
4	6	9	14	22	35	56 $\cdots$
7	10	15	23	36	57	91 $\cdots$
11	16	24	37	58	92	147 $\cdots$
12	17	25	38	59	93	148 $\cdots$
18	26	39	60	94	149	238 $\cdots$
19	27	40	61	95	150	239 $\cdots$
20	28	41	62	96	151	240 $\cdots$
29	42	63	97	152	241	385 $\cdots$
30	43	64	98	153	242	386 $\cdots$
31	44	65	99	154	243	387 $\cdots$
32	45	66	100	155	244	388 $\cdots$
33	46	67	101	156	245	389 $\cdots$
47	68	102	157	246	390	623 $\cdots$
$\vdots$	$\vdots$	$\vdots$	$\vdots$	$\vdots$	$\vdots$	$\ddots$

TABLE 12. F, *1–2-Fibonacci Array*, (194030). $S(2)-1$ of corresponding functions S in Table 9 provides a bijection. Cohort dual of *2–1-Fibonacci Array*, Table 15. Rows are sequences of left branchings in the *minimal Fibonacci tree*, Figure 5. Columns are right clades of the *minimal successor tree*, Figure 3. Arranged as a 1–2-Fibonacci cohort tableau in Table 28(i). Member of the branch quartet (Table 3, top left).

elements (not equivalence classes) of the free monoid $\{\kappa, \lambda\}^\star$ on $\{\kappa, \lambda\}$ and the positive integers. This yields an explicit formula for entries $\mathsf{F}_{n,k}$ of Table 12.

Proposition 4.16 (Constructive bijection between free monoid on $\{\kappa, \lambda\}$ and $\mathbb{Z}_+$)**.** *Let the first column of Table 9 list the standard representatives of all equivalence classes $S/\circ\kappa^\star \in \{\kappa, \lambda\}^\star/\circ\kappa^\star$ of $S \in \{\kappa, \lambda\}^\star$. This means that for $n = 0, 1, 2, \ldots$, the entry $S_{n,1}$ at position $(n, 1)$ of the table is either I or ends in λ. Moreover, let the entries in the first column of Table 9 be ordered such that $S_{n,1}(1) - 1 = n$, where Corollary 4.11 guarantees the existence and uniqueness of an equivalence class whose representatives S satisfy $S(1) = n$ for each $n = 1, 2, 3, \ldots$. Further, let $S_{n,k} = S_{n,1}\kappa^{k-1}$ give subsequent columns of Table 9, so that the number of κ's in the suffix of $S_{n,k}$ equals $k - 1$. Finally, let the corresponding entries of Table 12 give the values $\mathsf{F}_{n,k} \equiv S_{n,k}(2) - 1$ for $n = 0, 1, 2, \ldots$ and $k = 1, 2, 3 \ldots$. Then,*

(a): $\mathsf{F}_{n,k} \equiv S_{n,k}(2) - 1 = n + F_{F^{-1}(n)+k+1}$.

(b): *The map*

$$\begin{aligned} \{\kappa, \lambda\}^\star &\to \mathbb{Z}_+ \\ S &\mapsto S(2) - 1. \end{aligned}$$

is a bijection.

Proof. In Section 11. □

Remark 4.17. Proposition 4.16 derives a formula for $\mathsf{F}_{n,k}$ using the "free-monoid approach," that is, mapping the tabulation Table 12 of $\mathsf{F}_{n,k}$ to that of compositions in the free monoid $\{\kappa, \lambda\}^\star$, Table 9.

By contrast, Lemma 8.1 will derive the same formula using the "tree branch approach," that is, by defining the first column F_1 of $\mathsf{F}_{n,k}$ $(n = 1, 2, 3, \ldots)$ as the sequence of right children of $\mathbb{Z}_+$ in the minimal Fibonacci tree (Figure 5), and rows of $\mathsf{F}_{n,k}$ as sequences of all-left branchings in the tree. Equivalent descriptions of F also include the "tree clade approach" of Section 8.6.3 and the tableau manipulation approach of Section 8.2.2.

Remark 4.18. This section examined two maps between the free monoid $\{\kappa, \lambda\}^\star$ and the positive integers:

$$\begin{array}{rccc} \text{Corollary 4.11}: & \{\kappa,\lambda\}^\star\!\!\diagup\!\!\circ\kappa^\star & \to & \mathbb{Z}_+ \\ & S\!\diagup\!\circ\kappa^\star & \mapsto & S(1) \end{array}$$

$$\begin{array}{rccc} \text{Proposition 4.16}: & \{\kappa,\lambda\}^\star & \to & \mathbb{Z}_+ \\ & S & \mapsto & S(2)-1 \end{array}$$

Each column of Table 9 comprises one representative function from each equivalence class of $\{\kappa, \lambda\}^\star$. Moreover, the functions in column k are related in that they all share the suffix $\circ\kappa^{k-1}$, or equivalently are the k^{th} representives of their respective classes, with the 1^{st} column comprising the 1^{st} or standard representative of each class, the 2^{nd} column comprising the 2^{nd} representative of each class, and so forth.

The equivalence relation induces the natural isomorphism between any column of Table 9 (a complete set of class representatives) and the entire table. Thus, each column can be placed in a 1–2-Fibonacci cohort sequence or tableau — a fixed-M version of Table 11 — and placed into bijective correspondence with the positive integers as a sequence or tableau, Table 6(i), by the first map. The second map provides a bijection between the entirety of the array Table 9 and the array of the positive integers in Table 12.

Moreover, the composition of the two maps induces an isomorphism between any column of Table 12 and the entire table $(\mathbb{Z}_+)$. Although each column contains values $S(2)-1$ for a only subset of $\{\kappa, \lambda\}^\star$, the subset comprises a complete set of representatives for the classes $\{\kappa, \lambda\}^\star\!\diagup\!\circ\kappa^\star$. In turn, the values $S(1)$ for this subset fill the entire array. For example, take the third column of Table 12, $(3, 9, 15, 24, 25\ldots) \overset{S(2)-1}{\longmapsto}$ $(\kappa^2, \lambda\kappa^2, \kappa\lambda\kappa^2, \kappa^2\lambda\kappa^2, \lambda^2\kappa^2\ldots) \overset{\circ\kappa^\star}{\sim}$ $(\kappa^\star, M, \kappa M, \kappa^2 M, \lambda M\ldots) \overset{S(1)}{\longmapsto} (1, 2, 3, 4, 5\ldots)$, thus mapping entries in a column to their respective row indices (plus one). In Corollaries 8.17 and 8.18 this correspondence reappears, respectively, as a clade–tree order isomorphism for the minimal successor tree, and the induced column–clade isomorphism for between columns of T and F, and left, respectively, right clades of the tree.

Similarly, since rows of Table 12 are sequences of left branchings in the minimal Fibonacci tree, the value $p - p_\star$ for corresponding entries in Table 9 provides a bijection between any row and the entire table $(\mathbb{Z}_+)$, thus going from entries in a row to their respective column indices (minus one) and inducing a bijection between each branch and the entire tree, Figure 5. Remark 4.29 will discuss analogous column–array and row–array isomorphisms for the cohort-dual array, Table 15.

To recap, integer sequences S furnished with Fibonacci cohortizer F_{t+p} from their 1^{st} cohort can be described by two parameters: The parameter S_1 specifies where a sequence begins and the parameter p specifies how quickly it spreads out. All such sequences can be expressed as $S(n)$ for $n = 1, 2, 3, \ldots$ with $S \in \{\kappa, \lambda\}^\star$, or

differ from such an expression by an integer constant. Thus, the section focused on the specific examples of $\kappa(n) \equiv \lfloor n\phi \rfloor$ with $p = 1$ and $S(1) = 1$ and $\lambda(n) \equiv \lfloor n\phi^2 \rfloor$ with $p = 2$ and $S(2) = 2$ and compositions of these two.

To summarize the observations about Fibonacci cohort sequences under the specific cohortizer F_{t+p} and rate p positive, the foregoing discussion treated three canonical forms, equivalent over $\mathbb{Z}_+$: The cohort form (17) writes S as a combination $S_n = F_p\kappa(n) + F_{p-1}n - F_{p+1} + S_1$ of $\kappa(n)$ and n. The Wythoff-composition form is homogeneous, writing S as the representative of an S_1-class of compositions of κ and λ, and then matching p by initial applications of κ as required to determine a specific member of the class. For the equivalence classes, Proposition 4.7 ordered their standard class representatives I, λ, $\kappa\lambda$, $\kappa^2\lambda, \lambda^2$, $\kappa^3\lambda, \lambda\kappa\lambda, \kappa\lambda^2, \ldots$ by increasing values of $S(1)$, and arranged them in a tableau grouped by cohort (Table 11). Finally, the pure-κ form of Corollary 4.15 writes S as $S = \kappa^p + S_1 - 1$, a nested iteration of the floor function κ plus a constant.

Note that the equivalence of forms in the above discussion holds for elements $S_1, S_2, \ldots$ of the sequences, whereas the pure-κ form may not give the same value for a zeroth element S_0. For example, $\lambda(n) + 1 = \kappa^2(n) + 2$ for $n \geq 1$, although $\lambda(0) + 1 = 1 \neq 2 = \kappa^2(0) + 2$.

Starting with an example to motivate the discussion, the next subsection addresses the free monoid $\{\lfloor n/\phi \rfloor, \lfloor n/\phi^2 \rfloor\}^\star$, showing a duality with $\{\lfloor n\phi \rfloor, \lfloor n\phi^2 \rfloor\}^\star$.

4.1.6. *Free monoid on $\{\lfloor n/\phi \rfloor, \lfloor n/\phi^2 \rfloor\}$ under composition, and total orderings by the 2–1- and 1–2-Fibonacci outer cohort tableaux.*

Example 4.8. Negative values of the *rate* p in Proposition 4.2 produce what Kimberling and Stolarsky [23] call *slow Beatty sequences*. For $p = -1$, note that $\lfloor n/\phi \rfloor$ 060143 and $\lceil n/\phi \rceil$ 019446 are Fibonacci cohort sequences under cohortizer F_{t-1}, whereas $p = -2$ gives $\lfloor n/\phi^2 \rfloor$ 060144 and $\lceil n/\phi^2 \rceil$ 189663, cohortized by F_{t-2}, and $p = -3$ gives $\lfloor n/\phi \rfloor - \left\lfloor \frac{n}{1-\phi} \right\rfloor$ 060145, cohortized by F_{t-3}. These examples motivate the investigation that follows.

Consider the substitution of the cohortizer $F_{(t+p)^+}$ for F_{t+p}. When the recurrence (11) is modified to $S_{n-F_t} + F_{(t+p)^+}$, $F_{t+1} \leqslant n < F_{t+2}$, as Lemmas 4.17 and 4.18 allow, fewer simplifications can be made. Nonetheless, the following analogs of (21) and (23) hold.

Lemma 4.17 (Bounds on S_n, a Fibonacci cohort sequence under cohortizer $F_{(t+p)^+}$)**.** *Consider a Fibonacci cohort sequence from the 1^{st} cohort under $f(t) = F_{(t+p)^+}$. Then for $F_{t+1} \leqslant n < F_{t+2}$, $t = 2, 3, \ldots$:*

Lower Bound

$$
\begin{aligned}
S_n \geq S_1 + F_{(t+p+1)^+} &- \left\{ \begin{array}{ll} 1, & t+p \text{ even and } t+p \geq 0; \\ 0, & \text{otherwise.} \end{array} \right\} \\
&+ \left\{ \begin{array}{ll} 1, & t+p \text{ even and } p+1 \geq 0; \\ 0, & \text{otherwise.} \end{array} \right\} \\
&- \left\{ \begin{array}{ll} F_{(p+2)^+}, & t \text{ odd;} \\ F_{(p+1)^+}, & t \text{ even.} \end{array} \right\}
\end{aligned} \tag{29}
$$

Upper Bound

$$
\begin{aligned}
S_n \leq S_1 + F_{(t+p+2)^+} &- \left\{ \begin{array}{ll} 1, & t+p+1 \geq 0; \\ 0, & \textit{otherwise.} \end{array} \right\} \\
&+ \left\{ \begin{array}{ll} 1, & p+2 \geq 0; \\ 0, & \textit{otherwise.} \end{array} \right\} \\
&- F_{(p+3)^+}
\end{aligned} \tag{30}
$$

Proof. Analogous to the proof of Lemma 4.5. □

Further, for $S_1 = 0$, Lemma 4.18 demonstrates (a) that if the cohort index $t \leq 1-p$ then members of the cohort are children of 0, and conversely (b), that if a member of the sequence is a child of 0, then it must lie in a cohort C_t for $t \leq 2-p$.

Lemma 4.18. *For sequences S_n described in Lemma 4.17 and having $S_1 = 0$ and $p \leq -1$,* **(a)** *$t+p \leq 1$ implies $S_{n-F_t} = 0$ and* **(b)** *$S_{n-F_t} = 0$ implies $t+p \leq 2$.*

Proof. We will use Lemma 4.17 to show **(a)** and **(b)**.

(a): Consider the upper bound (30). First note that $S_1 = 0$ for any S that the proposition contemplates, thus, the first term of the right hand side of (30) vanishes. Next note that $p \leq -1$ causes the last two terms of the right hand side of (30) to cancel, that is, $\left\{ \begin{array}{ll} 1, & p+2 \geq 0; \\ 0, & \text{otherwise;} \end{array} \right\} - F_{(p+3)^+} = 0$. Finally, use the definition (11), substituting $S_n = S_{n-F_t} + F_{(t+p)^+}$ into the left hand side of (30), and rearrange the remaining terms to obtain $S_{n-F_t} \leq F_{(t+p+2)^+} - F_{(t+p)^+} - \left\{ \begin{array}{ll} 1, & t+p+1 \geq 0; \\ 0, & \text{otherwise;} \end{array} \right\}$. Now, for $t+p \leq 1$, the right hand side of the latter expression sums to zero, forcing $S_{n-F_t} = 0$, as required.

(b): Consider the lower bound (29). Again note that $S_1 = 0$ causes the first term of the right hand side of (29) to vanish. Further note that $p \leq -1$ causes the last two terms of the right hand side of (29) to cancel:

$$
\begin{aligned}
&\left\{ \begin{array}{ll} 1, & t+p \text{ even and } p+1 \geq 0; \\ 0, & \text{otherwise;} \end{array} \right\} - \left\{ \begin{array}{ll} F_{(p+2)^+}, & t \text{ odd;} \\ F_{(p+1)^+}, & t \text{ even;} \end{array} \right\} \\
&\qquad = \left\{ \begin{array}{ll} 1, & t \text{ odd and } p = -1; \\ 0, & \text{otherwise;} \end{array} \right\} - \left\{ \begin{array}{ll} 1, & t \text{ odd and } p = -1; \\ 0, & \text{otherwise;} \end{array} \right\} = 0.
\end{aligned}
$$

Finally, use the modified form of (11), subtracting $F_{(t+p)^+} = S_n - S_{n-F_t}$ from (29), to get $S_{n-F_t} = S_n - F_{(t+p)^+} \geq F_{(t+p+1)^+} - F_{(t+p)^+} - \left\{ \begin{array}{ll} 1, & t+p \text{ even and } t+p \geq 0; \\ 0, & \text{otherwise;} \end{array} \right\}$. Now, $S_{n-F_t} = 0$, forces the right hand side of the latter expression to zero, which can only hold for $t+p \leq 2$. □

Proposition 4.19 (Cohortizers for compositions of the forms η^h and $\eta^h\theta$)**.** *Let $\theta(n) = \lfloor n/\phi \rfloor$, $\eta(n) = \lfloor n/\phi^2 \rfloor$. If a composition S of θ's and η's takes the particular form $S = \eta^h\theta^q$, where h is a nonnegative integer and $q \in \{0,1\}$, then $S_1, S_2, S_3, \ldots \equiv S(1), S(2), S(3), \ldots$ is a Fibonacci cohort sequence from the 1^{st} cohort, under cohortizer $F_{(t+p)^+}$, where $p = -q - 2h$.*

Proof. Induction. First consider Proposition 4.2 and note that so long as $p \geq -2$, $F_{(t+p)^+}$ can replace F_{t+p} in that proposition and the corollaries that follow it. Next examine (16) and observe that $p = -1$ and $S_1 = 0$ are the unique parameter values

that give $S_n = \theta(n)$, and that $p = -2$ and $S_1 = 0$ are the unique parameter values that give $S_n = n - 1 - \theta(n) = \eta(n)$, verifying the proposition for cases $(p, q, h) = (-1, 1, 0)$, respectively, $(p, q, h) = (-2, 0, 1)$. Thus it remains to verify the proposition for arbitrary $p \leq -1$.

Before composition, the initial cases $p = -1$ and $p = -2$ give $\theta(1) = 0$ and $\eta(1) = 0$, respectively, and S_1 cannot increase with further compositions of η's and θ's, since 0 is a fixed-point of both η and θ. Thus, the proposed conditions on S imply those in the lemma, allowing the induction step to use Lemma 4.18.

For the induction step, first consider the composition, $T = \eta \circ S$, of η with an existing composition, S, of the form $S = \eta^h\theta$ or $S = \eta^h$. Let F_{t+p} cohortize S and let $F_{t+1} \leq n < F_{t+2}$. This gives

$$
\begin{aligned}
T_n &= \eta(S_n) \\
&= \left\lfloor (S_{n-F_t} + F_{(t+p)^+})/\phi^2 \right\rfloor \\
&= \begin{cases} S_{n-F_t} + F_{t+p} - 1 - \lfloor (S_{n-F_t} + F_{t+p})/\phi \rfloor, & S_{n-F_t} \geq 1 \text{ and } t+p \geq 2; \\ 0, & S_{n-F_t} = 0 \text{ and } t+p \leq 2; \end{cases} \qquad (31) \\
&= \begin{cases} S_{n-F_t} - 1 - \lfloor S_{n-F_t}/\phi \rfloor - F_{t+p-1} + F_{t+p}, & S_{n-F_t} \geq 1 \text{ and } t+p \geq 2; \\ 0, & S_{n-F_t} = 0 \text{ and } t+p \leq 2; \end{cases} \\
&= \begin{cases} S_{n-F_t} - 1 - \lfloor S_{n-F_t}/\phi \rfloor + F_{t+p-2}, & S_{n-F_t} \geq 1 \text{ and } t+p \geq 2; \\ 0, & S_{n-F_t} = 0 \text{ and } t+p \leq 2; \end{cases} \\
&= \left\lfloor (S_{n-F_t})/\phi^2 \right\rfloor + F_{(t+p-2)^+} \\
&= T_{n-F_t} + F_{(t+p-2)^+},
\end{aligned}
$$

as desired of the cohortizer for $T = \eta\eta^h\theta^q$ with $p = -q - 2h$, where the conditions on (31) follow from Lemma 4.18(a) (converse) and Lemma 4.18(b). □

Here again, the preamble to Section 4.1.6 uses the *rate* parameter p to quantify the speed of an integer sequence, including the two sequences generated by the two Wythoff^{-1} floor functions. In Proposition 4.19, the degree p continues to describe the speed of integer sequences — those generated by compositions of the Wythoff^{-1} pair previously considered. As in Section 4.1.5, parameter p will now be used for initial classification of these compositions into cohorts, with the number of leading zeroes of the Wythoff^{-1} compositions used to order the compositions within each cohort.

To remove the restrictions in Proposition 4.19, and treat general compositions in the free monoid $\{\theta, \eta\}^\star$, the succeeding results, some well-known, prepare the way forward.

Lemma 4.20. *For an irrational slope $\mu > 1$, the count of positive numbers of the form $0 < \lfloor m\mu \rfloor \leq n$ for integer m equals $\lfloor (n+1)/\mu \rfloor$.*

Proof. This well-known result can be shown using, say, that of Fraenkel, Mushkin, and Tassa [17]: For $\mu > 1$ irrational, the 0–1-indicator function $g_\mu(n)$ of the spectrum sequence $\lfloor m\mu \rfloor$ at integer n equals $f_{1/\mu}(n) \equiv \lfloor (n+1)/\mu \rfloor - \lfloor n/\mu \rfloor - \lfloor 1/\mu \rfloor = \lfloor (n+1)/\mu \rfloor - \lfloor n/\mu \rfloor$, where the latter equality follows from $0 < 1/\mu < 1$. This gives the telescoping series: $\sum_{m=1}^{n} g_\mu(m) = \sum_{m=1}^{n} (\lfloor (m+1)/\mu \rfloor - \lfloor m/\mu \rfloor) = \lfloor (n+1)/\mu \rfloor - \lfloor 1/\mu \rfloor = \lfloor (n+1)/\mu \rfloor$, as claimed. □

Proposition 4.21. *For any $\mu > 1$ irrational, the sequence $(\lfloor m/\mu \rfloor)_{m=1,2,3,\ldots}$ comprises $\lfloor \mu \rfloor$ zeroes, followed by $\lfloor 2\mu \rfloor - \lfloor \mu \rfloor$ ones, followed by $\lfloor 3\mu \rfloor - \lfloor 2\mu \rfloor$ twos, and*

so forth. That is, the sequence is non-decreasing and comprises $\lfloor (n+1)\mu \rfloor - \lfloor n\mu \rfloor$ *copies of each non-negative integer* n.

While the number of (initial) zeroes is always $\lfloor \mu \rfloor$*, for each positive integer* $n \geq 1$*, the number of copies* $\lfloor (n+1)\mu \rfloor - \lfloor n\mu \rfloor$ *of* n *is either* $\lfloor \mu \rfloor + 1$ *or* $\lfloor \mu \rfloor$.

Proof. To cite Fraenkel, Mushkin, and Tassa [17] once again, $g_\mu(m) = \lfloor (m+1)/\mu \rfloor - \lfloor m/\mu \rfloor - \lfloor 1/\mu \rfloor = \lfloor (m+1)/\mu \rfloor - \lfloor m/\mu \rfloor$, where the latter equality follows from $\mu > 1$. By the same telescoping series as in the proof of Lemma 4.20:

$$\begin{aligned}
&\vdots && \vdots \\
&\sum_{m=1}^{\lfloor n\mu \rfloor - 1} g_\mu(m) = \lfloor \lfloor n\mu \rfloor / \mu \rfloor && = n-1, \\
&\sum_{m=1}^{\lfloor n\mu \rfloor} g_\mu(m) = \lfloor (\lfloor n\mu \rfloor + 1)/\mu \rfloor && = n, \\
&\vdots && \vdots \\
&\sum_{m=1}^{\lfloor (n+1)\mu \rfloor - 1} g_\mu(m) = \lfloor \lfloor (n+1)\mu \rfloor / \mu \rfloor && = n, \\
&\sum_{m=1}^{\lfloor (n+1)\mu \rfloor} g_\mu(m) = \lfloor (\lfloor (n+1)\mu \rfloor + 1)/\mu \rfloor && = n+1, \\
&\vdots && \vdots
\end{aligned}$$

from which it is apparent that $\lfloor m/\mu \rfloor$ produces its first n for $m = \lfloor n\mu \rfloor + 1$ and its last n for $m = \lfloor (n+1)\mu \rfloor$, thus showing the desired result. □

Corollary 4.22. *For any* $\mu > 1$ *irrational, the sequence* $(\lfloor m/\mu \rfloor)_{m=-1,-2,-3,\ldots}$ *comprises* $\lfloor \mu \rfloor$ *minus ones, followed by* $\lfloor 2\mu \rfloor - \lfloor \mu \rfloor$ *minus twos, followed by* $\lfloor 3\mu \rfloor - \lfloor 2\mu \rfloor$ *minus threes, and so forth. That is, the sequence is non-increasing and comprises* $\lfloor -n\mu \rfloor - \lfloor -(n+1)\mu \rfloor$ *copies of each negative integer* n.

While the number of (initial) minus ones is always $\lfloor \mu \rfloor$*, for each negative integer* $n \leq -2$*, the number of copies* $\lfloor -n\mu \rfloor - \lfloor -(n+1)\mu \rfloor = \lfloor (n+1)\mu \rfloor - \lfloor n\mu \rfloor$ *of* n *is either* $\lfloor \mu \rfloor + 1$ *or* $\lfloor \mu \rfloor$.

Remark 4.19. In the following, recall the designation "lower Wythoff numbers" (000201) for those of the form $\kappa(n)$, $n = 1, 2, 3, \ldots$, and "upper Wythoff numbers" (001950), for those of the form $\lambda(n)$, $n = 1, 2, 3, \ldots$. Let $K = \kappa(\mathbb{Z}_+)$ and $\Lambda = \lambda(\mathbb{Z}_+)$ denote the complete sequences of lower, respectively, upper Wythoff numbers, for $n = 1, 2, 3, \ldots$, and, similarly, $\Theta = \theta(\mathbb{Z}_+)$, and $H = \eta(\mathbb{Z}_+)$ for the complete sequences of lower, respectively, upper Wythoff^{-1} numbers.

Consider $\theta(n) = \lfloor n/\phi \rfloor$ and $\eta(n) = \lfloor n/\phi^2 \rfloor$ in the context of Proposition 4.21. Then on the positive integers, the former has $\lfloor \phi \rfloor = 1$ leading zero while the latter has $\lfloor \phi^2 \rfloor = 2$ leading zeroes.

Further, the number of copies of each positive integer in the two sequences is given by $f_\phi(n) + 1 = \lfloor (n+1)\phi \rfloor - \lfloor n\phi \rfloor$ and $f_{\phi^2}(n) + 2 = \lfloor (n+1)\phi^2 \rfloor - \lfloor n\phi^2 \rfloor$, respectively. Since $f_\phi(n) = f_{\phi^2}(n) = g_\phi(n)$, the sequence Θ has runs of length two, respectively, one, of each lower, respectively, upper Wythoff number, while

the sequence H comprises runs of length three, respectively, two of each of each lower, respectively, upper Wythoff number.

The equalities $f_\phi(n) = f_{\phi^2}(n) = g_\phi(n)$ follow from the continued fraction expansions $\phi = [\bar{1}]$ and $\phi^2 = [2, \bar{1}]$, which give, respectively, convergents $\frac{F_{t+1}}{F_t}$ and $\frac{F_{t+2}}{F_t}$, for $t = 1, 2, 3, \ldots$ (See, *e.g.*, [29]).

Consider that in both sequences of convergents, the sequences of both numerators and denominators greater than one are $F_3, F_4, F_5, \ldots = 2, 3, 5, \ldots$. Also, $(f_\phi(1), f_\phi(2)) = (f_{\phi^2}(1), f_{\phi^2}(2)) = (g_\phi(1), g_\phi(2)) = (1, 0)$. Thus, calculation using Stolarsky's shift operators as described in [17] gives $f_\phi(n) = f_{\phi^2}(n) = g_\phi(n)$, for $n = 1, 2, 3, \ldots$.

Lemma 4.51 will show a similar results for the run lengths of Bergman and Bergman^{-1} pairs — a class of Beatty and Beatty^{-1} pairs that generalizes the Wythoff pair $\{\kappa, \lambda\}$ and Wythoff^{-1} pair $\{\theta, \eta\}$)

Lemma 4.23 (Recall well-known relations between κ, λ, θ and η)**.**

$$\eta\kappa(n) = \theta(n), n = 1, 2, 3, \ldots \tag{32}$$

$$\theta\kappa(n) = \eta\lambda(n) = n-1, n = 1, 2, 3, \ldots \tag{33}$$

$$\theta\lambda(n) = \kappa(n), n = 1, 2, 3, \ldots \tag{34}$$

In contrast to Proposition 4.19, Proposition 4.24, next, will employ the convention of p positive.

Proposition 4.24 (Runs in the sequence of values at positive integers, for a composition S of θ and η)**.** *Consider a composition $S \in \{\theta, \eta\}^\star$ of θ's and η's in any order. Evaluate this composition along the sequence of positive integers $n = 1, 2, 3, ...$ to obtain the sequence $S(n) = S(1), S(2), S(3), \ldots$. Let $p = q + 2h$, where q counts the number of applications of θ, and h the number of applications of η, respectively, made by S. Then, $S(n)$ begins with a leading run of N_0 zeroes, where $F_{p+2} - 1 \leq N_0 \leq F_{p+3} - 2$, followed by a run of length F_{p+2}, respectively, F_{p+1} of each lower Wythoff, respectively, upper Wythoff number.*

Proof. Induction. For the base cases, consider the length of runs in $\theta(n)$ and $\eta(n)$, $n = 1, 2, 3, \ldots$. As described in Remark 4.19, Θ comprises a single zero, followed by a run of length two, respectively, one, of each lower, respectively, upper Wythoff number, while H comprises a leading run of two zeroes, followed by runs of length three, respectively, two of each of each lower, respectively, upper Wythoff number.

Now suppose the proposition holds for $S(n)$, where S is a composition of q θ's and h η's. The reader can easily confirm that for any such S, the sequence $S(n)$, $n = 1, 2, 3, \ldots$ is nondecreasing. This property allows the remainder of the discussion to treat the values $S(n)$ equivalently as a multiset or as a sequence.

Case $T = \theta S$: By hypothesis, the sequence of values $T(n) = \theta S(n)$ will comprise the following: A run of length N_0 of the value $\theta(0) = 0$, followed by runs of length F_{p+2}, respectively, F_{p+1}, of each number of the form θK, respectively, $\theta\Lambda$. Now, write $T(n)$ as the multiset union of zero with multiplicity $N_0 + F_{p+2}$, the positive integers with multiplicity F_{p+2} (using (33)), and K with multiplicity F_{p+1}, (using (34)). Given that the positive integers equal, in turn, $K \cup \Lambda$, rewrite $T(n)$ as the multiset union of zero with multiplicity $N_0 + F_{p+2}$, K with multiplicity $F_{p+2} + F_{p+1} = F_{p+3}$, and Λ with multiplicity F_{p+2}. Since the composition of θ with S to form T increases p by one, the values $T(n)$ include K and Λ with the multiplicities claimed by the proposition. Also, the hypothesis $F_{p+2} - 1 \leq N_0 \leq F_{p+3} - 2$, F_{p+2}

implies that $F_{p+3} - 1 < F_{p+3} + F_p - 1 \leq N_0 + F_{p+2} \leq F_{p+3} + F_{p+2} - 2 = F_{p+4} - 2$, giving the desired bounds on the multiplicity of (leading) zeroes of $T(n)$. Thus, the induction holds for the new composition $T = \theta S$.

Case $T = \eta S$: On the other hand, the sequence of values $T(n) = \eta S(n)$ will comprise the following: A run of length N_0 of the value $\eta(0) = 0$, followed by runs of length F_{p+2}, respectively, F_{p+1}, of each number of the form ηK, respectively, $\eta\Lambda$. Now, write $T(n)$ as the multiset union of zero with multiplicity $N_0 + F_{p+1}$, Θ with multiplicity F_{p+2} (using (32)), and the positive integers with multiplicity F_{p+1} (using (33)). From the base case, recall the run–length encoding of Θ, and again use the decomposition of the positive integers into $K \cup \Lambda$. Thus, rewrite $T(n)$ as the multiset union of zero with multiplicity $N_0 + F_{p+2} + F_{p+1} = N_0 + F_{p+3}$, K with multiplicity $2F_{p+2} + F_{p+1} = F_{p+4}$, and Λ with multiplicity $F_{p+2} + F_{p+1} = F_{p+3}$. Since the composition of η with S to form T increases p by two, the values $T(n)$ include K and Λ with the multiplicities claimed by the proposition. Also, the hypothesis $F_{p+2} - 1 \leq N_0 \leq F_{p+3} - 2$ implies that $F_{p+4} - 1 \leq N_0 + F_{p+3} \leq 2F_{p+3} - 2 = F_{p+4} + F_{p+1} - 2 = F_{p+5} - 2$, the desired bounds on the multiplicity of (leading) zeroes of $T(n)$. Thus, the induction holds for the new composition $T = \eta S$. □

C_1								I
C_2								θ
C_3							η	θ^2
C_4						$\eta\theta$	$\theta\eta$	θ^3
C_5				η^2	$\eta\theta^2$	$\theta\eta\theta$	$\theta^2\eta$	θ^4
C_6	$\eta^2\theta$	$\eta\theta\eta$	$\eta\theta^3$	$\theta\eta^2$	$\theta\eta\theta^2$	$\theta^2\eta\theta$	$\theta^3\eta$	θ^5
⋮	⋮	⋮	⋮	⋮	⋮	⋮	⋮	⋮

TABLE 13. 2–1-Fibonacci (outer) cohort tableau of compositions $S \in \{\theta, \eta\}^\star$, ordered by increasing values of $N_0(S) + 1 = 1, 2, 3, \ldots$, which provides a bijection to Table 6(ii), and gathered into cohorts C_{p+1} by degree $p(S) = \underline{072649} - 1 = \underline{130233}_1 - 2 = 0, 1, 2, 2, 3, 3, 3, \ldots$. $\underline{112310}_0 = \underline{200648}_2 - 1 = 0,\ 1,\ 1, 2,\ 2, 2, 3, \ldots$ gives the number of symbols. Isomorph of Tables 7(ii), 22 and 32(ii). Planar graph isomorph of Figure 9.

Remark 4.20. Proposition 4.24 allows compositions $S \in \{\theta, \eta\}^\star$ to be written in a *2–1-Fibonacci outer cohort tableau*, Table 13, similar to Table 7(ii). Here, the compositions are arranged by increasing values of $N_0(S) + 1 = 1, 2, 3, \ldots$, beginning with $N_0(I) = 0$, and subsequently, $N_0(\theta) = 1$, $N_0(\eta) = 2$, $N_0(\theta^2) = 3$, $N_0(\theta\eta) = 4$, $N_0(\eta\theta) = 5$, $N_0(\theta^3) = 6$, and so forth. The tableau gathers the elements into cohorts C_{p+1} according to increasing value of the degree $p = 0, 1, 2, \ldots$, with one cohort per level $p + 1$, whilst the value of N_0 strictly increases throughout the tableau, with range $\{F_{p+2} - 1, \ldots, F_{p+3} - 2\}$ over cohort C_{p+1}. This illustrates Proposition 4.24, in particular, that $F_{p+2} - 1 \leq N_0 \leq F_{p+3} - 2$.

Remark 7.1 further examines the lexicography of this tableau, which isomorphic to the tableaux of "maximal Fibonacci gaps," Table 22, and branching functions in the maximal Fibonacci tree, Table 32(ii).

Now that Proposition 4.24 described the structure shown in Table 13, the algorithm of Proposition 4.25 will exploit this structure.

Proposition 4.25 (Inside-outward algorithm for $N_0(S)$, Number of Zeroes of Compositions S of θ and η on the positive integers)**.** *Let $S \in \{\theta, \eta\}^\star$, that is, a composition of θ's and η's in any order, and consider S from the inside outward. Then the following algorithm gives N_0, such that $S_1 = \cdots = S_{N_0} = 0$ and $S_{N_0+1} = 1$:*

Initialization: *Initialize p to 0 and initialize N_0 to 0.*

Main Step: *Then, until the last θ or η is applied, iterate as follows:*

$$p \longleftarrow \begin{cases} p+1, & \text{if } \theta \text{ is applied;} \\ p+2, & \text{if } \eta \text{ is applied;} \end{cases} \quad \text{and}$$
$$N_0 \leftarrow N_0 + F_{p+1}$$

Radix procedure (equivalent): *Write 1 for each θ applied and 01 for each η applied from the inside outward, and apply the resulting word in a basis of Fibonacci numbers $(F_2, F_3, \ldots)$ to obtain N_0.*

Proof. First prove the values used to initialize the algorithm. By Proposition 4.24, $(S(n))_{n=1,2,3,\ldots}$ begins with a leading run of N_0 zeroes, where $F_{p+2} - 1 \leq N_0 \leq F_{p+3} - 2$. This can be rewritten $F_{p+2} - 1 \leq N_0 < F_{p+3} - 1$, and further, as $F_{p+2} \leq N_0 + 1 < F_{p+3}$. This places S in cohort C_{p+1} of the 2–1-Fibonacci cohort tableau, Table 13. Thus, to prove the initial values used by the algorithm, it suffices to observe that $I(n)$ resides in the 1^{st} cohort of the table, having $p = 0$, and has no zeros on the positive integers, *i.e.*, $N_0(I) = 0$.

Secondly, prove the main step of the algorithm. At a given iteration of the main step, let R be the incumbent, partial composition of θ's and η's applied since initialization. Let the current iteration of the main step consider composition S, with either $S = \theta R$ or $S = \eta R$. By Proposition 4.24, if the incumbent R has degree p', then it has a run of length $F_{p'+2}$ of each lower Wythoff number, in particular of 1, and a run of length $F_{p'+1}$ of each upper Wythoff number, in particular of 2.

Thus, for $S = \theta R$, the application of θ to R increases q by 1, thus $p = p' + 1$ is the correct increment. Since $\theta(1) = 0$, the application of θ to R increases the number of (leading) zeros by $F_{p'+2} = F_{p+1}$, as claimed. For $S = \eta R$, the application of η to R increases h by 1, thus $p = p' + 2$ is the correct increment. Since $\eta(1) = \eta(2) = 0$, the application of η to R also increases the number of (leading) zeros by $F_{p'+2} + F_{p'+1} = F_{p'+3} = F_{p+1}$, as claimed. □

Remark 4.21. Since p increases with each step of the algorithm, the "most significant digits" of the resulting expansion of N_0 arise from the functions θ, η applied last.

Example 4.9. Consider $S = \theta^2\eta\theta\eta\theta$. Then successive steps of the algorithm give $(p, N_0) = (0, 0), (1, F_2), (3, F_2 + F_4), (4, F_2 + F_4 + F_5), (6, F_2 + F_4 + F_5 + F_7), (7, F_2 + F_4 + F_5 + F_7 + F_8), (8, F_2 + F_4 + F_5 + F_7 + F_8 + F_9) = (9, 77)$. Equivalently by the radix procedure, $\theta^2\eta\theta\eta\theta$ corresponds to $1 \cdot 01 \cdot 1 \cdot 01 \cdot 1 \cdot 1 = 10110111 = F_2 + F_4 + F_5 + F_7 + F_8 + F_9 = 77$.

Figure 7 shows the "outer" tree for actions of the algorithm on compositions of θ and η. Starting with $S = I$, the tree grows through successive applications of θ and η to S from the inside out, which form each left, respectively, right branch. For example, the branching sequence left–right–left–right corresponds to $S = \eta\theta\eta\theta$.

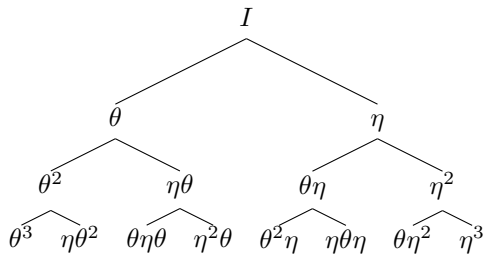

FIGURE 7. "Outer" binary tree of functions $S \in \{\theta, \eta\}^\star$ in the free monoid on $\{\theta, \eta\}^\star$. The algorithm of Proposition 4.25 follows this tree *downward* to calculate $N_0(S)$, which provides the bijection $N_0(S) + 1$ to Figure 8. Also, for prefix $L = \theta^\star\eta$, outer binary tree of suffix S' of each equivalence class $\{LS' \in \{\theta, \eta\}^\star \setminus \{\theta\}^\star | N_{-1}(LS') = N_{-1}(\eta S')\} \in \{\theta, \eta\}^\star / \theta^\star \circ$. The algorithm of Corollary 4.37 follows this tree *upward* to calculate $N_{-1}(LS)$, which provides the bijection $N_{-1}(LS) - 1$ to Figure 5. Blade dual of Figure 9.

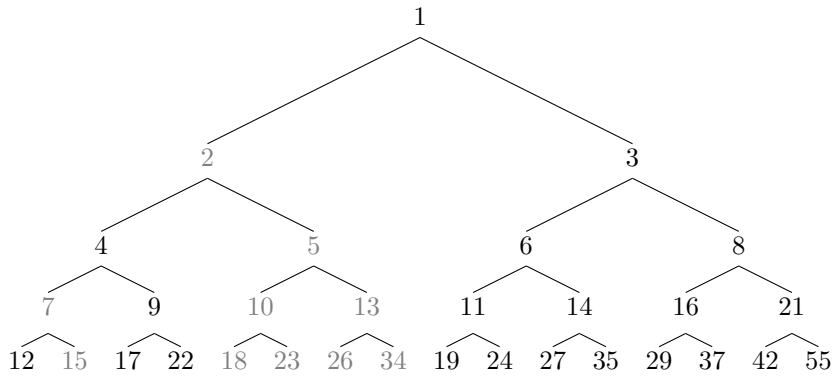

FIGURE 8. *Maximal Fibonacci Tree*. Corresponds bijectively to Figure 4 via $-S(-1)$ for compositions S shown therein. Corresponds bijectively to Figure 7 via $N_0(S) + 1$ for compositions S shown therein. Expanded in Figure 13. Blade dual of Figure 10 and 059893 permutes the two sequences. Cohort dual of Figures 5 and 14. 243571 (corrected) gives positions **P** of positive integers in the tree.

Now by the algorithm of Proposition 4.25, the sequence $S_n = \eta\theta\eta\theta(n)$ has number $N_0(S)$ of leading zeros equal to $F_2+F_4+F_5+F_7 = 22$. Thus, the index $N_0(S)+1$ of the *first nonzero element* S_{23} can be written $F_1 + F_2 + F_4 + F_5 + F_7 = 23$. The gaps between these Fibonacci indices give $(2-1, 4-2, 5-4, 7-5) = (1, 2, 1, 2)$. Evidently, a gap of 1 corresponds to a left branching while a gap of 2 corresponds to a right branching. Section 6 will revisit this pattern in Figure 17(iv).

Applying the algorithm of Proposition 4.25 level by level in Figure 7 gives F_1 on the first level, $F_1 + F_2$ and $F_1 + F_3$ on the second level, $F_1 + F_2 + F_3, F_1 + F_2 + F_4, F_1 + F_3 + F_4$, and $F_1 + F_3 + F_5$ on the third level, etc,... (Figure 13), as the index of the first nonzero element of $S = I, \theta, \eta, \theta^2, \eta\theta, \theta\eta, \eta^2, \ldots$, respectively, on the sequence positive integers. Figure 8 shows the result $1, 2, 3, 4, 5, 6, 8, 7, 9, 10, 13, 11, 14, 16, 21, \ldots$, not found in the OEIS [41] as of this writing.

Corollary 4.26 (Bijection between free monoid of Wythoff^{-1} compositions and positive integers)**.** *The map*

$$\begin{array}{ccc} \{\theta,\eta\}^\star & \to & \mathbb{Z}_+ \\ S & \mapsto & N_0(S)+1 \end{array}$$

is a bijection.

Proof. The algorithm of Proposition 4.25 gives the number of leading zeros $N_0(S)$ of S on the positive integers, for functions S in the free monoid $\{\theta,\eta\}^\star$ under composition. Whereas these functions include $S = I$, for which $N_0(I) = 0$, the range of $N_0(\{\theta,\eta\}^\star) = 0, 1, 2, \ldots$, the nonnegative integers. Thus $N_0(S) + 1$, the index of the first nonzero element of S on $\mathbb{Z}_+$, has the range $N_0(\{\theta,\eta\}^\star) + 1 = \mathbb{Z}_+$.

Moreover, the algorithm constructs the *lazy Fibonacci representation* of $N_0(S)$, since for $S \neq I$ the algorithm first applies either F_2 or F_3, depending on whether the innermost function is θ of η, respectively, and thereafter does not skip any two consecutive Fibonacci numbers. In the equivalent radix procedure, the substitution of 1 and 01 for θ and η, respectively, also ensures that the resulting representation does not skip any two consecutive Fibonacci numbers. Thus, the algorithm produces a distinct lazy Fibonacci representation for each distinct composition in $\{\theta,\eta\}^\star$. That each distinct $S \in \{\theta,\eta\}^\star$ has a distinct value of $N_0(S)$ follows from the uniqueness of the lazy Fibonacci representation, thus providing the bijection $\{\theta,\eta\}^\star \sim \mathbb{Z}_+$. □

Remark 4.22. Since the algorithm of Proposition 4.25 produces the lazy Fibonacci representation of $N_0(S)$ (Corollary 4.26), it also yields the *maximal Fibonacci expansion* of $N_0(S) + 1$ (Definition 6.1, Remark 6.1). Remark 6.7 will treat the recursive definition of this expansion (64) and the resulting binary tree, Figure 13. This offers a variant of the bijection between the free monoid $\{\theta,\eta\}^\star$ of compositions (Figure 7) and the positive integers $\mathbb{Z}_+$ (Figure 8). (Remark 4.28 will make an analogous observation about $N_{-1}(S)$.)

Lazy Fibonacci representation of N_0 also allows Proposition 4.25 to be applied in reverse. For example, to find an $S \in \{\theta,\eta\}^\star$ with exactly $N_0 = 17$ zeros on the positive integers, consider the lazy Fibonacci representation $17 = F_2 + F_4 + F_5 + F_6$ in Zeckendorf binary notation 10111, mapping $\{01, 1\} \mapsto \{\eta, \theta\}$ to obtain $\theta\eta\theta^2$, and finally reversing to obtain $\theta^2\eta\theta$, the $(17+1)^{\text{st}}$ element in Table 13.

Since both the lazy Fibonacci representation and maximal Fibonacci expansion skip no two consecutive bits, if F_t is the largest Fibonacci number in S, then $t-1$ is the largest bit used in encoding S by Proposition 4.25. Hence, the encoding of θS is that of S with an F_t appended, so that $N_0(\theta S) - N_0(S) = F_{t-1} + F_t - F_{t-1} = F_t$, and the encoding of ηS is that of S with an F_{t+1} appended, so that $N_0(\eta S) - N_0(S) = F_{t-1} + F_{t+1} - F_{t-1} = F_{t+1}$ (Figure 15(iv)).

Thus by correspondence with Figure 7, Proposition 4.25 effectively shows that each left, respectively, right child in Figure 8 corresponds to concatenating the maximal Fibonacci expansion (in Zeckendorf binary notation) of its parent with ·1, respectively, ·01 (Figure 16(iv)). For example, $4 = F_1 + F_2 + F_3 = 111$ has children $7 = 111 \cdot 1$ and $9 = 111 \cdot 01$. Section 6 investigates the branching in detail.

It will follow that for the free monoid of compositions $S \in \{\theta,\eta\}^\star$, the value $N_0 + 1 \in \mathbb{Z}_+$ — the least integer for which $S(N_0 + 1) > 0$ — provides a 2–1-Fibonacci outer cohort structure identical to that of the maximal Fibonacci expansion (Proposition 5.4), and the values of $N_0(S) + 1$ for compositions S in Table 13

are merely the positive integers in arranged in 2–1-Fibonacci cohort tableau (Table 6(ii)), this tableau also being isomorphic to Table 22, under $\{\theta, \eta\} \mapsto \{1, 2\}$ and with the order of symbols reversed in each element of the latter by notational convention (see Remark 7.1).

The correspondence between the tree of compositions in $\{\theta, \eta\}^\star$ (Figure 7) and the maximal Fibonacci tree (Figure 8) yields following results about the latter, analogous to Lemma 4.13 for the minimal Fibonacci tree.

Lemma 4.27 (Nodes and branches of the "outer" and "maximal Fibonacci" trees)**.** *Let $n \in \mathbb{Z}_+$ be a node in Figure 8. Then, there exists $t \geq 2$ such that $F_t \leq n < F_{t+1}$, and*

(a): *Either* **(i)** *t is even and the position of $n = F_t = N_0(\eta^{t/2-1}) + 1$, corresponds to that of $\eta^{t/2-1}$ in Figure 7, or* **(ii)** *there exists $m = N_0(R) + 1$ ancestor of n in Figure 8, with $m = n - F_t + F_{u-1}$, and the positions of m and n in Figure 8 correspond to those of R, respectively, $T = \eta^{(t-u-1)/2}\theta R$ in Figure 7, where $F_u \leq m < F_{u+1}$.*

(b): *For n in Figure 8 corresponding to S in Figure 7, the left and right children of n equal $n + F_t = N_0(\theta S) + 1$, respectively, $n + F_{t+1} = N_0(\eta S) + 1$, corresponding to θS, and ηS, respectively.*

Proof. In Section 11. □

Remark 4.23. Observing the form of T in Lemma 4.27(a)(ii) shows that if and only if n is not a Fibonacci number of even index, then T and n descend (in Figures 7 and 8), from ancestors R, respectively, m by a single left branching possibly followed by one or more right branchings ($^{(t-u-1)}/_2$ right branchings, to be precise). Thus, the ancestor m of n can be read from Figure 8 as the node on any previous level to the right of n and horizontally closest to it.

On the other hand, if and only if $n = F_t$ is a Fibonacci number of even index, then it is the right child of $m = F_t - F_{t-1} = F_{t-2}$ in Figure 8, its position corresponding to that of $\eta^{t/2-1}$, the right child of $\eta^{t/2-2}$ in Figure 7.

For example, the fourth level of the tree, has $7 = 4 + F_5 - F_{4-1}$, corresponding to $\theta^3 = \theta \circ \theta^2$; $9 = 2 + F_6 - F_{3-1}$, corresponding to $\eta\theta^2 = \eta\theta \circ \theta$; $10 = 5 + F_6 - F_{5-1}$, corresponding to $\theta\eta\theta = \theta \circ \eta\theta$; $13 = 1 + F_7 - F_{2-1}$, corresponding to $\eta^2\theta = \eta^2\theta \circ I$; $11 = 6 + F_7 - F_{5-1}$, corresponding to $\theta^2\eta = \theta \circ \theta\eta$; $14 = 3 + F_7 - F_{4-1}$, corresponding to $\eta\theta\eta = \eta\theta \circ \eta$; $16 = 8 + F_7 - F_{6-1}$, corresponding to $\theta\eta^2 = \theta \circ \eta^2$; and $21 = F_8$, corresponding to η^3.

Remark 4.24 (Sequences of all left branchings or all right branchings in Figures 7, 8)*.* Take the sequence of left branchings $S = (\eta\theta,\ \theta\eta\theta,\ \theta^2\eta\theta,\ \theta^3\eta\theta, \ldots)$ in Figure 7 corresponding to $N_0(S) + 1 = (5, 10, 18, 31 \ldots)$ in Figure 8. The algorithm of Proposition 4.25 gives $N_0(S) = (101, 1011, 10111, 101111, \ldots) = (F_2 + F_4,\ F_2 + F_4 + F_5,\ F_2 + F_4 + F_5 + F_6,\ F_2 + F_4 + F_5 + F_6 + F_7, \ldots)$ in Figure 13. By Lemma 4.27(b), a left branching in Figure 8 appends F_t to the maximal Fibonacci expansion, where F_t is the largest Fibonacci number not greater than the parent, or equivalently, appending $t + 1$ to its Fibonacci indices (see Definition 6.2 and Figure 16(iv)), or equivalently, appending 1 to its Fibonacci gaps (see Definition 6.3 and Figure 17(iv)). Indeed, each row $S_{n,1}, S_{n,2}, S_{n,3}, \ldots$ of Table 14 appears as a sequence of left branchings in Figure 7, and conversely. For corresponding values $N_0(S) + 1$,

I	θ	θ^2	θ^3	θ^4	$\theta^5\cdots$	
η	$\theta\eta$	$\theta^2\eta$	$\theta^3\eta$	$\theta^4\eta$	$\theta^5\eta\cdots$	
$\eta\theta$	$\theta\eta\theta$	$\theta^2\eta\theta$	$\theta^3\eta\theta$	$\theta^4\eta\theta$	$\theta^5\eta\theta\cdots$	
η^2	$\theta\eta^2$	$\theta^2\eta^2$	$\theta^3\eta^2$	$\theta^4\eta^2$	$\theta^5\eta^2\cdots$	
$\eta\theta^2$	$\theta\eta\theta^2$	$\theta^2\eta\theta^2$	$\theta^3\eta\theta^2$	$\theta^4\eta\theta^2$	$\theta^5\eta\theta^2\cdots$	
$\eta^2\theta$	$\theta\eta^2\theta$	$\theta^2\eta^2\theta$	$\theta^3\eta^2\theta$	$\theta^4\eta^2\theta$	$\theta^5\eta^2\theta\cdots$	
$\eta\theta\eta$	$\theta\eta\theta\eta$	$\theta^2\eta\theta\eta$	$\theta^3\eta\theta\eta$	$\theta^4\eta\theta\eta$	$\theta^5\eta\theta\eta\cdots$	
$\eta\theta^3$	$\theta\eta\theta^3$	$\theta^2\eta\theta^3$	$\theta^3\eta\theta^3$	$\theta^4\eta\theta^3$	$\theta^5\eta\theta^3\cdots$	
η^3	$\theta\eta^3$	$\theta^2\eta^3$	$\theta^3\eta^3$	$\theta^4\eta^3$	$\theta^5\eta^3\cdots$	
$\vdots$	$\vdots$	$\vdots$	$\vdots$	$\vdots$	$\vdots$	$\ddots$

TABLE 14. Array of elements $S \in \{\theta, \eta\}^\star$ of the free monoid on $\{\theta, \eta\}$, arranged with degree p increasing along rows and non-decreasing down columns, and $N_0(S)$ increasing across rows and down columns, and N_{-1}(S) constant along rows. Rows reproduce columns of Table 13. Column 1 arranges members of left subcohorts of Table 13, column 2 arranges members of left subcohorts of right subcohorts, and so forth (see Section 8.2.2). Column k lists the k^{th} representatives of the N_{-1}-equivalence classes in Table 16. Each row is a sequence of left branchings in the outer binary tree, Figure 7. Column k comprises the k^{th} right clade in the inner binary tree, Figure 9. $N_0(S) + 1$ provides a bijection to Table 15.

1	2	4	7	12	20	$\cdots$
3	6	11	19	32	53	$\cdots$
5	10	18	31	52	86	$\cdots$
8	16	29	50	84	139	$\cdots$
9	17	30	51	85	140	$\cdots$
13	26	47	81	136	225	$\cdots$
14	27	48	82	137	226	$\cdots$
15	28	49	83	138	227	$\cdots$
21	42	76	131	220	364	$\cdots$
$\vdots$	$\vdots$	$\vdots$	$\vdots$	$\vdots$	$\vdots$	$\ddots$

TABLE 15. ⊢, *2–1-Fibonacci array*. $N_0(S)+1$ of corresponding functions S in Table 14 provides a bijection. Cohort dual of *1–2-Fibonacci Array*, Table 12 (194030). Rows are sequences of left branchings in the *maximal Fibonacci tree*, Figure 8. Columns are left clades of *maximal successor tree*, Figure 10. Arranged as a 2–1-Fibonacci cohort tableau in Table 28(ii). Member of branch quartet (Table 3, top right).

all sequences of left branchings in Figure 8 appear as rows of ⊢, the 2–1-Fibonacci Array (Table 3, top right, and reproduced in Table 15), and conversely.

By contrast, consider the sequence of right branchings $S = (\theta\eta,\ \eta\theta\eta,\ \eta^2\theta\eta,\ \eta^3\theta\eta, \ldots)$ in Figure 7, corresponding to $N_0(S) + 1 = (6, 14, 35, 90 \ldots)$ in Figure 8. The algorithm of Proposition 4.25 gives $N_0(S) = (011,\ 01101,\ 0110101,\ 011010101, \ldots) = (F_2+F_3, F_2+F_3+F_5, F_2+F_3+F_5+F_7, F_2+F_3+F_5+F_7+F_9, \ldots)$. By Lemma 4.27(b), a right branching in Figure 8 appends F_{t+1} to the maximal Fibonacci expansion, where F_t is the largest Fibonacci number not greater the parent, or equivalently, appending $t+2$ to its Fibonacci indices (Figure 16(iv)), or equivalently, appending 2 to its Fibonacci gaps (Figure 17(iv)). Here, sequences of right branchings in Figure 8 appear as rows of $\dashv$, the 1–2-mirror Array (Table 3, bottom right), and conversely.

Section 8.3.1 will elaborate on gathering rows of the branch quartet arrays from tree branches, summarized in Figures 24(a)(i) and 25(b)(i). Proposition 8.5 will formalize the statements about gaps of the branch quartet arrays, with a summary in Remark 8.4.

Proposition 4.28 (Cohortizers and complementarity for Compositions in $\{\theta, \eta\}^\star$)**.** *Let sequence S and degree p be as in Proposition 4.24 and suppose that $(S(n))_{n=1,2,3,\ldots}$ has $N_0(S)$ leading zeroes (Proposition 4.25 gives an algorithm to calculate $N_0(S)$). Then for $n = 1, 2, 3, \ldots$, $S(n)$ is a Fibonacci cohort sequence of integers under cohortizer $F_{(t-p)^+}$ starting with element $S(N_0(S) - F_{p+2} + 2)$.*

Proof. First, recall from Proposition 4.24 the bounds $F_{p+2} - 1 \le N_0 \le F_{p+3} - 2$, which can be rewritten $F_{p+2} - 1 \le N_0 < F_{p+3} - 1$, and further, as $F_{p+2} \le N_0 + 1 < F_{p+3}$. Moreover, note from the proof of Proposition 4.24 that $\theta(n)$ has $p = 1$ and a single zero, satisfying with equality the lower bound $1 = F_{p+2} - 1 \le N_0$ on the number of zeroes N_0, whereas $\eta(n)$ has $p = 2$ and two leading zeroes, also satisfying with equality the lower bound $2 = F_{p+2} - 1 \le N_0$. Further observe that after applying η any number of times to either base case, the lower bound on N_0 continues to be satisfied with equality. That is, for $S = \eta^h\theta$ with $h = 0, 1, 2, \ldots$, $N_0(S) = N_0(\eta^h\theta) = F_{2h+3} - 1 = F_{q+2h+2} - 1 = F_{p+2} - 1$, while $S = \eta^h$ with $h = 1, 2, 3 \ldots$, $N_0(S) = N_0(\eta^h) = F_{2h+2} - 1 = F_{q+2h+2} - 1 = F_{p+2} - 1$.

Now, let T be a composition of θ's and η's in any order, and let N_0 be the number of zeroes of $T(n)$, with $F_{p+2} - 1 \le N_0 \le F_{p+3} - 2$. By Proposition 4.24, $(T(n))_{n=1,2,3,\ldots}$ includes K and Λ with the same multiplicity as $(S(n))_{n=1,2,3,\ldots}$, where S is some composition of the particular form $S = \eta^h\theta$ or $S = \eta^h$, and the only difference between $(S(n))_{n=1,2,3,\ldots}$ and $(T(n))_{n=1,2,3,\ldots}$ is that the latter has up to $(F_{p+3} - 2) - (F_{p+2} - 1) = F_{p+1} - 1$ additional leading zeroes.

However, Proposition 4.19 treated compositions of these particular forms and provided the cohortizer. Thus, it suffices to skip the first $N_0 - F_{p+2} + 1$ zeroes of $T(n)$ and apply this same cohortizer to the remaining sequence. □

Example 4.10 (Continuation of Example 4.9)**.** Consider $S = \theta^2\eta\theta\eta\theta$, having $p = 4 + 2 \times 2 = 8$. By Proposition 4.25, the first 77 elements of $S(n)$ on the positive integers are zero, that is, $S(1) = \cdots = S(77) = 0$. By Proposition 4.28, it suffices to skip the first $77 - F_{8+2} + 1 = 23$ elements of $S(n)$, to put the rest of the sequence in the form of Proposition 4.19. Thus, $S(n + 23)$ is a Fibonacci cohort sequence from the first element under cohortizer $F_{(t-8)^+}$, since, by Proposition 4.24, for $n = 1, 2, 3, \ldots$, $S(n + 23) = \theta^2\eta\theta\eta\theta(n + 23) = \eta^4(n) = \theta^p(n + F_{p+1} - 1) = \theta^8(n + F_9 - 1) = \theta^8(n + 33)$. Corollary 4.29 will generalize the latter equalities.

Example 4.11 (Complementary Equations)**.** To generalize Example 4.10, Proposition 4.28 generates pairwise equalities between compositions of Wythoff^{-1} functions over the positive integers by (i) matching p, and (ii) shifting the argument ("inside") by an integer to match N_0. Where this argument remains a nonnegative integer, following Table 13 and generating all complementary equations possible by Proposition 4.28 gives,

$$\begin{aligned}
&\text{For } p = 2,\\
&\qquad \eta(n) = \theta^2(n+1);\\
&\text{For } p = 3,\\
&\qquad \eta\theta(n) = \theta\eta(n+1) = \theta^3(n+2);\\
&\text{For } p = 4,\\
&\qquad \eta^2(n) = \eta\theta^2(n+1) = \theta\eta\theta(n+2) = \theta^2\eta(n+3) + \theta^4(n+4);\\
&\text{For } p = 5,\\
&\qquad \eta^2\theta(n) = \eta\theta\eta(n+1) = \eta\theta^3(n+2) = \theta\eta^2(n+3) = \theta\eta\theta^2(n+4)\\
&\qquad\qquad = \theta^2\eta\theta(n+5) = \theta^3\eta(n+6) = \theta^5(n+7);\\
&\qquad\quad \vdots
\end{aligned}$$

Corollary 4.29 (of Proposition 4.28, "Pure-θ" form of Fibonacci cohort sequence from 1$^{\text{st}}$ cohort)**.** *Let S be a Fibonacci cohort sequence under cohortizer $F_{(t-p)^+}$, $p > 0$ and having $N_0(S)$ initial zeroes. Then, $S(n) = \theta^p(n - N_0(S) + F_{p+3} - 2)$, for $n = 0, 1, 2, \ldots$.*

Proof. By construction, a pure-θ form exists for all p, shown in Table 13 as the rightmost entry in each row $p+1$, that is, the last entry in cohort C_{p+1}. It suffices to show that θ^p has $F_{p+3} - 2$ initial zeroes, the maximum number of zeroes for a composition with degree p, as given in Proposition 4.24. By the algorithm (Proposition 4.25), the number of zeroes of θ^p will equal $\sum_{k=2}^{p+1} F_k = \sum_{k=1}^{p+1} F_k - 1 = F_{p+3} - 2$, as claimed. □

Remark 4.25. Per Remark 4.24, consider that each row of Table 14 corresponds to a succession of left branchings in Figure 7, such that if $\epsilon_{n,k}$ is an entry of Table 14 with $k \geq 1$, then $\epsilon_{n,k+1} = \theta \circ \epsilon_{n,k}$. Row $n = 0$ of Table 14 begins at the root node of Figure 7. For subsequent rows $n \geq 1$ of Table 14, the first entry $\epsilon_{n,1}$ begins with an η and therefore corresponds to a node of Figure 7 that is the right child of an entry in some previous row $m < n$ of Table 14. Thus the remainder of row n in the table follows from $\epsilon_{n,1}$ by a succession of left branchings (See Remark 4.23). With the functions built up in this manner, no two functions $\epsilon_{n,k} \in \{\eta, \theta\}^\star$ of Table 14 can appear at the same node of Figure 7, and, therefore, cannot have the same value of $N_0 + 1$ in the corresponding maximal Fibonacci tree, Figure 8. Corollary 4.26 formalizes this observation using the lazy Fibonacci representation.

For the functions S in Table 14, tabulating the values $N_0(S) + 1$ gives the *2–1-Fibonacci array*, Table 15, which turns out to be an interspersion. Proposition 4.30 considers this array and expresses the bijection between functions in the free monoid $\{\theta, \eta\}^\star$ on $\{\theta, \eta\}$ and the positive integers, giving an explicit formula for entries $\vdash_{n,k}$ of Table 15.

Proposition 4.30 (Constructive bijection between free monoid on $\{\theta, \eta\}$ and $\mathbb{Z}_+$)**.** *Let the first column of Table 14 list all $S \in \{\theta, \eta\}$ that do not include the prefix θ on the outside. Thus for $n = 0, 1, 2, \ldots$, the entry $S_{n,1}$ at position $(n, 1)$ of the table is either I or includes the prefix η on the outside. Moreover, let the entries in the first column of Table 14 be ordered such that $N_0(S_{n,1}) = n$, where Proposition 4.25 guarantees the existence and uniqueness of composition S of θ's and η's satisfying $N_0(S) = n$ for each $n = 0, 1, 2, \ldots$ (Corollary 4.26). Further, let $S_{n,k} = \theta^{k-1} S_{n,1}$ give subsequent columns of Table 14, so that the number of θ's in the prefix of $S_{n,k}$ equals $k - 1$. Finally, let the corresponding entries of Table 15 give the values $\vdash_{n,k} \equiv N_0(S_{n,k}) + 1$ for $n = 0, 1, 2, \ldots$ and $k = 1, 2, 3 \ldots$. Then, $\vdash_{n,k} \equiv N_0(S_{n,k}) + 1 = n + F_{F^{-1}(n)+k+2} - F_{F^{-1}(n)+2}$.*

Proof. Recall Proposition 4.25 and Corollary 4.26.

Case (i): S in the first column of Table 14

Use the algorithm of Proposition 4.25 to calculate the values $N_0(S_{n,1})$. For $S_{n,1}$ in the first column of Table 14, observe that by construction, it is either $S_{0,1} = I$ or it $S_{n,1}$ begins in the prefix η. By Proposition 4.25, therefore, the lazy Fibonacci representation of $N_0(S_{n,1})$ for $n \geq 1$ must terminate in $\cdots 101$ (Corollary 4.26).

Now, in the lazy Fibonacci representation of m, the largest Fibonacci index is $F^{-1}(m) - 1$, thus the representation always includes $F_{F^{-1}(m)-1}$ and never includes $F_{F^{-1}(m)}$ (Remark 6.7). The zero in its penultimate position shows that the representation of $m = N_0(S_{n,1})$ produced by the algorithm for $n \geq 1$ also excludes $F_{F^{-1}(m)-2}$. The first column of Table 15 includes all such values in increasing order, by construction; thus for $n \geq 1$, the $\vdash_{n,1}$ are precisely the numbers of the form $n + F_{F^{-1}(n)+1}$, where $n = m - F_{F^{-1}(m)-1}$. Whereas $N_0(\vdash_{0,1}) = 0$, the formula claimed also gives the top element of the column, which begins $\vdash_{0,1} \equiv N_0(S_{0,1})+1 = N_0(I)+1 = 0+F_{F^{-1}(0)+1} = 1$ and continues to $\vdash_{1,1} \equiv N_0(S_{1,1})+1 = 1 + F_{F^{-1}(1)+1} = 1 + F_2 = 3$, etc. It suffices to note that $\vdash_{n,1} \equiv N_0(S_{n,1}) + 1 = n + F_{F^{-1}(n)+3} - F_{F^{-1}(n)+2} = n + F_{F^{-1}(n)+1}$.

Case (ii): S in column $k \geq 2$ of Table 14

By Proposition 4.24, S has $F_{p(S)+2}$ ones on $\mathbb{Z}_+$. Therefore, $N_0(\theta S_{n,1}) = N_0(S_{n,1}) + F_{p(S)+2}$. Moreover, $S_{n,k} = \theta^{k-1} S_{n,1}$ for $k \geq 1$ by construction, so that

$$\begin{array}{lll} N_0(\theta S_{n,1}) - N_0(S_{n,1}) & & = F_{p(S_{n,1})+2}, \\ N_0(\theta^2 S_{n,1}) - N_0(\theta S_{n,1}) & = F_{p(\theta S_{n,1})+2} & = F_{p(S_{n,1})+3}, \\ & \vdots & \vdots \\ N_0(\theta^{k-1} S_{n,1}) - N_0(\theta^{k-2} S_{n,1}) & = F_{p(\theta^{k-2} S_{n,1})+2} & = F_{p(\theta S_{n,1})+k}. \end{array}$$

The telescoping sum in the left-hand sides collapses when summed to give

$$\begin{aligned} N_0(\theta^{k-1} S_{n,1}) - N_0(S_{n,1}) &= \sum\nolimits_{h=2}^{k} F_{p(S_{n,1})+h} \\ &= \sum\nolimits_{h=1}^{p(S_{n,1})+k} F_h - \sum\nolimits_{h=1}^{p(S_{n,1})+1} \\ &= F_{p(S_{n,1})+k+2} - F_{p(S_{n,1})+3} \\ &= F_{F^{-1}(n)+k+2} - F_{F^{-1}(n)+3}, \end{aligned}$$

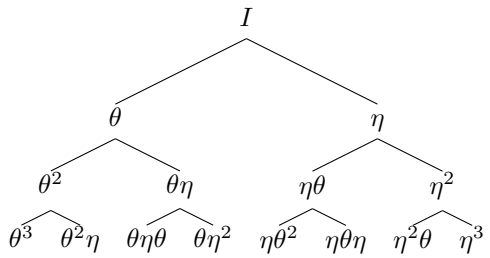

FIGURE 9. "Inner" binary tree of compositions $S \in \{\theta, \eta\}^\star$ in the free monoid on $\{\theta, \eta\}^\star$. As each iteration removes symbols from the incumbent composition from the inside outward, the algorithm of Proposition 4.25 follows this tree *upward* to calculate $N_0(S)$, which provides the bijection $N_0(S)+1$ to Figure 10. Planar graph isomorph of Table 13. Also, for prefix $L = \theta^\star\eta$, inner binary tree of suffix S' of each equivalence class $\{LS' \in \{\theta, \eta\}^\star \setminus \{\theta\}^\star | N_{-1}(LS') = N_{-1}(\eta S')\} \in \{\theta, \eta\}^\star / \theta^\star \circ$. As each iteration accumulates symbols from the outside inward, the algorithm of Corollary 4.37 follows this tree *downward* to calculate $N_{-1}(LS)$, which provides the bijection $N_{-1}(LS) - 1$ to Figure 3. Planar graph isomorph of (suffixes in) Table 16 with $C_0 = (\theta^\star)$ omitted. Blade dual of Figure 7.

which combined with the formula for the first column yields the desired result,

$$\begin{aligned} N_0(S_{n,k}) + 1 &= F_{F^{-1}(n)+k+2} - F_{F^{-1}(n)+3} + N_0(S_{n,1}) \\ &= F_{F^{-1}(n)+k+2} - F_{F^{-1}(n)+3} + n + F_{F^{-1}(n)+1} \\ &= n + F_{F^{-1}(n)+k+2} - F_{F^{-1}(n)+2}. \end{aligned}$$

□

Remark 4.26. Proposition 4.30 derives a formula for $\vdash_{n,k}$ using the "free-monoid approach," that is, mapping the tabulation Table 15 of $\vdash_{n,k}$ to that of compositions in the free monoid $\{\theta, \eta\}^\star$, Table 14.

By contrast, Lemma 8.1 will derive the same formula using the "tree branch approach," that is, by defining the first column $\vdash_1$ of $\vdash_{n,k}$ $(n = 1, 2, 3, \ldots)$ as the sequence of right children of $\mathbb{Z}_+$ in the maximal Fibonacci tree (Figure 8), and rows of $\vdash_{n,k}$ as sequences of all-left branchings in the tree. Equivalent descriptions of $\vdash$ also include the "tree clade approach" of Section 8.6.3 and the tableau manipulation approach of Section 8.2.2.

For completeness, Figures 9 and 10 show the "inner" versions of Figures 7, respectively, 8. Once again, the self-inverse tree blade permutation, 059893, transforms between Figures 8 and 10, the latter being the "maximal successor tree." Lemma 4.32 gives a formula for its left and right children in terms of their parent node, more elusive than the result (Remark 4.11) for the minimal successor tree.

Corollary 4.31 (of Proposition 4.21)**.** *Let the non-negative-integer-valued function $T(n)$ be non-decreasing on the non-negative integers, and let $N_0(T)$ give the number of its (initial) zero values on the positive integers. Let $T'(n) = T(\lfloor n/\mu \rfloor)$ for some irrational $\mu > 1$. Then $N_0(T') = \lfloor (N_0(T) + 1)\mu \rfloor$.*

Proof. By definition, $T(0), \ldots, T(N_0(T)) = 0$ and $T(N_0(T) + 1) > 0$. By Proposition 4.21, $N_0(T') = \sum_{m=0}^{N_0(T)} (\lfloor (m+1)\mu \rfloor - \lfloor m\mu \rfloor) = \lfloor (N_0(T) + 1)\mu \rfloor$, as claimed. □

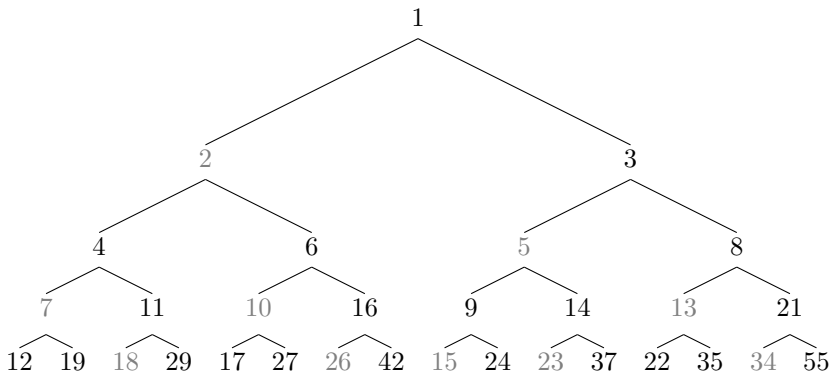

FIGURE 10. *Maximal successor tree* (232560). Corresponds bijectively to Figure 2 via $-S(-1)$ for compositions S shown therein. Corresponds bijectively to Figure 9 via $N_0(T)+1$ for compositions T shown therein. Blade dual of Figure 8 and 059893 permutes the two sequences. Cohort dual of Figure 3. Planar graph isomorph of the tableax in Table 6. 232559 gives positions $\bar{\mathbf{P}}$ of the positive integers in the tree.

Lemma 4.32. *In the Maximal successor tree, Figure 10, a node n has left and right children $\kappa(n)+1 = -\kappa(-n)$ and $\lambda(n)+1 = -\lambda(-n)$, respectively (Figure 15(ii)).*

Proof. Consider the bijection between composition T in Figure 9 and value $N_0(T)+1$ at the corresponding node in Figure 10. The branching rule claimed for Figure 10 now follows from a counting argument similar to that in Proposition 4.24.

In Figure 10, consider that node $N_0(T)+1$ has left, respectively, right children $N_0(T\theta)+1$ and $N_0(T\eta)+1$, for some T in Figure 9.

By Corollary 4.31, $N_0(T\theta) = \kappa(N_0(T)+1)$ and $N_0(T\eta) = \lambda(N_0(T)+1)$. In Figure 10, therefore, a node $n = N_0(T)+1$ — corresponding to node T in Figure 9 — has left, respectively, right children $\kappa(N_0(T)+1)+1 = \kappa(n)+1$ and $\lambda(N_0(T)+1)+1 = \lambda(n)+1$ as claimed. □

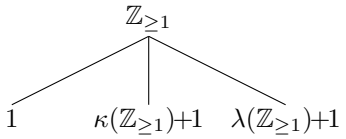

FIGURE 11. A partition of the positive integers into three non-intersecting subsequences: $\mathbb{Z}_{\geq 1} = \{1\} \cup [\kappa(\mathbb{Z}_{\geq 1})+1] \cup [\lambda(\mathbb{Z}_{\geq 1})+1]$

Proposition 4.33 (Figures 8 and 10 arrange the positive integers)**.** *Per Lem. 4.32, node n in Figure 10 has left child $\kappa(n)+1$ and right child of n $\lambda(n)+1$. Each level of Figure 10 merely rearranges the corresponding level of Figure 8. Consequently, these binary trees both arrange $\mathbb{Z}_{\geq 1}$.*

Proof. Consider the partition of the positive integers shown in Figure 11. The first two levels of Figure 10 (comprising its first three nodes) contain the first element of

each subsequence in the partition. That is, 1 at the root node, and $(\kappa(1), \lambda(1)) + 1 = (\min \kappa(\mathbb{Z}_{\geq 1}), \min \lambda(\mathbb{Z}_{\geq 1})) + 1 = (2, 3)$ at its (left, right) children. Note that considering the second level alone, the nodes contain the first elements of two subsequences that partition $\mathbb{Z}_{\geq 2}$.

Now consider the third level, $(\kappa(\kappa(1)+1), \lambda(\kappa(1)+1), \kappa(\lambda(1)+1), \lambda(\lambda(1)+1))+1 = (4, 6, 5, 8)$ of Figure 10, and rearrange this level to give $= (4, 5, 6, 8) = (\kappa(\kappa(1) + 1), \kappa(\lambda(1)+1), \lambda(\kappa(1)+1), \lambda(\lambda(1)+1))+1 = (\min \kappa(\kappa(\mathbb{Z}_{\geq 1})+1), \min \kappa(\lambda(\mathbb{Z}_{\geq 1})+1), \min \lambda(\kappa(\mathbb{Z}_{\geq 1}) + 1), \min \lambda(\lambda(\mathbb{Z}_{\geq 1}) + 1)) + 1$.

Collecting the nodes of levels 2 and 3 into two sets $\{\kappa(1), \kappa(\kappa(1) + 1), \kappa(\lambda(1) + 1)\} + 1 = \{\kappa(1), \min \kappa(\kappa(\mathbb{Z}_{\geq 1}) + 1), \min \kappa(\lambda(\mathbb{Z}_{\geq 1}) + 1)\} + 1$ and $\{\lambda(1), \lambda(\kappa(1) + 1), \lambda(\lambda(1) + 1)\} + 1 = \{\lambda(1), \min \lambda(\kappa(\mathbb{Z}_{\geq 1}) + 1), \min \lambda(\lambda(\mathbb{Z}_{\geq 1}) + 1)\} + 1$ shows that the partition of $\mathbb{Z}_{\geq 1}$ in Figure 11 was substituted for "1" in each node of the second level and the first element then taken, to form the third level.

The trees repeat this process *ad infinitum*, at each level effectively substituting the "1" at the inside of each expression with the partition of $\mathbb{Z}_{\geq 1}$ shown in Figure 11, and taking its smallest element to produce the next level. Thus applying the branching rule at each successive level descending from the root node 1 generates a tree that arranges the positive integers. □

Remark 4.27. Note from the partitions shown in Figure 11 that, without loss of generality, the spectrum sequences $\kappa(n) = \lfloor n\phi \rfloor$ and $\lambda(n) = \lfloor n\phi^2 \rfloor$ in Proposition 4.33 can be substituted by any pair of complementary spectrum sequences $\lfloor n\mu \rfloor$ and $\lambda(n) = \lfloor n\nu \rfloor$ with irrational slopes μ and ν satisfying $1 < \mu < 2 < \nu \equiv \frac{1}{1-1/\mu}$.

Corollary 9.2 further generalizes this observation.

Corollary 4.34 (of Corollary 4.22)**.** *Let function $T(n)$ be the negative-integer-valued on the negative integers and the sequence $(T(n))_{n=-1,-2,-3,\ldots}$ non-increasing, and let $N_{-1}(T)$ give the number of its (initial) minus-one values. Let $T'(n) = T(\lfloor n/\mu \rfloor)$ for some irrational $\mu > 1$. Then $N_{-1}(T') = \lfloor N_{-1}(T)\mu \rfloor$.*

Proof. By definition, $T(-1), \ldots, T(N_{-1}(T)) = -1$ and $T(N_{-1}(T) + 1) < -1$. By Corollary 4.22, $N_{-1}(T') = \sum_{m=-1}^{-N_{-1}(T)} (\lfloor -m\mu \rfloor - \lfloor -(m+1)\mu \rfloor) = \lfloor N_{-1}(T)\mu \rfloor$, as claimed. □

Proposition 4.35. *Let $S \in \{\lfloor n\mu \rfloor, \lfloor n\nu \rfloor\}^\star$ be a member of the free monoid on $\{\lfloor n\mu \rfloor, \lfloor n\nu \rfloor\}$ under composition and $T = \{\lfloor n/\mu \rfloor, \lfloor n/\nu \rfloor\}^\star$ a member of the free monoid on $\{\lfloor n/\mu \rfloor, \lfloor n/\nu \rfloor\}$ under composition. Let $\overleftrightarrow{S}$ be the reverse of S, that is, the individual applications of $\lfloor n\mu \rfloor$ and $\lfloor n\nu \rfloor$ of $S(n)$ composed in reverse order. Let $\overleftrightarrow{T}$ be the reverse of T, that is, the individual applications of $\lfloor n/\mu \rfloor$ and $\lfloor n/\nu \rfloor$ of $T(n)$ composed in reverse order. Define the "Beatty invert" operation* BeattyInvert *mapping compositions on a Beatty pair to compositions on the corresponding Beatty^{-1} pair in the obvious way:*

$$\begin{array}{rccc} \mathsf{BeattyInvert}: & \{\lfloor n\mu \rfloor, \lfloor n\nu \rfloor\}^\star & \to & \{\lfloor n/\mu \rfloor, \lfloor n/\nu \rfloor\}^\star \\ & (\lfloor n\mu \rfloor, \lfloor n\nu \rfloor) & \mapsto & (\lfloor n/\mu \rfloor, \lfloor n/\nu \rfloor) \end{array}$$

Then,

$$-S(-1) = N_0(\mathsf{BeattyInvert}(\overleftrightarrow{S})) + 1, \tag{35}$$

Or equivalently,

$$N_0(T) + 1 = -\mathsf{BeattyInvert}^{-1}(\overleftrightarrow{T})(-1), \tag{36}$$

Further, letting $LT = \lfloor T/\nu \rfloor$,

$$S(\lfloor \nu \rfloor) = N_{-1}(L\,\mathsf{BeattyInvert}(\overleftrightarrow{S})), \tag{37}$$

Or equivalently,

$$N_{-1}(LT) = \mathsf{BeattyInvert}^{-1}(\overleftrightarrow{T})(\lfloor \nu \rfloor), \tag{38}$$

Note that for irrational $1 < \mu < 2$*, the latter identities also hold for*

$$LT = \left\lfloor \ddots \left\lfloor \lfloor T/\nu \rfloor / \mu \right\rfloor \ddots / \mu \right\rfloor.$$

Proof. To show (35) by induction, first set S to the identity $S(n) = n$ so that $-S(-1) = 1$. Now $\mathsf{BeattyInvert}(\overleftrightarrow{S})(n) = n$, thus $N_0(\mathsf{BeattyInvert}(\overleftrightarrow{S})) + 1 = 0 + 1$, as desired. To be a bit more illustrative, consider $S(n) = \lfloor n\mu \rfloor$ so that $-S(-1) = \lfloor \mu \rfloor + 1$. Now $\mathsf{BeattyInvert}(\overleftrightarrow{S})(n) = \lfloor n/\mu \rfloor$, thus by Proposition 4.21, $N_0(\mathsf{BeattyInvert}(\overleftrightarrow{S})) + 1 = \lfloor \mu \rfloor + 1$, as desired. Both $\mu > 1$ and $\nu > 1$, so that the claim also holds for $S(n) = \lfloor n\nu \rfloor$.

Now suppose that for any $S \in \{\lfloor n\mu \rfloor, \lfloor n\nu \rfloor\}^\star$, composition of $\lfloor n\mu \rfloor$s and $\lfloor n\nu \rfloor$s, that $-S(-1) = N_0(\mathsf{BeattyInvert}(\overleftrightarrow{S}))+1$. Letting $T = \mathsf{BeattyInvert}(\overleftrightarrow{S})$ write $-S(-1) = N_0(T) + 1$. Now consider $S'(n) = \lfloor S(n)\mu \rfloor$. By Corollary 4.31 and the induction hypothesis, $N_0(\mathsf{BeattyInvert}(\overleftrightarrow{S'})) + 1 = \lfloor (N_0(T) + 1)\mu \rfloor + 1 = \lfloor -S(-1)\mu \rfloor + 1 = -S'(-1)$, thus completing the induction from S to S'. Both $\mu > 1$ and $\nu > 1$, so that induction from S to $\lfloor S\nu \rfloor$ also holds.

To show (37) by induction, first set S to the identity $S(n) = n$ so that $S(\lfloor \nu \rfloor) = \lfloor \nu \rfloor$. Now $\mathsf{BeattyInvert}(\overleftrightarrow{S})(n) = n$, thus $N_{-1}(L\,\mathsf{BeattyInvert}(\overleftrightarrow{S})) = N_{-1}(\lfloor n/\nu \rfloor) = \lfloor \nu \rfloor$, as desired, where the latter equality is due to Corollary 4.22.

To be a bit more illustrative, consider $S(n) = \lfloor n\mu \rfloor$ so that $S(\lfloor \nu \rfloor) = \lfloor \lfloor \nu \rfloor \mu \rfloor$. Now $\mathsf{BeattyInvert}(\overleftrightarrow{S})(n) = \lfloor n/\mu \rfloor$, thus by Corollary 4.22, $N_{-1}(L\,\mathsf{BeattyInvert}(\overleftrightarrow{S}))$ $= N_{-1}(\lfloor \lfloor n/\mu \rfloor / \nu \rfloor) = \sum_{m=-1}^{-\lfloor \nu \rfloor} (\lfloor -m\mu \rfloor - \lfloor -(m+1)\mu \rfloor) = \lfloor \lfloor \nu \rfloor \mu \rfloor$, as desired. Both $\mu > 1$ and $\nu > 1$, so that the claim also holds for $S(n) = \lfloor n\nu \rfloor$.

Now suppose that for any $S \in \{\lfloor n\mu \rfloor, \lfloor n\nu \rfloor\}^\star$, composition of $\lfloor n\mu \rfloor$s and $\lfloor n\nu \rfloor$s, that $S(\lfloor \nu \rfloor) = N_{-1}(L\,\mathsf{BeattyInvert}(\overleftrightarrow{S}))$. Letting $T = \mathsf{BeattyInvert}(\overleftrightarrow{S})$ write $S(\lfloor \nu \rfloor) = N_{-1}(LT)$. Now consider $S'(n) = \lfloor S(n)\mu \rfloor$ and $T'(n) = T(\lfloor n/\mu \rfloor)$. By Corollary 4.34 and the induction hypothesis, $N_{-1}(L\,\mathsf{BeattyInvert}(\overleftrightarrow{S'})) = N_{-1}(LT') = \lfloor N_{-1}(LT)\mu \rfloor$ $= \lfloor S(\lfloor \nu \rfloor)\mu \rfloor = S'(\lfloor \nu \rfloor)$, thus completing the induction from S to S'. Both $\mu > 1$ and $\nu > 1$, so that induction from S to $\lfloor S\nu \rfloor$ also holds.

For the final claim, note with reference to Corollary 4.22 that $N_{-1}(\lfloor T/\mu \rfloor) = N_{-1}(T) + \cdots + N_{-\lfloor \mu \rfloor}(T)$.

Thus, if $1 < \mu < 2$, then $N_{-1}(\lfloor T/\nu \rfloor) = N_{-1}\left(\left\lfloor \ddots \left\lfloor \lfloor T/\nu \rfloor / \mu \right\rfloor \ddots / \mu \right\rfloor\right)$. □

Proposition 4.36 (Runs in the sequence of values at negative integers, for a composition S of θ and η)**.** *Consider a composition* $S \in \{\theta, \eta\}^\star$ *of* θ*'s and* η*'s in any order. Evaluate this composition along the sequence of negative integers* $-1, -2, -3, \ldots$ *to obtain the sequence* $S(-1), S(-2), S(-3), \ldots$*. Let* $p = q + 2h$*, where* q *counts the number of applications of* θ*, and* h *the number of applications of* η*, respectively, made by* S*.*

Starting from the outside of $S(n)$ *(relative to an integer argument* n*), ignore any* θ*'s applied last (since* -1 *is a fixed point of* θ*,* $\theta(-1) = \lfloor -1/\phi \rfloor = -1$*, and, further,*

-1 is not an attractor for θ, since the neighboring value -2 is also a fixed point: $\theta(-2) = \lfloor -2/\phi \rfloor = -2$). Then, beginning with the last η applied, let h count this and prior applications of η's, and let $q_\star$ count the number of applications of θ's made prior to the last application of η. Refer to $p_\star = q_\star + 2h$ as the reduced degree *of S.*

Let $K_{-1} = \kappa(\mathbb{Z}_-)$ and $\Lambda_{-1} = \lambda(\mathbb{Z}_-)$ denote the complete sequences of κ, respectively, λ applied to the negative integers $-1, -2, -3, \ldots$. Then,

(a): *For $n = 1, 2, 3, \ldots$, $S(-n)$ begins with a leading run of $N_{-1}(S)$ minus-ones, where $F_{p_\star} < N_{-1}(S) \leq F_{p_\star+1}$, followed by a run of length F_{p+2}, respectively, F_{p+1} of each number of the form $K_{-1} = -K - 1$, respectively, $\Lambda_{-1} = -\Lambda - 1$.*

(b): *Further, let $L \equiv \theta^\star\eta$ so that $S = LS' = \theta^\star\eta S'$. Then $N_{-1}(L\theta S') = N_{-1}(S) + F_{p_\star-1}$ and $N_{-1}(L\eta S') = N_{-1}(S) + F_{p_\star+2}$*

Proof of **(a):** Similar to the proof of Proposition 4.24, first consider the length of runs in $\theta(-n)$ and $\eta(-n)$, $n = 1, 2, 3, \ldots$. Firstly, Θ_{-1} comprises a single minus-one, followed by a run of length two, respectively, one, of each number of the form $K_{-1} = -K - 1$, respectively, $\Lambda_{-1} = -\Lambda - 1$. Secondly, H_{-1} comprises a leading run of two minus-ones, followed by runs of length three, respectively, two of each of each number of the form $K_{-1} = -K - 1$, respectively, $\Lambda_{-1} = -\Lambda - 1$.

Thereafter, continue by induction to cases θS and ηS as in Proposition 4.24, using identities from Lemma 4.23 to complete the desired result. □

Proof of **(b):** Firstly, since $L = \theta^\star\eta$ maps -1 and -2 to -1, we have $N_{-1}(S) = N_{-1}(LS') = N_{-1}(S') + N_{-2}(S')$.

Case 1. $L\theta S'$: Further, since θ maps -2, and -3 to -2, $N_{-1}(L\theta S') = N_{-1}(\theta S') + N_{-2}(\theta S') = N_{-1}(S') + N_{-2}(S') + N_{-3}(S')$. Thus, $N_{-1}(L\theta S') - N_{-1}(S) = N_{-3}(S')$. Since $-3 \in \Lambda_{-1}$, by Part (a), $N_{-3}(S') = F_{p(S')+1}$. Now, observe that $p(S') = p_\star(S) - 2$. Thus, $N_{-1}(L\theta S') = N_{-1}(S) + N_{-3}(S') = N_{-1}(S) + F_{p(S')+1} = N_{-1}(S) + F_{p_\star-2+1} = N_{-1}(S) + F_{p_\star-1}$, as claimed.

Case 2. $L\eta S'$: Further, since η maps -3, -4, and -5 to -2, $N_{-1}(L\eta S') = N_{-1}(\eta S') + N_{-2}(\eta S') = N_{-1}(S') + N_{-2}(S') + N_{-3}(S') + N_{-4}(S') + N_{-5}(S')$. Thus, $N_{-1}(L\eta S') - N_{-1}(S) = N_{-3}(S') + N_{-4}(S') + N_{-5}(S')$. Since $-3 \in \Lambda_{-1}$ and $-4, -5 \in K_{-1}$, by Part (a), $N_{-3}(S') + N_{-4}(S') + N_{-5}(S') = F_{p(S')+1} + 2F_{p(S')+2} = F_{p(S')+4}$. Using $p(S') = p_\star(S) - 2$ gives $N_{-1}(L\eta S') = N_{-1}(S) + F_{p(S')+4} = N_{-1}(S) + F_{p_\star-2+4} = N_{-1}(S) + F_{p_\star+2}$, as claimed. □

Forming equivalence classes analogously to Proposition 4.7(b), Prop. 4.36(b) allows entire rows of Table 14 to be condensed to N_{-1}-equivalence classes $S/\theta^\star\circ \in \{\theta, \eta\}^\star/\theta^\star\circ$ and placed into a 1–2-Fibonacci outer cohort tableau (Table 16). The 0^{th} cohort $C_0 = (\theta^\star)$ comprises the 0^{th} equivalence class $\theta^\star$, corresponding to the zeroth (top) row of Table 14.

Likewise the 1^{st}, 2^{nd}, and 3^{rd} cohorts, respectively, $C_1 = (L)$, $C_2 = (L\theta)$, $C_3 = (L\theta^2, L\eta)$ comprise the equivalence classes $\theta^\star\eta$, $\theta^\star\eta\theta$, $\theta^\star\eta\theta^2$, and $\theta^\star\eta^2$, represented in rows 1, 2, 4, and 3, respectively of Table 14.

Take $\theta^0 = I$ as the standard representative of the 0^{th} equivalence class. Then beginning with the 1^{st} class, replace L in the tableau by η to obtain the standard representatives having $p = p_\star$ found in the first column of Table 14 (reading each cohort from right to left): I, η, $\eta\theta$, η^2, $\eta\theta^2, \ldots$. For subsequent columns $2, 3, 4, \ldots, k, \ldots$ of the table, replace L by $\theta\eta$, $\theta^2\eta$, $\theta^3\eta, \ldots$ $\theta^{k-1}\eta, \ldots$ to obtain class

C_0	$\theta^\star$							
C_1	L							
C_2	$L\theta$							
C_3	$L\theta^2$	$L\eta$						
C_4	$L\theta^3$	$L\theta\eta$	$L\eta\theta$					
C_5	$L\theta^4$	$L\theta^2\eta$	$L\theta\eta\theta$	$L\eta\theta^2$	$L\eta^2$			
C_6	$L\theta^5$	$L\theta^3\eta$	$L\theta^2\eta\theta$	$L\theta\eta\theta^2$	$L\theta\eta^2$	$L\eta\theta^3$	$L\eta\theta\eta$	$L\eta^2\theta$
$\vdots$	$\vdots$	$\vdots$	$\vdots$	$\vdots$	$\vdots$	$\vdots$	$\vdots$	$\vdots$

TABLE 16. 1–2-Fibonacci (outer) cohort tableau of equivalence classes $S/\theta^\star\circ \in \{\theta,\eta\}^\star/\theta^\star\circ$, (by left infix) from 0^{th} cohort, ordered by strictly increasing $N_{-1}(S)-1 = 0, 1, 2, 3\ldots$, which provides a bijection to Table 6(i), and gathered into cohorts $C_{p_\star-1}$ by reduced degree $p_\star$=130233 $= 0, 2, 3, 4, 4, \ldots$. Counting $L = \theta^\star\eta$ as one symbol, 135817$_{n+1}$ gives the number of symbols in the n^{th} element. With $C_0 = (\theta^\star)$ and prefix L omitted, planar graph isomorph of Figure 7. Isomorph of Table 32(i).

representatives having $p = p_\star + 1$, $p_\star + 2$, $p_\star + 3, \ldots$, $p_\star + k - 1$, respectively, (also taking θ^{k-1} to represent the 0^{th} class).

Thus, the tableau enumerates $N_{-1}(S)$-classes, that is, equivalence classes of compositions S having the same run length $N_{-1}(S)$ of -1 on $\mathbb{Z}_-$. Table 16 shows the equivalence classes sorted by increasing values of $N_{-1}(S)$, beginning with the 0^{th} equivalence class $\theta^\star$, for which $N_{-1}(\theta^\star) = 1$, the 1^{st} equivalence class $L = \theta^\star\eta$, for which $N_{-1}(L) = N_{-1}(\theta^\star\eta) = 2$, and subsequently, $N_{-1}(L\theta) = 3$, $N_{-1}(L\theta^2) = 4$, $N_{-1}(L\eta) = 5$, $N_{-1}(L\theta^3) = 6$, $N_{-1}(L\theta\eta) = 7$, $N_{-1}(L\eta\theta) = 8$, and so forth.

Observe that the tableau gathers the classes into cohorts according to increasing value of the reduced degree $p_\star$ = 130233 $= 0, 2, 3, 4, 4, \ldots$. The tableau displays one cohort per level. While the 0^{th} cohort has length 1 by convention, for $p_\star \geq 2$, cohort $C_{p_\star-1}$ appearing on level $p_\star-1$ of the tableau has length $F_{p_\star-1}$. The value of $N_{-1}(S)$ strictly increases throughout the tableau, with range $\{F_{p_\star} + 1, \ldots, F_{p_\star+1}\}$ over cohort $C_{p_\star-1}$, providing a bijection to Table 6(i). In particular, this illustrates Proposition 4.36(a), that $F_{p_\star} < N_{-1}(S) \leq F_{p_\star+1}$.

Table 16 illustrates properties that the remainder of Section 4 will reference, but whose formal proof is deferred to Section 5. Proposition 4.36 described the structure shown in Table 16. Now, the algorithm of Corollary 4.37 will exploit this structure.

Corollary 4.37 (of Proposition 4.36(b): Outside–inward algorithm for N_{-1} of $S \in \{\theta,\eta\}^\star$)**.** *For compositions S of θ's and η's,* the following algorithm gives $N_{-1}(S)$*:*

Initialization: *If $S = \theta^\star$, then $N_{-1}(S) \leftarrow 1$ and terminate.*

Otherwise starting from the outside and moving inward, ignore any θ's outside the final application of η (since subsequent applications of θ do not change the number of -1s in the codomain of S), and beginning with the outermost (last) application of η, let h count this and prior applications of

η's and let and $q_\star$ count prior applications of θ's. Let $p_\star = q_\star + 2h$ be the reduced degree, as in Proposition 4.36.

If $S = \eta$, then $N_{-1}(S) \leftarrow 2$ and terminate.

Otherwise initialize t to $p_\star - 2$ and initialize $N_{-1}(S)$ to 2, accounting for the final application of $\eta = 2$.

Main Step: *Then, starting with the next function inside the initial $\theta^\star\eta$ and until the innermost function is applied, iterate as follows:*

$$t \leftarrow\!\!- \left\{ \begin{array}{ll} t-1, & \text{if } \theta \text{ is applied;} \\ t-2, & \text{if } \eta \text{ is applied;} \end{array} \right.$$

and

$$S_1 \leftarrow S_1 + \left\{ \begin{array}{ll} F_{t+1}, & \text{if } \theta \text{ is applied;} \\ F_{t+4}, & \text{if } \eta \text{ is applied;} \end{array} \right.$$

Proposition 4.38 (Radix algorithm for N_{-1} of classes $S/\theta^\star\circ \in \{\theta,\eta\}^\star/\theta^\star\circ$)**.** *Consider S, a composition of θ's and η's. From the inside outward, write a 0 for each θ applied and 10 for each η applied. Treat the resulting word as Zeckendorf binary by applying the bits, as coefficients, in a basis of Fibonacci numbers $(F_2, F_3, F_4, \ldots)$ to obtain $N_{-1}(S) - 1$, where $N_{-1}(S)$ is the number of -1's of S on $\mathbb{Z}_-$.*

Example 4.12 (of Corollary 4.37)**.** Consider $S = \theta^\star\eta\theta\eta\theta$. Then $p_\star = 6$ and successive steps of the algorithm give $(t, N_{-1}(S)) = (4,2), (3, 2+F_4), (1, 2+F_4+F_5), (0, 2+F_4+F_5+F_1) = (0, 11)$.

Example 4.13 (of Proposition 4.38)**.** Encode $S = L\theta\eta\theta = \theta^\star\eta\theta\eta\theta$ as $0100100\ldots0 = 01001$, where order was reversed. Evaluate the latter to $F_3+F_6 = 2+8 = 10$. Thus, $N_{-1}(\theta^\star\eta\theta\eta\theta) - 1 = 10$, so that $S(-1) = \cdots = S(-11) = -1$ and $S(-12) = -2$.

Corollary 4.39 (Bijection between equivalence classes on free monoid of inverse Wythoff compositions and positive integers)**.** *The map*

$$\begin{array}{rcl} \{\theta,\eta\}^\star/\theta^\star\circ & \to & \mathbb{Z}_+ \\ S/\theta^\star\circ & \mapsto & N_{-1}(S)+1 \end{array}$$

is a bijection.

Proof. The algorithm of Proposition 4.38 gives the value of $N_{-1}(S)$ for functions S in the free monoid $\{\theta,\eta\}^\star$ under composition. Moreover, the algorithm constructs the value $N_{-1}(S)-1$ via lazy Fibonacci representation, since the encoding $\{\theta,\eta\} \mapsto \{0, 10\}$ ensures that it does not include any two consecutive Fibonacci numbers. Further, zeroes at the "most significant" end of the word do not affect the evaluation of $N_{-1}(S)$. Whereas the lazy expansion of $N_{-1}(S)-1$ is distinct up to final zeroes, corresponding to outer θs of S, two representatives of the same equivalence class have the same value of $N_{-1}(S)$.

With reference to Table 14, the algorithm produces a distinct value of $N_{-1}(S)$ for each row and the same value for all entries in the same row. That is, compositions $S, R \in \{\theta,\eta\}^\star$ representing two distinct equivalence classes $S/\theta^\star\circ, R/\theta^\star\circ \in \{\theta,\eta\}^\star/\theta^\star\circ$, respectively, have $N_{-1}(S) \neq N_{-1}(R)$. Thus, the algorithm produces a distinct lazy Fibonacci representation for each distinct class of compositions in $\{\theta,\eta\}^\star$. It follows from the uniqueness of the lazy Fibonacci representation that each distinct $S/\theta^\star\circ \in \{\theta,\eta\}^\star/\theta^\star\circ$ has a distinct value of $N_{-1}(S)$, thus providing the bijection $\{\theta,\eta\}^\star/\theta^\star\circ \sim \mathbb{Z}_+$. □

Remark 4.28. Proposition 4.38 constructs the lazy Fibonacci representation of $N_{-1}(S) - 1$, thus adding F_1 to this representation gives the minimal Fibonacci expansion (Definition 6.1) of $N_0(S)$ (Analogously to Remark 4.22 about $N_0(S)$).

Remark 4.29. To recap, the value of $N_0(S) + 1$ for a composition S in Figure 7 appears at the corresponding node in Figure 8. Hence, the map between the free monoid $\{\theta, \eta\}^\star$ and the positive integers is:

$$\begin{array}{rccc} \text{Proposition 4.30}: & \{\theta,\eta\}^\star & \to & \mathbb{Z}_+ \\ & S & \mapsto & N_0(S)+1 \end{array}$$

Corollary 4.39 also provided a map between equivalence classes and the positive integers:

$$\begin{array}{rccc} \text{Corollary 4.39}: & \{\theta,\eta\}^\star/\theta^\star\circ & \to & \mathbb{Z}_+ \\ & S/\theta^\star\circ & \mapsto & N_{-1}(S) \end{array}$$

Each column of Table 14 comprises a set of related functions, one from each equivalence class of $\{\theta, \eta\}^\star$. Naturally, the equivalence relation induces an isomorphism between any column of Table 14 and the entire table. Thus, each column can be placed in a 2–1-Fibonacci cohort tableau, a fixed-L version of the tableau for equivalence classes, Table 16. Consequently, the second map provides a bijection between any column of Table 14 and the positive integers, whereas the second map provides a bijection between the entirety of Table 14 and the positive integers.

Moreover, the composition of the two maps induces an isomorphism between any column of Table 15 and the entire table ($\mathbb{Z}_+$).Although each column contains values $N_0(S) + 1$ for a only subset of $\{\theta, \eta\}^\star$, the subset comprises a complete set of class representatives of the classes $\{\theta, \eta\}^\star/\theta^\star\circ$. In turn, the values $N_{-1}(S)$ for this subset fill the entire array. For example, take the third column of Table 15, $(4, 11, 18, 29, 30, \ldots) \overset{N_0(S)+1}{\longleftarrow} (\theta^2, \theta^2\eta, \theta^2\eta\theta, \theta^2\eta^2, \theta^2\eta\theta^2 \ldots) \overset{\theta^\star\circ}{\sim} (\theta^\star, L, L\theta, L\eta, L\theta^2 \ldots) \overset{N_{-1}(S)}{\longmapsto} (1, 2, 3, \mathbf{5}, \mathbf{4}, \ldots)$, thus going from entries in a column to (a permutation of) the sequence of positive integers $1, 2, 3, \ldots$. Observe that the latter sequence does *not* follow the respective row indices n (plus one) of the $\vdash_{n,k}$, rather it follows the sequence of positive integers with each cohort reversed (e.g., Table 6(i) with each cohort read from right to left). An order-preserving variant of this correspondence appears in Corollaries 8.17 and 8.18, respectively, as a clade–tree order isomorphism for the maximal successor tree and as a column–array order isomorphism intrinsic to $\dashv$ as well as $\vdash$.

Similarly, since rows of Table 15 are sequences of left branchings in the maximal Fibonacci tree, the value $p - p_\star$ for corresponding entries in Table 14 provides a bijection between any row and the entire table ($\mathbb{Z}_+$), thus going from entries in a row to their respective column indices (minus one) and inducing a bijection between each branch and the entire tree, Figure 8. Remark 4.18 discussed an analogous column–array and row–array isomorphisms for the cohort-dual array, Table 12.

To summarize the observations about Fibonacci cohort sequences S under cohortizer $F_{(t-p)^+}$ with rate p positive, such sequences are Fibonacci cohort from the 1st cohort and have two parameters: The parameter p specifies how slowly the sequence grows and parameter N_0 specifies the number of initial zeroes. The above discussion examined two canonical forms: The Wythoff^{-1}-composition form is homogeneous, writing S as a composition of θ and η, where Proposition 4.24 ordered the compositions by increasing values of N_0, as $I, \theta, \eta, \theta^2, \eta\theta, \theta\eta, \theta^3, \eta^2, \ldots$

and set them into a cohort tableau (Table 13), while Corollary 4.29 writes $S(n)$ in the pure-θ form $\theta^p(n - N_0(S) + F_{p+3} - 2)$.

In closing Sections 4.1.5 and 4.1.6, note that the main results of these sections can also be approached by a more abstract treatment. Section 5 will do this by treating the free monoids $\{\kappa, \lambda\}^\star$ and $\{\theta, \eta\}^\star$ using the "cohort calculus" on symbols:

- (Proposition 5.2): A bracket $\langle \circ\kappa, \circ\lambda \rangle$ cohortizes the free monoid $\{\kappa, \lambda\}^\star$ into a 1–2-Fibonacci inner cohort sequence (Definition 5.1). This means that the bracket produces a total order, generating all elements $S \in \{\kappa, \lambda\}^\star$ sequentially, in particular, with the value $S(2)$ increasing by 1 between successive elements S in the sequence, and that moreover, the bracket forms the cohorts (Table 10), with degree $p = t-1$ for all elements in cohort C_t, and p increasing by 1 between successive cohorts.
- (Corollary 5.3): A bracket $\langle \circ\kappa M, \circ\lambda M \rangle$, cohortizes the equivalence classes $S/\!\circ\kappa^\star$ of the free monoid $\{\kappa, \lambda\}^\star$ into a 1–2-Fibonacci inner cohort sequence (Definition 5.1). This means that the bracket produces a total order, generating all equivalence classes $S'M = S/\!\circ\kappa^\star \in \{\kappa, \lambda\}^\star/\!\circ\kappa^\star$ sequentially, in particular, with the value $S'M(1)$ increasing by 1 between successive classes $S'M$ in the sequence, and that moreover, the bracket forms the cohorts (Table 11), with reduced degree $p_\star = t + 1$ for all classes in cohort C_t, and $p_\star$ increasing by 1 between successive cohorts.
- (Proposition 5.4): A bracket $\langle \eta\circ, \theta\circ \rangle$ cohortizes the free monoid $\{\theta, \eta\}^\star$ into a 2–1-Fibonacci outer cohort sequence (Definition 5.1). This means that the bracket produces a total order, generating all elements $S \in \{\theta, \eta\}^\star$ sequentially, in particular, with the value $N_0(S)$ increasing by 1 between successive elements S in the sequence, and that moreover, the bracket forms the cohorts (Table 13), with degree $p = t-1$ for all elements in cohort C_t, and p increasing by 1 between successive cohorts.
- (Corollary 5.5): A bracket $\langle L\theta\circ, L\eta\circ \rangle$, cohortizes the equivalence classes $S/\!\theta^\star\circ$ of the free monoid $\{\theta, \eta\}^\star$ into a 1–2-Fibonacci outer cohort sequence (Definition 5.1). This means that the bracket produces a total order, generating all equivalence classes $LS' = S/\!\theta^\star\circ \in \{\theta, \eta\}^\star/\!\theta^\star\circ$ sequentially, in particular, with the value $N_{-1}(LS')$ increasing by 1 between successive classes LS' in the sequence, and that moreover, the bracket forms the cohorts (Table 16), with reduced degree $p_\star = t + 1$ for all classes in cohort C_t, and $p_\star$ increasing by 1 between successive cohorts.

The above results, together with Lemmas 5.6– 5.9, would provide a more abstract treatment for the main results of Sections 4.1.5 and 4.1.6.

4.1.7. *Free monoids on combined basis of Wythoff and Wythoff^{-1} functions.* The free monoid $\{\eta, \theta, \kappa, \lambda\}^\star$ on four generators is the subject of ongoing investigation [36]. Thus far, the investigation has yielded identities (generalized complementarities) that are not reducible in terms of the better-known identities shown in Lemma 4.23. Examples include,

$$\kappa^2 = \theta\kappa\lambda$$
$$\theta^2 = \eta\theta\kappa$$
$$\kappa\theta = \theta^2\kappa^2,$$

with inferences such as

$$\kappa\theta(n+1) = n + \kappa(n+1) - \kappa(n) - 2, n \geq 1$$

4.1.8. *Affine combinations of Fibonacci cohort sequences.*

Example 4.14. Any sequence nk of consecutive integer multiples of k, is a Fibonacci cohort sequence with respect to cohortizer $n + kF_t$. This motivates the following proposition.

Proposition 4.40 (Closure of collection of Fibonacci cohort sequences under affine combination)**.** *Consider an affine combination of Fibonacci Cohort sequences. Then this affine combination is a Fibonacci cohort sequence under the linear combination of the cohortizers formed with the same coefficients.*

Proof. Let $(R_n)_{n\geq 1}$ and $(S_n)_{n\geq 1}$ be Fibonacci cohort sequences under cohortizers $f(t)$ and $g(t)$, respectively. Suppose further that for all $n \geq 1$, $T_n = q + rR_n + sS_n$, where q, r and s are constants. Then, directly calculate from the relations (10) that $(T_n)_{n\geq 1}$ is a cohort sequence under $rf(t) + sg(t)$:

$$\begin{aligned}
T_{F_{t+1}} &= q + rR_{F_{t+1}} + sS_{F_{t+1}} \\
&= q + rR_{F_{t-1}} + sS_{F_{t-1}} + rf(t) + sg(t) \\
&= T_{F_{t-1}} + rf(t) + sg(t), \\
&\vdots \\
T_{F_{t+2}-1} &= q + rR_{F_{t+2}-1} + sS_{F_{t+2}-1} \\
&= q + rR_{F_{t+1}-1} + sS_{F_{t+1}-1} + rf(t) + sg(t) \\
&= T_{F_{t+1}-1} + rf(t) + sg(t),
\end{aligned}$$

□

Example 4.15 (Wythoff Array)**.** For constants r_0, r_1, r_2, and r_3, the function $f(t) = r_1F_t + r_2F_{t+1} + r_3F_{t+2}$ will cohortize any affine combination $r_0 + r_1n + r_2\kappa(n) + r_3\lambda(n)$ of $n, \kappa(n)$ and $\lambda(n)$, for $n = 1, 2, 3, \ldots$. In particular, for any column k of the Wythoff Array, take $r_0 = -F_k$, $r_1 = F_k$, $r_2 = F_{k+1}$, and $r_3 = 0$. For $k = 1, \ldots, 6$, the sequences 003622, 035336, 035337, 035338, 035339, and 035340 are Fibonacci cohort under cohortizers $F_t + F_{t+1} = F_{t+2}$, $F_t + 2F_{t+1} = F_{t+3}$, $2F_t + 3F_{t+1} = F_{t+4}$, $3F_t + 5F_{t+1} = F_{t+5}$, $5F_t + 8F_{t+1} = F_{t+6}$, and $8F_t + 13F_{t+1} = F_{t+7}$, respectively.

Remark 4.30. Example 4.15 produces the expression $F_{k+1}\kappa(n) + F_kn - F_k$ for columns of the Wythoff array, corresponding to a (2–1-) Fibonacci cohort sequence with rate $p = k + 1$ and initial element $S_1 = F_{k+1}$ as parameters in (17). The expression gives S_n considering the rows of array w indexed $n = 1, 2, 3, \ldots$, thus coinciding with the expression given in Section 4.1.4 for $w_{n-1,k}$. For rows indexed $n = 0, 1, 2, \ldots$, the expression becomes $w_{n,k} = F_{k+1}\kappa(n+1) + F_kn$ and appears at the top left of Table 4. The expressions for the Wythoff array obtained in Theorem 10 of Kimberling [22], in particular, and other formulations, in general, follow from the three canonical forms of Section 4.1.5, and can also be derived by harvesting its rows from branches of the minimal successor tree (Lemma 8.3).

Example 4.23 reformulates the columns of the Wythoff array as 1–2-Fibonacci cohort sequences.

Example 4.16 (Sums of η, θ, κ, and λ)**.** (2–1-) Fibonacci cohort sequences include $\kappa(n)+\theta(n) = 2\kappa(n)-n$ or $\underline{050140}_n$ under $2F(t+1)-F(t) = \underline{000204}_t$; $\lambda(n)+\eta(n) = 3n+2$ or $\underline{016789}_n$ under $3F_t = \underline{022086}_t = \underline{097135}_t$; $\kappa(n)+\eta(n) = 2n-1$ or $\underline{060747}_n$ under $2F_t = \underline{055389}_t$; and $\lambda(n)+\theta(n) = 2\kappa(n) = \underline{283233}_n$ also under $2F_t = \underline{055389}_t$.

4.1.9. *Base-ϕ representation and free-monoids on Bergman and Bergman^{-1} pairs.* Section 4.1.8 treated affine combinations of Fibonacci cohort sequences. As an application, consider the following.

Example 4.17 (Lucas cohortizers)**.** Observe that the sequence $\underline{050140}$ in [41], mentioned in Example 4.16 and beginning 1, 4, 5, 8, 11, 12, 15, 16, 19, 22, 23, 26 . . . is a 2–1-Fibonacci cohort sequence from the 1$^{\text{st}}$ cohort under cohortizer $L_t = F_{t-1}+F_{t+1}$. Thus, Proposition 4.40 indicates its decomposition into an element-wise sum of a Fibonacci cohort sequence with cohortizer F_{t-1} and another Fibonacci cohort sequence with cohortizer F_{t+1}. Substituting $p=-1$ into (17) gives $\kappa(n)-n+S_1$, while substituting $p=1$ into (17) gives $\kappa(n)-1+R_1$. The choice of $S_1+R_1=1$ in $2\kappa(n)-n-1+S_1+R_1$ confirms the formula $\underline{050140}(n) = 2\kappa(n)-n$, for $n = 1, 2, 3, \ldots$, matching the desired value 1 at $n=1$.

Its complement in the positive integers, $\underline{287775}$, begins: 2, 3, 6, 7, 9, 10, 13, 14, 17, 18, 20, 21, 24, 25, 27, 28, 31, 32, 35, 36, 38, 39, . . ., and decomposes into a complementary pair $\underline{054770}$ and $\underline{003231}$, both 2–1-Fibonacci cohort sequences from the 1$^{\text{st}}$ cohort under cohortizer $L_{t+1} = F_t + F_{t+2}$ (also see Remark 4.32).

Substituting $p=0$ and $p=2$, respectively, into (17) gives $n-1+S_1$ (a series of consecutive integers) and $\kappa(n)+n-2+R_1$. The choice of $S_1+R_1=2$ in $\kappa(n)+2n-3+S_1+R_1$ confirms the formula $\underline{054770}(n) = \kappa(n)+2n-1$, for $n = 1, 2, 3, \ldots$. The choice of $S_1+R_1=3$ in $\kappa(n)+2n-3+S_1+R_1$ confirms the formula $\underline{003231}(n) = \kappa(n)+2n$, for $n = 1, 2, 3, \ldots$.

Example 4.18 (Integers with and without 1 in the minimal base-ϕ representation)**.** Consider the base-ϕ representation of n as a sum $n = \sum_{i=-\infty}^{\infty} \varepsilon_i \phi^i$ of positive and negative powers of the golden ratio, where the coefficients — or *phigits* — satisfy $\varepsilon_i \in \{0, 1\}$ [5]. The minimal base-ϕ representation is that which minimizes $\sum \varepsilon_i$ and for which no two successive ε_i can equal 1 [24].

Sequence $\underline{214971}$ in [41] lists the positive integers whose minimal base-ϕ representation includes 1, that is, whose 0$^{\text{th}}$ phigit ε_0 equals one: 1, 4, 8, 11, 15, 19, 22, 26, 29, 33, 37, 40, 44, ... Its complement in the non-negative integers $\underline{195121}$ lists the positive integers whose minimal base-ϕ representation excludes 1, that is, whose 0$^{\text{th}}$ phigit ε_0 equals zero: 0, 2, 3, 5, 6, 7, 9, 10, 12, 13, 14, 16, 17, 18, 20, 21, 23, 24, 25, 27, 28, ...

The former sequence is a 2–1-Fibonacci cohort sequence from the 0$^{\text{th}}$ cohort under cohortizer $L_{t+1} = F_{t+2}+F_t$. Thus, Proposition 4.40 indicates its decomposition into an element-wise sum of a Fibonacci cohort sequence with cohortizer F_{t+2} and a Fibonacci cohort sequence with cohortizer F_t. Substituting $p=0$ into (17) gives $n-1+S_1$ (a series of consecutive integers), while substituting $p=2$ into (17) gives $\kappa(n)+n-2+R_1$. The choice of $S_1+R_1=4$ in $\kappa(n)+2n-3+S_1+R_1$ confirms the formula $\underline{214971}(n+1) = \kappa(n)+2n+1$, for $n = 0, 1, 2, \ldots$, matching the desired value 4 for $n=1$.

The latter sequence is a 2–1-Fibonacci cohort sequence from the 0$^{\text{th}}$ cohort under cohortizer $L_{t-1} = F_{t-2}+F_t$. Thus, Proposition 4.40 indicates its decomposition

into an element-wise sum of a Fibonacci cohort sequence with cohortizer F_{t-2} and a Fibonacci cohort sequence with cohortizer F_t. Substituting $p = 0$ into (17) gives $n-1+S_1$ (a series of consecutive integers), while substituting $p = -2$ into (17) gives $-\kappa(n)+2n-1+R_1$. The choice of $S_1+R_1 = 2$ in $3n-\kappa(n)-2+S_1+R_1$ confirms the formula $\underline{\texttt{195121}}(n) = 3n - \kappa(n)$, for $n = 0, 1, 2, \ldots$, matching the desired value 2 for $n = 1$.

Similarly, consider the sequence $\underline{\texttt{249115}}$: 1, 2, 4, 5, 6, 8, 9, 11, 12, 13, 15, 16, 17, 19, 20, 22, 23, 24, 26, 27, ... in in [41] and its complement in the positive integers $\underline{\texttt{003231}}$: 3, 7, 10, 14, 18, 21, 25, 28, 32, 36, 39, 43, 47, 50, 54, 57, 61, 65, 68, 72, ... Example 4.17 discussed the latter sequence, giving the formula $\underline{\texttt{003231}}(n) = \kappa(n) + 2n$.

The former sequence is a 2–1-Fibonacci cohort sequence from the 1st cohort under cohortizer $L_{t-1} = F_{t-2} + F_t$. Thus, Proposition 4.40 indicates its decomposition into an element-wise sum of a Fibonacci cohort sequence with cohortizer F_{t-2} and a Fibonacci cohort sequence with cohortizer F_t. Substituting $p = 0$ into (17) gives $n - 1 + S_1$ (a series of consecutive integers), while substituting $p = -2$ into (17) gives $-\kappa(n)+2n-1+R_1$. The choice of $S_1+R_1 = 1$ in $3n-\kappa(n)-2+S_1+R_1$ gives the additional formula $\underline{\texttt{249115}}(n) = 3n - \kappa(n) - 1$, for $n = 0, 1, 2, \ldots$, matching the desired value 1 for $n = 1$.

Considering Example 4.18, Proposition 4.40 thus simplifies the proof of a result conjectured by Baruchel [41] and proved by Dekking [11]. Proposition 4.42 provides this simplified proof, which requires only Lemma 4.41.

Lemma 4.41 (Lucas number of even index as an addend that preserves ε_0)**.** *Consider the minimal base-ϕ representation of S. That is $S = \sum_{i=-\infty}^{\infty} \varepsilon_i \phi^i$ where no two successive ε_i equal 1. Then,*

(a): *For integer $S \in [0, L_{2t+1}]$, the minimal base-ϕ representations of $S, S + L_{2t+2}$, $S + L_{2t+4}, S + L_{2t+6}, \ldots$ all have the same 0^{th} phigit (ε_0).*

(b): *For integer $S \in [0, L_{2t+1})$, the minimal base-ϕ representations of S and $S+L_{2t}$ have the same 0^{th} phigit (ε_0).*

Proof. The proof of Lemma 4.41 appears in Section 11, and recapitulates results of Sanchis and Sanchis [31]. □

Proposition 4.42 (Integers with and without 1 in the minimal base-ϕ representation)**.** *For $n = 0, 1, 2, \ldots$,*

(a): $\kappa(n) + 2n + 1 = \underline{\texttt{214971}}(n + 1)$ *gives the sequence of non-negative integers with $\varepsilon_0 = 1$ in the minimal base-ϕ representation. Conjectured by Baruchel in [41]. Proved by Dekking in [11].*

(b): $3n-\kappa(n) = \underline{\texttt{195121}}(n)$ *gives the sequence of non-negative integers with $\varepsilon_0 = 0$ in the minimal base-ϕ representation.*

Proof. Using the Fibonacci cohort structure identified in Example 4.18, claims **(a)** and **(b)** now follow easily by induction on t. Lemma 4.1 allows the induction step to be written as an increment by (sufficiently large) Lucas number of even index. In turn, Lemma 4.41 shows that the induction step preserves the value of the 0^{th} phigit, ε_0, in the minimal base-ϕ representation.

(a): Per Example 4.18, the formula describes a 2–1-Fibonacci cohort sequence S from the 0^{th} cohort under cohortizer L_{t+1}, a Lucas number. Since the Lucas numbers satisfy the Fibonacci property, Lemma 4.1 applies to this cohort sequence.

By Lemma 4.1(c), the last element of cohort C_t is $S_{F_{t+2}-1} = 1 + L_{t+3} - L_3 = L_{t+3} - 3 = \underline{027961}(t)$.

For t odd, the induction step $C_t = C_{t-2}C_{t-1} + L_{t+1}$ adds a Lucas number of even index to the elements S of cohorts C_{t-2} and C_{t-1}. By Lemma 4.1(c), these elements satisfy $S \leq L_{t+2} - 3 < L_{t+2}$. Further, by the induction hypothesis, the elements employ $\varepsilon_0 = 1$ in their minimal base-ϕ representation. Hence, by Lemma 4.41(b), elements $S + L_{t+1}$ of C_t also employ $\varepsilon_0 = 1$ in their minimal base-ϕ representation.

For t even, Lemma 4.1(a) allows us to write the induction step as $C_t = C_0C_1 \cdots C_{t-3}C_{t-2} + L_{t+2}$ — addition of a Lucas number of even index to the elements S of cohorts $C_0, \ldots, C_{t-2}$. By Lemma 4.1(c), these elements satisfy $S \leq L_{t+1} - 3 < L_{t+1}$. Further, by strong induction hypothesis, the elements employ $\varepsilon_0 = 1$ in their minimal base-ϕ representation. Hence, by Lemma 4.41(a), elements $S + L_{t+2}$ of C_t also employ $\varepsilon_0 = 1$ in their minimal base-ϕ representation.

(b): Per Example 4.18, the formula gives a 2–1-Fibonacci cohort sequence S from the 0^{th} cohort under cohortizer L_{t-1}, a Lucas number. Since the Lucas numbers satisfy the Fibonacci property, Lemma 4.1 applies to this cohort sequence.

By Lemma 4.1(c), the last element of cohort C_t is $S_{F_{t+2}-1} = 0 + L_{t+1} - L_1 = L_{t+1} - 1 = \underline{001610}(t)$.

For t odd, the induction step $C_t = C_{t-2}C_{t-1} + L_{t-1}$ adds a Lucas number of even index to the elements S of cohorts C_{t-2} and C_{t-1}. By Lemma 4.1(c), these elements satisfy $S \leq L_t - 1 < L_t$. Further, by the induction hypothesis, the elements have $\varepsilon_0 = 0$ in their minimal base-ϕ representation. Hence, by Lemma 4.41(b), elements $S + L_{t-1}$ of C_t also have $\varepsilon_0 = 0$ in their minimal base-ϕ representation.

For t even, Lemma 4.1(a) allows us to write the induction step as $C_t = C_0C_1 \cdots C_{t-3}C_{t-2} + L_t$ — addition of a Lucas number of even index to the elements S of cohorts $C_0, \ldots, C_{t-2}$. By Lemma 4.1(c), these elements satisfy $n \leq L_{t-1} - 1 < L_{t-1}$. Further, by strong induction hypothesis, the elements have $\varepsilon_0 = 0$ in their minimal base-ϕ representation. Hence, by Lemma 4.41(a), elements $S + L_t$ of C_t also have $\varepsilon_0 = 0$ in their minimal base-ϕ representation.

It remains only to show that the sequences of non-negative integers given by the two formulas indeed complement one another in $\mathbb{Z}_{\geq 0}$.

For any $t \geq 0$, consider the first t cohorts of the first sequence together with the first $t + 2$ cohorts of the second sequence. Including the 0^{th} element of each sequence, the tally gives F_{t+2} elements from the first sequence and F_{t+4} elements from the second, for a total of $F_{t+2} + F_{t+4} = L_{t+3}$ elements. By Lemma 4.1(c), the first partial sequence begins with 1 and ends with $1 + L_{t+3} - L_3 = L_{t+3} - 3$ while the second begins with 0 and ends with $L_{t+3} - 1$. The formulas in **(a)** and **(b)** show that both sequences strictly increase, and that, moreover, elements of the two sequences are distinct from one another. (To see this, consider $n > -1$ for which $\kappa(n) \geq n > \frac{n-1}{2}$. Thus $2\kappa(n) > n - 1$ and therefore $\kappa(n) + 2n + 1 > 3n - \kappa(n)$.) Hence, by pigeonhole principle, $\forall t \geq 0$, the first t cohorts of the first sequence together with the first $t + 2$ cohorts of the second sequence contain exactly the integers $0, \ldots, L_{t+3} - 1$. Hence the sequences complement one another in the set of non-negative integers

For an alternative argument, reformulate the two sequences as (one plus) a pair complementary of Beatty sequences (see Corollary 4.50): $\underline{214971}(n) = \left\lfloor \frac{5+\sqrt{5}}{2} n \right\rfloor + 1 = \kappa_2(n) + 1$ for $n \geq 0$ and $\underline{195121}(n) = \left\lfloor \frac{5-\sqrt{5}}{2} n \right\rfloor + 1 = \lambda_2(n) + 1$ for $n \geq 1$. □

4.1.10. *A Fibonacci cohort sequence from the* $2^1/_2$ *cohort.* A sequence can also begin to satisfy the Fibonacci cohort relations in the middle of a cohort. For example, each column of $\mathfrak{w}$, array 191436, tabulated at the bottom left of Table 4 satisfies (10) from the fourth element, that is, from the middle of the third cohort.

For this specific example, if the top row of $\mathfrak{w}$, which reads $1, 4, 12, 33, 88, 232, \ldots$, is replaced by the shifted version $0, 1, 4, 12, 33, 88, 232, \ldots$, (with a zero prepended), then each column k of the modified array $\hat{\mathfrak{w}}$ becomes a 2–1-Fibonacci cohort sequence from the 1^{st} cohort with degree $p = 2k-1$ and seed element $S_1 = \mathfrak{w}_{0,k-1} = F_{2k-1} - 1$, as described in Section 4.1.4. Substituting these parameters into (17) generates the expression $F_{2k-1}\kappa(n)+F_{2k-2}(n-1)-1$ for the modified array $\hat{\mathfrak{w}}$. The expression gives S_n considering the rows of array $\mathfrak{w}$ indexed $n = 1, 2, 3, \ldots$, thus coinciding with the expression given in Section 4.1.4 for $\hat{\mathfrak{w}}_{n-1,k}$. For rows indexed $n = 0, 1, 2, \ldots$, the expression becomes $\hat{\mathfrak{w}}_{n,k} = F_{2k-1}\kappa(n+1)+F_{2k-2}n-1$, as shown in Table 4 for rows $n \geq 1$. In particular, for the array so modified, each column $\hat{\mathfrak{w}}_{n-1,k} = S_n$ for $n = 1, 2, 3, \ldots$ satisfies all of the relations (10), as described in Section 4.1.4.

Example 4.23 reformulates the columns of arrays $\mathfrak{w}$ and $\hat{\mathfrak{w}}$ array as 1–2-Fibonacci cohort sequences.

4.2. **2–1- and 1–2-Fibonacci cohort sequences.** As foreshadowed by Remark 4.2, this section will examine the formulas $\langle 2, 1\rangle$ and $\langle 1, 2\rangle$ in the language of Rozenberg and Lindenmayer [30], and interplay between integer sequences that possess one or both of these structures.

4.2.1. *Definitions and examples.*

Definition 4.3 (2–1-Fibonacci Cohort Sequence)**.** Let the sequence $S_1, S_2, \ldots$ fall into cohorts, $C_1, C_2, \ldots, C_t, \ldots$, of lengths $|C_t| = F_t$, respectively. For a pair of left and right cohortizers $h_L(t)$ and $h_R(t)$, respectively, if elements in cohort C_t for $t = 3, 4, 5 \ldots$ satisfy relations

$$\begin{aligned} S_{F_{t+1}} &= S_{F_{t-1}} + h_L(t), \\ &\vdots \\ S_{2F_t-1} &= S_{F_t-1} + h_L(t), \\ S_{2F_t} &= S_{F_t} + h_R(t), \\ &\vdots \\ S_{F_{t+2}-1} &= S_{F_{t+1}-1} + h_R(t), \end{aligned} \tag{39}$$

then call the sequence a *2–1-Fibonacci cohort sequence* under cohortizer $\langle h_L, h_R\rangle$. Gathering (39) into a sequence of cohorts, rather than elements, gives $C_t = [C_{t-2} + h_L(t)] \oplus [C_{t-1} + h_R(t)]$, where h_L produces the left *subcohort* $C_{t-2} + h_L(t)$ of C_t and h_R produces the right subcohort $C_{t-1} + h_R(t)$ of C_t, and where the addition of $h_L(t)$ or $h_R(t)$ distributes to each to element of C_{t-2}, respectively, C_{t-1}. Note that a Fibonacci cohort sequence by Definition 4.1, above, is merely a 2–1-Fibonacci cohort sequence with $h_L \equiv h_R$.

Moreover, by analogy to Definition 4.2, let a 2–1-Fibonacci cohort sequence from the 1^{st} cohort include $S_2 = S_1 + h_R(2)$, in addition to (39).

Definition 4.4 (1–2-Fibonacci Cohort Sequence)**.** Define a *1–2-Fibonacci cohort sequence* analogously except that $C_t = [C_{t-1} + g_L(t)] \oplus [C_{t-2} + g_R(t)]$, that is, the left and right subcohorts $C_{t-1} + g_L(t)$ and $C_{t-2} + g_R(t)$ of C_t, respectively, obtain via the relations

$$\begin{aligned} S_{F_{t+1}} &= S_{F_t} + g_L(t), \\ &\vdots \\ S_{F_{t+1}+F_{t-1}-1} &= S_{F_{t+1}-1} + g_L(t), \\ S_{F_{t+1}+F_{t-1}} &= S_{F_{t-1}} + g_R(t), \\ &\vdots \\ S_{F_{t+2}-1} &= S_{F_t-1} + g_R(t), \end{aligned} \tag{40}$$

for each cohort C_t, $t = 3, 4, 5 \ldots$.

Moreover, by analogy to Definition 4.2, let a 1–2-Fibonacci cohort sequence from the 1st cohort include $S_2 = S_1 + g_L(2)$, in addition to (40).

The following define *subcohort* more precisely.

Definition 4.5. For cohort C_t of a 1–2-Fibonacci cohort sequence S, define its left and right *subcohorts* as the blocks of elements $C_{t_L} = (S_{F_{t+1}}, \ldots, S_{F_{t+1}+F_{t-1}-1})$, respectively $C_{t_R} = (S_{F_{t+1}+F_{t-1}}, \ldots, S_{F_{t+2}-1})$, containing F_{t-1}, respectively F_{t-2} elements.

Definition 4.6. For cohort C_t of a 2–1-Fibonacci cohort sequence S, define its left and right *subcohorts* as the blocks of elements $C_{t_L} = (S_{F_{t+1}}, \ldots, S_{2F_t-1})$, respectively $C_{t_R} = (S_{2F_t}, \ldots, S_{F_{t+2}-1})$, containing F_{t-2}, respectively F_{t-1} elements.

Example 4.19 (Examples of sequences with both 2–1- and 1–2-Fibonacci cohort structure)**.** Sequence $\underline{007895}_1$ is a 1–2-Fibonacci cohort sequence under cohortizer $\langle 0, 1\rangle$, and gives the number of terms in the minimal Fibonacci representation of n (compare Figures 5 and 14), whereas $\underline{112310}_0$ is a (2–1-) Fibonacci cohort sequence under cohortizer $\langle 1, 1\rangle$, and gives the number of terms in the lazy Fibonacci representation of n, as well as the number of symbols θ, η in the 2–1-Fibonacci cohort tableau, Table 13.

Sequence $\underline{102364}_1$ is a 1–2-Fibonacci cohort sequence under under cohortizer $\langle 1, 1\rangle$, and gives the number of symbols κ, λ in the 1–2-Fibonacci cohort tableau, Table 10, as well as the number of Fibonacci terms $< n$ not used in the minimal representation of n, whereas $\underline{200650}_2$ is a 2–1-Fibonacci cohort sequence under cohortizer $\langle 1, 0\rangle$ and gives the number of Fibonacci terms $< n$ not used in the lazy representation or maximal expansion of n.

Moreover, obtain any cohort C_t in $\underline{102364}_1$ by merely reversing cohort C_t in $\underline{112310}_0$, and obtain any cohort C_t in $\underline{200650}_2$ by reversing cohort C_t in $\underline{007895}_1$ and subtracting 1 from all elements. This duality resembles that between the 1–2-Fibonacci cohort tableaux, such as Tables 10, 11, and 16, and 2–1-Fibonacci cohort tableaux, such as Tables 13 and 22.

Finally, $\underline{200648}_2 = \underline{112310}_0 + 1$, a (2–1-) Fibonacci cohort sequence under cohortizer $\langle 1, 1\rangle$, gives the number of terms in the maximal Fibonacci expansion of the positive integers (Definition 6.1 tabulated in Table 20), whereas $\underline{135817}_2$ is a 1–2-Fibonacci cohort sequence under the same cohortizer that gives the number of symbols in Tables 11 and 16, counting each M and L as one symbol.

A 2–1-Fibonacci cohort sequence from the 0^{th} cohort with constant cohortizer 1 arises from the level of the maximal trees, Figures 8 or 10, on which $\vdash_{n,1}$, $\dashv_{n,1}$, $a_{n,1}$ or $\mathfrak{o}_{n,1}$ appear for $n = 0, 1, 2, \ldots$: 1, 2, 3, 3, 4, 4, 4, 5, 4, 5, 5, 5, 6, 5, 5, 6, 5, 6, 6, 6, 7, ... The sequence does not appear in [41] as of this writing, though it resembles 200648+1 except for the first element. More generally, for $n = 0, 1, 2, \ldots$ the same sequence of (shifted) tree levels obtains for any column k of any of these arrays:

$$\begin{aligned}
&\lfloor \log_2 \mathbf{P}(\vdash_{n,k}) \rfloor - k + 2 = \lfloor \log_2 \mathbf{P}(\dashv_{n,k}) \rfloor - k + 2 \\
&= \lfloor \log_2 \mathbf{P}(w_{n,k}) \rfloor - k + 2 = \lfloor \log_2 \mathbf{P}(\mathfrak{w}_{n,k}) \rfloor - k + 2 \\
&= \lfloor \log_2 \bar{\mathbf{P}}(\vdash_{n,k}) \rfloor - k + 2 = \lfloor \log_2 \bar{\mathbf{P}}(\dashv_{n,k}) \rfloor - k + 2 \\
&= \lfloor \log_2 \bar{\mathbf{P}}(w_{n,k}) \rfloor - k + 2 = \lfloor \log_2 \bar{\mathbf{P}}(\mathfrak{w}_{n,k}) \rfloor - k + 2,
\end{aligned}$$

indicative of the column–clade isomorphisms and clade–tree order isomorphisms described in Section 8.6.

Analogously, a 1–2-Fibonacci cohort sequence from the 0^{th} cohort with constant cohortizer 1 arises from the level of the minimal trees, Figures 3 or 5, on which $\mathsf{F}_{n,1}$, $\exists_{n,1}$, $w_{n,1}$ or $\mathfrak{w}_{n,1}$ appear for $n = 0, 1, 2, \ldots$: 1, 2, 3, 4, 3, 5, 4, 4, 6, 5, 5, 5, 4, 7, 6, 6, 6, 5, 6, 5, 5, ... The sequence does not appear in [41] as of this writing, though it resembles 135817+1 except for the first element. More generally, for $n = 0, 1, 2, \ldots$ the same sequence of (shifted) tree levels obtains for any column k of any of these arrays:

$$\begin{aligned}
&\lfloor \log_2 \mathbf{p}(\mathsf{F}_{n,k}) \rfloor - k + 2 = \lfloor \log_2 \mathbf{p}(\exists_{n,k}) \rfloor - k + 2 \\
&= \lfloor \log_2 \mathbf{p}(a_{n,k}) \rfloor - k + 2 = \lfloor \log_2 \mathbf{p}(\mathfrak{o}_{n,k}) \rfloor - k + 2 \\
&= \lfloor \log_2 \bar{\mathbf{p}}(\mathsf{F}_{n,k}) \rfloor - k + 2 = \lfloor \log_2 \bar{\mathbf{p}}(\exists_{n,k}) \rfloor - k + 2 \\
&= \lfloor \log_2 \bar{\mathbf{p}}(a_{n,k}) \rfloor - k + 2 = \lfloor \log_2 \bar{\mathbf{p}}(\mathfrak{o}_{n,k}) \rfloor - k + 2,
\end{aligned}$$

also indicative of the column–clade isomorphisms and clade–tree order isomorphisms described in Section 8.6. For the maximal and minimal Fibonacci trees, the tree-position functions $\mathbf{P}$ and $\mathbf{p}$ are themselves examples of 2–1-, respectively, 1–2-Fibonacci cohort sequences, albeit non-monotonic and linear catenative, rather than affine catenative (Section 6.6). Despite this exception, most integer sequences of interest to the present investigation are non-decreasing and of affine catenative, or else purely catenative, as in the following example.

Previously, Section 4.1.1 showed the Fibonacci word $\underline{096270}_0$ to be a (2–1-) Fibonacci cohort sequence. The "shift operators" defined by Stolarsky in [43] also generate this Fibonacci word (equivalent to $\underline{005614}_0$ with a 0 prepended). For $t = 3, 4, 5, \ldots$, each shift operator captures the first F_t letters from the result of the preceding shift operator and repeats these letters infinitely. When applied to the initial sequence $(1, 0)^\infty$, the shift operators produce the Fibonacci word in the limit (ibid, p. 475), specifically $\underline{005614}_0$, (equivalent to $\underline{096270}_1$). Proposition 4.43 shows how Stolarsky's shift operators construct a 1–2-Fibonacci cohort sequence (Definition 4.4).

Proposition 4.43 (Stolarsky's shift operators produce a 1–2-Fibonacci cohort sequence)**.** *Stolarsky's application of "certain shift operators" [43] to the initial sequence* $(1, 0)^\infty$*, generating the Fibonacci word* $(S_n)_{n=1}^\infty$*, implies that the sequence* $(S_{n+1})_{n=1}^\infty$ *is a 1–2-Fibonacci cohort sequence, under cohortizer* $\langle g_L, g_R \rangle = \langle 0, 0 \rangle$*.*

Proof. The initial sequence $(1,0)^\infty$ repeats F_3 letters indefinitely, and each repeating block comprises a subblock of F_2 letters ("1") followed by a subblock of F_1 letters ("0"). Now for any $t \geq 3$, begin with a sequence that repeats a block of F_t letters indefinitely, and split this repeating block into subblock of F_{t-1} letters followed by a subblock of F_{t-2} letters. In particular, the initial subblock of F_{t-1} letters will reappear after the first F_t letters. That is, $S_{F_t+1} = S_1, \ldots, S_{F_{t+1}} = S_{F_{t-1}}$. The subsequent shift operator will take the first F_{t+1} letters and repeat them indefinitely. In particular, it will copy the first F_t letters and repeat them after the first F_{t+1}. That is,

$$\begin{aligned} S_{F_{t+1}+1} &= S_1, \\ &\vdots \\ S_{F_{t+1}+F_{t-1}} &= S_{F_{t-1}}, \\ S_{F_{t+1}+F_{t-1}+1} &= S_{F_{t-1}+1}, \\ &\vdots \\ S_{F_{t+2}} &= S_{F_t}. \end{aligned}$$

Substituting identities from the prior shift operator into the right-hand-side of the first block of equations gives

$$\begin{aligned} S_{F_{t+1}+1} &= S_{F_t+1}, \\ &\vdots \\ S_{F_{t+1}+F_{t-1}} &= S_{F_{t+1}}, \\ S_{F_{t+1}+F_{t-1}+1} &= S_{F_{t-1}+1}, \\ &\vdots \\ S_{F_{t+2}} &= S_{F_t}, \end{aligned}$$

identities for letters $S_{F_{t+1}+1}$ through $S_{F_{t+2}}$. Observe that the next shift operator will repeat the first F_{t+2} letters, thus preserving the identities just written. Reexamining the identities, notice that they are merely an instance of (40) with $g_L(t) = g_R(t) = 0$, and with indices incremented by one. □

Interestingly, up to a difference in two initial letters, this Fibonacci word (096270 / 005614) and its binary inverse (189661 / 003849), possess both 2–1- and 1–2-Fibonacci cohort structure. Proposition 8.20 will identify 005614_0 as the sequence of *Wythoff signatures* for Fibonacci cohort series that totally order the compositions in the free monoids $\{\bar{\boldsymbol{l}}, \bar{\boldsymbol{r}}\}^\star$ and $\{\bar{\boldsymbol{L}}, \bar{\boldsymbol{R}}\}^\star$.

Meanwhile, the following section deals with sequences that behave similarly.

4.2.2. *"Doubly Fibonacci" cohort sequences.*

Example 4.20. Any sequence of consecutive integers, while a (2–1-) Fibonacci cohort sequence under cohortizer F_t, is also a 1–2-Fibonacci cohort sequence under the cohortizer $\langle F_{t-1}, F_{t+1} \rangle$. The result is intuitive, because consecutive elements change by 1, cohort lengths form a Fibonacci sequence (and hence the change in length between consecutive cohorts is also a Fibonacci number), and therefore the cohortizer comprises Fibonacci number(s) indexed by t. Moreover, the change

from 2–1-Fibonacci to 1–2-Fibonacci merely transposes the way these integers are gathered into cohorts. However, the following propositions extend the family of "doubly Fibonacci" cohort sequences in less intuitive ways.

Array	1–2-Fibonacci cohortizer $\langle g_L(t), \quad g_R(t)\rangle$	2–1-Fibonacci cohortizer $\langle h_L(t), \quad h_R(t)\rangle$
$\digamma_{n,k}$	$F_{t+k} + F_{t-1}, \quad F_{t+k+1} + F_{t+1}{}^{(\mathrm{R})}$	$F_{t+k+1} + F_t{}^{(\mathrm{L})}, \quad F_{t+k} + F_t$
$\daleth_{n,k}$	$F_{t+2k-1} - F_{t-1}{}^{(\mathrm{L})}, F_{t+2k} - F_{t-2}$	$F_{t+2k} - F_t, \quad F_{t+2k-1} - F_{t-3}{}^{(1)}$
$\vdash_{n,k}$	$F_{t+k+1} - F_t, \quad F_{t+k+2} - F_t{}^{(\mathrm{R})}$	$F_{t+k+2} - F_{t+1}{}^{(\mathrm{L})}, F_{t+k+1} - F_{t-1}$
$\dashv_{n,k}$	$F_{t+2k-2} + F_{t-3}, \quad F_{t+2k-1} + F_t{}^{(1)}$	$F_{t+2k-1} + F_{t-2}, \quad F_{t+2k-2} + F_{t-1}{}^{(\mathrm{R})}$
$w_{n,k}$	$F_{t+k} \quad F_{t+k+2}{}^{(\mathrm{R})}$	
$\mathfrak{w}_{n,k}$	$F_{t+2k-2}{}^{(\mathrm{L})} \quad F_{t+2k}$	
$a_{n,k}$		F_{t+k+1}
$\mathfrak{a}_{n,k}$		F_{t+2k-1}
$w_{n-1,k}$		F_{t+k+1}
$\mathfrak{w}_{n-1,k}$		$F_{t+2k-1}{}^{(4)}$
$a_{n+1,k}$	$F_{t+k} \quad F_{t+k+2}{}^{(\mathrm{R})}$	
$\mathfrak{a}_{n+1,k}$	$F_{t+2k-2} \quad F_{t+2k}{}^{(\mathrm{R})}$	

TABLE 17. Fibonacci cohortizers for columns k of the branch and clade quartet arrays. Notes: ${}^{(\mathrm{L})}S_1 = S_0 + g_L(1)$ or $S_1 = S_0 + h_L(1)$; ${}^{(\mathrm{R})}S_1 = S_0 + g_R(1)$ or $S_1 = S_0 + h_R(1)$; ${}^{(1)}$From the 1st cohort / 1st element only; ${}^{(4)}$From the 4th element only. See Propositions 4.44 and 4.45.

Proposition 4.44 (Sequences both 1–2- and 2–1-Fibonacci cohort)**.** *Let $S = S_1, S_2, S_3, \ldots$ be a 1–2-Fibonacci cohort sequence from the 1st cohort under cohortizer $\langle g_L(t), g_R(t)\rangle$. If there exists $\langle h_L(t), h_R(t)\rangle$ satisfying*

$$h_R(2) = g_L(2), \tag{41}$$

and for $t \geq 3$,

$$h_L(t) = g_L(t) + g_L(t-1), \tag{42}$$

$$h_L(t-1) + h_R(t) = g_L(t) + g_R(t-1), \tag{43}$$

$$h_R(t-1) + h_R(t) = g_R(t) \tag{44}$$

then S is also 2–1-Fibonacci cohort sequence from the 1st cohort under cohortizer $\langle h_L(t), h_R(t)\rangle$, and conversely.

Proof. Equality for the second cohort $C_2 = (S_2) = (S_1 + h_R(2)) = (S_1 + g_L(2))$ follows from (41). Equality for the third cohort $C_3 = (S_3, S_4) = (S_1 + h_L(3), S_2 + h_R(3)) = (S_1 + h_L(3), S_1 + h_R(2) + h_R(3)) = (S_2 + g_L(3), S_1 + g_R(3)) = (S_1 + g_L(3) + g_L(2), S_1 + g_R(3))$ follows from (42) and (44).

Suppose that equality holds through cohorts $\ldots, C_{t-3}, C_{t-2}, C_{t-1}$. Then, the first F_{t-2} elements of cohort C_t equal $C_{t-2} + h_L(t)$ using the 2–1-cohortizer, or using the 1–2-cohortizer, to $g_L(t)$ plus the first F_{t-2} elements of C_{t-1}, thus equaling $C_{t-2} + g_L(t) + g_L(t-1)$. Consequently, the first F_{t-2} elements of C_t satisfy the induction hypothesis by (42). The middle F_{t-3} elements of cohort C_t equal $h_R(t)$ plus the first F_{t-3} elements of C_{t-1}, thus equaling $C_{t-3} + h_L(t-1) + h_R(t)$ using the 2–1-cohortizer. Using the 1–2-cohortizer, The middle F_{t-3} elements of C_t equal $g_L(t)$ plus the last F_{t-3} elements of C_{t-1}, thus equaling $C_{t-3} + g_L(t) + g_R(t-1)$. Consequently, the middle F_{t-2} elements of C_t satisfy the induction hypothesis by

(43). Finally, the last F_{t-2} elements of cohort C_t equal $h_R(t)$ plus the last F_{t-2} elements of cohort C_{t-1}, thus equaling $C_{t-2} + h_R(t-1) + h_R(t)$ using the 2–1-cohortizer, or using the 1–2-cohortizer, to $C_{t-2} + g_R(t)$. Consequently, the last F_{t-2} elements of C_t satisfy the induction hypothesis by (44). □

Example 4.21 (Columns of the branch quartet arrays)**.** For the branch quartet arrays, columns k of ⊦ and ⊣ are 1–2-Fibonacci cohort sequences from the 0^{th} cohort under $\langle F_{t+k} + F_{t-1}, F_{t+k+1} + F_{t+1}\rangle$, respectively, $\langle F_{t+2k-1} - F_{t-1}, F_{t+2k} - F_{t-2}\rangle$, and are also 2–1-Fibonacci cohort sequences from the 1^{st} cohort under $\langle F_{t+k+1} + F_t, F_{t+k} + F_t\rangle$, respectively, $\langle F_{t+2k} - F_t, F_{t+2k-1} - F_{t-3}\rangle$, since the relations shown in Proposition 4.44 hold between the 2–1-cohortizers and the 1–2-cohortizers.

Similarly, columns k of ⊢ and ⊤ are 2–1-Fibonacci cohort sequences from the 0^{th} cohort under $\langle F_{t+k+2} - F_{t+1}, F_{t+k+1} - F_{t-1}\rangle$, respectively, $\langle F_{t+2k-1} + F_{t-2}, F_{t+2k-2} + F_{t-1}\rangle$, and are also 1–2-Fibonacci cohort sequences from the 1^{st} cohort under $\langle F_{t+k+1} - F_t, F_{t+k+2} - F_t\rangle$, respectively, $\langle F_{t+2k-2} + F_{t-3}, F_{t+2k-1} + F_t\rangle$, since the relations shown in Proposition 4.44 hold between the 1–2-cohortizers and the 2–1-cohortizers.

Further, in most of the above cases, the topmost entry in the column can be included, to complete a Fibonacci cohort sequence from the 0^{th} element, following conventions shown in the notes below Table 17.

Example 4.22. Sloane's 026273 and 058065_0 are both 1–2-Fibonacci cohort sequences under cohortizer $\langle g_L, g_R\rangle = \langle F_t, F_{t+2}\rangle$. However, prepend a -1 to 026273, and a -2 to 058065, and they become 2–1-Fibonacci cohort sequences under cohortizer $h_L(t) = h_R(t) = F_{t+1}$. Proposition 4.45, next, will generalize this observation.

Proposition 4.45 (Sequences 2–1- and 1–2-Fibonacci cohort under index shift)**.**

(a): *Let $S = S_1, S_2, S_3...$ be a 2–1-Fibonacci cohort sequence from the 1^{st} cohort under cohortizer $h_L(t) = h_R(t) = F_{t+p}$ or a 2–1-Fibonacci cohort sequence satisfying the relations with cohortizer $h_L(t) = h_R(t) = F_{t+p}$ from element $S_4 = S_2 + F_{p+3}$ and further satisfying $S_3 = S_2 + F_{p+1}$. Then, $S_2, S_3, S_4...$ is a 1–2-Fibonacci cohort sequence from the 1^{st} cohort under cohortizer $\langle g_L(t), g_R(t)\rangle = \langle F_{t+p-1}, F_{t+p+1}\rangle$.*

(b): *Conversely, let $S = S_1, S_2, S_3...$ be a 1–2-Fibonacci cohort sequence from the 1^{st} cohort under cohortizer $\langle g_L(t), g_R(t)\rangle = \langle F_{t+p-1}, F_{t+p+1}\rangle$. Then, $S_1 - F_{p+2}, S_1, S_2, S_3, \ldots$ is a 2–1-Fibonacci cohort sequence from the 1^{st} cohort under cohortizer $h_L(t) = h_R(t) = F_{t+p}$.*

Proof of Proposition 4.45: In Section 11. □

Example 4.23 (Columns of the clade quartet arrays)**.** Section 4.1.4 cited column k of the Wythoff array, $w_{n-1,k}$ for $n = 1, 2, 3, \ldots$ as being a 2–1-Fibonacci cohort sequence from the 1^{st} cohort with parameters $S_1 = w_{0,k} = F_{k+1}$ and $p = k + 1$ (hence cohortizer $h_L(t) = h_R(t) = F_{t+k+1}$). Thus by Proposition 4.45(a), $w_{n,k}$ for $n = 1, 2, 3, \ldots$ is a 1–2-Fibonacci cohort sequence from the 1^{st} cohort under $\langle g_L(t), g_R(t)\rangle = \langle F_{t+k}, F_{t+k+2}\rangle$. The 0^{th} element $w_{0,k}$ can be then prepended to the 1–2-Fibonacci cohort sequence using the convention $w_{1,k} = w_{0,k} + f_R(1) = w_{0,k} + F_{k+3}$ shown in the notes below Table 17, or equivalently, $w_{0,k} = w_{1,k} - F_{k+3} = F_{k+3} + F_{k+1} - F_{k+3} = F_{k+1}$, thus completing column k of the Wythoff array as a 1–2-Fibonacci cohort sequence from the 0^{th} cohort. Corollary 8.13 provides further properties of this structure.

Section 4.1.10 cited column k of the Wythoff mirror array, $\mathfrak{w}_{n-1,k}$ for $n = 1, 2, 3, \ldots$ as being a 2–1-Fibonacci cohort sequence satisfying the relations $C_t = C_{t-2}C_{t-1} + F_{t+2k-1}$ from the 4^{th} element $S_4 = \mathfrak{w}_{4-1,k} = \mathfrak{w}_{2-1,k} + F_{2k+2} = S_2 + F_{2k+2}$, further satisfying $\mathfrak{w}_{3-1,k} = \mathfrak{w}_{2-1,k} + F_{2k}$. The latter condition allowed Section 4.1.4 to treat $S_n = \hat{\mathfrak{w}}_{n-1,k} = \begin{cases} F_{2k-1} - 1, & n = 1; \\ \mathfrak{w}_{n-1,k}, & n \geq 2; \end{cases}$ as a 2–1-Fibonacci cohort sequence from the 1^{st} cohort with parameters $S_1 = F_{2k-1} - 1$ and $p = 2k - 1$ (hence cohortizer $h_L(t) = h_R(t) = F_{t+2k-1}$). Thus, $\mathfrak{w}_{n,k} = \hat{\mathfrak{w}}_{n,k}$ for $n = 1, 2, 3, \ldots$ is a 1–2-Fibonacci cohort sequence from the 1^{st} cohort under $\langle g_L(t), g_R(t)\rangle = \langle F_{t+2k-2}, F_{t+2k}\rangle$. The 0^{th} element $\mathfrak{w}_{0,k}$ can be then prepended to the 1–2-Fibonacci cohort sequence using the convention $\mathfrak{w}_{1,k} = \mathfrak{w}_{0,k}gf_L(1) = w_{0,k} + F_{2k-1}$ shown in the notes below Table 17, or equivalently, $\mathfrak{w}_{0,k} = \mathfrak{w}_{1,k} - F_{2k-1} = F_{2k+1} + F_{2k-1} - 1 - F_{2k-1} = F_{2k+1} - 1$, thus completing column k of the Wythoff mirror array as a 1–2-Fibonacci cohort sequence from the 0^{th} cohort.

Observe that for $n = 0, 1, 2, \ldots$ and $k = 1, 2, 3, \ldots$, the array $\hat{\mathfrak{w}}_{n,k} + 1 = F_{2k-1}\kappa(n+1) + F_{2k-2}n = \lambda^{k-1}\kappa(n+1)$ corresponds to Kimberling's "Wythoff difference array" (<u>080164</u>, see Example 9.4), hence each column k of $\hat{\mathfrak{w}}_{n-1,k}+1$ is a 2–1-Fibonacci cohort sequence from the 0^{th} cohort with cohortizer $h_L(t) = h_R(t) = F_{t+2k-1}$, and each column k of $\hat{\mathfrak{w}}_{n,k}+1$ is a 1–2-Fibonacci cohort sequence from the 0^{th} cohort under $\langle F_{t+2k-2}, F_{t+2k}\rangle$ with $S_1 = \hat{\mathfrak{w}}_{1,k}+1 = S_0+g_R(1) = \hat{\mathfrak{w}}_{0,k}+1+F_{2k+1}$.

Similarly, columns k of a and $\mathfrak{a}$ are 2–1-Fibonacci cohort sequences from the 0^{th} cohort. Excluding the topmost two entries ($a_{0,k}, a_{1,k}$, respectively, $\mathfrak{a}_{0,k}, \mathfrak{a}_{1,k}$), the columns are also 1–2-Fibonacci cohort sequences from the 1^{st} cohort. In the latter sequences, the second entry from the top of the column ($a_{1,k}$, respectively, $\mathfrak{a}_{1,k}$) can also be included, to complete a 1–2-Fibonacci cohort sequence from the 0^{th} element, following conventions shown in the notes below Table 17.

Example 4.24. Example 4.8 gave $\theta(n)$, $\eta(n)$, and $\lfloor n/\phi \rfloor - \left\lfloor \frac{n}{1-\phi} \right\rfloor$ as (2–1) Fibonacci cohort sequences under cohortizers F_{t-1}, F_{t-2}, and F_{t-3} respectively. Omitting the first element as per Proposition 4.45(a), the rest of the elements form 1–2-Fibonacci cohort sequences under the cohortizers $\langle F_{t-2}, F_t\rangle$, $\langle F_{t-3}, F_{t-1}\rangle$, and $\langle F_{t-4}, F_{t-2}\rangle$, respectively.

Example 4.25. A second type of sequence that exhibits both 2–1- and 1–2-Fibonacci cohort structure includes Sloane's <u>130312</u>, comprising F_t copies of each number F_t, and <u>087172</u>, comprising F_t copies of each number F_{t+1}. These sequences are 2–1-Fibonacci cohort via $\langle f_L, f_R\rangle = \langle F_{t-1}, F_{t-2}\rangle$ and $\langle f_L, f_R\rangle = \langle F_t, F_{t-1}\rangle$, respectively. However, they are also 1–2-Fibonacci cohort under $\langle f_L, f_R\rangle = \langle F_{t-2}, F_{t-1}\rangle$, respectively, $\langle f_L, f_R\rangle = \langle F_{t-1}, F_t\rangle$. Noting that $\underline{130312}(n) = \bar{\boldsymbol{R}}(n) - \bar{\boldsymbol{L}}(n)$, Remark 6.12 will present a related sequence $\bar{\boldsymbol{r}}(n) - \bar{\boldsymbol{l}}(n) = 2, 4, 6, 6, 10, 10, 10, 16, 16, 16, 16, 16, 26, 26, 26, 26, 26, 26, 26, 26, \ldots$ comprising F_t copies of $2F_{t+1}$, which has 2–1-Fibonacci cohortizer $\langle 2F_t, 2F_{t-1}\rangle$ and 1–2-Fibonacci cohortizer $\langle 2F_{t-1}, 2F_t\rangle$. Proposition 4.46, the proof of which is trivial, will generalize this observation.

Proposition 4.46 (Cohorts for sequences that repeat qF_{t+p} F_t many times)**.** *For p, q integer, the sequence of qF_{t+p} repeated F_t many times for $t = 1, 2, 3\ldots$ is a 2–1-Fibonacci cohort sequence and also a 1–2-Fibonacci cohort sequence, under the cohortizers $\langle f_L, f_R\rangle = \langle qF_{t+p-1}, qF_{t+p-2}\rangle$ and $\langle f_L, f_R\rangle = \langle qF_{t+p-2}, qF_{t+p-1}\rangle$, respectively.*

Example 4.26. Per Section 8.2.1, the para-Fibonacci sequence 066628, gives the row indices of $1, 2, 3, \ldots$ in Table 12. It is both a 1–2-Fibonacci cohort sequence under the cohortizer $\langle 0, F_{t-1}\rangle$ and a 2–1-Fibonacci cohort sequence under the cohortizer $\langle 0, F_{t-2}\rangle$.

4.2.3. *Left and right subcohorts of 2–1- and 1–2-Fibonacci cohort sequences.*

Proposition 4.47 (All left or all right subcohorts)**.** *Consider a Fibonacci cohort sequence S and form new sequences L by reversing and concatenating all left subcohorts and R by concatenating all right subcohorts of the original sequence.*

(a): *The reversed left subcohorts of a 2–1-Fibonacci cohort sequence from the 1^{st} cohort under cohortizer $\langle f_L(t), f_R(t)\rangle$ form a 1–2-Fibonacci cohort sequence from the 0^{th} cohort under cohortizer $\langle f_L(t+2) - f_L(t+1) + f_R(t), f_L(t+2)\rangle$.*

(b): *Right subcohorts of a 1–2-Fibonacci cohort sequence from the 1^{st} cohort under cohortizer $\langle f_L(t), f_R(t)\rangle$ form a 1–2-Fibonacci cohort sequence from the 0^{th} cohort under cohortizer $\langle f_R(t+2) - f_R(t+1) + f_L(t), f_R(t+2)\rangle$.*

Proof of Proposition 4.47: In Section 11 □

The mechanics of Proposition 4.47 may seem obscure, but are quite simple, as Remark 5.1 will explain in the context of its symbolic version Proposition 5.1.

Example 4.27 (First column of F from subcohorts)**.** As Section 8.1 will note, the first column of F comprises the right cohorts of 1–2-Fibonacci cohort sequence of positive integers, those numbers to the right of the staircase in Table 6(i). Whereas that entire tableau (the positive integers) is a 1–2-Fibonacci cohort sequence under $\langle F_{t-1}, F_{t+1}\rangle$ per Example 4.20, Proposition 4.47(b) gives that $\mathsf{F}_{n,1}$, for $n = 0, 1, 2, \ldots$ is a 1–2-Fibonacci cohort sequence from the 0^{th} cohort under $\langle F_{t+1} + F_{t-1}, F_{t+3}\rangle$.

Example 4.28 (Dual Fibonacci Cohort Sequences from subcohorts)**.** To further demonstrate Proposition 4.47(a), consider the 2–1-Fibonacci cohort sequence 0, 0, 1, 0, 2, 1, 0, 4, 3, 2, 1, 0, 7, 6, 5, 4, 3, 2, 1, 0, … under cohortizer $\langle F_{t-1}, 0\rangle$. Per Section 8.2.1, this para-Fibonacci sequence gives row indices of the positive integers in L.

Taking its reversed left subcohorts (and excluding its right subcohorts) yields the 1–2-Fibonacci cohort sequence from the 0^{th} cohort 0, 1, 2, 3, 4, 5, 6, 7, …, which is merely the nonnegative integers under cohortizer $\langle F_{t+1} - F_t + 0, F_{t+1}\rangle = \langle F_{t-1}, F_{t+1}\rangle$, as given in Example 4.20.

The same sequence is also 1–2-Fibonacci cohort under cohortizer $\langle F_{t-2}, 0\rangle$. Thus by Proposition 4.47(b), taking its right subcohorts (and excluding its left subcohorts) gives 0, 0, 0, 1, 0, 2, 1, 0, 4, 3, 2, 1, 0, 7, 6, 5, 4, 3, 2, 1, 0, …, or the original 1–2-Fibonacci cohort sequence with a 0 prepended as the 0^{th} element.

Consider the 1–2-Fibonacci cohort sequence 0, 0, 0, 1, 0, 1, 2, 0, 1, 2, 3, 4, 0, 1, 2, 3, 4, 5, 6, 7, … under cohortizer $\langle 0, F_{t-1}\rangle$ or 066628. Per Section 8.2.1, this para-Fibonacci sequence gives row indices of the positive integers in F.

By Proposition 4.47(b), taking its right subcohorts (and excluding its left subcohorts) yields the 1–2-Fibonacci cohort sequence from the 0^{th} cohort of the nonnegative integers with cohortizer $\langle F_{t+1} - F_t + 0, F_{t+1}\rangle = \langle F_{t-1}, F_{t+1}\rangle$.

As mentioned in Example 4.26, sequence 066628 is also a 2–1-Fibonacci cohort sequence under $\langle 0, F_{t-2}\rangle$. Thus by Proposition 4.47(a), taking its reversed left subcohorts (and excluding its right subcohorts) gives the sequence 0, 0, 0, 1, 0,

$2,1,0,\ 4,3,2,1,0,\ 7,6,5,4,3,2,1,0,\ldots$, (same as the sequence mentioned several paragraphs above), a 1–2-Fibonacci cohort sequence from the 0^{th} cohort under cohortizer $\langle F_{t-2}, 0\rangle$.

4.2.4. *Linear catenative sequences.* Section 6.6 describes a 2–1-Fibonacci cohort sequence 243571= $\mathbf{P}(n)$ and its 1–2-Fibonacci cohort dual $\mathbf{p}(\mathbf{n})$, which are linear catenative sequences, rather than affine ones, as the coefficients of previous terms in the cohortizer do not consist only of ones, but rather a mixture of ones and twos.

4.3. **Pell, Lucas, and general affine cohort sequences of integers.** Results of the preceding section on Fibonacci cohort sequences extend to a more general class of integer sequences. Like most of the Fibonacci cohort sequences previously examined, these cohort sequences will be affinely catenative. That is, each cohort C_t forms by concatenating previous cohorts (according to a specified formula), and then adding (elementwise) to this concatenation a scalar term (possibly) dependent on t. A proposed definition for this class of sequences, together with a few examples, motivates the discussion. Compared to the locally catenative sequences treated by [30], the present definition will preclude the emergence of "banded" and "cyclical" patterns, and only consider affine catenative recurrences where the lengths of cohorts strictly increase.

4.3.1. *General affine sequences of integers with cohorts of increasing size.*

Definition 4.7 (A general class of cohort sequences)**.** Let $T > 1$ be an integer and $\langle t_1, \ldots, t_k\rangle$ a composition (ordered partition) of T into $k > 1$ parts, with no zero parts, that is, $T = \sum_{i=1}^{k} t_i$ with $0 < t_i < T$, for all $i = 1, \ldots, k$, and let $d = \max_{i\in\{1,\ldots,k\}} t_i$ denote the largest part in the composition. Observe that $\langle t_1, \ldots, t_k\rangle$ is equivalent to the "formula" for local concatenation in the language of Rozenberg and Lindenmayer [30], and will provide the "lags" of the recurrence.

Next, let $1 < G_1 < G_2 < G_3 < \ldots$ be a strictly increasing integer sequence that gives the lengths of cohorts and that follows the recurrence $G_t = G_{t-t_1} + \ldots + G_{t-t_k}$, for $t > d$. For the lengths of cohorts to strictly increase, a sufficient condition is to require $1 \in \{t_1, \ldots, t_k\}$ (smallest part of T / shortest lag equal to one), together with $1 < G_1 < \cdots < G_d$ (strictly increasing lengths of "seed cohorts"). Initial examples here will satisfy this sufficient condition, though Section 4.3.3 will relax this requirement. Further, define the partial sums $D_t = \sum_{i=1}^{t} G_i$.

Finally, consider a right-infinite integer sequence S and cohorts:

$$\text{seed cohorts}\begin{cases} C_1 &\equiv (S_1, \ldots, S_{D_1}),\\ &\vdots\\ C_d &\equiv (S_{D_{d-1}+1}, \ldots, S_{D_d}),\\ C_{d+1} &\equiv (S_{D_d+1}, \ldots, S_{D_{d+1}}),\\ &\vdots\\ C_t &\equiv (S_{D_{t-1}+1}, \ldots, S_{D_t}). \end{cases}$$

In other words, let the ordered recurrence G decompose the sequence S into cohorts $C_1, C_2, \ldots, C_t, \ldots$, having lengths $|C_t| = G_t$. Further, allow G to break each cohort C_t into subcohorts C_{t_i} where $C_t = C_{t_1} \cdots C_{t_k}$, and the i^{th} subcohort C_{t_i} of cohort C_t has length equal to that of the $(t - t_i)^{\text{th}}$ cohort C_{t-t_i}, which is to say it has length $|C_{t_i}| = |C_{t-t_i}| = G_{t-t_i}$.

If for functions $\langle g_1(t), \ldots, g_k(t)\rangle$ depending only on t, each cohort C_t for $t = d+1, d+2, \ldots$ satisfies $C_t = C_{t_1}C_{t_2}\cdots C_{t_k} = [C_{t-t_1} + g_1(t)] \oplus [C_{t-t_2} + g_2(t)] \oplus \cdots \oplus [C_{t-t_k} + g_k(t)]$, then call the sequence S a t_1–t_2–$\cdots$–t_k–G cohort sequence and further, say that "$\langle g_1(t), \ldots, g_k(t)\rangle$ is a t_1–t_2–$\cdots$–t_k–G cohortizer of S.

Remark 4.31. In the following examples, the cohortizer functions $g_1(t), \ldots, g_k(t)$ will simply add one or more terms of the form G_{t+p}, as with many of the Fibonacci cohort sequences previously investigated.

4.3.2. *Pell cohort sequences.*

Example 4.29 (Consecutive integers as Pell cohort sequences of each possible formula)**.** Consider the sequence of Pell numbers (Sloane's 000129), given by the recurrence $P_t = P_{t-2} + 2P_{t-1}$ and beginning 1, 2, 5, 12, 29, 70, 169, 408, 985. Analogous to Examples 4.2 and 4.20 for Fibonacci cohort sequences, any sequence of consecutive integers is a 2–1–1-Pell cohort sequence under cohortizer $\langle P_{t-2} + P_{t-1}, P_{t-2} + P_{t-1}, P_t\rangle$, a 1–2–1-Pell cohort sequence under $\langle P_{t-1}, P_t, P_t\rangle$, and a 1–1–2-Pell cohort sequence under $\langle P_{t-1}, 2P_{t-1}, P_{t-1} + P_t\rangle$. Thus, in particular, the positive integers can be gathered into 2–1–1-Pell cohorts as

$$\begin{aligned}
C_1 &= (1),\\
C_2 &= (2,3),\\
C_3 &= [C_{3-2} + g_1(3)] \oplus [C_{3-1} + g_2(3)] \oplus [C_{3-1} + g_3(3)]\\
&= C_1C_2C_2 + (g_1, g_2, g_2, g_3, g_3)(3) = (1,2,3,2,3) + (3,3,3,5,5)\\
&= (4,5,6,7,8),\\
C_4 &= (2,3,4,5,6,7,8,4,5,6,7,8) + (7,7,7,7,7,7,7,12,12,12,12,12), \ldots;
\end{aligned}$$

into 1–2–1-Pell cohorts as

$$\begin{aligned}
C_1 &= (1),\\
C_2 &= (2,3),\\
C_3 &= [C_{3-1} + g_1(3)] \oplus [C_{3-2} + g_2(3)] \oplus [C_{3-1} + g_3(3)]\\
&= C_2C_1C_2 + (g_1, g_1, g_2, g_3, g_3)(3) = (2,3,1,2,3) + (2,2,5,5,5)\\
&= (4,5,6,7,8),\\
C_4 &= (4,5,6,7,8,2,3,4,5,6,7,8) + (5,5,5,5,5,12,12,12,12,12,12,12), \ldots;
\end{aligned}$$

and into 1–1–2-Pell cohorts as

$$\begin{aligned}
C_1 &= (1),\\
C_2 &= (2,3),\\
C_3 &= [C_{3-1} + g_1(3)] \oplus [C_{3-1} + g_2(3)] \oplus [C_{3-2} + g_3(3)]\\
&= C_2C_2C_1 + (g_1, g_1, g_2, g_2, g_3)(3) = (2,3,2,3,1) + (2,2,4,4,7)\\
&= (4,5,6,7,8),\\
C_4 &= (4,5,6,7,8,4,5,6,7,8,2,3) + (5,5,5,5,5,10,10,10,10,10,17,17), \ldots.
\end{aligned}$$

Example 4.30. As with Fibonacci cohort sequences (Example 4.2), shifting the rate p in the 1–2–1-Pell cohortizer of the integers cohorizes a family of related Beatty sequences. Specifically, $\langle P_t, P_{t+1}, P_{t+1}\rangle$ cohortizes the 1–2–1-Pell cohort sequence 003151 — the Beatty sequence $\lfloor n\chi\rfloor$, where $\chi \equiv 1 + \sqrt{2}$ — which begins

2, 4, 7, 9, 12, 14, 16, 19, 21, 24, 26, 28, 31, 33, 36, 38, 41, 43, 45, 48, ..., into cohorts beginning $C_1 = (2)$, $C_2 = (4, 7)$, $C_3 = C_{3_1}C_{3_2}C_{3_3} = [C_2 + g_1(3)] \oplus [C_1 + g_2(3)] \oplus [C_2 + g_3(3)] = (4 + P_3, 7 + P_3)(2 + P_4)(4 + P_4, 7 + P_4) = ((9, 12)(14)(16, 19))$, $C_4 = (21, 24, 26, 28, 31, 33, 36, 38, 41, 43, 45, 48), \ldots$.

With suitable choices for the three elements of the two seed cohorts $C_1 = (S_1)$ and $C_2 = (S_2, S_3)$, the same cohortizer forms 1–2–1-Pell cohort sequences 285075 ($\lfloor n\chi - \sqrt{2} \rfloor + 1$), 082845 ($\lfloor n\chi + \sqrt{2} \rfloor - 1$) and 080754 ($\lceil n\chi \rceil$).

Example 4.31. Shifting p further gives $\langle P_{t+1}, P_{t+2}, P_{t+2} \rangle$, which 1–2–1-Pell cohortizes Sloane's 188039 ($\lfloor \lfloor n\chi - \sqrt{2} \rfloor \chi \rfloor$), beginning 2, 7, 12, 19, 24, 31, 36, 41, 48, 53, 60, 65, 70, 77, 82, 89, 94, 101, 106, 111, ..., as well as 276879 ($\lfloor \lfloor n\chi - \sqrt{2} \rfloor \chi \rfloor - 1$), beginning 1, 6, 11, 18, 23, 30, 35, 40, 47, 52, 59, 64, 69, 76, 81, 88, 93, 100, 105, 110, ..., as well as 140868 ($\lfloor \lfloor n\chi \rfloor \chi \rfloor$), beginning 4, 9, 16, 21, 28, 33, 38, 45, 50, 57, 62, 67, 74, 79, 86, 91, 98, 103, 108, 115, ..., as well as 098021 ($\lfloor \lfloor n\chi \rfloor \chi \rfloor + 1$), beginning 5, 10, 17, 22, 29, 34, 39, 46, 51, 58, 63, 68, 75, 80, 87, 92, 99, 104, 109, 116, ...

Shifting p further still gives $\langle P_{t+2}, P_{t+3}, P_{t+3} \rangle$, which 1–2–1-Pell cohortizes Sloane's 187975 ($\lfloor \lfloor \lfloor n\chi \rfloor \chi \rfloor \chi \rfloor + 3 = \lfloor \lfloor n\chi \rfloor \chi^2 \rfloor + 1$).

Example 4.32. Shifting p in the 2–1–1-Pell cohortizer of integers gives $\langle P_{t-1} + P_t, P_{t-1} + P_t, P_{t+1} \rangle$, which cohortizes Sloane's 081841$_2$ ($\lfloor n\chi - {}^3\!/_2\sqrt{2} \rfloor + 2$), beginning 2, 4, 7, 9, 11, 14, 16, 19, 21, 24, 26, 28, 31, 33, 36, 38, 40, 43, 45, 48, ..., with the cohorts beginning $C_1 = (2)$, $C_2 = (4, 7)$, $C_3 = C_{3_1}C_{3_2}C_{3_3} = [C_1 + g_1(3)] \oplus [C_2 + g_2(3)] \oplus [C_2 + g_3(3)] = (2 + P_2 + P_3)(4 + P_2 + P_3, 7 + P_2 + P_3)(4 + P_4, 7 + P_4) = ((9)(11, 14)(16, 19))$, $C_4 = (21, 24, 26, 28, 31, 33, 36, 38, 40, 43, 45, 48), \ldots$. The same cohortizer applies to 064437 ($\lfloor n\chi - {}^3\!/_2\sqrt{2} \rfloor + 1$) as well as to 086377 ($\lfloor n\chi - {}^1\!/_2\sqrt{2} \rfloor$) and to 080652 ($\lfloor n\chi - {}^1\!/_2\sqrt{2} \rfloor + 1$).

Shifting p further still gives $\langle P_t + P_{t+1}, P_t + P_{t+1}, P_{t+2} \rangle$, which 2–1–1-Pell cohortizes 328987 ($\lfloor \lfloor n\chi - {}^1\!/_2\sqrt{2} \rfloor \chi - {}^1\!/_2\sqrt{2} \rfloor + 2$).

Example 4.33. Shifting p in the 1–1–2-Pell cohortizer of integers gives $\langle P_t, 2P_t, P_t + P_{t+1} \rangle$, which cohortizes the sequence $\lfloor n\chi + {}^1\!/_2\sqrt{2} \rfloor$, beginning 3, 5, 7, 10, 12, 15, 17, 20, 22, 24, 27, 29, 32, 34, 36, 39, 41, 44, 46, 48, ..., into 1–1–2-Pell cohorts beginning $C_1 = (3)$, $C_2 = (5, 7)$, $C_3 = C_{3_1}C_{3_2}C_{3_3} = [C_2 + g_1(3)] \oplus [C_2 + g_2(3)] \oplus [C_1 + g_3(3)] = (5 + P_3, 7 + P_3)(5 + 2P_3, 7 + 2P_3)(3 + P_3 + P_4) = ((10, 12)(15, 17)(20))$, $C_4 = (22, 24, 27, 29, 32, 34, 36, 39, 41, 44, 46, 48), \ldots$.

Shifting p further still gives $\langle P_{t+1}, 2P_{t+1}, P_{t+1} + P_{t+2} \rangle$, a 1–1–2-Pell cohortizer of $\lfloor \lfloor n\chi + {}^1\!/_2\sqrt{2} \rfloor \chi + {}^1\!/_2\sqrt{2} \rfloor$, $\lfloor \lfloor n\chi + {}^3\!/_2\sqrt{2} \rfloor \chi + {}^3\!/_2\sqrt{2} \rfloor$ and other sequences.

These examples motivate Conjecture 4.48.

Conjecture 4.48 (Pell Cohort Sequences)**.** *For $j \in \mathbb{Z}$, let $S(n) = \lfloor n\chi + {}^j\!/_2\sqrt{2} \rfloor$. Then, $S(n)$, $n = 1, 2, 3, \ldots$ is a Pell cohort sequence if and only if*

$j \in \{-9, -7, -5, -3, -1\}$, in which case $S^p(n)$ is a 2–1–1-Pell cohort sequence under cohortizer $\langle P_{t+p-2} + P_{t+p-1}, P_{t+p-2} + P_{t+p-1}, P_{t+p} \rangle$ for $p \in \mathbb{Z}_{\geq 0}$, or

$j \in \{-2, 0, 2, 4, 6\}$, in which case $S^p(n)$ is a 1–2–1-Pell cohort sequence under cohortizer $\langle P_{t+p-1}, P_{t+p}, P_{t+p} \rangle$ for $p \in \mathbb{Z}_{\geq 0}$, or

$j \in \{1, 3, 5, 7, 9, 11, 13\}$, in which case $S^p(n)$ is a 1–1–2-Pell cohort sequence under cohortizer $\langle P_{t+p-1}, 2P_{t+p-1}, P_{t+p-1} + P_{t+p} \rangle$ for $p \in \mathbb{Z}_{\geq 0}$.

Remark 8.1 briefly treats Pell cohort tableaux, the trees planar-graph isomorphic to them, and corresponding I–D arrays. While the remainder of the paper tends to

focus on (generalized) Fibonacci cohort sequences and related structures, Pell and more general cohort sequences remain objects of ongoing study [37].

Example 4.34 (Tribonacci cohort sequences)**.** Consider any integer sequence satisfying the Tribonacci recurrence $F_t^{(3)} = F_{t-3}^{(3)} + F_{t-2}^{(3)} + F_{t-1}^{(3)}$. Analogous to Examples 4.2 and 4.20 for Fibonacci cohort sequences, any sequence of consecutive integers is
a 1–2–3-Tribonacci cohort sequence under cohortizer $\langle F_{t-1}^{(3)}, 2F_{t-1}^{(3)} + F_{t-2}^{(3)}, F_{t+1}^{(3)} \rangle$,
a 1–3–2-Tribonacci cohort sequence under cohortizer $\langle F_{t-1}^{(3)}, F_t^{(3)}+F_{t-1}^{(3)}, F_t^{(3)}+F_{t-1}^{(3)}, \rangle$,
a 2–1–3-Tribonacci cohort sequence under cohortizer $\langle F_{t-1}^{(3)}+F_{t-2}^{(3)}, F_{t-1}^{(3)}+F_{t-2}^{(3)}, F_{t+1}^{(3)} \rangle$,
a 2–3–1-Tribonacci cohort sequence under cohortizer $\langle F_{t-1}^{(3)}+F_{t-2}^{(3)}, F_t^{(3)}+F_{t-2}^{(3)}, F_t^{(3)} \rangle$,
a 3–1–2-Tribonacci cohort sequence under cohortizer $\langle F_t^{(3)}, F_{t-1}^{(3)}+F_{t-3}^{(3)}, F_t^{(3)}+F_{t-1}^{(3)} \rangle$,
and a 3–2–1-Tribonacci cohort sequence under cohortizer $\langle F_t^{(3)}, F_t^{(3)}, F_t^{(3)} \rangle$. In each case, t can be substituted by $t+p$ for a fixed positive or negative integer shift p, to generate further sequences of interest.

4.3.3. *Lucas cohort sequences of integers.* In this section, Definition 4.7 will be relaxed to allow seed cohorts to initially decrease in length, so that cohort lengths $|C_t|$ for $t = 1, 2, 3, \ldots$ may follow the Lucas numbers $L_{t-1} = 2, 1, 3, 4, 7, 11, 18, 29, \ldots$.

Section 4.1.8 cited the complementary pair of Beatty sequences $\underline{\texttt{249115}}(n) = \left\lfloor \frac{5-\sqrt{5}}{2} n \right\rfloor$ and $\underline{\texttt{003231}}(n) = \left\lfloor \frac{5+\sqrt{5}}{2} n \right\rfloor$, for $n \geq 1$, recorded in the OEIS [41].

Now consider these Beatty sequences $\{\kappa_2(n), \lambda_2(n)\} \equiv \{\left\lfloor \frac{5-\sqrt{5}}{2} n \right\rfloor, \left\lfloor \frac{5+\sqrt{5}}{2} n \right\rfloor\}$ as the first (odd) extension of the complementary Wythoff sequences $\{\kappa(n), \lambda(n)\} \equiv \{\left\lfloor \frac{1+\sqrt{5}}{2} n \right\rfloor, \left\lfloor \frac{3+\sqrt{5}}{2} n \right\rfloor\} \equiv \{\kappa_1(n), \lambda_1(n)\}$. Continue this extension of Wythoff pairs.

Definition 4.8 (Bergman and Bergman^{-1} pairs)**.** For $b = 1, 2, 3, \ldots$, define

$$\{\kappa_b(n), \lambda_b(n)\} \equiv \{\left\lfloor \frac{2b+1+\sqrt{5}}{2b-1+\sqrt{5}} n \right\rfloor, \left\lfloor \frac{2b+1+\sqrt{5}}{2} n \right\rfloor\}, \tag{45}$$

and for $b \geq 2$ in particular, designate the resulting pairs of complementary Beatty sequences for $n = 1, 2, 3, \ldots$ *Bergman pairs*, after the connection cited in Section 4.1.9 of $\{\kappa_2(n), \lambda_2(n)\}$ to Bergman's "number system with an irrational base" [5].

Extend the Wythoff^{-1} pair $\{\theta(n), \eta(n)\} \equiv \{\left\lfloor \frac{2}{1+\sqrt{5}} n \right\rfloor, \left\lfloor \frac{2}{3+\sqrt{5}} n \right\rfloor\} \equiv \{\theta_1(n), \eta_1(n)\}$ likewise. For $b = 1, 2, 3, \ldots$, define

$$\{\theta_b(n), \eta_b(n)\} \equiv \{\left\lfloor \frac{2b-1+\sqrt{5}}{2b+1+\sqrt{5}} n \right\rfloor, \left\lfloor \frac{2}{2b+1+\sqrt{5}} n \right\rfloor\}, \tag{46}$$

and for $b \geq 2$ in particular, designate as *Bergman inverse pairs* or *Bergman^{-1} pairs* the resulting pairs of complementary Beatty sequences for $n = 1, 2, 3, \ldots$.

Proposition 4.49 shows relations for Bergman cohort sequences analogous to those of (11) for Fibonacci cohort sequences.

Proposition 4.49 (Bergman cohort relations)**.** *Consider Definition 4.8.*
(a): *For $n = 1, 2, 3, \ldots$, $\kappa_b(n)$ is a (generalized) Fibonacci cohort sequence with*
$|C_t| = F_{t-3} + bF_{t-2}$ *as cohort lengths, and*
$g(t) = F_{t-1} + bF_{t-2}$ *as cohortizer.*

Thus, $C_t = C_{t-2}C_{t-1} + g(t) = C_{t-2}C_{t-1} + F_{t-1} + bF_{t-2}$*, for* $t = 3, 4, 5, \ldots$*. That is, for* $t = 2, 3, 4, \ldots$*,*

$$\begin{aligned} \kappa_b(F_{t-2} + bF_{t-1}) &= \kappa_b(F_{t-4} + bF_{t-3}) + F_{t-1} + bF_{t-2}, \\ &\vdots \\ \kappa_b(F_{t-1} + bF_t - 1) &= \kappa_b(F_{t-2} + bF_{t-1} - 1) + F_{t-1} + bF_{t-2}. \end{aligned} \tag{47}$$

Further, $\kappa_b(n)$ *is a (generalized) Fibonacci cohort sequence from the* 1^{st} *cohort, whereas for the* 2^{nd} *cohort, always a singleton, (47) gives* $C_2 = (\kappa_b(b)) = (\kappa_b(b-1)+1)$*. That is, the singular element* $\kappa_b(b)$ *of* C_2 *succeeds* $\kappa_b(b-1)$*, the last of the* $b-1$ *elements of* C_1*.*

(b): *For* $n = 1, 2, 3, \ldots$*,* $\lambda_b(n)$ *is a Fibonacci cohort sequence from the* 1^{st} *cohort with* $g(t) = F_{t+1} + bF_t$ *as cohortizer.*
Thus for cohorts $C_t = (\lambda_b(F_{t+1}), \ldots, \lambda_b(F_{t+2} - 1))$*,*
$C_2 = C_1 + g(2) = C_1 + 2 + b$ *and for* $t = 3, 4, 5, \ldots$*,*
$C_t = C_{t-2}C_{t-1} + g(t) = C_{t-2}C_{t-1} + F_{t+1} + bF_t$*.*

Proof. Per Remark 4.4, the results here resemble that of Proposition 4.2. Whereas $\kappa_b(n)$ and $\lambda_b(n)$ are spectrum sequences, the cohortizers $g(t)$ and cohort lengths $|C_{t+1}|$ are merely the numerators and denominators, respectively, of convergents to the irrational base of each spectrum sequence.

Consider $\kappa_b(n)$, a spectrum sequence on the irrational base $\frac{2b+1+\sqrt{5}}{2b-1+\sqrt{5}} = \frac{\phi+b}{\phi+b-1}$, this base having the continued fraction expansion $[1, b, \bar{1}]$ and convergents $\frac{F_t+bF_{t-1}}{F_{t-2}+bF_{t-1}}$ for $t = 1, 2, 3, \ldots$ (See, *e.g.*, [29]).

Let $g(t) = \kappa_b(n) - \kappa_b(n - F_{t-3} - bF_{t-2})$ for $n \in [F_{t-2} + bF_{t-1}, F_{t-1} + bF_t)$. The substitution $j = n - F_{t-3} - bF_{t-2}$ gives $g(t) = \kappa_b(j + F_{t-3} + bF_{t-2}) - \kappa_b(j)$ for $j \in [F_{t-4}+bF_{t-3}, F_{t-2}+bF_{t-1})$. Considering the convergents of the irrational base, Lemma 2 of Fraenkel, Mushkin, and Tassa [17] gives $g(t) = F_{t-1} + bF_{t-2}$.

Consider $\lambda_b(n)$, a spectrum sequence on the irrational base $\frac{2b+1+\sqrt{5}}{2} = b+\phi$, this base having the continued fraction expansion $[b+1, \bar{1}]$ and convergents $b + \frac{F_{t+1}}{F_t} = \frac{F_{t+1}+bF_t}{F_t}$ for $t = 1, 2, 3, \ldots$.

Suppose that $g(t) = \lambda_b(n) - \lambda_b(n - F_t)$ for $n \in [F_{t+1}, F_{t+2})$. The substitution $j = n - F_t$ gives $g(t) = \lambda_b(j + F_t) - \lambda_b(n)$ for $j \in [F_{t-1}, F_{t+1})$. Considering the convergents of the irrational base, Lemma 2 of Fraenkel, Mushkin, and Tassa [17] gives $g(t) = F_{t+1} + bF_t$. □

Corollary 4.50 shows formulas for Bergman cohort sequences similar to those of Proposition 4.2 and Corollary 4.3 for Fibonacci cohort sequences. The proof of Corollary 4.42 applies these formulas.

Corollary 4.50 (Bergman cohort formulas)**.** *The following formulas hold:*

(a): *For* $b = 2$*,* $n = 1, 2, 3, \ldots$*,* $\kappa_b(n) = 3n - \kappa(n) - 1$*.*
(b): *For* $b = 1, 2, 3, \ldots$*,* $n = 1, 2, 3, \ldots$*,* $\lambda_b(n) = \kappa(n) + bn$*.*

Proof. From Proposition 4.49, note that κ_b has cohort lengths $|C_t| = F_t$ and cohortizer $g(t) = F_{t-2} + F_t = L_{t-1}$. Considering these parameters of the sequence, apply Proposition 4.40, analogously to Examples 4.17 and 4.18.

From Proposition 4.49, note that λ_b has cohort lengths $|C_t| = F_t$ and cohortizer $g(t) = F_{t+1} + bF_t$. Considering these parameters of the sequences, apply Proposition 4.40, analogously to Examples 4.17 and 4.18. □

Remark 4.32. Returning to the decomposition in Example 4.17, $\{\underline{050140}(n)\}_{n\geq 1} = K_2K_1$, hence its complement decomposes into $\Lambda_2 = \{\underline{003231}(n)\}_{n\geq 1}$ and $K_2\Lambda_1 = \{\underline{054770}(n)\}_{n\geq 1}$ (Figure 12).

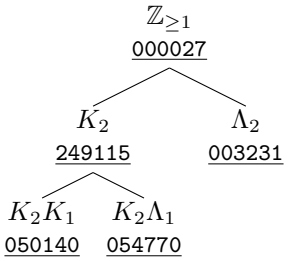

FIGURE 12. Partition of $\mathbb{Z}_{\geq 1}$ using complementary Bergman sequences for $b = 1, 2$.

Lemma 4.51. *Definitions 4.8 of the Bergman and Bergman^{-1} pairs (κ_b, λ_b), respectively, (θ_b, η_b) (45)–(46) imply the following related results.*

(i): *For $n = 1, 2, 3, \ldots$, the Beatty sequences $\kappa_b(n)$ and $\lambda_b(n)$ complement one another in the positive integers, hence, $\theta_b(n) + \eta_b(n) = n - 1$.*

(ii): *Θ_b comprises a single leading zero for $b \geq 1$, followed by runs of length one and two of each number in K_{b-1}, respectively, Λ_{b-1}.*

(iii): *H_b comprises a leading run of $b + 1$ zeroes for $b \geq -1$, followed by runs of length $b + 2$ and $b + 1$ of each of each lower Wythoff number (K_1), respectively, upper Wythoff number (Λ_1).*

(iv): *For integer $n \geq 1$*

$$\kappa_b(n) = n + \eta_{b-1}(n) \tag{48}$$

$$\lambda_b(n) = (b + 1)n + \theta_1(n) \tag{49}$$

Proof. In Section 11. □

The free monoids $\{\kappa_b, \lambda_b\}^\star$ on the "Bergman pair" $\{\kappa_b, \lambda_b\}$ under composition and the free monoid $\{\theta_b, \eta_b\}^\star$ on the "Bergman^{-1} pair" $\{\theta_b, \eta_b\}$ under composition provide one extension to the free monoids $\{\kappa, \lambda\}^\star$ and $\{\theta, \eta\}^\star$ discussed in Sections 4.1.5 and 4.1.6, respectively. The subject of ongoing investigation, Section 9.6 provides some preliminary observations about these free monoids.

4.3.4. *From the $\langle 1, 2\rangle$ and $\langle 2, 1\rangle$ toward the $\langle 1, 1\rangle$ formula.* A departure from the definitions and examples considered heretofore, Section 9.7 will discuss cohort series in which the present cohort C_t obtains using only some elements of the second previous cohort C_{t-2} together with the entirety of the previous cohort C_{t-1}, plus an additional copies of some elements of the latter. This is to say that, relative to the formula $\langle 1, 2\rangle$ or $\langle 2, 1\rangle$ for a Fibonacci cohort sequence, the prior cohorts in this new recurrence begin to overlap one another, approaching the formula $\langle 1, 1\rangle$, where each cohort obtains from two copies of the previous one, and cohort lengths double, $|C_t| = C_{t-1}$.

5. Cohort sequences of functions and equivalence classes thereof

The foregoing discussion treated cohort sequences of integers, and their construction by affine catenative recurrence. The discussion considered bijections between certain cohort sequences of integers and sequences of integer-valued, univariate functions $f : \mathbb{Z} \to \mathbb{Z}$, or equivalence classes of such functions. Specifically, Proposition 4.16(b) and Proposition 4.30 provided maps between the sequence of positive integers and functions in the free monoids $\{\kappa, \lambda\}^\star$ and $\{\theta, \eta\}^\star$, while Corollary 4.11 and Corollary 4.39 presented maps between the positive integers and the collections $\{\kappa, \lambda\}^\star / \circ\kappa^\star$, respectively, $\{\theta, \eta\}^\star / \theta^\star\circ$ of congruence classes of functions on these same free monoids.

The aforementioned maps induced a total order on $\{\kappa, \lambda\}^\star$ and also totally ordered the collection of its equivalence classes using the very same structure. Specifically, both Table 10 and Table 11 are ordered as 1–2-Fibonacci inner cohort sequences, like Table 7(i). In the case of $\{\theta, \eta\}^\star$, the maps induced total orders with two distinct structures, the member functions (Table 13) ordered as a 2–1-Fibonacci outer cohort sequence, like Table 7(iv), but the collection of equivalence classes of member functions (Table 16) ordered as a 1–2-Fibonacci outer cohort sequence, like Table 7(iii).

To motivate this section, consider that for $\{\kappa, \lambda\}^\star$, the functions on the inside of the composition have the most significant effect on the order of both elements and equivalence classes. For $\{\theta, \eta\}^\star$, the functions on the outside of the composition have the most significant effect on the order of elements, while those functions on the inside have the most significant effect on the order of equivalence classes.

For example, the precedence of both $\lambda\kappa \prec \kappa\lambda$ (Table 10) and $\lambda\kappa M \prec \kappa\lambda M$ (Table 11) agrees with the values $\lambda\kappa(2) = 7 < 8 = \kappa\lambda(2)$ and $\lambda\kappa M(1) = 7 < 8 = \kappa\lambda M(1)$, respectively, produced by the maps. While the precedence $\eta\theta \prec \theta\eta$ (Table 13) agrees with the values $N_0(\eta\theta) = 4 < 5 = N_0(\theta\eta)$, it differs from the precedence $L\eta\theta \succ L\theta\eta$ (Table 16), which follows the values $N_{-1}(L\eta\theta) = 8 > 7 = N_{-1}(L\theta\eta)$.

Seeking a more abstract treatment of these structures, this section reproduces the same total orders using a "cohort calculus" to generate the functions (or their equivalence classes) in order, rather than relying on explicit maps to $\mathbb{Z}_+$ to place the functions into order. While the operations for constructing a cohort of integers comprised the concatenation of previous cohorts and scalar addition, the cohort calculus for functions will also use concatenation to build up cohorts of increasing length, but will build up the elements of the sequence themselves using functional composition with a generating element of the monoid. This generating element serves the role of "cohortizer."

To formalize this cohort calculus for sequences of functions, Definition 5.1 extends Definitions 4.1, 4.2, 4.3 and 4.4 from sequences of integers to sequences of functions. The definition follows the types of Fibonacci cohort sequences of compositions by prefix and suffix shown in Figures 7. To encompass cohort sequences of equivalence classes, the definition also includes a variation where the cohortizer acts as an infix, which is to say that it builds up an existing composition by entering in the middle, adjacent to the kernel, not fully on the inside nor the outside. This proves useful for placing the collections $\{\kappa, \lambda\}^\star / \circ\kappa^\star$ and $\{\theta, \eta\}^\star / \theta^\star\circ$ of equivalence classes into total order. In this context, the operations $/L\circ$ and $/\circ R$ will refer, respectively, to the removal of kernel L from the outside (left) of a composition and

of kernel R from the inside (right) of a composition, respectively. The definition will employ labels such as "outer...by prefix" and "inner...by suffix," which may seem redundant at first, but because of the infix variations, this extra qualification proves necessary.

Definition 5.1 (Fibonacci Cohort Sequences of functions)**.** The following are defined by analogy to Definitions 4.1, 4.2, 4.3, and 4.4.

2–1-Fibonacci Outer Cohort Sequences of functions by prefix: By analogy to Definitions 4.1 and 4.3, decompose a sequence $f_1, f_2, \ldots, f_n, \ldots$ of functions into finite blocks of consecutive elements (cohorts), $C_1, C_2, \ldots, C_t, \ldots$ of increasing length $|C_t| = F_t$. If, for prefix functions f_L, f_R, the cohorts satisfy $C_t = f_L \circ C_{t-2} \oplus f_R \circ C_{t-1}$ for each cohort C_t, $t = 3, 4, \ldots$, where $C_{t-2} \oplus C_{t-1}$ is the concatenation of C_{t-2} and C_{t-1}, and the composition of f_L and f_R distributes to each element f_n of C_{t-2} and C_{t-1}, respectively, then designate $(f_n)_{n\geq 1}$ a *2–1-Fibonacci outer cohort sequence of functions by prefix under* $\langle f_L\circ, f_R\circ\rangle$, and designate $\langle f_L\circ, f_R\circ\rangle$ a *2–1-Fibonacci outer cohortizer* of $(f_n)_{n\geq 1}$.

2–1-Fibonacci Outer Cohort Sequences of functions by prefix from 1st cohort: By analogy to Definition 4.2, if f_1 and f_2 further satisfy $f_2 = f_R \circ f_1$ (so that $C_2 = f_R \circ C_1$), then designate the sequence a *2–1-Fibonacci outer cohort sequence of functions by prefix from the 1^{st} cohort.*

1–2-Fibonacci Inner Cohort Sequences of functions by suffix: If f_L, f_R serve as suffix functions and the cohorts instead satisfy $C_t = C_{t-1} \circ f_L \oplus C_{t-2} \circ f_R$, then by analogy to Definition 4.4, designate $(f_n)_{n\geq 1}$ a *1–2-Fibonacci inner cohort sequence of functions by suffix* under cohortizer $\langle \circ f_L, \circ f_R\rangle$.

1–2-Fibonacci Inner Cohort Sequences of functions by suffix from 1st cohort: By analogy to Definition 4.2, if f_1 and f_2 further satisfy $f_2 = f_1 \circ f_L$ (so that $C_2 = C_1 \circ f_L$), then designate the sequence a *1–2-Fibonacci inner cohort sequence of functions by suffix from the 1^{st} cohort.*

1–2-Fibonacci Outer Cohort Sequences of functions by left infix: For a variation in which the functions g_n have the decomposition $g_n = Lf_n$ and f_L, f_R serve as infix functions such that the cohortizer has the effect $g_n = Lf_n \mapsto Lf_Lf_n$, for $g_n \in C_{t-1}$ and $g_n = Lf_n \mapsto Lf_Rf_n$, for $g_n \in C_{t-2}$, then abbreviate the cohortizer $\langle Lf_L\circ, Lf_R\circ\rangle(g/L\circ)$ and designate the sequence a *1–2-Fibonacci outer cohort sequence of functions by left infix.*

1–2-Fibonacci Outer Cohort Sequences by left infix from the 1st or 0th cohort: If the latter further satisfies $g_2 = L \circ f_R \circ f_1$ for $g_1 = Lf_1$ (so that $C_2/L\circ = f_R\circ(C_1/L\circ)$), then designate the sequence a *1–2-Fibonacci outer cohort sequence of functions by left infix from the 1^{st} cohort*; and further, should the sequence have a zeroth element g_0, corresponding to the singleton zeroth cohort C_0, and satisfy $g_1 = f_L \circ g_0$, then designate the sequence a *1–2-Fibonacci outer cohort sequence of functions by left infix from the 0^{th} cohort.*

1–2-Fibonacci Inner Cohort Sequences of functions by right infix: For a variation in which the functions h_n have the decomposition $h_n = f_nR$ and f_L, f_R serve as infix functions such that the cohortizer has the effect $h_n = f_nR \mapsto f_nf_LR$, for $h_n \in C_{t-1}$ and $h_n = f_nR \mapsto f_nf_RR$, for $h_n \in C_{t-2}$, then abbreviate the

cohortizer $\langle \circ f_L R, \circ f_R R \rangle (h/\circ R)$ and designate the sequence a *1–2-Fibonacci inner cohort sequence of functions by right infix*.

1–2-Fibonacci Inner Cohort Sequences by right infix from 1st or 0th cohort: If the latter further satisfies $h_2 = f_1 \circ f_L \circ R$ for $h_1 = f_1 R$ (so that $C_2/\circ R = (C_1/\circ R) \circ f_L$), then designate the sequence a *1–2-Fibonacci inner cohort sequence of functions by right infix from the 1^{st} cohort*; and further, should the sequence have a zeroth element f_0, corresponding to the singleton zeroth cohort C_0, and satisfy $h_1 = h_0 \circ f_R$, then designate the sequence a *1–2-Fibonacci inner cohort sequence of functions by right infix from the 0^{th} cohort*.

Note that Definition 5.1 assumes that functions f_L and f_R do not vary with the parameter t that indexes the cohorts, though a more general treatment could allow it. The remainder of the section will be concerned only with Fibonacci cohort sequences of integer-valued, univariate functions and thus will restrict the functions f_L and f_R of the cohortizers in Definition 5.1 to integer-valued, univariate functions defined on $\mathbb{Z}$.

The following analog of Proposition 4.47 will examine relationships between some of the sequence types in Definition 5.1.

Proposition 5.1 (All left or all right subcohorts)**.** *For certain Fibonacci cohort sequences of functions $(f_n)_{n\geq 1}$, new Fibonacci cohort sequences $(g_n)_{n\geq 0}$ and $(h_n)_{n\geq 0}$ form either by (a) reversing and concatenating all left subcohorts, or (b) by concatenating all right subcohorts of the original sequence.*

(a): *For a 2–1-Fibonacci outer cohort sequence $(f_n)_{n\geq 1}$ by prefix from the 1^{st} cohort under $\langle f_L \circ, f_R \circ \rangle$, the reversed left subcohorts form a 1–2-Fibonacci outer cohort sequence $(g_n)_{n\geq 0}$ by left infix from the 0^{th} cohort under cohortizer $\langle f_L f_R \circ, f_L^2 \circ \rangle (g/f_L \circ)$. If f_L has a left inverse f_L^{-1}, the cohortizer can be written $\langle f_L f_R f_L^{-1} \circ, f_L \circ \rangle (g)$.*

(b): *For a 1–2-Fibonacci inner cohort sequence $(f_n)_{n\geq 1}$ by suffix from the 1^{st} cohort under $\langle \circ f_L, \circ f_R \rangle$, the right subcohorts form a 1–2-Fibonacci inner cohort sequence $(h_n)_{n\geq 0}$ by right infix from the 0^{th} cohort under cohortizer $\langle \circ f_L f_R, \circ f_R^2 \rangle$ $(h/\circ f_R)$. If f_R has a right inverse f_R^{-1}, the cohortizer can be written $\langle \circ f_R^{-1} f_L f_R, \circ f_R \rangle (h)$.*

Proof of Proposition 5.1: In Section 11 □

Remark 5.1. Note that part (a) of the proposition forms a 1–2-Fibonacci outer cohort sequence by left infix, setting $L = f_L$ as the "prefix" of g in the decomposition in Definition 5.1, while part (b) forms a 1–2-Fibonacci inner cohort sequence by right infix, setting $R = f_R$ as the "suffix" of g in the definition.

Also note that, where the functional inverses of f_L and f_R exist, the formulation of the cohortizers as $\langle f_L f_R f_L^{-1} \circ, f_L \circ \rangle$ and $\langle \circ f_R^{-1} f_L f_R, \circ f_R \rangle$ in parts (a) and (b), respectively, of Proposition 5.1 is analogous to the formulation of the cohortizers in Proposition 4.47, where new Fibonacci cohort sequences of integers obtain via cohortizers $\langle f_L(t+2) + f_R(t) - f_L(t+1), f_L(t+2) \rangle$, respectively, $\langle -f_R(t+1) + f_L(t) + f_R(t+2), f_R(t+2) \rangle$, which employ additive inverses $(-)$ rather than the functional inverses $(^{-1})$, and scalar addition instead of functional composition.

Proposition 5.1 can be explained most easily by referring to the tableaux archetypes in Figures 7(i)–(iv). First observe from the Figure that the cohort duality between the pairs of tableaux ((i), (ii)) and ((iii), (iv)) simply reverses the order

of elements in each cohort of the tableau, while the blade duality between the pairs of tableaux ((i), (iii)) and ((ii), (iv)) simply reverses the order of symbols in each element. Secondly, observe that in any tableau, a new cohort forms by concatenating the previous and second previous cohorts and applying a prefix (in the case of the "outer" tableaux (i) and (ii)) or a suffix (in the case of the "inner" tableaux (iii) and (iv)).

Thus by the recursive construction of the tableaux, taking the elements of all left cohorts or the elements of all right cohorts and dropping the cohortizer (the prefix in the case of the outer tableaux or the suffix in the case of the inner tableaux), will yield the original tableaux.

Finally, observe that Proposition 5.1(a) effectively composes two operations: It first takes the left subcohorts of the archetype in Figure 7(ii) and "drops" the cohortizer (by treating each element as an equivalence class), to yield a tableau of the same archetype. Then it reverses the order of elements to produce a tableau of the cohort-dual archetype in Figure 7(i). By contrast, Proposition 5.1(b) only does one operation: It takes the right subcohorts of the archetype in Figure 7(iii) and "drops" the cohortizer (by treating each element as an equivalence class), to yield a tableau of the same archetype.

Proposition 5.2 (Cohort sequence for functions $f \in \{\kappa, \lambda\}^\star$)**.** *Consider the free monoid $\{\kappa, \lambda\}^\star$ on generating set $\{\kappa, \lambda\}$ under composition. The compositions form a 1–2-Fibonacci inner cohort sequence of functions (by suffix) from the 1^{st} cohort under cohortizer $\langle \circ\kappa, \circ\lambda \rangle$, where the notation indicates the application of κ or λ on the inside, that is, $f \mapsto \langle f \circ \kappa, f \circ \lambda \rangle$, and the repeated application of the cohortizer provides a total order of $\{\kappa, \lambda\}^\star$ (Table 10).*

Moreover, between consecutive elements in this totally ordered set, the value of $f(2)$ increases by 1. Proposition 4.16(b) previously showed this map to be a bijection.

Proof. Using cohort notation, write the application of the cohortizer as $C_t = C_{t-1} \circ \kappa \oplus C_{t-2} \circ \lambda$, where $C_{t-1} \oplus C_{t-2}$ is the concatenation of prior cohorts C_{t-1} and C_{t-2}, and over which, composition with κ, respectively, λ, distributes to each element of the prior cohort. This gives $C_1 = (I)$, $C_2 = C_1 \circ \kappa = (I) \circ \kappa = (\kappa)$, $C_3 = C_2 \circ \kappa \oplus C_1 \circ \lambda = (\kappa) \circ \kappa \oplus (I) \circ \lambda = (\kappa^2) \oplus (\lambda) = (\kappa^2, \lambda)$, $C_4 = C_3 \circ \kappa \oplus C_2 \circ \lambda = (\kappa^2, \lambda) \circ \kappa \oplus (\kappa) \circ \lambda = (\kappa^3, \lambda\kappa) \oplus (\kappa\lambda) = (\kappa^3, \lambda\kappa, \kappa\lambda), \cdots$. Clearly, the repeated application of the cohortizer eventually yields all strings of any number of symbols κ, λ, thus generating $\{\kappa, \lambda\}^\star$.

Moreover, for the initial cohorts, $C_1(2) = (I)(2) = (2)$, $C_2(2) = (\kappa)(2) = (3)$, $C_3(2) = (\kappa^2, \lambda)(2) = (4, 5)$, $C_4(2) = (\kappa^3, \lambda\kappa, \kappa\lambda)(2) = (6, 7, 8), \ldots$, so that the value of $f(2)$ increases by 1 between successive elements of the initial cohorts.

Suppose this continues so that $C_{t-2} = (f_{F_{t-1}}, \ldots, f_{F_t-1})$ satisfies $C_{t-2}(2) = (F_{t-1} + 1, \ldots, F_t)$, and $C_{t-1} = (f_{F_t}, \ldots, f_{F_{t+1}-1})$ satisfies $C_{t-1}(2) = (F_t + 1, \ldots, F_{t+1})$. By the induction hypothesis then, $C_t = C_{t-1} \circ \kappa \oplus C_{t-2} \circ \lambda = (f_{F_t} \circ \kappa, \ldots, f_{F_{t+1}-1} \circ \kappa, f_{F_{t-1}} \circ \lambda, \ldots, f_{F_t-1} \circ \lambda)$. Since $\kappa(2) = 3$ and $\lambda(2) = 5$, this gives $C_t(2) = (f_{F_t}(3), \ldots, f_{F_{t+1}-1}(3), f_{F_{t-1}}(5), \ldots, f_{F_t-1}(5))$.

Proposition 4.7(b) gives $f(3) = f(2) + F_{t(f)}$ and $f(5) = f(2) + F_{t(f)+3}$, where $t(f)$ is the cohort index of f. Thus for $f \in C_{t-1}$, the former gives $f(3) = f(2) + F_{t-1}$, whilst for $f \in C_{t-2}$, the latter gives $f(5) = f(2) + F_{t-2+3} = f(2) + F_{t+1}$. Combining the two subcohorts gives $C_t(2) = (f_{F_t}(2) + F_{t-1}, \ \ldots, f_{F_{t+1}-1}(2) + F_{t-1}, f_{F_{t-1}}(2) + F_{t+1}, \ \ldots, f_{F_t-1}(2) + F_{t+1}) = (F_t + 1 + F_{t-1}, \ \ldots, F_{t+1} + F_{t-1}, \ F_{t-1} + 1 + F_{t+1}, \ldots, F_t + F_{t+1}) = (F_{t+1}+1, \ldots, F_{t+1}+F_{t-1}, F_{t+1}+F_{t-1}+1, \ldots, F_{t+2})$, as desired. □

Proposition 5.2 described a 1–2-Fibonacci inner cohort structure on the free monoid $\{\kappa, \lambda\}^\star$. Corollary 5.3 uses this result to characterize the cohortizer that places the set of equivalence classes $\{\kappa, \lambda\}^\star/\circ\,\kappa^\star$, into the 1–2-Fibonacci inner recursive cohort structure, as well. Corollary 5.3 thus provides a converse to Proposition 4.16(b), whereas the latter started with the cohort structure on the collection of equivalence classes to induce the cohort structure on the free monoid of compositions itself.

Corollary 5.3 (Cohort sequence for equivalence classes $f/\circ\,\kappa^\star$ of $\{\kappa, \lambda\}^\star$)**.** *Consider the free monoid $\{\kappa, \lambda\}^\star$ on generating set $\{\kappa, \lambda\}$ under composition. The equivalence classes, modulo application of $\kappa^\star$ on the inside, form a 1–2-Fibonacci inner cohort sequence (by right infix) from the 1^{st} cohort $D_1 = (\lambda\kappa^\star) \equiv (M)$ under cohortizer $\langle \circ\kappa M, \circ\lambda M\rangle$ $(f/\circ M)$, which has the action $f \mapsto \langle (f/\circ M)\circ\kappa M, (f/\circ M)\circ\lambda M\rangle$. The notation indicates the application of κ or λ as a right infix immediately outside M, and the repeated application of the cohortizer provides a total order of $\{\kappa, \lambda\}^\star/\circ\kappa^\star$ (Table 11).*

Moreover, between representatives h of consecutive classes in this total order, the value of $h(1)$ increases by 1. Corollary 4.11 previously showed this map to be a bijection.

Proof. Proposition 5.2, placed the set of functions $f \in \{\kappa, \lambda\}^\star$ into a 1–2-Fibonacci cohort sequence from the 1^{st} cohort under $\langle \circ\kappa, \circ\lambda\rangle$. In particular, the first cohort comprises the singleton I, and for each subsequent cohort, elements of its left subcohort end in suffix κ and elements of its right subcohort end in suffix λ. Thus, the set meets the conditions for the application of Proposition 5.1(b), with $f_L = \kappa$ and $f_R = \lambda$.

Consequently, Proposition 5.1(b) shows the set of standard class representatives $h = (f/\circ M)\circ\lambda$ to form a 1–2-Fibonacci cohort inner sequence of functions by right infix, with $f_L = \kappa$, and $f_R = R = \lambda$ under cohortizer $\langle \circ\kappa\lambda, \circ\lambda^2\rangle$ $(h/\circ\lambda)$ from the 0^{th} cohort $D_0 = (I)$, with $D_1 = (I\circ f_R) = (\lambda)$, $D_2 = ((\lambda/\circ f_R)\circ f_L f_R) = (\kappa\lambda)$, $D_3 = ((\kappa\lambda/\circ f_R)\circ f_L f_R, (\lambda/\circ f_R)\circ f_R^2) = (\kappa^2\lambda, \lambda^2)$, and so forth, where each function h_n for $n > 0$ ends in suffix $f_R = \lambda$, as desired.

To show that the value of $h(1)$ increases by 1 between representatives h_n of consecutive classes, examine the initial cohorts, $D_0(1) = (I)(1) = (1)$, $D_1(1) = (\lambda)(1) = (2)$, $D_2(1) = (\kappa\lambda)(1) = (3)$, $D_3(1) = (\kappa^2\lambda, \lambda^2)(1) = (4, 5)$, $D_4(1) = (\kappa^3\lambda, \lambda\kappa\lambda, \kappa\lambda^2)(1) = (6, 7, 8), \ldots$. For these initial cohorts, $h(1)$ indeed increases by 1 between consecutive elements h_n, and moreover the cohorts seem to take the form $D_t(1) = (F_{t+1} + 1, \ldots, F_{t+2})$. (Here, D temporarily refers to cohorts of class representatives, rather than cohorts of classes, though this distinction will soon be shown inconsequential).

Considering that each function h_n for $n > 0$ ends in suffix $f_R = \lambda$ and observing that $\lambda(1) = 2$, write for $t > 0$ that cohort t of standard class representatives $D_t(1) = (D_t/\circ\lambda)(\lambda(1)) = (D_t/\circ\lambda)(2)$. Now, the choice of h as right subcohorts of f, together with the underlying 1–2-Fibonacci cohort structure of f allows us to write $D_t/\circ\lambda = (h_{F_{t+1}}/\circ\lambda, \ldots, h_{F_{t+2}-1}/\circ\lambda) = (f_{F_{t+1}}, \ldots, f_{F_{t+2}-1})$, for $t \geq 1$ (see proof of Proposition 5.1(b), (140) – (141)).

Thus, it suffices for the value of $(h_n/\circ\lambda)(2) = f_n(2)$ to increase by 1 between successive elements f_n. As this was shown in Proposition 5.2, the progression noted above must continue such that cohort $D_t = (h_{F_{t+1}}, \ldots, h_{F_{t+2}-1})$ indeed satisfies $D_t(1) = (F_{t+1} + 1, \ldots, F_{t+2})$ for the standard class representatives.

To complete the proof, it suffices to observe that all representatives h of the same class $h\kappa^\star$ have the same value of $h(1)$, since $M(1) = \lambda\kappa^\star(1) = \lambda(1) = 2$. Clearly, modifying the cohortizer to $\langle \circ\kappa M, \circ\lambda M\rangle$ $(f \diagup \circ M)$ generates these classes in order, for which the substitution of λ for M returns the standard representative h. Thus, D can refer to cohorts of classes, so that the classes form a 1–2-Fibonacci inner cohort sequence by right infix, with $f_L = \kappa$, $f_R = \lambda$ and $R = M$.

As claimed, the recursion begins only with the 1^{st} cohort. Although the 0^{th} class $\kappa^\star$ does satisfy $\kappa^\star(1) = 1$, it does not relate to the 1^{st} cohort M in the way the definition prescribes, that is, $M \neq \kappa^\star\lambda$. □

Proposition 5.4 characterizes the cohortizer of $\{\theta, \eta\}^\star$ that places it into the 2–1-Fibonacci outer cohort structure.

Proposition 5.4 (Cohort sequence for functions $f \in \{\theta, \eta\}^\star$)**.** *Consider the free monoid $\{\theta, \eta\}^\star$ on generating set $\{\theta, \eta\}$ under composition. The compositions form a 2–1-Fibonacci outer cohort sequence of functions (by prefix) from the 1^{st} cohort under cohortizer $\langle \eta\circ, \theta\circ\rangle$, where the notation indicates the application of η or θ on the outside, that is, $f \mapsto \langle \eta \circ f, \theta \circ f\rangle$, and the repeated application of the cohortizer provides a total order of $\{\theta, \eta\}^\star$ (Table 13).*

Moreover, between consecutive elements in this totally ordered set, the value of $N_0(S)$ increases by 1. Corollary 4.26 previously showed this map to be a bijection.

Proof. Using cohort notation, write the application of the cohortizer as $C_t = \eta \circ C_{t-2} \oplus \theta \circ C_{t-1}$, where $C_{t-2} \oplus C_{t-1}$ is the concatenation of prior cohorts C_{t-2} and C_{t-1}, and, over which, composition with η, respectively, θ, distributes to each element of the cohort. This gives $C_1 = (I)$, $C_2 = \theta C_1 = \theta \circ (I) = (\theta)$, $C_3 = \eta \circ C_1 \oplus \theta \circ C_2 = \eta \circ (I) \oplus \theta \circ (\theta) = (\eta) \oplus (\theta^2) = (\eta, \theta^2)$, and $C_4 = \eta \circ C_2 \oplus \theta \circ C_3 = \eta \circ (\theta) \oplus \theta \circ (\eta, \theta^2) = (\eta\theta) \oplus (\theta\eta, \theta^2) = (\eta\theta, \theta\eta, \theta^3), \ldots$. Clearly, the repeated application of the cohortizer eventually yields all strings of any number of symbols θ, η, thus generating $\{\theta, \eta\}^\star$.

Moreover, for the initial cohorts, $N_0(C_1) = (N_0(I)) = (0)$, $N_0(C_2) = (N_0(\theta)) = (1)$, $N_0(C_3) = (N_0(\eta), N_0(\theta^2)) = (2, 3)$, $N_0(C_4) = (N_0(\eta\theta), N_0(\theta\eta), N_0(\theta^3)) = (4, 5, 6), \ldots$, so that the value of $N_0(f)$ increases by 1 between successive elements of initial cohorts.

Suppose this continues so that $C_{t-2} = (f_{F_{t-1}}, \ldots, f_{F_t-1})$ satisfies $N_0(C_{t-2}) = (F_{t-1} - 1, \ldots, F_t - 2)$ and $C_{t-1} = (f_{F_t}, \ldots, f_{F_{t+1}-1})$ satisfies $N_0(C_{t-1}) = (F_t - 1, \ldots, F_{t+1} - 2)$. From this hypothesis, induce that $C_t = (f_{F_{t+1}}, \ldots, f_{F_{t+2}-1})$ satisfies $N_0(C_t) = (F_{t+1} - 1, \ldots, F_{t+2} - 2)$, as follows.

Under the cohort structure described, $C_t = \eta\circ C_{t-2} \oplus \theta\circ C_{t-1} = (\eta\circ f_{F_{t-1}}, \ldots, \eta\circ f_{F_t-1}, \theta \circ f_{F_t}, \ldots, \theta \circ f_{F_{t+1}-1})$. Moreover, using Proposition 4.24, identify that $p(C_{t-2}) = t - 3$ and $p(C_{t-1}) = t - 2$, (where p is taken as the degree of any composition in the cohort), and observe that $N_1(f) = F_{p(f)+2}$ and $N_2(f) = F_{p(f)+1}$.

The left subcohort of C_t comprises elements ηf, where $f \in C_{t-2}$ and $N_0(\eta f) = N_0(f)+N_1(f)+N_2(f) = N_0(f)+F_{p(f)+2}+F_{p(f)+1} = N_0(f)+F_{p(f)+3} = N_0(f)+F_t$. The right subcohort of C_t comprises elements θf, where $f \in C_{t-1}$ and $N_0(\theta f) = N_0(f)+N_1(f) = N_0(f)+F_{p(f)+2} = N_0(f)+F_t$. Combining the two subcohorts gives $N_0(C_t) = \big(N_0(f_{F_{t-1}})+F_t, \ldots, N_0(f_{F_t-1})+F_t,\ \ N_0(f_{F_t})+F_t, \ldots, N_0(f_{F_{t+1}-1})+F_t\big)$ $= (F_{t-1}-1+F_t, \ldots, F_t-2+F_t, F_t-1+F_t, \ldots, F_{t+1}-2+F_t) = (F_{t+1}+1, \ldots, 2F_t-2,$ $2F_t - 1, \ldots, F_{t+2} - 2)$, as desired. □

Proposition 5.4 described a 2–1-Fibonacci outer cohort structure on the free monoid $\{\theta, \eta\}^\star$. Corollary 5.5 uses this result to characterize the cohortizer that places the set of equivalence classes$\{\theta, \eta\}^\star / \theta^\star\circ$, into the 1–2-Fibonacci outer cohort structure.

Corollary 5.5 (Cohort sequence for equivalence classes $f/\theta^\star\circ$ of $\{\theta, \eta\}^\star$)**.** *Consider the free monoid $\{\theta, \eta\}^\star$ on generating set $\{\theta, \eta\}$ under composition. The equivalence classes modulo application of $\theta^\star$ on the outside form a 1–2-Fibonacci outer cohort sequence of functions (by left infix) from the 1st cohort $D_1 = (\theta^\star\eta) \equiv (L)$ under cohortizer $\langle L\theta\circ, L\eta\circ\rangle(f/L\circ)$, which has the action $f \mapsto \langle L\theta \circ (f/L\circ), L\eta \circ (f/L\circ)\rangle$. The notation indicates the application of θ or η immediately inside L, and the repeated application of the cohortizer provides a total order of $\{\theta, \eta\}^\star/\theta^\star\circ$ (Table 16).*

Moreover, between representatives of consecutive classes in this totally ordered set, the value of $N_{-1}(S)$ increases by 1. Corollary 4.39 previously showed this map to be a bijection.

Proof. Proposition 5.4, placed the set of functions $f \in \{\theta, \eta\}^\star$ into a 2–1-Fibonacci cohort sequence from the 1st cohort under $\langle\eta\circ, \theta\circ\rangle$. In particular, elements of its left subcohorts begin with prefix η and elements of its right subcohorts begin with prefix θ. Thus, the set meets conditions for the application of Proposition 5.1(a), with $f_L = \eta$ and $f_R = \theta$.

Consequently, Proposition 5.1(a) shows the set of standard class representatives $g = \eta \circ (f/L\circ)$ to form a 1–2-Fibonacci cohort sequence of functions by left infix, with $f_L = L = \eta$, and $f_R = \theta$ under cohortizer $\langle\eta\theta\circ, \eta^2\rangle$ $(g/\eta\circ)$ from the 0th cohort $D_0 = (I)$, with $D_1 = (f_L \circ I) = (\eta)$, $D_2 = (f_L f_R \circ (\eta/f_L\circ)) = (\eta\theta)$, $D_3 = (f_L f_R\circ(\eta\theta/f_L\circ), f_L^2\circ(\eta/f_L\circ)) = (\eta\theta^2, \eta^2)$, and so forth, where each function g_n for $n > 0$ begins in prefix $f_L = \eta$, as desired. (Once again, D temporarily refers to cohorts of class representatives rather than of the classes themselves.)

To show that the value of $N_{-1}(g)$ increases by 1 between representatives g_n of consecutive classes, examine the initial cohorts, $N_{-1}(D_0) = (N_{-1}(I)) = (1)$, $N_{-1}(D_1) = (N_{-1}(\eta)) = (2)$, $N_{-1}(D_2) = (N_{-1}(\eta\theta)) = (3)$, $N_{-1}(D_3) = (N_{-1}(\eta\theta^2)$, $N_{-1}(\eta^2)) = (4, 5)$, $N_{-1}(D_4) = (N_{-1}(\eta\theta^3), N_{-1}(\eta\theta\eta), N_{-1}(\eta^2\theta)) = (6, 7, 8), \ldots$. For these initial cohorts, $N_{-1}(g)$ indeed increases by 1 between consecutive elements g_n.

Suppose the progression continues such that $D_{t-2} = (g_{F_{t-1}}, \ldots, g_{F_t-1})$ satisfies $N_{-1}(D_{t-2}) = (F_{t-1}+1, \ldots, F_t)$ and $D_{t-1} = (g_{F_t}, \ldots, g_{F_{t+1}-1})$ satisfies $N_{-1}(D_{t-1})$ $= (F_t + 1, \ldots, F_{t+1})$. From this hypothesis, induce that $D_t = (g_{F_{t+1}}, \ldots, g_{F_{t+2}-1})$ satisfies $N_{-1}(D_t) = (F_{t+1} + 1, \ldots, F_{t+2})$, as follows.

Recall from Proposition 4.36(a) that $F_{p_\star} < N_{-1}(S) \leq F_{p_\star+1}$. By hypothesis, then, $p_\star(D_{t-2}) = t - 1$ and $p_\star(D_{t-1}) = t$ (where $p_\star$ is taken as the reduced degree of any composition in the cohort). Also recall that each function g_n for $n > 0$ begins with prefix $f_L = \eta$ and that Proposition 4.36(b) gives $N_{-1}(\eta\theta(g/\eta\circ)) = N_{-1}(g) + F_{p_\star(g)-1}$ and $N_{-1}(\eta^2(g/\eta\circ)) = N_{-1}(g) + F_{p_\star(g)+2}$.

Under the cohort structure described, $D_t = \eta\theta(D_{t-1}/\eta\circ) \oplus \eta^2(D_{t-2}/\eta\circ)$. The left subcohort of D_t comprises elements $\eta\theta(g/\eta\circ)$, where $g \in D_{t-2}$ and N_{-1} $(\eta\theta(g/\eta\circ)) = N_{-1}(g) + F_{p_\star(g)-1} = N_{-1}(g) + F_{t-1}$. The right subcohort of D_t comprises elements $\eta^2(g/\eta\circ)$, where $g \in C_{t-1}$ and $N_{-1}(\eta^2(g/\eta\circ)) = N_{-1}(g) + F_{p_\star(g)+2}$ $= N_{-1}(g) + F_{t+1}$.

Combining the two subcohorts gives $N_{-1}(D_t) = [N_{-1}(D_{t-1}) + F_{t-1}] \oplus [N_{-1}$ $(D_{t-2}) + F_{t+1}] = (F_t + 1 + F_{t-1}, \ldots, F_{t+1} + F_{t-1}, F_{t-1} + 1 + F_{t+1}, \ldots, F_t + F_{t+1})$

$= (F_{t+1}+1, \ldots, F_{t+1}+F_{t-1},\ F_{t+1}+F_{t-1}+1, \ldots, F_{t+2})$, as desired, showing that the progression noted above continues for the standard class representatives.

To complete the proof, it suffices to observe that all representatives g of the same class $\theta^\star g$ have the same value of $N_{-1}(g)$. Recall that -1 is a fixed point of θ, since $\theta(-1) = -1$, and, further, that -1 is not an attractor for θ, since the neighboring value -2 is also a fixed point: $\theta(-2) = -2$. Therefore, $N_{-1}(L(g/\eta\circ)) = N_{-1}(\theta^\star g) = N_{-1}(g)$. Clearly, modifying the cohortizer to $\langle L\theta\circ, L\eta\circ\rangle\ (f/L\circ)$ generates these classes in order, for which the substitution of η for L returns the standard representative g. Thus D can refer to cohorts of classes, so that the classes form a 1–2-Fibonacci cohort sequence by left infix, with $f_L = \theta$, $f_R = \eta$ and $L = \theta^\star\eta$.

As claimed, the recursion begins only with the 1^{st} cohort. Although the 0^{th} class $\theta^\star$ does satisfy $N_{-1}(\theta^\star) = 1$, it does not relate to the 1^{st} cohort L in the way the definition prescribes, that is, $L \neq \eta\theta^\star$. □

As an application of this more abstract approach, the main results of Sections 4.1.5 and 4.1.6 could have used the following lemmas about subcohorts.

Lemma 5.6 (Cohort and subcohort of composition $S \in \{\kappa, \lambda\}^\star$)**.** *Suppose that composition S lies in cohort C_{p+1} of the 1–2-Fibonacci cohort tableau, Table 10, and refer to Definition 4.5.*

(a): *For $p(S) \geq 1$, consider that either $S = R\kappa$ or $S = R\lambda$, for some composition R lying in a previous cohort. Then, in the former case, S lies in the left subcohort of cohort C_{p+1}, while in the latter case, S lies in the right subcohort of cohort C_{p+1}.*

(b): *For $p(S) \geq 0$, whereas S resides in C_{p+1}, $S\kappa$ lies in the left subcohort of cohort C_{p+2}, with $S\kappa(2) - S(2) = F_{p+1}$, while $S\lambda$ lies in the right subcohort of cohort C_{p+3}, with $S\lambda(2) - S(2) = F_{p+4}$.*

*Proof of **(b)** (Proof of **(a)** follows by a simple change of index):* The proof will reference the cohort structure of Table 10 whose formal proof defers to Proposition 5.2. In particular, from the proof of Corollary 4.8, S lies in cohort C_{p+1}, where $p = p(S)$.

In the case of $S\kappa$, the length of cohort C_{p+1} is F_{p+1}, precisely equal to the stated displacement within the tableau between $S(2)$ and $S\kappa(2)$, placing the latter in the left subcohort of cohort C_{p+2}.

In the case of $S\lambda$, the combined length of cohorts C_{p+1}, C_{p+2}, and the left subcohort of C_{p+3} is $F_{p+1} + 2F_{p+2} = F_{p+4}$, precisely equal to the stated displacement within the tableau between $S(2)$ and $S\lambda(2)$, placing the latter in the right subcohort of cohort C_{p+3}. □

Lemma 5.7 (Cohort and subcohort of class $S \in \{\kappa, \lambda\}^\star/\circ\,\kappa^\star$)**.** *Suppose that class $S = S'M$ lies in cohort $C_{p_\star - 1}$ of Table 11 and refer to Definition 4.5.*

(a): *For $p_\star(S) \geq 2$, consider that either $S'M = R'\kappa M$ or $S'M = R'\lambda M$, for some class $R'M$ lying in a previous cohort. Then, in the former case, S lies in the left subcohort of cohort $C_{p_\star - 1}$, while in the latter case, S lies in the right subcohort of cohort $C_{p_\star - 1}$.*

(b): *For $p_\star(S) \geq 0$, $S'\kappa M$ lies in the left subcohort of cohort $C_{p_\star}$, with $S'\kappa M(1) - S'M(1) = S'\kappa(2) - S'(2) = F_{p_\star - 1}$, while $S'\lambda M$ lies in the right subcohort of cohort $C_{p_\star + 1}$, with $S'\lambda M(1) - S'M(1) = S'\lambda(2) - S'(2) = F_{p_\star + 2}$.*

*Proof of **(a)** (Proof of **(b)** follows by a simple change of index):* The proof will reference the cohort structure of Table 11, whose formal proof defers to Corollary 5.3.

The proof of Corollary 4.8 specifically treated $S = S'M$ lying in cohort $C_{p_\star-1}$, considering the cases $S'M = R'\kappa M$ and $S' = R'\lambda M$.

In the former case, $R = R'M$ lies in cohort $C_{p_\star-2}$, whose length is $|C_{p_\star-2}| = F_{p_\star-2}$. In this case, the algorithm increments the value of $S(1)$ by $F_{t_2} = F_{t_1-1} = F_{p_\star-2}$, precisely the displacement within the tableau between $R'_2 = R'M(1)$ and $S'_2 = S'M(1)$, placing the latter in the left subcohort of cohort $C_{p_\star-1}$.

In the latter case, $R = R'M$ lies in cohort $C_{p_\star-3}$, whose length is $|C_{p_\star-3}| = F_{p_\star-3}$. In this case, the algorithm increments the value of $S(1)$ by $F_{t_2+3} = F_{t_1+1} = F_{p_\star}$, precisely the displacement within the tableau between $R'_2 = R'M(1)$ and $S'_2 = S'M(1)$. Now the displacement $F_{p_\star} = F_{p_\star-2} + F_{p_\star-1}$ equals the combined lengths of cohorts $C_{p_\star-2}$ and $C_{p_\star-1}$, placing $S'_2 = S'M(1)$ in the right subcohort of cohort $C_{p_\star-1}$. □

Lemma 5.8 (Cohort and subcohort of composition $S \in \{\theta, \eta\}^\star$)**.** *Suppose that composition S lies in cohort C_{p+1} of the 2–1-Fibonacci cohort tableau, Table 13, and refer to Definition 4.6.*

(a): *For $p(S) \geq 1$, consider that either $S = \theta R$ or $S = \eta R$, for some composition R lying in a previous cohort. Then, in the former case, S lies in the right subcohort of cohort C_{p+1}, while in the latter case, S lies in the left subcohort of cohort C_{p+1}.*

(b): *For $p(S) \geq 0$, θS lies in the right subcohort of cohort C_{p+2}, with $N_0(\theta S) - N_0(R) = F_{p+2}$, while ηS lies in the left subcohort of cohort C_{p+3}, with $N_0(\eta S) - N_0(S) = F_{p+3}$.*

*Proof of **(b)** (Proof of **(a)** follows by a simple change of index):* The proof will reference the cohort structure of Table 11 whose formal proof defers to Proposition 5.4. In particular, from the proof of Proposition 4.25, S lies in cohort C_{p+1}, where $p = p(S)$.

In the case of θS, the length of cohort C_{p+2} is F_{p+2}, precisely equal to the stated displacement within the tableau between $N_0(S)$ and $N_0(\theta S)$, placing the latter in the right subcohort of cohort C_{p+2}.

In the case of ηS, the combined length of cohorts C_{p+1} and C_{p+2} is F_{p+3}, precisely equal to the stated displacement within the tableau between $N_0(S)$ and $N_0(\eta S)$, placing the latter in the left subcohort of cohort C_{p+3}. □

Lemma 5.9 (Cohort and subcohort of class $S/\theta^\star\circ \in \{\theta, \eta\}^\star/\theta^\star\circ$)**.** *Suppose that class $S = LS'$ lies in cohort $C_{p_\star-1}$ of the 1–2-Fibonacci cohort tableau, Table 16, and refer to Definition 4.5.*

(a): *For $p_\star(S) \geq 2$, consider that either $LS' = L\theta R'$ or $LS' = L\eta R'$, for some class LR' lying in a previous cohort. Then, in the former case, S lies in the left subcohort of cohort $C_{p_\star-1}$, while in the latter case, S lies in the right subcohort of cohort $C_{p_\star-1}$.*

(b): *For $p_\star(S) \geq 0$, $L\theta S'$ lies in the left subcohort of cohort $C_{p_\star}$, with $N_{-1}(L\theta S') - N_{-1}(LS') = F_{p_\star-1}$, while $L\eta S'$ lies in the right subcohort of cohort $C_{p_\star+1}$, with $N_{-1}(L\eta S') - N_{-1}(LS') = F_{p_\star+2}$.*

Proof. The proof will reference the cohort structure of Table 16, whose formal proof defers to Corollary 5.5. In all other aspects, the proof is analogous to that of Lemma 5.7, using Propositions 4.36 and 4.38. □

6. Fibonacci Numeration and Binary Trees

6.1. **Fibonacci expansions, successors, and gaps.** The following discussion will reference three (3) expansions of an integer by Fibonacci numbers:

- The minimal or greedy representation,
- the lazy Fibonacci representation, and the
- *maximal Fibonacci expansion.*

The minimal and lazy representations follow their historical definitions, whereas the following defines the maximal Fibonacci expansion.

Definition 6.1. (Maximal Fibonacci Expansion) The maximal Fibonacci expansion of $n \in \mathbb{Z}_+$ as $n = \sum_{i=1}^{r} \varepsilon_i F_i$, (where $\varepsilon_i \in \{0, 1\}$, $i = 1, \ldots, r$), *maximizes* the sum of coefficients $\sum_{i=1}^{r} \varepsilon_i$ while allowing both $\varepsilon_1 = 1$ and $\varepsilon_2 = 1$. When it requires just one of F_1 or F_2, the expansion uses F_1 by convention, that is, $\varepsilon_1 = 1$ and $\varepsilon_2 = 0$. As a convention, take the maximal expansion of zero to be the empty sum $\varepsilon_i = 0$, $\forall i$.

The lazy Fibonacci representation (Sloane's 104326) has a long history [1], [3], [6], [14], [13], [21], [26], [42], and has also been called "maximal Fibonacci *bit* representation" and "dual Fibonacci representation." By contrast, the maximal *expansion*, although unique as given by Definition 6.1, is not a "representation" in the usual sense, since it allows both ε_1 and ε_2 — two bits corresponding to elements F_1 and F_2 of equal value — to be nonzero, rather than using a basis comprised of distinct elements. The maximal expansion obtains directly from the lazy expansion, however.

Remark 6.1. The maximal expansion of n obtains by prepending F_1 to the lazy Fibonacci representation of $n - 1$ (50). It follows that the maximal expansion of $n \geq 1$ always includes F_1 (and may include F_2, as well). Thus for $n \geq 1$, $\varepsilon_1 \equiv 1$ in Definition 6.1. Since the lazy Fibonacci representation never includes F_1, the existence and uniqueness of the maximal expansion follow immediately from those of the lazy Fibonacci representation, the latter established by Brown [6].

Definition 6.2. Writing a Fibonacci expansion as $n = \sum_{j=1}^{s} F_{t_j}$, with $1 \leq t_1 < t_2 < \cdots < t_s$, define the *Fibonacci indices* of n as the tuple of indices $(t_1, t_2, \ldots, t_s)$ of Fibonacci numbers in the expansion.

Remark 6.2. The paper employs the convention of writing indices from smallest (on the left), rightward to the greatest because Proposition 7.5 will identify these indices with a "genealogy" $v_{n,k}$ that lists in order the sequence of replications used to place a particular square $S_{n,k}$ in the quilt, according to the construction method described in Part 1 of the paper [38]. The tuple of indices may also be written as the word $t_1 t_2 \cdots t_s$. For convenience, let $\mathbf{f}(n)$, $\mathbf{F}(n)$ and $\mathbf{F}_\star(n)$ produce the Fibonacci indices for the minimal representation, lazy representation and maximal expansion, respectively, of integer n.

When using a binary word to display the indices, the paper distinguishes between "Zeckendorf binary notation," using bits $F_2 F_3 F_4 \cdots$ and "maximal Fibonacci binary notation," using bits $F_1 F_2 F_3 \cdots$. Both employ 1s at bits $t_1, t_2, \ldots, t_s$ and 0s for all other bits, the zero bits being $\{2, \ldots, t_s\} \setminus \{t_1, \ldots, t_s\}$ in the case of Zeckendorf binary and $\{1, \ldots, t_s\} \setminus \{t_1, \ldots, t_s\}$ in the case of maximal Fibonacci binary.

When juxtaposing tuples, to avoid confusion between parenthesis that indicate tuples and those indicating the argument of a function, the discussion uses $C \oplus D \equiv CD$ interchangeably. In this context, the use of "direct sum" $\oplus$ provides a reasonable notation for juxtaposition of tuples, since the tuples $\mathbf{f}(n)$, $\mathbf{F}(n)$, $\mathbf{F}_\star(n)$ refer to spaces spanned by basis elements F_i (Remark 6.1).

Using the notation introduced by Remark 6.2, observe that Definition 6.1 of maximal expansion reads (in terms of lazy representation):

$$\mathbf{F}_\star(n) \equiv (1) \oplus \mathbf{F}(n-1). \tag{50}$$

Definition 6.3. Further, with respect to Fibonacci indices, define the *Fibonacci gaps* of integer n to be the tuple of differences

$$(\partial_1, \ldots, \partial_r) = \begin{cases} (), & t_1 = 1, s = 1; \\ (t_2 - t_1, t_3 - t_2, \ldots, t_s - t_{s-1}), & t_1 = 1, s > 1; \\ (t_1, t_2 - t_1, t_3 - t_2, \ldots, t_s - t_{s-1}), & t_1 > 1, s \geqslant 1. \end{cases}$$

The tuple of gaps may also be written as the word $\partial_1 \cdots \partial_r$.

Remark 6.3. To match the definition of Fibonacci indices given by Definition 6.2, the Fibonacci gaps of Definition 6.3 also run from the least significant index (on the left), rightward to the most significant, when taking the differences of successive indices. Clearly, the cases in Definition 6.3 are crafted to encompass all three expansions.

For convenience, let $\boldsymbol{\partial}(n)$, $\boldsymbol{\nabla}(n)$ and $\boldsymbol{\nabla}_\star(n)$ produce the tuple of Fibonacci gaps for the minimal representation, lazy representation and maximal expansion, respectively, of integer n. In the notation previously defined, Definition 6.3 of gaps becomes $\boldsymbol{\partial}(n) = \mathbf{f}(n) - [(0) \oplus \mathbf{f}(n) \setminus t_s]$, $\boldsymbol{\nabla}(n) = \mathbf{F}(n) - [(0) \oplus \mathbf{F}(n) \setminus t_s]$, and $\boldsymbol{\nabla}_\star(n) = [\mathbf{F}_\star(n) \ominus (t_1)] - [\mathbf{F}_\star(n) \setminus t_s]$, where the latter gives the empty tuple $\boldsymbol{\nabla}_\star(1) = ()$ for $n = 1$ since $\mathbf{F}_\star(1) = (1)$. In regard to the cardinality r of the tuple in Definition 6.3, observe that $|\boldsymbol{\nabla}_\star(n)| = s - 1$, while $|\boldsymbol{\partial}(n)| = s$ and $|\boldsymbol{\nabla}(n)| = s$.

Definition 6.4 (Fibonacci Successor and Predecessor)**.** Let $n = \sum_j F_{t_j}$ be a Zeckendorf representation, (*e.g.*, minimal or lazy), of integer n. Then, the *Fibonacci successor function* σ assigns a successor $\sigma(n) = \sum_j F_{t_j+1}$ to n. By extension, let $\sigma_\star$ denote the successor computed from maximal expansion.

Likewise, the *Fibonacci predecessor function* $\sigma^{-1}(n) = \sum_{\{j | t_j - 1 \geq 1\}} F_{t_j - 1}$ assigns a predecessor to integer n. Let $\sigma_\star^{-1}$ denote the predecessor computed from maximal expansion.

The following discussion requires a few identities involving Fibonacci successors.

Lemma 6.1. *Properties of Fibonacci successors*

$$\begin{aligned} \sigma(n) &= \lfloor (n+1)\phi^2 \rfloor - (n+1) - 1 \\ &= \lfloor (n+1)\phi \rfloor - 1 \\ &= \lfloor (n+1)/\phi \rfloor + (n+1) - 1 \\ &= \lfloor (n+1)/\phi \rfloor + n = \kappa(n+1) - 1, n = 1, 2, \ldots; \end{aligned} \tag{51}$$

$$\sigma^p(n) = F_p \sigma(n) + F_{p-1} n. \tag{52}$$

Proof. For (51), see entry for 022342 in [41]. For (52), see [8]. □

Remark 6.4. Note that for $p = 2$ in particular, (52) can be written $\sigma^2(n) = \lambda(n + 1) - 2$, analogous to the last equality, $\sigma(n) = \kappa(n + 1) - 1$, of (51).

Corollary 6.2 (of Proposition 4.2. Fibonacci cohort sequences and Fibonacci successors)**.** *Combining Lemma 6.1 with the cohort formula (17) for a Fibonacci cohort sequence from the* 1^{st} *cohort under cohortizer* F_{t+p} *with rate* $p \geq 0$ *gives*

$$S_n - S_1 = \sigma^p(n - 1).$$

Remark 6.5. The Fibonacci successor and Fibonacci predecessor of an integer are independent of the choice of *representation* (in a basis of *distinct* Fibonacci numbers [9]). However, different successors or predecessors may arise when computed from maximal expansion. For example, the minimal representation and maximal expansions of "3," respectively F_4 and $F_1 + F_3$ equal one another, but their respective successors $\sigma(3) = F_5 \neq F_2 + F_4 = \sigma_\star(3)$ do not, nor do their respective predecessors $\sigma^{-1}(3) = F_3 \neq F_2 = \sigma_\star^{-1}(3)$. Proposition 6.3 formulates the successor operator computed from maximal expansion.

Proposition 6.3 (Maximal Fibonacci Successors)**.** *For* $p \geq 0$, $\sigma_\star^p(n) = F_p \lfloor n\phi \rfloor + F_{p-1}n - (F_{p+1} - 1)$. *In particular,* $\sigma_\star(n) = \lfloor n\phi \rfloor \equiv \kappa(n)$. *Hence for* $p \geq 0$, *a Fibonacci cohort sequence from the* 1^{st} *cohort under cohortizer* F_{t+p}, *also can be written* $S_n - S_1 = \sigma_\star^p(n) - 1 = \kappa^p(n) - 1$, $n = 1, 2, 3, \ldots$, *the latter formulation given in Corollary 4.15.*

Proof. First note that by the definition of maximal expansion (50), $\sigma_\star(n) = \sigma(n - 1) + 1$. Thus, by (51), $\sigma_\star(n) = \sigma(n - 1) + 1 = \lfloor ((n - 1) + 1)/\phi \rfloor + (n - 1) + 1 = \lfloor n/\phi \rfloor + n = \lfloor n\phi \rfloor$. Next, using $\sigma^2(n) = \sigma(n) + n$, the particular case of (52) for $p = 2$ gives

$$\begin{aligned}
\sigma_\star^2(n) &= \sigma_\star(\sigma(n - 1) + 1) \\
&= \sigma((\sigma(n - 1) + 1) - 1) + 1 \\
&= \sigma(\sigma(n - 1)) + 1 \\
&= \sigma^2(n - 1) + 1 \\
&= \sigma(n - 1) + n \\
&= \sigma_\star(n) + n - 1
\end{aligned}$$

Continue this reasoning to powers $p > 2$, to obtain $\sigma_\star^p(n) = \kappa^p(n) = F_p\sigma_\star(n) + F_{p-1}n - (F_{p+1} - 1)$. □

Remark 6.6. Note, in particular, that for $p = 2$, the result of Proposition 6.3 can be written $\sigma_\star^2(n) = \lambda(n) - 1$, analogous to the equality, $\sigma_\star(n) = \kappa(n)$.

With the maximal Fibonacci successor and predecessor introduced, the following corollary revisits the cohort formula (1) for the quilt interspersion array (Tables 1(a) and 4, top right).

Corollary 6.4 (Maximal Fibonacci successors and the quilt interspersion)**.** *Combining Proposition 6.3 with Proposition 3.2 gives, among other relations:*

$$\begin{aligned}
\sigma_\star^k(n) &= a_{n,k-1} - 2(F_{k+1} - 1), \text{ and, conversely,} \\
a_{n,k} &= \sigma_\star^{k+1}(n) + 2(F_{k+2} - 1).
\end{aligned} \tag{53}$$

Corollary 6.2 suggests that, via successors, Fibonacci cohort sequences also relate to the *Fibonacci Multiplication* of two nonnegative integers as defined by Knuth [25], which uses the minimal Fibonacci representation of the two multiplicands.

Proposition 6.5 (Cohort sequences and Knuth's Fibonacci multiplication)**.** *Let* $\circledcirc$ *denote* Fibonacci Multiplication *in the sense of Knuth [25]. Consider* S_n*, a (2–1-) Fibonacci cohort sequence from the* 1^{st} *cohort under cohortizer* F_{t+p}*,* $p \geq 0$*, with first element* S_1*. Then,* $n \geq 1$*,*

$$S_n = \begin{cases} S_1 + (n-1) \circledcirc F_p + (n-1), & p = 0; \\ S_1 + (n-1) \circledcirc F_p - (n-1), & p = 1; \\ S_1 + (n-1) \circledcirc F_p, & p \geqslant 2. \end{cases}$$

Proof. In all three cases, setting $n = 1$ yields S_1, as desired.

For $p = 0$, both $S_1 + (n-1) \circledcirc F_p + (n-1)$, above, and the right hand side of (16) reduce to $S_1 + (n-1)$.

Now for $p \geq 2$ and $n \geq 2$, $S_1 + (n-1) \circledcirc F_p = S_1 + \sigma^p(n-1)$, for which (52) gives $S_1 + \sigma^p(n-1) = S_1 + F_p\sigma(n-1) + F_{p-1}(n-1)$. By (51), this becomes $S_1 + F_p[(n-1) + \lfloor n/\phi \rfloor] + F_{p-1}(n-1) = S_1 + F_p \lfloor n/\phi \rfloor + F_{p+1}(n-1)$, identical to the right hand side of (16).

Finally, for $p = 1$ and $n \geq 2$, $S_1 + (n-1) \circledcirc F_1 - (n-1) = S_1 + (n-1) \circledcirc 1 - (n-1) = S_1 + (n-1) \circledcirc F_2 - (n-1)$, where the latter identity follows from the fact that the Zeckendorf representation does not use F_1. Hence, even when $p = 1$, the product $(n-1) \circledcirc F_1$ still equals $\sigma^2(n-1)$. Thus, for $p = 1$, the formula gives $S_n = S_1 + \sigma^2(n-1) - (n-1) = S_1 + \sigma(n-1) = S_1 + (n-1) + \lfloor n/\phi \rfloor$, identical to the right hand side of (16) for $p = 1$. □

Lemma 6.6 (Linearity of p^{th} successor on a line segment)**.** *For integers* $p \geq 0$*,* $t \geq 2$ *and* $m \in [-F_t, F_{t+1} - 2]$*, let* $x = F_t + m$ *and* $y = F_{t+1} - 2 - m$*. Then*

$$\sigma^p(x) + \sigma^p(y) = \sigma^p(x+y) = F_{t+p+2} - F_{p+3}.$$

For $p = 1$ *and* $p = 2$ *in particular,*

$$\sigma(F_t + m) + \sigma(F_{t+1} - 2 - m) = \sigma(F_{t+2} - 2) = F_{t+3} - 3, \quad \text{for } t \geq 2, m = -F_t, \ldots, F_{t+1} - 2; \tag{54}$$

$$\sigma^2(F_{u-1} + n) + \sigma^2(F_u - 2 - n) = \sigma^2(F_{u+1} - 2) = F_{u+3} - 5, \quad \text{for } u \geq 3, n = -F_{u-1}, \ldots, F_u - 2; \tag{55}$$

which can be written, respectively, as

$$\kappa(F_t + m + 1) + \kappa(F_{t+1} - 1 - m) = F_{t+3} - 1, \quad \text{for } t \geq 2, m = -F_t, \ldots, F_{t+1} - 2; \tag{56}$$

$$\lambda(F_{u-1} + n + 1) + \lambda(F_u - 1 - n) = F_{u+3} - 1, \quad \text{for } u \geq 3, n = -F_{u-1}, \ldots, F_u - 2. \tag{57}$$

Proof. For the first equality, $\sigma^p(x) + \sigma^p(y) = \sigma^p(x+y)$, it suffices to show that x and y have Fibonacci representations with no common bits. To this end, consider the parameter m in three separate intervals: $m \in [-F_t, -1]$, $m \in [0, F_{t-1} - 1]$, and $m \in [F_{t-1}, F_{t+1} - 2]$.

For $m \in [-F_t, -1]$, $x = F_t + m \in [0, F_t - 1] = [0,\ \ F_{t-1} + F_{t-3} + F_{t-5} + \cdots]$ and $y = F_{t+1} - 2 - m \in [F_{t+2} - 2, F_{t+1} - 1] = [F_t + F_{t-1} + F_{t-2} + \cdots,$ $F_t + F_{t-2} + F_{t-4} + \cdots]$. At both ends of the interval, the representations of x and y share no bits. Moreover, since the sum $x+y = F_{t+2}-2$ remains constant, the bits added to increase x over the interval can simply be removed from the representation $F_t + F_{t-1} + F_{t-2} + \cdots$ to decrease y, so that at each value of $m \in [-F_t, -1]$ the sets of bits used to represent x and y remain disjoint.

For $m \in [0, F_{t-1} - 1]$, $x = F_t + m \in [F_t, F_{t+1} - 1] = [F_t,\ \ F_t + F_{t-2} + F_{t-4} + \cdots]$ and $y = F_{t+1} - 2 - m \in [F_{t+1} - 2, F_t - 1] = [F_{t-1} + F_{t-2} + F_{t-3} + \cdots,$ $F_{t-1} + F_{t-3} + F_{t-5} + \cdots]$. At both ends of the interval, the representations of x and y share no bits. Moreover, since the sum $x + y = F_{t+2} - 2$ remains constant, the bits added to increase x over the interval can simply be removed from the representation $F_{t-1} + F_{t-2} + F_{t-3} + \cdots$ to decrease y, so that at each value of $m \in [0, F_{t-1} - 1]$ the sets of bits used to represent x and y remain disjoint.

Finally, for $m \in [F_{t-1}, F_{t+1} - 2]$, $x = F_t + m \in [F_{t+1}, F_{t+2} - 2] = [F_{t+1},$ $F_{t+1} + F_t - 2] = [F_{t+1},\ \ F_{t+1} + F_{t-2} + F_{t-3} + F_{t-4} + \cdots]$ and $y = F_{t+1} - 2 - m$ $\in [F_t - 2, 0] = [F_{t-2} + F_{t-3} + F_{t-4} + \cdots,\ \ 0]$. At both ends of the interval, the representations of x and y share no bits. Moreover, since the sum $x + y = F_{t+2} - 2$ remains constant, the bits added to increase x over the interval can simply be removed from the representation $F_{t-2} + F_{t-3} + F_{t-4} + \cdots$ to decrease y, so that at each value of $m \in [F_{t-1}, F_{t+1} - 2]$ the sets of bits used to represent x and y remain disjoint.

For the second equality, represent $x + y = F_{t+2} - 2$ as $F_t + F_{t-1} + F_{t-2} + \cdots$. Thus, the first successor of $x + y$ will lose the bit $t = 2$, the second will be deficient of both $t = 2$ and $t = 3$, and so forth, such that the p^{th} successor will be $F_{t+p+2} - 2 - F_2 - F_3 - F_4 - \cdots - F_{p+1} = F_{t+p+2} - 2 - (F_{p+3} - 2) = F_{t+p+2} - F_{p+3}$, from which (54) and (55) follow.

Formulas (56) and (57) then follow from (54) and (55), respectively, via Lemma 6.1 and change of variable (see also Remark 6.4). □

Lemma 6.7 (Successor Gap Properties)**.**

$$\text{(58)} \qquad \text{++}\boldsymbol{\partial}(n) = \boldsymbol{\partial}(\sigma(n)) \qquad = \boldsymbol{\partial}(\kappa(n+1) - 1),$$

$$\text{(59)} \qquad (2)\boldsymbol{\partial}(n) = \boldsymbol{\partial}(\sigma^2(n) + 1) \ = \boldsymbol{\partial}(\lambda(n+1) - 1),$$

$$\text{(60)} \qquad (1)\boldsymbol{\nabla}_\star(n) = \boldsymbol{\nabla}_\star(\sigma_\star(n) + 1) = \boldsymbol{\nabla}_\star(\kappa(n) + 1),$$

$$\text{(61)} \qquad (2)\boldsymbol{\nabla}_\star(n) = \boldsymbol{\nabla}_\star(\sigma_\star^2(n) + 2) = \boldsymbol{\nabla}_\star(\lambda(n) + 1),$$

and for suitable $U \in \{1, 2\}^\star$ *writing*

$$\boldsymbol{\nabla}_\star(n) \qquad = (2)^h(1)U, \ \textit{implies}$$

$$\text{(62)} \qquad \boldsymbol{\nabla}_\star(\sigma_\star(n)) = \boldsymbol{\nabla}_\star(\kappa(n)) = (11)^h(2)U.$$

Proof. The former equalities (58)–(61) merely take properties of successors discussed above and restate them in terms of gaps. Similarly, for the first equality of (62), consider that $\sigma_\star(n) = \kappa(n)$ (Proposition 6.3).

Now as to the last equality of (62), recall Definition 6.3. In the case $h = 0$, $\boldsymbol{\nabla}_\star(n) = (1)U = (t_2 - t_1, \ldots, t_s - t_{s-1}) = (1, t_3 - 2, t_4 - t_3, \ldots, t_s - t_{s-1})$, so that $\boldsymbol{F}_\star(n) = (t_1, \ldots, t_s) = (1, 2, t_3, \ldots, t_s)$. Thus, $\sigma_\star(n) = F_{t_1+1} + \cdots + F_{t_s+1}$ $= F_2 + F_3 + F_{t_3+1} + \cdots + F_{t_s+1}$, whose maximal Fibonacci indices reduce back

to $\boldsymbol{F}_\star(\sigma_\star(n)) = (1, 3, t_3 + 1, \ldots, t_s + 1)$, corresponding to maximal Fibonacci gaps $\boldsymbol{\nabla}_\star(\sigma_\star(n)) = (2, t_3 - 2, t_4 - t_3, \ldots, t_s - t_{s-1}) = (2)U$, as per (62).

In the case $h \geq 1$, the gaps $\boldsymbol{\nabla}_\star(n) = (2)^h(1)U = (2, \ldots, 2, 1, t_{h+3} - t_{h+2}, \ldots, t_s - t_{s-1})$ imply that $t_i = 2i - 1$, for $i = 1, \ldots, h + 1$, and $t_{h+2} = 2h + 2$, so that $\boldsymbol{F}_\star(n) = (1, 3, 5, \ldots, 2h+1\ 2h+2, t_{h+3}, \ldots, t_s)$. Thus, $\sigma_\star(n) = F_{t_1+1} + \cdots + F_{t_s+1} = F_2 + F_4 + F_6 + \cdots + F_{2h+2} + F_{2h+3} + F_{t_{h+3}+1} + \cdots + F_{t_s+1}$, whose maximal Fibonacci indices reduce back to $\boldsymbol{F}_\star(\sigma_\star(n)) = (1, 2, 3, 4, 5, \ldots, 2h, 2h + 1,\ 2h + 3,\ t_{h+3} + 1, \ldots, t_s + 1)$, corresponding to maximal Fibonacci gaps $\boldsymbol{\nabla}_\star(\sigma_\star(n)) = (1, \ldots, 1,\ 2,\ t_{h+3} - t_{h+2}, \ldots, t_s - t_{s-1}) = (11)^h(2)U$, as per (62). □

6.2. **Self-similarity of maximal Fibonacci expansion.** Ferns [14] observed that for n satisfying $F_t - 1 \leq n < F_{t+1} - 1$, lazy Fibonacci representation of n obtains by appending F_{t-1} to that of $n - F_{t-1}$. In the present notation,

$$\mathbf{F}(n) = \mathbf{F}(n - F_{t-1}) \oplus (t - 1). \tag{63}$$

For the maximal Fibonacci expansion of Definition 6.1, the corresponding observation takes a form that is simpler still (Proposition 6.8).

Proposition 6.8 (Self-similarity of Maximal Fibonacci Expansion)**.** *For integer $t \geq 1$, if integer n satisfies $F_{t+1} \leq n < F_{t+2}$ then the maximal Fibonacci expansion of n satisfies*

$$\mathbf{F}_\star(n) = \mathbf{F}_\star(n - F_t) \oplus (t). \tag{64}$$

Proof. For $t = 1$ the proposition holds, since only $n = 1$ satisfies $F_2 \leq n < F_3$, and since by definition $\mathbf{F}_\star(1 - F_1) = \mathbf{F}_\star(0) = ()$, it implies $\mathbf{F}_\star(1) = (1) = \mathbf{F}_\star(1 - F_1) \oplus (1)$. Next, using strong induction, suppose the proposition true for $n = 1, 2, \ldots, N - 1$, and for integer N satisfying $F_{t+1} \leq N < F_{t+2}$, proceed to show the equivalence of $\mathbf{F}_\star(N)$ and $\mathbf{F}_\star(N - F_t) \oplus (t)$, by showing in particular that "Case (i)" where $t \in \mathbf{F}_\star(N)$ and $t + 1 \notin \mathbf{F}_\star(N)$ must hold, thus contradicting the other conceivable cases.

Case (i): $t \in \mathbf{F}_\star(N)$ and $t + 1 \notin \mathbf{F}_\star(N)$:
Since $N - F_t \leq N - 1$, by hypothesis $\mathbf{F}_\star(N - F_t)$ satisfies (64), so that $\mathbf{F}_\star(N - F_t) = \mathbf{F}_\star(N - F_t - F_{t-1}) \oplus (t - 1)$ proving $t - 1$ to be the largest index in $\mathbf{F}_\star(N - F_t)$ and thus $\mathbf{F}_\star(N) = \mathbf{F}_\star(N - F_t) \oplus (t)$ to be maximal.

Case (ii): $t, t + 1 \notin \mathbf{F}_\star(N)$:
These conditions imply that $\mathbf{max}\ \mathbf{F}_\star(N) \leq t - 1$. Consequently, we have $\sum_{i \in \mathbf{F}_\star(N)} F_i \leq \sum_{i=1}^{t-1} F_i = F_{t+1} - 1 < F_{t+1} \leq N$, contradicting $\sum_{i \in \mathbf{F}_\star(N)} F_i = N$.

Cases (iii)-(iv): For Cases (iii)-(iv), note that $F_{t+1} \leq N < F_{t+2}$ implies $F_{t-1} \leq N - F_t < F_{t+1}$.

Case (iii): $t \notin \mathbf{F}_\star(N)$, $t + 1 \in \mathbf{F}_\star(N)$, and $F_t \leq N - F_t < F_{t+1}$:
Since $N - F_{t+1} \leq N - 1$, the induction hypothesis defines $\mathbf{F}_\star(N - F_{t+1})$ and thus defines $\mathbf{F}_\star(N) = \mathbf{F}_\star(N - F_{t+1}) \oplus (t + 1)$. Also, the condition $F_t \leq N - F_t < F_{t+1}$ likewise implies that $\mathbf{F}_\star(N - F_t) = \mathbf{F}_\star(N - F_t - F_{t-1}) \oplus (t - 1) = \mathbf{F}_\star(N - F_{t+1}) \oplus (t - 1)$. Consequently $\mathbf{F}_\star(N - F_t) \oplus (t) = \mathbf{F}_\star(N - F_{t+1}) \oplus (t - 1, t)$, hence $|\mathbf{F}_\star(N)| = |\mathbf{F}_\star(N - F_{t+1}) \oplus (t + 1)| < |\mathbf{F}_\star(N - F_{t+1}) \oplus (t - 1, t)| = |\mathbf{F}_\star(N - F_t) \oplus (t)|$, contradicting $\mathbf{F}_\star(N)$ maximal.

Case (iv): $t \notin \mathbf{F}_\star(N)$, $t + 1 \in \mathbf{F}_\star(N)$, and $F_{t-1} \leq N - F_t < F_t$:
The condition $N - F_t < F_t$ implies $N - F_{t+1} < F_{t-2}$ and thus $t - 1 \notin$

$\mathbf{F}_\star(N) \ominus (t+1)$. However, this, together with $t \notin \mathbf{F}_\star(N)$, implies that the pair $(t-1, t)$ could replace $t+1$ in $\mathbf{F}_\star(N)$, again contradicting $\mathbf{F}_\star(N)$ maximal.

□

Remark 6.7 (Largest Fibonacci number in Maximal Expansion). Consider the proof of Proposition 6.8. In particular, since **Case (i)** holds,

$$F_{F^{-1}(n)} \notin \mathbf{F}_\star(n) \text{ and } F_{F^{-1}(n)-1} \in \mathbf{F}_\star(n). \tag{65}$$

As a restatement of (65), for n satisfying $F_t \leq n < F_{t+1}$, $|\mathbf{F}_\star(n)|_\infty = t-1$. As a further restatement of (65) in words, the largest Fibonacci index in the maximal expansion of n is $F^{-1}(n) - 1$. Since this expansion does not skip any two consecutive Fibonacci indices, we can increment the expansion stepwise by either of two procedures: Appending F_t to the expansion, or appending F_{t+1} to the expansion. Performing the two procedures repeatedly, writing the result of the former (latter) procedure to the left (right) child of n, gives the tree, Figure 13. Observe that both left and right branching increases the number of addends by one, thus balancing the number of addends of all nodes on the same level of the tree. Listing in series the number of addends in maximal Fibonacci expansion for integers in the tree going from left to right on each successive level gives 070939, whereas, as the caption notes, 200648_{n+1} gives the number of addends used to expand n.

Now, recall that by Lemma 4.27(b), a left, respectively, right branch of the maximal Fibonacci tree, Figure 8, corresponds to the addition of F_t, respectively, F_{t+1} to the parent node n, where $F_t \leq n < F_{t+1}$. This shows the equivalence of the trees, Figures 8 and 13.

The existence of this rooted tree indicates that the maximal expansion is a closer analog to minimal representation than the lazy representation. Using self-similarity to express the maximal expansion allows the positive integers to be positioned in a single binary tree, Figure 8, in contrast to the two separate binary trees needed for the lazy Fibonacci representation (see the entry for 095903 in [41]). Remark 6.8 further explores the analogy between maximal expansion and minimal representation.

For n satisfying $F_t \leq n < F_{t+1}$, the left child $n + F_t$ and the right child $n + F_{t+1}$ expand neatly as $\mathbf{F}_\star(n+F_t) = \mathbf{F}_\star(n) \oplus (t)$, respectively, $\mathbf{F}_\star(n+F_{t+1}) = \mathbf{F}_\star(n) \oplus (t+1)$. Thus, in terms of gaps, we may write the branching rule, for $F_t \leq n < F_{t+1}$, as

$$\begin{aligned} \boldsymbol{\nabla}_\star(n) \oplus (1) &= \boldsymbol{\nabla}_\star(n + F_t), \\ \boldsymbol{\nabla}_\star(n) \oplus (2) &= \boldsymbol{\nabla}_\star(n + F_{t+1}), \end{aligned} \tag{66}$$

as shown in Figure 17(iv).

Considering the nodal position of n in the tree, it follows that if 1's and 2's are used to encode the sequence of left and right branchings, respectively, required to reach n from the root node 1, then the tuple of 1's and 2's that encode node n is precisely $\boldsymbol{\nabla}_\star(n)$.

In particular, at each level ℓ of the tree, gaps $\boldsymbol{\nabla}_\star(n)$ for integers on that level of the tree from left to right are indeed the tuples $(1,2)^{\ell-1}$ written in lexicographic order, where $(1,2)^\ell$ indicates all ℓ-tuples on $\{1,2\}$. For example, the third level of the tree comprises elements $(4,5,6,8)$, which have maximal Fibonacci indices $(\mathbf{F}_\star(4), \mathbf{F}_\star(5), \mathbf{F}_\star(6), \mathbf{F}_\star(8)) = ((1,2,3), (1,2,4), (1,3,4), (1,3,5))$, and which exhibit

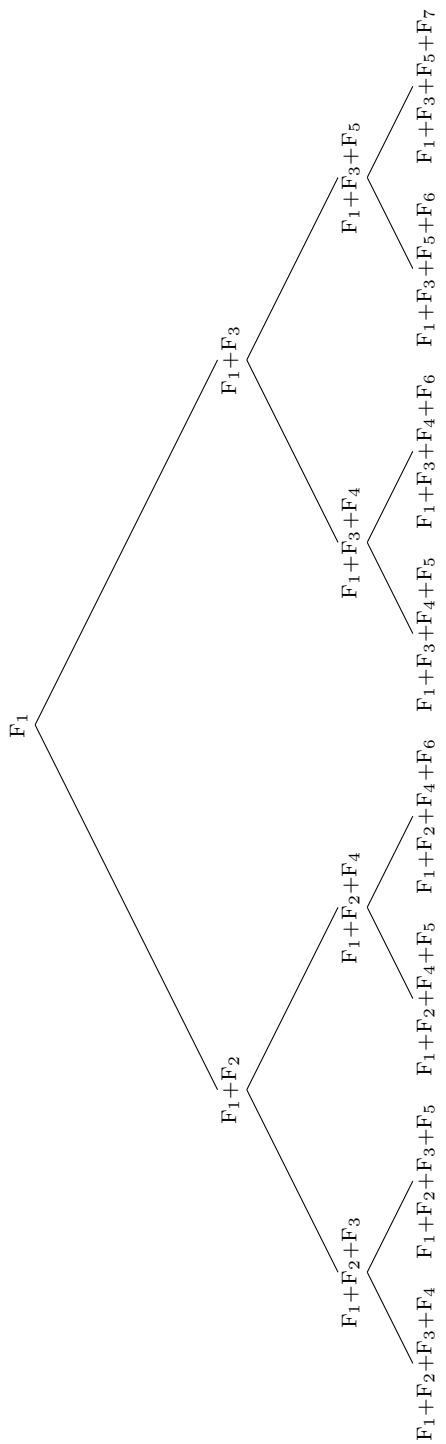

FIGURE 13. Positive integers arranged by self-symmetry of maximal Fibonacci expansion (64). Evaluates to Figure 8. Cohort dual of Figures 5 and 14. $\underline{200648}_{n+1}$ gives number of terms in n. $\underline{113473}_n = \underline{070939}_n = \underline{029837}_{n+1}$ gives the number of terms level by level down the tree.

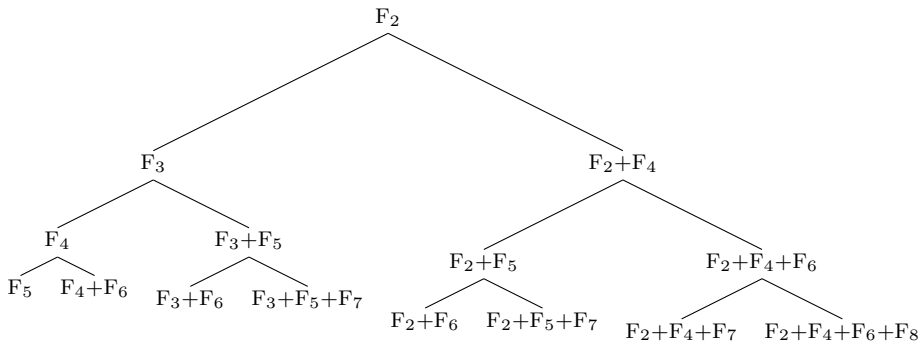

FIGURE 14. Minimal Fibonacci representation (67) of positive integers arranged by self-symmetry. Evaluates to Figure 5. Cohort dual of Figures 8 and 13. $\underline{\texttt{007895}}_n$ gives number of terms in n. $\underline{\texttt{000120}}_n$ gives the number of terms level by level down the tree.

gaps ($\boldsymbol{\nabla}_\star(4)$, $\boldsymbol{\nabla}_\star(5)$, $\boldsymbol{\nabla}_\star(6)$, $\boldsymbol{\nabla}_\star(8)$) $= (11, 12, 21, 22) = (1, 2)^2$, in turn. In all, listing the series of maximal Fibonacci gaps for integers in the tree going from left to right on each successive level gives $\underline{\texttt{007931}}$.

Only the other hand, by writing the elements themselves going from left to right on each successive level of the tree (Figure 8), the resulting permutation of the positive integers, 1, 2, 3, 4, 5, 6, 8, 7, 9, 10, 13, 11, 14, 16, 21,..., is equivalent to $1+\underline{\texttt{095903}}_{n-1}$, where $\underline{\texttt{095903}}$ is a lexical ordering of the lazy Fibonacci representation. This equivalence comes as no surprise given that the maximal expansion of n obtains by adding F_1 to the lazy representation of $n-1$, as Remark 6.1, above, notes.

Thus in the maximal Fibonacci tree, Figure 8, calculate the maximal Fibonacci indices of a node by taking the path downward to reach the node from the root of the tree and encoding the branching via left $\mapsto 1$ and right $\mapsto 2$.

For example, consider the nodes "10," "22," "24," and "29" in Figure 8. The downward paths from the root of the tree have branching sequences "l-r-l," "l-l-r-r," "r-l-l-r," and "r-r-l-l," respectively, encoded as 121, 1122, 2112 and 2211. Taking these encodings as maximal Fibonacci gaps gives the maximal Fibonacci indices $(1, 2, 4, 5)$, $(1, 2, 3, 5, 7)$, $(1, 3, 4, 5, 7)$, and $(1, 3, 5, 6, 7)$, which evaluate correctly, *e.g.*, $F_1 + F_3 + F_5 + F_6 + F_7 = 29$.

Conversely, in the maximal successor tree, Figure 10, calculate the maximal Fibonacci indices of a node by taking the path upward from the node back to the root of the tree and encoding the (parent-to-child) branching.

Considering the nodes "10," "22," "24," and "29" in Figure 10, the upward paths back to the root of the tree follow (parent-to-child) branching sequences "l-r-l," "l-l-r-r," "r-l-l-r," and "r-r-l-l," the same as the downward paths to the same values in the minimal tree.

To tackle the recursive evolution of these gaps, Section 7 introduces cohort sequences of tuples, which complements the discussion of Fibonacci expansions.

6.3. **Self-similarity of minimal Fibonacci representation.**

Remark 6.8. Recall that for the minimal Fibonacci representation, $F_t \leq n < F_{t+1}$ implies that

$$\mathbf{f}(n) = \mathbf{f}(n - F_t) \oplus (t) \tag{67}$$

(see [14], p. 23). When it comes to self-similarity, therefore, the maximal expansion (64) provides a closer analog to minimal representation, (67), than does the lazy representation (63). Comparing the self-similarity relation for the maximal expansion (64) with that of minimal representation (67), only the index of the Fibonacci numbers in the limits of the inequality changes.

Analogously to (65), the recurrence (67) implies

$$F_{F^{-1}(n)} \in \mathbf{f}(n) \text{ and } F_{F^{-1}(n)-1} \notin \mathbf{f}(n), \tag{68}$$

where the second statement holds, since otherwise n would contain $F_{t-1}+F_t = F_{t+1}$, contradicting the assumption that F_t is the largest Fibonacci number not greater than n.

Restating (68), for n satisfying $F_t \leq n < F_{t+1}$, $|\mathbf{f}(n)|_\infty = t$. In words, the largest Fibonacci index in the minimal representation of n is $F^{-1}(n)$. Since this representation does not contain any two consecutive Fibonacci indices, we can increment the representation stepwise by either of two procedures: Replacing F_t with F_{t+1} in the representation, or appending F_{t+2} to the representation. Performing the two procedures repeatedly, writing the result of the former (latter) procedure to the left (right) child of n, gives the tree, Figure 14. Observe that each left branching preserves the number of addends, whereas each right branching increases the number of addends by one. Listing in series the number of addends in maximal Fibonacci expansion for integers in the tree going from left to right on each successive level gives $\underline{000120}$, whereas, as the caption notes, $\underline{007895}_n$ gives the number of addends used to represent n.

Now, recall that by Lemma 4.13(b), a left, respectively, right branch of the minimal Fibonacci tree, Figure 5, corresponds to the addition of F_{t-1}, respectively, F_{t+2} to the parent node n, where $F_t \leq n < F_{t+1}$. Clearly, then, the trees of Figures 5 and 14 are equal, whereas $F_t + F_{t-1} = F_{t+1}$ substitutes F_t in the left child.

In terms of gaps, we may write the branching rule, for $F_t < n \leq F_{t+1}$, as

$$\begin{aligned} \boldsymbol{\partial}(n)\texttt{++} &= \boldsymbol{\partial}(n + F_{t-1}), \\ \boldsymbol{\partial}(n) \oplus (2) &= \boldsymbol{\partial}(n + F_{t+2}), \end{aligned} \tag{69}$$

for left, respectively, right branching of the minimal Fibonacci tree, as shown in Figure 17(iii).

Here again, the upward path from any value n back to the root of the minimal successor tree (Figure 3) has the same (parent-to-child) branching sequence as the downward path from the root node to the same values in the minimal Fibonacci tree.

For example, to reach the node "20" in Figure 5, follow the downward path with branching"l-r-r" from the root of the tree, and conversely, to reach the root node in the minimal successor tree, follow the upward path with (parent-to-child) branching "l-r-r" from the node "20."

6.4. **The quartet of binary trees.**

Remark 6.9 (Branching in the quartet of trees). Previewed together in Figure 5, individually Figures 3, 5, 8 and 10 presented the minimal successor tree, minimal Fibonacci tree, maximal Fibonacci tree, and maximal successor tree, respectively. Table 16 summarizes the branching of the four trees schematically in terms of binary notation, (either Zeckendorf or "maximal Fibonacci"), with the leftmost bit corresponding to F_2 in the case of the minimal trees (Zeckendorf binary), and to F_1 in the case of the maximal trees (maximal Fibonacci binary, see Remark 6.2).

In the notational convention used here, "succession" (Figures 16(i) and (ii)) attains by prepending onto the binary form of the parent to produce a child, that is, an "inner" operation of pushing a prefix onto its the least-significant end.

The branching shown in Figure 16(i) for the minimal successor tree holds for the parent node in any Fibonacci representation (Remark 4.11), while for the minimal Fibonacci tree, the branching shown in Figure 16(iii) holds for the parent node in minimal Fibonacci representation, and not *e.g.*, in lazy Fibonacci representation (Remark 4.13).

In the maximal trees, for the branching in Figures 16(ii) and (iv), values of the nodes employ maximal Fibonacci binary notation, which includes the bit for F_1.

Following directly from Figure 16, Figure 17 translates the branching from binary notation to gaps. In particular, Figures 17(iii) and (iv) show the expressions (69) and (66) noted in Remarks 6.8, respectively, 6.7. Section 8.5 uses gaps to consider how sequences of left branchings in Figures 17(iii) and (iv) generate rows (constant n) of the arrays F and L, respectively, while sequences of right branchings generate rows of the arrays $\exists$, respectively, $\exists$ (see Remark 8.4).

The schematic in Figure 15 shows the same branching as a function of the parent n. The expressions in Figure 15(i) in terms of κ and λ follow from the bijection between Figures 2 and 3 (see Remark 4.11), while those in Figure 15(ii) are given in Lemma 4.32.

True to their names, in both of the successor trees branching produces some type of successor in Fibonacci numeration. The expressions in Figures 15(i) and (ii) using Fibonacci successors follow from Lemma 6.1 (see Remark 6.4), respectively, Proposition 6.3 (see Remark 6.6). Alternatively, the expressions obtain from the branching of gaps given in Figures 17(i) and (ii), via identities (58)–(59), respectively, (60)–(61) of Lemma 6.7.

Figures 15(iii) and (iv) follow from Lemmas 4.13(b) and 4.27(b), respectively.

Proposition 6.9 (Successor branching and Wythoff numbers)**.** *The following claims relate to the successor branching functions:*

(i): *For maximal successor branching,* $\bar{\boldsymbol{L}}K = \Lambda$*, and, consequently,* $\{1\} \cup \bar{\boldsymbol{L}}\Lambda \cup \bar{\boldsymbol{R}}K \cup \bar{\boldsymbol{R}}\Lambda = K$*, where any pair of terms in the union has empty intersection.*

(ii): $\bar{\boldsymbol{L}}\kappa(n) = \bar{\boldsymbol{l}}\kappa(n) = \lambda(n)$*, where the former equality holds for integers* $n \neq 0$ *and the latter equality holds for all integers* n*.*

(iii): *For minimal successor branching,* $\bar{\boldsymbol{l}}K = \Lambda$*, and, consequently,* $\{1\} \cup \bar{\boldsymbol{l}}\Lambda \cup \bar{\boldsymbol{r}}K \cup \bar{\boldsymbol{r}}\Lambda = K$*, and in particular,* $\{1\} \cup \bar{\boldsymbol{r}}K \cup \bar{\boldsymbol{r}}\Lambda = K^2$ *and* $\bar{\boldsymbol{l}}\Lambda = K\Lambda$*, where any pair of terms in the union has empty intersection.*

(iv): $\bar{\boldsymbol{L}}\lambda(n) - 1 = \bar{\boldsymbol{l}}\lambda(n) = \kappa\lambda(n)$ *for all integers* n*.*

(v): $\bar{\boldsymbol{R}}\kappa(n) = \bar{\boldsymbol{r}}\kappa(n) - 1 = \kappa\lambda(n)$*, where the former equality holds for integers* $n \neq 0$ *and the latter equality holds for all integers* n*.*

(vi): $\bar{\boldsymbol{r}}\lambda(n) = \bar{\boldsymbol{R}}\lambda(n) = \lambda^2(n) + 1$ *for all integers* n*.*

(i) minimal successor tree (Fig. 3)

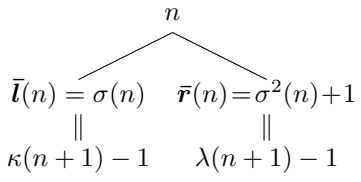

(ii) maximal successor tree (Fig. 10)

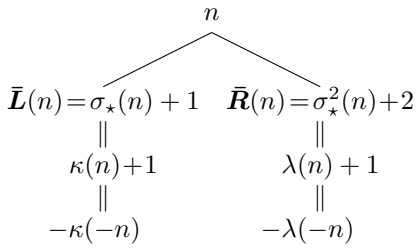

(iii) minimal Fibonacci tree (Fig. 5)

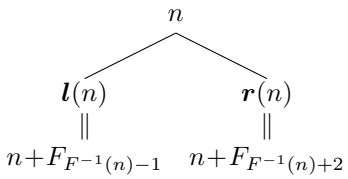

(iv) maximal Fibonacci tree (Fig. 8)

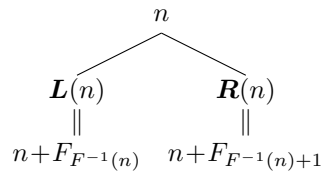

FIGURE 15. Branching in Figures 3, 5, 8 and 10, as integer-valued functions.

(i) minimal successor tree (Fig. 3) in Fibonacci representation (any)

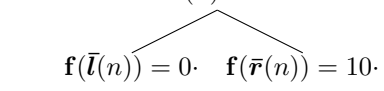

(ii) maximal successor tree (Fig. 10) in maximal Fibonacci Expansion

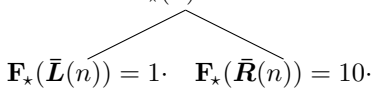

(iii) minimal Fibonacci tree (Fig. 5) in minimal Fibonacci representation

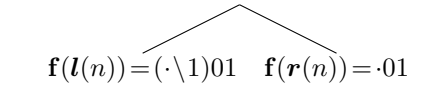

(iv) maximal Fibonacci tree (Fig. 8) in maximal Fibonacci Expansion

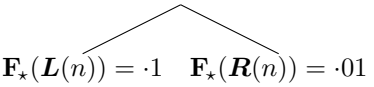

FIGURE 16. Branching in Figures 3 and 5 in Zeckendorf binary notation, and Figures 8 and 10 in maximal Fibonacci binary notation (includes a bit for F_1).

Proof. The proofs will consider partitions of the positive integers by complementary Wythoff sequences (or shifts of such partitions) and the well-known identity for integer $m \geq 1$,

$$\lfloor m\mu \rfloor = \sum_{i=0}^{m-1} \lfloor \mu + {}^{i}\!/_{m} \rfloor \,. \tag{70}$$

(i): Firstly, $\mathbb{Z}_+$ partitions into $\{1\} \cup [K+1] \cup [\Lambda+1] = \{1\} \cup [K^2+1] \cup [K\Lambda+1] \cup [\Lambda K+1] \cup [\Lambda^2+1]$. By complementarity (see, *e.g.*, Example 4.7), $\kappa^2(n) + 1 = \lambda(n)$ for integer $n \neq 0$, so that $\bar{\boldsymbol{L}}K = \Lambda$, and further, $1 \in K$. Thus $\{1\} \cup \bar{\boldsymbol{L}}\Lambda \cup \bar{\boldsymbol{R}}K \cup \bar{\boldsymbol{R}}\Lambda = K$. Note in particular that $\bar{\boldsymbol{L}}\Lambda = K\Lambda + 1 \subset K$.

(ii): Part **(i)** demonstrated the first equality, namely $\bar{\boldsymbol{L}}\kappa(n) = \lambda(n)$ for $n \neq 0$. For the second equality, identity (70) allows us to write

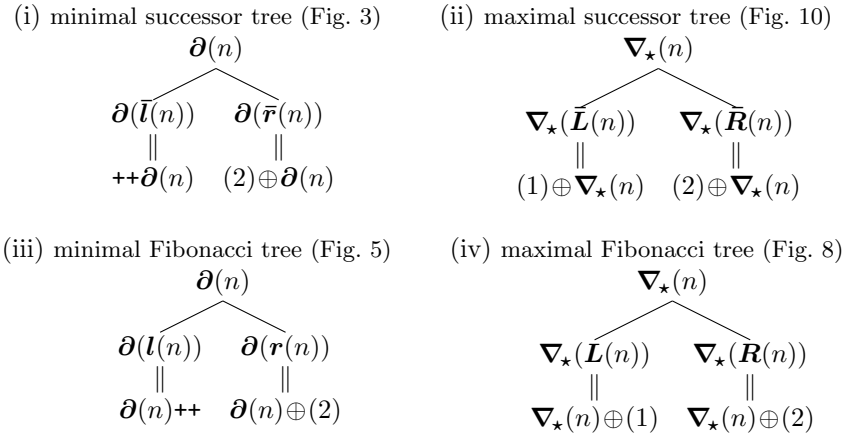

FIGURE 17. Branching in Figures 3, 5, 8 and 10, as gaps in Fibonacci numeration.

$\bar{\boldsymbol{L}}\kappa(n) - \bar{\boldsymbol{l}}\kappa(n)$
$= \kappa^2(n) + 1 - (\kappa(\kappa(n)+1) - 1)$
$= 2 + \sum_{i=0}^{\kappa(n)-1} \lfloor \phi + {}^{i}\!/_{\kappa(n)} \rfloor - \sum_{i=0}^{\kappa(n)} \lfloor \phi + {}^{i}\!/_{\kappa(n)+1} \rfloor$
$= 2 - \lfloor \phi + {}^{\kappa(n)}\!/_{\kappa(n)+1} \rfloor + \sum_{i=0}^{\kappa(n)-1} (\lfloor \phi + {}^{i}\!/_{\kappa(n)} \rfloor - \lfloor \phi + {}^{i}\!/_{\kappa(n)+1} \rfloor)$,

for which the $i = 0^{\text{th}}$ term of the summation is null. Now for the full expression, the first two terms generally cancel since

$$\lfloor \phi + {}^{\kappa(n)}\!/_{\kappa(n)+1} \rfloor = \begin{cases} 2, & n \neq 0; \\ 1, & n = 0. \end{cases}$$

Further, the summation can have at most one nonzero term, since $i < \kappa(n)$ and, therefore $\frac{i+1}{\kappa(n)+1} > \frac{i}{\kappa(n)} \geq \frac{i}{\kappa(n)+1}$. Whereas $\frac{i}{\kappa(n)+1} \leq \frac{i}{\kappa(n)} < 1$ and $\phi \approx 1.618$, a nonzero term $\lfloor \phi + {}^{i}\!/_{\kappa(n)} \rfloor - \lfloor \phi + {}^{i}\!/_{\kappa(n)+1} \rfloor$ implies that $\phi + {}^{i}\!/_{\kappa(n)+1} < 2 < \phi + {}^{i}\!/_{\kappa(n)}$ or equivalently, ${}^{i}\!/_{\kappa(n)+1} < 2 - \phi < {}^{i}\!/_{\kappa(n)}$. Substituting $2 - \phi = {}^{1}\!/_{\phi^2}$ gives $\kappa(n) < i\phi^2 < \kappa(n) + 1$, which implies that $\kappa(n) = \lfloor i\phi^2 \rfloor \equiv \lambda(i)$ — a contradiction for integer $i \neq 0$.

Hence, $\bar{\boldsymbol{L}}\kappa(n) - \bar{\boldsymbol{l}}\kappa(n) = \begin{cases} 0, & n \neq 0; \\ 1, & n = 0. \end{cases}$ Since $\bar{\boldsymbol{l}}\kappa(0) = \lambda(0) = 0$, this completes the proof that $\bar{\boldsymbol{l}}\kappa(n) = \lambda(n)$ for n integer.

(iii): Firstly, $\mathbb{Z}_{\geq 0}$ partitions into $[K-1] \cup [\Lambda - 1] = \{0\} \cup [K(K+1)-1] \cup [K(\Lambda+1)-1] \cup [\Lambda - 1] = \{0\} \cup [K(K+1)-1] \cup [K(\Lambda+1)-1] \cup K^2 = \{0\} \cup \bar{\boldsymbol{l}}K \cup \bar{\boldsymbol{l}}\Lambda \cup K^2$, so that $\mathbb{Z}_{\geq 1}$ partitions into $\bar{\boldsymbol{l}}K \cup \bar{\boldsymbol{l}}\Lambda \cup K^2 = \Lambda \cup K\Lambda \cup K^2$, from whence $\bar{\boldsymbol{r}}K \cup \bar{\boldsymbol{r}}\Lambda = K^2 \subset K$, and $\bar{\boldsymbol{l}}K \cup \bar{\boldsymbol{l}}\Lambda = \Lambda \cup K\Lambda$, where in all cases any pair of terms in the unions has empty intersection. Finally, combining this with $\bar{\boldsymbol{l}}K = \Lambda$ from **(ii)** gives $\bar{\boldsymbol{l}}\Lambda = K\Lambda$.

(iv)–(vi): Analogous to **(ii)**.

□

6.5. **Trees and Fibonacci cohort structure.** As previously observed, infinite Fibonacci cohort sequences from the 1^{st} cohort and their corresponding Fibonacci cohort tableaux have only two subcohorts per cohort, and are thus graph isomorphic to infinite, regular, single-rooted binary trees, with arcs defined by the Fibonacci cohort relations.

Consider the 1–2-Fibonacci relations in Definition 4.4. Specifying the cohortizer $\langle f_L(t), f_R(t)\rangle = \langle F_{t-1}, F_{t+1}\rangle$ places the positive integers into 1–2-Fibonacci cohort sequence as shown in the tableau Table 6(i). Taking the elements $S_1 = 1, S_2 = 2, S_3 = 3, \ldots$ of the tableau as "nodes" and the relations as "arcs" between pairs of nodes provides a graph isomorphism with the binary tree of Figure 5. Similarly, the 2–1-Fibonacci cohort relations provide a graph isomorphism between the tableau Table 6(ii) and the binary tree of Figure 8. In both cases, the isomorphism places the nodes of a binary tree into the sequence of the positive integers in their usual order.

Thus, investigation of the branching structure for the maximal and minimal Fibonacci trees in Sections 6.2 and 6.3, respectively, allows the identification of these trees with the 2–1- and 1–2-Fibonacci cohort structures, respectively.

Lemma 6.10 (Fibonacci cohort of children in the Fibonacci trees)**.** *Consider the binary trees of positive integers, Figures 5 and 8:*

(i): *Let $\boldsymbol{l}(n)$, respectively $\boldsymbol{r}(n)$ be the left and right children of integer n in the minimal Fibonacci tree, Figure 5. Now consider the 1–2-Fibonacci cohort sequence S under cohortizer $\langle \boldsymbol{l}, \boldsymbol{r}\rangle$, such that $C_t = \boldsymbol{l}(C_{t-1})\boldsymbol{r}(C_{t-2})$, and, in particular, $C_2 = \boldsymbol{l}(C_1)$. Then, setting $S_1 = 1$ makes S the positive integers in sequence, with cohorts as shown in Table 6(i).*

(ii): *Let $\boldsymbol{L}(n)$, respectively $\boldsymbol{R}(n)$ be the left and right children of integer n in the maximal Fibonacci tree, Figure 8. Now consider the 2–1-Fibonacci cohort sequence S under cohortizer $\langle \boldsymbol{R}, \boldsymbol{L}\rangle$, such that $C_t = \boldsymbol{R}(C_{t-2})\boldsymbol{L}(C_{t-1})$, and, in particular, $C_2 = \boldsymbol{L}(C_1)$. Then, setting $S_1 = 1$ makes S the positive integers in sequence, with cohorts as shown in Table 6(ii).*

Proof. **(i)**: The branching rule for the minimal Fibonacci tree as formulated in Remark 6.8, gives $\boldsymbol{l}(n) = n + F_{t-1}$ and $\boldsymbol{r}(n) = n + F_{t+2}$, for parent $F_t \le n < F_{t+1}$ (Figure 15(iii)).

Using induction, develop the properties of such a sequence. Consider elements $(S_{F_t}, \ldots, S_{F_{t+1}-1})$ of cohort C_{t-1} and elements $(S_{F_{t-1}}, \ldots, S_{F_t-1})$ of cohort C_{t-2}. By hypothesis, suppose for elements of C_{t-1}, that $F_t \le S_{F_t}, \ldots, S_{F_{t+1}-1} < F_{t+1}$, and for elements of C_{t-2}, that $F_{t-1} \le S_{F_{t-1}}, \ldots, S_{F_t-1} < F_t$. Then, $C_t = \boldsymbol{l}(C_{t-1})$ $\boldsymbol{r}(C_{t-2}) = S_{F_t} + F_{t-1}, \ldots, S_{F_{t+1}-1} + F_{t-1}, S_{F_{t-1}} + F_{t+1}, \ldots, S_{F_t-1} + F_{t+1}$. This shows the cohortizer equal to $\langle F_{t-1}, F_{t+1}\rangle$, and that elements of left subcohort of C_t satisfy $F_{t+1} = F_t + F_{t-1} \le S_{F_{t+1}}, \ldots, S_{F_{t+1}+F_{t-2}-1} < F_{t+1} + F_{t-1} < F_{t+2}$, and that elements of the right subcohort of C_t also satisfy $F_{t+1} < F_{t-1} + F_{t+1} \le S_{F_t+F_{t-2}}, \ldots, S_{F_{t+2}-1} + F_t < F_t + F_{t+1} = F_{t+2}$, proving the induction hypothesis.

From Example 4.20, recall the formulation of any sequence of successive integers as a 1–2-Fibonacci cohort sequence under the cohortizer $\langle F_{t-1}, F_{t+1}\rangle$, and observe for the base case $S_1 = 1$, that $F_2 = S_1 < F_3$ and that $C_2 = \boldsymbol{l}(C_1) = S_1 + F_2 = 2$. Thus the 1–2-Fibonacci cohortizer $\langle \boldsymbol{l}, \boldsymbol{r}\rangle$ produces the sequence of positive integers.

Conversely, start with the cohort sequence and take the difference between elements of cohort C_t and those of $C_{t-1}C_{t-2}$ to give $C_t - C_{t-1}C_{t-2} = (F_{t+1}, \ldots, F_{t+2} - 1) - (F_t, \ldots, F_{t+1} - 1, F_{t-1}, \ldots, F_t - 1) = (F_{t-1}, \ldots, F_{t-1}, F_{t+1}, \ldots, F_{t+1})$, and consider that for $F_t \le n < F_{t+1}$, the addition of F_{t-1} produces the left child of n in the minimal Fibonacci tree, whereas for $F_{t-1} \le n < F_t$ the addition of F_{t+1} produces the right child of n, so that cohort C_t is the juxtaposition of the left children of cohort C_{t-1} with the right children of cohort C_{t-2}.

(ii): The branching rule for the maximal Fibonacci tree as formulated in Remark 6.7, gives $\boldsymbol{L}(n) = n + F_t$ and $\boldsymbol{R}(n) = n + F_{t+1}$, for parent $F_t \leq n < F_{t+1}$ (Figure 15(iv)).

Using induction, develop the properties of such a sequence. Consider elements $(S_{F_{t-1}}, \ldots, S_{F_t-1})$ of cohort C_{t-2} and elements $(S_{F_t}, \ldots, S_{F_{t+1}-1})$ of cohort C_{t-1}. By hypothesis, suppose for elements of C_{t-2}, that $F_{t-1} \leq S_{F_{t-1}}, \ldots, S_{F_t-1} < F_t$, and for elements of C_{t-1}, that $F_t \leq S_{F_t}, \ldots, S_{F_{t+1}-1} < F_{t+1}$. Then, $C_t = \boldsymbol{R}(C_{t-2})$ $\boldsymbol{L}(C_{t-1}) = S_{F_{t-1}} + F_t, \ldots, S_{F_t-1} + F_t, S_{F_t} + F_t, \ldots, S_{F_{t+1}-1} + F_t$. This shows the cohortizer equal to F_t, and that elements of left subcohort of C_t satisfy $F_{t+1} = F_{t-1} + F_t \leq S_{F_{t+1}}, \ldots, S_{F_{t+1}+F_{t-2}-1} < F_t + F_t < F_{t+2}$, and that elements of the right subcohort of C_t also satisfy $F_{t+1} < F_t + F_t \leq S_{F_t+F_{t-2}}, \ldots, S_{F_{t+2}-1} + F_t < F_{t+1} + F_t = F_{t+2}$, proving the induction hypothesis.

From Example 4.2 recall the formulation of any sequence of successive integers as a 2–1-Fibonacci cohort sequence under F_t, and observe for the base case $S_1 = 1$, that $F_2 = S_1 < F_3$ and that $C_2 = \boldsymbol{L}(C_1) = S_1 + F_2 = 2$. Thus the 2–1-Fibonacci cohortizer $\langle \boldsymbol{R}, \boldsymbol{L} \rangle$ produces the sequence of positive integers.

Conversely, start with the cohort sequence and take the difference between elements of cohort C_t and those of $C_{t-2}C_{t-1}$ to give $C_t - C_{t-2}C_{t-1} = (F_{t+1}, \ldots, F_{t+2} - 1) - (F_{t-1}, \ldots, F_t - 1, F_t, \ldots, F_{t+1} - 1) = (F_t, \ldots, F_t)$, and consider that for $F_{t-1} \leq n < F_t$ the addition of F_t produces the right child of n in the maximal Fibonacci tree, whereas for $F_t \leq n < F_{t+1}$ the addition of F_t produces the left child of n in the maximal Fibonacci tree, so that cohort C_t is the juxtaposition of the right children of cohort C_{t-2} with the left children of cohort C_{t-1}. □

Restating Lemma 6.10(i), the minimal Fibonacci tree arranges the t^{th} cohort C_t of the positive integers so that the values $(F_{t+1}, \ldots, F_{t+1} + F_{t-1} - 1)$ of its left subcohort are found at the left children of the respective values $(F_t, \ldots, F_{t+1} - 1)$ of the prior cohort C_{t-1} and that the values $(F_{t+1} + F_{t-1}, \ldots, F_{t+2} - 1)$ of its right subcohort are found at the right children of the respective the values $(F_{t-1}, \ldots, F_t - 1)$ of the second-prior cohort C_{t-2}.

Restating Lemma 6.10(ii), the maximal Fibonacci tree arranges the t^{th} cohort C_t of the positive integers so that the values $(F_{t+1}, \ldots, F_{t+1} + F_{t-2} - 1)$ of its left subcohort are found at the right children of the respective values $(F_{t-1}, \ldots, F_t - 1)$ of the second-prior cohort C_{t-2} and that the values $(F_{t+1} + F_{t-2}, \ldots, F_{t+2} - 1)$ of its right subcohort are found at the left children of the respective values $(F_t, \ldots, F_{t+1} - 1)$ of the prior cohort C_{t-1}.

From Remark 4.11, recall the branching of the minimal successor tree from its correspondence to Figure 2 via the algorithm of Corollary 4.8. From Lemma 4.32, recall the branching of the maximal successor tree. Figures 15(i) and (ii) summarize the two branching schemes.

Lemma 6.11 (Fibonacci cohort of children in the successor trees)**.** *Consider the branching from parent node to children in the minimal and maximal successor trees, Figures 3 and 10, respectively, and observe that*

$$F_{t+1} \leq \bar{\boldsymbol{l}}(n) \leq \bar{\boldsymbol{L}}(n) < F_{t+2}, \text{ for } F_t \leq n < F_{t+1}; \text{ and} \tag{71}$$

$$F_{t+1} \leq \bar{\boldsymbol{R}}(n) \leq \bar{\boldsymbol{r}}(n) < F_{t+2}, \text{ for } F_{t-1} \leq n < F_t. \tag{72}$$

Thus in either tree, a parent in the interval $[F_t, F_{t+1} - 1]$ *for* $t \geq 2$ *begets a left child in the interval* $[F_{t+1}, F_{t+2} - 1]$*, whereas a parent in the interval* $[F_{t-1}, F_t - 1]$

for $t \geq 3$ also begets a right child in the interval $[F_{t+1}, F_{t+2} - 1]$, or

$$\bar{\boldsymbol{l}}(\{F_t, \ldots, F_{t+1} - 1\}) \subset \{F_{t+1}, \ldots, F_{t+2} - 1\}$$
$$\bar{\boldsymbol{r}}(\{F_{t-1}, \ldots, F_t - 1\}) \subset \{F_{t+1}, \ldots, F_{t+2} - 1\},$$
$$\bar{\boldsymbol{L}}(\{F_t, \ldots, F_{t+1} - 1\}) \subset \{F_{t+1}, \ldots, F_{t+2} - 1\}$$
$$\bar{\boldsymbol{R}}(\{F_{t-1}, \ldots, F_t - 1\}) \subset \{F_{t+1}, \ldots, F_{t+2} - 1\}.$$

By pigeonhole principle, therefore, for $t \geq 2$, each cohort $C_t = \{F_{t+1}, \ldots, F_{t+2} - 1\}$ of the positive integers exactly comprises the left children of the previous cohort $C_{t-1} = \{F_t, \ldots, F_{t+1} - 1\}$ interleaved with, for $t \geq 3$, the right children of the second previous cohort $C_{t-2} = \{F_{t-1}, \ldots, F_t - 1\}$, in either tree.

Proof. Via Lemma 6.1 (also see Remark 6.4 and Figure 15(i) and (ii)), the relations

$$F_{t+1} \leq \kappa(n+1) - 1 \leq \kappa(n) + 1 < F_{t+2}, \text{ for } F_t \leq n < F_{t+1}; \text{ and} \tag{73}$$

$$F_{t+1} \leq \lambda(n) + 1 \leq \lambda(n+1) - 1 < F_{t+2}, \text{ for } F_{t-1} \leq n < F_t; \tag{74}$$

are equivalent to (71), respectively, (72). To show that $\kappa(n+1) - 1 \geq F_{t+1}$ in (73), use the identities

$$0 \leq m\phi - \kappa(m) < 1, \text{ and} \tag{75}$$

$$F_{h+1} - \phi F_h = (-\tfrac{1}{\phi})^h. \tag{76}$$

First, let $m = F_t + 1$ in (75) and manipulate

$$0 \leq \phi(F_t + 1) - \kappa(F_t + 1) < 1$$

into

$$\phi F_t + \phi - 2 < \kappa(F_t + 1) - 1 \leq \phi F_t + \phi - 1.$$

Then letting $h = t$ in (76), use the latter to yield

$$F_{t+1} - (-\tfrac{1}{\phi})^t + \phi - 2 < \kappa(F_t + 1) - 1 \leq F_{t+1} - (-\tfrac{1}{\phi})^t + \phi - 1.$$

Evaluating the bounds on this integer quantity shows that $\kappa(F_t + 1) - 1 = F_{t+1}$, for $t \geq 2$.

By similar arguments, obtain the remaining bounds on the complete set of left successor branching claimed for $t \geq 2$:

$$\kappa(F_t + 1) - 1 = F_{t+1},$$
$$\kappa(F_t) + 1 = \begin{cases} F_{t+1}, & t \text{ even}; \\ F_{t+1} + 1, & t \text{ odd}; \end{cases}$$
$$\kappa(F_{t+1}) - 1 = \begin{cases} F_{t+2} - 1, & t \text{ even}; \\ F_{t+2} - 2, & t \text{ odd}; \end{cases}$$
$$\kappa(F_{t+1} - 1) + 1 = F_{t+2} - 1,$$

and bounds on the complete set of right successor branching claimed for $t \geq 3$:

$$\lambda(F_{t-1}) + 1 = \begin{cases} F_{t+1}, & t \text{ odd}; \\ F_{t+1} + 1, & t \text{ even}; \end{cases}$$
$$\lambda(F_{t-1} + 1) - 1 = F_{t+1} + 1,$$
$$\lambda(F_t - 1) + 1 = F_{t+2} - 2$$
$$\lambda(F_t) - 1 = \begin{cases} F_{t+2} - 1, & t \text{ odd}; \\ F_{t+2} - 2, & t \text{ even}. \end{cases}$$

□

6.6. **Positions in trees.** Lemma 6.10 begs the question of whether the sequences of nodal positions **p** and **P** in the minimal and maximal Fibonacci trees exhibit Fibonacci cohort structure.

In the Fibonacci trees, the positions of the positive integers turn out to be Fibonacci cohort sequences (Table 18) that are non-affine, but rather linear catenative sequences. This follows immediately from Lemma 6.10 since for the node at position $\mathbf{p}(n)$ ($\mathbf{P}(n)$) in the minimal (maximal) tree, its left and right children are found at positions $2\mathbf{p}(n)$, respectively, $2\mathbf{p}(n)+1$ ($2\mathbf{P}(n)$, respectively, $2\mathbf{P}(n)+1$). Being non-affine, results of Section 4.2 do not apply to these sequences.

(i)

C_1	1								
C_2	2								
C_3	4	3							
C_4	8	6	5						
C_5	16	12	10	9	7				
C_6	32	24	20	18	14	17	13	11	

(ii)

								1	C_1
							2	2	C_2
						3	4	3	C_3
					5	6	8	4	C_4
				7	9	10	12	16	C_5
11	13	17	14	18	20	24	32	6	C_6

TABLE 18. (i) and (ii): Positions $\mathbf{p}(n)$ and $\mathbf{P}(\mathbf{n})$ of n within the minimal, respectively maximal Fibonacci trees, Figures 5 and 8. The tableau on the right equals an "irregular triangle array" of Kimberling (243571 in [41], corrected here). For both tableaux, cohort C_t gives tree positions for integers in the interval $[F_{t+1}, F_{t+2}-1]$. The sequences are linear-catenative, rather than affine-catenative, whereas cohortizers $\mathbf{p}(n) \mapsto \langle 2\mathbf{p}(n), 2\mathbf{p}(n)+1\rangle$ and $\mathbf{P}(n) \mapsto \langle 2\mathbf{P}(n)+1, 2\mathbf{P}(n)\rangle$ form the 1–2- and 2–1-Fibonacci cohort sequences at left and right, respectively.

6.6.1. *Positions in Fibonacci trees, and cohort-dual arrays of the branch quartet.*

Proposition 6.12 (Positions in minimal and maximal Fibonacci trees)**.** *Label the nodal positions in a binary tree from the root level downward and from left-to-right on each level, with the nodes on level r thus labeled $(2^{r-1}, \ldots, 2^r-1)$ (Figure 18).*

Then for $t = 1, 2, 3, \ldots$, the set of integers $\{F_{t+1}, \ldots, F_{t+2}-1\}$ has the same set of nodal positions in the minimal and maximal Fibonacci trees, Figures 5 and 8. In particular, for each $t = 1, 2, 3, \ldots$ the sequence of nodal positions of $C_t = (F_{t+1}, \ldots, F_{t+2}-1)$ in the minimal Fibonacci tree is merely the reverse of that in the maximal Fibonacci tree. That is,

$$(\mathbf{p}(F_{t+1}), \ldots, \mathbf{p}(F_{t+2}-1)) = (\mathbf{P}(F_{t+2}-1), \ldots, \mathbf{P}(F_{t+1})).$$

Moreover, the nodal positions in the minimal and maximal Fibonacci trees are given by the 1–2-, respectively 2–1-Fibonacci cohort sequences under cohortizers $\mathbf{p}(n) \mapsto \langle 2\mathbf{p}(n), 2\mathbf{p}(n)+1\rangle$ and $\mathbf{p}(n) \mapsto \langle 2\mathbf{p}(n)+1, 2\mathbf{p}(n)\rangle$ (Tables 18(i) and (ii), respectively).

Proof. It suffices to show the latter claim, as it implies the former. Comparing Table 18(i) and (ii) with Figures 5 and 8, respectively, observe that the claim holds for the first few cohorts and proceed by induction.

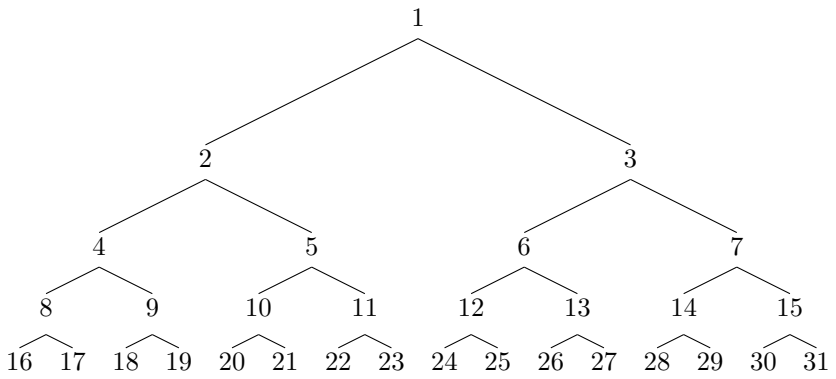

FIGURE 18. Tree of nodal positions in an infinite binary tree. Single root on level 1. Positions $\{2^{r-1}, \ldots, 2^r - 1\}$ from left to right on level $r = 1, 2, 3, \ldots$. A limiting tree for branching rules that use Beatty pairs, as their irrational slopes approach 2 (Corollary 9.2). Blade dual of Figure 21. Sequences of left or right branchings give rows of I–D arrays shown in Table 41. Sequences of left or right clades give columns of I–D arrays shown in Table 41. Siblings of the same parent node are adjacent integers, thus minimizing an aggregate measure of distance over binary trees that arrange $\mathbb{Z}_+$.

Without loss of generality, for a binary tree with nodal positions $\mathbf{p}$ counted as the claim describes, the left and right children of the node in position $\mathbf{p}(n)$ occupy positions $2\mathbf{p}(n)$ and $2\mathbf{p}(n) + 1$, respectively.

Let $\mathbf{p}$ and $\mathbf{P}$ denote the position(s) of integers in the minimal, respectively, maximal Fibonacci trees. Then in particular,

$$\mathbf{p}(\boldsymbol{l}(n)) = 2\mathbf{p}(n) \text{ and } \mathbf{p}(\boldsymbol{r}(n)) = 2\mathbf{p}(n) + 1; \tag{77}$$

$$\mathbf{P}(\boldsymbol{L}(n)) = 2\mathbf{P}(n) \text{ and } \mathbf{P}(\boldsymbol{R}(n)) = 2\mathbf{P}(n) + 1. \tag{78}$$

Now for the minimal Fibonacci tree, Lemma 6.10(i) showed the bracket $\langle \boldsymbol{l}, \boldsymbol{r} \rangle$ to be a 1–2-Fibonacci cohortizer for the integers, forming cohorts via $C_t = \boldsymbol{l}(C_{t-1})\ \boldsymbol{r}(C_{t-2})$. Thus,

$$\begin{aligned} &\mathbf{p}(C_t) \\ =&\mathbf{p}(\boldsymbol{l}(C_{t-1})) \oplus \mathbf{p}(\boldsymbol{r}(C_{t-2})) \\ =&2\mathbf{p}(C_{t-1}) \oplus [2\mathbf{p}(C_{t-2}) + 1]\,. \end{aligned} \tag{79}$$

This shows that the change in elements from one cohort to the next induces the cohort structure on the tree positions $\mathbf{p}$ that the Corollary claims, thus proving the induction step. For the maximal Fibonacci tree, Lemma 6.10(ii) showed the bracket $\langle \boldsymbol{R}, \boldsymbol{L} \rangle$ to be a 2–1-Fibonacci cohortizer for the integers, forming cohorts via $C_t = \boldsymbol{R}(C_{t-2})\ \boldsymbol{L}(C_{t-1})$. Thus,

$$\begin{aligned} &\mathbf{P}(C_t) \\ =&\mathbf{P}(\boldsymbol{R}(C_{t-2})) \oplus \mathbf{P}(\boldsymbol{L}(C_{t-1})) \\ =&\,[2\mathbf{P}(C_{t-2}) + 1] \oplus 2\mathbf{P}(C_{t-1}). \end{aligned} \tag{80}$$

This shows that the change in elements from one cohort to the next induces the cohort structure on the tree positions $\mathbf{P}$ that the Corollary claims, thus proving the

induction step for the last claim. For the former claim, suppose that $\mathbf{P}(C_{t-2})$ is the reverse of $\mathbf{p}(C_{t-2})$ and that $\mathbf{P}(C_{t-1})$ is the reverse of $\mathbf{p}(C_{t-1})$. Then (79) and (80) imply that $\mathbf{P}(C_t)$ is the reverse of $\mathbf{p}(C_t)$, as desired. □

Corollary 6.13 (Cohort index for the pairs of cohort-dual entries in the branch quartet.)**.** *Consider the pairs of cohort-dual arrays in the branch quartet. Suppose that for all $n \geq 0, k \geq 1$, $\mathbf{p}(\mathsf{F}_{n,k}) = \mathbf{P}(\mathsf{L}_{n,k})$. Then by Proposition 6.12,*

$$F^{-1}(\mathsf{F}_{n,k}) = F^{-1}(\mathsf{L}_{n,k})$$

Similarly, suppose that for all $n \geq 0, k \geq 1$, $\mathbf{p}(\mathsf{T}_{n,k}) = \mathbf{P}(\mathsf{J}_{n,k})$. Then by Proposition 6.12,

$$F^{-1}(\mathsf{T}_{n,k}) = F^{-1}(\mathsf{J}_{n,k}).$$

That is, corresponding entries at positions (n, k) of the respective arrays are members of the same Fibonacci cohort of the positive integers.

6.6.2. *Positions in successor trees, and cohort-dual arrays of the clade quartet.*

Remark 6.10. Analogously to (77) and (78) in the Fibonacci trees, in the successor trees,

$$\bar{\mathbf{p}}(\bar{\boldsymbol{l}}(n)) = 2\bar{\mathbf{p}}\,(n) \text{ and } \bar{\mathbf{p}}(\bar{\boldsymbol{r}}(n)) = 2\bar{\mathbf{p}}\,(n) + 1; \tag{81}$$

$$\bar{\mathbf{P}}(\bar{\boldsymbol{L}}(n)) = 2\bar{\mathbf{P}}(n) \text{ and } \bar{\mathbf{P}}(\bar{\boldsymbol{R}}(n)) = 2\bar{\mathbf{P}}(n) + 1. \tag{82}$$

Moreover, as with the Fibonacci trees, cohort C_t of the integers within the successor trees does comprise the left children of cohort C_{t-1} and right children of cohort C_{t-2}. However, C_t is not a simple juxtaposition of the two as in Lemma 6.10, but rather an interleaving of the left children of cohort C_{t-1} with the right children of cohort C_{t-2}.

For the minimal and maximal successor trees (Figures 3 and 10), the branching functions involve successors and thus do not consist of simple postfix (outer) operations, but rather prefixed (inner) operations. Hence, the recursive structure of positions in the minimal and maximal successor trees does not lend itself to posterior calculation as with the recursive cohort structure of the Fibonacci trees evidenced by formulas (79) and (80) and tabulated in Tables 18. Nevertheless, Lemma 6.11 provided bounds on cohort membership for a child node in the successor trees that shall prove useful.

Proposition 6.14. *For $t = 1, 2, 3, \ldots$, the set of integers $\{F_{t+1}, \ldots, F_{t+2} - 1\}$ has the same set of nodal positions in the minimal and maximal successor trees, Figures 3 and 10. In particular, for each $t = 1, 2, 3, \ldots$ the set of nodal positions of $(F_{t+1}, \ldots, F_{t+2} - 1)$ in the minimal successor tree is merely the reverse of that in the maximal successor tree. That is,*

$$(\bar{\mathbf{p}}(F_{t+1}), \ldots, \bar{\mathbf{p}}(F_{t+2} - 1)) = (\bar{\mathbf{P}}(F_{t+2} - 1), \ldots, \bar{\mathbf{P}}(F_{t+1})).$$

Proof. Lemma 6.11 showed that the C_t comprises an interleaving of $\bar{\boldsymbol{l}}(C_{t-1})$ and $\bar{\boldsymbol{r}}(C_{t-2})$, and equivalently, an interleaving of $\bar{\boldsymbol{L}}(C_{t-1})$ and $\bar{\boldsymbol{R}}(C_{t-2})$. Thus argue as follows:

Step 1: Consider a pair of elements at opposite positions in the tuple $C_{t-1} = (F_t, \ldots, F_{t+1} - 1)$ and show that applying $\bar{\boldsymbol{l}}$ to one element of the pair and $\bar{\boldsymbol{L}}$ to the other produces a pair of elements at opposite positions in the tuple $C_t = (F_{t+1}, \ldots, F_{t+2} - 1)$.

Similarly, for a pair of elements at opposite positions in the tuple $C_{u-2} = (F_{u-1}, \ldots, F_u - 1)$, show that applying $\bar{\boldsymbol{r}}$ to one element of the pair and $\bar{\boldsymbol{R}}$ to the other also produces a pair of elements at opposite positions in the tuple $C_u = (F_{u+1}, \ldots, F_{u+2} - 1)$.

That is, for integers $t \geq 2$, $u \geq 3$, $m \in [0, F_{t-1} - 1]$, and $n \in [0, F_{u-2} - 1]$, show that

$$\bar{\boldsymbol{l}}(F_t + m) - F_{t+1} = F_{t+2} - 1 - \bar{\boldsymbol{L}}(F_{t+1} - 1 - m),$$
$$\bar{\boldsymbol{r}}(F_{u-1} + n) - F_{u+1} = F_{u+2} - 1 - \bar{\boldsymbol{R}}(F_u - 1 - n).$$

Or more simply,

$$\bar{\boldsymbol{l}}(F_t + m) + \bar{\boldsymbol{L}}(F_{t+1} - 1 - m) = F_{t+3} - 1,$$
$$\bar{\boldsymbol{r}}(F_{u-1} + n) + \bar{\boldsymbol{R}}(F_u - 1 - n) = F_{u+3} - 1.$$

Or, equivalently by Lemma 6.1,

$$\kappa(F_t + m + 1) - 1 + \kappa(F_{t+1} - 1 - m) + 1 = F_{t+3} - 1,$$
$$\lambda(F_{u-1} + n + 1) - 1 + \lambda(F_u - 1 - n) + 1 = F_{u+3} - 1.$$

Or more simply,

$$\kappa(F_t + m + 1) + \kappa(F_{t+1} - 1 - m) = F_{t+3} - 1,$$
$$\lambda(F_{u-1} + n + 1) + \lambda(F_u - 1 - n) = F_{u+3} - 1.$$

The latter are identical to (56) and (57), which were shown in Lemma 6.6 for the more general case $m \in [-F_t, F_{t+1} - 2]$, and $n \in [-F_{u-1}, F_u - 2]$.

Step 2: Considering a pair of elements at opposite positions in the tuple C_t, use Step 1 to trace the parentage of the pair — either to a pair with opposite positions in C_{t-2} or a pair with opposite positions in C_{t-1}. Then induce that the positions of the respective children remain opposite in the two trees, so that considering collectively the positions of all such pairs of children, the $\bar{\mathbf{p}}(\bar{\boldsymbol{r}}(C_{t-2}))$ are the reverse of the $\bar{\mathbf{P}}(\bar{\boldsymbol{R}}(C_{t-2}))$, and the $\bar{\mathbf{p}}(\bar{\boldsymbol{l}}(C_{t-1}))$ are the reverse of the $\bar{\mathbf{P}}(\bar{\boldsymbol{L}}(C_{t-1}))$, and consequently $\bar{\mathbf{p}}(C_t)$ as a whole are the reverse of $\bar{\mathbf{P}}(C_t)$. That is, under the hypothesis (I.H.) that

$$\bar{\mathbf{p}}(F_{t-1} + n) = \bar{\mathbf{P}}(F_t - 1 - n), \quad n = 0, 1, 2, \ldots, F_{t-2} - 1;$$
$$\bar{\mathbf{p}}(F_t + m) = \bar{\mathbf{P}}(F_{t+1} - 1 - m), m = 0, 1, 2, \ldots, F_{t-1} - 1;$$

for C_{t-2} and C_{t-1}, respectively, induction to C_t gives,

$$\bar{\mathbf{p}}(\bar{\boldsymbol{r}}(F_{t-1} + n)) \overset{(81)}{=} 2\bar{\mathbf{p}}(F_{t-1} + n) + 1 \overset{\text{I.H.}}{=} 2\bar{\mathbf{P}}(F_t - 1 - n) + 1 \overset{(82)}{=} \bar{\mathbf{P}}(\bar{\boldsymbol{R}}(F_t - 1 - n)),$$
$$\bar{\mathbf{p}}(\bar{\boldsymbol{l}}(F_t + m)) \overset{(81)}{=} 2\bar{\mathbf{p}}(F_t + m) \overset{I.H.}{=} 2\bar{\mathbf{P}}(F_{t+1} - 1 - m) \overset{(82)}{=} \bar{\mathbf{P}}(\bar{\boldsymbol{L}}(F_{t+1} - 1 - m)),$$

where the pairs $(\bar{\boldsymbol{r}}(F_{t-1} + n), \bar{\boldsymbol{R}}(F_t - 1 - n))$ and $(\bar{\boldsymbol{l}}(F_t + m), \bar{\boldsymbol{L}}(F_{t+1} - 1 - m))$ were shown in Step 1 to reside in opposite positions within the tuple C_t. □

Remark 6.11. Note that 048679 and 232559 appear to give the positions $\bar{\mathbf{p}}(n)$ and $\bar{\mathbf{P}}(n)$ of positive integers n in the minimal and maximal successor trees, Figures 3, respectively, 10, though neither series possesses a complete Fibonacci cohort structure. Corollary 6.22 will say more about these tree positions.

Corollary 6.15 (Cohort index for the pairs of cohort-dual entries in the clade quartet.)**.** *Consider the pairs of cohort-dual arrays in the clade quartet. Suppose that for all* $n \geq 0, k \geq 1$, $\bar{\mathbf{p}}(w_{n,k}) = \bar{\mathbf{P}}(a_{n,k})$. *Then by Proposition 6.14,*

$$F^{-1}(w_{n,k}) = F^{-1}(a_{n,k})$$

Similarly, suppose that for all $n \geq 0, k \geq 1$, $\bar{\mathbf{p}}(\mathfrak{w}_{n,k}) = \bar{\mathbf{P}}(\mathfrak{a}_{n,k})$. *Then by Proposition 6.14,*

$$F^{-1}(\mathfrak{w}_{n,k}) = F^{-1}(\mathfrak{a}_{n,k}).$$

That is, corresponding entries in positions (n, k) *of the respective arrays are members of the same cohort of the integers.*

6.6.3. *Positions in blade-dual trees, and blade-dual arrays of the octet.*

Lemma 6.16 (Cohort index in Fibonacci and successor trees)**.**

$$\{\mathbf{p}(F_{t+1}), \ldots, \mathbf{p}(F_{t+2} - 1)\} = \{\bar{\mathbf{p}}(F_{t+1}), \ldots, \bar{\mathbf{p}}(F_{t+2} - 1)\}$$
$$\{\mathbf{P}(F_{t+1}), \ldots, \mathbf{P}(F_{t+2} - 1)\} = \left\{\bar{\mathbf{P}}(F_{t+1}), \ldots, \bar{\mathbf{P}}(F_{t+2} - 1)\right\}$$

Proof. Without loss of generality, demonstrate the first claim by induction on t, noting the identical cohort structure of $\mathbf{p}$ and $\bar{\mathbf{p}}$. By Proposition 6.12,

$$\begin{aligned}\{\mathbf{p}(F_{t+1}), \ldots, \ & \mathbf{p}(F_{t+2} - 1)\} \\ &= \{\mathbf{p}(\boldsymbol{l}(F_t)), \ldots, \mathbf{p}(\boldsymbol{l}(F_{t+1} - 1)), \mathbf{p}(\boldsymbol{r}(F_{t-1})), \ldots, \mathbf{p}(\boldsymbol{r}(F_t - 1))\} \\ &= \{2\mathbf{p}(F_t), \ldots, 2\mathbf{p}(F_{t+1} - 1), 2\mathbf{p}(F_{t-1}) + 1, \ldots, 2\mathbf{p}(F_t - 1) + 1\}.\end{aligned}$$

Whereas, by Proposition 6.14,

$$\begin{aligned}\{\bar{\mathbf{p}}(F_{t+1}), \ldots, \ & \bar{\mathbf{p}}(F_{t+2} - 1)\} \\ &= \{\bar{\mathbf{p}}(\boldsymbol{l}(F_t)), \ldots, \bar{\mathbf{p}}(\boldsymbol{l}(F_{t+1} - 1)), \bar{\mathbf{p}}(\boldsymbol{r}(F_{t-1})), \ldots, \bar{\mathbf{p}}(\boldsymbol{r}(F_t - 1))\} \\ &= \{2\bar{\mathbf{p}}(F_t), \ldots, 2\bar{\mathbf{p}}(F_{t+1} - 1), 2\bar{\mathbf{p}}(F_{t-1}) + 1, \ldots, 2\bar{\mathbf{p}}(F_t - 1) + 1\}.\end{aligned}$$

Demonstrate the second claim similarly, noting the identical makeup of corresponding cohorts in $\mathbf{P}$ and $\bar{\mathbf{P}}$. □

Corollary 6.17. *For the pairs of blade-dual arrays in the branch and clade quartets, the statements for all* $n \geq 0, k \geq 1$,

$$\begin{aligned}\mathbf{p}(\mathsf{F}_{n,k}) &= \bar{\mathbf{p}}(w_{n,k}), \\ \mathbf{p}(\mathsf{T}_{n,k}) &= \bar{\mathbf{p}}(\mathfrak{w}_{n,k}), \\ \mathbf{P}(\mathsf{L}_{n,k}) &= \bar{\mathbf{P}}(a_{n,k}), \\ \mathbf{P}(\mathsf{J}_{n,k}) &= \bar{\mathbf{P}}(\mathfrak{a}_{n,k}),\end{aligned}$$

imply, respectively,

$$\begin{aligned}F^{-1}(\mathsf{F}_{n,k}) &= F^{-1}(w_{n,k}), \\ F^{-1}(\mathsf{T}_{n,k}) &= F^{-1}(\mathfrak{w}_{n,k}), \\ F^{-1}(\mathsf{L}_{n,k}) &= F^{-1}(a_{n,k}), \\ F^{-1}(\mathsf{J}_{n,k}) &= F^{-1}(\mathfrak{a}_{n,k}).\end{aligned}$$

Proof. Follows from Lemmas 6.16. □

For the equalities demonstrated in Corollaries 6.13, 6.15, and 6.17, Proposition 6.18 will quantify the cohort index of the array entries.

Proposition 6.18 (Cohort index of array entries in the branch and clade quartets)**.** *Assume that the premises of Corollaries 6.13, 6.15, and 6.17 hold. Then for $k \geq 1$, the formulas*

$$\mathsf{F}_{n,k} = \quad n + F_{F^{-1}(n)+k+1}$$
$$\beth_{n,k} = \begin{cases} F_{2k}, & n = 0; \\ n + F_{F^{-1}(n)+2k-1} - F_{F^{-1}(n)-1}, & n > 0. \end{cases}$$

imply, respectively,

$$(83)\quad F^{-1}(\mathsf{F}_{n,k}) = F^{-1}(\mathsf{L}_{n,k}) = F^{-1}(w_{n,k}) = F^{-1}(a_{n,k}) = \ F^{-1}(n) + \ k+1, n \geq 0.$$

$$(84)\quad F^{-1}(\daleth_{n,k}) = F^{-1}(\beth_{n,k}) = F^{-1}(\mathfrak{w}_{n,k}) = F^{-1}(\mathfrak{v}_{n,k}) = \begin{cases} 2k, & n = 0; \\ F^{-1}(n)+2k-1, & n \geq 1. \end{cases}$$

Proof. First, write (83) using the formula for $\mathsf{F}_{n,k}$ to obtain $F^{-1}(n + F_{F^{-1}(n)+k+1})$ $= F^{-1}(n)+k+1$. Make the substitution $y = F^{-1}(n)+k+1$ to obtain $F^{-1}(n+F_y) = y$. This equality requires $n < F_{y-1} = F_{F^{-1}(n)+k}$, which is clearly true for all $k > 1$.

Next, write (84) using the formula for $\beth_{n,k}$. The case $n = 0$ is trivial, whereas $F^{-1}(F_{2k}) = 2k$. For $n \geq 1$, it gives $F^{-1}(n+F_{F^{-1}(n)+2k-1} - F_{F^{-1}(n)-1}) = F^{-1}(n)+$ $2k-1$. Make the substitution $y = F^{-1}(n)+2k-1$ to obtain $F^{-1}(n+F_y - F_{y-2k}) = y$. This equality requires $F_{y-2k} \leq n < F_{y-1} + F_{y-2k}$. The upper bound fails for $k = 0$, since $n \not< F_{y-1} + F_y = F_{y+1} = F_{F^{-1}(n)} = n$, but holds for all $k \geq 1$, since $n < F_{y-1} + F_{y-2k} \leq F_{y-1} + F_{y-2} = F_y = F_{F^{-1}(n)+1}$. The lower bound however, requires $n \geq 1$ just as claimed, since $F_{y-2k} = F_{F^{-1}(n)-1} \leq n$ only for $n \geq 1$. □

6.7. **Planar graph isomorphism between trees and tableaux.**

6.7.1. *Successor trees' planar graph isomorphism to Fibonacci cohort tableaux.* The following demonstrates that arcs of the minimal, respectively, maximal successor trees (Figures 3 and 10) can be stretched so as to arrange the nodes of each tree into the respective Fibonacci cohort tableau (Tables 6) without crossing arcs in the plane.

Lemma 6.19 (Decomposition of successor-tree branching into horizontal and vertical tableau displacement)**.** *With reference to the Fibonacci cohort tableaux of positive integers $n \in \mathbb{Z}_+$ (Tables 6), in the 1–2-Fibonacci cohort tableau (Table 6(i))*

$$(85)\qquad \bar{\boldsymbol{l}}(n) = \boldsymbol{l}(n) \ + \theta(n + 1 - F_{F^{-1}(n)}),$$

$$(86)\qquad \bar{\boldsymbol{r}}(n) = \boldsymbol{l}^2(n) + \kappa(n + 1 - F_{F^{-1}(n)});$$

and in the 2–1-Fibonacci cohort tableau (Table 6(ii))

$$\bar{\boldsymbol{L}}(n) = \boldsymbol{L}(n) \ - \theta(F_{F^{-1}(n)+1} - n),$$
$$\bar{\boldsymbol{R}}(n) = \boldsymbol{L}^2(n) - \kappa(F_{F^{-1}(n)+1} - n);$$

where for each equality, the first term on the right-hand side provides a vertical-only displacement from n within the tableau and the second term on the right-hand side provides a horizontal-only displacement from n within the tableau.

Proof. In Section 11. □

Corollary 6.20 (of Lemmas 6.11 and 6.19)**.**

$$F_{F^{-1}(n)+1} \leq \ \boldsymbol{l}(n) \leq \ \bar{\boldsymbol{l}}(n) \leq \bar{\boldsymbol{L}}(n) \leq \boldsymbol{L}(n) < F_{F^{-1}(n)+2};$$
$$F_{F^{-1}(n)+2} \leq \boldsymbol{R}(n) \leq \bar{\boldsymbol{R}}(n) \leq \bar{\boldsymbol{r}}(n) \leq \boldsymbol{r}(n) < F_{F^{-1}(n)+3}.$$

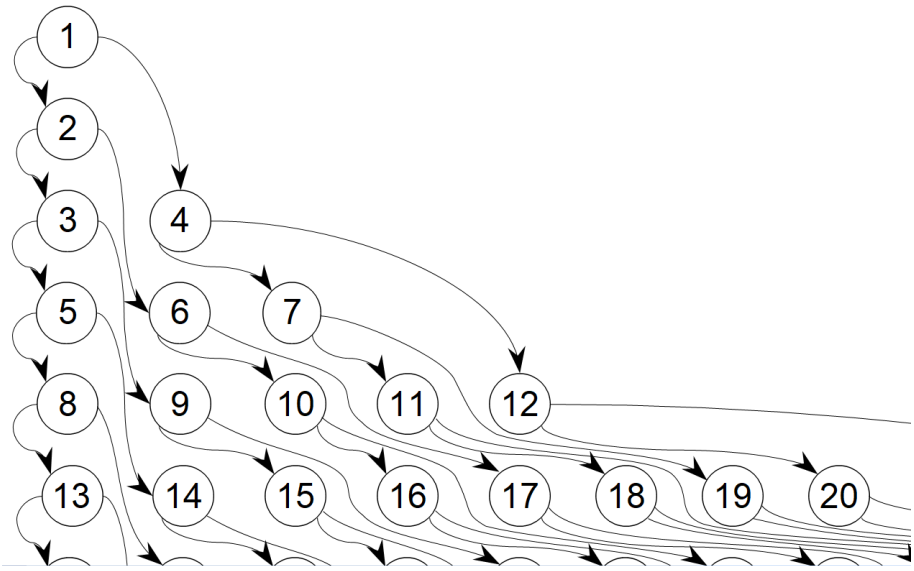

FIGURE 19. 1–2-Fibonacci cohort tableau (Table 6(i)) with arcs of $(n, \bar{\boldsymbol{l}}(n))$ and $(n, \bar{\boldsymbol{r}}(n))$the minimal successor tree (Figure 3) superimposed: A planar graph isomorphism

Proof. Follows from Lemmas 6.11 and 6.19, as well as the definitions of $\boldsymbol{l}$, $\boldsymbol{r}$, $\boldsymbol{L}$, and $\boldsymbol{R}$, noting that $\boldsymbol{l}(n) = n + F_{F^{-1}(n)-1} \in [F_{F^{-1}(n)+1}, F_{F^{-1}(n)+1} + F_{F^{-1}(n)-1})$, $\boldsymbol{L}(n) = n + F_{F^{-1}(n)} \in [2F_{F^{-1}(n)}, F_{F^{-1}(n)+2})$, $\boldsymbol{R}(n) = n + F_{F^{-1}(n)+1} \in [F_{F^{-1}(n)+2}, 2F_{F^{-1}(n)+1})$, and $\boldsymbol{r}(n) = n + F_{F^{-1}(n)+2} \in [F_{F^{-1}(n)} + F_{F^{-1}(n)+2}, F_{F^{-1}(n)+3})$. □

Remark 6.12. Note that $\bar{\boldsymbol{R}}(n) - \bar{\boldsymbol{L}}(n) = \underline{130312}(n)$, comprises F_t copies of each number F_t, while $\bar{\boldsymbol{r}}(n) - \bar{\boldsymbol{l}}(n)$ comprises F_t copies of each number $2F_{t+1}$.

Proposition 6.21 (Planar graph isomorphism between successor trees and Fibonacci cohort tableaux)**.** *The graph isomorphism between either successor tree, Figure 3 or 10, and its corresponding Fibonacci cohort tableau of the positive integers, Table 6(i), respectively, (ii), is a* planar *graph isomorphism. That is, taking the elements $S_1 = 1, S_2 = 2, S_3 = 1, \ldots$ of the tableau as "nodes," the arcs of the tree transfer to the tableau without crossing arcs.*

Proof for the minimal successor tree. Consider the 1–2-Fibonacci cohort tableau of $\mathbb{Z}_+$, Table 6(i).

Figure 19 shows the arcs of the minimal successor tree, Figure 3, transferred to the tableau. For each node n, the figure shows the (oriented) arcs $(n, \bar{\boldsymbol{l}}(n))$ and $(n, \bar{\boldsymbol{r}}(n))$. For $n \in [F_{t+1}, F_{t+2})$, (71) and (72) show, respectively, that $\bar{\boldsymbol{l}}(n) \in [F_{t+2}, F_{t+3})$ and $\bar{\boldsymbol{r}}(n) \in [F_{t+3}, F_{t+4})$. That is, for n in cohort C_t, $\bar{\boldsymbol{l}}(n)$ and $\bar{\boldsymbol{r}}(n)$ lie in cohorts C_{t+1} and C_{t+2}, respectively

Refer to the decomposition of $\bar{\boldsymbol{l}}$ given by Lemma 6.19. Observe that $\bar{\boldsymbol{l}}$ displaces n in the tableau horizontally by $\theta(n + 1 - F_{F^{-1}(n)}) = \theta(n + 1 - F_{t+1})$ and that this displacement is nonnegative and nondecreasing on $[F_{t+1}, F_{t+2})$, for each $t = 1, 2, 3, \ldots$. Thus, in connecting nodes $m, n \in [F_{t+1}, F_{t+2})$ to the respective nodes

$\bar{\boldsymbol{l}}(m), \bar{\boldsymbol{l}}(n) \in [F_{t+2}, F_{t+3})$, the arcs $(m, \bar{\boldsymbol{l}}(m))$ and $(n, \bar{\boldsymbol{l}}(n))$ will not intersect one another.

Further, observe that $\bar{\boldsymbol{r}}$ displaces n in the tableau horizontally by $\kappa(n+1-F_{F^{-1}(n)}) = \kappa(n+1-F_{t+1})$, that this displacement is positive and increasing on $[F_{t+1}, F_{t+2})$, for each $t = 1, 2, 3, \ldots$, and further, this displacement satisfies the inequality $\kappa(n+1-F_{t+1}) > \theta(n+1-F_{t+1})$. Hence, as Figure 19 shows, on its descent from node $n \in [F_{t+1}, F_{t+2})$ to node $\bar{\boldsymbol{r}}(n) \in [F_{t+3}, F_{t+4})$ the arc $(n, \bar{\boldsymbol{r}}(n))$ will follow alongside the arc $(n, \bar{\boldsymbol{l}}(n))$, always keeping to the right of the latter. If $\bar{\boldsymbol{l}}(n)+1 \in [F_{t+2}, F_{t+3})$, *i.e.*, if $\bar{\boldsymbol{l}}(n)$ has a right neighbor in C_{t+1}, then the arc will then also pass between nodes $\bar{\boldsymbol{l}}(n)$ and $\bar{\boldsymbol{l}}(n)+1$ to reach node $\bar{\boldsymbol{r}}(n)$ without intersecting any arc $(m, \bar{\boldsymbol{l}}(m))$ nor any other arc $(m, \bar{\boldsymbol{r}}(m))$, for $m \in [F_{t+1}, F_{t+2})$.

Thus, arcs descending from nodes in the *same* cohort never cross, and it remains only to show that the arcs descending from a node in cohort C_t can reach cohort C_{t+2} without crossing an arc that descends from a node in cohort C_{t+1}. In particular, for $n \in [F_{t+1}, F_{t+2})$ of cohort C_t, the arc $(n, \bar{\boldsymbol{r}}(n))$, where $\bar{\boldsymbol{r}}(n) \in [F_{t+3}, F_{t+4})$ must not intersect any arc $(m, \bar{\boldsymbol{l}}(m))$ or $(m, \bar{\boldsymbol{r}}(m))$ for $m \in [F_{t+2}, F_{t+3})$. Once again, since the horizontal displacement $\kappa(n+1-F_{t+1}) > \theta(n+1-F_{t+1})$ is positive and increasing on $[F_{t+2}, F_{t+3})$, it suffices to show that the arc $(n, \bar{\boldsymbol{r}}(n))$ does not intersect the arc $(\bar{\boldsymbol{l}}(n)+1, \bar{\boldsymbol{l}}(\bar{\boldsymbol{l}}(n)+1))$, the latter being the arc whose origin and destination both have the least possible horizontal displacement from those of $(n, \bar{\boldsymbol{r}}(n))$, whilst originating to the right of it.

For the two arcs to avoid intersection, it suffices to have $\bar{\boldsymbol{l}}(\bar{\boldsymbol{l}}(n)+1) - \bar{\boldsymbol{r}}(n) \geq 0$, so that the destination of the latter arc is also to the right of the former. Whereas the graphs are 3-regular, however, a node can only have at most one entering arc (it is either the root node, or a left child, or a right child). Thus the inequality must be satisfied strictly, if satisfied at all. Substituting the definitions of $\bar{\boldsymbol{l}}$ and $\bar{\boldsymbol{r}}$, the condition for non-intersection of the arcs becomes $\kappa(\kappa(n+1)-1+1+1)-1-(\lambda(n+1)-1) = \kappa(\kappa(n+1)+1) - \lambda(n+1) \geq 0$. Let $m = \kappa(\kappa(n+1)+1)$ in (75), and manipulate

$$0 \leq \phi(\kappa(n+1)+1) - \kappa(\kappa(n+1)+1) < 1,$$

into

$$\phi - 1 + \phi\kappa(n+1) < \kappa(\kappa(n+1)+1) \leq \phi + \phi\kappa(n+1).$$

Also, let $m = \kappa^2(n+1)$ in (75) and manipulate

$$0 \leq \phi\kappa(n+1) - \kappa^2(n+1) < 1$$

into

$$\kappa^2(n+1) \leq \phi\kappa(n+1) < 1 + \kappa^2(n+1).$$

Combining these gives

$$\begin{aligned} \phi - 1 + \kappa^2(n+1) \leq \phi - 1 + \phi\kappa(n+1) & \\ < \kappa(\kappa(n+1)+1) & \\ \leq \phi + \phi\kappa(n+1) < \phi + 1 + \kappa^2(n+1), & \end{aligned}$$

thus,

$$\phi - 1 < \kappa(\kappa(n+1)+1) - \kappa^2(n+1) < \phi + 1.$$

Since $n+1 \geq 1$, substitute in the complementary equation $\kappa^2+1 = \lambda$ (Example 4.7), to give

$$-0.382 \approx \phi - 2 < \kappa(\kappa(n+1)+1) - 1 - (\lambda(n+1)-1) < \phi \approx 1.618.$$

Thus, as desired, the integer quantity $\kappa(\kappa(n+1)+1)-1-(\lambda(n+1)-1)$ is either 0 or 1. Again, whereas the graphs are 3-regular, in fact, $\kappa(\kappa(n+1)+1)-1-(\lambda(n+1)-1) = 1$, strictly satisfying the desired inequality. Note that the complementary equation introduced as a substitution is valid for $n \geq 0$.

Proof for the maximal successor tree is analogous. □

Proposition 6.21 implies a stronger version of Proposition 6.14: For each Fibonacci cohort of the positive integers, not only are its tree positions reversed from one another in the two successor trees, but the positions are in order, horizontally increasing (decreasing) for the minimal (maximal) successor tree. Figure 19 makes this easy to visualize, whereas it is impossible to switch the horizontal positions of two nodes on the same row (cohort) without crossing arcs. Thus the tree preserves their left-to-right order.

Corollary 6.22 (of Proposition 6.21. Cohorts horizontally ordered within successor trees)**.** *For $t = 1, 2, 3, \ldots$,*

$$\{\log_2 \bar{\mathbf{p}}(F_{t+1})\} = \{\log_2 \bar{\mathbf{P}}(F_{t+2}-1)\} < \cdots < \{\log_2 \bar{\mathbf{p}}(F_{t+2}-1)\} = \{\log_2 \bar{\mathbf{P}}(F_{t+1})\}.$$

6.7.2. *Fibonacci trees' planar graph isomorphism to successor cohort tableaux.*

Remark 6.13. Does Corollary 6.22 have an analog for the Fibonacci trees? Note that while Proposition 6.12 identified the positions of positive integers in the Fibonacci trees, a more subtle question deals with the relative horizontal positions of a set of integers from left to right within each of the trees. Specifically, for each $t = 1, 2, 3, \ldots$, how is the t^{th} cohort of the positive integers $C_t = (F_{t+1}, \ldots, F_{t+2}-1)$ ordered from left to right within each of the Fibonacci trees? Since level r of a tree contains positions $\{2^{r-1}, \ldots, 2^r - 1\}$, the left-to-right order of the nodal positions of a set of integers therefore follows the fractional part of the base-2 log of the respective positions.

For example, take $t = 6$ and consider the left–to–right order of $C_5 = (13, 14, 15, 16, 17, 18, 19, 20)$ in Figure 5. Table 18(i) would gives the positions $\mathbf{p}(C_6) = (32, 24, 20, 18, 14, 17, 13, 11)$. Taking the fractional part of the base-2 logs of these positions obtain $\{\log_2 \mathbf{p}(13)\} < \{\log_2 \mathbf{p}(18)\} < \{\log_2 \mathbf{p}(16)\} < \{\log_2 \mathbf{p}(15)\} < \{\log_2 \mathbf{p}(20)\} < \{\log_2 \mathbf{p}(14)\} < \{\log_2 \mathbf{p}(19)\} < \{\log_2 \mathbf{p}(17)\}$ (approximately $0 < 0.09 < 0.17 < 0.32 < 0.46 < 0.58 < 0.7 < 0.81$), making the left-to-right order $(13, 18, 16, 15, 20, 14, 19, 17)$.

Figure 19 furnished the 1–2-Fibonacci cohort tableau of the positive integers (Table 6(i)) with arcs that correspond to those of the minimal successor tree, thus converting the tableau into an infinite, regular, single-rooted binary tree. Since no arcs crossed, the two trees were planar graph isomorphs of one another. This begs the question: What tableaux are in planar graph isomorphism with the Fibonacci trees?

Table 19(i) and (ii) shows the *successor tableaux* that are planar graph isomorphs of the minimal, respectively, maximal Fibonacci trees. The tableaux can

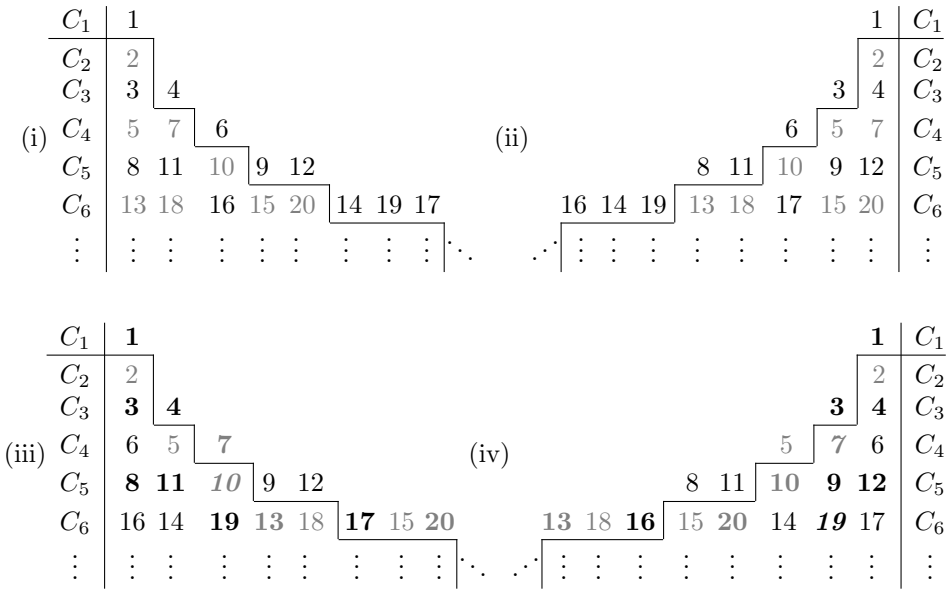

TABLE 19. Successor cohort tableaux: With the 1–2-Fibonacci cohort relations and 2–1-Fibonacci cohort relations superimposed as arcs on (i) and (ii), respectively, these tableaux become infinite, regular, single-rooted binary trees that are planar graph isomorphic to the minimal (i) and maximal (ii) Fibonacci trees. Thus (i) and (ii) are blade duals of Tables 6(i) and (ii), respectively. In (i) and (ii), each element aligns directly above its left child from the minimal (i) or maximal (ii) successor tree. Hence columns of (i) and (ii) give rows of w and a, respectively, comparable to the respective "diatomic" tableaux in Tables 40(i) and (ii). In (iii) and (iv), each element lies in the same column as its right child from the maximal (iii) or minimal (iv) successor tree, in the second cohort below. Thus, split columns of (iii) and (iv) give rows of $\mathfrak{w}$ and $\mathfrak{w}$, respectively. Compare this "cohort tableau" method — that uses columns and split columns of tableaux to obtain rows of the clade quartet — with that for the branch quartet (Table 6).

be furnished with arcs corresponding to the 1–2-, respectively, 2–1-Fibonacci cohort relations (Example 4.20), without crossing arcs.

Table 19(i) appears to permute each cohort by sorting the fractional part of the base-2 logs of its positions within the binary tree, in the manner that Remark 6.13 suggests. However, Section 7.3 describes the *intra-cohort blade* permutations of Tables 19(i) and (ii) directly, without reference to tree positions. Section 8.2.4 will revisit the successor tableaux in the context of the clade quartet.

6.8. **Branching palindromes and node coincidences between trees.**

Remark 6.14 (Double-left branching). From the definition of branching shown in 15(iii) and (iv), observe that $\boldsymbol{L}^2 = \boldsymbol{r}$, that is, two consecutive left branchings in the maximal Fibonacci tree yields the same value as a right branching from the same value in the minimal Fibonacci tree, since $F_{F^{-1}(n)} + F_{F^{-1}(n)+1} = F_{F^{-1}(n)+2}$. Conversely, $\boldsymbol{l}^2 = \boldsymbol{R}$, that is, two consecutive left branchings in the minimal Fibonacci tree yields the same value as a right branching from the same value in the maximal

Fibonacci tree, since, $F_{F^{-1}(n)-1} + F_{F^{-1}(n)} = F_{F^{-1}(n)+1}$. For example, a double-left branching from "1" in Figure 8 yields "4," whereas a single right branching from "1" in Figure 5 also yields "4." Conversely, a double-left branching from "1" in Figure 5 yields "3", whereas a single right branching from in Figure 8 also yields "3."

The effect of double-left branching can also be visualized in the tableaux. The operation $\boldsymbol{L}$ maps an element of cohort C_t to the element directly below it in (the same horizontal position and in cohort C_{t+1} of) a 2–1-Fibonacci cohort tableau. Now, in a 1–2-Fibonacci cohort tableau, $\boldsymbol{l}$ maps an element of cohort C_t to the element directly below it (in cohort C_{t+1} and in the same horizontal position), whilst the operation $\boldsymbol{r}$ maps an element of cohort C_t to the corresponding element in the right subcohort of cohort C_{t+2} in the 1–2-Fibonacci cohort tableau, that is, to the second cohort below and displaced to the right by F_{t+1}, or the length of the left subcohort of cohort C_{t+1}. Transferred to the 2–1-Fibonacci cohort tableau, the same displacement takes an element of cohort C_t to the second element directly below it (in the same horizontal position) and in cohort C_{t+2}. Hence, a comparison of the two tableaux provides a visualization of the identity $\boldsymbol{L}^2 = \boldsymbol{r}$, and can be employed similarly to visualize $\boldsymbol{l}^2 = \boldsymbol{R}$.

For branching in the successor trees as shown in 15(i) and (ii), the effect of double-left branching is not as uniform as it is in the Fibonacci trees. Nonetheless, Lemma 6.9 shows that the effect holds for lower Wythoff numbers, which may be stated as follows:

Corollary 6.23 (of Proposition 6.9: Blade-dual identities and Wythoff signature of branching functions in successor trees)**.**

$$\vec{\boldsymbol{l}}^2\kappa = \bar{\boldsymbol{R}}\kappa \quad = \kappa\lambda \quad \subset K \text{ and} \tag{87}$$

$$\bar{\boldsymbol{L}}^2\kappa = \bar{\boldsymbol{r}}\kappa \quad = \kappa\lambda + 1 \subset K \tag{88}$$

$$\bar{\boldsymbol{r}}\bar{\boldsymbol{l}}\kappa = \bar{\boldsymbol{R}}\bar{\boldsymbol{L}}\kappa = \lambda^2 + 1 \subset K \tag{89}$$

More generally,

$$\vec{\boldsymbol{l}}^k\kappa = \begin{cases} \bar{\boldsymbol{L}}\bar{\boldsymbol{R}}^{(k-1)/2}\kappa & \subseteq \Lambda, \quad k \geq 1 \text{ odd}; \\ \bar{\boldsymbol{R}}^{k/2}\kappa & \subset K, \quad k \geq 2 \text{ even}; \end{cases} \tag{90}$$

with equality only for $k = 1$ *and*

$$\bar{\boldsymbol{L}}^k\kappa = \begin{cases} \bar{\boldsymbol{l}}\bar{\boldsymbol{r}}^{(k-1)/2}\kappa & \subseteq \Lambda, \quad k \geq 1 \text{ odd}; \\ \bar{\boldsymbol{r}}^{k/2}\kappa & \subset K, \quad k \geq 2 \text{ even}; \end{cases} \tag{91}$$

with equality only for $k = 1$.

Lemma 8.19 and Proposition 8.20 will exploit the double-left branching of the successor trees given in Corollary 6.23.

Remark 6.15 (Coincidences in the minimal and maximal Fibonacci trees). Similarly to the previous remark, consider the branching shown in 15(iii) and (iv) and observe that a right branching from n followed by a left branching yields the same value in either Fibonacci tree: $\boldsymbol{l}(\boldsymbol{r}(n)) = \boldsymbol{L}(\boldsymbol{R}(n)) = n + F_{F^{-1}(n)+3}$. In the minimal Fibonacci tree, for $F_t \leq n < F_{t+1}$, the right child of node n satisfies $F_t + F_{t+2} \leq \boldsymbol{r}(n) = n + F_{t+2} < F_{t+3}$, hence $\boldsymbol{l}(\boldsymbol{r}(n)) = n + F_{t+2} + F_{t+1} = n + F_{t+3}$. In the maximal Fibonacci tree, for $F_t \leq n < F_{t+1}$, the right child of node n satisfies $F_{t+2} \leq \boldsymbol{R}(n) = n + F_{t+1} < 2F_{t+1}$, hence $\boldsymbol{L}(\boldsymbol{R}(n)) = n + F_{t+1} + F_{t+2} = n + F_{t+3}$.

Noting further that "1" and "2" have the same positions in Figures 5 and 8, that is, $\mathbf{p}(1) = \mathbf{P}(1) = 1$ and $\mathbf{p}(2) = \mathbf{P}(2) = 2$, observe that these two nodes generate two sequences of coincident nodes between the two trees, both of which skip levels of the trees, alternating levels between the two sets. For $k = 1, 2, 3 \ldots$, the sequence $(\boldsymbol{lr})^{k-1}(1) = (\boldsymbol{LR})^{k-1}(1) = \sum_{j=1}^{k} F_{3j-1} = 1/2(F_{3k+1} - 1)$, or 049651, descending from grandparent to grandchild starting with "1," appears at positions $\mathbf{p}((\boldsymbol{lr})^{k-1}(1)) = \mathbf{P}((\boldsymbol{LR})^{k-1}(1)) = 4^{k-1} + 2/3(4^{k-1} - 1)$, or 020989, and the sequence $(\boldsymbol{lr})^{k-1}(2) = (\boldsymbol{LR})^{k-1}(2) = \sum_{j=1}^{k} F_{3j} = 1/2(F_{3k+2} - 1)$, or 099919, descending from grandparent to grandchild starting with "2," appears at positions $\mathbf{p}((\boldsymbol{lr})^{k-1}(2)) = \mathbf{P}((\boldsymbol{LR})^{k-1}(2)) = 2 \times 4^{k-1} + 2/3(4^{k-1} - 1)$, or 020988. Collectively, the coincident nodes occur at positions 061547.

Remark 6.16 (Coincident chain in the minimal and maximal successor trees). The sequences of values given in the previous remark and appearing at coincident positions in the two Fibonacci trees, also appear at coincident positions in the two successor trees. Whereas their positions in the successor trees are different from those in the Fibonacci trees, however, the two coincident sequences form a single chain of descent in each of the successor trees. The former sequence of values $(\bar{\boldsymbol{r}}\bar{\boldsymbol{l}})^{k-1}(1) = (\bar{\boldsymbol{R}}\bar{\boldsymbol{L}})^{k-1}(1) = \sum_{j=1}^{k} F_{3j-1} = 1/2(F_{3k+1} - 1)$, or 049651, appears at positions $\bar{\mathbf{p}}((\bar{\boldsymbol{r}}\bar{\boldsymbol{l}})^{k-1}(1)) = \bar{\mathbf{P}}((\bar{\boldsymbol{R}}\bar{\boldsymbol{L}})^{k-1}(1)) = 4^{k-1} + 1/3(4^{k-1} - 1)$, or 002450, while the latter sequence of values $(\bar{\boldsymbol{l}}\bar{\boldsymbol{r}})^{k-1}(2) = (\bar{\boldsymbol{L}}\bar{\boldsymbol{R}})^{k-1}(2) = \sum_{j=1}^{k} F_{3j} = 1/2(F_{3k+2} - 1)$, or 099919, appears at the same positions $\bar{\mathbf{p}}((\bar{\boldsymbol{l}}\bar{\boldsymbol{r}})^{k-1}(2)) = \bar{\mathbf{P}}((\bar{\boldsymbol{L}}\bar{\boldsymbol{R}})^{k-1}(2)) = 2 \times 4^{k-1} + 2/3(4^{k-1} - 1)$, or 020988, as in the Fibonacci trees. In the successor trees, however, since the latter are right children of the former, whilst the former are left children of the latter, together the two sequences form a zigzagging chain of descent. Observe this from $\mathbf{2} \times 002450_k = \mathbf{2}(4^{k-1} + 1/3(4^{k-1} - 1)) = 2 \times 4^{k-1} + 2/3(4^{k-1} - 1) = 020988_k$ and $\mathbf{2} \times 020988_k + 1 = \mathbf{2}(2 \times 4^{k-1} + 2/3(4^{k-1} - 1)) + 1 = 4^k + 1/3(4^k - 1)) = 002450_{k+1}$, for $k = 1, 2, 3, \ldots$. Collectively, the chain of coincident nodes occupies positions 000975.

Remark 6.17. Consider the commutative diagram in Figure 20, where $\mathbf{B}(n) \equiv$ 059893$(n) = 1,\ 2, 3,\ 4, 6, 5, 7,\ 8, 12, 10, 14,\ 9, 13, 11, 15,\ 16, 24, 20, 28, 18, 26, 22, 30, 17, 25, 21, 29, 19, 27, 23, 31, \ldots$ is the self-inverse tree blade permutation, and $\mathbf{C}(n) = 1,\ 2, 4,\ 3, 8, 6, 16,\ 5, 12, 10, 32,\ 9, 24, 18, 64, 7, 20, 14, 48,\ 17, 40, 34, 128, 13, 36, 26, 96, 33, 72, 66, 256, \ldots$ and $\mathbf{D}(n) = 1, 2, 4, 3, 5, 8, 16, 6, 12, 10, 20, 9, 17, 32, 64, 7, 13, 24, 48, 11, 21, 40, 80, 18, 36, 34, 68, 33, 65, 128, 256, \ldots$ are self-inverse permutations not found in the OEIS [41] as of this writing.

Observe that Remarks 6.15 and 6.16 described fixed-points of $\mathbf{C}$ and $\mathbf{D}$, respectively. Now, fixed points of $\mathbf{B}$ occur at $1,\ 2, 3,\ 4, 7, 8, 10,\ 13, 15, 16, 22, 25, 31, 32, 36, 42, 46, 49, 53, 59, 63, 64, 76, 82, 94, 97, 109, 115, 127, 128, 136, \ldots$, given by 329395, previously noted by Kimberling to coincide with the palindromes in left-to-right binary enumeration (081242), or equivalently, palindromic sequences of left-right branching in the trees.

It is at these positions at which values coincide in the two minimal trees, Figures 3 and 5 as well as in the two maximal trees, Figures 8 and 10, these being the sequences of values $1,\ 2, 3,\ 4, 5, 8, 10,\ 12, 13, 19, 21, 24, 28, 30, 33,\ 34, 44, 48, 55, 60, 66, 70, 75, 77, 82, 88, 89, 105, 112, 124, 140, \ldots$, respectively, $1,\ 2, 3, 4,\ 7, 8, 10,\ 12, 14, 20, 21, 24, 26, 30, 33,\ 40, 44, 54, 55, 61, 66, 68, 73, 77, 83, 88, 92, 108, 120, 127, 143, \ldots$, neither located in the OEIS [41] as of this writing.

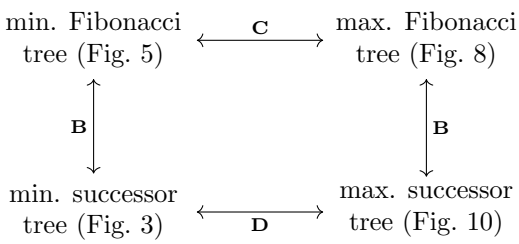

FIGURE 20. Remark 6.17: Commutative diagram for the quartet of trees, Table 5

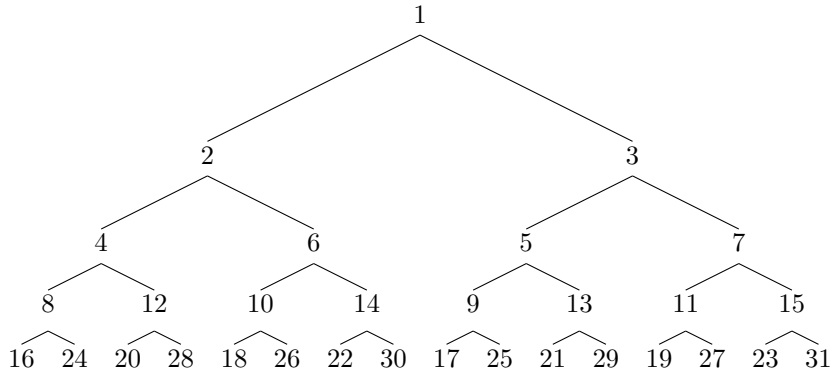

FIGURE 21. The Blade tree, 059893. Blade dual of Figure 18. Sequences of left or right branchings give rows of I–D arrays shown in Table 41. Sequences of left or right clades give columns of I–D arrays shown in Table 41. Siblings of the same parent node grow ever closer in 2-adic distance, thus minimizing an aggregate measure of 2-adic distance over binary trees that arrange $\mathbb{Z}_+$.

6.8.1. *The blade permutation and Blade tree.* At this point, the self-inverse permutation $\mathbf{B}(n) \equiv$ 059893(n) deserves explanation, and its entry in the OEIS [41] derives it from binary numeration. For the blade permutation, first write each positive integer in binary representation. Then whilst holding fixed the most significant digit of the representation, reverse the remaining digits and evaluate. (The most significant digit the one on the right, in the present notational convention. See Remark 6.2.) Consider for example, the 4^{th} level of the tree, Figure 18. This level of the tree contains the values $(2^{4-1}, \ldots, 2^4-1) = (8, 9, 10, 11, 12, 13, 14, 15)$, which can be written $(0001, 1001, 0101, 1101, 0011, 1011, 0111, 1111)$ on the basis $(1, 2, 4, 8)$. Reversing all but the most significant digit gives $(0001, 0011, 0101, 0111, 1001, 1011, 1101, 1111)$, which evaluates to $(\mathbf{B}(8), \ldots, \mathbf{B}(15)) = (8, 12, 10, 14, 9, 13, 11, 15)$.

As previously mentioned, the blade permutation quite usefully turns Fibonacci trees (Figures 5 and 8) into successor trees (Figures 3 and 10), respectively, and vice versa. For the tree of positions Figure 18, its blade dual, shown in Figure 21, illustrates what can be simply (and fittingly) called the *Blade tree*.

At the end of the next section, a derivation analogous to that of the blade permutation, substituting Fibonacci numeration in place of binary numeration, will produce the permutations of the positive integers listed in Tables 19(i) and (ii).

Section 7.3 will designate these permutations *intra-cohort blades*. First, however, the several types of Fibonacci numeration warrant further exploration.

Remark 6.18 (2-adic distance in the Blade tree). Observe that with successive levels of the Blade tree (Figure 21), siblings of the same parent node grow ever closer in 2-adic distance. This implies that the Blade tree minimizes a measure of central tendency of the 2-adic distance between neighboring nodes over the space of binary-tree arrangements of the positive integers.

A similar observation can be made about its blade dual, the Positions tree (Figure 18), which minimizes an aggregate measure of distance between (values of) neighboring nodes in the usual metric.

7. Cohort Sequences of Tuples and Compositions of Integers

Section 4 treated cohort sequences of integers and their construction by affine catenative recurrence. In that context, the operations for constructing a cohort comprised the concatenation of prior cohorts and modifying their individual elements by scalar addition. Extending the context to cohort sequences whose elements are tuples (words), these elements also fall into cohorts whose length increases via recursive concatenation of prior cohorts. Rather than scalar addition, however, new elements form from prior ones using two other operations: Extension of an existing tuple (word) by pushing a new element (letter) onto one of its ends, written $\oplus$, and increment, written `++`, of the element (letter) at one end of an existing tuple (word) (By assumption, the tupled elements / letters come from an ordered set / alphabet).

The Fibonacci expansions in Section 6 motivate the extension of Definitions 4.1, 4.2, 4.3 and 4.4 from sequences of integers to sequences of tuples. Moreover, Definition 7.1 allows the sequences of tuples to be placed into total order via direct comparison of the tuples, without relying on an explicit isomorphism between the tuples and the positive integers.

Propositions 7.1 and 7.6 use cohorts to enumerate restricted compositions of integers, thus providing constructive proofs of known combinatorial results. These results on compositions relate back to the quilt via Corollary 7.2 and Proposition 7.5.

Definition 7.1 (Fibonacci Cohort Sequences of Tuples or Words)**.** By analogy to Definitions 4.1 and 4.3, decompose a sequence $T_1, T_2, \ldots, T_n, \ldots$ of tuples into finite blocks of consecutive tuples (cohorts), $C_1, C_2, \ldots, C_t, \ldots$ of increasing length $|C_t| = F_t$. If for $f_L(t), f_R(t)$, tuple-valued functions of tuples, also depending on t, the cohorts satisfy $C_t = f_L(C_{t-2})f_R(C_{t-1})$ for each cohort C_t, $t = 3, 4, \ldots$, where $C_{t-2}C_{t-1}$ is the juxtaposition of C_{t-2} and C_{t-1}, and $f_L(t), f_R(t)$ distribute to each individual tuple T_n, then designate $(T_n)_{n\geq 1}$ a *2–1-Fibonacci cohort sequence of tuples under* $\langle f_L(t), f_R(t)\rangle$, and designate $\langle f_L(t), f_R(t)\rangle$ a *Fibonacci cohortizer* of $(T_n)_{n\geq 1}$.

If $f_L \equiv f_R$ in the above, then abbreviate the designation to *Fibonacci cohort sequence of tuples* under cohortizer $f(t) = f_L(t) = f_R(t)$. Then, by analogy to Definition 4.2, if the cohorts further satisfy $C_2 = f(C_1)$, then the sequence is a *Fibonacci cohort sequence of tuples from the* 1^{st} *cohort*; and further, should the sequence have a zeroth element T_0, corresponding to the singleton zeroth cohort C_0, and satisfy $C_1 = f(C_0)$, then designate the sequence a *Fibonacci cohort sequence of*

tuples from the 0^{th} cohort. (Note that the unique element of cohort C_0 may itself be — and often is — the empty tuple () or empty word ε).

Finally, if the cohorts instead satisfy $C_t = f_L(C_{t-1})f_R(C_{t-2})$, then by analogy to Definition 4.4, designate $(T_n)_{n\geq 1}$ a *1–2-Fibonacci cohort sequence of tuples under* $\langle f_L(t), f_R(t)\rangle$.

The remainder of the discussion of Fibonacci cohort sequences of tuples will mostly restrict the cohortizer operator $f(t)$ of Definition 7.1 to the particular "outer" forms $f(t)(T) \equiv T \oplus U$ and $f(t)(T) \equiv T\texttt{++}$ of extension, respectively, increment. For example, for the tuple $T = (t_1, \ldots, t_n)$ and singleton $U = (u_1)$, consider $T \oplus U = (t_1, \ldots, t_n, u_1)$ and $T\texttt{++} = (t_1, \ldots, t_{n-1}, t_n + 1)$. These outer forms of the cohortizer operate on the "most significant" end of the tuple, by appending an element onto it or incrementing the last element.

Occasionally the development will also consider the "inner" versions $f(t)(T) \equiv U \oplus T = (u_1, t_1, \ldots, t_n)$ and $f(t)(T) \equiv \texttt{++}T = (t_1 + 1, t_2 \ldots, t_n)$ of extension, respectively, increment, in which the cohortizer operates on the "least significant" end of the tuple by prepending an element onto it or incrementing the first element.

Because the cohortizer generally includes the operation of extension, this construction of cohort sequences of tuples could rightly be described as an "extensive catenative recurrence."

7.1. **Cohort sequences in maximal expansion & integer compositions.**

Example 7.1. Consider the sequence $(\mathbf{F}_\star(n))_{n\geq 1}$ of maximal Fibonacci indices of the positive integers under cohortizer $f(t)(T) = T \oplus (t)$ (Definition 6.2). Then, the 2–1-Fibonacci cohort structure of the integers themselves, under cohortizer F_t (Example 4.2), induces a corresponding structure on the tuple of maximal Fibonacci indices, which follows from Proposition 6.8. Table 20 shows the sequence of tuples in a cohort tableau.

For example, the integer "12" appears at the end of cohort C_5 and its maximal expansion $12 = F_1 + F_2 + F_3 + F_4 + F_5$ can be written as the juxtaposition of tuples $(1, 2, 3, 4)(5) = (1, 2, 3, 4, \mathbf{5}) = \mathbf{F}_\star(12)$, to emphasize its origin in the expansion of "7" from the end of cohort C_4 via $\mathbf{F}_\star(12) = \mathbf{F}_\star(7) \oplus (5) = (1, 2, 3, 4)(5)$.

C_1					(1)
C_2					$(1, \mathbf{2})$
C_3				$(1, \mathbf{3})$	$(1, 2, \mathbf{3})$
C_4			$(1, 2, \mathbf{4})$	$(1, 3, \mathbf{4})$	$(1, 2, 3, \mathbf{4})$
C_5	$(1, 3, \mathbf{5})$	$(1, 2, 3, \mathbf{5})$	$(1, 2, 4, \mathbf{5})$	$(1, 3, 4, \mathbf{5})$	$(1, 2, 3, 4, \mathbf{5})$
$\vdots$	$\vdots$	$\vdots$	$\vdots$	$\vdots$	$\vdots$

TABLE 20. 2–1-Fibonacci outer cohort tableau of maximal Fibonacci indices $\mathbf{F}_\star(n)$

Table 21 shows the same expansion in maximal Fibonacci binary notation (see Remark 6.2), making it apparent that each left subcohort (above the staircase) forms by appending ·01 to elements of the second previous cohort, and that each right subcohort (below the staircase) forms by appending ·1 to elements of the previous cohort.

C_1						1
C_2						1**1**
C_3					1**01**	11**1**
C_4				11**01**	101**1**	111**1**
C_5	101**01**	111**01**		1101**1**	1011**1**	1111**1**
⋮	⋮	⋮	⋮	⋮	⋮	⋮

TABLE 21. 2–1-Fibonacci outer cohort tableau of the sequence of positive integers in maximal Fibonacci binary notation

Example 7.2. The maximal Fibonacci gaps of the positive integers $\boldsymbol{\nabla}_\star(n)$ (Definition 6.3) form a 2–1-Fibonacci cohort sequence under cohortizer $\langle f_L, f_R\rangle = \langle \oplus 2, \oplus 1\rangle$ with cohots $C_1 = ()$, $C_2 = (1)$, $C_3 = (2, 11)$, $C_4 = (12, 21, 111)$, $C_5 = (22, 112, 121, 211, 1111)$, $C_6 = (122, 212, 1112, 221, 1121, 1211, 2111, 11111), \ldots$. Table 22 shows the elements written as words, rather than tuples, to emphasize the relationship of its lexicography to that of other Fibonacci cohort tableaux, Tables 13 and 32 (isomorphism) and Tables 10, 11, 16 (duality).

C_1								ε
C_2								1
C_3							2	1^2
C_4						12	21	1^3
C_5				2^2	1^22	121	21^2	1^4
C_6	12^2	212	1^32	2^21	1^221	121^2	21^3	1^5
⋮	⋮	⋮	⋮	⋮	⋮			

TABLE 22. 2–1-Fibonacci outer cohort tableau of maximal Fibonacci gaps $\boldsymbol{\nabla}_\star(n)$. Isomorph of Tables 13 and 32(ii). Cohort dual of Tables 10, 11, and 16

Remark 7.1. Tables 20, 21, and 22 exhibit 2–1-Fibonacci *outer* cohort tableaux, the same structure exhibited in Table 7(ii). Because of the notational convention of writing indices from least to greatest significance, (explained in Remark 6.2), symbols 1 and 2 in Table 22 appear reverse order relative to symbols l and r in Table 7(ii). Nevertheless, the tableaux for maximal Fibonacci expansion take the outer form, whereas they originate in the binary trees Figures 8 and 13, whose values equal $N_0(S)+1$ for compositions of θ and η at the corresponding nodes of the outer binary tree, Figure 7 or alternatively, as the images of 1 under compositions of the branching functions $\boldsymbol{L}$ and $\boldsymbol{R}$ in an outer binary tree (not depicted). Tables 13 and 32(ii) show, respectively, the compositions of θ and η and the compositions of $\boldsymbol{L}$ and $\boldsymbol{R}$, both as 2–1-Fibonacci outer cohort tableaux. Table 22 is isomorphic to these.

Remark 7.2. The words in Table 22 are out of lexicographic order ($\prec$). As a sequence, therefore, it is not the same as Sloane's 114034. For example, while

the sequence of integers $14 < 15 < 16$ increases, that of their maximal Fibonacci gaps $(\boldsymbol{\nabla}_\star(14), \boldsymbol{\nabla}_\star(15), \boldsymbol{\nabla}_\star(16)) = (212, 1112, 221)$ is not monotonic with respect to (reverse) lexicographic order: $212 \succ 1112 \prec 221$.

By construction (Proposition 6.8), elements in Table 20 do not skip more than one index. Correspondingly, those in Table 21 do not contain more than one consecutive zero, while the gaps in Table 22 comprise only ones and twos (1s and 2s). Proposition 7.1 shows the converse: All strings of ones and twos are contained in the maximal Fibonacci gaps for the positive integers, $\{1, 2\}^\star = \boldsymbol{\nabla}_\star(\mathbb{Z}_+)$. Further, while F_t is equal to the number of compositions of $t-1$ using only ones and twos [2], the maximal Fibonacci gaps provide a bijection between the positive integers and the set of all such restricted compositions.

Proposition 7.1 (Maximal Fibonacci gaps as restricted compositions)**.** *For $t = 1, 2, \ldots$, an integer n satisfies $F_{t+1} \leq n < F_{t+2}$ if and only if $\boldsymbol{\nabla}_\star(n)$ is a composition of $t-1$ using only ones and twos.*

If: Example 7.2 shows that the proposition holds for the first few values of n. Suppose the proposition true for all $1 \leq n < F_{t+1}$, and let $\boldsymbol{\nabla}_\star(n)$ be a composition of $t-1$ using only ones and twos. In particular, its last element is either 1 or 2.

In the former case, removing the final 1 yields $\boldsymbol{\nabla}_\star(n) \setminus (1)$, a composition of $t-2$ using only ones and twos. By hypothesis, m such that $\boldsymbol{\nabla}_\star(m) = \boldsymbol{\nabla}_\star(n) \setminus (1)$ satisfies $F_t \leq m < F_{t+1}$. By (65), the last Fibonacci index of m is $t-1$. Thus $n = m + F_t$, and consequently $F_{t+1} < F_t + F_t \leq n < F_t + F_{t+1} = F_{t+2}$.

In the latter case, removing the final 2 yields $\boldsymbol{\nabla}_\star(n) \setminus (2)$, a composition of $t-3$ using only ones and twos. By hypothesis, m such that $\boldsymbol{\nabla}_\star(m) = \boldsymbol{\nabla}_\star(n) \setminus (2)$ satisfies $F_{t-1} \leq m < F_t$. By (65), the last Fibonacci index of m is $t-2$. Thus $n = m + F_t$, and consequently $F_{t+1} = F_{t-1} + F_t \leq n < F_t + F_t < F_{t+2}$. □

Only If: Observe that for $F_{t+1} \leq n < F_{t+2}$, either $F_{t-1} \leq n - F_t < F_t$ or $F_t \leq n - F_t < F_{t+1}$.

In the former case, $\boldsymbol{\nabla}_\star(n - F_t)$ is a composition of $t-3$, by hypothesis. By (65), the last index of $\mathbf{F}_\star(n - F_t)$, is $t-2$. Thus the concatenation $\mathbf{F}_\star(n) = \mathbf{F}_\star(n - F_t) \oplus (t)$ corresponds to $\boldsymbol{\nabla}_\star(n) = \boldsymbol{\nabla}_\star(n - F_t) \oplus (2)$, making $\boldsymbol{\nabla}_\star(n)$ a composition of $t-3+2 = t-1$.

In the latter case, $\boldsymbol{\nabla}_\star(n - F_t)$ is a composition of $t-2$, by hypothesis. By (65), the last index of $\mathbf{F}_\star(n - F_t)$, is $t-1$. Thus the concatenation $\mathbf{F}_\star(n) = \mathbf{F}_\star(n - F_t) \oplus (t)$ corresponds to $\boldsymbol{\nabla}_\star(n) = \boldsymbol{\nabla}_\star(n - F_t) \oplus (1)$, making $\boldsymbol{\nabla}_\star(n)$ a composition of $t-2+1 = t-1$. □

7.1.1. *Fibonacci gaps and Fibonacci indices in the quilt black quartet.* In Corollary 7.2, the quilt coordinates $a_{n,k}$ (Table 1) reappear as restricted compositions of an integer via their maximal Fibonacci gaps $\boldsymbol{\nabla}_\star(a_{n,k})$. Moreover, the composition corresponding to $a_{n,k+1}$ will comprise a "1" prepended to the composition corresponding to $a_{n,k}$ (92).

Corollary 7.2 (Gaps of sequence a of the quilt, Figure 1, as compositions)**.** *For $n \geq 0$:*

(i): *$\boldsymbol{\nabla}_\star(a_{n,k})$ is a composition of $F^{-1}(n) + k - 1$ using only ones and twos.*

(ii): *Let $S_{n,k}$ be any quilt square strictly south of the spine ($n > 0$) and $S_{0,h}$ the spinal square due west of $S_{n,k}$ in Figure 1. Then $F^{-1}(n) + k - 1 = h$, or, in*

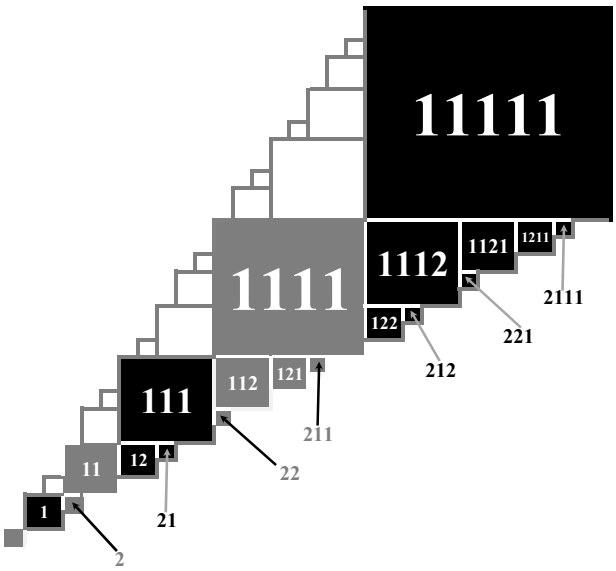

FIGURE 22. Compositions using only 1s and 2s in the quilt (Figure 1), computed from the genealogies that arise in a "cloning method" for constructing the quilt [38], whereby the 1st clone of a square receives a suffix of 1 and the 2nd clone of a square receives a suffix of 2. Only squares $S_{n,1}$ of the smallest cardinal size $F_2 \times F_2$ have labels that begin with 2. Each larger square $S_{n,k+1}$, constitutes an "upsized" clone of $S_{n,k}$. Whereas the latter two squares appear in "similar" contexts, the label for $S_{n,k+1}$ merely prepends a 1 to that of $S_{n,k}$, for $k = 1, 2, 3, ...$

light of part **(i)**, $\boldsymbol{\nabla}_\star(a_{n,k})$ *is a composition of* h *using only ones and twos. Moreover, for the next spinal square* $S_{0,h+1}$*, which lies due north of* $S_{n,k}$*,* $\boldsymbol{\nabla}_\star(a_{0,h+1})$ *is also a composition of* h *using only ones and twos.*

Proof. **(i)**: From Proposition 7.1, $\boldsymbol{\nabla}_\star(a_{n,k})$ is a composition of $F^{-1}(a_{n,k}) - 2$ using only ones and twos. By (83), $F^{-1}(a_{n,k}) - 2 = F^{-1}(n) + k + 1 - 2 = F^{-1}(n) + k - 1$.

(ii): By the structure of Figure 1, $a_{n,k} \neq a_{0,h}$ for $n \neq 0$ (since only the 0^{th} square of each size lies on the diagonal), and $a_{0,h} = F_{h+2} - 1$ and $b_{0,h} = F_{h+3} - 1$, by particular cases of Proposition 3.2, (1), respectively, (2). Thus, $F_{h+2} \leq a_{n,k} < F_{h+3}$. By Proposition 7.1, the inequality holds if and only if $\boldsymbol{\nabla}_\star(a_{n,k})$ is a composition of h using only ones and twos. However, Part **(i)** also shows $\boldsymbol{\nabla}_\star(a_{n,k})$ to be composition of $F^{-1}(n)+k-1$ using only ones and twos. Thus, $F^{-1}(n)+k-1 = h$. That the result also holds for $S_{0,h+1}$ is trivial, since $F^{-1}(0) + h + 1 - 1 = h$. □

Example 7.3. Corollary 7.2 showed that the quilt's black squares provide visualization of restricted compositions of integers (those using only twos and ones), with square $S_{n,k}$ corresponding to a restricted composition of $F^{-1}(n) + k - 1$. That is, spinal square $S_{0,F^{-1}(n)+k}$ and all black quilt squares directly south of it graphically illustrate all compositions of $F^{-1}(n) + k - 1$ that use 1s and 2s (Figure 22).

Consider ($S_{3,2}$, $S_{5,1}$, $S_{1,4}$, $S_{6,1}$, $S_{2,3}$, $S_{4,2}$, $S_{7,1}$, $S_{0,6}$), the collection of squares found due east of spinal square $S_{0,5}$ in Figure 1 together with $S_{0,6}$ found immediately northeast of $S_{0,5}$. These have the respective corner coordinates ($a_{3,2}$,

$a_{5,1}$, $a_{1,4}$, $a_{6,1}$, $a_{2,3}$, $a_{4,2}$, $a_{7,1}$, $a_{0,6}$) = (13,14,15,16,17,18,19,20). These, in turn, have maximal Fibonacci indices ($\mathbf{F}_\star(13)$, $\mathbf{F}_\star(14)$, $\mathbf{F}_\star(15)$, $\mathbf{F}_\star(16)$, $\mathbf{F}_\star(17)$, $\mathbf{F}_\star(18)$, $\mathbf{F}_\star(19)$, $\mathbf{F}_\star(20)$) = ((1,2,4,6), (1,3,4,6), (1,2,3,4,6), (1,3,5,6), (1,2,3,5,6), (1,2,4,5,6), (1,3,4,5,6), (1,2,3,4,5,6)). Finally, these indices have gaps ($\boldsymbol{\nabla}_\star(13)$, $\boldsymbol{\nabla}_\star(14)$, $\boldsymbol{\nabla}_\star(15)$, $\boldsymbol{\nabla}_\star(16)$, $\boldsymbol{\nabla}_\star(17)$, $\boldsymbol{\nabla}_\star(18)$, $\boldsymbol{\nabla}_\star(19)$, $\boldsymbol{\nabla}_\star(20)$) = ((1,2,2), (2,1,2), (1,1,1,2), (2,2,1), (1,1,2,1), (1,2,1,1), (2,1,1,1), (1,1,1,1,1)), comprising the set of all compositions of 5 that use only ones and twos.

Part 2 [39]

Proposition 7.3 futher investigates the Fibonacci gaps for the quilt black quartet (Table 1).

Proposition 7.3 (Gaps of quilt square corner coordinates a, b, c and d)**.** *Gaps of Quilt Corners a, b, c and d (Table 1) can be written as follows:*

$$(a)\text{: } \boldsymbol{\nabla}_\star(a_{n,k}) = \begin{cases} (1)^{k-1}, & n=0; \\ (1)^{k-1}(2)\boldsymbol{\nabla}_\star(n) = (1)^{k-1}\boldsymbol{\nabla}_\star(\lambda(n)+1), & n>0. \end{cases}$$

$$(b)\text{: } \boldsymbol{\nabla}_\star(b_{n,k}) = \begin{cases} (), & n=0, k=1; \\ (2)(1)^{k-2}, & n=0, k>1; \\ (2)(1)^{k-1}\boldsymbol{\nabla}_\star(n), & n>0, k\geq 1. \end{cases}$$

$$(c)\text{: } \boldsymbol{\nabla}_\star(c_{n,k}) = \begin{cases} (1)^{k-1}, & n=0; \\ (1)^{k+1}\boldsymbol{\nabla}_\star(\kappa(n)), & n>0. \end{cases}$$

$$(d)\text{: } \boldsymbol{\nabla}_\star(d_{n,k}) = \begin{cases} 2(1)^{k-2}, & n=0, k>1; \\ (1)^2\boldsymbol{\nabla}_\star(\kappa(n)), & n\geq 0, k=1; \\ 2(1)^{k-2}(2)\boldsymbol{\nabla}_\star(n), & n>0, k>1. \end{cases}$$

Proof of (a) (Proofs of (b), (c) and (d) are similar): We show separately that the Fibonacci expansions corresponding to the gaps on the right hand side are maximal and that these expansions evaluate to $a_{n,k}$.

Maximal:

Clearly, the expressions $(1)^{k-1}$ and $(1)^{k-1}(2)\boldsymbol{\nabla}_\star(n)$ for gaps of $a_{n,k}$ contain only entries in $\{1,2\}$ and start with 1, hence the corresponding indices $(1,2,\ldots,k)$ and $(1,\ldots,k)\oplus[k+1+\mathbf{F}_\star(n)]$, for $n=0$, respectively, $n>0$, are maximal.

Correct Evaluation:

The proof uses properties (50), (51), and (52).

Case $n>0$: Using (50), rewrite $(1,\ldots,k)\oplus[k+1+\mathbf{F}_\star(n)]$ as $(1,\ldots,k)\oplus(k+2)\oplus[k+1+\mathbf{F}(n-1)]$, where $\mathbf{F}_\star$ refers to indices for maximal expansion and $\mathbf{F}$ those for lazy representation. Recalling that $\sigma(n)$ is invariant with respect to choice of representation, evaluate this expansion to $\sum_{i=1}^{k} F_i + F_{k+2} + \sigma^{k+1}(n-1)$. Using (52), rewrite it as $2F_{k+2} + (n-1)F_k + \sigma(n-1)F_{k+1} - 1$. Then, using (51) to rewrite it as $2F_{k+2} + (n-1)F_k + (n-1+\lfloor n/\phi \rfloor)F_{k+1} - 1$, observe that it further reduces to $(n+1)F_{k+2} + \lfloor n/\phi \rfloor F_{k+1} - 1$, the expression for $a_{n,k}$ given in Proposition 3.2.

Case $n=0$: Indices $(1,\ldots,k)$ evaluate to $\sum_{i=1}^{k} F_i = F_{k+2} - 1 = a_{0,k}$, as desired.

For the last equality, observe from Proposition 6.3 that $\lambda(n) = \sigma(\kappa(n)) = \sigma(\sigma_\star(n)) = \sigma(\sigma(n-1)+1)$. So, if $\mathbf{F}_\star(n) = (1, t_2 \ldots, t_s)$, then $\mathbf{F}_\star(\lambda(n)+1) = (1, 3, t_2+2 \ldots, t_s+2)$, and $\boldsymbol{\nabla}_\star(\lambda(n)+1) = (2, t_2-1, t_3-t_2, \ldots, t_s-t_{s-1}) = (2)\boldsymbol{\nabla}_\star(n)$, demonstrating the latter equality.

□

Corollary 7.4 (Children of $a_{n,k}$ in the maximal succesor tree and their gaps)**.**

$$\begin{aligned}(92)\qquad &\boldsymbol{\nabla}_\star(\bar{\boldsymbol{L}}(a_{n,k})) = (1)\boldsymbol{\nabla}_\star(a_{n,k}) = \boldsymbol{\nabla}_\star(a_{n,k+1})\\ &\boldsymbol{\nabla}_\star(\bar{\boldsymbol{R}}(a_{0,k})) = (2)\boldsymbol{\nabla}_\star(a_{0,k}) = \boldsymbol{\nabla}_\star(a_{F_{k+2}-1,1})\\ &\boldsymbol{\nabla}_\star(\bar{\boldsymbol{R}}(a_{n,k})) = (2)\boldsymbol{\nabla}_\star(a_{n,k}) = \boldsymbol{\nabla}_\star(a_{a_{n,k},1}), n > 0\end{aligned}$$

Proof. The first result follows immediately from Proposition 7.3(a), while the second and third also employ Proposition 6.3 and Corollary 6.4. □

Example 7.4. Recall that Part 1 of the paper [38] used the term *genealogy* and notation $v_{n,k}$ as the tuple of integers that lists (in order) the sequence of replications used to place a particular square $S_{n,k}$ in the quilt, this sequence ordered according to the method of constructing the quilt discussed therein.

Now for $k = 1, 2, 3, 4, 5, 6, 7$, respectively, take the sequence $(v_{n,k})_{n\geq 0}$ of genealogies for the squares of size F_{k+1}, and use the genealogies as coefficients in maximal Fibonacci binary notation to obtain the natural numbers 000027, the Lower Wythoff sequence 000201, the Upper Wythoff sequence 001950, Wythoff AB numbers 003623, Wythoff BB numbers 101864, Wythoff ABB numbers 134862, and Wythoff BBB numbers 134864, respectively. The following result generalizes the example.

Proposition 7.5 (Maximal Fibonacci indices of quilt genealogies)**.** *Example 7.4 motivates the following claims:*

(i): *Genealogies for the smallest-sized squares $S_{n,1}$ in the quilt give the maximal Fibonacci indices of n. That is, $v_{n,1} = \mathbf{F}_\star(n)$.*

(ii): *The genealogy for a larger square $S_{n,k}$ with $k > 1$ equals $k-1$ plus the genealogy for the n^{th} square of size 1. That is, $v_{n,k} = v_{n,1} + (k-1, \ldots, k-1)$, $k > 1$.*

(iii): *Let $V_{n,k}$ apply $v_{n,k}$ as coefficients to a basis in maximal Fibonacci binary notation,* i.e.*, $V_{n,k} = v_{n,k} \cdot (F_1, F_2 \ldots)$. Then, $V_{n,k} = F_{k-1}\lfloor n\phi \rfloor + F_{k-2}\, n$.*

(iv): *In particular, $V_{n,1} = n$, $V_{n,2} = \lfloor n\phi \rfloor$, and for $n \geq 2$, $V_{n,k} = V_{n,k-1} + V_{n,k-2}$.*

(v): $V_{n,k} = \begin{cases} \lambda^{(k-1)/2}(n), & k \text{ odd};\\ \kappa\lambda^{(k-2)/2}(n), & k \text{ even}. \end{cases}$

Proof. By Part 1 of the paper [38],

$$\begin{aligned}(93)\qquad &v_{n,k} = v_{n-F_t,k} \oplus (t+k-1), F_{t+1} \leq n < F_{t+2}, t = 1, 2, \ldots,\\ &v_{n,0} = ()\end{aligned}$$

(i): For $k = 1$, (93) becomes

$$v_{n,1} = v_{n-F_t,1} \oplus (t), \qquad F_{t+1} \leq n < F_{t+2}, t = 1, 2, \ldots,$$

showing the recurrence to be identical to (64).

(ii): Follows by induction from (93) and **(i)**.

(iii): Recurrence (93) shows $V_{n,k}$ to be a Fibonacci cohort sequence over n from the 1st cohort, with $S_1 = V_{1,k} = F_k$ and cohortizer F_{t+k-1}. Thus, by (17), $V_{n,k} = F_{k-1}\lfloor n\phi \rfloor + F_{k-2}n$.

(iv): Follows from **(iii)**.

(v): Follows from **(iii)** and (27).

□

Remark 7.3. By Proposition 7.5(v), $V_{n,p+1}$ gives the last composition in each cohort $C_1, C_2, \ldots, C_{p+1}, \ldots$ of Table 10, and $V_{M,p_\star-1}$ gives the last element of each cohort $C_1, C_2, \ldots, C_{p_\star-1}, \ldots$ in Table 11 (see Remark 4.9), with $V_{M,0}$ for cohort C_0. In addition, observe that for the quilt white array (β) of Table 2, the cohort formula (6) is homogeneous and gives $\beta_{n,k} = V_{n,k+1}$.

7.2. **Cohort sequences in minimal representation & integer compositions.**

Example 7.5. The minimal Fibonacci indices $\mathbf{f}(n)$ of the integers $n = 1, 2, \ldots$ form a 1–2-Fibonacci cohort sequence of tuples under cohortizer $\langle f_L, f_R\rangle = \langle \texttt{++}, \oplus(t+1)\rangle$, where ++ indicates the increment of the last element of the tuple argument of f_L.

The 1–2-Fibonacci cohort structure of the integers themselves, under cohortizer $\langle F_{t-1}, F_{t+1}\rangle$ (Example 4.20), induces a corresponding structure on the tuple of minimal Fibonacci indices. This is more evident from the similarity in the alternative notation $\langle \ominus(t) \oplus (t+1), \oplus(t+1)\rangle$ for the 1–2-Fibonacci cohortizer of the tuples to that of the 1–2-Fibonacci cohortizer of the integers, $\langle -F_t + F_{t+1}, F_{t+1}\rangle$.

The sequence of cohorts reads $C_1 = (2)$, $C_2 = (3)$, $C_3 = (4, 24)$, $C_4 = (5, 25, 35)$, $C_5 = (6, 26, 36, 46, 246)$, $C_6 = (7, 27, 37, 47, 247, 57, 257, 357)$,.... Table 23 shows the sequence of tuples.

C_1	(2)				
C_2	(3)				
C_3	(4)	(2, 4)			
C_4	(5)	(2, 5)	(3, 5)		
C_5	(6)	(2, 6)	(3, 6)	(4, 6)	(2, 4, 6)
⋮	⋮	⋮	⋮	⋮	⋮

TABLE 23. 1–2-Fibonacci outer cohort tableau of minimal Fibonacci indices $\mathbf{f}(n)$

C_1	1				
C_2	**0**1				
C_3	0**0**1	1**01**			
C_4	00**0**1	10**0**1	01**01**		
C_5	000**0**1	100**0**1	010**0**1	001**01**	101**01**
⋮	⋮	⋮	⋮	⋮	⋮

TABLE 24. 1–2-Fibonacci outer cohort tableau of the sequence of positive integers in Zeckendorf binary notation

Table 24 shows the same expansion as words in Zeckendorf binary notation, making it apparent that each left subcohort (below the staircase) forms by substituting ·01 for the final 1 of elements of the previous cohort, and that each right subcohort (above the staircase) forms by appending ·01 to elements of the second previous cohort.

Example 7.6. The minimal Fibonacci gaps $\boldsymbol{\partial}(n)$ of the positive integers $n = 1, 2, \ldots$ form a 1–2-Fibonacci cohort sequence under cohortizer $\langle f_L, f_R \rangle = \langle \mathsf{++}, \oplus(2) \rangle$.

The sequence of cohorts reads $C_1 = (2)$, $C_2 = (3)$, $C_3 = (4, 22)$, $C_4 = (5, 23, 32)$, $C_5 = (6, 24, 33, 42, 222)$, $C_6 = (7, 25, 34, 43, 223, 52, 232, 322)$,.... Table 25 displays the sequence.

C_1	(2)				
C_2	(3)				
C_3	(4)	(2, 2)			
C_4	(5)	(2, 3)	(3, 2)		
C_5	(6)	(2, 4)	(3, 3)	(4, 2)	(2, 2, 2)
⋮	⋮	⋮	⋮	⋮	⋮

TABLE 25. 1–2-Fibonacci outer cohort tableau of minimal Fibonacci gaps $\boldsymbol{\partial}(n)$

Written as words, the elements in this sequence are out of lexicographic order. For example, while the sequence of integers $16 < 17 < 18$ increases, that of their minimal Fibonacci gaps $(\boldsymbol{\partial}(16), \boldsymbol{\partial}(17), \boldsymbol{\partial}(18)) = (43, 223, 52)$ is *not* monotonic with respect to (reverse) lexicographic order: $43 \succ 223 \prec 52$.

By construction (67), elements in Table 23 do not contain any two consecutive indices. Correspondingly, those in Table 24 do not contain more than two consecutive ones (1s), while the gaps in Table 25 do not contain any ones (1s) at all. Proposition 7.6 shows the converse: All strings of integers greater than one are contained in the minimal Fibonacci gaps of the positive integers, $Z^{\star}_{\geq 2} = \boldsymbol{\partial}(\mathbb{Z}_+)$. Further, while F_t is equal to the number of compositions of $t+1$ with no part equal to one [19], the minimal Fibonacci gaps provide a bijection between the positive integers and the set of all such restricted compositions.

Proposition 7.6 (Minimal Fibonacci Gaps as Restricted Compositions)**.** *For $t = 1, 2, \ldots$, an integer n with minimal Fibonacci gaps $\boldsymbol{\partial}(n) = (\partial_1, \ldots \partial_r)$, satisfies $F_{t+1} \leqslant n < F_{t+2}$ if and only if $(\partial_1, \partial_2 \ldots, \partial_r)$ is a composition of $t+1$ without ones.*

If: Example 7.6 shows the proposition to hold for the first few values of n. For some n, let $\boldsymbol{\partial}(n) = (\partial_1, \ldots \partial_r)$ be a composition of $t+1$ without ones. Define $m < n$ to be the integer having minimal Fibonacci gaps $\boldsymbol{\partial}(m) = \boldsymbol{\partial}(n) \setminus (\partial_r)$, and observe that $(\partial_1, \partial_2 \ldots, \partial_{r-1})$ is a composition of $t + 1 - \partial_r$ without ones. By hypothesis, $F_{t+1-\partial_r} \leqslant m < F_{t+2-\partial_r}$. Thus, $\mathbf{f}(m)$ terminates in $t + 1 - \partial_r$ and consequently, $\mathbf{f}(n)$ terminates in $t + 1$. Thus $F_{t+1} \leqslant n < F_{t+2}$. □

Only If: Let n satisfy $F_{t+1} \leqslant n < F_{t+2}$, thus $0 \leqslant n - F_{t+1} < F_t$. In particular, there exists an $s \leq t-2$ such that $F_{s+1} \leqslant n - F_{t+1} < F_{s+2} \leq F_t$. By hypothesis, $\boldsymbol{\partial}(n - F_{t+1})$ is a composition of $s+1$ without ones. By (67), $\mathbf{f}(n) = \mathbf{f}(n - F_{t+1}) \oplus (t+1)$. Since $\mathbf{f}(n - F_{t+1})$ must terminate in $s+1$, $\boldsymbol{\partial}(n)$ must terminate in $(t+1)-(s+1) = t-s$. Therefore, $\boldsymbol{\partial}(n)$ is a composition of $(s+1)+(t-s) = t+1$. Moreover, $F_{s+2} \leq F_t$ gives $t - s \geq 2$. Thus the terminal element ∂_r is not a 1. □

7.3. **Intra-cohort blades and palindromes.** Recall the successor tableaux of the positive integers, where Tables 19(i) and (ii) were displayed as left-, respectively, right-justified cohort tableaux. Section 6.13 observed these tableaux to be planar-graph isomorphic to the minimal, respectively, maximal Fibonacci trees. Moreover, the former of these was described in Remark 6.13 as having each cohort reordered according to the fractional part of the base-2 log of the respective positions in the minimal Fibonacci tree, $\mathrm{frac}(\log_2 \mathbf{p}(n))$.

This begs the question of how one might generate the sequence in Tables 19(i) without reference to tree positions, and further, how to generate the sequence in Tables 19(ii) at all. In fact, generating these sequences resembles the generation of the blade permutation described in Section 6.8.1, with the base-2 representation substituted by the minimal Fibonacci representation and maximal Fibonacci expansion, respectively. Consequently, the paper will refer to these as the *minimal intra-cohort blade* and *maximal intra-cohort blade* permutations. Generation of the intra-cohort blades now follows:

For the minimal intra-cohort blade permutation, first write the minimal Fibonacci representation in maximal Fibonacci binary notation, by prepending a digit (always zero) for F_1. Then holding fixed the most significant digit (the one on the right), reverse the remaining digits and evaluate. For example, the 6^{th} cohort of the positive integers $C_t = (13, 14, 15, 16, 17, 18, 19, 20)$ can be written $(0000001, 0100001, 0010001, 0001001, 0101001, 0000101, 0100101, 0010101)$ on the basis $(1, 1, 2, 3, 5, 8, 13)$. Reversing all but the most significant digit gives $(0000001, 0000101, 0001001, 0010001, 0010101, 0100001, 0100101, 0101001)$, which evaluates to $(13, 18, 16, 15, 20, 14, 19, 17)$. (Note, the permutation could also be accomplished in minimal Fibonacci binary expansion by holding fixed the *two* most significant digits (the two on the right) and reversing the remaining digits).

For the maximal intra-cohort blade permutation, first write the maximal Fibonacci expansion in maximal Fibonacci binary notation. Then holding fixed the most significant digit (the one on the right), as well as the least significant digit (the one on the left — in the F_1 place, which is always one), reverse the remaining digits in between and evaluate. For example, the 6^{th} cohort of the positive integers $C_t = (13, 14, 15, 16, 17, 18, 19, 20)$ can be written $(110101, 101101, 111101, 101011, 111011, 110111, 101111, 111111)$ on the basis $(1, 1, 2, 3, 5, 8)$. Reversing all but the most and least significant digits gives $(101011, 101101, 101111, 110101, 110111, 111011, 111101, 111111)$, which evaluates to $(16, 14, 19, 13, 18, 17, 15, 20)$. Neither of these self-inverse permutations 1, 2, 3, 4, 5, 7, 6, 8, 11, 10, 9, 12, 13, 18, 16, 15, 20, 14, 19, 17, 21, 29, 26, 24, 32, 23, 31, 28, 22, 30, 27, 25, 33, ... nor 1, 2, 3, 4, 6, 5, 7, 8, 11, 10, 9, 12, 16, 14, 19, 13, 18, 17, 15, 20, 21, 29, 27, 24, 32, 26, 23, 31, 22, 30, 28, 25, 33, ... is found in the OEIS [41] as of this writing. As noted in Remark 6.17, neither are their respective palindromes 1, 2, 3, 4, 5, 8, 10, 12, 13, 19, 21, 24, 28, 30, 33, 34, 44, 48, 55, 60, 66, 70, 75, 77, 82, 88, 89, 105, 112, 124, 140, 144, 152, ... nor 1, 2, 3, 4, 7, 8, 10, 12, 14, 20, 21, 24, 26, 30, 33, 40, 44, 54, 55, 61, 66, 68, 73, 77, 83, 88, 92, 108, 120, 127, 143, 144, 152, ... found in the OEIS, these sequences of palindromes being values which coincide in the pairs of minimal (Figures 3 & 5), respectively, maximal (Figures 8 & 10) trees.

8. The Branch Quartet and the Clade Quartet

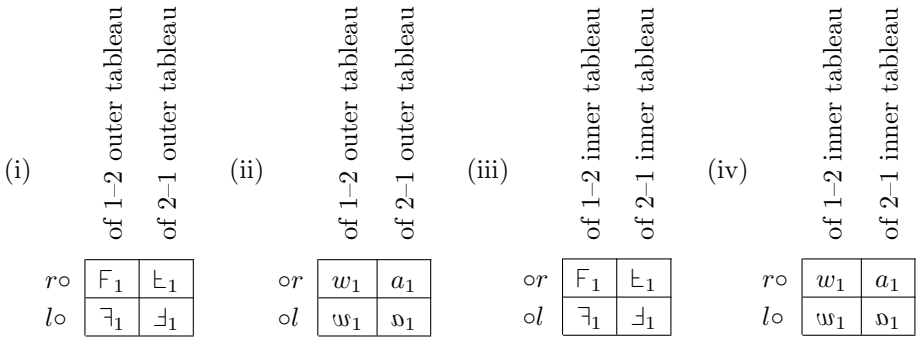

Figure 23. First column of the quartet arrays as index of prefix- or suffix-restricted elements in the 1–2- and 2–1-Fibonacci outer and 1–2- and 2–1-Fibonacci inner cohort tableaux, Tables 7(i), (ii), (iii), and (iv), respectively.

8.1. **First columns of the branch and clade quartet arrays.** Tables 7 exhibited four types of Fibonacci tableaux of compositions in a free monoid on two symbols l and r. With respect to these tableaux, the first column of each array in the branch and clade quartets indexes a distinct set of elements with a common restriction on prefix or suffix. For example, the first column of F indexes compositions with prefix $r\circ$ in the 1–2-Fibonacci outer cohort tableau, Table 7(i), and (equivalently) those with suffix $\circ r$ in the 1–2-Fibonacci inner cohort tableau, Table 7(iii), including the identity I in both cases. Figure 23 shows the makeup of the first column of each array in the octet (Tables 3 & 4) with respect to each of the four tableaux. In each case, the top left entry, 1, (in row $n = 0$) of the array indexes the first element, I, of the tableau, while the sequence of remaining elements in rows $n = 1, 2, 3, \ldots$ of column $k = 1$ index elements of the tableau with the restriction shown in the Figure.

Thus using the cohort calculus to obtain the first column of each array from the archetypes in Table 7, Kimberling's dispersion properties [20] allow the completion of each row, (by repeated application of the ordered complement of the 1st column), yielding an interspersion–dispersion array with the desired first column, and hence a method of generating the arrays of the octet.

Remark 8.1 (Pell cohort tableaux and related sextets of interspersions). The Pell cohort sequences of integers described in Section 4.3 prompt a consideration of Pell cohort sequences of words on three letters, $\{l, m, r\}^\star$, say. The use of three letters allows the cohort calculus to generate the complete lexicon without repeating words. Similar to the Pell cohort sequences of integers, the Pell tableaux follow a 2–1–1-, 1–2–1-, or 1–1–2-Pell cohort structure, and similarly to the Fibonacci tableaux of words (Tables 7), generators can be applied on the outside or the inside. Associated to each tableau is a sextet of increasing positive integer sequences that describe the positions of words starting or ending with l, m, and r. Consider, for example, for the 1–2–1-Pell outer cohort sequence beginning I, l, r, l^2, lr, m, rl, r^2, l^3, l^2r, lm, lrl, lr^2, ml, mr, $rl^2, rlr, rm, r^2l, r^3, \ldots$ (Table 26(i)). The words that end with m appear to be indexed by the 1–2–1-Pell cohort sequence of integers 276879 (Table 26(ii)). For

(i)

C_1	$\boldsymbol{I}$												
C_2	l	r											
C_3	l^2	lr	$\boldsymbol{m}$	rl	r^2								
C_4	l^3	l^2r	$\boldsymbol{lm}$	lrl	lr^2	ml	mr	rl^2	rlr	$\boldsymbol{rm}$	r^2l	r^3	
$\vdots$	$\vdots$	$\vdots$	$\vdots$	$\vdots$	$\vdots$	$\vdots$	$\vdots$	$\vdots$	$\vdots$	$\vdots$	$\vdots$	$\ddots$	

(ii)

C_1	1												
C_2	6	11											
C_3	18	23	30	35	40								
C_4	47	52	59	64	69	76	81	88	93	100	105	110	
$\vdots$	$\vdots$	$\vdots$	$\vdots$	$\vdots$	$\vdots$	$\vdots$	$\vdots$	$\vdots$	$\vdots$	$\vdots$	$\vdots$	$\ddots$	

TABLE 26. 1–2–1-Pell cohort tableaux: (i) Outer cohortizer on three symbols, (ii) Integer sequence 276879, cohortized by $\langle P_{t+1}, P_{t+2}, P_{t+2}\rangle$ (see Section 4.3), indexes those words in (i) ending with "m."

the analogous 2–1–1-Pell outer cohort sequence of words in $\{l, m, r\}^\star$, beginning I, l, r, m, l^2, lr, rl, r^2, ml, mr, lm, l^3, l^2r, lrl, lr^2, $rm, rl^2, rlr, r^2l, r^3, \ldots$, the 2–1–1-Pell cohort sequence of integers 064437 appears to index the words that end with r. Research continues into Pell and more general cohort tableaux and related interspersions [37].

Observe that for Pell cohort sequences the cohort tableau shown in Table 26(i) continues to take the form of a tetrangle or irregular triangle array but with natural isomorphism not only to binary trees, but also to infinite, regular, single-rooted ternary trees, in which each parent node begets a **l**eft, a **m**iddle, and a **r**ight child. On the other hand, columns of Table 26(ii) could be taken as successions of all-left branchings in a binary tree, thus also furnishing such tableaux with a map to binary trees, via *e.g.*, the grafting procedure of Remark 9.3.

8.2. **Cohort-tableau approach to constructing the quartets.**

8.2.1. *Para-Fibonacci sequences in the branch quartet.* Recall the branch quartet of interspersion arrays shown in Table 3 (clockwise from the top left, ⊦, ⊢, ⊣, and ⊣). (For the first two of these of these arrays, Tables 12 (⊦) and 15 (⊢) provide additional rows and columns.)

According to 1996 correspondence between John Conway and Neil Sloane (reproduced in [41] as "Notes on the Para-Fibonacci and related sequences" under the entry for 019586), Conway proposed the name *para-Fibonacci sequence* doubly inspired by the words "parameter" and "paraphrase," citing Kimberling's earlier baptism of 003603 as the "paraphrase of the Fibonacci sequence." In its original context, the name referred to the sequence of row indices of w in which each positive integer appears. The name spread to other sequences of row and column indices of the positive integers in an I–D array. The present text now considers the sequences of row and column indices of the positive integers in each of the four member arrays of the branch quartet.

$$\text{(i) } C_t = \begin{array}{c|c} C_{t-1} \oplus (F_{t-1}, \ldots, F_t - 1) & (F_{t-1}, \ldots, F_t - 1) \oplus C_{t-1} \\ \hline (F_t, \ldots, F_{t+1} - 1) \oplus C_{t-2} & C_{t-2} \oplus (F_t, \ldots, F_{t+1} - 1) \end{array}$$

$$\text{(ii) } C_t = \begin{array}{c|c} [C_{t-1} + 1] \oplus (\overbrace{1, \ldots, 1}^{F_{t-2}}) & (\overbrace{1, \ldots, 1}^{F_{t-2}}) \oplus [C_{t-1} + 1] \\ \hline (\overbrace{1, \ldots, 1}^{F_{t-1}}) \oplus [C_{t-2} + 1] & [C_{t-2} + 1] \oplus (\overbrace{1, \ldots, 1}^{F_{t-1}}) \end{array}$$

TABLE 27. Structure of cohort C_t in the row (i) and column indices (ii) of the positive integers in sequence, for the branch quartet of interspersion arrays (Table 3). In each of tables (i) and (ii), clockwise from the top left, ⊢, ⊨, ⊣, and ⊰.

First, observe that sequence 066628 = 0, 0, 0, 1, 0, 1, 2, 0, 1, 2, 3, 4, ... gives indices of rows in ⊢ for the sequence of positive integers. Indeed, this sequence exhibits a 1–2-Fibonacci cohort structure under cohortizer $\langle 0, F_{t-1} \rangle$, that is, a constant left cohortizer $f_L(t) = 0$ and right cohorts comprising the nonnegative integers in sequence. Thus, cohorts for the row index sequence can be written $C_t = C_{t-1} \oplus [C_{t-2} + F_{t-1}]$, equivalently as $C_t = C_{t-1} \oplus (F_{t-1}, \ldots, F_t - 1)$ as in Table 27(i), upper left, or still more simply as $C_t = (0, \ldots, F_t - 1)$. Remark 8.11 obtains this sequence by setting $F_1 = 0$ in Table 33(i).

Moving on to the column indices of $1, 2, 3, \ldots$ in ⊢ gives the sequence 1, 2, 3, 1, 4, 2, 1, 5, 3, 2, 1, 1, ..., which does not appear in the OEIS [41] as of this writing. It too exhibits a type of 1–2-Fibonacci cohort structure with a constant left cohortizer $f_L(t) = 1$ and right cohorts comprised of ones (1s), that is, $n \mapsto \langle n + 1, 1 \rangle$. Its cohorts can be written $C_t = [C_{t-1} + 1] \oplus (1, \ldots, 1)$ as in Table 27(ii), upper left.

In ⊨, the row indices 0, 0, 1, 0, 2, 1, 0, 3, 4, 2, 1, 0, ... of the positive integers exhibit a 2–1-Fibonacci cohort structure under cohortizer $\langle F_{t-1}, 0 \rangle$. That is, with a constant right cohortizer $f_R(t) = 0$ and left cohorts comprising the nonnegative integers in sequence. Its cohorts can be written $C_t = (F_{t-1}, \ldots, F_t - 1) \oplus C_{t-1}$, as in Table 27(i), upper right.

Moving on to the column indices 1, 2, 1, 3, 1, 2, 4, 1, 1, 2, 3, 5 ... of the positive integers in ⊨ also reveals a 2–1-Fibonacci cohort structure with a constant right cohortizer $f_R(t) = 1$ and left cohorts comprised of ones (1s), that is, $n \mapsto \langle 1, n+1 \rangle$. Its cohorts can be written $C_t = (1, \ldots, 1) \oplus [C_{t-1} + 1]$, as in Table 27(ii), upper right.

Tables 27(i) and (ii) summarize the results for row, respectively, column indices of $\mathbb{Z}_+$ in the arrays of the branch quartet, also including ⊰ and ⊣ at the bottom left and right of the tables, respectively. Table 27(ii) shows that cohorts of column indices for ⊢ and ⊨ contain the same elements in reverse order. Similarly, respective cohorts C_t of column indices in ⊰ and ⊣ are the reverse of one another.

Section 4.1.4 described columns of the branch and clade quartet arrays as Fibonacci cohort sequences, giving explicit cohort-based formulas. Thus it comes as no surprise that the sequences of row indices of the integers exhibit the Fibonacci cohort property. However, the fact that the column indices also exhibit the Fibonacci cohort property suggests a close relationship between the rows of the underlying arrays and Fibonacci cohort tableaux, hence a possible transformation between tableaux and the arrays themselves.

8.2.2. *Fibonacci cohort tableaux and the branch quartet.* How then does the branch quartet relate to the Fibonacci cohort tableaux of the positive integers in Table 6? More specifically, can the four arrays obtain directly from these Fibonacci cohort tableaux? In an attempt to answer the question, this section will develop a fourth procedure, the "cohort tableau approach," to generate rows of the branch and clade quartet arrays.

(i)

C_1	$\mathsf{F}_{0,1}$										$\mathsf{L}_{0,1}$	C_1
C_2	$\mathsf{F}_{0,2}$										$\mathsf{L}_{0,2}$	C_2
C_3	$\mathsf{F}_{0,3}$	$\mathsf{F}_{1,1}$								$\mathsf{L}_{1,1}$	$\mathsf{L}_{0,3}$	C_3
C_4	$\mathsf{F}_{0,4}$	$\mathsf{F}_{1,2}$	$\mathsf{F}_{2,1}$				(ii)		$\mathsf{L}_{2,1}$	$\mathsf{L}_{1,2}$	$\mathsf{L}_{0,4}$	C_4
C_5	$\mathsf{F}_{0,5}$	$\mathsf{F}_{1,3}$	$\mathsf{F}_{2,2}$	$\mathsf{F}_{3,1}$	$\mathsf{F}_{4,1}$		$\mathsf{L}_{3,1}$	$\mathsf{L}_{4,1}$	$\mathsf{L}_{2,2}$	$\mathsf{L}_{1,3}$	$\mathsf{L}_{0,5}$	C_5
$\vdots$	$\vdots$	$\vdots$	$\vdots$	$\vdots$	$\vdots$	$\cdots$	$\vdots$	$\vdots$	$\vdots$	$\vdots$	$\vdots$	$\vdots$

(iii)

C_1	$\dashv_{\mathbf{0,1}}$										$\exists_{\mathbf{0,1}}$	C_1
C_2	$\dashv_{1,1}$										$\exists_{1,1}$	C_2
C_3	$\dashv_{\mathbf{0,2}}$	$\dashv_{\mathbf{2,1}}$								$\exists_{\mathbf{2,1}}$	$\exists_{\mathbf{0,2}}$	C_3
C_4	$\dashv_{1,2}$	$\dashv_{3,1}$	$\dashv_{\mathbf{4,1}}$				(iv)		$\exists_{\mathbf{3,1}}$	$\exists_{4,1}$	$\exists_{1,2}$	C_4
C_5	$\dashv_{\mathbf{0,3}}$	$\dashv_{\mathbf{2,2}}$	$\dashv_{5,1}$	$\dashv_{\mathbf{6,1}}$	$\dashv_{\mathbf{7,1}}$		$\exists_{\mathbf{5,1}}$	$\exists_{\mathbf{6,1}}$	$\exists_{7,1}$	$\exists_{\mathbf{2,2}}$	$\exists_{\mathbf{0,3}}$	C_5
$\vdots$	$\vdots$	$\vdots$	$\vdots$	$\vdots$	$\vdots$	$\cdots$	$\vdots$	$\vdots$	$\vdots$	$\vdots$	$\vdots$	$\vdots$

TABLE 28. Entries of the branch quartet (Table 3), (i) F, (ii) L, (iii) $\dashv$, (iv) $\exists$ transferred to 1–2-, or 2–1-Fibonacci cohort tableaux of positive integers (Table 6)

$C_{1,1}$	$C_{2,1}$	$C_{3,1}$	$C_{4,1}$	$C_{5,1}\ \cdots$
$C_{3,2}$	$C_{4,2}$	$C_{5,2}$	$C_{6,2}$	$C_{7,2}\ \cdots$
$C_{4,3}$	$C_{5,3}$	$C_{6,3}$	$C_{7,3}$	$C_{8,3}\ \cdots$
$C_{5,4}$	$C_{6,4}$	$C_{7,4}$	$C_{8,4}$	$C_{9,4}\ \cdots$
$C_{5,5}$	$C_{6,5}$	$C_{7,5}$	$C_{8,5}$	$C_{9,5}\ \cdots$
$C_{6,6}$	$C_{7,6}$	$C_{8,6}$	$C_{9,6}$	$C_{10,6}\ \cdots$
$C_{6,7}$	$C_{7,7}$	$C_{8,7}$	$C_{9,7}$	$C_{10,7}\ \cdots$
$C_{6,8}$	$C_{7,8}$	$C_{8,8}$	$C_{9,8}$	$C_{10,8}\ \cdots$

TABLE 29. Rearrangement of the 1–2-Fibonacci cohort tableau, Table 6(i), to form F, the 1–2-Fibonacci Array (Table 12). The pair of indices reference the cohort of the tableau (first index) and rank within the cohort (second index) counted from left to right. Converse of Table 28(i)

1–2-Fibonacci array (F), row description To investigate the relationship between the Fibonacci cohort tableaux and the arrays of the branch quartet, first display the row and column indices for each $z \in \mathbb{Z}_+$ in a Fibonacci cohort tableau of $\mathbb{Z}_+$ (Tables 28). (Conversely, for an array of the quartet, its entries can be written as pair of indices that reference a cohort and rank within the cohort in a 1–2- or 2–1-Fibonacci array of $\mathbb{Z}_+$. Tables 29 and 30 illustrate this for F and $\dashv$, respectively).

Beginning with Table 28(i), recall that the row indices of $z = 1, 2, 3, \ldots$ in F exhibit the Fibonacci cohort structure $C_t = (0, \ldots, F_t - 1)$ discussed above and shown in Table 27(i), top left. Similarly the column indices of $z = 1, 2, 3, \ldots$ in F exhibit the 1–2-Fibonacci cohort structure $C_t = [C_{t-1} + 1] \oplus (1, \ldots, 1)$ discussed above and shown in Table 27(ii), top left. Together, these form the pairs of indices shown in Table 28(i).

Now consider the left subcohorts — those elements below the staircase in Table 28(i) — and observe the indices of F. In the left subcohort of cohort C_t, the first index of each element merely repeats the first index of the element in cohort C_{t-1} aligned directly above it in the tableau, while the second index increments by one the second index of the element aligned directly above it. This shows that each column in the tableau continues a row of F throughout the left subcohorts.

By construction, each column of the tableau begins with an element above the staircase, that is, an element of a right subcohort. Thus it remains only to observe that the row start $\mathsf{F}_{n,1}$ for each row n of Table 12 appears somewhere in a right subcohort of Table 28(i). The cohort structure assures this, whereas the first index for elements of the right subcohort of cohort C_t is $F_{t-1}, \ldots, F_t - 1$, such that over the course of successive cohorts $C_1, C_2, C_3, \ldots, C_t, \ldots$ in the tableau, the first index of elements in the right subcohorts will enumerate all rows $n = 0, 1, 2, \ldots$ in sequence. Meanwhile the second index, 1, of any entry in a right subcohort — represented collectively by "$1, \ldots, 1$" in Table 27(ii) — consistently points to the leftmost column $k = 1$ in the array, that is, the start $\mathsf{F}_{n,1}$ of row n in Table 12.

It follows that the rows of the 1–2-Fibonacci array from top to bottom are merely the columns of the tableau Table 6(i) from left to right . As a method to generate rows of F, then, it suffices to take columns from the Table 6(i) in sequence from left to right, and transpose them directly to form rows of F from top to bottom.

2–1-Fibonacci array (E), row description Moving on to Table 28(ii), note that the row indices of $z = 1, 2, 3, \ldots$ in E exhibit the 2–1-Fibonacci cohort structure $C_t = (F_{t-1}, \ldots, F_t - 1) \oplus C_{t-1}$ discussed above and shown in Table 27(i). Similarly the column indices of $z = 1, 2, 3, \ldots$ in E exhibit the 1–2-Fibonacci cohort structure $C_t = (1, \ldots, 1) \oplus [C_{t-1} + 1]$ discussed above and shown in Table 27(ii). Together, these form the pairs of indices shown in Table 28(ii).

Consider the right subcohorts — those elements below the staircase in Table 28(ii) — and consider the indices of E. Here again, the first index of any element in the right subcohort of cohort C_t merely repeats the first index of the element in cohort C_{t-1} aligned directly above it in the tableau, while the second index increments by one the second index of the element aligned directly above it. This shows that each column in the tableau continues a row of E throughout the right subcohorts.

Thus it remains to observe that the row start $\mathsf{E}_{n,1}$ for each row n in Table 15 appears somewhere in a left subcohort of Table 28(ii). The cohort structure assures this, whereas the first index for elements of the left subcohort of cohort C_t is $F_{t-1}, \ldots, F_t - 1$, such that over the course of successive cohorts $C_1, C_2, C_3, \ldots, C_t, \ldots$ in the tableau, the first index of elements in the left subcohorts will enumerate rows $n = 0, 1, 2, \ldots$ in sequence. Meanwhile the column indices for the left subcohort, $1, \ldots, 1$, consistently point to the leftmost column $k = 1$, that is, the start $\mathsf{E}_{n,1}$ of row n in Table 15.

It follows that the set of rows of the 2–1-Fibonacci array equals the set of columns of the tableau Table 6(ii), (though the top-to-bottom order of the former does not quite correspond to the right-to-left order of the latter). As a method to generate rows of ⊧, then, it suffices to take columns from the Table 6(ii) and transpose them to form the rows of ⊧, reordering them as required.

Column description of ⫞ and ⫟

$C_{1,1}$	$C_{3,1}$	$C_{5,1}$	$C_{7,1}$	$C_{9,1}\cdots$
$C_{2,1}$	$C_{4,1}$	$C_{6,1}$	$C_{8,1}$	$C_{10,1}\cdots$
$C_{3,2}$	$C_{5,2}$	$C_{7,2}$	$C_{9,2}$	$C_{11,2}\cdots$
$C_{4,2}$	$C_{6,2}$	$C_{8,2}$	$C_{10,2}$	$C_{12,2}\cdots$
$C_{4,3}$	$C_{6,3}$	$C_{8,3}$	$C_{10,3}$	$C_{12,3}\cdots$
$C_{5,3}$	$C_{7,3}$	$C_{9,3}$	$C_{11,3}$	$C_{13,3}\cdots$
$C_{5,4}$	$C_{7,4}$	$C_{9,4}$	$C_{11,4}$	$C_{13,4}\cdots$
$C_{5,5}$	$C_{7,5}$	$C_{9,5}$	$C_{11,5}$	$C_{13,5}\cdots$

TABLE 30. Rearrangement of the 1–2-Fibonacci cohort tableau, Table 6(i), to form ⫞, the 2–1-mirror Array (Table 3 at bottom right). The pair of indices reference the cohort of the tableau (first index) and rank within the cohort (second index) counted from left to right. Converse of Table 28(iii)

The foregoing discussion described a "cohort tableau approach" for generating arrays ⊦ and ⊧ by taking columns from the 1–2- and 2–1-Fibonacci cohort tableaux of positive integers, respectively, Tables 6(i) and (ii), transposing them from vertical horizontal to form the rows of the respective arrays, and, in the case of ⊧, reordering them as necessary.

An extension of this approach produces the "mirror arrays," ⫞ and ⫟, found at the bottom of Table 3. Obtain the rows of ⫞ by taking "split columns" of the 1–2-Fibonacci tableau, Table 6(i), that is, elements of *alternate* cohorts, in columns of the tableau running from left to right. Refer to Table 28(iii). Accordingly, Table 28(iii) shows the cohorts of ⫞ aligned to the left (though the sequences of row and column indices in ⫞ for the sequence of positive integers have a 2–1-Fibonacci cohort structure, as presented at the bottom right of Tables 27(i) and (ii), respectively.

Similarly, obtain the rows of ⫟ by taking split columns of the 2–1-Fibonacci Array, Table 6(ii). Accordingly, Table 28(iv) displays ⫟ aligned to the right — a similar change of tableau alignment — whereas the tableau aligns the values to the right, though the sequences of row and column indices in ⫟ for the sequence positive integers, have a 1–2-Fibonacci cohort structure, as presented at the bottom left of Tables 27(i) and (ii), respectively.

The alignment highlights the split-columns method for generating rows of and ⫞ and ⫟. Returning to Tables 27(i) and (ii) (bottom right of each), consider the left subcohorts for the sequences of row, respectively, column indices of $z = 1, 2, 3, \ldots$ in ⫞. For the left subcohort of cohort C_t, the row indices merely repeat those of the second previous cohort C_{t-2}, while the column indices increment by one those of the second previous cohort C_{t-2}. Consequently, Table 28(iii) opts to align the columns of ⫞ to the left of the tableau, placing the left subcohort of cohort C_t directly below cohort C_{t-2} from which it derives.

This shows that any element of a left subcohort in the tableau continues a sequence started in the same column in the second cohort above it, and that this sequence is a row of $\exists$. Thus, it suffices to "split" these columns, taking elements from alternate cohorts in the tableau, to obtain rows of $\exists$. Here again, to see that the method indeed yields *all* rows of $\exists$, observe that the formulation $(F_t, \ldots, F_{t+1} - 1)$ of right subcohorts of the sequence of row indices gives $n = 0, 1, 2, \ldots$ and that the formulation $(1, \ldots, 1)$ of right subcohorts of the sequence of column indices gives $k = 1$, so that the row start $\exists_{n,1}$ for each row n appears in some right subcohort (above the staircase) of Table 28(iii).

Referring to the bottom-left of Tables 27(i) and (ii), consider the right subcohorts for the sequences of row, respectively, column indices of $z = 1, 2, 3, \ldots$ in $\nexists$. For the right subcohort of cohort C_t, the row indices merely repeat those of the second previous cohort C_{t-2}, while the column indices increment by one those of the second previous cohort C_{t-2}. Consequently, Table 28(iv) opts to align the columns of $\nexists$ to the right, placing the right subcohort of cohort C_t directly below cohort C_{t-2} from which it derives.

This shows that any element of a right subcohort in the tableau continues a sequence started in same column in the second cohort above it, and that this sequence is a row of $\nexists$. As before, it suffices to "split" these columns, taking elements from alternate cohorts, to obtain rows of $\nexists$. Yet again, the formulation of left subcohorts of row and column indices ensures that the row start $\nexists_{n,1}$ for each row n appears in some left subcohort (above the staircase) of Table 28(iv).

Figure 24(b)(i) summarizes this Fibonacci-cohort-tableau approach to constructing the branch quartet.

Column description of $\digamma$ and $\vdash$ Conversely to the above description of rows, and also following a cohort tableau approach, a description of the columns of $\digamma$ proceeds as follows: Each cohort of the 1–2-Fibonacci cohort tableau (Table 6(i)) distributes among columns of the 1–2-Fibonacci array (Table 12) by placing the right subcohorts in the first column of the array, the right subcohorts of the left subcohorts in the second column of the array, etc. Table 29 reformulates each entry of array $\digamma$ using a pair of indices that reference a cohort of the tableau (first index) and rank within the cohort (second index).

Recall from Definition 4.1 that cohort C_t has length $|C_t| = F_t$. Then, for distribution among the columns of the array, cohort t of the tableau partitions into subcohorts, sub-subcohorts, etc., of lengths

$$\begin{aligned} F_t &= F_{t-1} + F_{t-2} \\ &= (F_{t-2} + F_{t-3}) + F_{t-2} \\ &= ((F_{t-3} + F_{t-4}) + F_{t-3}) + F_{t-2} \\ &= (((F_{t-4} + F_{t-5}) + F_{t-4}) + F_{t-3}) + F_{t-2} \\ &\;\;\vdots \\ &= (\cdots((1 + F_1) + F_2) + \cdots + F_{t-3}) + F_{t-2}, \end{aligned}$$

with F_{t-2} elements from each cohort C_t distributed to the first column of the array (provided that $t \geq 3$), F_{t-3} elements distributed to the second column (provided that $t \geq 4$), and so forth. Thus, for $k \leq t - 2$, a run of F_{t-k-1} elements from cohort C_t is placed in column k of the array, and the remaining block of F_{t-k}

elements to its left in the cohort is further partitioned, if possible. Now, $|C_t| = F_t = 1 + \sum_{k=1}^{t-2} F_k = 1 + \sum_{k=1}^{t-2} F_{t-k-1}$. Thus for $t \geq 3$, element $C_{t,2} = F_{t+1} + 1$ of cohort C_t is placed in column $k = t - 2$ of the array. Subsequently, for $t \geq 1$, the leftmost element $C_{t,1} = F_{t+1}$ is all that remains of cohort C_t, and is placed in (row $n = 0$ of) column $k = t$.

With reference to the 1–2-Fibonacci cohort tableau, Table 29 seems to show that $\digamma_{n,k} = C_{F^{-1}(n)+k,n+1}$, where the first index would follow from (83), while the second index follows from the partition just described.

For $\vdash$ on the other hand, values in the first column of the 2–1-Fibonacci array, Table 15, are precisely the values in the left subcohorts of the 2–1-Fibonacci cohort tableau, Table 6(ii).

The array distributes each cohort of the tableau, placing the left subcohort in the first column of the array, the left subcohort of the right subcohort in column two of the array, etc. Thus, for distribution among the columns of the array, cohort t of the tableau partitions into subcohorts, sub-subcohorts, etc., of lengths

$$\begin{aligned} F_t &= F_{t-2} + F_{t-1} \\ &= F_{t-2} + (F_{t-3} + F_{t-2}) \\ &= F_{t-2} + (F_{t-3} + (F_{t-4} + F_{t-3})) \\ &= F_{t-2} + (F_{t-3} + (F_{t-4} + (F_{t-5} + F_{t-4}))) \\ &\vdots \\ &= F_{t-2} + (F_{t-3} + \cdots + (F_2 + (F_1 + 1)) \cdots), \end{aligned}$$

with F_{t-2} elements from each cohort C_t distributed to the first column of the array (provided that $t \geq 3$), F_{t-3} elements distributed to the second column (provided that $t \geq 4$), and so forth. Thus, for $k \leq t - 2$, a run of F_{t-k-1} elements from cohort C_t is placed in column k of the array, and the remaining block of F_{t-k} elements to its right in the cohort is further partitioned, if possible. Now, $|C_t| = F_t = 1 + \sum_{k=1}^{t-2} F_k = 1 + \sum_{k=1}^{t-2} F_{t-k-1}$. Thus for $t \geq 3$, element $C_{t,F_t-1} = F_{t+2} - 2$ of cohort C_t is placed in column $k = t - 2$ of the array. Subsequently, for $t \geq 1$, only the rightmost element $C_{t,F_t} = F_{t+2} - 1$ of cohort C_t remains, and is placed in (row $n = 0$ of) column $k = t$.

Column description of $\dashv$ and $\dashv$ A similar description can be derived for the mirror arrays of the branch quartet. Table 30 shows the converse of Table 28(iii), the array $\dashv$ with its elements indexed to the 1–2-Fibonacci cohort tableau of the positive integers, Table 6(i).

With reference to the 1–2-Fibonacci cohort tableau, the first row of Table 30 seems to follow $\dashv_{n,k} = C_{2k-1,1}$, the second row $\dashv_{n,k} = C_{F^{-1}(n)+2k-2,1}$, and the remaining rows $\dashv_{n,k} = C_{F^{-1}(n)+2k-2,n+1-(F^{-1}(n)-2)}$, where in each case the first index follows from (84), while the second index follows from the alternating pattern of Table 28(iii).

8.2.3. *Para-Fibonacci sequences in the clade quartet.* Recall the clade quartet of interspersion arrays shown in Table 4, clockwise from the top left, w, a, $\mathfrak{d}$, and $\mathfrak{w}$. Consider the sequences of row and column indices of $\mathbb{Z}_+$ in each of the four member arrays. Beginning with w, observe that sequence $\underline{019586} = \underline{003603} - 1$ gives row indices $0, 0, 0, 1, 0, 2, 1, 0, 3, 2, 1, 4, 0, 5, 3, 2, 6, 1, 7, 4, \ldots$ for the sequence of positive integers. Indeed, this sequence exhibits a 1–2-Fibonacci cohort structure,

(i) $C_t =$

$\boldsymbol{l}(C_{t-1})\oplus\boldsymbol{r}(C_{t-2})$, $\boldsymbol{l}(0)\equiv 0$, $\boldsymbol{r}(0)\equiv 1$	$\boldsymbol{R}(C_{t-2})\oplus\boldsymbol{L}(C_{t-1})$, $\boldsymbol{L}(0)\equiv 0$, $\boldsymbol{R}(0)\equiv 1$
$\boldsymbol{l}(C_{t-1})\oplus\boldsymbol{r}(C_{t-2})$, $\boldsymbol{l}(0)\equiv 1$, $\boldsymbol{r}(0)\equiv 0$	$\boldsymbol{R}(C_{t-2})\oplus\boldsymbol{L}(C_{t-1})$, $\boldsymbol{L}(0)\equiv 1$, $\boldsymbol{R}(0)\equiv 0$

(ii) $C_t =$

$\texttt{++}C_{t-1}\oplus C_{t-2}$	$C_{t-2}\oplus C_{t-1}\texttt{++}$
$\begin{cases} C_{t-1}\oplus C_{t-2}\texttt{++}, & t \text{ odd};\\ C_{t-1}\oplus C_{t-2}, & t \text{ even}. \end{cases}$	$\begin{cases} \texttt{++}C_{t-2}\oplus C_{t-1}, & t \text{ odd};\\ C_{t-2}\oplus C_{t-1}, & t \text{ even}. \end{cases}$

TABLE 31. Structure of cohort C_t in the row (i) and column indices (ii) of the positive integers in sequence, for the clade quartet of interspersion arrays (Table 4). In each of tables (i) and (ii), clockwise from the top left, w, a, $\mathfrak{a}$, and $\mathfrak{w}$.

with cohorts $C_t = \boldsymbol{l}(C_{t-1})\oplus\boldsymbol{r}(C_{t-2})$, where $\boldsymbol{l}(n)$ and $\boldsymbol{r}(n)$ represent left and right branching, respectively in the minimal Fibonacci tree, taking $\boldsymbol{l}(0)\equiv 0$ and $\boldsymbol{r}(0)\equiv 1$. Thus, its cohortizer can be written $\langle \boldsymbol{l}, \boldsymbol{r}\rangle$.

Moving on to the column indices in w for the sequence of positive integers, observe that sequence 035612 gives column indices 1, 2, 3, 1, 4, 1, 2, 5, 1, 2, 3, 1, 6, 1, 2, 3, 1, 4, 1, 2, ... It too exhibits a 1–2-Fibonacci cohort structure with cohorts $C_t = \texttt{++}C_{t-1}\oplus C_{t-2}$. Thus its cohortizer can be written $\langle \texttt{++}, I\rangle$.

In a, the row indices 0, 0, 1, 0, 1, 2, 0, 3, 1, 2, 4, 0, 3, 5, 1, 6, 2, 4, 7, 0, ... of the positive integers in natural order exhibit a 2–1-Fibonacci cohort structure, with cohorts $C_t = \boldsymbol{R}(C_{t-2})\oplus\boldsymbol{L}(C_{t-1})$, where $\boldsymbol{L}(n)$ and $\boldsymbol{R}(n)$ represent left and right branching, respectively in the maximal Fibonacci tree, taking $\boldsymbol{L}(0)\equiv 0$ and $\boldsymbol{R}(0)\equiv 1$. The sequence equals 167198 $- 1$. Thus, its cohortizer can be written $\langle \boldsymbol{R}, \boldsymbol{L}\rangle$. Remark 8.9 obtains this sequence by setting $A_1 = 0$ in Table 32.

Moving on to the column indices in a for the sequence of positive integers, observe that sequence 083368 provides the indices 1, 2, 1, 3, 2, 1, 4, 1, 3, 2, 1, 5, 2, 1, 4, 1, 3, 2, 1, 6, ..., revealing a 2–1-Fibonacci cohort structure $C_t = C_{t-2}\oplus C_{t-1}\texttt{++}$. Thus, its cohortizer can be written $\langle I, \texttt{++}\rangle$.

Tables 31(i) and (ii) summarize the results for row, respectively, column indices of $\mathbb{Z}_+$ in the arrays of the clade quartet, also including $\mathfrak{w}$ and $\mathfrak{a}$ at the bottom left and right of the tables, respectively. Table 31(ii) shows that cohorts of column indices for w and a contain the same elements in reverse order. Similarly, respective cohorts C_t of column indices in $\mathfrak{w}$ and $\mathfrak{a}$ are the reverse of one another.

8.2.4. *Successor tableaux and the clade quartet.* Section 4.1.4 described columns of the clade quartet arrays as Fibonacci cohort sequences, giving explicit cohort-based formulas. Thus it comes as no surprise that the sequences of row indices of the integers in these arrays exhibit the Fibonacci cohort property. The fact that the column indices also exhibit some sort of Fibonacci cohort property suggests a relationship between the rows of the underlying arrays and cohort tableaux, hence a possible transformation between tableaux and the arrays themselves. However, the recurrences in Table 31(ii) are *not* Fibonacci cohort relations. Rather, the increment (++) in the recurrence affords special treatment to a single element of a prior cohort. This special treatment reappears in Lemma 8.19(iii) & (iv), in the context of the pairs of branching functions $(\boldsymbol{l}, \boldsymbol{r})$ and $(\boldsymbol{L}, \boldsymbol{R})$.

This motivates a comparison of the column index sequences for F and w. An examination shows that each cohort of one rearranges the corresponding cohort of the other, with cohort C_t of either sequence containing F_{t-k-1} copies of $k = 1, \ldots, t$.

Per Table 27(ii), the column index sequence for F has cohortizer $[C_{t-1}+1] \oplus \overbrace{(1,\ldots,1)}^{F_{t-2}}$, which shows each cohort to be non-increasing, thus taking the generic form $C_t = (\overbrace{t}^{(t\geq 1)}_{F_{-1}}, \overbrace{t-2}^{(t\geq 3)}_{F_1}, \overbrace{t-3}^{(t\geq 4)}_{F_2}, \overbrace{t-4,t-4}^{(t\geq 5)}_{F_3}, \overbrace{t-5,t-5,t-5}^{(t\geq 6)}_{F_4}, \overbrace{t-6,t-6,t-6,t-6,t-6}^{(t\geq 7)}_{F_5}, \ldots)$ and containing F_{t-k-1} copies of $k = 1,\ldots,t$.

By contrast, the column index sequence for w has cohortizer $\mathsf{{+}{+}}C_{t-1} \oplus C_{t-2}$ according to Table 27(ii), which gives each cohort generically as $C_t = (t) \oplus C_1 \oplus \cdots \oplus C_{t-2}$. Equivalently, the recurrence $S_m = \begin{cases} F^{-1}(m) - 1, & m \text{ a Fibonacci number;} \\ S_{m-F^{-1}(m)}, & \text{otherwise;} \end{cases}$ gives the individual elements of the sequence for $m \geq 1$. This makes it possible to infer by strong induction that each cohort C_t contains the number of copies F_{t-k-1} of each integer k, as claimed above. The latter formulation also follows from the recursive structure of each column k of $w_{n,k}$ for $n \geq 1$ (98), whereby $F_{k+1} = w_{0,k}$ is the first integer to fall in column k, following which k recurs as a column index according to the expression shown.

How then does the clade quartet relate to cohort tableaux and which tableaux are they? Table 19 provides the answer. Just as the branch quartet arrays can be generated (Tables 28) from the Fibonacci cohort tableaux (Tables 6), in a fully analogous procedure, rows of the clade quartet arrays arise from columns (or split columns) of the successor tableaux (Table 19).

Figure 24(b)(ii) summarizes this Fibonacci-cohort-tableau approach to constructing the clade quartet.

8.3. **Tree branch (or prefix) approach to constructing the quartets.**

8.3.1. *Tree branch (or prefix) approach to constructing the branch quartet.* Propositions 4.16(a) and 4.30 gave the formulas for F, respectively L shown in the upper half of Table 3, while similar results of the free-monoid approach yield the formulas for $\mathsf{\exists}$, and $\mathsf{\exists}$ shown in the lower half of the table. Whereas these formulas obtained from counting arguments in the tableaux of compositions in a free-monoid ("free-monoid approach," Figure 25(a)(i)), the same formulas obtain by defining the quartet arrays in terms of branching functions (Figures 15(iii) & (iv)) in the minimal and maximal Fibonacci trees, Figures 5, respectively, 8.

For the minimal and maximal Fibonacci arrays, the first column, $1, \boldsymbol{r}(1), \boldsymbol{r}(2), \boldsymbol{r}(3), \ldots$ ($1, \boldsymbol{R}(1), \boldsymbol{R}(2), \boldsymbol{R}(3), \ldots$), employs the right children of the integers $1, 2, 3, \ldots$ in the minimal, respectively, maximal Fibonacci tree, and rows of the arrays are sequences of all-left branchings in the minimal, respectively, maximal Fibonacci tree.

For the minimal and maximal mirror arrays, the first column, $1, \boldsymbol{l}(1), \boldsymbol{l}(2), \boldsymbol{l}(3), \ldots$ ($1, \boldsymbol{L}(1), \boldsymbol{L}(2), \boldsymbol{L}(3), \ldots$), employs the left children of the integers $1, 2, 3, \ldots$ in the minimal, respectively, maximal Fibonacci tree, and rows of the arrays are sequences of all-right branchings in the minimal, respectively, maximal Fibonacci tree.

Figure 24(a)(i) summarizes this "tree approach" to the branch quartet, from which Lemma 8.1 follows.

Lemma 8.1 (Formulas for the branch quartet)**.** *Using the "tree approach" of harvesting branches (Figure 24(b)(i)), write the branch quartet (Table 3) as:*

(F): $\mathsf{F}_{n,k} = \quad n + F_{F^{-1}(n)+k+1} \qquad\qquad n \geq 0.$

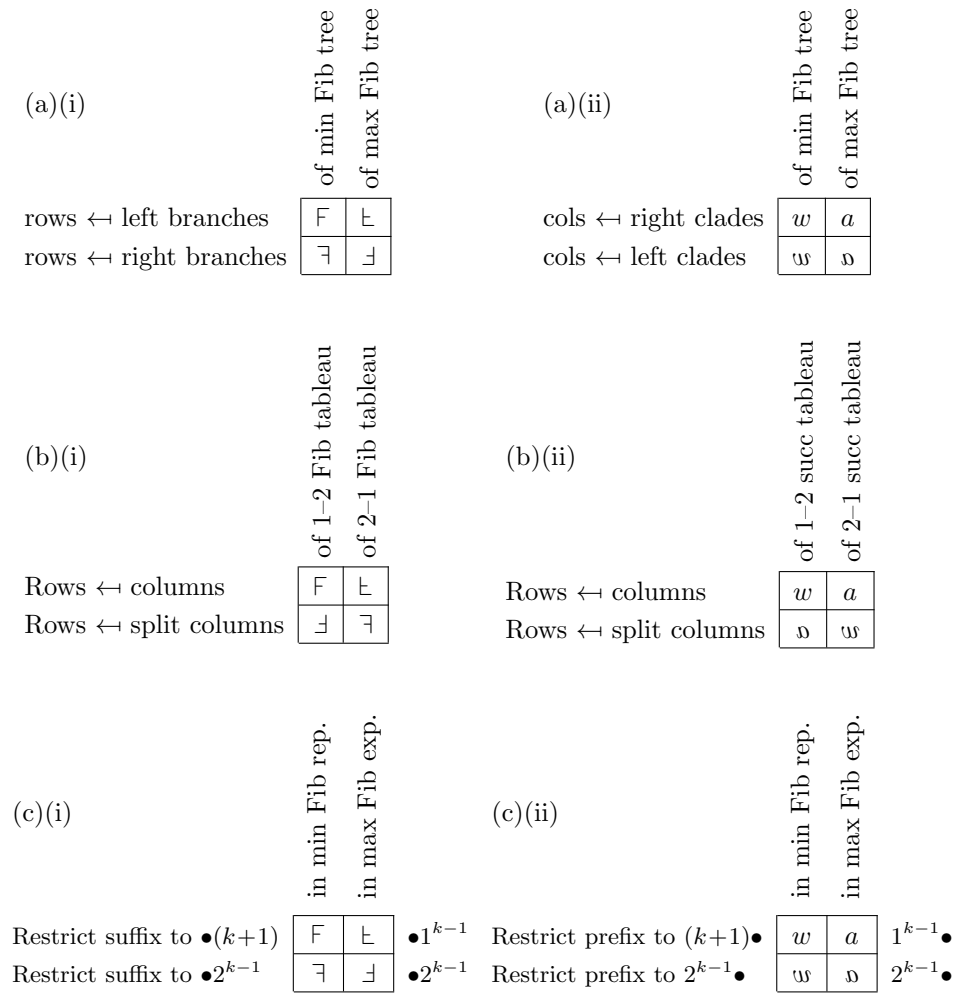

FIGURE 24. At left: (i) Branch quartet (Table 3). At right: (ii) Clade quartet (Table 4). At top: (a) "Tree approach": Generation of rows (columns) by gathering branches (clades) of binary trees of integers (Figures 5 and 8). At middle: (b) "Cohort-tableau approach": In (b)(i), Branch quartet rows obtain by manipulating 1–2- or 2–1-Fibonacci cohort tableaux, Tables 6 (see Table 28). In (b)(ii), Clade quartet columns obtain by manipulating 1–2- or 2–1-successor tableaux, Tables 19. At bottom: (c) "Numeration approach": Generation of column k by restricting gaps in a Fibonacci numeration system.

$$(\text{⊣}):\ \text{⊣}_{n,k} = \begin{cases} F_{2k+1} - 1, & n = 0; \\ n + F_{F^{-1}(n)+2k} - 2F_{F^{-1}(n)}, & n > 0. \end{cases}$$

$$(\text{⊢}):\ \text{⊢}_{n,k} = n + F_{F^{-1}(n)+k+2} - F_{F^{-1}(n)+2} \quad n \geq 0.$$

$$(\text{⊥}):\ \text{⊥}_{n,k} = \begin{cases} F_{2k}, & n = 0; \\ n + F_{F^{-1}(n)+2k-1} - F_{F^{-1}(n)-1}, & n > 0. \end{cases}$$

Proof of Lemma 8.1: In Section 11 □

Remark 8.2. Figure 25(b)(i) presents the formulas of Lemma 8.1 as $S(n)$ in terms of compositions S of branching functions $\boldsymbol{l}$ and $\boldsymbol{r}$ or $\boldsymbol{L}$ and $\boldsymbol{R}$. Further, one can substitute the row index n in this formulation by an expression of the form $n = N(1)$, where the composition $N \in \{\boldsymbol{l}, \boldsymbol{r}\}^\star$ takes the form described in Lemma 6.10(i). This substitution leaves the expressions for F and $\mathsf{\exists}$ in a form where each entry of the array is the image of 1 under some composition $SN \in \{\boldsymbol{l}, \boldsymbol{r}\}^\star$. To furnish the compositions N, Table 32(i) arranges the free monoid $\{\boldsymbol{l}, \boldsymbol{r}\}^\star$ as a 1–2-Fibonacci outer cohort sequence, such that the n^{th} element NW_1 of the tableau evaluates to n, when setting $W_1 = 1$.

Similarly, in the formulation presented in Figure 25(b)(i), one can substitute the row index n by an expression of the form $n = N(1)$, where the composition $N \in \{\boldsymbol{L}, \boldsymbol{R}\}^\star$ takes the form described in Lemma 6.10(ii), thus leaving the expressions for L and $\mathsf{\exists}$ in a form where each entry of the array is the image of 1 under some composition $SN \in \{\boldsymbol{L}, \boldsymbol{R}\}^\star$. To furnish the compositions N, Table 32(ii) arranges the free monoid $\{\boldsymbol{L}, \boldsymbol{R}\}^\star$ as a 2–1-Fibonacci outer cohort sequence, such that the n^{th} element NA_1 of the tableau evaluates to n, when setting $A_1 = 1$.

Proposition 8.2 (Adjacent Fibonacci tree positions of mirror duals in the branch quartet)**.** *For the branch quartet of arrays given in Table 3:*

$$(\mathsf{F} \text{ and } \mathsf{\exists})\text{: } \mathbf{p}(\mathsf{\exists}_{n,k}) = \begin{cases} 2\mathbf{p}(\mathsf{F}_{n,k}) - 1, & n = 0; \\ \mathbf{p}(\mathsf{F}_{n,k}) - 1, & n > 0. \end{cases}$$

$$(\mathsf{L} \text{ and } \mathsf{\exists})\text{: } \mathbf{P}(\mathsf{\exists}_{n,k}) = \begin{cases} 2\mathbf{P}(\mathsf{L}_{n,k}) - 1, & n = 0; \\ \mathbf{P}(\mathsf{L}_{n,k}) - 1, & n > 0. \end{cases}$$

Proof. Case $n = 0$:

By construction, for $k = 1, 2, 3, \ldots$, $\mathsf{F}_{0,k}$ and $\mathsf{L}_{0,k}$ are sequences of all-left branchings in the minimal, respectively, maximal Fibonacci trees, with $\mathsf{F}_{0,1} = \mathsf{L}_{0,1} = 1$. Also, for $k = 1, 2, 3, \ldots$, $\mathsf{\exists}_{0,k}$ and $\mathsf{\exists}_{0,k}$ are sequences of all-right branchings in the minimal, respectively, maximal Fibonacci trees, with $\mathsf{\exists}_{0,1} = \mathsf{\exists}_{0,1} = 1$. Consequently, $\mathbf{p}(\mathsf{F}_{0,k}) = \mathbf{P}(\mathsf{L}_{0,k}) = 2^{k-1}$ and $\mathbf{p}(\mathsf{\exists}_{0,k}) = \mathbf{P}(\mathsf{\exists}_{0,k}) = 2^k - 1$, thus proving the claim for $n = 0$.

Case $n > 0$:

By construction, for $n > 1$, $\mathsf{\exists}_{n,1} = \boldsymbol{l}(n)$ and $\mathsf{F}_{n,1} = \boldsymbol{r}(n)$ are children of the same parent in the minimal Fibonacci tree, so that $\mathbf{p}(\mathsf{\exists}_{n,1}) = 2\mathbf{p}(n)$ and $\mathbf{p}(\mathsf{F}_{n,1}) = 2\mathbf{p}(n) + 1$, and the claim holds for $n > 1$ and $k = 1$.

Moreover, the sequences of all-right, respectively, all-left branchings give $\mathsf{\exists}_{n,k} = \boldsymbol{r}^{k-1}(\mathsf{\exists}_{n,1})$ and $\mathsf{F}_{n,k} = \boldsymbol{l}^{k-1}(\mathsf{F}_{n,1})$. By induction, therefore, if $\mathbf{p}(\mathsf{\exists}_{n,k}) = \mathbf{p}(\mathsf{F}_{n,k}) - 1$ for some $n > 0$, then $\mathbf{p}(\mathsf{F}_{n,k+1}) = \mathbf{p}(\boldsymbol{l}(\mathsf{F}_{n,k})) = 2\mathbf{p}(\mathsf{F}_{n,k})$ and $\mathbf{p}(\mathsf{\exists}_{n,k+1}) = \mathbf{p}(\boldsymbol{r}(\mathsf{\exists}_{n,k})) = 2\mathbf{p}(\mathsf{\exists}_{n,k}) + 1 = 2(\mathbf{p}(\mathsf{F}_{n,k}) - 1) + 1 = 2\mathbf{p}(\mathsf{F}_{n,k}) - 1 = \mathbf{p}(\mathsf{F}_{n,k+1}) - 1$, proving the claim.

Similarly, for $n > 1$, $\mathsf{\exists}_{n,1} = \boldsymbol{L}(n)$ and $\mathsf{L}_{n,1} = \boldsymbol{R}(n)$ are children of the same parent in the maximal Fibonacci tree, so that $\mathbf{P}(\mathsf{\exists}_{n,1}) = 2\mathbf{P}(n)$ and $\mathbf{P}(\mathsf{L}_{n,1}) = 2\mathbf{P}(n) + 1$, and the claim holds for $n > 1$ and $k = 1$.

Moreover, the sequences of all-right, respectively, all-left branchings give $\mathsf{\exists}_{n,k} = \boldsymbol{R}^{k-1}(\mathsf{\exists}_{n,1})$ and $\mathsf{L}_{n,k} = \boldsymbol{L}^{k-1}(\mathsf{L}_{n,1})$. By induction, therefore, if $\mathbf{P}(\mathsf{\exists}_{n,k}) = \mathbf{P}(\mathsf{L}_{n,k}) - 1$ for some $n > 0$, then $\mathbf{P}(\mathsf{L}_{n,k+1}) = \mathbf{P}(\boldsymbol{L}(\mathsf{L}_{n,k})) = 2\mathbf{P}(\mathsf{L}_{n,k})$ and $\mathbf{P}(\mathsf{\exists}_{n,k+1}) = \mathbf{P}(\boldsymbol{R}(\mathsf{\exists}_{n,k})) = 2\mathbf{P}(\mathsf{\exists}_{n,k}) + 1 = 2(\mathbf{P}(\mathsf{L}_{n,k}) - 1) + 1 = 2\mathbf{P}(\mathsf{L}_{n,k}) - 1 = \mathbf{P}(\mathsf{L}_{n,k+1}) - 1$, proving the claim. □

8.3.2. *Tree branch (or prefix) approach to constructing the clade quartet.* For the Wythoff and quilt arrays, the first column, $1, \bar{\boldsymbol{r}}(1), \bar{\boldsymbol{r}}(2), \bar{\boldsymbol{r}}(3), \ldots$ $(1, \bar{\boldsymbol{R}}(1), \bar{\boldsymbol{R}}(2), \bar{\boldsymbol{R}}(3), \ldots)$, employs right children of the integers $1, 2, 3, \ldots$ in the minimal, respectively, maximal successor tree, and rows of the arrays are sequences of all-left branchings in the minimal, respectively, maximal successor tree.

For the Wythoff and quilt mirror arrays, the first column, $1, \bar{\boldsymbol{l}}(1), \bar{\boldsymbol{l}}(2), \bar{\boldsymbol{l}}(3), \ldots$ $(1, \bar{\boldsymbol{L}}(1), \bar{\boldsymbol{L}}(2), \bar{\boldsymbol{L}}(3), \ldots)$, employs left children of the integers $1, 2, 3, \ldots$ in the minimal, respectively, maximal successor tree, and, rows of the arrays are sequences of all-right branchings in the minimal, respectively, maximal successor tree.

Figure 24(b)(ii) summarizes this "tree approach" to the clade quartet, from which Lemma 8.3 follows.

Lemma 8.3 (Formulas for the clade quartet)**.** *Using the "tree approach" of harvesting branches (Figure 24(b)(ii)), write the clade quartet (Table 4) as:*

(*w***):** $w_{n,k} = F_{k+1}\kappa(n+1) + F_k n, n \geq 0.$

(ɯ): $\mathfrak{w}_{n,k} = \begin{cases} F_{2k+1} - 1, & n = 0; \\ F_{2k-1}\kappa(n+1) + F_{2k-2}n - 1, & n \geq 1. \end{cases}$

(*a***):** $a_{n,k} = F_{k+1}\kappa(n) + F_k n + F_{k+2} - 1, n \geq 0.$

(ɒ): $\mathfrak{o}_{n,k} = F_{2k-1}\kappa(n) + F_{2k-2}n + F_{2k}, n \geq 0.$

Proof of Lemma 8.3: In Section 11 □

Remark 8.3. Figure 25(b)(ii) presents the formulas of Lemma 8.3 as $S(n)$ in terms of compositions S of branching functions $\bar{\boldsymbol{l}}$ and $\bar{\boldsymbol{r}}$ or $\bar{\boldsymbol{L}}$ and $\bar{\boldsymbol{R}}$. Further, one can substitute the row index n in the latter formulation by an expression of the form $n = N(1)$ for some composition $N \in \{\bar{\boldsymbol{l}}, \bar{\boldsymbol{r}}\}^\star$. This substitution leaves the expressions for w and $\mathfrak{w}$ in a form where each entry of the array is the image of 1 under some composition $SN \in \{\bar{\boldsymbol{l}}, \bar{\boldsymbol{r}}\}^\star$. To supply the compositions N, Table 33(i) arranges the free monoid $\{\bar{\boldsymbol{l}}, \bar{\boldsymbol{r}}\}^\star$ as a 1–2-Fibonacci inner cohort sequence, such that the n^{th} element NF_1 of the tableau evaluates to n, when setting $F_1 = 1$.

Similarly, the row index n converts to an expression of the form $N(1)$ for some composition $N \in \{\bar{\boldsymbol{L}}, \bar{\boldsymbol{R}}\}^\star$, thus leaving the expressions for a and $\mathfrak{o}$ in a form where each element of the array is the image of 1 under some composition $SN \in \{\bar{\boldsymbol{L}}, \bar{\boldsymbol{R}}\}^\star$. To supply the compositions N, Table 33(ii) arranges the free monoid $\{\bar{\boldsymbol{L}}, \bar{\boldsymbol{R}}\}^\star$ as a 2–1-Fibonacci inner cohort sequence, such that the n^{th} element $N\mathfrak{L}_1$ of the tableau evaluates to n, when setting $\mathfrak{L}_1 = 1$.

Proposition 8.4 (Adjacent successor tree positions of mirror duals in the clade quartet)**.** *For the clade quartet of arrays given in Table 4:*

(*w* **and ɯ):** $\bar{\mathbf{p}}(\mathfrak{w}_{n,k}) = \begin{cases} 2\bar{\mathbf{p}}(w_{n,k}) - 1, & n = 0; \\ \bar{\mathbf{p}}(w_{n,k}) - 1, & n > 0. \end{cases}$

(*a* **and ɒ):** $\bar{\mathbf{P}}(\mathfrak{o}_{n,k}) = \begin{cases} 2\bar{\mathbf{P}}(a_{n,k}) - 1, & n = 0; \\ \bar{\mathbf{P}}(a_{n,k}) - 1, & n > 0. \end{cases}$

Proof of Proposition 8.4. Analogous to that of Proposition 8.2. □

8.4. **Free-monoid approach to constructing the quartets.** To describe the eight arrays of the branch and clade quartets, Tables 3, respectively, 4 gave the necessary restrictions on compositions in the free monoids $\{\kappa, \lambda\}^\star$ (suffix for F and $\exists$, and prefix for w and $\mathfrak{w}$) and $\{\theta, \eta\}^\star$ (prefix for L and $\exists$, and suffix for a and $\mathfrak{o}$), required to place each composition of the free monoid into an array *column*. The

resulting arrays of compositions generate the arrays of values via the isomorphisms of Proposition 4.16(b) and Corollary 4.26. This section completes the description of these arrays of compositions by giving the restriction on *rows* for the complete octet (Figures 25(a)(i) and (a)(ii)).

(An alternative approach using the free monoids $\{\boldsymbol{l}, \boldsymbol{r}\}^\star$, $\{\boldsymbol{L}, \boldsymbol{R}\}^\star$, $\{\bar{\boldsymbol{l}}, \bar{\boldsymbol{r}}\}^\star$, and $\{\bar{\boldsymbol{L}}, \bar{\boldsymbol{R}}\}^\star$, provides greater symmetry in as much as the columns of all arrays in the octet can be described by either a prefix restriction, Figures 25(b)(i) and (b)(ii), or by a suffix description, Figures 25(c)(i) and (c)(ii). Also see Remarks 8.2 and 8.3.)

8.4.1. *Free-monoid approach to constructing the branch quartet.* To describe the branch quartet, Table 3 indicated the restrictions on the suffix of compositions in $\{\kappa, \lambda\}^\star$ for $\digamma$ and $\exists$, or the prefix of compositions in $\{\theta, \eta\}^\star$ for $\vdash$ and $\dashv$ (Figure 25(a)(i)). From Section 8.1, recall the description of the arrays' first columns as cohort tableaux. Similar to that description, this present section indicates the restrictions on the prefix of compositions in $\{\kappa, \lambda\}^\star$ and suffix of compositions in $\{\theta, \eta\}^\star$ to forms that occur only in specific subcohorts of the corresponding 1–2-Fibonacci inner and 2–1-Fibonacci outer cohort tableaux, respectively, thus completing the description of the "free-monoid approach."

Section 4.1.5 constructed the array $\digamma$ by first gathering compositions $S \in \{\kappa, \lambda\}^\star$ with the same value of $S(1)$ into rows (equivalence classes), the value of $S(1)$ increasing from one row to the next, and then sorting each row according to increasing value of $S(2) - 1$. Table 9 showed this array of compositions S, for which the corresponding array of values $S(2) - 1$ gave $\digamma$.

In terms of the free monoid on $\{\kappa, \lambda\}$, a common suffix of entries characterizes the columns of Table 9, with entries in each column $k = 1, 2, 3, \ldots$ sharing the suffix $\circ\kappa^{k-1}$. A common prefix of entries characterizes each row of Table 9, with entries in row $n = 0, 1, 2, \ldots$ sharing as prefix the ${\digamma_{n,1}}^{\text{st}}$ element in the tableau, Table 10, that is, the n^{th} element terminating in λ (see Figure 23(iii)), or equivalently, the n^{th} element lying in a right subcohort of the tableau (where I counts as the 0^{th} element terminating in λ and lying in a right subcohort): $I, \lambda, \kappa\lambda, \kappa^2\lambda, \lambda^2, \kappa^3\lambda, \lambda\kappa\lambda, \kappa\lambda^2, \ldots$.

By analogy, $\exists$ arises from values $S(2) - 1$ for an array of compositions $S \in \{\kappa, \lambda\}^\star$, in which entries of each column $k = 1, 2, 3, \ldots$ share the suffix $\circ\lambda^{k-1}$. Entries in each row $n = 0, 1, 2, \ldots$ of this array of compositions share as prefix the ${\exists_{n,1}}^{\text{st}}$ element in Table 10, that is, the n^{th} element terminating in κ (see Figure 23(iii)), or equivalently, the n^{th} element lying in a left subcohort of the tableau (where I counts as the 0^{th} element terminating in κ and lying in a left subcohort): $I, \kappa, \kappa^2, \kappa^3, \lambda\kappa, \kappa^4, \lambda\kappa^2, \kappa\lambda\kappa, \ldots$.

Section 4.1.6 constructed the array $\vdash$ by gathering compositions $S \in \{\theta, \eta\}^\star$ with the same value of $N_{-1}(S)$ into rows (equivalence classes), and then sorting the columns so that the value of $N_0(S) + 1$ increases along each row. Table 14 showed this array of compositions S, for which the corresponding array of values $N_0(S) + 1$ gave $\vdash$.

In terms of the free monoid on $\{\theta, \eta\}$, a common prefix of entries characterizes the columns of Table 14, with entries in each column $k = 1, 2, 3, \ldots$ sharing the prefix $\theta^{k-1}\circ$. A common suffix of entries characterizes each row of Table 14, with entries in row $n = 0, 1, 2, \ldots$ sharing as suffix the ${\vdash_{n,1}}^{\text{st}}$ element in Table 13, that is, the n^{th} element beginning in η (see Figure 23(i)), or equivalently, the n^{th} element lying in a left subcohort of the tableau (where I counts as the 0^{th} element beginning in θ, and lying in a left subcohort): $I, \eta, \eta\theta, \eta^2, \eta\theta^2, \eta^2\theta, \eta\theta\eta, \eta\theta^3, \ldots$.

By analogy, $\exists$ arises from values $N_0(S)+1$ for an array of compositions $S \in \{\theta,\eta\}^\star$, in which entries of each column $k = 1,2,3,\ldots$ share the prefix $\eta^{k-1}\circ$. Entries in each row $n = 0,1,2,\ldots$ of this array of compositions share as suffix the ${\exists_{n,1}}^{\text{st}}$ element in Table 13, that is, the n^{th} element beginning in θ (see Figure 23(i)), or equivalently, the n^{th} element lying in a right subcohort of the tableau (where I counts as the 0^{th} element beginning in θ, and lying in a right subcohort): $I, \theta, \theta^2, \theta\eta, \theta^3, \theta\eta\theta, \theta^2\eta, \theta^4, \ldots$.

The "cohort-tableau approach" of Section 8.2.2 implicitly enforced the latter restrictions when generating the branch quartet from cohort tableaux of the positive integers. The method transposes right and left subcohorts of the 1–2-Fibonacci tableau to the first columns of $\digamma$ and $\exists$, respectively, while transposing left and right subcohorts of the 2–1-Fibonacci tableau to the first columns of $\vdash$ and $\dashv$, respectively. Thus, via the bijections of Proposition 4.16(b) and Corollary 4.26, the cohort tableau approach implicitly restricts the corresponding compositions in the free monoid, precisely as though the cohort-tableau approach had been applied to the tableaux of compositions in Tables 10 and 13 to obtain Tables 9 and 14, and the bijection subsequently applied to yield the integer arrays $\digamma$ and $\vdash$.

8.4.2. *Free-monoid approach to constructing the clade quartet.* By analogy to the branch quartet, the clade quartet (Table 4) also arises from values $S(2)-1$ for arrays of compositions $S \in \{\kappa,\lambda\}^\star$ (for w and $\mathfrak{w}$) and values $N_0(S)+1$ for arrays of compositions $S \in \{\theta,\eta\}^\star$ (for a and $\mathfrak{a}$) (Figures 25(a)(ii)).

For the array of compositions $S \in \{\kappa,\lambda\}^\star$ that gives rise via $S(2)-1$ to the array of values w, entries of each column $k = 1,2,3,\ldots$ share the prefix $\kappa^{k-1}\circ$. Entries in each row $n = 0,1,2,\ldots$ of this array of compositions share as suffix the ${w_{n,1}}^{\text{st}}$ element in Table 10, that is, the n^{th} element beginning in λ (where I counts as the 0^{th} element beginning in λ) (see Figure 23(iv)), or equivalently for $n \geq 1$, the suffix is $\lambda S'$, where S' is the n^{th} element of the tableau: $I, \lambda, \lambda\kappa, \lambda\kappa^2, \lambda^2, \lambda\kappa^3, \lambda^2\kappa, \lambda\kappa\lambda, \ldots$.

Analogously, $\mathfrak{w}$ arises from values $S(2)-1$ for an array of compositions $S \in \{\kappa,\lambda\}^\star$, in which entries of each column $k = 1,2,3,\ldots$ share the prefix $\lambda^{k-1}\circ$. Entries in each row $n = 0,1,2,\ldots$ of this array of compositions share as suffix the ${\mathfrak{w}_{n,1}}^{\text{st}}$ element in Table 10, that is, the n^{th} element beginning in κ (where I counts as the 0^{th} element beginning in κ) (see Figure 23(iv)), or equivalently for $n \geq 1$, the suffix is $\kappa S'$, where S' is the n^{th} element of the tableau: $I, \kappa, \kappa^2, \kappa^3, \kappa\lambda, \kappa^4, \kappa\lambda\kappa, \kappa^2\lambda, \ldots$.

For the array of compositions $S \in \{\theta,\eta\}^\star$ that gives rise via $N_0(S)+1$ to the array of values a, entries of each column $k = 1,2,3,\ldots$ share the suffix $\circ\theta^{k-1}$. Entries in each row $n = 0,1,2,\ldots$ of this array of compositions share as prefix the ${a_{n,1}}^{\text{st}}$ element in Table 13, that is, the n^{th} element terminating in η (where I counts as the 0^{th} element terminating in η) (see Figure 23(ii)), or equivalently for $n \geq 1$, the prefix is $S'\eta$, where S' is the n^{th} element of the tableau: $I, \eta, \theta\eta, \eta^2, \theta^2\eta, \eta\theta\eta, \theta\eta^2, \theta^3\eta, \ldots$.

Analogously, $\mathfrak{a}$ arises from values $N_0(S)+1$ for an array of compositions $S \in \{\theta,\eta\}^\star$, in which entries of each column $k = 1,2,3,\ldots$ share the suffix $\circ\eta^{k-1}$. Entries in each row $n = 0,1,2,\ldots$ of this array of compositions share as prefix the ${\mathfrak{a}_{n,1}}^{\text{st}}$ element in Table 13, that is, the n^{th} element terminating in θ (where I counts as the 0^{th} element terminating in η) (see Figure 23(ii)), or equivalently for $n \geq 1$, the prefix is $S'\eta$, where S' is the n^{th} element of the tableau: $I, \theta, \theta^2, \eta\theta, \eta\theta^2, \theta\eta\theta, \theta^4, \eta^2\theta, \ldots$.

8.5. **Numeration approach to constructing the quartets.** To describe the eight interspersions of the branch and clade quartets, Tables 3 and 4 indicated

the necessary restrictions on the gaps of positive integers in minimal Fibonacci representation (suffix for $\digamma$ and $\daleth$, and prefix for w and $\mathfrak{w}$), and maximal Fibonacci expansion (suffix for $\vdash$ and $\dashv$, and prefix for a and $\mathfrak{a}$), required to place each positive integer into a *column* of each array. This section completes the description of the arrays by giving the restriction on *rows*.

The "numeration approach" to constructing the quartets (Figure 24(c)(i) & (c)(ii)) follows from the "tree approach," (Figure 24(a)(i) & (a)(ii)) which relates the rows of each array to the collection of all-left or all-right branchings in one of four trees. Figure 16 shows the branching for each of the four trees in one of the two radix notations.

Figures 13 and 14 expand the maximal and minimal Fibonacci trees in the maximal Fibonacci expansion and minimal Fibonacci representation, respectively, showing the self-symmetry of each tree that lends itself to recursive calculation in one of the two numeration systems. The Fibonacci trees expand from each parent node by adding or modifying one term at a time, allowing all-left or all-right branchings to be written as Fibonacci outer cohort sequences.

By contrast, the successor trees do not lend themselves to this type of iterative calculation in the numeration systems. Rather, true to their name, branching in the successor trees shifts all terms in the expansion of the parent node (Figure 16(i) and (ii)). Instead of the Fibonacci indices themselves, therefore, Fibonacci gaps (Figure 17) provide a more convenient way to characterize the array entries in the numeration systems, with reference to either the Fibonacci trees or the successor trees.

8.5.1. *Fibonacci gaps in the branch and clade quartets.* Lemma 6.1 and Proposition 6.3 gave identities for $\sigma^p(n)$ and $\sigma^p_\star(n)$, the iterated successors of n in minimal Fibonacci representation and maximal Fibonacci expansion, respectively (see Remarks 6.4 and 6.6). Lemma 6.7 reformulated these results on Fibonacci successors in terms of Fibonacci gaps, which prove useful to the following results.

Proposition 8.5 (Gaps of the branch quartet)**.** *Gaps for the branch quartet of arrays (Table 3) may be written as follows:*

$$\textbf{1–2-Fibonacci Array:}\quad \boldsymbol{\partial}(\digamma_{n,k}) = \begin{cases} (k+1), & n=0;\\ \boldsymbol{\partial}(n)(k+1), & n>0. \end{cases}$$

$$\textbf{1–2-mirror Array:}\quad \boldsymbol{\partial}(\daleth_{n,k}) = \begin{cases} (2)^k, & n=0;\\ [\boldsymbol{\partial}(n)\text{++}](2)^{k-1}, & n>0. \end{cases}$$

$$\textbf{2–1-Fibonacci Array:}\quad \boldsymbol{\nabla}_\star(\vdash_{n,k}) = \begin{cases} (1)^{k-1}, & n=0;\\ \boldsymbol{\nabla}_\star(n)(2)(1)^{k-1}, & n>0. \end{cases}$$

$$\textbf{2–1-mirror Array:}\quad \boldsymbol{\nabla}_\star(\dashv_{n,k}) = \begin{cases} (2)^{k-1}, & n=0;\\ \boldsymbol{\nabla}_\star(n)(1)(2)^{k-1}, & n>0. \end{cases}$$

Proof of Proposition 8.5: In Section 11 □

Corollary 6.4 related $a_{n,k}$ to maximal Fibonacci Successors. Proposition 7.3 gave maximal Fibonacci gaps for all corner coordinates $a_{n,k}$, $b_{n,k}$, $c_{n,k}$, and $d_{n,k}$ of black squares in the quilt (Figure 1). Proposition 8.6 now characterizes the gaps for the other interspersions of the clade quartet.

Proposition 8.6 (Gaps of the clade quartet)**.** *Gaps for the clade quartet of arrays (Table 4) may be written as follows:*

$$(w)\text{:}\quad \boldsymbol{\partial}(w_{n,k}) = \begin{cases} (k\ +\ 1), & n=0;\\ (k\ +\ 1)\boldsymbol{\partial}(n), & n>0. \end{cases}$$

$$(\mathfrak{w})\text{:}\quad \boldsymbol{\partial}(\mathfrak{w}_{n,k}) = \begin{cases} (2)^k, & n=0;\\ (2)^{k-1}[\boldsymbol{+\!+\partial}(n)] \ = (2)^{k-1}\boldsymbol{\partial}(\kappa(n+1)-1), & n>0; \end{cases}$$

$$(a)\text{:}\ \boldsymbol{\nabla}_\star(a_{n,k}) = \begin{cases} (1)^{k-1}, & n=0;\\ (1)^{k-1}(2)\boldsymbol{\nabla}_\star(n) = (1)^{k-1}\boldsymbol{\nabla}_\star(\lambda(n)+1), & n>0. \end{cases}$$

$$(\mathfrak{a})\text{:}\ \boldsymbol{\nabla}_\star(\mathfrak{a}_{n,k}) = \begin{cases} (2)^{k-1}, & n=0;\\ (2)^{k-1}(1)\boldsymbol{\nabla}_\star(n) = (2)^{k-1}\boldsymbol{\nabla}_\star(\kappa(n)+1), & n>0. \end{cases}$$

Proof of Proposition 8.6: In Section 11 □

The foregoing propositions notated gaps as tuples. Where no confusion exists, gaps can also be notated as words. (Such is always the case with maximal Fibonacci gaps, which, by definition, consist only of 1s and 2s.)

8.5.2. *Numeration approach to constructing the branch quartet (Figure 24(c)(i)).*

Remark 8.4 (Interpretation of Proposition 8.5). For the array ⊦, minimal Fibonacci gaps for entries of each column $k = 1, 2, 3, \ldots$ share the suffix $\bullet(k+1)$. Gaps for entries in each row $n = 0, 1, 2, \ldots$ of ⊦ share as prefix the n^{th} element in Table 25 (where the empty tuple () counts as the 0^{th} element): $\bullet, 2, 3, 4, 22, 5, 23, 32, 6, 24, \ldots$.

For the array ⊣, minimal Fibonacci gaps for entries of each column $k = 2, 3, 4, \ldots$ share the suffix $\bullet 2^{k-1}$. Gaps for entries in each row $n = 0, 1, 2, \ldots$ of ⊣ share as prefix the ${\dashv_{n,1}}^{\text{st}}$ element in Table 25, equivalently for $n \geq 1$, the n^{th} element not terminating in 2 or the n^{th} element lying in a left subcohort of the tableau: $2, 3, 4, 5, 23, 6, 24, 33, 7, 25, \ldots$.

For the array ⊢, maximal Fibonacci gaps for entries of each column $k = 2, 3, 4, \ldots$ share the suffix $\bullet 1^{k-1}$. Entries in each row $n = 0, 1, 2, \ldots$ of ⊢ share as prefix the ${\vdash_{n,1}}^{\text{st}}$ element in Table 22, equivalently for $n \geq 1$, the n^{th} element terminating in 2 or the $n+1^{\text{st}}$ element lying in a left subcohort of the tableau: $\bullet, 2, 12, 22, 112, 122, 212, 1112, 222, 1122, \ldots$.

For the array ⊥, maximal Fibonacci gaps for entries of each column $k = 2, 3, 4, \ldots$ share the suffix $\bullet 2^{k-1}$. Entries in each row $n = 0, 1, 2, \ldots$ of ⊥ share as prefix the ${\perp_{n,1}}^{\text{st}}$ element in Table 22, equivalently for $n \geq 1$, the n^{th} element terminating in 1 or or the n^{th} element lying in a right subcohort of the tableau: $\bullet, 1, 11, 21, 111, 121, 211, 1111, 221, 1121, \ldots$.

8.5.3. *Numeration approach to constructing the clade quartet (Figure 24(c)(ii)).*

Remark 8.5 (Interpretation of Proposition 8.6). For the array w, minimal Fibonacci gaps for entries of each column $k = 1, 2, 3, \ldots$ share the prefix $(k+1)\bullet$. Gaps for entries in each row $n = 0, 1, 2, \ldots$ of ⊦ share as suffix the n^{th} element in Table 25 (where the empty tuple () counts as the 0^{th} element): $\bullet, 2, 3, 4, 22, 5, 23, 32, 6, 24, \ldots$.

For the array $\mathfrak{w}$, minimal Fibonacci gaps for entries of each column $k = 2, 3, 4, \ldots$ share the prefix $2^{k-1}\bullet$. Gaps for entries in each row $n = 0, 1, 2, \ldots$ of $\mathfrak{w}$ share as suffix the ${\mathfrak{w}_{n,1}}^{\text{st}}$ element in Table 25, equivalently the n^{th} element not beginning with 2: $2, 3, 4, 5, 32, 6, 33, 42, 7, 34, \ldots$.

For the array a, maximal Fibonacci gaps for entries of each column $k = 2, 3, 4, \ldots$ share the prefix $1^{k-1}\bullet$. Entries in each row $n = 0, 1, 2, \ldots$ of a share as suffix the ${a_{n,1}}^{\text{st}}$ element in Table 22, equivalently for $n \geq 1$, the n^{th} element beginning in 2: $\bullet, 2, 21, 22, 211, 212, 221, 2111, 222, 2112, \ldots$.

For the array $\mathfrak{o}$, maximal Fibonacci gaps for entries of each column $k = 2, 3, 4, \ldots$ share the prefix $2^{k-1}\bullet$. Entries in each row $n = 0, 1, 2, \ldots$ of $\mathfrak{o}$ share as suffix the $\mathfrak{o}_{n,1}{}^{\text{st}}$ element in Table 22, equivalently for $n \geq 1$, the n^{th} element beginning in 1: $\bullet, 1, 11, 12, 111, 112, 121, 1111, 122, 1112, \ldots$.

8.6. **Tree clade (or suffix) approach to constructing the quartets.**

Remark 8.6 (Introduction and motivation for the tree-clade approach). As its caption describes, Table 11 sequences the equivalence classes of compositions $S \in \{\kappa, \lambda\}^\star$ in such a way that the image $S_n(1)$ of 1 under the n^{th} composition S_n in this sequence gives the positive integer n. Now let $M = \lambda\kappa^{k-1}$ (and substitute κ^{k-1} for the 0^{th} element $\kappa^\star$ of the tableau). Then for the n^{th} composition S_n in the resulting tableau, $S_n(2) - 1 = \mathsf{F}_{n,k}$. That is, besides giving the positive integers in sequence, the tableau can also produce any given column of the array F. Similarly, let $M = \kappa\lambda^{k-1}$ (and substitute λ^{k-1} for the 0^{th} element $\kappa^\star$ of the tableau). Then, $S_n(2) - 1 = \mathsf{\exists}_{n,k}$. Finally, let $M = \begin{cases} \kappa^2\lambda^{\frac{k-1}{2}}, & k \text{ odd}; \\ \lambda\kappa\lambda^{\frac{k-2}{2}}, & k \text{ even}; \end{cases}$ (and substitute $\begin{cases} \lambda^{\frac{k-1}{2}}, & k \text{ odd}; \\ \kappa\lambda^{\frac{k-2}{2}}, & k \text{ even}; \end{cases}$ for the 0^{th} element $\kappa^\star$ of the tableau). Then, $S_n(2) - 1 = \mathsf{L}_{n,k}$.

Thus, using a sequence of compositions from $\{\kappa, \lambda\}^\star$ in the order generated by the cohort calculus of Section 5 and presented in Tables 10 and 11, it is possible to formulate suffixes such that the images of a constant value under the sequence gives the integers, or (one plus) any column of F, $\mathsf{\exists}$, or L. The idea can be simplified and extended to all eight arrays of the branch and clade quartets using the pairs $\{\bar{\boldsymbol{l}}, \bar{\boldsymbol{r}}\}$, $\{\bar{\boldsymbol{L}}, \bar{\boldsymbol{R}}\}$, $\{\boldsymbol{l}, \boldsymbol{r}\}$, and $\{\boldsymbol{L}, \boldsymbol{R}\}$ of tree branching functions, rather than $\{\kappa, \lambda\}$.

In contrast to the tree branch (or prefix) approach of Section 8.3, this section will discuss a self-similarity of the eight arrays of the clade and branch quartets, Corollaries 8.11 and 8.18, respectively, in the form of column–clade isomorphism. Here, a tree partitions into a sequence of clades, each of which corresponds to a different column of the array. This differs from the natural column–array order isomorphisms for F and L previously described in Remarks 4.18 respectively 4.29.

For the column–clade isomorphism, all entries in a given column of the array appear as nodes in the same clade of the tree, and only in that clade. Conversely, the values of all nodes in a given clade of the tree appear in the same column of the array and only in that column.

Moreover, each clade also exhibits a clade–tree order isomorphism. That is, the clade maps to the whole tree (Corollaries 8.10 and 8.17) according to the following procedure: Lookup each node of the clade in the array, find its row index, and substitute this row index for the value of the node itself. The result will be a copy of the whole tree, with its root node grafted to the root of the clade. Figures 26 and 27 illustrate the idea.

Definition 8.1 describes the decomposition of a tree into clades suitable for the order isomorphism, as well as a decomposition into *half-clades* suitable for a second order isomorphism presented in Section 8.6.4. Previously, the paper mentioned "gathering left or right clades" from the Fibonacci trees (Figures 5 and 8) as a means of generating columns of the arrays shown in Table 4, and gathering left or right clades from the successor trees (Figures 3 and 10) as a means of generating

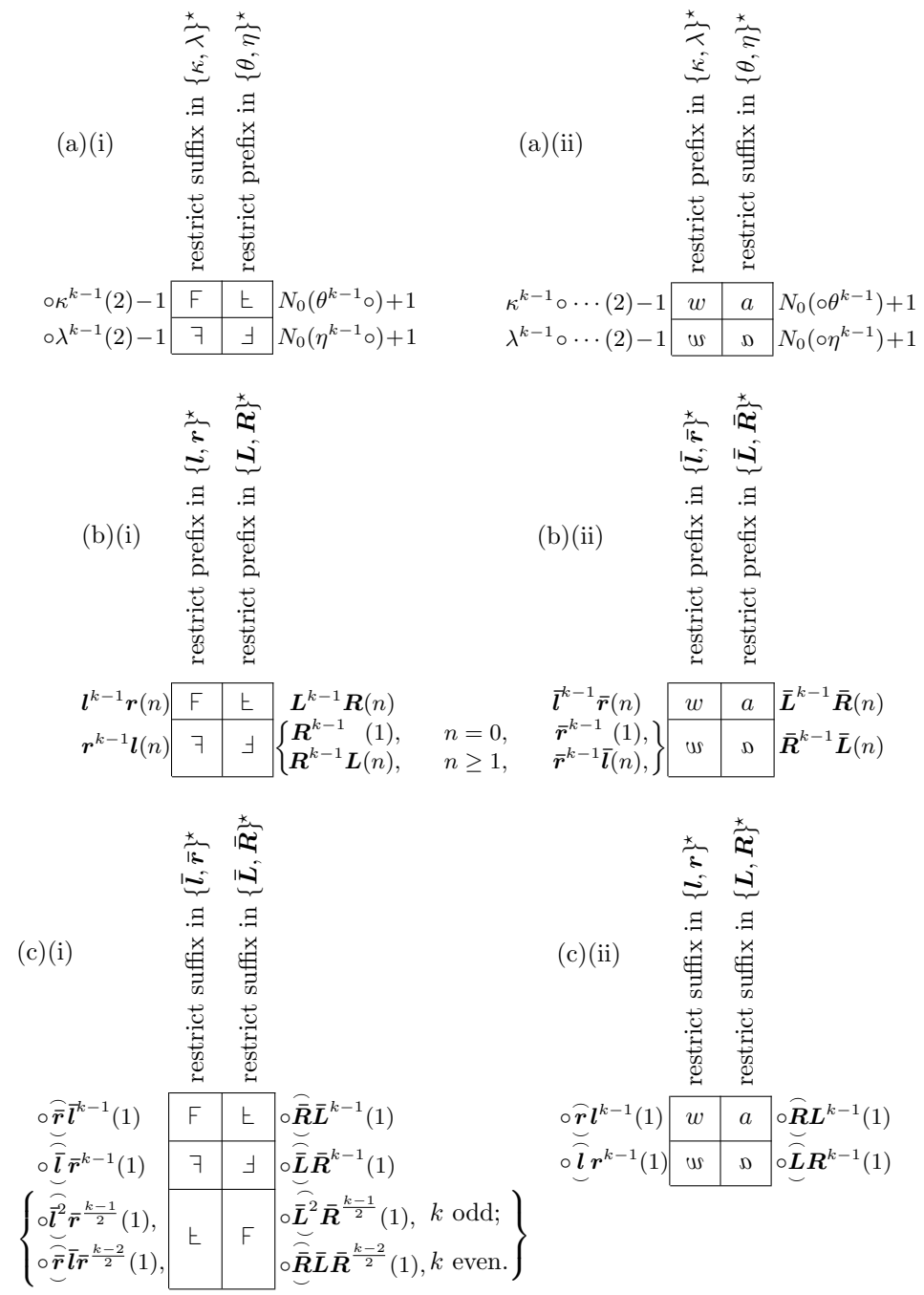

FIGURE 25. "Free-monoid" approaches: At left: (i) Branch quartet (Table 3); At right: (ii) Clade quartet (Table 4). At top: (a) "Clades to columns" Generate column k by restricting Wythoff or Wythoff^{-1} compositions. At middle: (b) "Branches to rows": Generate row n by prefix restriction on compositions of branching functions (Figure 15). At bottom: (c) "Clades to columns": Generate column k by suffix restriction on compositions of branching functions. Functions in rotated parenthesis omitted for row $n = 0$.

columns of the arrays shown in Tables 3. It serves the succeeding discussion to provide a precise definition of left and right clades.

Definition 8.1 (Tree clades and half-clades)**.** Consider that an infinite, regular, single-rooted binary tree has its nodes or vertices (Figure 18) at positions

Tree positions	on level of the tree
2^0	1
$2^1, 2^2-1$	2
$2^2, \ldots, 2^3-1$	3
$\vdots$	$\vdots$
$2^{\ell-1}, \ldots, 2^\ell-1$	ℓ
$\vdots$	$\vdots$

Then for $k = 1, 2, 3, \ldots$, define the k^{th} *left clade* as the subtree comprising

Tree positions	on level *of the clade*
2^k-1	0
$2^{k+1}-2$	1
$2^{k+2}-2^2, 2^{k+2}-2^1-1$	2
$2^{k+3}-2^3, \ldots, 2^{k+3}-2^2-1$	3
$\vdots$	$\vdots$
$2^{k+\ell}-2^\ell, \ldots, 2^{k+\ell}-2^{\ell-1}-1$	ℓ
$\vdots$	$\vdots$

Define the k^{th} *right clade* as the subtree comprising

Tree positions	on level *of the clade*
2^{k-1}	0
2^k+1	1
$2^{k+1}+2^1, 2^{k+1}+2^2-1$	2
$2^{k+2}+2^2, \ldots, 2^{k+2}+2^3-1$	3
$\vdots$	$\vdots$
$2^{k+\ell-1}+2^{\ell-1}, \ldots, 2^{k+\ell-1}+2^\ell-1$	ℓ
$\vdots$	$\vdots$

Finally, define the k^{th} *left half-clade* (Figure 28) as the subtree comprising

For k odd, tree positions	on level *of the half-clade*
$2^{\frac{k+1}{2}}-1$	0
$2^{\frac{k+5}{2}}-4$	1
$2^{\frac{k+7}{2}}-8, 2^{\frac{k+7}{2}}-7$	2
$2^{\frac{k+9}{2}}-16, \ldots, 2^{\frac{k+9}{2}}-13$	3
$\vdots$	$\vdots$
$2^{\frac{k+2\ell+3}{2}}-2^{\ell+1}, \ldots, 2^{\frac{k+2\ell+3}{2}}-3\times 2^{\ell-1}-1$	ℓ
$\vdots$	$\vdots$

For k even, tree positions	on level *of the half-clade*
$2^{\frac{k+2}{2}} - 2$	0
$2^{\frac{k+4}{2}} - 3$	1
$2^{\frac{k+6}{2}} - 6, 2^{\frac{k+6}{2}} - 5$	2
$2^{\frac{k+8}{2}} - 12, \ldots, 2^{\frac{k+8}{2}} - 9$	3
$\vdots$	$\vdots$
$2^{\frac{k+2\ell+2}{2}} - 3 \times 2^{\ell-1}, \ldots, 2^{\frac{k+2\ell+2}{2}} - 2^{\ell} - 1$	ℓ
$\vdots$	$\vdots$

Note the convention here considers the root node of the tree to be on level 1, whereas clades have a 0^{th} level containing their planted root. The inclusion of this root makes the clades only weakly binary overall, though from the 1^{st} level downward, the clades are strongly binary. For k even, the k^{th} left half-clade "resembles" (is isomorphic as an unlabeled tree to) a right clade in this regard, whilst for k odd, the k^{th} half-clade is a disconnected graph comprising an isolated 0^{th} node together with a complete binary tree (see Figure 28). The clade–tree order isomorphisms will ignore the planted root of the clades considering only the strongly binary subtree from level 1 downward. In Proposition 8.20, a half-clade–tree order isomorphism will similarly ignore the 0^{th} node for half-clades, whilst a clade-to-half-clade splitting property will include the 0^{th} nodes when splitting the k^{th} left clade into the $2k - 1^{\text{st}}$ and $2k^{\text{th}}$ left half-clades.

Remark 8.7. Example: Successive left clades of the maximal Fibonacci tree In Figure 8, the 1^{st} left clade comprises the left half of the tree together with the root node 1 at position $\mathbf{P}(1) = 2^1 - 1 = 1$ of the tree. Removing 1 from the tree by pruning this root node together with its left child, the node 2 at position $\mathbf{P}(2) = 2^{1+1} - 2 = 2$, and all descendants of the latter, leaves a subtree, comprising 3, root node of the remaining subtree, at original tree position $\mathbf{P}(3) = 2^2 - 1 = 3$, and all of its descendants.

The 2^{nd} left clade appears as the left half of the resultant subtree, node 6 at position $\mathbf{P}(6) = 2^{2+1} - 2 = 6$ and all its descendants, together with the zeroth node 3 of the clade. . ..

Thus, after pruning the 1^{st},. . .,$k - 1^{\text{st}}$ left clades from the tree, the k^{th} left clade appears as the left half of the remaining subtree together with the root of the remaining subtree (having position $2^k - 1$ in the greater tree).

Corollary 8.11 will identify this sequence of clades with the columns of $\mathfrak{o}$.

Example: Successive right clades of the minimal Fibonacci tree In Figure 5, the 1^{st} right clade comprises the right half of the tree together with the root node 1 at position $\mathbf{p}(1) = 2^{1-1} = 1$ of the tree. Removing 1 from the tree by pruning this root node together with its right child, the node 4 at position $\mathbf{p}(4) = 2^1 + 1 = 3$, and all descendants of the latter, leaves a subtree, comprising 2, root node of the remaining subtree, at original tree position $\mathbf{p}(2) = 2^{2-1} = 2$, and all of its descendants.

The 2^{nd} right clade appears as the right half of the resultant subtree, node 7 at position $\mathbf{P}(7) = 2^2 + 1 = 5$ and all its descendants, together with the zeroth node 2 of the clade. . ..

Thus, after pruning the 1^{st},. . .,$k - 1^{\text{st}}$ right clades from the tree, the k^{th} right clade appears as the right half of the remaining subtree together with the root of the remaining subtree (having position 2^{k-1} in the greater tree).

Corollary 8.11 will identify this sequence of clades with the columns of w.

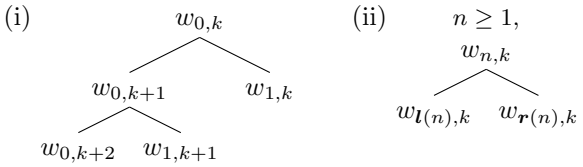

FIGURE 26. Branching diagram for relative position of elements $w_{n,k}$ in Figure 5

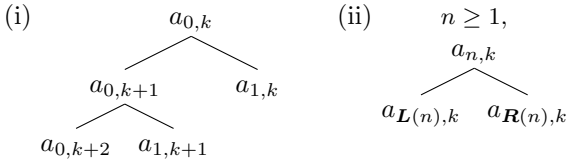

FIGURE 27. Branching diagram for relative position of elements $a_{n,k}$ in Figure 8

8.6.1. *Tree clade (or suffix) approach to constructing the clade quartet.* Consider an array of the clade quartet, Table 4. The successive entries in rows zero, respectively, one of the array appear on levels zero, respectively, one of left or right clades in the minimal or maximal Fibonacci trees (Figures 5 or 8):

Proposition 8.7 (Rows zero and one of the clade quartet arrays and Fibonacci tree branching)**.** *Consider the arrays w, $\mathfrak{w}$, a, and $\mathfrak{a}$ of the clade quartet (Table 4).*

Rows zero and one relate as follows, column $k = 1, 2, 3, \ldots$:

(w): $\boldsymbol{l}(w_{0,k}) = w_{0,k+1}$ *and* $\boldsymbol{r}(w_{0,k}) = w_{1,k}$,
($\mathfrak{w}$): $\boldsymbol{l}(\mathfrak{w}_{0,k}) = \mathfrak{w}_{1,k}$ *and* $\boldsymbol{r}(\mathfrak{w}_{0,k}) = \mathfrak{w}_{0,k+1}$,
(a): $\boldsymbol{L}(a_{0,k}) = a_{0,k+1}$ *and* $\boldsymbol{R}(a_{0,k}) = a_{1,k}$,
($\mathfrak{a}$): $\boldsymbol{L}(\mathfrak{a}_{0,k}) = \mathfrak{a}_{1,k}$ *and* $\boldsymbol{R}(\mathfrak{a}_{0,k}) = \mathfrak{a}_{0,k+1}$.

Proof of (w). (Proofs of ($\mathfrak{w}$), (a), and ($\mathfrak{a}$) are similar). Approach the claims about rows zero and one directly from the formula of Lemma 8.3, and the definition of branching in the respective trees. Figures 15(iii) shows the branching for w and $\mathfrak{w}$, while Figure 15(iv) shows the branching for a and $\mathfrak{a}$.

For the former claim, $\boldsymbol{l}(w_{0,k}) = w_{0,k} + F_{F^{-1}(w_{0,k})-1} = F_{k+1} + F_{F^{-1}(F_{k+1})-1} = F_{k+1} + F_{k+1-1} = F_{k+1} + F_k = F_{k+2} = w_{0,k+1}$.

For the latter claim, $\boldsymbol{r}(w_{0,k}) = w_{0,k} + F_{F^{-1}(w_{0,k})+2} = F_{k+1} + F_{F^{-1}(F_{k+1})+2} = F_{k+1} + F_{k+1+2} = F_{k+1} + F_{k+3} = w_{1,k}$.

For the later two pairs of identities, it is illustrative to consider the expanded Figure 14, which was shown to equal Figure 5 by Lemma 4.13(b). □

Figures 26(i) and 27(i) illustrate Proposition 8.7 for w, respectively, a. Further, Proposition 8.7 suggests that

Rows zero and one of w equal the sequences of nodes at the left, respectively, second from left on each level of Figure 5 (branching diagram, Figure 26(i)).

Rows zero and one of $\mathfrak{w}$ equal the sequences of nodes at the right, respectively, second from right on each level of Figure 5.

Rows zero and one of a equal the sequences of nodes at the left, respectively, second from left on each level of Figure 8 (branching diagram, Figure 27(i)).

Rows zero and one of $\mathfrak{a}$ equal the sequences of nodes at the right, respectively, second from right on each level of Figure 8.

Corollary 8.8 captures this observation formally.

Corollary 8.8 (Fibonacci tree positions for rows zero and one of the clade quartet)**.** *For arrays w, and $\mathfrak{w}$, respectively, a, and $\mathfrak{a}$ rows zero and one can be found in the minimal, respectively, maximal Fibonacci tree at the following positions:*

(w): $\mathbf{p}(w_{0,k}) = 2^{k-1}$ *and* $\mathbf{p}(w_{1,k}) = 2^k + 1$,
$(\mathfrak{w})$: $\mathbf{p}(\mathfrak{w}_{0,k}) = 2^k - 1$ *and* $\mathbf{p}(\mathfrak{w}_{1,k}) = 2^{k+1} - 2$,
(a): $\mathbf{P}(a_{0,k}) = 2^{k-1}$ *and* $\mathbf{P}(a_{1,k}) = 2^k + 1$,
$(\mathfrak{a})$: $\mathbf{P}(\mathfrak{a}_{0,k}) = 2^k - 1$ *and* $\mathbf{P}(\mathfrak{a}_{1,k}) = 2^{k+1} - 2$.

Proof. Consider w, whereas $\mathfrak{w}$, a, and $\mathfrak{a}$ are analogous.

To approach the claims directly, begin at the root of the binary tree with the node $1 = w_{0,1} = \mathfrak{w}_{0,1} = a_{0,1} = \mathfrak{a}_{0,1}$ and combine the results of Proposition 8.7 with the identities (77) or (78) for positions of left and right children, as required, to obtain the position of $w_{0,k}$, $\mathfrak{w}_{0,k}$, $a_{0,k}$, $\mathfrak{a}_{0,k}$, for $k = 2, 3, 4, \ldots$.

Alternatively, approach the claims using Fibonacci gaps. By Proposition 8.6, for $n = 0$, the gaps of $w_{0,k}$ are $\boldsymbol{\partial}(w_{0,k}) = (k + 1)$. Also in terms of gaps, left branching in the minimal Fibonacci tree follows $\boldsymbol{\partial}(\boldsymbol{l}(m)) = \boldsymbol{\partial}(m)\texttt{++}$, as Figure 17(iii) illustrates. Whereas $w_{0,1} = 1$, the root node of the tree, it follows immediately that $w_{0,1}, w_{0,2}, w_{0,3}, \ldots$ corresponds to a sequence of all-left branching in the tree, proving the former claim, that is, $\mathbf{p}(w_{0,k}) = 2^{k-1}$.

Combining this result with (77) or (78), as required, the position $\mathbf{p}(w_{1,k})$ of $w_{1,k}$ then follows by Proposition 8.7, (and similarly for $\mathfrak{w}_{1,k}$, $a_{1,k}$, or $\mathfrak{a}_{1,k}$). □

Proposition 8.9 (Closure under Fibonacci tree branching for columns of arrays in clade quartet)**.** *Columns of w and $\mathfrak{w}$ are closed under the branching functions $\boldsymbol{l}$ and $\boldsymbol{r}$ of the minimal Fibonacci tree and columns of a and $\mathfrak{a}$ are closed under branching functions $\boldsymbol{L}$ and $\boldsymbol{R}$ of the maximal Fibonacci tree.*

In particular, for $n > 0$, columns $k = 1, 2, 3, \ldots$ of the arrays satisfy:

(w): $\boldsymbol{l}(w_{n,k}) = w_{\boldsymbol{l}(n),k}$ *and* $\boldsymbol{r}(w_{n,k}) = w_{\boldsymbol{r}(n),k}$,
$(\mathfrak{w})$: $\boldsymbol{l}(\mathfrak{w}_{n,k}) = \mathfrak{w}_{\boldsymbol{l}(n),k}$ *and* $\boldsymbol{r}(\mathfrak{w}_{n,k}) = \mathfrak{w}_{\boldsymbol{r}(n),k}$,
(a): $\boldsymbol{L}(a_{n,k}) = a_{\boldsymbol{L}(n),k}$ *and* $\boldsymbol{R}(a_{n,k}) = a_{\boldsymbol{R}(n),k}$,
$(\mathfrak{a})$: $\boldsymbol{L}(\mathfrak{a}_{n,k}) = \mathfrak{a}_{\boldsymbol{L}(n),k}$ *and* $\boldsymbol{R}(\mathfrak{a}_{n,k}) = \mathfrak{a}_{\boldsymbol{R}(n),k}$.

Proof of (w). (Proofs of $(\mathfrak{w})$, (a), and $(\mathfrak{a})$ are similar).

Approach the claims about rows $n > 0$ using Fibonacci gaps. By the uniqueness of the minimal Fibonacci representation, it suffices to show equality of the gaps of the left-hand side to the gaps of the right-hand side. Figure 15(iii) illustrates the branching for w and $\mathfrak{w}$.

As shown in the corresponding Figure 17(iii), gaps of the left and right children, $\boldsymbol{l}(n)$ and $\boldsymbol{r}(n)$ of n, respectively, are $\boldsymbol{\partial}(n)\texttt{++}$ and $\boldsymbol{\partial}(n)(2)$, respectively. By Proposition 8.6, for $n > 0$, the gaps of $w_{n,k}$ are $\boldsymbol{\partial}(w_{n,k}) = (k+1)\boldsymbol{\partial}(n)$. Hence, gaps of the left and right children, $\boldsymbol{l}(w_{n,k})$ and $\boldsymbol{r}(w_{n,k})$ of $w_{n,k}$, respectively, are $(k+1)\boldsymbol{\partial}(n)\texttt{++}$ and $(k+1)\boldsymbol{\partial}(n)(2)$, respectively.

In the former case, $\boldsymbol{\partial}(\boldsymbol{l}(w_{n,k})) = \boldsymbol{\partial}(w_{n,k})\texttt{++} = (k+1)\boldsymbol{\partial}(n)\texttt{++} = (k+1)\boldsymbol{\partial}(\boldsymbol{l}(n))$ $= (k+1)\boldsymbol{\partial}(n + F_{F^{-1}(n)-1}) = \boldsymbol{\partial}(w_{n+F_{F^{-1}(n)-1},k}) = \boldsymbol{\partial}(w_{\boldsymbol{l}(n),k})$, thus proving the former claim.

In the latter case, $\boldsymbol{\partial}(\boldsymbol{r}(w_{n,k})) = \boldsymbol{\partial}(w_{n,k})\oplus(2) = (k+1)\boldsymbol{\partial}(n)\oplus(2) = (k+1)\boldsymbol{\partial}(\boldsymbol{r}(n))$ $= (k+1)\boldsymbol{\partial}(n+F_{F^{-1}(n)+2}) = \boldsymbol{\partial}(w_{n+F_{F^{-1}(n)+2},k}) = \boldsymbol{\partial}(w_{\boldsymbol{r}(n),k})$, thus proving the latter claim. □

Figures 26(ii) and 27(ii) illustrate Proposition 8.9 for w, respectively, a.

Now, Corollary 8.8 showed the position $\mathbf{p}(w_{1,k})$ of $w_{1,k}$ in the minimal Fibonacci tree to be $2^k + 1$. Further, Proposition 8.9 implies that the position of $w_{n,k}$ in the tree relative to that of $w_{1,k}$ is the same as the position of n relative to that of 1, as in both cases, the latter node descends from its ancestor via the same sequence of left and right branchings. Hence, the following result.

Corollary 8.10 (Clade–tree order isomorphism for the Fibonacci trees)**.** *Consider the clade quartet arrays $w, \mathfrak{w}, a,$ and $\mathfrak{a}$ (Table 4).*

For $n > 0$, let $\mathbf{p}(n) = 2^{\ell-1}+h$ on level ℓ with horizontal offset $0 \le h < 2^{\ell-1}$. Then, for each $k = 1, 2, 3, \ldots$, the clades $\{w_{n,k}\}_{n>0}$ and $\{\mathfrak{w}_{n,k}\}_{n>0}$ satisfy:

$$(w)\text{:}\quad \mathbf{p}(w_{n,k}) = 2^{k+\ell-1} + 2^{\ell-1} + h,$$
$$(\mathfrak{w})\text{:}\quad \mathbf{p}(\mathfrak{w}_{n,k}) = 2^{k+\ell} \quad - 2^{\ell} \quad + h.$$

For $n > 0$, let $\mathbf{P}(n) = 2^{\ell-1}+h$ on level ℓ with horizontal offset $0 \le h < 2^{\ell-1}$. Then, for each $k = 1, 2, 3, \ldots$, the clades $\{a_{n,k}\}_{n>0}$ and $\{\mathfrak{a}_{n,k}\}_{n>0}$ satisfy:

$$(a)\text{:}\quad \mathbf{P}(a_{n,k}) = 2^{k+\ell-1} + 2^{\ell-1} + h,$$
$$(\mathfrak{a})\text{:}\quad \mathbf{P}(\mathfrak{a}_{n,k}) = 2^{k+\ell} \quad - 2^{\ell} \quad + h.$$

Alternatively, for each $k = 1, 2, 3, \ldots$, the Fibonacci tree positions corresponding to column k of a clade quartet array can be expressed in terms of the position of $n \ge 1$ as:

$$\mathbf{p}(w_{n,k}) = \mathbf{p}(n) + 2^{k+\lfloor \log_2 \mathbf{p}(n) \rfloor}, \tag{94}$$

$$\begin{aligned}\mathbf{p}(\mathfrak{w}_{n,k}) &= \mathbf{p}(n) + 2^{k+\lfloor \log_2 \mathbf{p}(n) \rfloor + 1} - 3 \times 2^{\lfloor \log_2 \mathbf{p}(n) \rfloor}, \\ &= \mathbf{p}(n) + (2^{k+1} - 3)2^{\lfloor \log_2 \mathbf{p}(n) \rfloor}, \text{ respectively,}\end{aligned} \tag{95}$$

$$\mathbf{P}(a_{n,k}) = \mathbf{P}(n) + 2^{k+\lfloor \log_2 \mathbf{P}(n) \rfloor}, \tag{96}$$

$$\begin{aligned}\mathbf{P}(\mathfrak{a}_{n,k}) &= \mathbf{P}(n) + 2^{k+\lfloor \log_2 \mathbf{P}(n) \rfloor + 1} - 3 \times 2^{\lfloor \log_2 \mathbf{P}(n) \rfloor}, \\ &= \mathbf{P}(n) + (2^{k+1} - 3)2^{\lfloor \log_2 \mathbf{P}(n) \rfloor}.\end{aligned} \tag{97}$$

Proof of levels $n > 1$ (Corollary 8.8 treated level $n = 1$.) For the remaining levels $n > 1$ of the k^{th} clade, begin at level one with $w_{1,k}$, $\mathfrak{w}_{1,k}$, $a_{1,k}$, or $\mathfrak{a}_{1,k}$. Next, combine the results of Proposition 8.9 with (77) or (78), as required, to show the remaining levels by induction on n.

Considering the case of (w) (whereas the others are analogous) and taking $n > 0$ and $k = 1, 2, 3, \ldots$, suppose that the claim is true through level ℓ and proceed by induction to level $\ell+1$. That is, suppose that for any integer m in position $\mathbf{p}(m) = 2^{\ell-1}+h$ for $0 \le h < 2^{\ell-1}$ on level ℓ of the tree, we have $\mathbf{p}(w_{m,k}) = 2^{k+\ell-1}+2^{\ell-1}+h$.

Now a node with value n at position $\mathbf{p}(n)$ on level $\ell+1$ of the tree must be either the left or right child of some node with value m at position $\mathbf{p}(m)$ on level ℓ of the tree. That is, either $\mathbf{p}(n) = \mathbf{p}(\boldsymbol{l}(m)) = 2\mathbf{p}(m)$ or $\mathbf{p}(n) = \mathbf{p}(\boldsymbol{r}(m)) = 2\mathbf{p}(m) + 1$. Now, the former case gives $\mathbf{p}(n) = 2^{\ell} + 2h$ with $0 \le 2h \le 2^{\ell} - 2 < 2^{\ell} - 1$, whereas the latter case gives $\mathbf{p}(n) = 2^{\ell} + 2h + 1$ with $0 < 1 \le 2h + 1 \le 2^{\ell} - 1 < 2^{\ell}$. This

makes it possible to write that $\mathbf{p}(n) = 2^\ell + h'$ with $0 \leq h' < 2^\ell$, where either $h' = 2h$ or $h' = 2h + 1$.

Now the hypothesis gives a node with value $w_{m,k}$ at position $\mathbf{p}(w_{m,k}) = 2^{k+\ell-1} + 2^{\ell-1} + h$ on level $\ell + k$ of the tree. Thus its children are $\boldsymbol{l}(w_{m,k})$ and $\boldsymbol{r}(w_{m,k})$ on level $\ell + k + 1$ of the tree at respective positions $\mathbf{p}(\boldsymbol{l}(w_{m,k})) = 2^{k+\ell} + 2^\ell + 2h = \mathbf{p}(\boldsymbol{l}(m)) + 2^{k+\ell}$ and $\mathbf{p}(\boldsymbol{r}(w_{m,k})) = 2^{k+\ell} + 2^\ell + 2h + 1 = \mathbf{p}(\boldsymbol{r}(m)) + 2^{k+\ell}$. Here again, it is possible to write that a child of $w_{m,k}$ has position $2^{k+\ell} + 2^\ell + h'$, where either $h' = 2h$ or $h' = 2h + 1$ and $0 \leq h' < 2^\ell$.

Now using Proposition 8.9, note that $\boldsymbol{l}(w_{m,k}) = w_{\boldsymbol{l}(m),k}$ and $\boldsymbol{r}(w_{m,k}) = w_{\boldsymbol{r}(m),k}$. Consequently, in the case $n = \boldsymbol{l}(m)$, this gives $w_{n,k} = w_{\boldsymbol{l}(m),k}$ and thus $\mathbf{p}(w_{n,k}) = \mathbf{p}(w_{\boldsymbol{l}(m),k}) = \mathbf{p}(\boldsymbol{l}(w_{m,k})) = \mathbf{p}(\boldsymbol{l}(m)) + 2^{k+\ell} = \mathbf{p}(n) + 2^{k+\ell}$, as desired. Similarly, in the case $n = \boldsymbol{r}(m)$, this gives $w_{n,k} = w_{\boldsymbol{r}(m),k}$ and thus $\mathbf{p}(w_{n,k}) = \mathbf{p}(w_{\boldsymbol{r}(m),k}) = \mathbf{p}(\boldsymbol{r}(w_{m,k})) = \mathbf{p}(\boldsymbol{r}(m)) + 2^{k+\ell} = \mathbf{p}(n) + 2^{k+\ell}$, as desired. □

Remark 8.8. Examine the foregoing results. Consider that for $n \geq 0, k \geq 1$, entries of $a_{n,k}$, respectively, $\mathfrak{w}_{n,k}$ are found within the maximal Fibonacci tree in the same positions at which the corresponding entries of $w_{n,k}$, respectively, $\mathfrak{w}_{n,k}$ are found within the tree's cohort dual, the minimal Fibonacci tree, Figure 5.

Corollary 8.8 showed that node zero of the k^{th} right clade of the minimal Fibonacci tree (at position 2^{k-1}) has value $w_{0,k}$ and node 1 at position $2^k + 1$ has value $w_{1,k}$, whereas Proposition 8.9 showed that the collection $\{w_{n,k}\}_{n>0}$ of the $n = 1^{\text{st}}$ and subsequent entries of any column k of w are closed under the functions $\boldsymbol{l}$ and $\boldsymbol{r}$, the latter being injections from $\{w_{n,k}\}_{n>0}$ to $\{w_{n,k}\}_{n>0}$ for each k. Thus if $m = w_{n,k}$ (or $m = \mathfrak{w}_{n,k}$) for $n > 0$, then $\boldsymbol{l}(m)$ and $\boldsymbol{r}(m)$ lie in the same right (left) clade of the tree.

Conversely, given branching functions $\boldsymbol{l}$ and $\boldsymbol{r}$ of the minimal Fibonacci tree, Corollary 8.10 implies that $\forall w_{n,k}, \exists S \in \{\boldsymbol{l}, \boldsymbol{r}\}^\star$ such that $S(w_{1,k}) = w_{n,k}$, where $\mathbf{p}(w_{1,k}) = 2^k + 1$ by Corollary 8.8. Consequently, all entries in the k^{th} column of w appear in the k^{th} right clade of the minimal Fibonacci tree and vice versa.

For the same S, moreover, the Corollary implies that $S(1) = n$, and effectively demonstrates an order isomorphism between (the 1^{st} and subsequent levels of) the k^{th} right (left) clade and the full tree. That is, each right (left) clade "straightens" into a column of one of the clade quartet arrays via the same rearrangement of the full tree that enumerates the positive integers in sequence.

Consider the restriction on the prefix of Fibonacci gaps associated with a column of a clade quartet array. Table 4 shows these restrictions. The aforementioned clade–tree order isomorphism also preserves the gap prefix restriction present in node 1 of the clade when branching from it. For example, consider w, for which Proposition 8.6 gives $\boldsymbol{\partial}(w_{n,k}) = (k+1)\boldsymbol{\partial}(n)$. Start at level zero of any right clade of the minimal Fibonacci tree. Using Proposition 8.7, the node with gaps $\boldsymbol{\partial}(w_{0,k}) = (k+1)$ begets left and right children with gaps $\boldsymbol{\partial}(w_{0,k+1}) = (k+2)$ and $\boldsymbol{\partial}(w_{1,k}) = (k+1, 2)$, respectively.

In particular, consider the first right clade $k = 1$ and continue down the remainder of the clade. Using Proposition 8.9, obtain $\boldsymbol{\partial}(\boldsymbol{r}(w_{0,k})) = \boldsymbol{\partial}(w_{0,k}) \oplus (2) = (k+1, 2) = (2, 2)$ for level one of the clade. Now, for level two of the clade, obtain the pair $\boldsymbol{\partial}(\boldsymbol{l}(\boldsymbol{r}(w_{0,k}))) = (2,2)\texttt{++} = (2,3)$ and $\boldsymbol{\partial}(\boldsymbol{r}(\boldsymbol{r}(w_{0,k}))) = (2,2) \oplus (2) = (2,2,2)$.

Continue this branching and observe the resulting gaps. It shows that the first right clade of the minimal Fibonacci tree contains only elements in the first column w_1 of $w_{n,k}$, whereas for its 0^{th} level $\boldsymbol{\partial}(w_{0,1}) = \boldsymbol{\partial}(1) = (2)$, for its 1^{st} level $\boldsymbol{\partial}(\boldsymbol{r}(w_{0,1})) = (2) \oplus (2) = (2,2)$, and for its 2^{nd} level $(\boldsymbol{\partial}(\boldsymbol{l}(\boldsymbol{r}(w_{0,1}))), \boldsymbol{\partial}(\boldsymbol{r}(\boldsymbol{r}(w_{0,1}))) = ((2,3),(2,2,2))$. Whereas further branching either increments the last element of the gaps or pushes a new last element onto the end, for succeeding levels of the 1^{st} clade, gaps always begin with $\partial_1 = 2$. Since $\boldsymbol{\partial}(w_{n,k}) = (k+1)\boldsymbol{\partial}(n)$, the first right clade contains only elements $w_{n,1}$ of the 1^{st} column of w.

This reasoning, together with the foregoing results, leads to the following conclusion.

Corollary 8.11 (Column–clade isomorphism between the clade quartet and Fibonacci trees)**.** *Consider the clade quartet arrays $w, \mathfrak{w}, a,$ and $\mathfrak{a}$ (Table 4). For columns $k = 1, 2, 3, \ldots$:*

(w): *The k^{th} column w_k and k^{th} right clade of the minimal Fibonacci tree contain exactly the same entries.*

($\mathfrak{w}$): *The k^{th} column $\mathfrak{w}_k$ and k^{th} left clade of the minimal Fibonacci tree contain exactly the same entries.*

(a): *The k^{th} column a_k and k^{th} right clade of the maximal Fibonacci tree contain exactly the same entries.*

($\mathfrak{a}$): *The k^{th} column $\mathfrak{a}_k$ and k^{th} left clade of the maximal Fibonacci tree contain exactly the same entries.*

Proof. Approach the claims using Fibonacci gaps as described above. This approach suffices, given the uniqueness of the minimal Fibonacci representation and the maximal Fibonacci expansion.

Consider the formulas for gaps of the clade quartet given in Proposition 8.6. For w and $\mathfrak{w}$, respectively, a and $\mathfrak{a}$, Figures 15(iii), respectively, (iv) illustrate the tree branching in terms of these gaps.

The remainder of the exposition is for w, though the reasoning is analogous for the other four arrays.

Consider the succession of left children $\boldsymbol{l}^{k-1}(w_{0,1})$ (Figure 26(i)) and observe for the k^{th} right clade of the minimal Fibonacci tree, that level zero comprises $w_{0,k}$. Corollary 8.8 gives $\mathbf{p}(w_{0,k}) = 2^{k-1}$. Further, consider that level one of the k^{th} right clade comprises $w_{1,k}$, for which Corollary 8.8 gives $\mathbf{p}(w_{1,k}) = 2^k + 1$.

To recap, the 0^{th} level of the clade consists of $w_{0,k}$, the 1^{st} level consists of $w_{1,k}$, the 2^{nd} level consists of the pair with gaps $(\boldsymbol{\partial}(\boldsymbol{l}(w_{1,k})),\ \boldsymbol{\partial}(\boldsymbol{r}(w_{1,k}))) = (\boldsymbol{\partial}(w_{1,k})\mathbf{{+}{+}},\ \boldsymbol{\partial}(w_{1,k}) \oplus (2)) = ((k+1)\boldsymbol{\partial}(n)\mathbf{{+}{+}},\ (k+1)\boldsymbol{\partial}(n) \oplus (2))$, and so forth. Further branching either increments the last element of the gaps or pushes a new last element onto the end. Thus, for succeeding levels of the clade, gaps always begin with prefix $\partial_1 = k+1$. Since $\boldsymbol{\partial}(w_{n,k}) = (k+1)\boldsymbol{\partial}(n)$, the k^{th} right clade contains only elements $w_{n,k}$ of the k^{th} column of w.

Now since the above holds for all $k \in \mathbb{Z}_+$, and since both the array w and the minimal Fibonacci tree arrange $\mathbb{Z}_+$, by pigeonhole principle, the k^{th} right clade contains *all* entries $w_{n,k}$ of the k^{th} column of w, and no entry $w_{n,h}$ of any other column $h \neq k$ of w. Conversely, column k of w contains all nodal values in the k^{th} right clade of the minimal Fibonacci tree and no nodal value from any other right clade in the tree. □

(i)

W_0							
W_1							
$\boldsymbol{l}\ W_1$							
$\boldsymbol{l}^2W_1$	$\boldsymbol{r}W_1$						
$\boldsymbol{l}^3W_1$	$\boldsymbol{l}\ \boldsymbol{r}W_1$	$\boldsymbol{rl}W_1$					
$\boldsymbol{l}^4W_1$	$\boldsymbol{l}^2\boldsymbol{r}W_1$	$\boldsymbol{l}\ \boldsymbol{rl}W_1$	$\boldsymbol{rl}^2W_1$	$\boldsymbol{r}^2W_1$			
$\boldsymbol{l}^5W_1$	$\boldsymbol{l}^3\boldsymbol{r}W_1$	$\boldsymbol{l}^2\boldsymbol{rl}W_1$	$\boldsymbol{lrl}^2W_1$	$\boldsymbol{lr}^2W_1$	$\boldsymbol{rl}^3W_1$	$\boldsymbol{rlr}W_1$	$\boldsymbol{r}^2\boldsymbol{l}W_1$
$\vdots$	$\vdots$	$\vdots$	$\vdots$	$\vdots$	$\vdots$	$\vdots$	$\vdots$

(ii)

							A_0
							A_1
							$\boldsymbol{L}\ A_1$
						$\boldsymbol{R}A_1$	$\boldsymbol{L}^2A_1$
					$\boldsymbol{RL}A_1$	$\boldsymbol{L}\ \boldsymbol{R}A_1$	$\boldsymbol{L}^3A_1$
				$\boldsymbol{R}^2A_1$	$\boldsymbol{RL}^2A_1$	$\boldsymbol{L}\ \boldsymbol{RL}A_1$	$\boldsymbol{L}^2\boldsymbol{R}A_1$	$\boldsymbol{L}^4A_1$
$\boldsymbol{R}^2\boldsymbol{L}A_1$	$\boldsymbol{RLR}A_1$	$\boldsymbol{RL}^3A_1$	$\boldsymbol{LR}^2A_1$	$\boldsymbol{LRL}^2A_1$	$\boldsymbol{L}^2\boldsymbol{RL}A_1$	$\boldsymbol{L}^3\boldsymbol{R}A_1$	$\boldsymbol{L}^5A_1$
$\vdots$	$\vdots$	$\vdots$	$\vdots$	$\vdots$	$\vdots$	$\vdots$	$\vdots$

TABLE 32. (i): Branching sequences in the minimal Fibonacci tree, ordered as a 1–2-Fibonacci outer cohort tableau (by prefix). Setting $W_0 = 0$ and $W_1 = 1$, the tableau lists the nonnegative integers (Lemma 6.10(i)). Setting $W_0 = \boldsymbol{l}^{k-1}(1)$ and $W_1 = \boldsymbol{rl}^{k-1}(1)$, the tableau lists entries in column k of w. Setting $W_0 = \boldsymbol{r}^{k-1}(1)$ and $W_1 = \boldsymbol{lr}^{k-1}(1)$, the tableau lists entries in column k of $\mathfrak{w}$. (ii): Branching sequences in the maximal Fibonacci tree, ordered as a 2–1-Fibonacci outer cohort tableau (by prefix). Setting $A_0 = 0$ and $A_1 = 1$, the tableau lists the nonnegative integers (Lemma 6.10(ii)). Setting $A_0 = \boldsymbol{L}^{k-1}(1)$ and $A_1 = \boldsymbol{RL}^{k-1}(1)$, the tableau lists entries in column k of a. Setting $A_0 = \boldsymbol{R}^{k-1}(1)$ and $A_1 = \boldsymbol{LR}^{k-1}(1)$, the tableau lists entries in column k of $\mathfrak{a}$. See Table 25(c)(ii)

Example 8.1 (Array row indices for first few clade levels)**.** Jointly, Corollaries 8.10 and 8.11 say that

Column k of array w is isomorphic to the k^{th} right clade of the minimal Fibonacci tree which is order isomorphic, in turn, to the entire tree (array). For $k = 1, 2, \ldots, K \ldots$, the complete subtree descending from $w_{1,k}$ is isomorphic to the entire tree, in the following sense. For $k = 1, 2, 3, \ldots$, Corollary 8.8 gives that $\boldsymbol{p}(w_{1,k}) = 2^{k-1} + 1$ contains the first degree-three node in the k^{th} right clade. For all $n > 0$, if $F_t \leq n < F_{t+1}$, then the left and right children of $w_{n,k}$ are $w_{n+F_{t-1},k}$, respectively, $w_{n+F_{t+2},k}$.

That is, the first level of the clade comprises $w_{1,k}$, the second $w_{2,k}$, $w_{4,k}$, the third, $w_{3,k}$, $w_{7,k}$, $w_{6,k}$, $w_{12,k}$, and so forth (Branching Diagram, Figure 26(ii)).

Column k of array $\mathfrak{w}$ is isomorphic to the k^{th} left clade of the minimal Fibonacci tree which is order isomorphic, in turn, to the entire tree (array). For $k = 1, 2, \ldots, K \ldots$, the complete subtree descending from $\mathfrak{w}_{1,k}$ is isomorphic to the entire tree, in the

following sense. For all $n > 0$, if $F_t \leq n < F_{t+1}$, then the left and right children of $\mathfrak{w}_{n,k}$ are $\mathfrak{w}_{n+F_{t-1},k}$, respectively, $\mathfrak{w}_{n+F_{t+2},k}$.

That is, the first level of the clade comprises $\mathfrak{w}_{1,k}$, the second $\mathfrak{w}_{2,k}$, $\mathfrak{w}_{4,k}$, the third, $\mathfrak{w}_{3,k}$, $\mathfrak{w}_{7,k}$, $\mathfrak{w}_{6,k}$, $\mathfrak{w}_{12,k}$, and so forth.

Column k of array a is isomorphic to the k^{th} right clade of the maximal Fibonacci tree which is order isomorphic, in turn, to the entire tree (array). For $k = 1, 2, \ldots, K \ldots$, the complete subtree descending from $a_{1,k}$ is isomorphic to the entire tree, in the following sense. For all $n > 0$, if $F_t \leq n < F_{t+1}$, then the left and right children of $a_{n,k}$ are $a_{n+F_t,k}$, respectively, $a_{n+F_{t+1},k}$.

That is, the first level of the clade comprises $a_{1,k}$, the second $a_{2,k}$, $a_{3,k}$, the third, $a_{4,k}$, $a_{5,k}$, $a_{6,k}$, $a_{8,k}$, and so forth (Branching Diagram, Figure 27(ii)).

Column k of array $\mathfrak{v}$ is isomorphic to the k^{th} left clade of the maximal Fibonacci tree which is order isomorphic, in turn, to the entire tree (array). For $k = 1, 2, \ldots, K \ldots$, the complete subtree descending from $\mathfrak{v}_{1,k}$ is isomorphic to the entire tree, in the following sense. For all $n > 0$, if $F_t \leq n < F_{t+1}$, then the left and right children of $\mathfrak{v}_{n,k}$ are $\mathfrak{v}_{n+F_t,k}$, respectively, $\mathfrak{v}_{n+F_{t+1},k}$.

That is, the first level of the clade comprises $\mathfrak{v}_{1,k}$, the second $\mathfrak{v}_{2,k}$, $\mathfrak{v}_{3,k}$, the third, $\mathfrak{v}_{4,k}$, $\mathfrak{v}_{5,k}$, $\mathfrak{v}_{6,k}$, $\mathfrak{v}_{8,k}$, and so forth.

Remark 8.9 (Fibonacci outer cohort tableaux of $\{\boldsymbol{l}, \boldsymbol{r}\}^\star$ and $\{\boldsymbol{L}, \boldsymbol{R}\}^\star$ (Tables 32)). Recall from Corollary 8.10 that $\forall w_{n,k}, \exists S \in \{\boldsymbol{l}, \boldsymbol{r}\}^\star$ such that $S(w_{1,k}) = w_{n,k}$, and $S(1) = n$. Further, the Corollary gives that $\forall \mathfrak{w}_{n,k}, \exists S \in \{\boldsymbol{l}, \boldsymbol{r}\}^\star$ such that $S(\mathfrak{w}_{1,k}) = \mathfrak{w}_{n,k}$ and that $S(1) = n$. Proposition 8.9 and Corollary 8.10 imply that the two compositions S are identical and Table 32(i) provides a partial listing of the $S \in \{\boldsymbol{l}, \boldsymbol{r}\}^\star$, ordered in 1–2-Fibonacci cohort sequence from the 1^{st} cohort (with a 0^{th} cohort added as well). More precisely, the cohorts of this sequence obtain recursively via the 1–2-Fibonacci outer cohortizer $C_t = \boldsymbol{l}(C_{t-1})\boldsymbol{r}(C_{t-2})$ as described in Lemma 6.10(i).

Moreover, the table includes a 0^{th} element that can be set to $w_{0,k}$, $\mathfrak{w}_{0,k}$, or 0, as required to complete a 1–2-Fibonacci cohort sequence from the 0^{th} cohort of $(w_{n,k})_{n=0,1,2,\ldots}$, $(\mathfrak{w}_{n,k})_{n=0,1,2,\ldots}$, or $(n)_{n=0,1,2,\ldots}$, respectively.

Similarly, Table 32(ii) provides a partial listing of functions $T \in \{\boldsymbol{L}, \boldsymbol{R}\}^\star$ such that $T(a_{1,k}) = a_{n,k}$, $T(\mathfrak{v}_{1,k}) = \mathfrak{v}_{n,k}$, and $T(1) = n$. The functions are ordered in 2–1-Fibonacci cohort sequence from the 1^{st} cohort. That is, the cohorts of this sequence obtain recursively via the 2–1-Fibonacci outer cohortizer $D_t = \boldsymbol{R}(D_{t-2})\boldsymbol{L}(D_{t-1})$ as described in Lemma 6.10(ii).

Moreover, the table includes a 0^{th} element that can be set to $a_{0,k}$, $\mathfrak{v}_{0,k}$, or 0, as required to form a 2–1-Fibonacci cohort sequence from the 0^{th} cohort of $(a_{n,k})_{n=0,1,2,\ldots}$, $(\mathfrak{v}_{n,k})_{n=0,1,2,\ldots}$, or $(n)_{n=0,1,2,\ldots}$, respectively.

As a further curiosity, setting $W_1 = 0$ in the former table (and ignoring the 0^{th} element W_0) yields the sequence 0, 1, 2, 1, 3, 2, 4, 5, 3, 6, 7, 4, 8, 5, 9, 10, 6, 11, 7, 12 ..., or 026272 with a zero prepended, having 1–2-Fibonacci cohort structure $\boldsymbol{l}(C_{t-1}) \oplus \boldsymbol{r}(C_{t-2})$, taking $\boldsymbol{l}(0) \equiv \boldsymbol{r}(0) \equiv 1$. Analogously, setting $A_1 = 0$ in the latter table (and ignoring the 0^{th} element A_0) yields the para-Fibonacci sequence 0, 0, 1, 0, 1, 2, 0, 3, 1, 2, 4, 0, 3, 5, 1, 6, 2, 4, 7, 0 ... that has a 2–1-Fibonacci cohort structure and gives the row of $a_{n,k}$ containing each positive integer, as Section 8.2.3 described.

Contrast the description of the clade quartet arrays given here with that given in Section 8.3.2 by comparing Figures 25(b)(ii) and (c)(ii).

8.6.2. *Additional structure of the clade quartet arrays.*

Proposition 8.12 (Additional structure of the clade quartet arrays)**.** *For $n > 0$, $k = 1, 2, 3, \ldots$,*

As a counterpart to Proposition 8.9:

(w): $\boldsymbol{R}(w_{n,k}) = w_{\boldsymbol{R}(n),k}$ *and* $w_{\boldsymbol{L}(n)-1,k} = w_{n-1,k} + F_{F^{-1}(n)+k+1}$,

(a): $\boldsymbol{r}(a_{n,k}) = a_{\boldsymbol{r}(n),k}$ *and* $a_{\boldsymbol{l}(n)+1,k} = a_{n+1,k} + F_{F^{-1}(n)+k}$,

Proof. For w, the first property requires that $0 = w_{\boldsymbol{R}(n),k} - \boldsymbol{R}(w_{n,k}) = w_{n+F_{F^{-1}(n)+1},k} - w_{n,k} - F_{F^{-1}(w_{n,k})+1} = w_{n+F_{F^{-1}(n)+1},k} - w_{n,k} - F_{F^{-1}(n)+k+2} = F_{k+1}[\kappa(n+1+F_{F^{-1}(n)+1}) - \kappa(n+1)] + F_k(F_{F^{-1}(n)+1}) - F_{F^{-1}(n)+k+2}$, where the last equality uses the cohort-based formula for $w_{n,k}$ and the penultimate equality is due to Proposition 6.18. Next observe that by Bunder and Tognetti [7] and / or Fraenkel, Mushkin, and Tassa [17], that $\kappa(n+1+F_{F^{-1}(n)+1}) - \kappa(n+1) = F_{F^{-1}(n)+2}$, so that it suffices to have $F_{k+1}F_{F^{-1}(n)+2} + F_kF_{F^{-1}(n)+1} = F_{F^{-1}(n)+k+2}$. The latter equality holds by a known identity of Fibonacci numbers.

For w, the second property requires that $0 = w_{\boldsymbol{L}(n)-1,k} - w_{n-1,k} - F_{F^{-1}(n)+k+1} = w_{n-1+F_{F^{-1}(n)},k} - w_{n-1,k} - F_{F^{-1}(n)+k+1} = F_{k+1}[\kappa(n-1+F_{F^{-1}(n)}) - \kappa(n-1)] + F_kF_{F^{-1}(n)} - F_{F^{-1}(n)+k+1}$, where the last equality uses the cohort-based formula for $w_{n,k}$ and the penultimate equality is due to Proposition 6.18. Next observe that by Bunder and Tognetti and / or Fraenkel, Mushkin, and Tassa, that $\kappa(n-1+F_{F^{-1}(n)}) - \kappa(n-1) = F_{F^{-1}(n)+1}$ for $n \geq 2$, so that it suffices to have $F_{k+1}F_{F^{-1}(n)+1} + F_kF_{F^{-1}(n)} = F_{F^{-1}(n)+k+1}$. The latter equality holds by a known identity of Fibonacci numbers. Finally, for $n = 1$, show the property by directly evaluating $w_{\boldsymbol{L}(1)-1,k} - w_{0,k} - F_{F^{-1}(1)+k+1} = w_{1,k} - w_{0,k} - F_{k+3} = F_{k+1}[\kappa(2) - \kappa(1)] + F_k - F_{k+3} = 2F_{k+1} + F_k - F_{k+3} = 0$.

For a, the first property requires that $0 = a_{\boldsymbol{r}(n),k} - \boldsymbol{r}(a_{n,k}) = a_{n+F_{F^{-1}(n)+2},k} - a_{n,k} - F_{F^{-1}(a_{n,k})+2} = a_{n+F_{F^{-1}(n)+2},k} - a_{n,k} - F_{F^{-1}(n)+k+3} = F_{k+1}[\kappa(n+F_{F^{-1}(n)+2}) - \kappa(n)] + F_kF_{F^{-1}(n)+2} - F_{F^{-1}(n)+k+3}$, where the last equality uses the cohort-based formula for $a_{n,k}$ and the penultimate equality is due to Proposition 6.18. Next observe that by Bunder and Tognetti and / or Fraenkel, Mushkin, and Tassa, that $\kappa(n+F_{F^{-1}(n)+2}) - \kappa(n) = F_{F^{-1}(n)+3}$, so that it suffices to have $F_{k+1}F_{F^{-1}(n)+3} + F_kF_{F^{-1}(n)+2} = F_{F^{-1}(n)+k+3}$. The latter equality holds by a known identity of Fibonacci numbers.

For a, the second property requires that $0 = a_{\boldsymbol{l}(n)+1,k} - a_{n+1,k} - F_{F^{-1}(n)+k} = a_{n+1+F_{F^{-1}(n)-1},k} - a_{n+1,k} - F_{F^{-1}(n)+k} = F_{k+1}[\kappa(n+1+F_{F^{-1}(n)-1}) - \kappa(n+1)] + F_k[F_{F^{-1}(n)-1}] - F_{F^{-1}(n)+k}$, where the last equality uses the cohort-based formula for $a_{n,k}$ and the penultimate equality is due to Proposition 6.18. Next observe that by Bunder and Tognetti and / or Fraenkel, Mushkin, and Tassa, that $\kappa(n+1+F_{F^{-1}(n)-1}) - \kappa(n+1) = F_{F^{-1}(n)}$, so that it suffices to have $F_{k+1}F_{F^{-1}(n)} + F_kF_{F^{-1}(n)-1} = F_{F^{-1}(n)+k}$. The latter equality holds by a known identity of Fibonacci numbers. □

As an example of the first property, consider that $\boldsymbol{r}(a_{1,1}) = a_{\boldsymbol{r}(1),1} = a_{4,1} = 11$, whereas $\boldsymbol{r}(1) = 4$, matching $\boldsymbol{r}(3) = 11$.

Corollary 8.13. *(of Proposition 8.12) For $n > 0$, $k = 1, 2, 3, \ldots$:*

$$w_{n,k} - F_{F^{-1}(w_{n,k})} = w_{n-F_{F^{-1}(n)},k} \tag{98}$$

$$a_{n+1,k} - F_{F^{-1}(a_{n,k})} = a_{n+1-F_{F^{-1}(n)},k} \tag{99}$$

Table 17 gave a 1–2-Fibonacci cohortizer for each column k of $w_{n,k}$ as $\langle F_{t+k}, F_{t+k+2}\rangle$, with first element $w_{1,k} = F_{k+1} + F_{k+3}$. Corollary 8.13 allows the interpretation of each column k of $w_{n,k}$ for $n > 0$ as the sum of two 1–2-Fibonacci cohort sequences, with the sum of cohortizers for these two sequences equal to the aforementioned cohortizer of the sum, analogous to Proposition 4.40. The first sequence, comprising the elements $S_n = w_{n-F_{F^{-1}(n)},k}$, begins with $S_1 = F_{k+1}$, has cohortizer $\langle 0, F_{t+k}\rangle$, and is non-monotonic: Each cohort "starts over again" from F_{k+1}. The second sequence, comprising the elements $S_n = F_{F^{-1}(w_{n,k})}$, begins with $S_1 = F_{k+3}$ and has cohortizer $\langle F_{t+k}, F_{t+k+1}\rangle$; it is nondecreasing.

These additional properties of clade quartet arrays prove material to the "mutual dispersion" property given in (106).

8.6.3. *Tree clade (or suffix) approach to constructing the branch quartet.* In the following, let $\bar{\boldsymbol{l}}(n)$ and $\bar{\boldsymbol{r}}(n)$ denote the left and right children, respectively, of node n in the minimal successor tree (Figure 3) and let $\bar{\boldsymbol{L}}(n)$ and $\bar{\boldsymbol{R}}(n)$ denote the left and right children, respectively, of node n in the maximal successor tree (Figure 10). Let $\bar{\mathbf{p}}(n)$ and $\bar{\mathbf{P}}(n)$ denote the position of node n in the minimal, respectively, maximal successor trees. The following results and their proofs are analogous to those of the previous section.

Proposition 8.14 (Rows zero and one of the branch quartet arrays and successor tree branching)**.** *Consider the arrays* $\mathsf{F}, \mathsf{\exists}, \mathsf{L}, \mathsf{\exists}$ *of the branch quartet (Table 3). Rows zero and one relate as follows, column* $k = 1, 2, 3, \ldots$*:*

(F): $\bar{\boldsymbol{l}}(\mathsf{F}_{0,k}) = \mathsf{F}_{0,k+1}$ *and* $\bar{\boldsymbol{r}}(\mathsf{F}_{0,k}) = \mathsf{F}_{1,k}$,
($\mathsf{\exists}$): $\bar{\boldsymbol{l}}(\mathsf{\exists}_{0,k}) = \mathsf{\exists}_{1,k}$ *and* $\bar{\boldsymbol{r}}(\mathsf{\exists}_{0,k}) = \mathsf{\exists}_{0,k+1}$,
(L): $\bar{\boldsymbol{L}}(\mathsf{L}_{0,k}) = \mathsf{L}_{0,k+1}$ *and* $\bar{\boldsymbol{R}}(\mathsf{L}_{0,k}) = \mathsf{L}_{1,k}$,
($\mathsf{\exists}$): $\bar{\boldsymbol{L}}(\mathsf{\exists}_{0,k}) = \mathsf{\exists}_{1,k}$ *and* $\bar{\boldsymbol{R}}(\mathsf{\exists}_{0,k}) = \mathsf{\exists}_{0,k+1}$.

Corollary 8.15 (Successor tree positions for rows zero and one of the branch quartet)**.** *For arrays* F*, and* $\mathsf{\exists}$*, respectively,* L*, and* $\mathsf{\exists}$ *rows zero and one can be found in the minimal, respectively, maximal successor tree at the following positions:*

(F): $\bar{\mathbf{p}}(\mathsf{F}_{0,k}) = 2^{k-1}$ *and* $\bar{\mathbf{p}}(\mathsf{F}_{1,k}) = 2^k + 1$,
($\mathsf{\exists}$): $\bar{\mathbf{p}}(\mathsf{\exists}_{0,k}) = 2^k - 1$ *and* $\bar{\mathbf{p}}(\mathsf{\exists}_{1,k}) = 2^{k+1} - 2$,
(L): $\bar{\mathbf{P}}(\mathsf{L}_{0,k}) = 2^{k-1}$ *and* $\bar{\mathbf{P}}(\mathsf{L}_{1,k}) = 2^k + 1$,
($\mathsf{\exists}$): $\bar{\mathbf{P}}(\mathsf{\exists}_{0,k}) = 2^k - 1$ *and* $\bar{\mathbf{P}}(\mathsf{\exists}_{1,k}) = 2^{k+1} - 2$.

Proposition 8.16 (Closure under successor tree branching for columns of arrays in branch quartet)**.** *Columns of* F *and* $\mathsf{\exists}$ *are closed under the branching functions* $\bar{\boldsymbol{l}}$ *and* $\bar{\boldsymbol{r}}$ *of the minimal successor tree and columns of* L *and* $\mathsf{\exists}$ *are closed under branching functions* $\bar{\boldsymbol{L}}$ *and* $\bar{\boldsymbol{R}}$ *of the maximal successor tree.*

In particular, for $n > 0$*, columns* $k = 1, 2, 3, \ldots$ *of the arrays satisfy:*

(F): $\bar{\boldsymbol{l}}(\mathsf{F}_{n,k}) = \mathsf{F}_{\bar{\boldsymbol{l}}(n),k}$ *and* $\bar{\boldsymbol{r}}(\mathsf{F}_{n,k}) = \mathsf{F}_{\bar{\boldsymbol{r}}(n),k}$,
($\mathsf{\exists}$): $\bar{\boldsymbol{l}}(\mathsf{\exists}_{n,k}) = \mathsf{\exists}_{\bar{\boldsymbol{l}}(n),k}$ *and* $\bar{\boldsymbol{r}}(\mathsf{\exists}_{n,k}) = \mathsf{\exists}_{\bar{\boldsymbol{r}}(n),k}$,
(L): $\bar{\boldsymbol{L}}(\mathsf{L}_{n,k}) = \mathsf{L}_{\bar{\boldsymbol{L}}(n),k}$ *and* $\bar{\boldsymbol{R}}(\mathsf{L}_{n,k}) = \mathsf{L}_{\bar{\boldsymbol{R}}(n),k}$,
($\mathsf{\exists}$): $\bar{\boldsymbol{L}}(\mathsf{\exists}_{n,k}) = \mathsf{\exists}_{\bar{\boldsymbol{L}}(n),k}$ *and* $\bar{\boldsymbol{R}}(\mathsf{\exists}_{n,k}) = \mathsf{\exists}_{\bar{\boldsymbol{R}}(n),k}$.

Corollary 8.17 (Clade–tree order isomorphisms for the successor trees)**.** *Consider the branch quartet arrays* $\mathsf{F}, \mathsf{\exists}, \mathsf{L}$*, and* $\mathsf{\exists}$ *(Table 3).*

For $n > 0$*, let* $\bar{\mathbf{p}}(n) = 2^{\ell-1} + h$ *on level* ℓ *with horizontal offset* $0 \le h < 2^{\ell-1}$*. Then, for each* $k = 1, 2, 3, \ldots$*, the clades* $\{\mathsf{F}_{n,k}\}_{n>0}$ *and* $\{\mathsf{\exists}_{n,k}\}_{n>0}$ *satisfy:*

(⊢): $\bar{\mathbf{p}}(⊢_{n,k}) = 2^{k+\ell-1} + 2^{\ell-1} + h,$
(⊣): $\bar{\mathbf{p}}(⊣_{n,k}) = 2^{k+\ell} \quad - 2^{\ell} \quad + h.$

For $n > 0$, let $\bar{\mathbf{P}}(n) = 2^{\ell-1} + h$ on level ℓ with horizontal offset $0 \le h < 2^{\ell-1}$. Then, for each $k = 1, 2, 3, \ldots$, the clades $\{⊢_{n,k}\}_{n>0}$ and $\{⊣_{n,k}\}_{n>0}$ satisfy:

(⊢): $\bar{\mathbf{P}}(⊢_{n,k}) = 2^{k+\ell-1} + 2^{\ell-1} + h,$
(⊣): $\bar{\mathbf{P}}(⊣_{n,k}) = 2^{k+\ell} \quad - 2^{\ell} \quad + h.$

Alternatively, for each $k = 1, 2, 3, \ldots$, the successor tree positions for values in column k of a branch quartet array can be expressed in terms of the position of $n \ge 1$ as:

$$\bar{\mathbf{p}}(⊢_{n,k}) = \bar{\mathbf{p}}(n) + 2^{k+\lfloor \log_2 \bar{\mathbf{p}}(n) \rfloor}, \tag{100}$$

$$\begin{aligned} \bar{\mathbf{p}}(⊣_{n,k}) &= \bar{\mathbf{p}}(n) + 2^{k+\lfloor \log_2 \bar{\mathbf{p}}(n) \rfloor + 1} - 3 \times 2^{\lfloor \log_2 \bar{\mathbf{p}}(n) \rfloor}, \\ &= \bar{\mathbf{p}}(n) + (2^{k+1} - 3) 2^{\lfloor \log_2 \bar{\mathbf{p}}(n) \rfloor}, \end{aligned} \tag{101}$$

$$\bar{\mathbf{P}}(⊢_{n,k}) = \bar{\mathbf{P}}(n) + 2^{k+\lfloor \log_2 \bar{\mathbf{P}}(n) \rfloor}, \tag{102}$$

$$\begin{aligned} \bar{\mathbf{P}}(⊣_{n,k}) &= \bar{\mathbf{P}}(n) + 2^{k+\lfloor \log_2 \bar{\mathbf{P}}(n) \rfloor + 1} - 3 \times 2^{\lfloor \log_2 \bar{\mathbf{P}}(n) \rfloor}, \\ &= \bar{\mathbf{P}}(n) + (2^{k+1} - 3) 2^{\lfloor \log_2 \bar{\mathbf{P}}(n) \rfloor}. \end{aligned} \tag{103}$$

Remark 8.10. Examining the foregoing results, consider that for $n \ge 0, k \ge 1$, entries of $⊢_{n,k}$, respectively, $⊣_{n,k}$ are found within the maximal successor tree in the same positions at which the corresponding entries of $⊢_{n,k}$, respectively, $⊣_{n,k}$ are found within the minimal successor tree. Proposition 8.20 will assert, moreover, that entries of column k of $⊢_{n,k}$ are found in the maximal successor tree in the same positions at which entries of column k of $⊢_{n,k}$ are found in the minimal successor tree.

Corollary 8.18 (Column–clade isomorphism between the branch quartet and successor trees)**.** *Consider the clade quartet arrays $⊢, ⊣, ⊢, \text{and } ⊣$ (Table 3). For columns $k = 1, 2, 3, \ldots$:*

(⊢): *The k^{th} column $⊢_k$ and k^{th} right clade of the minimal successor tree contain exactly the same entries.*
(⊣): *The k^{th} column $⊣_k$ and k^{th} left clade of the minimal successor tree contain exactly the same entries.*
(⊢): *The k^{th} column $⊢_k$ and k^{th} right clade of the maximal successor tree contain exactly the same entries.*
(⊣): *The k^{th} column $⊣_k$ and k^{th} left clade of the maximal successor tree contain exactly the same entries.*

Remark 8.11 (Fibonacci inner cohort tableaux of $\{\bar{\boldsymbol{l}}, \bar{\boldsymbol{r}}\}^\star$ and $\{\bar{\boldsymbol{L}}, \bar{\boldsymbol{R}}\}^\star$ (Tables 33)). Proposition 8.16 and Corollary 8.17 provide that $\forall ⊢_{n,k}, \exists S \in \{\bar{\boldsymbol{l}}, \bar{\boldsymbol{r}}\}^\star$ such that $S(⊢_{1,k}) = ⊢_{n,k}$, and $S(1) = n$, and moreover, that $\forall ⊣_{n,k}, \exists S \in \{\bar{\boldsymbol{l}}, \bar{\boldsymbol{r}}\}^\star$ such that $S(⊣_{1,k}) = ⊣_{n,k}$ and that $S(1) = n$. Proposition 8.16 and Corollary 8.17 imply that the two compositions S are identical and Table 33(i) provides a partial listing of the $S \in \{\bar{\boldsymbol{l}}, \bar{\boldsymbol{r}}\}^\star$, ordered in 1–2-Fibonacci cohort sequence from the 1^{st} cohort. That is, the cohorts of this sequence obtain recursively via the 1–2-Fibonacci inner cohortizer $C_t = C_{t-1} \circ \bar{\boldsymbol{l}} \oplus C_{t-2} \circ \bar{\boldsymbol{r}}$.

(i)

F_0							
F_1							
$\bar{\boldsymbol{l}}F_1$							
$\bar{\boldsymbol{l}}^2F_1$	$\bar{\boldsymbol{r}}F_1$						
$\bar{\boldsymbol{l}}^3F_1$	$\bar{\boldsymbol{r}}\bar{\boldsymbol{l}}F_1$	$\bar{\boldsymbol{l}}\bar{\boldsymbol{r}}F_1$					
$\bar{\boldsymbol{l}}^4F_1$	$\bar{\boldsymbol{r}}\bar{\boldsymbol{l}}^2F_1$	$\bar{\boldsymbol{l}}\bar{\boldsymbol{r}}\bar{\boldsymbol{l}}F_1$	$\bar{\boldsymbol{l}}^2\bar{\boldsymbol{r}}F_1$	$\bar{\boldsymbol{r}}^2F_1$			
$\bar{\boldsymbol{l}}^5F_1$	$\bar{\boldsymbol{r}}\bar{\boldsymbol{l}}^3F_1$	$\bar{\boldsymbol{l}}\bar{\boldsymbol{r}}\bar{\boldsymbol{l}}^2F_1$	$\bar{\boldsymbol{l}}^2\bar{\boldsymbol{r}}\bar{\boldsymbol{l}}F_1$	$\bar{\boldsymbol{r}}^2\bar{\boldsymbol{l}}F_1$	$\bar{\boldsymbol{l}}^3\bar{\boldsymbol{r}}F_1$	$\bar{\boldsymbol{r}}\bar{\boldsymbol{l}}\bar{\boldsymbol{r}}F_1$	$\bar{\boldsymbol{l}}\bar{\boldsymbol{r}}^2F_1$
⋮	⋮	⋮	⋮	⋮	⋮	⋮	⋮

(ii)

							$\mathbb{L}_0$
							$\mathbb{L}_1$
							$\bar{\boldsymbol{L}}\mathbb{L}_1$
						$\bar{\boldsymbol{R}}\mathbb{L}_1$	$\bar{\boldsymbol{L}}^2\mathbb{L}_1$
					$\bar{\boldsymbol{L}}\bar{\boldsymbol{R}}\mathbb{L}_1$	$\bar{\boldsymbol{R}}\bar{\boldsymbol{L}}\mathbb{L}_1$	$\bar{\boldsymbol{L}}^3\mathbb{L}_1$
		$\bar{\boldsymbol{R}}^2\mathbb{L}_1$	$\bar{\boldsymbol{L}}^2\bar{\boldsymbol{R}}\mathbb{L}_1$	$\bar{\boldsymbol{L}}\bar{\boldsymbol{R}}\bar{\boldsymbol{L}}\mathbb{L}_1$	$\bar{\boldsymbol{R}}\bar{\boldsymbol{L}}^2\mathbb{L}_1$	$\bar{\boldsymbol{L}}^4\mathbb{L}_1$
$\bar{\boldsymbol{L}}\bar{\boldsymbol{R}}^2\mathbb{L}_1$	$\bar{\boldsymbol{R}}\bar{\boldsymbol{L}}\bar{\boldsymbol{R}}\mathbb{L}_1$	$\bar{\boldsymbol{L}}^3\bar{\boldsymbol{R}}\mathbb{L}_1$	$\bar{\boldsymbol{R}}^2\bar{\boldsymbol{L}}\mathbb{L}_1$	$\bar{\boldsymbol{L}}^2\bar{\boldsymbol{R}}\bar{\boldsymbol{L}}\mathbb{L}_1$	$\bar{\boldsymbol{L}}\bar{\boldsymbol{R}}\bar{\boldsymbol{L}}^2\mathbb{L}_1$	$\bar{\boldsymbol{R}}\bar{\boldsymbol{L}}^3\mathbb{L}_1$	$\bar{\boldsymbol{L}}^5\mathbb{L}_1$
⋮	⋮	⋮	⋮	⋮	⋮	⋮	⋮

TABLE 33. (i): Branching sequences in the minimal successor tree, ordered as a 1–2-Fibonacci inner cohort tableau (by suffix / right infix). Setting $F_0 = 0$ and $F_1 = 1$, the tableau lists the nonnegative integers. Setting $F_0 = \bar{\boldsymbol{l}}^{k-1}(1)$ and $F_1 = \bar{\boldsymbol{r}}\bar{\boldsymbol{l}}^{k-1}(1)$, the tableau lists entries in column k of F. Setting $F_0 = \bar{\boldsymbol{r}}^{k-1}(1)$ and $F_1 = \bar{\boldsymbol{l}}\bar{\boldsymbol{r}}^{k-1}(1)$, the tableau lists entries in column k of $\mathsf{\exists}$. (ii): Branching sequences in the maximal successor tree, ordered as a 2–1-Fibonacci inner cohort tableau (by suffix / right infix). Setting $\mathbb{L}_0 = 0$ and $\mathbb{L}_1 = 1$, the tableau lists the nonnegative integers. Setting $\mathbb{L}_0 = \bar{\boldsymbol{L}}^{k-1}(1)$ and $\mathbb{L}_1 = \bar{\boldsymbol{R}}\bar{\boldsymbol{L}}^{k-1}(1)$, the tableau lists entries in column k of $\mathbb{L}$. Setting $F_0 = \bar{\boldsymbol{R}}^{k-1}(1)$ and $F_1 = \bar{\boldsymbol{L}}\bar{\boldsymbol{R}}^{k-1}(1)$, the tableau lists entries in column k of $\exists$. See Table 25(c)(i)

Moreover, the table includes a 0^{th} element that can be set to $\mathsf{F}_{0,k}$, $\mathsf{\exists}_{0,k}$, or 0, as required, to complete a 1–2-Fibonacci cohort sequence from the 0^{th} cohort of $(\mathsf{F}_{n,k})_{n=0,1,2,\ldots}$, $(\mathsf{\exists}_{n,k})_{n=0,1,2,\ldots}$, or $(n)_{n=0,1,2,\ldots}$, respectively.

Similarly, Table 33(ii) provides a partial listing of functions $T \in \{\bar{\boldsymbol{L}}, \bar{\boldsymbol{R}}\}^\star$ such that $T(\mathbb{L}_{1,k}) = \mathbb{L}_{n,k}$, $T(\exists_{1,k}) = \exists_{n,k}$, and $T(1) = n$. The functions are ordered in 2–1-Fibonacci cohort sequence from the 1^{st} cohort. That is, the cohorts of this sequence obtain recursively via the 2–1-Fibonacci inner cohortizer $D_t = D_{t-2} \circ \bar{\boldsymbol{R}} \oplus D_{t-1}\bar{\boldsymbol{L}}$.

Moreover, the table includes a 0^{th} element that can be set to $\mathbb{L}_{0,k}$, $\exists_{0,k}$, or 0, as required, to complete a 2–1-Fibonacci cohort sequence from the 0^{th} cohort of $(\mathbb{L}_{n,k})_{n=0,1,2,\ldots}$, $(\exists_{n,k})_{n=0,1,2,\ldots}$, or $(n)_{n=0,1,2,\ldots}$, respectively.

Curiously, setting $F_1 = 0$ in the former table (and ignoring the 0^{th} element F_0) yields the para-Fibonacci sequence 0, 0, 0, 1, 0, 1, 2, 0, 1, 2, 3, 4, 0, 1, 2, 3, 4, 5, 6, 7 . . .,

or 066628, that has a 1–2-Fibonacci cohort structure and indexes the row of $\mathsf{F}_{n,k}$ containing each positive integer, as Section 8.2.1 described. Analogously, setting $\mathfrak{L}_1 = 0$ in the latter table (and ignoring the 0^{th} element $\mathfrak{L}_0$) yields the sequence 0, 1, 1, 2, 2, 3, 4, 3, 4, 5, 6, 7, 5, 6, 7, 8, 9, 10, 11, 12, . . ., with 2–1-Fibonacci cohortizer $\langle F_{t-2}, F_{t-1}\rangle$.

As a further curiosity, setting $F_0 = \mathfrak{L}_{0,k}$ and $F_1 = \mathfrak{L}_{1,k}$ in Table 33(i) generates the entries in column k of $\mathfrak{L}$, while setting $\mathfrak{L}_0 = \mathsf{F}_{0,k}$ and $\mathfrak{L}_1 = \mathsf{F}_{1,k}$ in Table 33(ii) generates the entries in column k of F. Thus, the tableaux generate columns of the 1–2- and 2–1-Fibonacci arrays from either the minimal *or* the maximal successor tree branching functions (Proposition 8.20). Section 8.6.4, next, will explore this additional structure of the successor trees and branch quartet arrayas. This observation also proves material to the "mutual dispersion" property shown in (105).

Contrast the description of the branch quartet arrays given here with that given in Section 8.3.1 by comparing Figures 25(b)(i) and (c)(i).

The column–array isomorphisms of the branch quartet described in Corollary 8.18 also invite comparison with the column–array isomorphisms of F and $\mathfrak{L}$ described in Remarks 4.18, respectively, 4.29, via the free monoids $\{\kappa, \lambda\}^\star$ and $\{\theta, \eta\}^\star$, and their equivalence classes. The last of these did not preserve order, whereas for example, $(\mathfrak{L}_{3,3}, \mathfrak{L}_{4,3}) = (29, 30) = (N_0(\theta^2\eta^2) + 1, N_0(\theta^2\eta\theta^2) + 1)$ and $(\theta^2\eta^2, \theta^2\eta\theta^2) \overset{\theta^\star\circ}{\sim} (L\eta, L\theta^2)$, for which $(N_{-1}(L\eta), N_{-1}(L\theta^2)) = (5, 4)$. By contrast, Corollaries 8.17 and 8.18 are based on an isomorphism between a tree and a clade thereof that preserves the usual order of integers.

8.6.4. *Additional structure of the branch quartet arrays.* For the branch quartet arrays, Proposition 8.20 explores properties analogous to those of Proposition 8.12, showing such properties to hold not only for right branching, as in the case of the clade quartet, but also for left branching.

The last observation in Remark 8.11 motivates the following claims.

Definition 8.2. Let S be a (positive-integer-valued) function on the positive integers. Define the *Wythoff signature* of S as $\begin{cases} 1, & SK \subseteq K; \\ 0, & SK \subseteq \Lambda; \\ \text{undefined}, & \text{otherwise.} \end{cases}$

Lemma 8.19 (Lower (K) and upper Wythoff numbers (Λ) in each Fibonacci cohort of $\mathbb{Z}_+$)**.** *For $t = 1, 2, 3, \ldots$, let $K_t = \{n \in [F_{t+1}, F_{t+2}) | \exists m \in \mathbb{Z}_+ \text{ s.t. } n = \kappa(m)\}$ and $\Lambda_t = \{n \in [F_{t+1}, F_{t+2}) | \exists m \in \mathbb{Z}_+ \text{ s.t. } n = \lambda(m)\}$ be the lower and upper Wythoff numbers, respectively, in each Fibonacci cohort $C_t = [F_{t+1}, F_{t+2})$ of the positive integers, with $K_0 = \Lambda_0 = \Lambda_1 = \emptyset$ and $K_1 = \{1\}$. Then, for $t \geq 2$,*

(i): *In the minimal successor tree, $K_t = \bar{\boldsymbol{l}}\Lambda_{t-1} \cup \bar{\boldsymbol{r}}K_{t-2} \cup \bar{\boldsymbol{r}}\Lambda_{t-2}$, where each pair has empty intersection, and $\Lambda_t = \bar{\boldsymbol{l}}K_{t-1}$.*

(ii): *In the maximal successor tree, $K_t = \bar{\boldsymbol{L}}\Lambda_{t-1} \cup \bar{\boldsymbol{R}}K_{t-2} \cup \bar{\boldsymbol{R}}\Lambda_{t-2}$, where each pair has empty intersection, and $\Lambda_t = \bar{\boldsymbol{L}}K_{t-1}$.*

(iii): *In the minimal Fibonacci tree, all nodes of the k^{th} right clade comprise lower Wythoff numbers for k odd and upper Wythoff numbers for k even. Equivalently,*

$$K_t = \begin{cases} \boldsymbol{r}K_{t-2} \cup \boldsymbol{l}K_{t-1} \cup \{\boldsymbol{l}(F_t)\}, & t \text{ odd}; \\ \boldsymbol{r}K_{t-2} \cup \boldsymbol{l}(K_{t-1} \setminus \{F_t\}), & t \text{ even}; \end{cases}$$

$$\Lambda_t = \begin{cases} \boldsymbol{r}\Lambda_{t-2} \cup \boldsymbol{l}(\Lambda_{t-1} \setminus \{F_t\}), & t \text{ odd}; \\ \boldsymbol{r}\Lambda_{t-2} \cup \boldsymbol{l}\Lambda_{t-1} \cup \{\boldsymbol{l}(F_t)\}, & t \text{ even}; \end{cases}$$

(iv): *In the maximal Fibonacci tree, all nodes of the k^{th} right clade comprise lower Wythoff numbers for k odd and upper Wythoff numbers for k even. Equivalently,*

$$K_t = \begin{cases} \boldsymbol{R}K_{t-2} \cup \boldsymbol{L}K_{t-1} \cup \boldsymbol{L}(\{F_{t+1}-1\}), & t \text{ odd}; \\ \boldsymbol{R}K_{t-2} \cup \boldsymbol{L}(K_{t-1} \setminus \{F_{t+1}-1\}), & t \text{ even}; \end{cases}$$

$$\Lambda_t = \begin{cases} \boldsymbol{R}\Lambda_{t-2} \cup \boldsymbol{L}(\Lambda_{t-1} \setminus \{F_{t+1}-1\}), & t \text{ odd}; \\ \boldsymbol{R}\Lambda_{t-2} \cup \boldsymbol{L}\Lambda_{t-1} \cup \{\boldsymbol{L}(F_{t+1}-1)\}, & t \text{ even}; \end{cases}$$

(v): $|K_t| = F_{t-1} + (-1)^{t-1} = \underline{008346}(t-1)$ *and* $|\Lambda_t| = F_{t-2} + (-1)^{t-2} = \underline{008346}(t-2)$.

(vi): *For the successor trees,* $\bar{\boldsymbol{l}}\Lambda_{t-1} = \bar{\boldsymbol{R}}K_{t-2}$, $\bar{\boldsymbol{L}}\Lambda_{t-1} = \bar{\boldsymbol{r}}K_{t-2}$, *and* $\bar{\boldsymbol{r}}\Lambda_{t-2} = \bar{\boldsymbol{R}}\Lambda_{t-2}$.

Proof. —

(i)–(ii): The Wythoff signatures of $\bar{\boldsymbol{l}}$ and $\bar{\boldsymbol{r}}$, respectively, $\bar{\boldsymbol{L}}$ and $\bar{\boldsymbol{R}}$, follow from Proposition 6.9(iii) and (i), respectively. To assign the correct cohort of origin use Lemma 6.11 or Corollary 6.20, whereby $C_t = \bar{\boldsymbol{l}}(C_{t-1}) \cup \bar{\boldsymbol{r}}(C_{t-2})$ and $C_t = \bar{\boldsymbol{L}}(C_{t-1}) \cup \bar{\boldsymbol{R}}(C_{t-2})$.

(iii): Consider both alternative formulations: The Wythoff array in terms of pairs of branching functions $(\bar{\boldsymbol{l}}, \bar{\boldsymbol{r}})$ and in terms of branching functions $(\boldsymbol{l}, \boldsymbol{r})$ (see Figures 25(b)(ii) and (c)(ii), respectively).

In the first formulation, $w_{n,k} = \bar{\boldsymbol{l}}^{k-1}\bar{\boldsymbol{r}}(n)$. Thus, by Proposition 6.9(iii), the first column of w given by $\bar{\boldsymbol{r}}(n)$ comprises only lower Wythoff numbers, $w_{n,1} = \bar{\boldsymbol{r}}(n) \subset K$. Hence by (90), $w_{n,k} \in \begin{cases} K, & k \text{ odd}; \\ \Lambda, & k \text{ even}. \end{cases}$

In the second formulation, observe from Corollary 8.11 that each column $\{w_{n,k}\}_{n=0,1,2,\ldots}$ comprises the k^{th} right clade of the Minimal Fibonacci tree, that is, a subtree including $F_{k+1} = \boldsymbol{l}^{k-1}(F_2) = \boldsymbol{l}^{k-1}(1)$ and the complete tree descending from its right child $\boldsymbol{r}(F_{k+1})$ by application of some branching sequence in $(\boldsymbol{l}, \boldsymbol{r})^\star$. Hence, the set of values at nodes throughout each clade is either entirely $\subset K$ or entirely $\subset \Lambda$, the Wythoff signature of right clades $k = 1, 2, 3, \ldots$ alternating according to the parity of k.

Use Lemma 6.10 or Corollary 6.20 to assign the correct cohort of origin to the subsets of cohort C_t via $C_t = \boldsymbol{l}(C_{t-1}) \cup \boldsymbol{r}(C_{t-2})$.

Combining the two formulations, note that the right child of $n \in K_{t-2} \subset C_{t-2}$ is $\boldsymbol{r}(n) \in K_t$ and the right child of $n \in \Lambda_{t-2} \subset C_{t-2}$ is $\boldsymbol{r}(n) \in \Lambda_t$, each right child $\boldsymbol{r}(n)$ having the same Wythoff signature as its parent, n, as both belong to the same right clade. By contrast, the left child of $n \in K_{t-1} \subset C_{t-1}$ is $\boldsymbol{l}(n) \in \begin{cases} \Lambda_t, & n = F_t \text{ for } t \text{ even}; \\ K_t, & \text{otherwise}; \end{cases}$ and thus its Wythoff signature differs from that of its parent, when and only when n and $\boldsymbol{l}(n)$ lie in different right clades. Thus K_t and Λ_t can be defined by the given recursion, exactly as claimed.

(iv): Analogous to **(iii)**, considering the formulation of the Quilt Array $a_{n,k}$ as $a_{n,k} = \bar{\boldsymbol{L}}^{k-1}\bar{\boldsymbol{R}}(n)$ (see Figure 25(b)(ii)), the application of (91), and matching each column of a with the corresponding right clade of the Maximal Fibonacci tree (Figure 25(c)(ii)).

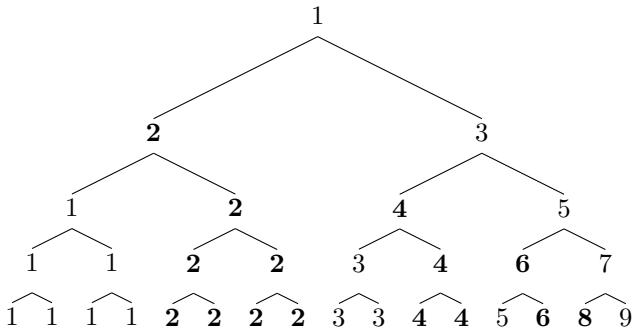

FIGURE 28. A binary tree, split into its left half-clades. In the minimal successor tree (Figure 3), nodes labeled k here contain entries of the k^{th} column of ⊧. In the maximal successor tree (Figure 10), nodes labeled k here contain entries of the k^{th} column of ⊩. Nodes labeled $2k-1$ and those labeled $2k$ together make up the k^{th} left clade, corresponding to column k of ⫞ (⫟) in the minimal (maximal) successor tree.

(v): Follows by induction from any of **(i)**, **(ii)**, **(iii)**, or **(iv)**.

(vi): From **(v)**, the cardinality of sets Λ_t lags that of sets K_t, by one cohort. Thus, $|K_{t-2}| = |\Lambda_{t-1}|$ confirming the cohort index in the identities. To complete the first two identities, combine Propositions 6.9(iv) and (v). Proposition 6.9(vi) completes the latter identity.

□

Tables and figures use darker typeface for lower Wythoff numbers (K) and lighter typeface for upper Wythoff numbers (Λ). The contrasting typeface provides a means to visualize the results of Lemma 8.19. For example, columns of w and a in Table 4 alternate light and dark, matching Figures 5 and 8, in which every second right clade is lighter, in agreement with Lemma 8.19(iii) and (iv), respectively. In Figures 3 and 10, left branchings alternate light and dark, and right branchings are all dark, agreeing with Lemma 8.19(i), respectively, (ii). In a Fibonacci cohort recurrence, the treatment of an element depends only on which prior cohort (C_{t-1} or C_{t-2}) it came from. By contrast, Lemma 8.19(iii) and (iv) affords special treatment to a specific element (F_t) of every other cohort, depending on the parity of t. Section 8.2.4 will revisit this pattern.

The following proposition presents three related results. The first result is a *half-clade-to-half-clade order isomorphism* for ⊩ and ⊧. In contrast to Corollaries 8.15 and 8.17, here, column k of ⊩ appears within the *maximal* successor tree, whilst column k of ⊧ appears within the *minimal* successor tree. Entries for the k^{th} column of the two arrays once again appear in the same tree positions within opposite trees. Moreover, for each column, a distinct subtree once again comprises all entries of the column, with the exception of the zeroth entries $⊩_{0,k}$ or $⊧_{0,k}$ for all k odd.

The second result shows a *clade / column splitting* property. By means of this property, splitting the left clades of the minimal successor tree into left half-clades corresponds to columns of ⫞ split into pairs of adjacent columns of ⊧. Similarly in the maximal successor tree, a split of the left clades into left half-clades corresponds to columns of ⫟ split into pairs of adjacent columns of ⊩. In Definition 8.1, the left

clades are infinite, weakly-binary trees having a 0^{th} node of degree 1. In splitting clades of the minimal successor tree, the k^{th} left clade, which comprises column k of $\exists$, splits into two half-clades, namely the $2k-1^{\text{st}}$ and $2k^{\text{th}}$ left half-clades (Figure 28).

The $2k-1^{\text{st}}$ left half-clade includes the orphaned node at position 2^k-1 as its 0^{th} node, together with its 1^{st} node at position $2^{k+2}-2^2$ and all descendants of the latter. The $2k^{\text{th}}$ left half-clade includes the node at position $2^{k+1}-2$ as its 0^{th} node, together with its 1^{st} node at position $2^{k+2}-2^1-1$ and all descendants of the latter. Thus in the minimal successor tree, the $2k-1^{\text{st}}$ left half-clade comprises column $2k-1$ of $\vdash$ and the $2k^{\text{th}}$ left half-clade comprises column $2k$ of $\vdash$.

Similarly in the maximal successor tree, the k^{th} left clade, which comprises column k of $\dashv$, splits into two half-clades (same Figure 28). The $2k-1^{\text{st}}$ left half-clade includes the orphaned node at position 2^k-1 as its 0^{th} node, together with its 1^{st} node at position $2^{k+2}-2^2$ and all descendants of the latter. The $2k^{\text{th}}$ left half-clade includes the node at position $2^{k+1}-2$ as its 0^{th} node, together with its 1^{st} node at position $2^{k+2}-2^1-1$ and all descendants of the latter. Thus the $2k-1^{\text{st}}$ left half-clade comprises column $2k-1$ of $\vdash$ and the $2k^{\text{th}}$ left half-clade comprises column $2k$ of $\vdash$.

The third result is a *column–cohort splitting* property for array columns. By means of this property, splitting the k^{th} left clade into the aforementioned odd-$(2k-1)$ and even-indexed $(2k)$ half-clades corresponds to splitting column k of $\exists(\dashv)$ into the concatenated sequences of its left and right subcohorts, respectively, considering a column of $\exists(\dashv)$ written as a 1–2- (2–1-) Fibonacci cohort tableau.

To write column k of $\exists$ as a 1–2-Fibonacci tableau, start from the 0^{th} cohort, writing one entry in cohort 0 and F_t entries in each cohort C_t for $t \geq 1$. The left subcohorts of the tableau (including the 0^{th} element) will give column $2k-1$ of $\vdash$ and the right subcohorts give column $2k$ of $\vdash$. Analogously, writing column k of $\dashv$ as a 2–1-Fibonacci tableau from the 0^{th} cohort, with one entry in cohort 0 and F_t entries in each cohort C_t for $t \geq 1$, the right subcohorts in the tableau (including the 0^{th} element) give column $2k-1$ of $\vdash$ and the left subcohorts give column $2k$ of $\vdash$.

Proposition 8.20 (Half-clade-to-half-clade order isomorphism and clade / column / cohort splitting for the branch mirror arrays)**.** —

Let $S_1, S_2, \ldots, S_n, \ldots \in \{\bar{\boldsymbol{l}}, \bar{\boldsymbol{r}}\}^\star$ be the sequence of prefixes of elements in Table 33(i), (which breaks the sequence into Fibonacci cohorts according to the cohort calculus).

Let $T_1, T_2, \ldots, T_n, \ldots \in \{\bar{\boldsymbol{L}}, \bar{\boldsymbol{R}}\}^\star$ be the sequence of prefixes of elements in Table 33(ii), (which breaks the sequence into Fibonacci cohorts according to the cohort calculus).

By Proposition 8.16 and Corollary 8.17, the former sequence generates columns of the branch quartet arrays $\vdash$ and $\exists$ (Table 3, at left) via $\vdash_{n,k} = S_n\vdash_{1,k} = S_n\bar{\boldsymbol{r}}\bar{\boldsymbol{l}}^{k-1}(1)$ and $\exists_{n,k} = S_n\exists_{1,k} = S_n\bar{\boldsymbol{l}}\bar{\boldsymbol{r}}^{k-1}(1)$, whilst the latter sequence generates columns of the branch quartet arrays $\vdash$ and $\dashv$ (Table 3, at right) via $\vdash_{n,k} = T_n\vdash_{1,k} = T_n\bar{\boldsymbol{R}}\bar{\boldsymbol{L}}^{k-1}(1)$ and $\dashv_{n,k} = T_n\dashv_{1,k} = T_n\bar{\boldsymbol{L}}\bar{\boldsymbol{R}}^{k-1}(1)$. In addition:

(i): *The two sequences yield the same values when applied to a lower Wythoff number. That is, $S_n\kappa = T_n\kappa$.*

(ii): *On the set K of lower Wythoff numbers, the range of each composition satisfies either $S_nK = T_nK \subset K$ or $S_nK = T_nK \subseteq \Lambda$, and the resulting sequence of Wythoff signatures (Definition 8.2) of the sequence S_n or T_n equals the Fibonacci word $\underline{005614}_0$.*

(iii): *As a counterpart to Proposition 8.14,*

$$(\vdash): \quad \bar{\boldsymbol{l}}(\vdash_{0,k}) = \begin{cases} \vdash_{0,k+1}, & k \text{ odd}; \\ \vdash_{1,k-1}, & k \text{ even}; \end{cases}$$

$$\bar{\boldsymbol{r}}(\vdash_{0,k}) = \begin{cases} \vdash_{0,k+2}, & k \text{ odd}; \\ \vdash_{1,k}, & k \text{ even}; \end{cases}$$

$$(\digamma): \quad \bar{\boldsymbol{L}}(\digamma_{0,k}) = \begin{cases} \digamma_{0,k+1}, & k \text{ odd}; \\ \digamma_{1,k-1}, & k \text{ even}; \end{cases}$$

$$\bar{\boldsymbol{R}}(\digamma_{0,k}) = \begin{cases} \digamma_{0,k+2}, & k \text{ odd}; \\ \digamma_{1,k}, & k \text{ even}; \end{cases}$$

(iv): *As a counterpart to Corollary 8.15,*

$$(\vdash): \quad \bar{\mathbf{p}}(\vdash_{0,k}) = \begin{cases} 2^{\frac{k+1}{2}} - 1, & k \text{ odd}; \\ 2^{\frac{k+2}{2}} - 2, & k \text{ even}; \end{cases}$$

$$\bar{\mathbf{p}}(\vdash_{1,k}) = \begin{cases} 2^{\frac{k+5}{2}} - 4, & k \text{ odd}; \\ 2^{\frac{k+4}{2}} - 3, & k \text{ even}; \end{cases}$$

$$(\digamma): \quad \bar{\mathbf{P}}(\digamma_{0,k}) = \begin{cases} 2^{\frac{k+1}{2}} - 1, & k \text{ odd}; \\ 2^{\frac{k+2}{2}} - 2, & k \text{ even}; \end{cases}$$

$$\bar{\mathbf{P}}(\digamma_{1,k}) = \begin{cases} 2^{\frac{k+5}{2}} - 4, & k \text{ odd}; \\ 2^{\frac{k+4}{2}} - 3, & k \text{ even}; \end{cases}$$

(v): *As a counterpart to Proposition 8.16 for $n > 0$, $k = 1, 2, 3, \ldots$:*

$(\vdash)$: $\bar{\boldsymbol{l}}(\vdash_{n,k}) = \vdash_{\bar{\boldsymbol{l}}(n),k}$ *and* $\bar{\boldsymbol{r}}(\vdash_{n,k}) = \vdash_{\bar{\boldsymbol{r}}(n),k}$,

$(\digamma)$: $\bar{\boldsymbol{L}}(\digamma_{n,k}) = \digamma_{\bar{\boldsymbol{L}}(n),k}$ *and* $\bar{\boldsymbol{R}}(\digamma_{n,k}) = \digamma_{\bar{\boldsymbol{R}}(n),k}$,.

(vi): *As a counterpart to Corollary 8.17*

For $n > 0$, let $\bar{\mathbf{p}}(n) = 2^{\ell-1} + h$ for $0 \le h < 2^{\ell-1}$. Then for $k = 1, 2, 3, \ldots$:

$$(\vdash): \bar{\mathbf{p}}(\vdash_{n,k}) = \begin{cases} 2^{\frac{k+5}{2}+l-1} - 4 \times 2^{\ell-1} + h, & k \text{ odd}; \\ 2^{\frac{k+4}{2}+l-1} - 3 \times 2^{\ell-1} + h, & k \text{ even}; \end{cases}$$

For $n > 0$, let $\bar{\mathbf{P}}(n) = 2^{\ell-1} + h$ for $0 \le h < 2^{\ell-1}$. Then for $k = 1, 2, 3, \ldots$:

$$(\digamma): \bar{\mathbf{P}}(\digamma_{n,k}) = \begin{cases} 2^{\frac{k+5}{2}+\ell-1} - 4 \times 2^{\ell-1} + h, & k \text{ odd}; \\ 2^{\frac{k+4}{2}+\ell-1} - 3 \times 2^{\ell-1} + h, & k \text{ even}; \end{cases}$$

(vii): *(Clade / column splitting) As a counterpart to Corollary 8.18, for $k = 1, 2, 3, \ldots$:*

$(\vdash)$: *Columns $\vdash_{2k-1}$ and $\vdash_{2k}$ together contain exactly the same entries as column $\dashv_k$, which contains, in turn, exactly the same entries as the k^{th} left clade of the minimal successor tree.*

(⊦): *Columns* $⊦_{2k-1}$ *and* $⊦_{2k}$ *together contain exactly the same entries as column* $⊣_k$*, which contains, in turn, exactly the same entries as the* k^{th} *left clade of the maximal successor tree.*

(viii): *(Column–cohort splitting)*

(⊨): *When evaluated at* $⊨_{1,k}$*, an entry in the* 1^{st} *row of the 2–1-Fibonacci array, the* S_n *generate the subsequent entries* $⊨_{2,k}, ⊨_{3,k}, \ldots$ *in column* k *of* $⊨$*, that is,* $⊨_{n,k} = S_n ⊨_{1,k}$*. Moreover, the* S_n *also generate any column* k *of* $⊨$ *when evaluated at the* 0^{th} *or* 1^{st} *entries of the appropriate column of the 1–2-Mirror array* $⫪$*. Specifically,*

$$⊨_{n,k} = \begin{cases} & ⫪_{0,(k+1)/2}, & n = 0 \text{ and } k \geq 1 \text{ odd}; \\ & ⫪_{1,k/2}, & n = 0 \text{ and } k \geq 2 \text{ even}; \\ S_n \bar{\boldsymbol{l}}\, ⫪_{1,(k+1)/2} & = ⫪_{⫪_{n,1},(k+1)/2}, & n \geq 1 \text{ and } k \geq 1 \text{ odd}; \\ S_n \bar{\boldsymbol{r}}\, ⫪_{1,k/2} & = ⫪_{⊦_{n,1},k/2}, & n \geq 0 \text{ and } k \geq 2 \text{ even}. \end{cases}$$

This shows that odd and even columns of the 2–1-Fibonacci array $⊨$ *obtain from all-left, respectively, all-right subcohorts of the 1–2-Fibonacci cohorts of columns of the 1–2-Mirror array* $⫪$*. Conversely, each column* $k' = 1, 2, 3, \ldots$ *of* $⫪$ *splits into two consecutive columns* $2k'-1$ *and* $2k'$ *of* $⊨$*.*

(⊦): *When evaluated at* $⊦_{1,k}$*, an entry in the* 1^{st} *row of the 1–2-Fibonacci array, the* T_n *generate the subsequent entries* $⊦_{2,k}, ⊦_{3,k}, \ldots$ *in column* k *of* $⊦$*, that is,* $⊦_{n,k} = T_n ⊦_{1,k}$*. Moreover, the* T_n *also generate any column* k *of* $⊦$ *when evaluated at the* 0^{th} *or* 1^{st} *entries in the appropriate column of the 2–1-Mirror array* $⊣$*. Specifically,*

$$⊦_{n,k} = \begin{cases} & ⊣_{0,(k+1)/2}, & n = 0 \text{ and } k \geq 1 \text{ odd}; \\ & ⊣_{1,k/2}, & n = 0 \text{ and } k \geq 2 \text{ even}; \\ T_n \bar{\boldsymbol{R}} ⊣_{1,(k+1)/2} & = ⊣_{⊣_{n,1},(k+1)/2}, & n \geq 1 \text{ and } k \geq 1 \text{ odd}; \\ T_n \bar{\boldsymbol{L}}\, ⊣_{1,k/2} & = ⊣_{⊨_{n,1},k/2}, & n \geq 0 \text{ and } k \geq 2 \text{ even}. \end{cases}$$

This shows that odd and even columns of the 1–2-Fibonacci array $⊦$ *obtain from all-right, respectively, all-left subcohorts of the 2–1-Fibonacci cohorts of columns of the 2–1-Mirror array* $⊣$*. Conversely, each column* $k' = 1, 2, 3, \ldots$ *of* $⊣$ *splits into two consecutive columns* $2k'-1$ *and* $2k'$ *of* $⊦$*.*

Proof. In Section 11. □

By construction, for a node with value m in the minimal or maximal Fibonacci or successor trees:

$$1 \leq m < \boldsymbol{l}(m) < \boldsymbol{r}(m). \tag{104}$$

Infinitely many binary trees arrange the positive integers while satisfying this property. (Section 9.9.1 will quantify by computer experiments the number of finite binary trees satisfying this property while arranging the first n positive integers $1, 2, 3, \ldots, n$.) For any such tree, all-left or all-right branchings can be harvested and ordered as rows into arrays. The left or right clades of any such tree can also be harvested and ordered as columns into arrays. It is not necessarily true, however, that *both* the tree-branch method *and* the tree-clade method produce I–D arrays from the *same* tree satisfying (104). This section distinguished the branch

and clade quartet arrays in as much as all four pairs of blade-dual arrays are I–D arrays.

Proposition 9.9 will give a sufficient condition for blade duality to preserve the I–D property of arrays, or alternatively, for arrays produced via the tree-clade approach from a tree satisfying (104) to be I–D arrays. This condition will require only one clade in the tree to satisfy clade–tree order isomorphism. By contrast, *any* clade in one of the Fibonacci or successor trees is order isomorphic to the full tree (Corollaries 8.10 and 8.17). Section 9.9.1 will also quantify by computer experiments the numbers of trees that arrange sequences $1, 2, 3, \ldots, n$ of the first n positive integers whilst satisfying a single clade–tree order isomorphism or whilst satisfying complete clade–tree order isomorphism.

8.7. **Mutual dispersion properties of dual arrays in the octet.** The following shows results about mutual dispersions between dual arrays in the two quartets. In the case of mirror-dual arrays, the proof uses the "tree clade method" of constructing the arrays, without explicitly using the fact that the arrays are I–D arrays. In the case of cohort-dual arrays, the proof uses the "tree branch method" of constructing the arrays.

8.7.1. *Mutual dispersion property of mirror duals.* For an I–D array with infinitely many rows, the mirror dual is the same as what Kimberling called the "inverse I–D array," from which the mutual dispersion of first columns immediately follows. Proposition 8.21 explicitly formulates the mutual dispersion relationship between the pairs of mirror-dual arrays in the octet, so as to provide a (limited) analogy to the less intuitive mutual dispersion between certain pairs of cohort-dual arrays in the octet (Proposition 8.22).

Consider mirror duality within the Branch Quartet (Table 3) and Clade Quartet (Table 4). In any of these arrays, all entries of a column $k \geq 2$ are found within the first column of its mirror dual. Moreover, its own previous column indexes its entries in the first column of the mirror dual, and reciprocally, giving the following property.

Proposition 8.21 (Mutual dispersion property of all mirror duals in the octet)**.**

$$\begin{aligned}
&\mathsf{F}_{n,k} = \mathsf{ㅋ}_{\mathsf{F}_{n,k-1},1},\ k \geq 2;\ \textit{and}\ \ \mathsf{ㅋ}_{n,k} = \mathsf{F}_{\mathsf{ㅋ}_{n,k-1},1},\ k \geq 2;\\
&\mathsf{L}_{n,k} = \mathsf{ㅓ}_{\mathsf{L}_{n,k-1},1},\ k \geq 2;\ \textit{and}\ \ \mathsf{ㅓ}_{n,k} = \mathsf{L}_{\mathsf{ㅓ}_{n,k-1},1},\ k \geq 2;\\
&w_{n,k} = \mathfrak{w}_{w_{n,k-1},1}, k \geq 2;\ \textit{and}\ \mathfrak{w}_{n,k} = w_{\mathfrak{w}_{n,k-1},1}, k \geq 2;\\
&a_{n,k} = \mathfrak{a}_{a_{n,k-1},1},\ k \geq 2;\ \textit{and}\ \ \mathfrak{a}_{n,k} = a_{\mathfrak{a}_{n,k-1},1},\ k \geq 2.
\end{aligned}$$

Proof for F *(others are similar):* Corollary 8.18 imples $\{1\} \cup \{\mathsf{F}_{n,k}\}_{k\geq 2} = \{\mathsf{ㅋ}_{n,1}\}$. Thus, the equality is true set-wise, and it remains to show equality between individual pairs of entries in the two arrays with the indices claimed. Show this entry-wise equality by induction.

Case $n = 0$: For the base case, observe that $\mathsf{F}_{0,2} = 2 = \mathsf{ㅋ}_{1,1} = \mathsf{ㅋ}_{\mathsf{F}_{0,2-1},1}$. Now suppose that $\mathsf{F}_{0,k-1} = \mathsf{ㅋ}_{\mathsf{F}_{0,k-2},1}$ for some $k \geq 3$ and proceed by induction on k. From Proposition 8.14, $\mathsf{F}_{0,k} = \bar{\boldsymbol{l}}(\mathsf{F}_{0,k-1})$ and from Proposition 8.16 $\mathsf{ㅋ}_{\mathsf{F}_{0,k-1},1} = \mathsf{ㅋ}_{\bar{\boldsymbol{l}}(\mathsf{F}_{0,k-2}),1} = \bar{\boldsymbol{l}}(\mathsf{ㅋ}_{\mathsf{F}_{0,k-2},1})$, where $\mathsf{F}_{0,k-2} > 0$ meets the condition of the Proposition. Thus it follows from the induction hypothesis that $\mathsf{F}_{0,k} = \mathsf{ㅋ}_{\mathsf{F}_{0,k-1},1}$ for all $k \geq 2$.

Case $n = 1$: It follows from case $n = 0$ and Proposition 8.14 that $\mathsf{F}_{1,k} = \bar{\boldsymbol{r}}(\mathsf{F}_{0,k}) = \bar{\boldsymbol{r}}(\mathsf{ㅋ}_{\mathsf{F}_{0,k-1},1}) = \mathsf{ㅋ}_{\bar{\boldsymbol{r}}(\mathsf{F}_{0,k-1}),1} = \mathsf{ㅋ}_{\mathsf{F}_{1,k-1},1}$ for all $k \geq 2$.

Case $n > 0$: Consider case $n = 1$, where the result holds for all $k \geq 2$, and the fact that any $n > 0$ obtains from 1 by repeated application of $\bar{\boldsymbol{l}}$ and $\bar{\boldsymbol{r}}$. Thus for induction from n to $\bar{\boldsymbol{l}}(n)$ and $\bar{\boldsymbol{r}}(n)$, consider $\mathsf{F}_{\bar{\boldsymbol{l}}(n),k} = \bar{\boldsymbol{l}}(\mathsf{F}_{n,k}) = \bar{\boldsymbol{l}}(\exists_{\mathsf{F}_{n,k-1},1}) = \exists_{\bar{\boldsymbol{l}}(\mathsf{F}_{n,k-1}),1} = \exists_{\mathsf{F}_{\bar{\boldsymbol{l}}(n),k-1},1}$ and $\mathsf{F}_{\bar{\boldsymbol{r}}(n),k} = \bar{\boldsymbol{r}}(\mathsf{F}_{n,k})\bar{\boldsymbol{r}}(\exists_{\mathsf{F}_{n,k-1},1}) = \exists_{\bar{\boldsymbol{r}}(\mathsf{F}_{n,k-1}),1} = \exists_{\mathsf{F}_{\bar{\boldsymbol{r}}(n),k-1},1}$, where the equalities follow from Proposition 8.16 and induction from case $n = 1$.

Using the formulas in Tables 3 & 4, Part 3 of this paper [40] gives a different proof for the mutual dispersion property of mirror-dual arrays in the octet. □

Althought Proposition 8.21 follows from the fact that "mirror dual" I–D arrays are inverse I–D arrays as defined by Kimberling [20] for I–D arrays with infinitely many rows (see Remark 9.3), Proposition 8.22 will show analogous mutual dispersion properties for certain cohort dual I–D arrays of the branch and clade quartets.

8.7.2. *Mutual dispersion property of cohort duals.* A mutual-dispersion property also emerges between certain pairs of cohort-dual arrays in the branch quartet and clade quartets.

Proposition 8.22 (Mutual dispersion property of certain cohort duals in the octet)**.**

$$\mathsf{F}_{n,k} = \ \vdash_{\mathsf{F}_{n,k-2},1}, k \geq 3; \qquad \textit{and } \vdash_{n,k} = \ \mathsf{F}_{\vdash_{n,k-2},1}, k \geq 3; \tag{105}$$

$$w_{n,k} = \begin{cases} a_{w_{n,k-2},1}, k \geq 3, \textit{ odd}; \\ a_{w_{n,k-3},2}, k \geq 4, \textit{ even}; \end{cases} \textit{ and } a_{n,k} = \begin{cases} w_{a_{n,k-2},1}, k \geq 3, \textit{ odd}; \\ w_{a_{n,k-3},2}, k \geq 4, \textit{ even}; \end{cases} \tag{106}$$

Proof for F *(others are similar):* From Remark 6.14, consider that $\boldsymbol{R} = \boldsymbol{l}^2$. Thus, with reference to Figure 25(b)(i), $\vdash_{n,1} = \begin{cases} 1\,, & n = 0 \\ \boldsymbol{R}(n), & n \geq 1 \end{cases} = \begin{cases} 1\,, & n = 0 \\ \boldsymbol{l}^2(n), & n \geq 1 \end{cases}$, while for $k \geq 3$, $\mathsf{F}_{n,k} = \boldsymbol{l}^2(m)$, where $m = \begin{cases} \boldsymbol{l}^{k-3}\,(1), & n = 0 \\ \boldsymbol{l}^{k-3}\boldsymbol{r}(n), & n \geq 1 \end{cases} = \mathsf{F}_{n,k-2}$, where the last equality follows from substitution into the formulation given in Figure 25(b)(i).

Using the formulas in Tables 3 & 4, Part 3 of this paper [40] gives a different proof for the mutual dispersion property of clade-dual arrays in the octet. □

In the present context, it is interesting to note that blade duality alters the mutual dispersion between pairs of cohort-dual arrays from a property of first columns (105) to a property of the first two columns (106). Example 9.1 will show other properties of the "mutual-dispersion" type.

9. Tree Extensions and Generalizations

This section provides a brief summary of ongoing attempts to extend and generalize the minimal and maximal Fibonacci trees and the numeration systems they characterize, the minimal and maximal successor trees, and the cohort tableaux and interspersion–dispersion arrays associated with these trees.

In particular, this section will consider three techniques for arranging the positive integers into binary trees rooted at 1:

- Section 9.1: Start with a linear recurrence relation and use it to generate cohort lengths as presented in Section 4.3. Next, break the positive integers into cohorts of these lengths, writing each block on a successive level of a (dense) cohort tableau (like those in Tables 6, 34, 39, and 42(i) and (iii)). Finally,

construct a binary tree by grafting together columns of the tableau as straight (all-left) branchings, according to the procedure Remark 9.3 describes.

- Section 9.2: Consider the Fibonacci numeration systems (Sections 6.2 and 6.3) that form the basis of branching rules (Figures 15(iv) and (iii)) in the maximal and minimal Fibonacci trees. Extrapolate these numeration systems to develop branching rules for additional "numeration trees."
- Section 9.5: Consider pairs of floor functions $\bar{l}(n) = \lfloor \mu n \rfloor$ and $\bar{r}(n) = \lfloor \nu n \rfloor$ with irrational slopes $1 < \mu < 2$ and $\nu = {}^{1}\!/_{(1-\frac{1}{\mu})}$, and employ these Beatty pairs (not just the Wythoff pair with $\mu = \phi$) in branching rules for binary trees. Moreover, considering the shift between maximal and minimal successor branching — Figures 15(iv) and (iii), also Remarks 4.27 and 4.12 — extrapolate (Corollary 9.2) and interpolate (Remark 9.1), "shifting" the branching rules so as to develop additional trees for each Beatty pair.

Using trees constructed by any of the above techniques, the associated I–D arrays then follow by taking straight (all-left or all-right) tree branches as array rows, and ordering the rows so as to satisfy Kimberling's Third Interspersion Property (I3) [20].

9.1. **Cohort shift of dense tableaux.** For this variation, the dense Fibonacci cohort tableaux of the positive integers (Tables 6) undergo a shift in cohort lengths. On one hand, the cohort lengths $|C_1| = F_1, |C_2| = F_2, |C_3| = F_3, \cdots$ successively shift to the left, (meaning that elements of smaller value appear in cohorts of greater length), such that $|C_1| = F_2, |C_2| = F_3, |C_3| = F_4, \cdots$ for the first leftward shift, then $|C_1| = F_3, |C_2| = F_4, |C_3| = F_5, \cdots$ for the second leftward shift, and so forth, to produce a family of shifted 1–2-Fibonacci and 2–1 Fibonacci tableaux (Tables 34), and their corresponding binary trees (Figures 29) and I–D arrays (Tables 35 and 36).

Clark Kimberling previously contributed several of these arrays to the OEIS. For example, the first left shift just described produces 194056 (Table 35) and the second produces 194059 (Table 36). On the other hand, cohort lengths may also shift to the right by successively prepending additional cohorts of cardinality 1, such that $|C_1| = 1, |C_2| = F_1, |C_3| = F_2, |C_4| = F_3, \cdots$ for the first rightward shift, then $|C_1| = 1, |C_2| = 1, |C_3| = F_1, |C_4| = F_2, |C_5| = F_3, \cdots$ for the second rightward shift, and so forth.

Observe that branching in the first left shift, listed in Table 36 (at middle left) with the rule $n \mapsto (l(n), r(n)) = (n + F_{F^{-1}(n+1)-1}, n - 1 + F_{F^{-1}(n)+2})$ gives $l(n) = \boldsymbol{l}(n+1) - 1 =$ 183544$(n+1)$, a 2–1-Fibonacci cohort sequence under $\langle F_{t+1}, F_{t+1} - F_{t-3} \rangle$ and $r(n) = \boldsymbol{r}(n) - 1 =$ 183545(n), a 2–1-Fibonacci cohort sequence under $\langle F_{t+3} - F_{t-1}, F_{t+2} \rangle$. Similarly, the second shift (at bottom left) uses $(l(n), r(n)) = (\boldsymbol{l}(n+2) - 2, \boldsymbol{r}(n) - 2)$ with the same cohortizers. For the cohort-dual trees, the first shift (at middle right of the table) uses $l(n) = \boldsymbol{L}(n+1) - 1 =$ 133512$(n+1)$ and $r(n) = \boldsymbol{R}(n) - 1$, while the second shift (at bottom right) uses $(l(n), r(n)) = (\boldsymbol{L}(n+2) - 2, \boldsymbol{R}(n) - 2)$, in each case the left and right branching functions being 2–1-Fibonacci cohort sequences under $\langle F_{t+2} - F_{t-1}, F_{t+1} \rangle$, respectively, $\langle F_{t+2}, F_{t+2} - F_{t-1} \rangle$.

9.2. **Extrapolated Fibonacci Numeration.** For parent node n satisfying $F_t \leq n < F_{t+1}$ the pairs of children in the maximal, respectively, minimal Fibonacci

(i)

1													
2	3												
4	5	6											
7	8	9	10	11									
12	13	14	15	16	17	18	19						
20	21	22	23	24	25	26	27	28	29	30	31	32	
⋮	⋮	⋮	⋮	⋮	⋮	⋮	⋮	⋮	⋮	⋮	⋮	⋮	⋱

(ii)

													1
												2	3
											4	5	6
										7	8	9	10	11
									12	13	14	15	16	17	18	19
20	21	22	23	24	25	26	27	28	29	30	31	32				
⋰	⋮	⋮	⋮	⋮	⋮	⋮	⋮	⋮	⋮	⋮	⋮	⋮	⋮

(iii)

1	2												
3	4	5											
6	7	8	9	10									
11	12	13	14	15	16	17	18						
19	20	21	22	23	24	25	26	27	28	29	30	31	
⋮	⋮	⋮	⋮	⋮	⋮	⋮	⋮	⋮	⋮	⋮	⋮	⋮	⋱

(iv)

												1	2
											3	4	5
										6	7	8	9	10
									11	12	13	14	15	16	17	18
19	20	21	22	23	24	25	26	27	28	29	30	31				
⋰	⋮	⋮	⋮	⋮	⋮	⋮	⋮	⋮	⋮	⋮	⋮	⋮	⋮	⋮	⋮	⋮

TABLE 34. "Leftward shifted" versions of the Fibonacci Tableaux of positive integers (Tables 6): 1st leftward shift of the (i) 1–2- and (ii) 2–1-Fibonacci cohort tableaux; 2nd leftward shift of the (iii) 1–2- and (iv) 2–1-Fibonacci cohort tableaux. Figure 29 shows the corresponding binary trees, while Tables 35 and 36 show the corresponding I–D arrays (and their mirror duals) for (i) and (ii), respectively, (iii) and (iv).

trees, were $(n+F_t, n+F_{t+1})$ (Remark 6.7) and $(n+F_{t-1}, n+F_{t+2})$ (Remark 6.8), respectively. Extrapolating this pattern suggests additional binary trees based on the branching pairs $(n+F_{t-2}, n+F_{t+3})$, $(n+F_{t-3}, n+F_{t+4}), \ldots$, $(n+F_{t-p}, n+F_{t+p+1}), \ldots$.

To yield a tree arranging all positive integers, however, the latter branching rules must be modified due to the degeneracy $n+F_{t-p} < n+1$ that may occur for certain $n < F_{p+1}$. As examples: For $p = 2$, without modification the left child $n+F_{t-2}$ of $n = 1$ would itself be 1, while for $p = 3$, without modification the left child $n+F_{t-3}$ of $n = 2$ would equal 2. The branching rules can be modified by forcing the left child of n to $n+1$ as required to "patch" the degeneracy and produce a binary tree that arranges the positive integers. With their branching rules so modified, these additional trees extrapolate the maximal and minimal Fibonacci trees to a 1-parameter family of "Fibonacci numeration trees" [34].

The family starts with the maximal Fibonacci tree, it being more "balanced" on each level than the minimal Fibonacci tree or any subsequent tree of the family. Balance in the sense of Remark 6.7 means that the tree of maximal Fibonacci expansions, Figure 13, has the same number of addends for all nodes on the same level of the tree. Balance also can be reckoned in the sense of Corollary 6.20, that the left and right children of n are closer to one another in value in the maximal Fibonacci tree than in the minimal Fibonacci tree, or $\boldsymbol{R}(n) - \boldsymbol{L}(n) < \boldsymbol{r}(n) - \boldsymbol{l}(n)$.

As the family extends from the maximal Fibonacci tree to the minimal Fibonacci tree and beyond, each subsequent Fibonacci numeration tree yields an additional pair of mirror-dual interspersion arrays, obtained by taking sequences of all-left and all-right branchings of the tree. For the first several further extensions ($p = 2, 3$),

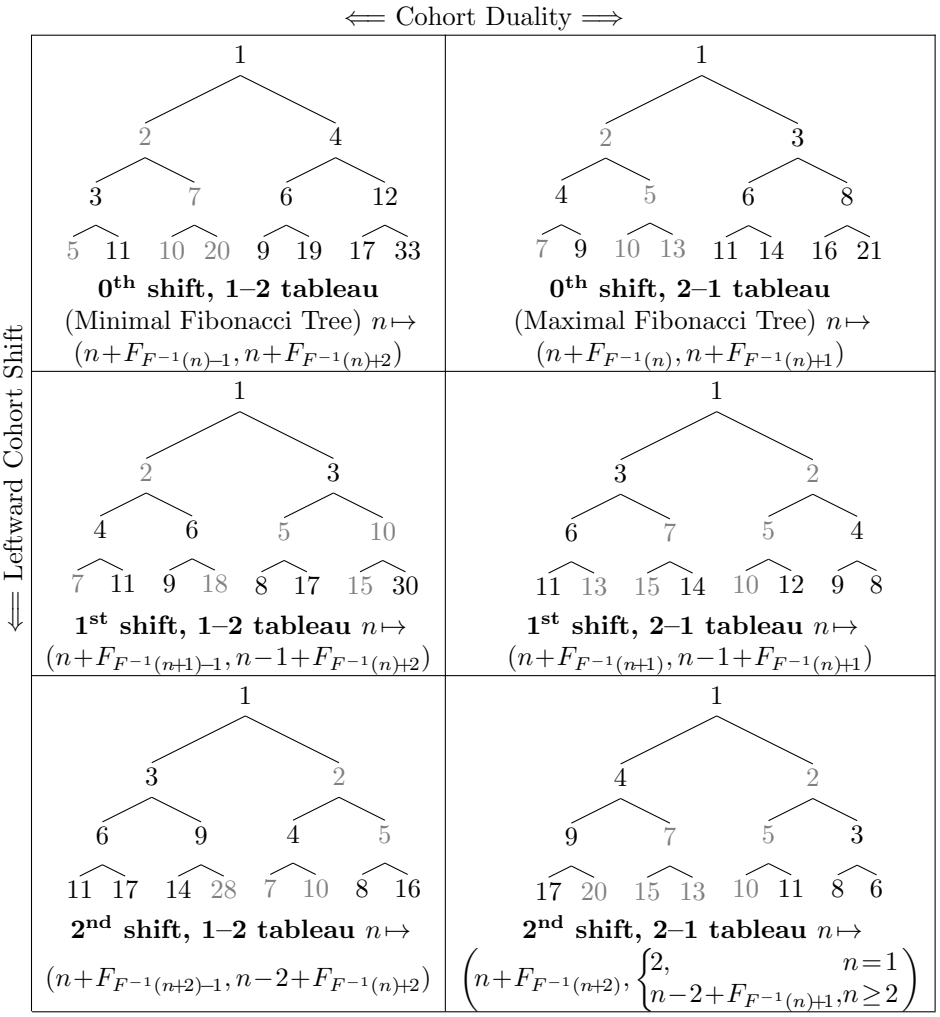

FIGURE 29. Binary trees of $\mathbb{Z}_+$ descending from 1 via the branching rules shown, corresponding to leftward shifts of the 1–2- and 2–1-Fibonacci cohort tableaux, at the left, respectively, right. At the top: 0^{th} shift of tableaux (Tables 6); in the middle: 1^{st} leftward shift of tableaux (Tables 34(i) and (ii)); at the bottom: 2^{nd} leftward shift of tableaux (Tables 34(iii) and (iv)). Whereas the branch quartet (Table 3) corresponds to the pair of trees at the top, Tables 35 and 36 show I-D arrays corresponding to the pairs at the middle, respectively, bottom.

a second tree and second pair of mirror-dual I–D arrays obtain via cohort duality, to complete a quartet of I–D arrays analogous to the branch quartet of Table 3.

Figure 30 shows the second extension tree. Figure 31 shows its cohort-dual tree, in which n has left and right children $n + F_{F^{-1}(\lfloor n/2 \rfloor)-1}$ and $n + 2F_{F^{-1}(n)+2}$, respectively. Table 37 shows the quartet of arrays that result. Tableaux for the second extension ($p = 2$) have cohort lengths $|C_1| = 1$ and $|C_{2t}| = |C_{2t+1}| = F_t$ for

$\Longleftarrow$ Cohort Duality $\Longrightarrow$

$\Uparrow$ Mirror Duality $\Uparrow$	1	2	4	7	12	20	1	3	6	11	19	32
	3	5	8	13	21	34	2	5	10	18	31	52
	6	9	14	22	35	56	4	9	17	30	51	85
	10	15	23	36	57	91	7	15	28	49	83	138
	11	16	24	37	58	92	8	16	29	50	84	139
	17	25	38	59	93	148	12	25	46	80	135	224
	18	26	39	60	94	149	13	26	47	81	136	225
	19	27	40	61	95	150	14	27	48	82	137	226
	28	41	62	96	151	240	20	41	75	130	219	363
	29	42	63	97	152	241	21	42	76	131	220	364
	1st left shift 1–2 (194056)						**1st left shift 2–1**					
$\Downarrow$ Mirror Duality $\Downarrow$	1	3	10	30	84	227	1	2	4	8	20	40
	2	6	18	51	139	371	3	7	14	34	88	176
	4	11	31	85	228	604	5	12	24	57	145	377
	5	17	50	138	370	979	6	13	33	66	154	386
	7	19	52	140	372	981	9	21	54	108	251	627
	8	28	82	225	601	1587	10	22	55	143	286	662
	9	29	83	226	602	1588	11	23	56	144	376	752
	12	32	86	229	605	1591	15	35	89	232	464	1073
	13	46	134	366	975	2571	16	36	90	233	609	1218
	14	47	135	367	976	2572	17	37	91	234	610	1596
	1st left shift 1–2 mirror						**1st left shift 2–1 mirror**					

TABLE 35. First quartet of arrays from "leftward shifted" Fibonacci tableaux. Rows of the arrays at the top left (top right) are columns of the 1–2- (2–1)-Fibonacci cohort tableau of the positive integers with cohort lengths $|C_t| = F_{t+1}$ for $t = 1, 2, 3, \cdots$ (Tables 34(i), respectively, (ii)). Each array at the bottom is the mirror dual of that above it: Rows of each array at the bottom are sequences of right branchings in that tree (Figure 29, middle row) for which the rows of the array above it are sequences of left branchings.

$t = 1, 2, 3, \ldots$ (Tables 39(i) and (ii)). Analogously, tableaux for the third extension ($p = 3$) have cohort lengths $|C_1| = |C_2| = 1$ and $|C_{3t}| = |C_{3t+1}| = |C_{3t+2}| = F_t$ for $t = 1, 2, 3, \ldots$ (Tables 39(iii) and (iv)). Figure 32 shows the third extension tree and Figure 33 its cohort-dual tree, the latter employing left and right branching functions $n + F_{F^{-1}(\lfloor n/3 \rfloor)-1}$ and $n + 3F_{F^{-1}(n)+2}$. This pair of trees produces the quartet of I–D arrays in Table 38.

Note that the branching formulation of the cohort-dual trees differs from that of the "numeration trees" themselves. Rather, the branching rules for the two cohort-dual trees extrapolate forward via $n \mapsto (l(n), r(n)) = (n + F_{F^{-1}(\lfloor n/p \rfloor)-1}, n + pF_{F^{-1}(n)+2})$, where p the *depth* of the extrapolation, forming cohorts whose lengths follow the pattern $|C_{pt}| = \cdots = |C_{p(t+1)-1}| = F_t$ for $t = 1, 2, 3, \ldots$, together with "seed" cohorts of lengths $|C_t| = 1$ for $t < p$. Extrapolating backwards to $p = 1$, gives the branching rule $n \mapsto (n + F_{F^{-1}(\lfloor n/1 \rfloor)-1}, n + 1 \times F_{F^{-1}(n)+2}) =$

$\Longleftarrow$ Cohort Duality $\Longrightarrow$

$\Uparrow$ Mirror Duality $\Downarrow$												
1	3	6	11	19	32	1	4	9	17	30	51
2	4	7	12	20	33	2	5	10	18	31	52
5	8	13	21	34	55	3	8	16	29	50	84
9	14	22	35	56	90	6	14	27	48	82	137
10	15	23	36	57	91	7	15	28	49	83	138
16	24	37	58	92	147	11	24	45	79	134	223
17	25	38	59	93	148	12	25	46	80	135	224
18	26	39	60	94	149	13	26	47	81	136	225
27	40	61	95	150	239	19	40	74	129	218	362
28	41	62	96	151	240	20	41	75	130	219	363
2nd left shift 1–2 (194059)						**2nd left shift 2–1**					
1	2	5	16	48	135	1	2	3	6	12	23
3	9	28	81	223	598	4	7	13	32	64	151
4	10	29	82	224	599	5	11	22	54	107	249
6	17	49	136	367	975	8	19	38	91	233	608
7	18	50	137	368	976	9	20	39	92	234	609
8	27	80	222	597	1582	10	21	53	106	248	623
11	30	83	225	600	1585	14	33	65	152	383	991
12	31	84	226	601	1586	15	34	87	174	405	1013
13	45	132	363	971	2566	16	35	88	175	406	1014
14	46	133	364	972	2567	17	36	89	231	462	1070
2nd left shift 1–2 mirror						**2nd left shift 2–1 mirror**					

TABLE 36. Second quartet of arrays from "leftward shifted" Fibonacci tableaux. Rows of the arrays at the top left (top right) are columns of the 1–2- (2–1)-Fibonacci cohort tableau of the positive integers with cohort lengths $|C_t| = F_{t+2}$ for $t = 1, 2, 3, \cdots$ (Tables 34(iii), respectively, (iv)). Each array at the bottom is the mirror dual of that above it: Rows of each array at the bottom are sequences of right branchings in that tree (Figure 29, bottom row) for which the rows of the array above it are sequences of left branchings.

$(n + F_{F^{-1}(\lfloor n \rfloor)-1}, n + F_{F^{-1}(n)+2})$ — the branching rule for the minimal Fibonacci tree itself.

Example 9.1 (Additional properties of the Fibonacci numeration I–D arrays)**.** As shown in [34], the branch quartet arrays and the Fibonacci$^{(2)}$ and Fibonacci$^{(3)}$ arrays given in Tables 3, 37 and 38, respectively, exhibit the following properties (*Depth* will refer to the degree of extrapolation of the underlying Fibonacci numeration system: 1 for the maximal and minimal Fibonacci trees, 2 for the system in shown in Figure 30, and 3 for that shown in Figure 32):

Ex. 9.1, continued: Coincidence of columns in cohort duals of the same Fibonacci numeration depth (for rows $n \geq 0$):

$$\vdash_{n,k} = \vdash_{n,k},\ k = 2;\ \text{and}\ \vdash^{(2)}_{n,k} = \vdash^{(2)}_{n,k},\ k = 3, 4;\ \text{and}\ \vdash^{(3)}_{n,k} = \vdash^{(3)}_{n,k},\ k = 4, 5, 6.$$

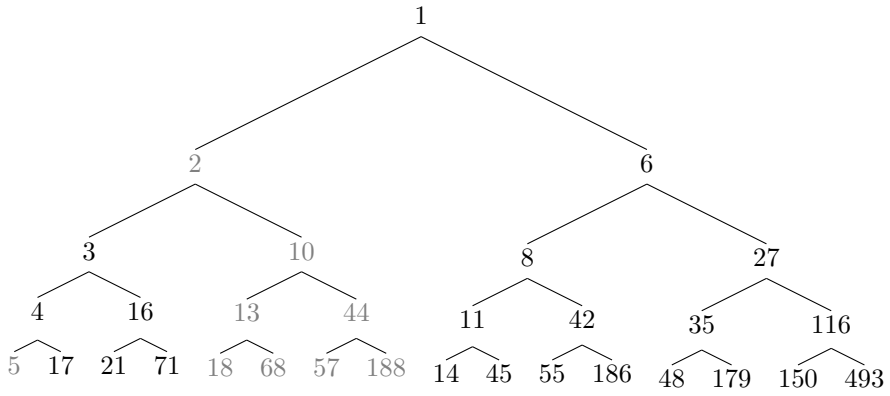

FIGURE 30. Second Fibonacci numeration tree "extrapolated" from the maximal Fibonacci tree and beyond the minimal Fibonacci tree. The left child of n is 2 for $n = 1$ and $n + F_{F^{-1}(n)-2}$ otherwise. The right child of n is $n + F_{F^{-1}(n)+3}$. Cohort dual tree of Figure 31. Sequences of all-left (all-right) branchings are rows of the arrays at the top (bottom) left of Table 37.

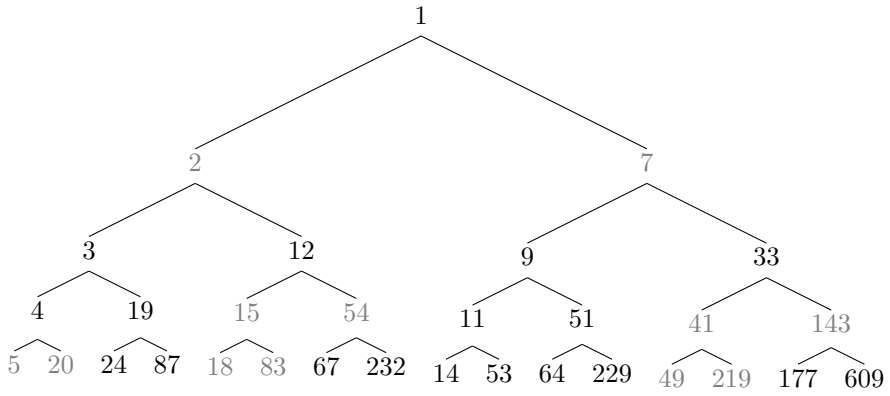

FIGURE 31. Cohort dual of the second "extrapolated" Fibonacci numeration tree (Figure 30). The left child of n is $n + F_{F^{-1}(\lfloor n/2 \rfloor)-1}$. The right child of n is $n + 2F_{F^{-1}(n)+2}$. Sequences of all-left (all-right) branchings are rows of the arrays at the top (bottom) right of Table 37.

Ex. 9.1, continued: Periodic coincidence of columns between arrays of differing Fibonacci numeration depth (for $k \geq 1$):

$$\vdash^{(2)}_{n,2k-1} = \begin{cases} \vdash_{n,k+1} - F_k, & n = 0; \\ \vdash_{n,k+1}, & n \geq 1; \end{cases} \text{ and } \mathsf{F}^{(2)}_{n,2k} = \begin{cases} \mathsf{F}_{n,k+2} - F_k, & n = 0; \\ \mathsf{F}_{n,k+2}, & n \geq 1; \end{cases}$$

$$\vdash^{(3)}_{n,3k-1} = \begin{cases} \vdash_{n,k+2} - 2F_k, & n = 0; \\ \vdash_{n,k+2}, & n \geq 1; \end{cases} \text{ and } \mathsf{F}^{(3)}_{n,3k} = \begin{cases} \mathsf{F}_{n,k+3} - 2F_k, & n = 0; \\ \mathsf{F}_{n,k+3}, & n \geq 1; \end{cases}$$

$\Longleftarrow$ Cohort Duality $\Longrightarrow$

$\Longleftarrow$ Mirror Duality $\Longrightarrow$

1	2	3	4	5	7	1	2	3	4	5	6
6	8	11	14	19	24	7	9	11	14	17	22
10	13	18	23	31	39	12	15	18	23	28	36
16	21	29	37	50	63	19	24	29	37	45	58
17	22	30	38	51	64	20	25	30	38	46	59
26	34	47	60	81	102	31	39	47	60	73	94
27	35	48	61	82	103	32	40	48	61	74	95
28	36	49	62	83	104	33	41	49	62	75	96
42	55	76	97	131	165	50	63	76	97	118	152
43	56	77	98	132	166	51	64	77	98	119	153
2nd extrapolated numeration $\vdash^{(2)}$						**2nd num. ext. cohort dual** $\digamma^{(2)}$					
1	6	27	116	493	2090	1	7	33	143	609	2583
2	10	44	188	798	3382	2	12	54	232	986	4180
3	16	71	304	1291	5472	3	19	87	375	1595	6763
4	17	72	305	1292	5473	4	20	88	376	1596	6764
5	26	115	492	2089	8854	5	31	141	607	2581	10943
7	28	117	494	2091	8856	6	32	142	608	2582	10944
8	42	186	796	3380	14326	8	50	228	982	4176	17706
9	43	187	797	3381	14327	9	51	229	983	4177	17707
11	45	189	799	3383	14329	10	52	230	984	4178	17708
12	46	190	800	3384	14330	11	53	231	985	4179	17709
2nd extrapolated num. mirror $\dashv^{(2)}$						**2nd ext. num. coh. dual mir.** $\urcorner^{(2)}$					

TABLE 37. Quartet of interspersion arrays, corresponding to the second Fibonacci numeration tree "extrapolated" from the maximal Fibonacci tree and beyond the minimal Fibonacci tree. Figure 30 shows this binary tree, for which sequences of all-left (all-right) branchings give rows of the arrays at the top (bottom) left. Rows of the arrays at the top (bottom) right are sequences of all-left (all-right) branchings in the cohort-dual tree Figure 31. Rows of arrays at the top left and right are columns of the tableaux in Tables 39(i), respectively, (ii). Example 9.1 mentions the coincidence of the 3rd and 4th columns of $\vdash^{(2)}$ and $\digamma^{(2)}$.

Ex. 9.1, continued: Irregular coincidence of columns between arrays of differing Fibonacci numeration depth and Fibonacci cohort structure (for rows $n \geq 1$):

$$\vdash^{(2)}_{n,1} = \digamma_{n,2}, \vdash^{(2)}_{n,4} = \digamma_{n,4}, \ \digamma^{(2)}_{n,3} = \vdash_{n,3};$$
$$\vdash^{(3)}_{n,1} = \digamma_{n,3}, \vdash^{(3)}_{n,6} = \digamma_{n,5}, \ \digamma^{(3)}_{n,5} = \vdash_{n,4};$$
$$\vdash^{(3)}_{n,1} = \digamma^{(2)}_{n,2}, \vdash^{(3)}_{n,2} = \digamma^{(2)}_{n,3}, \ \vdash^{(3)}_{n,6} = \digamma^{(2)}_{n,6}, \vdash^{(3)}_{n,7} = \digamma^{(2)}_{n,7};$$
$$\digamma^{(3)}_{n,3} = \vdash^{(2)}_{n,4}, \digamma^{(3)}_{n,5} = \vdash^{(2)}_{n,5}, \digamma^{(3)}_{n,10} = \vdash^{(2)}_{n,8}.$$

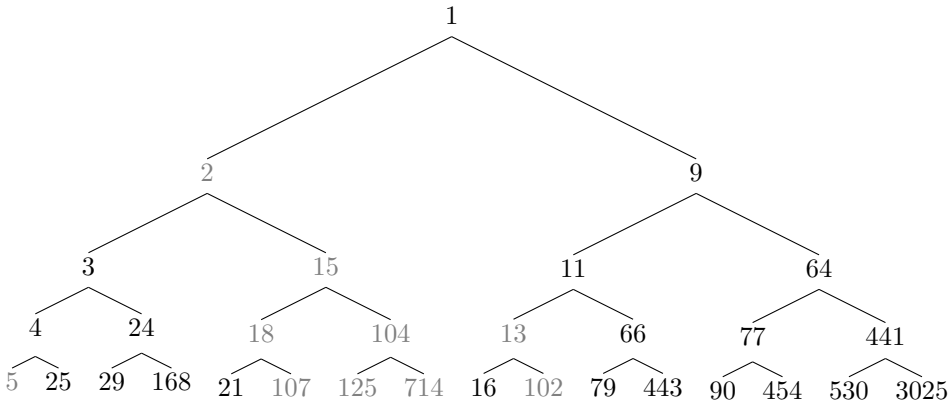

FIGURE 32. Third Fibonacci numeration tree "extrapolated" from the maximal Fibonacci tree and beyond the minimal Fibonacci tree. The left child of n is 3 for $n = 2$ and $n + F_{F^{-1}(n)-3}$ otherwise. The right child of n is $n + F_{F^{-1}(n)+4}$. Cohort dual tree of Figure 33. Sequences of all-left (all-right) branchings are rows of the arrays at the top (bottom) left of Table 38.

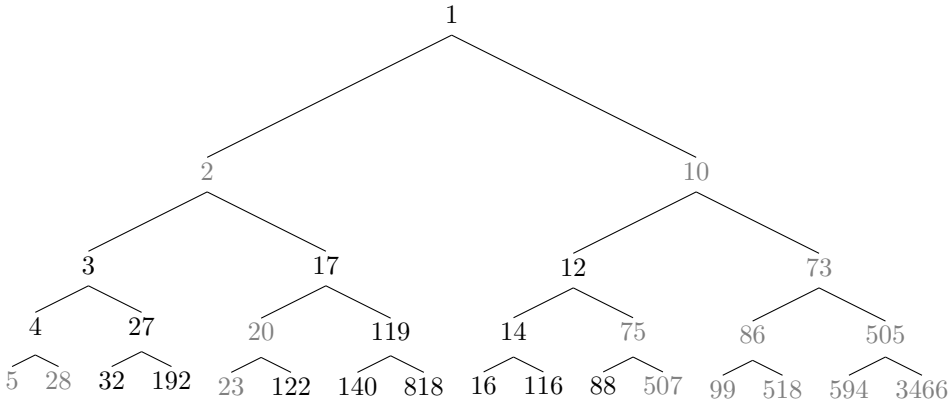

FIGURE 33. Cohort dual of the third "extrapolated" Fibonacci numeration tree (Figure 32). The left child of n is $n + F_{F^{-1}(\lfloor n/3 \rfloor)-1}$. The right child of n is $n + 3F_{F^{-1}(n)+2}$. Sequences of all-left (all-right) branchings are rows of the arrays at the top (bottom) right of Table 38.

⟸ Cohort Duality ⟹

⟸ Mirror Duality ⟹

1	2	3	4	5	6	1	2	3	4	5	6
9	11	13	16	19	22	10	12	14	16	19	22
15	18	21	26	31	36	17	20	23	26	31	36
24	29	34	42	50	58	27	32	37	42	50	58
25	30	35	43	51	59	28	33	38	43	51	59
39	47	55	68	81	94	44	52	60	68	81	94
40	48	56	69	82	95	45	53	61	69	82	95
41	49	57	70	83	96	46	54	62	70	83	96
63	76	89	110	131	152	71	84	97	110	131	152
64	77	90	111	132	153	72	85	98	111	132	153
3rd extrapolated numeration $\vdash^{(3)}$						**3rd ext. num. cohort dual** $\digamma^{(3)}$					
1	9	64	441	3025	20736	1	10	73	505	3466	23761
2	15	104	714	4895	33552	2	17	119	818	5609	38447
3	24	168	1155	7920	54288	3	27	192	1323	9075	62208
4	25	169	1156	7921	54289	4	28	193	1324	9076	62209
5	39	272	1869	12815	87840	5	44	311	2141	14684	100655
6	40	273	1870	12816	87841	6	45	312	2142	14685	100656
7	41	274	1871	12817	87842	7	46	313	2143	14686	100657
8	63	440	3024	20735	142128	8	71	503	3464	23759	162863
10	65	442	3026	20737	142130	9	72	504	3465	23760	162864
11	66	443	3027	20738	142131	11	74	506	3467	23762	162866
3rd extrapolated num. mirror $\dashv^{(3)}$						**3rd ext. num. coh. dual mir.** $\dashv^{(3)}$					

TABLE 38. Quartet of interspersion arrays, corresponding to the third Fibonacci numeration tree "extrapolated" from the maximal Fibonacci tree and beyond the minimal Fibonacci tree. Figure 32 shows this binary tree, for which sequences of all-left (all-right) branchings give rows of the arrays at the top (bottom) left. Rows of the arrays at the top (bottom) right are sequences of all-left (all-right) branchings in the cohort-dual tree Figure 33. Rows of arrays at the top left and right are columns of the tableaux in Tables 39(iii), respectively, (iv). Example 9.1 mentions the coincidence of the 4^{th}, 5^{th}, and 6^{th} columns of $\vdash^{(3)}$ and $\digamma^{(3)}$.

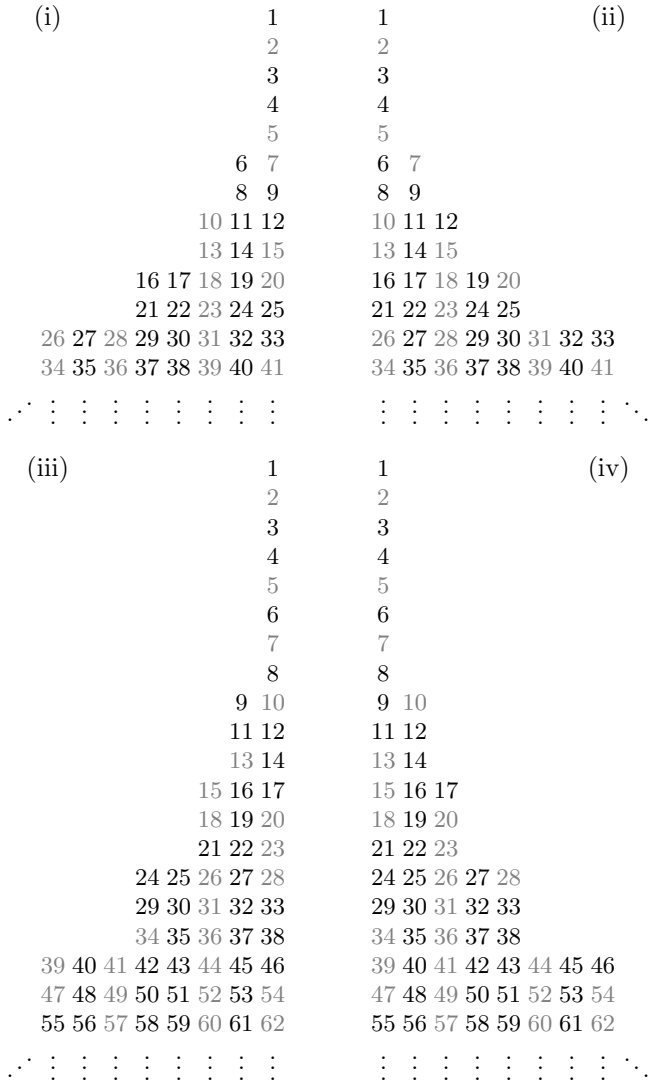

TABLE 39. (i) Cohort tableaux of positive integers for the 2nd extrapolated Fibonacci numeration tree (Figure 30); (ii) and its cohort dual (Figure 31). For (i) and (ii), cohort lengths are $|C_1| = 1$ and $|C_{2t}| = |C_{2t+1}| = F_t$ for $t = 1, 2, 3, \ldots$. Columns are rows of I–D arrays at top of Table 37. (iii) Cohort tableaux of positive integers for the 3rd extrapolated Fibonacci numeration tree (Figure 32); (iv) and its cohort dual (Figure 33). For (iii) and (iv), cohort lengths are $|C_1| = |C_2| = 1$ and $|C_{3t}| = |C_{3t+1}| = |C_{3t+2}| = F_t$ for $t = 1, 2, 3, \ldots$. Columns are rows of I–D arrays at top of Table 38.

Ex. 9.1, continued: Mutual dispersion of cohort duals, analogously to (106), (for $k \geq 1$):

$$\mathsf{L}^{(2)}_{n,2k+5} = \begin{cases} \mathsf{F}^{(2)}_{\mathsf{L}^{(2)}_{n,2k-1},1} - F_{k-1} - F_{k+2}, & n = 0,\ k \geq 2; \\ \mathsf{F}^{(2)}_{\mathsf{L}^{(2)}_{n,2k-1},1}, & n \geq 1,\ k \geq 1; \end{cases}$$

$$\mathsf{L}^{(2)}_{n,2k+6} = \begin{cases} \mathsf{F}^{(2)}_{\mathsf{L}^{(2)}_{n,2k-1},2} - F_{k-1} - F_{k+2}, & n = 0,\ k \geq 2; \\ \mathsf{F}^{(2)}_{\mathsf{L}^{(2)}_{n,2k-1},2}, & n \geq 1,\ k \geq 1; \end{cases}$$

$$\mathsf{F}^{(2)}_{n,2k+7} = \begin{cases} \mathsf{L}^{(2)}_{\mathsf{F}^{(2)}_{n,2k},1} + F_k + F_{k+2}, & n = 0,\ k \geq 1; \\ \mathsf{L}^{(2)}_{\mathsf{F}^{(2)}_{n,2k},1}, & n \geq 1,\ k \geq 1; \end{cases}$$

$$\mathsf{F}^{(2)}_{n,2k+8} = \begin{cases} \mathsf{L}^{(2)}_{\mathsf{F}^{(2)}_{n,2k},2} + F_k + F_{k+2}, & n = 0,\ k \geq 1; \\ \mathsf{L}^{(2)}_{\mathsf{F}^{(2)}_{n,2k},2}, & n \geq 1,\ k \geq 1; \end{cases}$$

$$\mathsf{L}^{(3)}_{n,3k+10} = \begin{cases} \mathsf{F}^{(3)}_{\mathsf{L}^{(3)}_{n,3k-1},1} - F_{k-1} - F_{k+5} + F_{k+2}, & n = 0,\ k \geq 2; \\ \mathsf{F}^{(3)}_{\mathsf{L}^{(3)}_{n,3k-1},1}, & n \geq 1,\ k \geq 1; \end{cases}$$

$$\mathsf{L}^{(3)}_{n,3k+11} = \begin{cases} \mathsf{F}^{(3)}_{\mathsf{L}^{(3)}_{n,3k-1},2} - F_{k-1} - F_{k+5}, & n = 0,\ k \geq 2; \\ \mathsf{F}^{(3)}_{\mathsf{L}^{(3)}_{n,3k-1},2}, & n \geq 1,\ k \geq 1; \end{cases}$$

$$\mathsf{L}^{(3)}_{n,3k+12} = \begin{cases} \mathsf{F}^{(3)}_{\mathsf{L}^{(3)}_{n,3k-1},3} - F_{k-1} - F_{k+5}, & n = 0,\ k \geq 2; \\ \mathsf{F}^{(3)}_{\mathsf{L}^{(3)}_{n,3k-1},3}, & n \geq 1,\ k \geq 1; \end{cases}$$

$$\mathsf{F}^{(3)}_{n,3k+13} = \begin{cases} \mathsf{L}^{(3)}_{\mathsf{F}^{(3)}_{n,3k},1} - F_{k-1} + F_{k+4}, & n = 0,\ k \geq 1; \\ \mathsf{L}^{(3)}_{\mathsf{F}^{(3)}_{n,3k},1}, & n \geq 1,\ k \geq 1; \end{cases}$$

$$\mathsf{F}^{(3)}_{n,3k+14} = \begin{cases} \mathsf{L}^{(3)}_{\mathsf{F}^{(3)}_{n,3k},2} - F_{k-1} + F_{k+4}, & n = 0,\ k \geq 1; \\ \mathsf{L}^{(3)}_{\mathsf{F}^{(3)}_{n,3k},2}, & n \geq 1,\ k \geq 1; \end{cases}$$

$$\mathsf{F}^{(3)}_{n,3k+15} = \begin{cases} \mathsf{L}^{(3)}_{\mathsf{F}^{(3)}_{n,3k},3} - F_{k-1} + F_{k+4}, & n = 0,\ k \geq 1; \\ \mathsf{L}^{(3)}_{\mathsf{F}^{(3)}_{n,3k},3}, & n \geq 1,\ k \geq 1; \end{cases}$$

9.3. **Diatomic tableaux and "clade-type" I–D Arrays.** Rearrange columns of each of the successor tableaux, Tables 19(i) and (ii), so as to place the elements in each cohort in increasing order from left to right. Tables 40(i) and (ii) show the results. As the ordered tableaux continue downward to successive cohorts, new columns start not just at one end of each successive cohort, but also in the interior of the cohort, thus pushing the existing columns farther apart. As new cohorts are tabulated, earlier cohorts grow ever sparser due to the interpolation of new columns. Thus, "diatomic tableaux" provides an apt name for this type of construction, inspired by Lehmer's 1929 tabulation of an 1855 series by Stern [28].

Definition 9.1 ([Tentative] Branch-type and clade-type I–D arrays)**.** As tentative definitions, let a *dense tableau* designate a tableau of the positive integers in

(i)

C_1	1																															C_1
C_2	2																															C_2
C_3	3							4																								C_3
C_4	5				6			7																								C_4
C_5	8		9		10			11			12																					C_5
C_6	13		14	15		16		17	18		19	20																				C_6
C_7	21	22	23	24	25	26	27	28	29	30	31	32	33																			C_7
⋮	⋮	⋮	⋮	⋮	⋮	⋮	⋮	⋮	⋮	⋮	⋮	⋮	⋮	⋱																		⋮

(ii)

C_1																																1	C_1
C_2																																2	C_2
C_3															3																	4	C_3
C_4															5			6														7	C_4
C_5							8								9			10			11				12								C_5
C_6					13	14				15	16				17			18	19				20										C_6
C_7	21	22	23	24	25	26	27	28	29	30	31	32	33																					C_7
⋮	⋮	⋮	⋮	⋮	⋮	⋮	⋮	⋮	⋮	⋮	⋮	⋮	⋮		⋱																			⋮

TABLE 40. Fibonacci cohort "diatomic" tableaux — (i) and (ii) — order each cohort of the corresponding "dense," partially-deranged tableaux (Tables 19(i), respectively, (ii)), aligning each element directly above its left child from the minimal (i) or maximal (ii) successor tree. Columns of (i) and (ii) give rows of w and a, respectively.

their natural order with nondecreasing cohort (row) lengths and the entire tableau aligned either to the left (Examples: Tables 6(i), 34(i) and (iii), 39(ii) and (iv), 42(i)) or to the right (Examples: Table 6(ii), 34(ii) and (iv), 39(i) and (iii), 42(iii)).

Let a *branch-type I–D array* designate *either* an I–D array whose rows may be arranged as columns of a dense tableau, *or* the mirror dual of such an array. Example: Rows of the branch quartet arrays (Table 3) may be arranged as columns of the (dense) Fibonacci cohort tableaux (Tables 6) as indicated by Table 28.

By contrast, let a *clade-type I–D array* designate an I–D array whose rows cannot be arranged as columns of a dense tableau, *nor* can those of its mirror dual. Example: Rows of the clade quartet arrays (Table 4) may be arranged as columns of partially-deranged tableaux (Tables 19), or as columns of diatomic tableaux (Tables 40), but not as dense tableau of the positive integers arranged in their natural order.

9.4. **The Blade Quartet of I–D Arrays.** Referring to the "Positions tree" and the Blade tree (Figures 18 and 21, respectively), Table 41 shows the I–D arrays that obtain by taking all-left or all-right branchings or left clades or right clades in the two trees. The OEIS records two of these as 054582 and 191448.

An examination of the associated tableaux, Table 42, indicates that for the blade quartet, mirror duality and cohort duality are equivalent, whereas each cohort occupies a full level of the associated tree, so that mirroring the tree corresponds to mirroring the structure of each cohort. Cohort lengths follow $|C_t| = 2^{t-1}$ for $t = 1, 2, 3, \ldots$.

Remarks 4.12 and 4.27 described the binary trees of the positive integers descending from root node 1 and constructed via branching rules that use a Beatty pair $\lfloor n\mu \rfloor$ and $\lfloor n\nu \rfloor$. As the irrational slopes μ and ν of the Beatty pair approach 2 from the left, respectively, right, the Positions tree (Figure 18) also provides the "limiting tree."

Like the Fibonacci and successor trees, the Blade and Positions trees exhibit complete clade–tree order isomorphism, meaning that elements in any left or right clade are ordered identically to one another and to the tree itself. It may be that the Positions tree forms a "kinship" with the successor trees, whereas $[1; 1, 1, 1, \ldots]$ gives the continued fraction expansion of ϕ while $1.111\cdots$ gives the binary decimal expansion of a number approaching 2 from below.

Section 9.5 now describes how branching rules can generate multiple, distinct trees for each Beatty pair by "shifting" the rule (Corollary 9.2).

⟸ Blade Duality ⟹

Right clades of Positions tree						Right clades of Blade tree					
1	2	4	8	16	32	1	2	4	8	16	32
3	5	9	17	33	65	3	6	12	24	48	96
6	10	18	34	66	130	5	10	20	40	80	160
7	11	19	35	67	131	7	14	28	56	112	224
12	20	36	68	132	260	9	18	36	72	144	288
13	21	37	69	133	261	11	22	44	88	176	352
14	22	38	70	134	262	13	26	52	104	208	416
15	23	39	71	135	263	15	30	60	120	240	480
24	40	72	136	264	520	17	34	68	136	272	544
25	41	73	137	265	521	19	38	76	152	304	608
Blade Array						**Positions Array (054582)**					
1	3	7	15	31	63	1	3	7	15	31	63
2	6	14	30	62	126	2	5	11	23	47	95
4	12	28	60	124	252	4	9	19	39	79	159
5	13	29	61	125	253	6	13	27	55	111	223
8	24	56	120	248	504	8	17	35	71	143	287
9	25	57	121	249	505	10	21	43	87	175	351
10	26	58	122	250	506	12	25	51	103	207	415
11	27	59	123	251	507	14	29	59	119	239	479
16	48	112	240	496	1008	16	33	67	135	271	543
17	49	113	241	497	1009	18	37	75	151	303	607
Blade Mirror						**Positions Mirror (191448)**					
Left clades of Positions tree						Left clades of Blade tree					

⟸ Mirror Duality = Cohort Duality ⟹

All-left paths in Blade tree / Cols of 1–2 dense tableau

All-right paths in Blade tree / Cols of 2–1 dense tableau

All-left paths in Positions tree / Cols of 1–2 diatomic tableau

All-right paths in Positions tree / Cols of 2–1 diatomic tableau

TABLE 41. The Blade Quartet comprising two branch-type I–D arrays, the Blade array (dispersion of 004754) and Blade mirror (dispersion of 004755), and two clade-type I–D arrays, the "Positions array" and "Positions mirror." At left, rows equal straight paths in the Blade tree (Figure 21) and columns equal clades of the Positions tree (Figure 18). At right, rows equal straight paths in the Positions tree and columns equal clades of the Blade tree. For each of the four arrays, rows are columns of the tableau in the corresponding position of Table 42.

9.5. **Shifted branching rules that use Beatty pairs.** —
Remarks 4.12 and 4.27 considered pairs of complementary spectrum sequences $\lfloor n\mu \rfloor$ and $\lfloor n\nu \rfloor$ with irrational slopes μ and ν that satisfy $\frac{1}{\mu} + \frac{1}{\nu} = 1$. Depending on the value of the slope, the Remarks identified either one or two binary-tree arrangements of the positive integers descending from root node 1 and employing the Beatty pair in the branching rule for the trees. In the case where two binary-trees shared the same Beatty pair, the branching rules of the trees were based on two distinct partitions of the positive integers, and it possible to extend the list of available

(i)

```
 1
 2  3
 4  5  6  7
 8  9 10 11 12 13 14 15
16 17 18 19 20 21 22 23 24 25 26 27 28 29 30 31
```

(ii)

```
 1
 2                 3
 4        5        6        7
 8     9  10    11  12    13  14    15
16 17 18 19 20 21 22 23 24 25 26 27 28 29 30 31
```

(iii)

```
                                                 1
                                              2  3
                                           4  5  6  7
                                        8  9 10 11 12 13 14 15
16 17 18 19 20 21 22 23 24 25 26 27 28 29 30 31
```

(iv)

```
                                                 1
                                              2  3
                                        4     5     6     7
                                     8     9    10    11    12    13    14    15
16 17 18 19 20 21 22 23 24 25 26 27 28 29 30 31
```

TABLE 42. I–D arrays of the Blade Quartet, Table 41, rearranged as two dense tableaux (i) and (iii) and two diatomic tableaux (ii) and (iv). All are planar graph isomorphic to the Positions tree. For the diatomic tableaux (ii) and (iv), columns can also be reordered to yield partially-deranged, dense tableaux that are planar graph isomorphic to the Blade tree.

partitions according to the proximity of the slopes μ and ν to 2, as follows: $\mathbb{Z}_{\geq 1} =$

$$\begin{aligned}
&\{1\} \cup [\lfloor \mu \mathbb{Z}_{\geq 1} \rfloor + 1] \quad \cup \quad [\lfloor \nu \mathbb{Z}_{\geq 1} \rfloor + 1] && \text{for} \quad 1 < \mu < 2 < \nu < \infty, \\
&\{1\} \cup [\lfloor \mu \mathbb{Z}_{\geq 2} \rfloor - 1] \quad \cup \quad [\lfloor \nu \mathbb{Z}_{\geq 2} \rfloor - 1] && \text{for} \quad 3/2 < \mu < 2 < \nu < 3, \\
&\{1\} \cup [\lfloor \mu \mathbb{Z}_{\geq 3} \rfloor - 3] \quad \cup \quad [\lfloor \nu \mathbb{Z}_{\geq 3} \rfloor - 3] && \text{for} \quad 5/3 < \mu < 2 < \nu < 5/2, \\
&\quad \vdots \qquad\qquad \vdots \qquad\qquad \vdots && \quad \vdots \qquad \vdots \qquad\qquad \vdots \\
&\{1\} \cup [\lfloor \mu \mathbb{Z}_{\geq m} \rfloor - 2m + 3] \cup [\lfloor \nu \mathbb{Z}_{\geq m} \rfloor - 2m + 3] && \text{for} \quad \tfrac{2m-1}{m} < \mu < 2 < \nu < \tfrac{2m-1}{m-1},
\end{aligned}$$

where on each line, the intersection between any of the three sets is empty, so that for $\frac{2\bar{m}-1}{\bar{m}} < \mu < 2$, a binary tree rooted at 1 and employing the branching rule $n \mapsto (\lfloor (n+m-1)\mu \rfloor - 2m + 3, \lfloor (n+m-1)\nu \rfloor - 2m + 3)$ for any integer $m = 1, \ldots, \bar{m}$ provides an arrangement of $\mathbb{Z}_{\geq 1}$. Remarks 4.27 and 4.12 treated the first ($m = 1$) and second ($m = 2$) partitions, respectively. Lemma 9.1 formally shows the existence of the remaining partitions.

Lemma 9.1 (Partitions of the positive integers by shifting Beatty pairs)**.** *For integer $m \geq 2$, let $\frac{2m-1}{m} < \mu < 2$ be an irrational. Then for $\nu \equiv \frac{1}{(1-\frac{1}{\mu})}$, $\mathbb{Z}_{\geq 1} = \{1\} \cup [\lfloor \mu \mathbb{Z}_{\geq m} \rfloor - 2m + 3] \cup [\lfloor \nu \mathbb{Z}_{\geq m} \rfloor - 2m + 3]$, and pairwise intersections of sets in the union are empty. To wit, $1 \notin [\lfloor \mu \mathbb{Z}_{\geq m} \rfloor - 2m + 3]$, $1 \notin [\lfloor \nu \mathbb{Z}_{\geq m} \rfloor - 2m + 3]$, and $[\lfloor \mu \mathbb{Z}_{\geq m} \rfloor - 2m + 3] \cap [\lfloor \nu \mathbb{Z}_{\geq m} \rfloor - 2m + 3] = \emptyset$.*

Proof. By the definition of ν, for $n = 1, 2, 3, \ldots$ the complementary spectrum sequences $\lfloor \mu n \rfloor$ and $\lfloor \nu n \rfloor$ partition the positive integers. Thus, $\lfloor \mu \mathbb{Z}_{\geq m} \rfloor \cap \lfloor \nu \mathbb{Z}_{\geq m} \rfloor = \emptyset$, and moreover, $\lfloor \mu \mathbb{Z}_{\geq m} \rfloor \cup \lfloor \nu \mathbb{Z}_{\geq m} \rfloor = Z_{\geq 1} \backslash \{\lfloor \mu \rfloor, \ldots, \lfloor \mu(m-1) \rfloor, \lfloor \nu \rfloor, \ldots, \lfloor \nu(m-1) \rfloor\}$. Now since $\frac{2m-1}{m} < \mu < 2$, $2m - 3 = \left\lfloor \frac{(2m-1)(m-1)}{m} \right\rfloor \leq \lfloor \mu(m-1) \rfloor < 2m - 2$, where the nonstrict inequality must hold with equality. Thus, $\lfloor \mu \rfloor = 1 < \cdots < \lfloor \mu(m-1) \rfloor = 2m - 3$.

Further, since $2 < \nu < \frac{2m-1}{m-1}$, then $2(m-1) \leq \lfloor \nu(m-1) \rfloor < 2m - 1$, where the nonstrict equality must hold with equality. Thus, $\lfloor \nu \rfloor = 2 < \cdots < \lfloor \nu(m-1) \rfloor =$

$2m-2$. Consequently, $\lfloor \mu\mathbb{Z}_{\geq m} \rfloor \cup \lfloor \nu\mathbb{Z}_{\geq m} \rfloor = \mathbb{Z}_{\geq 2m-1}$ with $\lfloor \mu\mathbb{Z}_{\geq m} \rfloor \cap \lfloor \nu\mathbb{Z}_{\geq m} \rfloor = \emptyset$. By subtracting $2m-3$ from each, the two resulting sets partition $\mathbb{Z}_{\geq 2}$ as claimed. □

Corollary 9.2 (of Proposition 4.12)**.** *For integer $m \geq 1$ and irrational slopes $^{2m-1}/_{m} < \mu < 2$ and $\nu \equiv {}^{1}/_{(1-\frac{1}{\mu})}$, a binary tree rooted at 1 employing the branching rule $n \mapsto (\lfloor (n+m-1)\mu \rfloor - 2m+3, \lfloor (n+m-1)\nu \rfloor - 2m+3)$ arranges the positive integers. Distinct integers m satisfying $1 \leq m < \bar{m} = \frac{1}{2-\mu}$ yield distinct trees.*

Proof. Using the partitions of the positive integers given in Lemma 9.1, it follows that each tree arranges the positive integers by the same argument as in the proof of Proposition 4.12.

To show that any two such trees are distinct, consider two trees whose branching rules employ the distinct integer parameters m_1 and m_2 with $1 \leq m_1 < m_2 \leq \bar{m}$, and let $n \geq m_1$.

In the first tree, node $n - m_1 + 1$ has left child $\lfloor (n - m_1 + 1 + m_1 - 1)\mu \rfloor - 2m_1 + 3 = \lfloor n\mu \rfloor - 2m_1 + 3$, while in the second tree, node $n - m_1 + 1$ has left child $\lfloor (n - m_1 + 1 + m_2 - 1)\mu \rfloor - 2m_2 + 3 = \lfloor (n + (m_2 - m_1))\mu \rfloor - 2m_2 + 3$.

Thus, equality of the two trees requires that $\lfloor (n + (m_2 - m_1))\mu \rfloor - \lfloor n\mu \rfloor = 2(m_2 - m_1)$, for all $n \geq m_1$, which is impossible for μ irrational (see, *e.g.*, Lemma 2 of [17]). □

Remark 9.1 (The "shifts" as non-homogeneous Beatty pairs). Writing the shifted branching rule of Corollary 9.2 as $n \mapsto (\lfloor n\mu + (m-1)\mu \rfloor - 2m+3, \lfloor n\nu + (m-1)\nu \rfloor - 2m+3)$ makes it apparent that $\lfloor n\mu + (m-1)\mu \rfloor$ and $\lfloor n\nu + (m-1)\nu \rfloor$ are instances of the *non-homogeneous* Beatty pairs studied by Fraenkel in [15]. This begs several questions: How do the partitions defined by Lemma 9.1 fare relative to the criteria given in [15] and what happens for half-integer values of m?

Firstly, the sets $\{\lfloor n\mu + (m-1)\mu \rfloor \,|n \in \mathbb{Z}\}$ and $\{\lfloor n\nu + (m-1)\nu \rfloor \,|n \in \mathbb{Z}\}$ are $(2-m)$-*upper complementary*. Though $n = 1-m$ gives zero in both sets, thereafter, for $n = 2-m$, $3-m$, $4-m, \ldots$, the sets complement one another in the positive integers, with $n = 2-m$ giving 1 in the first set, whereas $\lfloor (2-m)\mu + (m-1)\mu \rfloor = \lfloor \mu \rfloor = 1$.

For $(2-m)$-upper complementarity, the first criterion in [15] demands that $\frac{(m-1)\mu}{\mu} + \frac{(m-1)\nu}{\nu} = \lfloor (2-m)\mu + (m-1)\mu \rfloor - 2(2-m) + 1$, which clearly holds. The second criterion in [15] holds trivially: Since $n = 1-m$ is the only integer value of $n\nu + (m-1)\nu$, it requires only that $1 - m < 2 - m$.

For m a half integer, the sets $\{\lfloor n\mu + (m-1)\mu \rfloor \,|n \in \mathbb{Z}\}$ and $\{\lfloor n\nu + (m-1)\nu \rfloor \,|n \in \mathbb{Z}\}$ are fully complementary, since there are no integer values of n for which $n\nu + (m-1)\nu$ is an integer (ν being irrational).

Thus for half-integer values of m, results analogous to Lemma 9.1 and Corollary 9.2 do hold, producing partitions, respectively, binary trees of $\mathbb{Z}_{\geq 1}$. These half-integer confections are distinct from one another and from those shifted by integral values of m, provided that $\frac{1}{2} \leq m < \frac{1}{2-\mu}$. Example 9.9 treats such a case.

Example 9.2 (Slopes involving $\sqrt{2}$)**.** Consider the pair of slopes $\mu = \frac{3+\sqrt{2}}{1+\sqrt{2}}$ and $\nu = \frac{3+\sqrt{2}}{2}$. Since $^{2m-1}/_{m} < \mu < 2 < \nu < {}^{2m-1}/_{m-1}$ for $m = 1, 2, 3$ and 4, this pair of slopes yields four distinct binary-tree arrangements of the positive integers based on the branching rules $n \mapsto (\lfloor n\mu \rfloor + 1, \lfloor n\nu \rfloor + 1)$, $n \mapsto (\lfloor (n+1)\mu \rfloor - 1, \lfloor (n+1)\nu \rfloor - 1)$, $n \mapsto (\lfloor (n+2)\mu \rfloor - 3, \lfloor (n+2)\nu \rfloor - 3)$, and $n \mapsto (\lfloor (n+3)\mu \rfloor - 5, \lfloor (n+3)\nu \rfloor - 5)$ from root node 1, and four corresponding mirror-dual pairs of I–D arrays (Table 43).

$\Longleftarrow$ Mirror Duality $\Longrightarrow$

$\Longleftarrow$ Shifting of a branching rule that uses the pair of slopes $(\frac{3+\sqrt{2}}{1+\sqrt{2}}, \frac{3+\sqrt{2}}{2})$

1	2	4	8	15	28	1	3	7	16	36	80
3	6	11	21	39	72	2	5	12	27	60	133
5	10	19	35	64	118	4	9	20	45	100	221
7	13	24	44	81	149	6	14	31	69	153	338
9	17	32	59	108	198	8	18	40	89	197	435
12	22	41	75	138	253	10	23	51	113	250	552
14	26	48	88	161	295	11	25	56	124	274	605
16	30	55	101	185	339	13	29	65	144	318	702
18	33	61	112	205	375	15	34	76	168	371	819
20	37	68	125	229	419	17	38	84	186	411	908
1st Beatty shift						**1st Beatty shift mirror**					
1	2	4	8	15	28	1	3	7	16	36	80
3	6	11	20	37	68	2	5	12	27	60	133
5	9	17	31	57	105	4	10	23	51	113	250
7	13	24	44	81	148	6	14	32	71	157	347
10	19	35	64	117	214	8	18	40	89	197	436
12	22	41	75	137	251	9	21	47	104	230	508
14	26	48	88	161	295	11	25	56	124	274	605
16	30	55	101	185	339	13	29	65	144	319	705
18	33	61	112	205	375	15	34	76	168	372	822
21	39	72	132	242	443	17	38	85	188	416	919
2nd Beatty shift						**2nd Beatty shift mirror**					
1	2	4	7	13	24	1	3	8	19	43	96
3	6	11	20	37	68	2	5	12	27	61	136
5	9	17	31	57	104	4	10	23	52	116	257
8	15	28	51	93	170	6	14	32	72	160	354
10	18	33	60	110	201	7	16	36	80	177	392
12	22	40	73	134	245	9	21	47	105	233	515
14	26	48	88	161	295	11	25	56	125	277	612
16	29	53	97	178	326	13	30	67	149	330	729
19	35	64	117	214	391	15	34	76	169	374	826
21	39	71	130	238	435	17	38	85	189	418	923
3rd Beatty shift						**3rd Beatty shift mirror**					
1	2	4	7	13	24	1	3	8	19	43	96
3	5	9	16	29	53	2	6	14	32	72	160
6	11	20	37	68	124	4	10	23	52	116	257
8	15	27	49	90	165	5	12	28	63	140	310
10	18	33	60	110	201	7	17	39	87	193	427
12	22	40	73	133	243	9	21	47	105	233	515
14	26	48	88	161	294	11	25	56	125	277	612
17	31	57	104	190	347	13	30	67	149	330	729
19	35	64	117	214	391	15	34	76	169	374	827
21	38	69	126	230	421	16	36	81	180	398	880
4th Beatty shift						**4th Beatty shift mirror**					

TABLE 43. Four pairs of I–D arrays arising from binary trees (not depicted) related to one another by "shifting" the branching rule. The branching rule of each tree uses the pair of slopes $(\mu, \nu) = (\frac{3+\sqrt{2}}{1+\sqrt{2}}, \frac{3+\sqrt{2}}{2})$. Shifts $m = 1, 2, 3, 4$, produce distinct arrangements of the positive integers into trees rooted at 1, based on branching node n into left and right children $\lfloor (n+m-1)\mu \rfloor - 2m + 3$, respectively, $\lfloor \lfloor (n+m-1)\nu \rfloor - 2m + 3$. Rows of the array at the left (right) are straight all-left (all-right) branchings in each tree.

Example 9.3 (Slopes involving $\sqrt{3}$)**.** For $\mu = \frac{3+\sqrt{3}}{1+\sqrt{3}}$ and $\nu = \frac{3+\sqrt{3}}{2}$, Corollary 9.2 produces three trees, and the OEIS [41] records several of the corresponding I–D arrays (Table 44). For example, with the branching rule $n \mapsto (\lfloor n\mu \rfloor + 1, \lfloor n\nu \rfloor + 1)$ descending from 1, all-left branchings of the resulting binary tree give (rows of) 191443. The second branching rule $n \mapsto (\lfloor (n+1)\mu \rfloor - 1, \lfloor (n+1)\nu \rfloor - 1)$, similarly gives rise to an interspersion array, not recorded in the OEIS at present, whereas for the third branching rule $n \mapsto (\lfloor (n+2)\mu \rfloor - 3, \lfloor (n+2)\nu \rfloor - 3)$, all-left branchings of the resulting binary tree produce (the rows of) 191442. For each tree, all-right branchings produce (rows of) the array at the right, it being the mirror dual of the corresponding array to its left.

Note that the closer the irrational slope μ approaches 2 from the left (and ν approaches 2 from the right), the greater the number of distinct binary tree arrangements of the positive integers can be produced using the same (μ, ν) pair.

On the other hand, Section 9.4 already noted that as μ and ν get arbitrarily close to 2 (from the left and right, respectively), branching rules converges to $n \mapsto (2n, 2n+1)$, for all values of m in Corollary 9.2, and thus, the resulting binary trees approach the Positions tree, Figure 18. Indeed, for $t = 1, 2, 3, \ldots$, cohort lengths $|C_t| = 2^{t-1}$ for the positions tree follow the recurrence $|C_t| = 2|C_{t-1}|$, whereas each cohort C_t alternates left and right branchings of elements S from the prior cohort as $C_t = (S_{2^{t-1}}, \ldots, S_{2^t-1}) = (2S_{2^{t-2}}, 2S_{2^{t-2}} + 1, \ldots, 2S_{2^{t-1}-1}, 2S_{2^{t-1}-1} + 1)$.

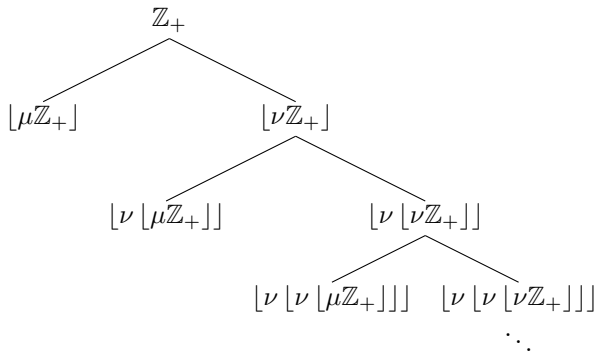

FIGURE 34. Leaves of the tree partition the positive integers into subsequences: $\mathbb{Z}_+ = \lfloor \mu\mathbb{Z}_+ \rfloor \cup \lfloor \nu \lfloor \mu\mathbb{Z}_+ \rfloor \rfloor \cup \lfloor \nu \lfloor \nu \lfloor \mu\mathbb{Z}_+ \rfloor \rfloor \rfloor \cup \cdots$, for a complementary pair of irrational slopes $1 < \mu < 2$ and $\nu \equiv 1/(1-\frac{1}{\mu})$.

9.5.1. *A branching rule that uses unshifted Beatty pairs.*

Proposition 9.3 (A branching rule that uses unshifted Beatty pairs)**.** *Consider a conjugate pair of irrational slopes $1 < \mu < 2$ and $\nu \equiv 1/(1-\frac{1}{\mu})$. Let $\bar{l}(n) = \lfloor n\mu \rfloor$ and $\bar{r}(n) = \lfloor n\nu \rfloor$. Then, in addition to the binary tree arrangements of $\mathbb{Z}_+$ identified in Corollary 9.2, the tree descending from 1 having as straight all-left branchings $\bar{l}(n), \bar{r}\bar{l}(n), \bar{r}^2\bar{l}(n), \ldots$, for $n = 1, 2, 3, \ldots$ also arranges the positive integers. Moreover, the corresponding array with entries $\bar{r}^{k-1}\bar{l}(n+1)$, for rows $n = 0, 1, 2, \ldots$ and columns $k = 1, 2, 3, \ldots$ is an I–D array.*

Proof. Consider the partition of $\mathbb{Z}_+$ into the sequences shown in Figure 34. Because $\mu < \nu$, each left child (leaf) in the Figure contains the least element of its parent,

$\Longleftarrow$ Mirror Duality $\Longrightarrow$

$\Longleftarrow$ Shifting of a branching rule that uses the pair of slopes $(\frac{3+\sqrt{3}}{1+\sqrt{3}}, \frac{3+\sqrt{3}}{2})$

1	2	4	7	13	23	1	3	8	19	45	107
3	6	11	20	35	61	2	5	12	29	69	164
5	9	16	28	49	85	4	10	24	57	135	320
8	14	25	44	77	134	6	15	36	86	204	483
10	18	32	56	97	169	7	17	41	98	232	549
12	21	37	65	113	196	9	22	53	126	299	708
15	26	46	80	139	241	11	27	64	152	360	852
17	30	52	91	158	274	13	31	74	176	417	987
19	33	58	101	175	304	14	34	81	192	455	1077
22	39	68	118	205	356	16	38	90	213	504	1193
1st Beatty shift (191443)						**1st Beatty shift mirror**					
1	2	4	7	12	21	1	3	8	20	48	114
3	5	9	16	28	49	2	6	15	36	86	204
6	11	19	33	57	99	4	10	25	60	143	339
8	14	24	42	73	127	5	13	32	77	183	434
10	18	31	54	94	163	7	17	41	98	233	552
13	23	40	70	121	210	9	22	53	126	299	708
15	26	45	78	135	234	11	27	65	155	368	872
17	30	52	90	156	270	12	29	69	164	389	921
20	35	61	106	184	319	14	34	81	193	458	1085
22	38	66	115	199	345	16	39	93	221	524	1241
2nd Beatty shift						**2nd Beatty shift mirror**					
1	2	3	5	9	16	1	4	11	27	65	155
4	7	12	21	36	62	2	6	15	37	89	212
6	10	17	29	50	87	3	8	20	49	117	278
8	14	24	42	73	126	5	13	32	77	183	434
11	19	33	57	99	171	7	18	44	105	250	593
13	22	38	66	114	197	9	23	56	134	318	754
15	26	45	78	135	234	10	25	60	143	340	806
18	31	54	93	161	279	12	30	72	172	408	967
20	35	61	106	184	319	14	34	82	195	463	1097
23	40	69	119	206	357	16	39	94	224	531	1258
3rd Beatty shift (191442)						**3rd Beatty shift mirror**					

TABLE 44. Three pairs of I–D arrays arising from binary trees (not depicted) related to one another by "shifting" the branching rule. The branching rule of each tree uses the pair of slopes $(\mu, \nu) = (\frac{3+\sqrt{3}}{1+\sqrt{3}}, \frac{3+\sqrt{3}}{2})$. Shifts $m = 1, 2, 3$, produce distinct arrangements of the positive integers into trees rooted at 1, based on branching node n into left and right children $\lfloor (n+m-1)\mu \rfloor - 2m+3$, respectively, $\lfloor (n+m-1)\nu \rfloor - 2m+3$. Rows of the array at the left (right) are straight all-left (all-right) branchings in each tree.

and in particular, $1 \in \lfloor \mu \mathbb{Z}_+ \rfloor$. Take the least element of each leaf in the figure as a subsequence $\bar{l}(1), \bar{r}\bar{l}(1), \bar{r}^2\bar{l}(1), \ldots$, the second-least element of each leaf as a subsequence $\bar{l}(2), \bar{r}\bar{l}(2), \bar{r}^2\bar{l}(2), \ldots$, and so forth. Observe that $\bar{l}(1) < \bar{l}(2) < \bar{l}(3) < \cdots$.

To grow a tree arranging the positive integers, rooted at 1 with one integer per node, use the first subsequence as the straight all-left branching descending from

the root node 1, then graft the second subsequence onto 1 as its right child and the straight all-left branching descending therefrom. For $n = 3, 4, 5, \ldots$, continue attaching each subsequence $\bar{l}(n), \bar{r}\bar{l}(n), \bar{r}^2\bar{l}(n), \ldots$ to the tree by grafting it onto the node of least value that does not already have a right child (a "mex-equivalent" construction of the tree, see Remark 9.3).

Thus for $k = 1, 2, 3, \ldots$, the k^{th} leaf in Figure 34 corresponds to a column of an array that comprises successive entries $\bar{r}^{k-1}\bar{l}(n+1)$, on rows $n = 0, 1, 2, \ldots$. In terms of Kimberling's dispersion properties [20], the first column $\bar{l}(1), \bar{l}(2), \bar{l}(3), \ldots$ of the array strictly increases (property D1), the element at the top of the second column (and to the immediate right of $\bar{l}(1) = \lfloor \mu \rfloor = 1$) is $\bar{r}\bar{l}(1) = \min \lfloor \nu \mathbb{Z}_+ \rfloor = \lfloor \nu \rfloor \geq 2$, the least element of the complement of the first column (D2), and the second and subsequent columns of the array comprise $\lfloor \nu \mathbb{Z}_+ \rfloor$, the complement of the first column $\lfloor \mu \mathbb{Z}_+ \rfloor$ (D3). Thus as an ordered sequence, the second and subsequent columns of the array give $\bar{r}(m)$ for $m = 1, 2, 3, \ldots$, so that $\bar{r}(\bar{r}^{k-2}\bar{l}(n+1)) = \bar{r}^{k-1}\bar{l}(n+1)$ (D4). Consequently, $\big(\bar{r}^{k-1}\bar{l}(n+1)\big)$, for rows $n = 0, 1, 2, \ldots$ and columns $k = 1, 2, 3, \ldots$ produces an I–D array. □

Example 9.4 (Wythoff difference quartet)**.** The I–D array 080164 at the bottom right of Table 45 exemplifies Proposition 9.3, in as much as its first column equals $\lfloor \phi \mathbb{Z}_+ \rfloor$, its second column equals $\lfloor \phi^2 \lfloor \phi \mathbb{Z}_+ \rfloor \rfloor$, its third column equals $\lfloor \phi^2 \lfloor \phi^2 \lfloor \phi \mathbb{Z}_+ \rfloor \rfloor \rfloor$, and so forth (leaves of the tree in Figure 34 for $\mu = \phi$). Example 4.23 gives cohortizers for its columns. The OEIS calls this array the "Wythoff difference array" [41]. Applying cohort duality and mirror duality allows for completion of the "Wythoff difference quartet."

9.6. **Bergman Pairs.** (Slopes involving $\sqrt{5}$) Definition 4.8 gave Bergman pairs $\{\kappa_b, \lambda_b\}$ (45) and Bergman inverse pairs $\{\theta_b, \eta_b\}$ (46), where $b = 1$ are the Wythoff and inverse Wythoff pairs. For $b \geq 1$, the pairs of slopes $(\frac{2b+1+\sqrt{5}}{2b-1+\sqrt{5}}, \frac{2b+1+\sqrt{5}}{2})$ $= (\frac{\phi+b}{\phi+b-1}, \phi+b)$ have the continued fraction expansions $\frac{\phi+b}{\phi+b-1} = [1, b, \bar{1}]$ and $\phi+b = [b+1, \bar{1}]$, respectively. The repeating 1 in the continued fraction expansions tends to engender nice properties and simple proofs thereof (*e.g.*, Lemma 4.51). Compared with the families of Beatty pairs mentioned in Example 9.2, $(\frac{2b+1+\sqrt{2}}{2b-1+\sqrt{2}}, \frac{2b+1+\sqrt{2}}{2})$, and Example 9.3, $(\frac{2b+1+\sqrt{3}}{2b-1+\sqrt{3}}, \frac{2b+1+\sqrt{3}}{2})$, the family of Bergman pairs thus seems more attractive for investigation. As the first "Bergman extension" of the pair κ and λ, consider $b = 2$ and by analogy to the maximum successor tree (Figure 10), the Bergman$_2$ tree of the positive integers, Figure 35, descending from root node 1 via $\bar{l}(n) = \kappa_2(n) + 1 = -\kappa_2(-n)$ and $\bar{r}(n) = \lambda_2(n) + 1 = -\lambda_2(-n)$. Sequences of all-left or all-right branchings in the Bergman$_2$ tree provide, respectively, the Bergman$_2$ array and Bergman$_2$ mirror array (Table 46), two I–D arrays associated to the tree.

The nature of the analogy is as follows. Take compositions S in the free monoid $\{\kappa_2, \lambda_2\}^\star$ and arrange them as an outer binary tree rooted at the identity. Then $-S(-1)$ provides a bijection to Figure 35. Equivalently, take compositions T in the free monoid $\{\theta_2, \eta_2\}^\star$ and arrange them as an inner binary tree rooted at the identity. Then $N_0(T) + 1$ provides a bijection to Figure 35. (Existence of these bijections follows from Proposition 4.35, wherein $T = \mathsf{BeattyInvert}(\overleftrightarrow{S})$ and $S = \mathsf{BeattyInvert}^{-1}(\overleftrightarrow{T})$.)

$\Longleftarrow$ Cohort Duality $\Longrightarrow$

$\Longleftrightarrow$ Mirror Duality $\Longleftrightarrow$

1	2	4	7	12	20	1	3	6	11	19	32
3	6	10	17	28	46	2	4	8	14	24	40
5	9	15	25	41	67	5	9	16	27	45	74
8	14	23	38	62	101	7	12	21	35	58	95
11	19	31	51	83	135	10	17	29	48	79	129
13	22	36	59	96	156	13	22	37	61	100	163
16	27	44	72	117	190	15	25	42	69	113	184
18	30	49	80	130	211	18	30	50	82	134	218
21	35	57	93	151	245	20	33	55	90	147	239
24	40	65	106	172	279	23	38	63	103	168	273
$F_{k+2}-1,\ n=0;$					(175004)	$F_{k+3}-2,\ n=0;$					(191428)
$F_{k+1}\kappa(n+1)+F_k n-1, n\geq 1.$						$F_{k+1}\kappa(n)+F_k n+F_{k+2}-2, n\geq 1.$					
1	3	8	21	55	144	1	2	5	13	34	89
2	5	13	34	89	233	3	7	18	47	123	322
4	11	29	76	199	521	4	10	26	68	178	466
6	16	42	110	288	754	6	15	39	102	267	699
7	18	47	123	322	843	8	20	52	136	356	932
9	24	63	165	432	1131	9	23	60	157	411	1076
10	26	68	178	466	1220	11	28	73	191	500	1309
12	32	84	220	576	1508	12	31	81	212	555	1453
14	37	97	254	665	1741	14	36	94	246	644	1686
15	39	102	267	699	1830	16	41	107	280	733	1919
$F_{2k}\quad[\kappa(n+2)-2]$					$n\geq 0.$	$\lambda^{k-1}\kappa(n+1)$					(080164)
$-F_{2k-2}[\kappa(n+1)-(n+1)],$						$=F_{2k-1}\kappa(n+1)+F_{2k-2}n, n\geq 0.$					

TABLE 45. "Wythoff Difference quartet" of I–D arrays. (Rows of) arrays on the left obtain from (straight all-left or all-right branchings in) a tree of the positive integers descending from 1 with branching rule $n \mapsto (\kappa(n+2)-2, \lambda(n+1)-2)$. Arrays on the right obtain from a tree of the positive integers descending from 1 with branching rule $n \mapsto (\kappa(n+1), \lambda(n))$.

By analogy to $\underline{200648}_2$ for $b=1$, for $b=2$, if the compositions in either $\{\kappa_2, \lambda_2\}^\star$ or $\{\theta_2, \eta_2\}^\star$ are placed in sequence according the corresponding value in Figure 35, the number of symbols in the composition — or equivalently, the level of the tree in which integer n appears — forms the sequence 1, 2, 3, 2, 4, 3, 5, 3, 4, 6, 4, 4, 5, 7, 3, 5, 5, 6, 5, 8, 4, 4, 6, 6, 7, 6, 6, 9,..., not found in the OEIS [41] as of this writing, and not following an identifiable recurrence.

Despite the convenient form of the continued fraction expansions for $\frac{\phi+b}{\phi+b-1}$ and $\phi+b$, which, with their repeating 1s, resemble that of ϕ, not all the nice properties of the free monoid $\{\kappa_b, \lambda_b\}^\star$ for $b=1$ extend to the Bergman family for $b>1$. For $b=1$, the 2–1-Fibonacci cohort tableau (Table 6(ii)) grouped the positive integers into cohorts according to the "degree" of the composition that produced them (Table 13). In that context, a composition with t symbols first occurs at the end of cohort t, $n=F_{t+2}-1$ being the least n for which $\underline{200648}(n+1)=t$. This gives cohort lengths $|C_t|=F_t$ for $t=1,2,3,\ldots$. Applying the same reasoning to

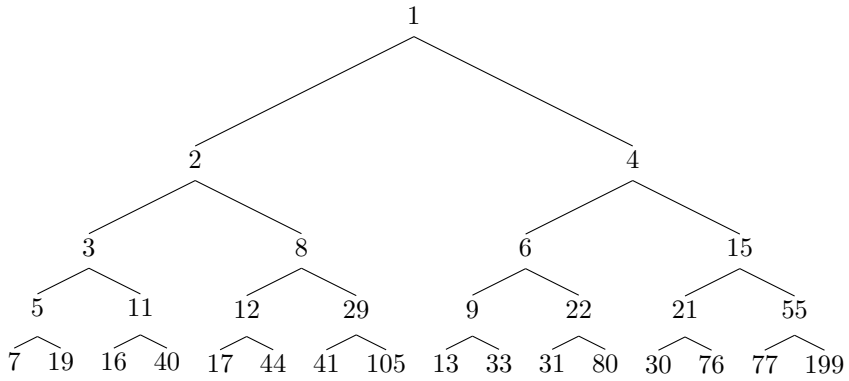

FIGURE 35. *Bergman$_2$ tree*, grown using branching rule $n \mapsto (\bar{l}, \bar{r}) = (\kappa_2(n) + 1, \lambda_2(n) + 1)$. Sequences of left, respectively, right branchings give rows of the Bergman$_2$ array and Bergman$_2$ mirror array, respectively (Table 46).

$\Longleftarrow$ Mirror Duality $\Longrightarrow$

1	2	3	5	7	10	1	4	15	55	199	720
4	6	9	13	18	25	2	8	29	105	380	1375
8	12	17	24	34	47	3	11	40	145	525	1900
11	16	23	32	45	63	5	19	69	250	905	3275
15	21	30	42	59	82	6	22	80	290	1050	3799
19	27	38	53	74	103	7	26	95	344	1245	4505
22	31	43	60	83	115	9	33	120	435	1574	5695
26	36	50	70	97	135	10	37	134	485	1755	6350
29	41	57	79	110	153	12	44	160	579	2095	7580
33	46	64	89	123	170	13	48	174	630	2280	8250
Bergman$_2$ Array						**Bergman$_2$ Mirror**					

TABLE 46. Bergman$_2$ pair of interspersion arrays, rows are sequences of all-left or all-right branchings in the Bergman$_2$ tree, Figure 35.

compositions in $\{\kappa_2, \lambda_2\}^\star$ or $\{\theta_2, \eta_2\}^\star$ would give cohort lengths 1, 1, 2, 2, 3, 4, 6, 8, 11, 15, 21, 29, 40, 56, 77, 106, 147, 203, 280, 387, 535, 740, 1022, 1413, 1952, 2698, 3728, 5152, 7120, 9840, 13598, 18792, 25970, 35890, 49599, 68544,.... For $b = 3$, the lengths would be 1, 1, 1, 2, 2, 3, 4, 5, 6, 8, 10, 13, 16, 21, 26, 34, 43, 55, 70, 89, 114, 146, 186, 237, 303, 387, 494, 630, 804, 1026, 1310, 1672, 2134, 2724, 3477, 4438,....

However, since these sequences do not arise from integer recurrence relations (apparently), they deviate from Definition 4.7 of a (generalized) cohort sequence. Consequently, when breaking the sequence of consecutive positive integers into blocks of these lengths, *pseudo-cohorts* might be a fitting name for these blocks, as the lengths of the blocks do not satisfy an integer recurrence relation. As with cohorts, pseudo-cohorts allow the tabulation of diatomic or (partially-disordered) dense tableaux and their cohort-dual tableaux.

For $b = 1$, moreover, κ_1^t occurs at the beginning of each cohort C_{t+1} in Table 10, while λ_1^t occurs at the end of cohort C_{2t+1}, whereas the relationship $-\lambda_1^t(-1) = -\kappa_1^{2t+1}(-1) - 1$ holds for $t = 1, 2, 3, \ldots$. Further, θ_1^t occurs at the end of each cohort C_{t+1} in Table 13, while η_1^t occurs at the beginning of cohort C_{2t+1}, whereas $N_0(\eta_1^t) = N_0(\theta_1^{2t-1}) + 1$ holds for $t = 1, 2, 3, \ldots$. In both instances, powers of the left and right branching functions intersperse regularly: Two consecutive powers of the left branching function occur between each power of the right branching function. Hence, the "degree" p of a composition in either $\{\kappa_1, \lambda_1\}^\star$ or $\{\theta_1, \eta_1\}^\star$ was straightforward to calculate: Add the sum of powers of the left branching function to twice the sum of powers of the right branching function, as in Propositions 4.7 and 4.24.

When considering a composition in the free monoids $\{\kappa_b, \lambda_b\}^\star$ or $\{\theta_b, \eta_b\}^\star$ for $b \geq 2$, however, the notion of its degree becomes illusive (or its value irrational), as the integer series $-\kappa_2^t(-1)$ and $-\lambda_2^t(-1)$, for example, intersperse irregularly.

In short, the free monoids $\{\kappa_b, \lambda_b\}^\star$ generated by Bergman pairs for $b > 1$, like those generated by the pairs of irrational slopes given in Examples 9.2 and 9.3, lack two nice properties of $\{\kappa, \lambda\}^\star$: (1) A regular interspersion of powers of the right branching function with those of the left branching function, (and a corresponding definition of "degree" for those compositions involving both $\bar{l}$ and $\bar{r}$), and (2) Cohort lengths that follow a linear recurrence. Moreover, blade duality fails to preserve the I–D properties of the arrays in Tables 43, 44, and 46, unlike those in Tables 3, 4, and 41 for which (3) blade-dual arrays of the I–D arrays are also I–D arrays.

9.7. **Between the Golden Ratio and Two — A search for three properties.** As a musing about research directions, consider a sequence of irrational slopes starting with ϕ and approaching 2, and the corresponding binary trees starting with the maximal and minimal successor trees and approaching the Positions tree. Ideally, the intermediate trees would share certain nice properties of the starting and ending trees. Let $\phi \leq \mu < 2$ and $\nu \equiv {}^1/_{(1-\frac{1}{\mu})}$ be a pair of irrational slopes.

The first of property desired is a regular interspersion of powers of the right branching function with those of the left branching function and the resulting ability to define the degree of a composition in $\{\bar{l}, \bar{r}\}^\star$ as an integer, or at minimum, as a rational number.

Repeatedly applying the left and **right** branching functions, examine the resulting the sequences $1, \bar{l}(1), \bar{l}^2(1), \bar{l}^3(1), \ldots$ and $1, \bar{r}(1), \bar{r}^2(1), \bar{r}^3(1), \ldots$ of all-left and **all-right** branchings, respectively, that descend from 1 in the Positions tree. The interspersion is one to one: $1 = \mathbf{1} < 2 < \mathbf{3} < 4 < \mathbf{7} < 8 < \mathbf{15} < 16 < \mathbf{31} < 32 < \cdots$. In particular, $\bar{r}^t(1) = \bar{l}^{t+1}(1) - 1$, $t \geq 0$. For the Positions tree, moreover, these sequences of all-left and all-right branchings (and the entire tree in general), are invariant under the shifts of the branching functions that Section 9.5 describes.

For $\mu = \phi$, consider the maximal successor tree. The sequence of **all-right** branchings intersperses regularly with that of the all-left branchings in so far as each power ≥ 1 of the nested **right** branching function ($\bar{\boldsymbol{R}}$) on 1 falls immediately *after* each second power of the nested left branching function ($\bar{\boldsymbol{L}}$) on 1: $\mathbf{1} = 1 < 2 < \mathbf{3} < 4 < 7 < \mathbf{8} < 12 < 20 < \mathbf{21} < 33 < 54 < \mathbf{55} < 88 < 143 < \mathbf{144} < 232 < \cdots$. In particular, $\bar{\boldsymbol{R}}^t(1) = \bar{\boldsymbol{L}}^{2t-1}(1) + 1$, $t \geq 1$.

Here, one shift of the branching function does exist, by either Corollary 9.2, in general, or by Proposition 4.12, in particular (see also Remark 4.12). Applying this

one available shift transforms of the maximal successor tree into the minimal successor tree, the latter having left and right branching functions $\bar{\boldsymbol{l}}(n) = \lfloor (n+1)\mu \rfloor - 1$, respectively, $\bar{\boldsymbol{r}}(n) = \lfloor (n+1)\nu \rfloor - 1$. Though the shift changes the images of 1, it preserves the property of a regular two-to-one interspersion of the sequences, whereas every other power of the nested left branching function ($\bar{\boldsymbol{l}}$) on 1 falls immediately *before* each power > 1 of the nested **right** branching function ($\bar{\boldsymbol{r}}$) on 1: $1 = \mathbf{1} < 2 < 3 < \mathbf{4} < 5 < 8 < \mathbf{12} < 13 < 21 < \mathbf{33} < 34 < 55 < \mathbf{88} < 89 < \cdots$. In particular, $\bar{\boldsymbol{r}}^t(1) = \bar{\boldsymbol{l}}^{2t+1}(1) - 1$, $t \geq 0$.

Secondly, the cohort lengths $|C_{t+1}| = \bar{l}^{t+1}(1) - \bar{l}^t(1)$, $t \geq 0$ follow a recurrence that evolves from $|C_{t+2}| = |C_{t+1}| + |C_t|$, $t \geq 1$ (the Fibonacci recurrence) for the successor trees ($\mu = \phi$), to $|C_{t+1}| = 2|C_t|$, $t \geq 1$ (a geometric doubling) for the Positions tree ($\mu \to 2$). Ideally then, for each intermediate μ in the sequence starting with ϕ and approaching 2, the first differences $\bar{l}^{t+1}(1) - \bar{l}^t(1)$ of the image of 1 under powers of the branching function using μ would also follow a (homogeneous) linear recurrence. Equivalently, the sequence $1, \bar{l}(1), \bar{l}^2(1), \bar{l}^3(1), \ldots, \bar{l}^t(1), \ldots$ would follow a (possibly non-homogeneous) linear recurrence.

Thirdly, the blade-dual trees for maximal and minimal successor trees and for the Positions tree all yield I–D arrays. Blade duality does not always preserve the interspersion–dispersion property, though. Rather, the original tree must satisfy an additional condition beyond the I–D properties (Section 9.9.1). Thus, preserving the I–D property under blade duality also finds its way onto the wish list for the "missing link" between the branch and clade quartets, on the one hand, and the blade quartet, on the other, seeking to maintain parallels with both of these.

In the quest for a series of slopes that engender these three properties, the paper next considers two different series of slopes, a "roots-based extension" of ϕ (Section 9.7.1) and Fibonacci n-step constants (Section 9.7.2) as candidates.

9.7.1. *Roots-based extension.* In an effort to find slopes that satisfy the desired properties, extend the golden ratio ϕ by considering solutions of $1/\phi_s + 1/\phi_s^s = 1$ for values of s other than 2. Before searching for slopes ϕ_s that would approach 2 and have nice properties (the eventual goal), first understand what happens for slopes that approach 1 (from above) by taking $s > 2$ integer. For example, the powers $s = 3, 4, 5, \ldots$ give solutions $\phi_3 \approx 1.46557, \phi_4 \approx 1.38028, \phi_5 \approx 1.32472, \ldots$. (The reader can encounter, *e.g.*, the Beatty sequence for $\lfloor n\phi_3 \rfloor$ at `138251`). Next, consider rational numbers $s > 1$, starting with $s = 3/2$, which gives $\phi_{3/2} \approx 1.75488$, as an initial foray in the other direction — the territory between ϕ and 2.

Note that in these cases the Beatty pairs take the form $\{\lfloor n\mu \rfloor, \lfloor n\nu \rfloor\} = \{\lfloor n\phi_s \rfloor, \lfloor n\phi_s^s \rfloor\}$ and that each Beatty pair yields one or more branching rules via the shift of Section 9.5, depending on the value of ϕ_s. In the cases $s > 2$ integer specifically, the available branching rules are limited to one per Beatty pair, namely $n \mapsto (\bar{l}(n), \bar{r}(n)) = (\lfloor n\phi_s \rfloor + 1, \lfloor n\phi_s^s \rfloor + 1)$.

Conjecture 9.4 (Regular interspersion of powers in the roots-based extensions)**.** *Let ϕ_s represent the largest positive, real solution of $\phi_s^{-1} + \phi_s^{-s} = 1$, or equivalently, the largest positive, real zero of $\phi_s^s - \phi_s^{s-1} - 1$, such that $\phi_2 = \phi \approx 1.61803$, $\phi_3 \approx 1.46557$, $\phi_4 \approx 1.38028$ and so forth. Let $\bar{l}(n) = \lfloor n\phi_s \rfloor + 1$ and $\bar{r}(n) = \lfloor n\phi_s^s \rfloor + 1$.*

Then, for $s > 0$ integer, there exists a non-negative integer "warm-up period" $\bar{t} \geq 0$ and a non-negative integer offset $0 \leq u < s$ such that

$$\bar{l}^{st-u-1}(1) < \bar{r}^t(1) < \bar{l}^{st-u}(1), \tag{107}$$

for each integer $t > \bar{t}$.

By extension, for a reduced fraction p/q with $0 < p/q < 1$, let $\phi_{q/p}$ represent the largest positive, real solution of $\phi_{q/p}^{-1} + \phi_{q/p}^{-q/p} = 1$, or equivalently, the largest positive, real zero of $\phi_{q/p}^{q-p}(\phi_{q/p} - 1)^p - 1$. Calculate that, e.g., *$\phi_{7/4} \approx 1.67821$, $\phi_{5/3} \approx 1.70161$, $\phi_{8/5} \approx 1.72179$, $\phi_{3/2} \approx 1.75488$, $\phi_{7/5} \approx 1.79191$, $\phi_{4/3} \approx 1.81917$, $\phi_{5/4} \approx 1.85667$, and so forth. For integer $1 \leq m < \frac{1}{2-\phi_s}$, let $\bar{l}(n) = \lfloor (n+m-1)\phi_{q/p} \rfloor - 2m + 3$ and $\bar{r}(n) = \lfloor (n+m-1)\psi_s \rfloor - 2m + 3$.*

Then for each m satisfying $1 \leq m < \frac{1}{2-\phi_s}$, there exists a non-negative integer "warm-up period" $\bar{t} \geq 0$ and integer offsets u and v such that

$$\bar{l}^{\lfloor \frac{q}{p}(t-v) \rfloor - u - 1}(1) < \bar{r}^t(1) < \bar{l}^{\lfloor \frac{q}{p}(t-v) \rfloor - u}(1), \tag{108}$$

for each integer $t > \bar{t}$. For suitable $\bar{t}$, moreover, (108) continues to hold under the (repeated) substitution of $u \pm q$ and $v \mp p$ for u and v, respectively.

Example 9.5 (Regular interspersion in the roots-based extensions)**.** As examples supporting Conjecture 9.4, first consider $\phi_5 \approx 1.32472$ and the inequality (107) with offset $u = 1$ and no warm-up period ($\bar{t} = 0$), so that the images of 1 under powers of the left and **right** branching functions $\bar{l}(n) = \lfloor n\phi_5 \rfloor + 1$ and $\bar{r}(n) = \lfloor n\phi_5^5 \rfloor + 1$, respectively, seem to intersperse regularly in the ratio of five to one:

$\mathbf{1} = 1 < 2 < 3 < 4 < \mathbf{5} < 6 < 8 < 11 < 15 < 20 < \mathbf{21} < 27 < 36 < 48 < 64 < 85 < \mathbf{86} < 113 < \cdots < \bar{l}^{5t-2}(1) < \bar{r}^t(1) < \bar{l}^{5t-1}(1) < \cdots$, for $t > \bar{t} = 0$.

Similarly, the slope $\phi_6 \approx 1.2852$ seems to produce a regular interspersion having a ratio of six to one, considering offset $u = 3$ and warm-up period of $\bar{t} = 1$:

$\mathbf{1} = 1 < 2 < 3 < 4 < \mathbf{5} < 6 < 8 < 11 < 15 < 20 < \mathbf{23} < 26 < 34 < 44 < 57 < 74 < 96 < \mathbf{104} < 124 < 160 < 206 < 265 < 341 < 439 < \mathbf{469} < 565 < \cdots < \bar{l}^{6t-4}(1) < \bar{r}^t(1) < \bar{l}^{6t-3}(1) < \cdots$, for $t > \bar{t} = 1$.

Finally, for $s = 3/2$, slope $\phi_{3/2} \approx 1.75488$ and $\bar{m} = \lfloor 1/(2 - \phi_{3/2}) \rfloor = 4$, so that $\bar{l}(n) = \lfloor (n+m-1)\phi_{3/2} \rfloor - 2m + 3$ and $\bar{r}(n) = \left\lfloor (n+m-1)\phi_{3/2}^{3/2} \right\rfloor - 2m + 3$ can be defined for $m = 1, 2, 3, 4$, all of which appear to intersperse regularly in the ratio of three to two:

$\mathbf{1} = 1 < 2 < \mathbf{3} < 4 < \mathbf{7} < 8 < 15 < \mathbf{17} < 27 < \mathbf{40} < 48 < 85 < \mathbf{93} < 150 < \mathbf{217} < 264 < 464 < \mathbf{505} < 815 < \cdots < \bar{l}^{\lfloor \frac{3}{2}(t+1) \rfloor - 2}(1) < \bar{r}^t(1) < \bar{l}^{\lfloor \frac{3}{2}(t+1) \rfloor - 1}(1) < \cdots$, for $t > \bar{t} = 0$, for $m = 1$;

$\mathbf{1} = 1 < 2 < \mathbf{3} < 4 < 7 < \mathbf{8} < 13 < \mathbf{19} < 23 < 41 < \mathbf{45} < 72 < \mathbf{105} < 127 < 223 < \mathbf{245} < 392 < \mathbf{570} < 688 < 1208 < \mathbf{1326} < 2120 < \cdots < \bar{l}^{\lfloor \frac{3}{2}t \rfloor}(1) < \bar{r}^t(1) < \bar{l}^{\lfloor \frac{3}{2}t \rfloor + 1}(1) < \cdots$, for $t > \bar{t} = 0$, for $m = 2$;

$1 < 2 < \mathbf{3} < 4 < 7 < \mathbf{8} < 12 < \mathbf{20} < 21 < 37 < \mathbf{48} < 65 < \mathbf{113} < 114 < 200 < \mathbf{264} < 351 < \mathbf{615} < 616 < 1081 < \mathbf{1431} < 1897 < \cdots < \bar{l}^{\lfloor \frac{3}{2}t \rfloor}(1) < \bar{r}^t(1) < \bar{l}^{\lfloor \frac{3}{2}t \rfloor + 1}(1)$, for $t > \bar{t} = 0$, for $m = 3$;

$\mathbf{1} = 1 < 2 < 3 < \mathbf{4} < 5 < 9 < \mathbf{11} < 16 < \mathbf{27} < 28 < 49 < \mathbf{64} < 86 < \mathbf{150} < 151 < 265 < \mathbf{350} < 465 < \mathbf{815} < 816 < 1432 < \mathbf{1896} < 2513 < \cdots < \bar{l}^{\lfloor \frac{3}{2}t \rfloor + 1}(1) < \bar{r}^t(1) < \bar{l}^{\lfloor \frac{3}{2}t \rfloor + 2}(1)$, for $t > \bar{t} = 0$, for $m = 4$.

Conjecture 9.5 (Regular & irregular recurrence in the roots-based extension)**.** *Beginning with $s = 1, 2, 3, \ldots$ integer, let ϕ_s represent the largest positive, real*

solution of $\phi_s^{-1} + \phi_s^{-s} = 1$, or equivalently, the largest positive, real zero of $\phi_s^s - \phi_s^{s-1} - 1$.

Further, considering each algebraic number ϕ_s as the constant slope of a floor function $\lfloor n\phi_s \rfloor$, apply the shift described in Section 9.5, writing $\bar{l}_{s,m}(n) = \lfloor (n+m-1)\phi_s \rfloor - 2m + 3$ for each integer $m = 1, \ldots, \lfloor 1/(2-\phi_s) \rfloor$. For example, $\bar{l}_{2,1}(n) = \lfloor n\phi \rfloor + 1$, $\bar{l}_{2,2}(n) = \lfloor (n+1)\phi \rfloor - 1$.

When the $\bar{l}_{s,m}$ are invariant under the shift of m, drop the second index m, writing only $\bar{l}_s$ in the case of $\bar{l}_1(n) = \bar{l}_{1,1}(n) = \bar{l}_{1,2}(n) = \bar{l}_{1,3}(n) = \cdots = 2n + 1$. Also drop the second index whenever $\bar{m} = \lfloor 1/(2-\phi_s) \rfloor = 1$, as in $\bar{l}_3(n) = \bar{l}_{3,1}(n) = \lfloor n\phi_3 \rfloor + 1$, $\bar{l}_4(n) = \bar{l}_{4,1}(n) = \lfloor n\phi_4 \rfloor + 1$, and so forth.

Now consider sequences of the form $1, \bar{l}_{s,m}(1), \bar{l}^2_{s,m}(1), \ldots, \bar{l}^t_{s,m}(1), \ldots$.

For $s = 2$, the sequence of images of 1 under repeated applications of $\bar{l}_{2,1}$ satisfies for $t \geq 2$ the non-homogeneous linear difference equation

$$\bar{l}^t_{2,1}(1) = \bar{l}^{t-1}_{2,1}(1) + \bar{l}^{t-2}_{2,1}(1) + 1,$$

whilst under $\bar{l}_{2,2}$ it satisfies the homogeneous linear difference equation

$$\bar{l}^t_{2,2}(1) = \bar{l}^{t-1}_{2,2}(1) + \bar{l}^{t-2}_{2,2}(1).$$

Prior sections have amply demonstrated these first two recurrences. Further, for $s = 1$ (trivially) as well as for $s = 3, 4, 5$, the image of 1 under repeated application of $\bar{l}_s$ satisfies for $t \geq s$ the non-homogeneous linear difference equation

$$\bar{l}^t_s(1) = \bar{l}^{t-1}_s(1) + \bar{l}^{t-s}_s(1) + 1.$$

For integer $s \geq 6$, however, the sequence of images of 1 under repeated applications of $\bar{l}_s = \lfloor n\phi_s \rfloor + 1$ does not *satisfy any linear difference equation.*

Finally, for $s = 3/2$, repeatedly applying any of the branching functions $\bar{l}_{3/2,1}, \ldots, \bar{l}_{3/2,4}$ to 1 produces a sequence that satisfies for $t \geq 4$ a linear difference equation:

$$\bar{l}^t_{3/2,1}(1) = \bar{l}^{t-1}_{3/2,1}(1) + \bar{l}^{t-2}_{3/2,1}(1) + \bar{l}^{t-4}_{3/2,1} + 2 = \underline{289692}(t+2) \quad \textit{(non-homogeneous)}$$

$$\bar{l}^t_{3/2,2}(1) = \bar{l}^{t-1}_{3/2,2}(1) + \bar{l}^{t-2}_{3/2,2}(1) + \bar{l}^{t-4}_{3/2,2} + 1 \quad \textit{(non-homogeneous)}$$

$$\bar{l}^t_{3/2,3}(1) = \bar{l}^{t-1}_{3/2,3}(1) + \bar{l}^{t-2}_{3/2,3}(1) + \bar{l}^{t-4}_{3/2,3} = \underline{005251}(t+3) \quad \textit{(homogeneous)}$$

$$\bar{l}^t_{3/2,4}(1) = \bar{l}^{t-1}_{3/2,4}(1) + \bar{l}^{t-2}_{3/2,4}(1) + \bar{l}^{t-4}_{3/2,4} = \underline{005314}(t+1) \quad \textit{(homogeneous)}$$

For any other reduced fraction $0 < p/q < 1$ with $p > 1$, however, considering the branching function $\bar{l}_{q/p,m}(n) = \lfloor (n+m-1)\phi_{q/p} \rfloor - 2m + 3$ for any integer shift $1 \leq m < \frac{1}{2-\phi_{q/p}}$, the sequence $1, \bar{l}_{q/p,m}(1), \bar{l}^2_{q/p,m}(1), \ldots, \bar{l}^t_{q/p,m}(1), \ldots$, that is, the sequence of images of 1 under iterated applications of $\bar{l}_{q/p,m}$, does not *satisfy any linear difference equation.*

Example 9.6 (Continuation of Example 9.5): Recurrence in the roots-based extension)**.** For $\bar{l}(n) = \lfloor n\phi_5 \rfloor + 1$, the sequence $1, \bar{l}_5(1), \bar{l}^2_5(1), \ldots, \bar{l}^t_5(1), \ldots = 1,$ 2, 3, 4, 6, 8, 11, 15, 20, 27, 36, 48, 64, 85, 113, 150, 199, 264, 350, 464, 615, 815, 1080, 1431, 1896, 2512, 3328, 4409, 5841, $\cdots, \bar{l}^t_5(1) \cdots$ appears to satisfy $\bar{l}^t_5(1) = \bar{l}^{t-1}_5(1) + \bar{l}^{t-5}_5(1) + 1$, for $t \geq 5$.

For $\bar{l}(n) = \lfloor n\phi_{3/2} \rfloor + 1$, the sequence 1, 2, 4, 8, 15, 27, 48, 85, 150, 264, 464, 815, 1431, 2512, 4409, 7738, 13580, 23832, 41823, 73395, 128800, $\cdots, \bar{l}^t_{3/2,1}(1), \cdots$ seemingly follows $\bar{l}^t_{3/2,1}(1) = \bar{l}^{t-1}_{3/2,1}(1) + \bar{l}^{t-2}_{3/2,1}(1) + \bar{l}^{t-4}_{3/2,1} + 2$, for $t \geq 4$.

For $\bar{l}(n) = \lfloor (n+1)\phi_{3/2} \rfloor - 1$, the sequence 1, 2, 4, 7, 13, 23, 41, 72, 127, 223, 392, 688, 1208, 2120, 3721, 6530, 11460, 20111, 35293, 61935, 108689, $\cdots$, $\bar{l}^t_{3/2,2}(1), \cdots$ seemingly follows $\bar{l}^t_{3/2,2}(1) = \bar{l}^{t-1}_{3/2,2}(1) + \bar{l}^{t-2}_{3/2,2}(1) + \bar{l}^{t-4}_{3/2,2} + 1$, for $t \geq 4$.

For $\bar{l}(n) = \lfloor (n+2)\phi_{3/2} \rfloor - 3$, the sequence 1, 2, 4, 7, 12, 21, 37, 65, 114, 200, 351, 616, 1081, 1897, 3329, 5842, 10252, 17991, 31572, 55405, 97229, $\cdots$, $\bar{l}^t_{3/2,3}(1), \cdots$ seemingly follows $\bar{l}^t_{3/2,3}(1) = \bar{l}^{t-1}_{3/2,3}(1) + \bar{l}^{t-2}_{3/2,3}(1) + \bar{l}^{t-4}_{3/2,3}$, for $t \geq 4$.

For $\bar{l}(n) = \lfloor (n+3)\phi_{3/2} \rfloor - 5$, the sequence 1, 2, 3, 5, 9, 16, 28, 49, 86, 151, 265, 465, 816, 1432, 2513, 4410, 7739, 13581, 23833, 41824, 73396 $\cdots$, $\bar{l}^t_{3/2,3}(1), \cdots$ seemingly follows $\bar{l}^t_{3/2,3}(1) = \bar{l}^{t-1}_{3/2,3}(1) + \bar{l}^{t-2}_{3/2,3}(1) + \bar{l}^{t-4}_{3/2,3}$, for $t \geq 4$.

Remark 9.2. Conjecture 9.5 deals with the sequences of nested application of shifted Beatty functions (floor functions that use irrational slopes). For some slopes, the Conjecture gives recurrences that the sequences of nested application satisfy. The Conjecture also identifies other slopes for which such recurrences seem not to exist. The difference between the slopes for which recurrences were identified and the slopes for which recurrences do not exist may be that in the former case, not only is the slope the "largest positive, real zero" of the given polynomial, but it is the *only* zero of the polynomial outside the unit circle in the complex plane. For all $s \geq 6$, the polynomial $\phi_s^s - \phi_s^{s-1} - 1$ seems to have multiple zeroes outside the unit circle, while for all reduced fractions $p/q \in (0,1)$ other than $p/q = 2/3$, the polynomial $\phi_{q/p}^{q-p}(\phi_{q/p} - 1)^p - 1$ seems to have multiple zeroes outside the unit circle. If this is indeed the case, the Conjecture would follow from [12] (see also [32]).

9.7.2. *Fibonacci s-step constants.*

Conjecture 9.6 (Fibonacci s-step constants)**.** *For $s = 1, 2, 3, \ldots$, let $\phi^{(s)}$ represent the positive, real zero of the polynomial $x^s - \sum_{i=0}^{s-1} x^s$, such that $\phi^{(1)} = 1$, $\phi^{(2)} = \phi$, and $\phi^{(3)}$, $\phi^{(4)}$, $\phi^{(5)}$, $\phi^{(6)}$, $\phi^{(7)}$, $\phi^{(8)}$ are the "tribonacci," "tetranacci," "pentanacci," "hexanacci," "heptanacci," and "octanacci" constants, respectively, and so forth.*

Further, considering each constant $\phi^{(s)}$ as the slope of a floor function $\lfloor n\phi^{(s)} \rfloor$ and letting $\bar{m}^{(s)} = \lfloor 1/(2 - \phi^{(s)}) \rfloor$, apply the Beatty shift described in Section 9.5 to write $\bar{l}_{(s),m}(n) = \lfloor (n+m-1)\phi^{(s)} \rfloor - 2m + 3$ for each integer $m = 1, \ldots, \bar{m}^{(s)}$, so that $\bar{l}_{(1),1}(n) = n + 1$; $\bar{l}_{(2),1}(n) = \lfloor n\phi \rfloor + 1$, $\bar{l}_{(2),2}(n) = \lfloor (n+1)\phi \rfloor - 1$; $\bar{l}_{(3),1}(n) = \lfloor n\phi^{(3)} \rfloor + 1$, $\bar{l}_{(3),2}(n) = \lfloor (n+1)\phi^{(3)} \rfloor - 1$, $\bar{l}_{(3),3}(n) = \lfloor (n+2)\phi^{(3)} \rfloor - 3$, $\bar{l}_{(3),4}(n) = \lfloor (n+3)\phi^{(3)} \rfloor - 5$, $\bar{l}_{(3),5}(n) = \lfloor (n+4)\phi^{(3)} \rfloor - 7$, $\bar{l}_{(3),6}(n) = \lfloor (n+5)\phi^{(3)} \rfloor - 9$, and so forth.

Then for each $s = 1, 2, 3, \ldots$, the sequence $1, \bar{l}_{(s),m}(1), \bar{l}^2_{(s),m}(1), \ldots, \bar{l}^t_{(s),m}(1), \ldots$, that is, the image of 1 under the repeated application of any of the $\bar{m}^{(s)}$ functions $\bar{l}_{(s),m}$, satisfies for $t \geq s$ exactly one of the s linear difference equations ($j = 2, \ldots, s$):

$$\left.\begin{aligned} \bar{l}^{t}_{(s),1}(1) &= \textstyle\sum_{i=1}^{s} \bar{l}^{t-i}_{(s),1}(1) + 1, \\ &\vdots \\ \bar{l}^{t}_{(s),\bar{m}^{(s)}-2^{r-1}+1}(1) &= \textstyle\sum_{i=1}^{s} \bar{l}^{t-i}_{(s),\bar{m}^{(s)}-2^{s-1}+1}(1) + 1; \end{aligned}\right\} \bar{m}^{(s)} - 2^{s-1} + 1$$

$$\left.\begin{aligned} \bar{l}^{t}_{(s),\bar{m}^{(s)}-2^{r-1}+2}(1) &= \textstyle\sum_{i=1}^{s} \bar{l}^{t-i}_{(s),\bar{m}^{(s)}-2^{s-1}+2}(1), \\ &\vdots \\ \bar{l}^{t}_{(s),\bar{m}^{(s)}-2^{s-2}+1}(1) &= \textstyle\sum_{i=1}^{s} \bar{l}^{t-i}_{(s),\bar{m}^{(s)}-2^{s-2}+1}(1); \end{aligned}\right\} \begin{cases} 2^{s-2},\ s \geq 2, \\ 0,\ s < 2; \end{cases}$$

$$\vdots$$

$$\left.\begin{aligned} \bar{l}^{t}_{(s),\bar{m}^{(s)}-2^{s-j+1}+2}(1) &= \textstyle\sum_{i=1}^{s} \bar{l}^{t-i}_{(s),\bar{m}^{(s)}-2^{s-j+1}+2}(1) - j + 2, \\ &\vdots \\ \bar{l}^{t}_{(s),\bar{m}^{(s)}-2^{s-j}+1}(1) &= \textstyle\sum_{i=1}^{s} \bar{l}^{t-i}_{(s),\bar{m}^{(s)}-2^{s-j}+1}(1) - j + 2; \end{aligned}\right\} \begin{cases} 2^{s-j},\ s \geq j, \\ 0,\ s < j; \end{cases}$$

$$\vdots$$

$$\left.\begin{aligned} \bar{l}^{t}_{(s),\bar{m}^{(s)}}(1) &= \textstyle\sum_{i=1}^{s} \bar{l}^{t-i}_{(s),\bar{m}^{(s)}}(1) - s + 2. \end{aligned}\right\} \begin{cases} 1,\ s \geq 2, \\ 0,\ s < 2. \end{cases}$$

Moreover, throughout each block above, the sequences themselves are identical:

$\bar{l}^{t}_{(s),1}(1) = \cdots = \bar{l}^{t}_{(s),\bar{m}^{(s)}-2^{s-1}+1}(1)$*, for all* $t \geq 0$*, and*

$\bar{l}^{t}_{(s),\bar{m}^{(s)}-2^{s-j+1}+2}(1) = \cdots = \bar{l}^{t}_{(s),\bar{m}^{(s)}-2^{s-j}+1}(1)$*, for all* $t \geq 0$*, for* $j = 2, \ldots, r$*.*

Example 9.7 (Tribonacci constant $\phi^{(3)}$)**.** Given the tribonacci constant $\phi^{(3)} \approx 1.83929$, Conjecture 9.6 states that, whereas $\bar{m}^{(3)} - 2^{3-1} + 1 = 6 - 4 + 1 = 3$, the first three shifted branching functions $\bar{l}_{(3),1} = \left\lfloor n\phi^{(3)} \right\rfloor + 1$, $\bar{l}_{(3),2} = \left\lfloor (n+1)\phi^{(3)} \right\rfloor - 1$ and $\bar{l}_{(3),3} = \left\lfloor (n+2)\phi^{(3)} \right\rfloor - 3$, give identical sequences of images of 1 under their iterated applications, satisfying, moreover, the same non-homogeneous linear difference equation $\bar{l}^{t}_{(3),1}(1) = \bar{l}^{t-1}_{(3),1}(1) + \bar{l}^{t-2}_{(3),1}(1) + \bar{l}^{t-3}_{(3),1}(1) + 1 = \bar{l}^{t}_{(3),2}(1) = \bar{l}^{t-1}_{(3),2}(1) + \bar{l}^{t-2}_{(3),2}(1) + \bar{l}^{t-3}_{(3),2}(1) + 1 = \bar{l}^{t}_{(3),3}(1) = \bar{l}^{t-1}_{(3),3}(1) + \bar{l}^{t-2}_{(3),3}(1) + \bar{l}^{t-3}_{(3),3}(1) + 1 = \underline{008937}$.

For the next 2^{3-2} or two branching functions, $\bar{l}_{(3),4} = \left\lfloor (n+3)\phi^{(3)} \right\rfloor - 5$ and $\bar{l}_{(3),5} = \left\lfloor (n+4)\phi^{(3)} \right\rfloor - 7$, the sequences of images of 1 under their iterated applications appear to be identical and to satisfy the same homogeneous linear difference equation $\bar{l}^{t}_{(3),4}(1) = \bar{l}^{t-1}_{(3),4}(1) + \bar{l}^{t-2}_{(3),4}(1) + \bar{l}^{t-3}_{(3),4}(1) = \bar{l}^{t}_{(3),5}(1) = \bar{l}^{t-1}_{(3),5}(1) + \bar{l}^{t-2}_{(3),5}(1) + \bar{l}^{t-3}_{(3),5}(1) = \underline{000073}$.

Finally, the sixth Beatty shift $\bar{l}_{(3),6} = \left\lfloor (n+5)\phi^{(3)} \right\rfloor - 9$, upon iterative application to 1, generates a sequence that appears to follow the non-homogeneous linear difference equation $\bar{l}^{t}_{(3),6}(1) = \bar{l}^{t-1}_{(3),6}(1) + \bar{l}^{t-2}_{(3),6}(1) + \bar{l}^{t-3}_{(3),6}(1) - 1 = \underline{192804}$.

Corollary 9.7 (Fibonacci s-step cohorts)**.** *With* C_t *as the cohort containing* $\bar{l}^{t}_{(s),m}$ *and* $|C_t| = \bar{l}^{t}_{(s),m}(1) - \bar{l}^{t-1}_{(s),m}(1)$ *being the length of said cohort, Conjecture 9.6 (if true) implies the (homogeneous) recurrence* $|C_t| = \sum_{i=1}^{s} |C_{t-s}|$ *for lengths of cohorts* $t > s$*, consistent with Definition 4.7 of a (generalized) cohort sequence.*

Example 9.8 (Continuation of Example 9.7)**.** For $t = 1, 2, 3, \ldots$, $\bar{l}^{t}_{(3),1}(1) - \bar{l}^{t-1}_{(3),1}(1) = \bar{l}^{t}_{(3),2}(1) - \bar{l}^{t-1}_{(3),2}(1) = \bar{l}^{t}_{(3),3}(1) - \bar{l}^{t-1}_{(3),3}(1) = \underline{000073}(t+1)$, $\bar{l}^{t}_{(3),4}(1) - \bar{l}^{t-1}_{(3),4}(1) = \bar{l}^{t}_{(3),5}(1) - \bar{l}^{t-1}_{(3),5}(1) = \underline{001590}(t+1)$, and $l^{t}_{(3),6}(1) - \bar{l}^{t-1}_{(3),6}(1) = \underline{000073}(t)$, such that all six sequences of successive differences seem to coincide with a version of

the Tribonacci sequence, each of the three versions using a different triple of "seed" elements (Example 4.34).

Conjecture 9.8 (Irregular interspersion of branching functions that use Fibonacci s-step constants as slopes)**.** *For the Fibonacci s-step constants $\phi^{(s)}$ described above, the sequences $1, \bar{l}_{(s),m}(1), \bar{l}^2_{(s),m}(1), \ldots, \bar{l}^t_{(s),m}(1), \ldots$ and $1, \bar{r}_{(s),m}(1), \bar{r}^2_{(s),m}(1), \ldots, \bar{r}^t_{(s),m}(1), \ldots$ do not intersperse regularly for $s \geq 3$. That is, the interspersion pattern is non-repeating.*

9.8. **Cohort, mirror, and blade duality — A tentative formalization.**

9.8.1. *Mirror Duality.*

Remark 9.3 (Mirror duals of (relaxed) I–D arrays). To any array satisfying interspersion properties (I2) and (I3) of [20] and whose rows partition *a subset of the positive integers* — a relaxed version of property (I1) — associate a tree, constructed as follows:

> Take the entry at the top left of the array as the root node of the tree, and the remainder of the first row as the sequence of all-left branchings descending from the root node. Thereafter, starting with the root node, consider the incumbent node at each stage to be the node of least value that has no right child. (Observe that this choice of incumbent node resembles the "minimum excluded" or mex operation often used for I–D arrays and other number-theoretic constructions.) Place each subsequent row of the array as a sequence of all-left branchings in the tree, grafting the first entry in the row onto the incumbent node as its right child.
>
> The mirror dual of the original array obtains by taking as its rows sequences of all-right branchings in the tree, these rows ordered as required to satisfy (I3), thus reversing left and right or "mirroring" the tree.

Rather than using rows of an I–D array, the tree can also be grafted from columns of a dense cohort tableau. (Remark 9.4 revisits this assemblage).

Note that that grafting branches in an order different from that just described produces a degenerate tree such as that shown in Figure 38, and that sequences of all-right branchings in a degenerate tree produce rows of an array that does *not* satisfy the I–D properties.

For an interspersion–dispersion array (I–D array) with infinitely many rows, what Kimberling termed the "inverse I–D array" equals the mirror dual as defined here. The present naming convention avoids confusion with several other types of duality discussed herein (cohort dual, blade dual). Take for example the mirror-dual pair $w_{n,k}$ and $\mathfrak{w}_{n,k}$, for $n = 0, 1, 2, \ldots$ and $k = 1, 2, 3, \ldots$. Per dispersion property (D3), their respective "dispersed sequences" are $S_n = \mathfrak{w}_{n,1}$ and $T_n = w_{n,1}$, respectively, for $n = 1, 2, 3, \ldots$, and S and T complement the first columns of w, respectively, $\mathfrak{w}$ (Proposition 8.21).

Defining the minimal successor tree (Figure 3) via left- and right-branching functions $\bar{\boldsymbol{l}}(n) = S_n = \mathfrak{w}_{n,1}$ and $\bar{\boldsymbol{r}}(n) = T_n = w_{n,1}$, $n = 1, 2, 3, \ldots$. Sequences of all-left branchings in the tree give rows of w, while sequences of all-right branchings give rows of $\mathfrak{w}$. Hence, Kimberling's inversion for I–D arrays with infinitely many rows

is equivalent to constructing the infinite binary tree from one of the I–D arrays by the grafting procedure just given and forming the other array by gathering tree branches from the opposite side.

The relaxation of property (I1), permits the analogous inversion or "mirroring" of *interspersioid–dispersoid* arrays [40] such as the quilt spectrum array $(d_{n,k})$ reproduced in Table 1. Since $d_{n,k} = \kappa(a_{n,k})$, $n = 0, 1, 2, \ldots$, $k = 1, 2, 3, \ldots$, its structure on K_+ is similar to that of $(a_{n,k})$ on $\mathbb{Z}_+$.

9.8.2. *Cohort Duality.* Whereas rows of the cohort-dual arrays w and a correspond to columns of the diatomic tableaux, Table 40, the latter constitute a pair of cohort-dual tableaux, just as Tables 6(i) and (ii) do. With the dense tableaux (Tables 6), cohort duality involves a change between left-aligned and right-aligned rows. For the more general cohort duality exhibited by the pair of diatomic tableaux, the spacing between columns reverses left and right, as a comparison of Tables 40(i) and (ii) shows. This suggests the following definition of cohort duality.

Definition 9.2 ([Tentative] Cohort-dual tableaux, cohort-dual I–D arrays, and cohort-dual trees)**.** As a tentative definition, let cohort dual tableaux obtain from one another by maintaining all elements in all cohorts of the tableau in the same left to right order and horizontally mirroring the structure of element spacing. In the case of a pair of cohort-dual tableaux of the positive integers, designate the pair of I–D arrays whose rows are columns of the respective tableaux as *cohort-dual I–D arrays* and designate as *cohort-dual trees* the pair of binary trees whose sequences of all-left branchings are columns of the respective cohort-dual tableaux (Remark 9.3 detailed how to construct these trees by grafting rows of the cohort-dual I–D arrays in a way consistent with Kimberling's third interspersion property [20]. Up to ordering, rows of each array are identical to columns of the associated tableau.)

Remark 9.4 (Cohort duals)*.* Notice that the operation of Definition 9.2 only mirrors the "tableaux structure" and does *not* mirror the elements of each cohort. Moreover, it is the only dual-forming procedure considered here that operates on cohorts and tableaux, hence "cohort duality" provides a suitable name. By contrast, the paper treats several different "dual" operations on trees (Remarks 9.3 and 9.5); the first of these completely mirrors the tree in effect, an operation aptly named "mirror duality."

Columns of the two dense tableaux in Table 6 are sequences of all-left branchings in the minimal and maximal Fibonacci trees (Figures 5 and 8). Meanwhile, columns of the the diatomic tableaux, Table 40, provide sequences of straight branchings in the successor trees. Within either pair of tableaux, applying Definition 9.2 to transform from one tableau to another thus induces a transformation between the corresponding (cohort-dual) "minimal" and "maximal" trees.

A glance at branching rules for the successor trees (Figures 15(i) and (ii)) might suggest that cohort duality has to do with a shift between $m = 1$ and $m = 2$ of branching functions that use Beatty pairs (Section 9.5). However, the "shift of branching rules that use Beatty pairs" with (left) slope $1 < \mu < 2$ does not yield a pair of trees in general, but may yield only one tree or multiple trees, with each integer shift $1 \leq m < 1/(2-\mu)$ or half-integer shift $1/2 \leq m < 1/(2-\mu)$ producing a distinct tree.

Glancing at the branching rules for the Fibonacci trees (Figures 15(iii) and (iv)), cohort duality between them might appear to correspond to the "Fibonacci numeration shift" of Section 9.2. However, the deceptive appearance does not extend beyond this pair of trees, whereas each tree (Figures 30 and 32) has its own cohort dual (Figures 31 and 33, respectively), which does not employ a branching rule of the same type. Rather, the cohort-dual trees for the extrapolated Fibonacci numeration use branching rules $n \mapsto (l(n), r(n)) = (n + F_{F^{-1}(\lfloor n/p \rfloor)-1}, n + pF_{F^{-1}(n)+2})$, where p is the depth of extrapolation as indicated in Example 9.1. Extrapolating backwards to $p = 1$, gives the branching rule $n \mapsto (n + F_{F^{-1}(\lfloor n/1 \rfloor)-1}, n + 1 \times F_{F^{-1}(n)+2})$ $= (n + F_{F^{-1}(\lfloor n \rfloor)-1}, n + F_{F^{-1}(n)+2})$ — the branching rule for the minimal Fibonacci tree — which would imply that the latter is its own cohort-dual, in contrast to Definition 9.2.

As a final deceptive analogy, it might be tempting to define cohort duality on the basis of mutual dispersion properties between pairs of cohort-dual I–D arrays (Proposition 8.22), which is somehow analogous to mutual-dispersion between pairs of mirror-dual I–D arrays (Proposition 8.21). However, mutual dispersion turns out to hold only for specific cohort-dual pairs of arrays in the two quartets, and its formulations as (105) and (106) differ slightly between the quartets. There is no obvious, systematic way to describe mutual dispersion between other cohort-duals pairs of I–D arrays, and when mutual dispersion does appear, its formulation can be altogether more intricate (Example 9.1).

9.8.3. *Blade Duality.*

Remark 9.5 (Blade duals of I–D arrays). Remarks 9.3 and 9.4 summarized the relationship between I–D arrays with infinitely many rows and their corresponding infinite binary trees. For arrays of the branch and clade quartets, blade-dual arrays are also interspersions. However, blade duality between trees, a switching of all-left (all-right) branchings with right (left) clades, often fails to preserve the I–D properties of arrays associated with the trees, so that blade duals of interspersions are not necessarily interspersions. Put differently, applying the tree blade permutation, 059893, to a binary tree built from an I–D array does produce a binary tree, but the arrays derived from this "blade-dual" tree do not necessarily inherit the I–D properties of the original array.

Beyond the branch and clade quartets, the "blade quartet" described in Section 9.4 provides another example of arrays for which blade duality preserves the interspersion property. With the latter as the sole exception, however, the other I–D arrays introduced here in Section 9 do not have I–D arrays as their blade duals.

A much studied I–D array, the Stolarsky array, shown as a tree in Figure 36, provides a further counterexample. Permuting this tree by the tree blade permutation, neither the "blade-dual" array nor the "blade mirror" array is an I–D array.

For the blade-dual (Figure 38) of the "mean successor tree" (Figure 37), the blade-dual array (Table 47 at bottom left) is an I–D array, whereas the "blade mirror" array (Table 47 at bottom right) is not.

Characterizing the class of interspersions whose blade duals are also interspersions forms part of ongoing research.

This prompts the development in Section 9.9.1 of a sufficient condition for an I–D array to have as its blade dual another I–D array. Using a specific formulation of an I–D array, Proposition 9.9 presents a sufficient condition (109) for its blade dual

to also be an I–D array, and this condition turns out to be a single left-clade–tree order isomorphism. (This condition is less restrictive than the complete clade–tree order isomorphism present in the Fibonacci and successor trees — associated with the octet — as well as in the Blade and Position trees.)

This propels Section 9.9 in the direction of computational experiments in generating trees, as well the tabulation of sieves for finding numbers that are powerfree in "floor functions" and shifted floor functions. That section reports on initial investigations into binary-tree arrangements of the integers satisfying (104) plus single or multiple clade–tree order isomorphisms by means of the computational tests on finite binary trees. For the trees of integers the paper has (mostly) dealt with so far, a finite version arranges the integers $\{1, \ldots, n\}$ in such a way that the values of nodes satisfy the desired criteria. For each n, the text presents the number of trees experimentally satisfying (104), the number of trees satisfying (104) plus the single clade–tree order isomorphism of the kind necessary for blade duality to preserve the I–D properties (109), and finally, the number of trees satisfying (104) plus complete clade–tree order isomorphism, like the Fibonacci, successor, and Positions / Blade trees.

Having found binary trees that satisfy the desired conditions, it will be interesting to know whether such a tree — or its blade dual — has formulation via (shifted) branching rules that use Beatty pairs $n \mapsto (\bar{l}(n), \bar{r}(n)) = (\lfloor (n+m-1)\mu \rfloor - 2m + 3, \lfloor (n+m-1)\nu \rfloor - 2m + 3)$, as in Section 9.5, descending from the root node 1. In this case, the outermost nodes $\bar{l}^t(1)$ and $\bar{r}^t(1)$ are invariant under blade duality, and by (104), these are consistently the smallest and largest values on level $t-1$ of both the original tree and its blade dual.

Thus, if their exists a sequence of trees "connecting the dots" between those based on $\mu = \phi$ (successor) and that based on $\mu \to 2$ (Positions), a necessary condition would exclude from the set of outermost nodes (of levels 3 and greater) of each tree those integers that do not obtain via $\bar{l}^t(1)$ and $\bar{r}^t(1)$ for $t \geq 2$, or conversely, exclude from the set of inside nodes (of levels 3 and greater) those integers that require at least one application of $\bar{l}$ *and* one of $\bar{r}$ to obtain from 1 via (multiple) branching. Since the latter use Beatty pairs, the following question — dealing with the "unshifted" Beatty pairs themselves — emerges as even more fundamental.

For slopes $1 < \mu < 2$ and $\nu = 1/(1 - 1/\mu)$: Which positive integers N are necessarily "floor-powerfree numbers," meaning that if N obtains from 1 by a composition in $\{\lfloor n\mu \rfloor, \lfloor n\nu \rfloor\}^t$ for $t \geq 2$, then N requires at least one application of $\lfloor n\mu \rfloor$ and one application of $\lfloor n\nu \rfloor$ to obtain from 1? More succinctly, which positive integers cannot be expressed as a (not trivially) nested floor function with a single slope?

By means of sieves, Section 9.9.2 will address this basic question about floor-powerfree numbers, as well as the practical question about "branching function powers" not expressible as $\bar{l}^t(1)$ for $t \geq 2$, where $\bar{l}(n) = \lfloor (n+m-1)\mu \rfloor - 2m + 3$.

9.9. **A condition for blade duality and a sieve for floor-powerfree.**

9.9.1. *Blade-dual conditions for I–D arrays.* Consider an "outer" binary tree arrangement of the positive integers descending from root node 1 by branching rules of the form described in Section 9.5. That is, for irrational slopes $1 < \mu < 2$ and ν satisfying $\frac{1}{\mu} + \frac{1}{\nu} = 1$, the tree employs branching functions $\bar{l}(n) = (\lfloor (n+m-1)\mu \rfloor - 2m+3$ and $\bar{r} = \lfloor (n+m-1)\nu \rfloor - 2m+3)$ for fixed integer m satisfying $1 \leq m < \frac{1}{2-\mu}$.

Now, consider the I–D array whose rows comprise sequences of all-left branchings of this tree. Its topmost (0^{th}) row will have entries $\bar{l}^{k-1}(1)$ in columns $k = 1, 2, 3, \ldots$. In particular, by the formula for $\bar{l}$ and the domain to which μ was restricted, $\bar{l}(1) = 2$ for the second entry of the topmost row (left child of root node 1 in the tree). Thus the array satisfies Kimberling's second dispersion property (D2). Its remaining rows will take the form $\bar{l}^{k-1}\bar{r}(n)$ for $n = 1, 2, 3, \ldots$ and $k = 1, 2, 3, \ldots$, or alternatively, $\bar{l}^{k-1}\bar{r}T_n(1) = \bar{l}^{k-1}\bar{r}(n)$ for some compositions $T_1, T_2, T_3, \ldots, T_n, \ldots \in \{\bar{l}, \bar{r}\}^\star$ of $\bar{l}$ and $\bar{r}$ that satisfy $2 < \bar{r}T_1(1) < \bar{r}T_2(1) < \bar{r}T_3(1) < \cdots < \bar{r}T_n(1) < \cdots$. By the ordering chosen for the T_n, the first column $(1, \bar{r}T_1(1), \bar{r}T_2(1), \bar{r}T_3(1), \ldots)$ strictly increases, satisfying Kimberling's first dispersion property (D1). The results of Section 9.5 show that entries $\bar{l}^{k-1}\bar{r}T_n(1)$ of the remaining columns $k = 2, 3, 4 \ldots$ have at least one outer $\bar{l}$, complementing those of the first column, $\bar{r}T_n(1)$ with no outer $\bar{l}$, and moreover, $\bar{l}$ increases on its integer argument by definition, thus satisfying Kimberling's third dispersion property (D3). Finally, for rows $n = 1, 2, 3, \ldots$, adjacent entries in the same row read $\bar{l}^k\bar{r}T_n(1) = \bar{l} \circ \bar{l}^{k-1}\bar{r}T_n(1)$ for $k = 2, 3, 4 \ldots$, satisfying Kimberling's fourth dispersion property (D4).

Next, consider the blade dual I–D array whose rows comprise sequences of all-left branchings of the blade-dual tree. Being an "inner" binary tree descending from root node 1, the blade-dual tree differs from the original tree in as much the branching functions $\bar{l}$ and $\bar{r}$ apply on the inside when descending a path through the tree (equivalently, the blade-dual tree obtains from permuting the original tree as a sequence by the tree-blade permutation, `059893` — see Section 6.8.1). Let l and r be the "outer" version of branching functions for the blade-dual tree.

Observe that the the two arrays will have the same top (0^{th}) row, whereas the sequence of all-left branchings $l^{k-1}(1) = \bar{l}^{k-1}(1)$ in the two trees is indifferent to the order in $\bar{l}$ are applied and thus identical for $k = 1, 2, 3, \ldots$. In particular, $l(1) = \bar{l}(1) = 2$ which completes property (D2). Further, for $n = 1, 2, 3, \ldots$, the rest of the first column of the blade-dual array will comprise $r(n)$ for $n = 1, 2, 3, \ldots$, or alternatively, $S_n\bar{r}(1) = r(n)$ for some compositions $S_1, S_2, S_3, \ldots, S_n, \ldots \in \{\bar{l}, \bar{r}\}^\star$ of $\bar{l}$ and $\bar{r}$ satisfying $2 < S_1\bar{r}(1) < S_2\bar{r}(1) < S_3\bar{r}(1) < \cdots < S_n\bar{r}(1) < \cdots$. By the order chosen for the S_n, the first column $(1, S_1\bar{r}(1), S_2\bar{r}(1), S_3\bar{r}(1), \ldots)$ strictly increases, satisfying (D1). Moreover, the remaining rows $n = 1, 2, 3, \ldots$ take the complete form $S_n\bar{r}\bar{l}^{k-1}(1)$.

Again by Section 9.5, entries $S_n\bar{r}\bar{l}^{k-1}(1)$ of the remaining columns $k = 2, 3, 4 \ldots$ have at least one inner $\bar{l}$, complementing those of the first column, $S_n\bar{r}(1)$ with no inner $\bar{l}$, a necessary condition for (D3). Now, the right neighbor of an entry in the blade-dual array can be written $S_n\bar{r}\bar{l}^k(1) = r(S_n\bar{r}\bar{l}^{k-1}(1))$, for $k = 1, 2, 3, \ldots$. Equivalently, $S_n\bar{r}\bar{l}^{k-1}\bar{l}(1) = S_n\bar{r}\bar{l}^{k-1}(2) = r(S_n\bar{r}\bar{l}^{k-1}(1))$. Letting $S_n\bar{r}\bar{l}^{k-1} = R_n \in \{\bar{l}, \bar{r}\}^\star$, define r via $R_n(2) = rR_n(1)$. With r so defined, property (D4) follows, and it remains only to complete the sufficient condition for (D3), namely that r strictly increase on the sequence of positive integers, or $r(1) < r(2) < r(3) < \cdots$.

As an equivalent condition, first sort the R_n according to the image of 1 under each: $R_1(1) < R_2(1) < R_3(1) < \cdots$, and then require $R_1(2) < R_2(2) < R_3(2) < \cdots$. Whereas, the R_n are arbitrary compositions in $\{\bar{l}, \bar{r}\}^\star$ such that $\{R_n\}_{n=1,2,3,\ldots} = \{\bar{l}, \bar{r}\}^\star$, the condition requires $R_i(1) < R_j(1) \implies R_i(2) < R_j(2)$ for all $i, j \in \mathbb{Z}_{\geq 1}$, or equivalently the following:

Proposition 9.9 (Sufficient condition for the blade-dual to be an I–D array)**.** *For irrational slopes $1 < \mu < 2$ and ν satisfying $\frac{1}{\mu} + \frac{1}{\nu} = 1$, define $\bar{l}(n) =$*

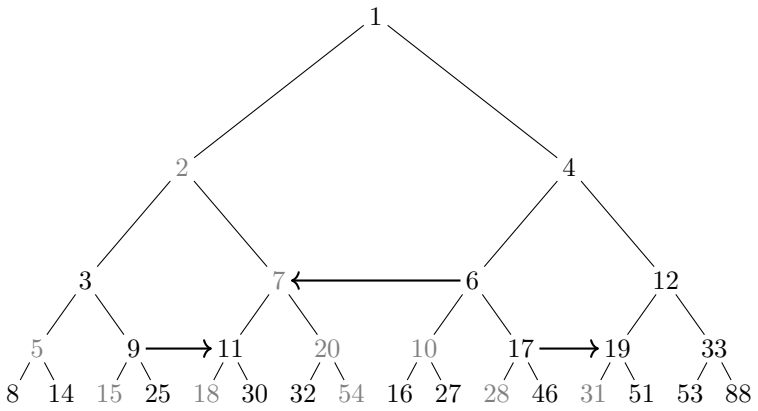

FIGURE 36. *Stolarsky tree* grown from branching rule $n \mapsto (\bar{l}(n), \bar{r}(n)) = (\lfloor n\phi - 1/2 \rfloor + 1, \lfloor n\phi^2 + \phi/2 \rfloor + 1)$. Sequences of left branchings are rows of the Stolarsky array (035506). Sequences of right branchings are rows of the Stolarsky mirror array (035507). The blade-dual of the Stolarsky array, constructed from the tree using the set of its right clades as columns, does not inherit the I–D properties of the original array, as evidenced by the opposing directions of arrows that show node labels $7 > 6$ of the tree ordered differently than those of its 1st left clade ($9 > 11$), in contrast to (109). Neither will the blade mirror array of the Stolarsky array inherit its I–D property, since node labels ($17 > 19$) of the 1st right clade are also ordered differently than those of the tree.

$(\lfloor (n+m-1)\mu \rfloor - 2m + 3$ *and* $\bar{r} = \lfloor (n+m-1)\nu \rfloor - 2m + 3)$ *for fixed integer* m *satisfying* $1 \leq m < \frac{1}{2-\mu}$. *Further, define the I–D array* $\begin{pmatrix} \bar{l}^{k-1}(1),\ n = 0; \\ \bar{l}^{k-1}\bar{r}(n),\ n \geq 1. \end{pmatrix}_{\substack{n=0,1,2,\ldots \\ k=1,2,3,\ldots}}$ *Then, sufficient conditions for its blade dual array to have Kimberling's I–D properties are:*

$$R(1) < S(1) \implies R(2) < S(2) \text{ for all } R, S \in \{\bar{l}, \bar{r}\}^\star. \tag{109}$$

With the exception of the blade quartet shown in Table 41, none of the other I–D arrays previously introduced here in Section 9 has a blade-dual that is also an I–D array. As well, many of these arrays do not satisfy the assumptions of Proposition 9.9, not having been generated by the specific formulation of Section 9.5. It is worth noting that important I–D arrays not treated in this present context also have blade duals that are not I–D arrays. For example, the blade dual of the Stolarsky array is not an I–D array (see Figure 36). For this reason, the sieve of the next subsection provides an initial approach for identifying whether a tree is the blade dual of one with the particular formulation of Section 9, or another predefined branching rule type.

For binary-tree arrangements of the 1st n positive integers satisfying (104), computational experiments counted 000111$(n) = 1, 1, 2, 5, 16, 61, 272, 1385, 7936, 50521, 353792, \ldots$ trees.

For binary-tree arrangements of the 1st n positive integers satisfying, in addition to (104), the right-hand counterpart of (109), that is, order isomorphism between

the tree and its 1st *right* clade, computational experiments counted $\underline{000110}(n-1) = 1, 1, 2, 5, 15, 52, 203, 877, 4140, 21147, 115975\ldots$ trees.

For binary-tree arrangements of the 1st n positive integers satisfying (109) in addition to (104), computational experiments counted $\underline{000667}(n-2) = 1, 1, 2, 4, 9, 24, 77, 294, 1309, 6664, 38177, \ldots$ trees.

For binary-tree arrangements of the 1st n positive integers satisfying complete clade–tree order isomorphism in addition to (104), computational experiments counted $\underline{011782}(n-1) = 1, 1, 2, 4, 8, 16, 32, 64, 128, 256, 512, \ldots$ trees, or 2^{n-2} for $n \geq 2$.

Example 9.9 (The half-integer shift of a branching rule that uses Beatty pairs)**.** The shift $m = 3/2$, gives the branching rule $n \mapsto (\lfloor (n+1/2)\phi \rfloor, \lfloor (n+1/2)\phi^2 \rfloor)$, which grows the "mean successor tree" shown in Figure 37. Unlike the Stolarsky tree, (Figure 36), the mean successor tree does satisfy (109), but does not satisfy the comparable clade–tree order isomorphism for the 1st right clade, as demonstrated by the arrows in the Figure.

Also of note, the images of 1 under iterated powers of the left and **right** branching functions in Figure 37 intersperse regularly in a ratio of two to one: $\mathbf{1} = 1 < 2 < \mathbf{3} < 4 < 7 < \mathbf{9} < 12 < 20 < \mathbf{24} < 33 < 54 < \mathbf{64} < 88 < 143 < \mathbf{168} < 232 < 376 < \mathbf{441} < 609 < 986 < \mathbf{1155} < 1596 < 2583 < \mathbf{3025} < 4180 < 6764 < \mathbf{7920} < 10945 < 17710 < \mathbf{20736} < 28656 < \cdots$. Apparently, for $t = 1, 2, 3, \ldots$, the difference $\bar{l}^{2t}(1) - \bar{r}^{t}(1)$ equals $\underline{064831}(t)$ while for $t = 0, 1, 2, \ldots$ the difference $\bar{r}^{t+1}(1) - \bar{l}^{2t+1}(1)$ equals $\underline{166516}_1(t+1)$, with the additional inferences that $\underline{166516}(t+1) = \underline{064831}(t)+1$ and that $\underline{166516}(t+1)+\underline{064831}(t) = \underline{061646}(t)$.

Figure 38 shows the blade dual of the mean successor tree. Sequences of all-left (all-right) branchings in the two trees yield the arrays at the left (right) of Table 47. The array at the bottom left of the Table is the 2–1-Fibonacci array, $\vdash$. The array at the bottom right of the table is *not* an I–D array, but several of its rows seem to match sequences of interest to researchers:

The first, second, and third rows appear to be $\underline{064831}$, $\underline{059840}$, and $\underline{107840}$, respectively, which would give these integer sequences as the images of 1, 2, and 4, under the sequence of iterated powers of $r(n) = F_{F^{-1}(n)+3} - n - 1$.

9.9.2. *A sieve for floor-powerfree.* Part of this ongoing investigation [35], Table 48 presents a sieve for generating "floor-powerfree" integers, *i.e.* those not expressible as the image of 1 under multiple iterations of $\lfloor n\mu \rfloor$ for any $\mu > 1$. Though presenting the sieve with only minimal discussion, its construction is simple, and the table leaves certain fractions unreduced, while displaying others in bold font, thus providing the reader with a blueprint to reproduce the sieve. Though not addressed to this specific question, [18] may prove instrumental for finding these floor-powerfree numbers without recourse to a sieve, as it characterizes $\lfloor n\mu \rfloor$ based on the parity of its final zeroes in a numeration system that uses convergents to μ.

Analogous to that for the simple floor function, tabulations for shifted branching functions appear in Tables 49 and 50, the latter of which also serves as a sieve for branching-function-powerfree numbers of the $m = 2$ type. When generating trees computationally as described in Section 9.9.1, preparing these tables in advance simplifies the work of identifying and eliminating trees whose blade duals do not use as branching functions shifted Beatty pairs or some other predefined type of branching rule.

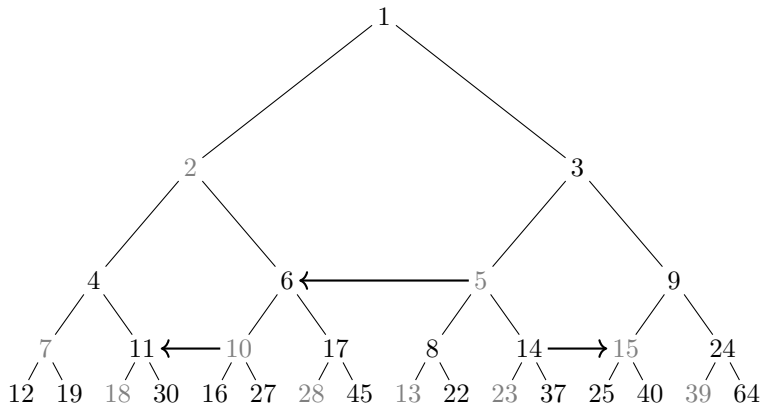

FIGURE 37. The "mean successor tree" grown using the branching rule $n \mapsto (\lfloor (n + 1/2)\phi \rfloor, \lfloor (n + 1/2)\phi^2 \rfloor)$ (shift $m = 3/2$ of the Wythoff pair). Sequences of all-left (all-right) branchings are rows of arrays at the top left (right) of Table 47. Sequences of right (left) clades are columns of arrays at bottom of Table 47, only one of which is an I–D array. Arrows indicate the presence of clade–tree isomorphism for the 1st left clade and its absence for the 1st right clade. Blade dual of Figure 38.

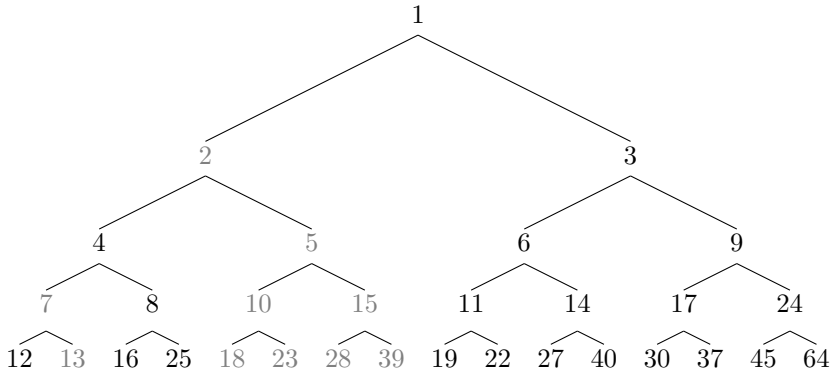

FIGURE 38. Blade dual of Figure 37, grown using the branching rule $n \mapsto (l(n), r(n)) = (n + F_{F^{-1}(n)}, F_{F^{-1}(n)+3} - n - 1)$. Here, $r(n)$ is non-monotonic. Sequences of all-left (all-right) branchings are rows of arrays at the bottom left (right) of Table 47. Sequences of right (left) clades are columns of arrays at top of Table 47.

For example, considering a slope $\mu \geq \frac{3}{2}$, Figures 39(i) and (ii) show the possible values for the outermost nodes of the trees generated by the branching functions $n \mapsto (\lfloor n\mu \rfloor + 1, \lfloor n\nu \rfloor + 1)$ and $n \mapsto (\lfloor (n + 1)\mu \rfloor - 1, \lfloor (n + 1)\nu \rfloor - 1)$, respectively.

To conclude this topic, ongoing work continues to search for the potential "missing link" between the octet of branch and clade arrays (Tables 3 & 4) and the quartet of blade arrays (Table 41).

In view of the foregoing, the kinship of the Fibonacci trees ($\mu = \phi$) and the Positions tree ($\mu \to 2$) vis-à-vis blade duality may prove unique the former has

$\Longleftarrow$ Mirror Duality $\Longrightarrow$

1	2	4	7	12	20	1	3	9	24	64	168
3	5	8	13	21	34	2	6	17	45	119	312
6	10	16	26	42	68	4	11	30	79	208	545
9	15	25	41	67	109	5	14	37	98	257	674
11	18	29	47	76	123	7	19	51	134	352	922
14	23	38	62	101	164	8	22	58	153	401	1051
17	28	46	75	122	198	10	27	71	187	490	1284
19	31	50	81	131	212	12	32	85	223	585	1532
22	36	59	96	156	253	13	35	92	242	634	1661
24	39	63	102	165	267	15	40	106	278	729	1909
1	2	4	7	12	20	1	3	9	24	64	168
3	6	11	19	32	53	2	**5**	**15**	39	104	272
5	10	18	31	52	86	4	8	25	63	169	440
8	16	29	50	84	139	**6**	**14**	40	103	273	713
9	17	30	51	85	140	7	13	41	102	274	712
13	26	47	81	136	225	10	23	65	167	442	1154
14	27	48	82	137	226	11	22	66	166	443	1153
15	28	49	83	138	227	12	21	67	165	444	1152
21	42	76	131	220	364	16	38	105	271	715	1868
22	43	77	132	221	365	17	37	106	270	716	1867
2–1-Fibonacci Array($\vdash$) $n + F_{F^{-1}(n)+k+2} - F_{F^{-1}(n)+2}$						Not an I–D array					

$\Longleftarrow$ Blade Duality $\Longrightarrow$

TABLE 47. In the "mean successor quartet," three of four arrays are I–D arrays. Rows of arrays at the top obtain from sequences of all-left or all-right branching in a tree, Figure 37, descending from 1 with branching rule $n \mapsto (\lfloor (n + 1/2)\phi \rfloor, \lfloor (n + 1/2)\phi^2 \rfloor)$. Rows of arrays at the bottom obtain from sequences of all-left or all-right branching in its blade-dual: a degenerate tree, Figure 38, descending from 1 with branching rule $n \mapsto (n + F_{F^{-1}(n)}, F_{F^{-1}(n)+3} - n - 1)$.

continued fraction expansion $[1; 1, 1, 1, \ldots]$ whilst the latter has binary decimal expansion $1.111\cdots$. For now, though, the search continues for other kin.

Candidates for branching functions include floor functions using as slopes algebraic numbers in $(\phi, 2)$, particularly those with no conjugates outside the unit circle. Also, the shifted branching functions that use Beatty pairs of Section 9.5 encompass only some of the *N-upper complementary* pairs of sets studied by Fraenkel in [15] (see Remark 9.1). Thus the "non-homogeneous" or "2-parameter" extensions of Beatty pairs (treated in [15] and further works by Fraenkel and others) also merit further investigation as candidate floor functions for $\bar{l}$. It may be that branching functions exhibiting blade duality and the other desired properties require an altogether different formulation. This too forms part of the ongoing research program in [35].

μ:	1	2											
1^{st}:	1	2											
μ:	**1**	**2**											
2^{nd}:	1	4											
μ:	**1**	**2**					$\frac{9}{4}$						
3^{rd}:	1	8					9						
μ:	**1**	**2**		$\frac{17}{8}$			$\mathbf{\frac{9}{4}}$		$\frac{21}{9}$			$\frac{22}{9}$	
4^{th}:	1	16		17			20		21			22	
μ:	**1**	**2**	$\frac{33}{16}$	$\mathbf{\frac{17}{8}}$	$\frac{37}{17}$	$\frac{38}{17}$	$\mathbf{\frac{9}{4}}$	$\frac{46}{20}$	$\mathbf{\frac{7}{3}}$	$\frac{50}{21}$	$\frac{51}{21}$	$\mathbf{\frac{22}{9}}$	$\frac{54}{22}$
5^{th}:	1	32	33	36	37	38	45	46	49	50	51	53	54
	⋮	⋮	⋮	⋮	⋮	⋮	⋮	⋮	⋮	⋮	⋮	⋮	⋮

μ:													
1^{st}:													
μ:	$\frac{5}{2}$												
2^{nd}:	5												
μ:	$\mathbf{\frac{5}{2}}$				$\frac{13}{5}$								
3^{rd}:	12				13								
μ:	$\mathbf{\frac{5}{2}}$			$\frac{31}{12}$	$\mathbf{\frac{13}{5}}$		$\frac{34}{13}$				$\frac{35}{13}$		
4^{th}:	30			31	33		34				35		
μ:	$\mathbf{\frac{5}{2}}$	$\frac{76}{30}$	$\frac{77}{30}$	$\mathbf{\frac{31}{12}}$	$\mathbf{\frac{13}{5}}$	$\frac{86}{33}$	$\mathbf{\frac{34}{13}}$	$\frac{89}{34}$	$\frac{90}{34}$	$\frac{91}{34}$	$\mathbf{\frac{35}{13}}$	$\frac{95}{35}$	$\frac{96}{35}$
5^{th}:	75	76	77	80	85	86	88	89	90	91	94	95	96
	⋮	⋮	⋮	⋮	⋮	⋮	⋮	⋮	⋮	⋮	⋮	⋮	⋮

μ:													3	…
1^{st}:													3	…
μ:													**3**	…
2^{nd}:													9	…
μ:			$\frac{14}{5}$										**3**	…
3^{rd}:			14										27	…
μ:	$\frac{36}{13}$		$\mathbf{\frac{14}{5}}$			$\frac{40}{14}$				$\frac{41}{14}$			**3**	…
4^{th}:	36		39			40				41			81	…
μ:	$\frac{36}{13}$	$\frac{100}{36}$	$\mathbf{\frac{14}{5}}$	$\frac{110}{39}$	$\frac{111}{39}$	$\mathbf{\frac{20}{7}}$	$\frac{115}{40}$	$\frac{116}{40}$	$\frac{117}{40}$	$\mathbf{\frac{41}{14}}$	$\frac{121}{41}$	$\frac{122}{41}$	**3**	…
5^{th}:	99	100	109	110	111	114	115	116	117	120	121	122	243	…
	⋮	⋮	⋮	⋮	⋮	⋮	⋮	⋮	⋮	⋮	⋮	⋮	⋮	⋱

"Floor-powerfree numbers," passing the sieve (below the line) of 2^{nd} floor powers, 3^{rd} floor powers, 4^{th} floor powers, etc. for any slope $\mu \geq 1$: 2, 3, 6, 7, 15, 23, 24, 44, 47, 48, 56, 57, 58, 59, 60, 61, 62, 63, 79, 97, 98, 113, 143, 167, 184, 185, 186, 210, 211, 212, 213, 214, 215, 222, 223, 247, 287, 320, 321, 356, 381, 462, 463, 474, 475, 481, 482, 483, 507, 508, 520, 521, 522, 553, 559, 604, 623, 661, 662, 671, 717, 718, 719, 720, 817, 819, 820, 839, 936, 941, 942, 943, 944, 945, 946, 947, 993, 994, 995, 1015, 1016, 1017,…

Table 48. A sieve for finding "floor-powerfree numbers" by successively sifting out floor powers greater than or equal to two (those below the line) of any slope μ, that is, floor squares, floor cubes, floor quartics, etc. of all slopes μ. Each line beginning with "μ" in the table shows the least μ that yields the integer below it, when applied as the slope of a floor function nested with the power shown at left.

μ:	1									2																														3	…
1^{st}:	2									3																														4	…
μ:	$\mathbf{1}$				$\frac{3}{2}$					$\mathbf{2}$								$\frac{7}{3}$											$\frac{8}{3}$											$\mathbf{3}$	…
2^{nd}:	3				4					7								8											9											13	…
μ:	$\mathbf{1}$		$\frac{4}{3}$		$\frac{\mathbf{3}}{\mathbf{2}}$			$\frac{7}{4}$		$\mathbf{2}$			$\frac{15}{7}$			$\frac{16}{7}$		$\frac{\mathbf{7}}{\mathbf{3}}$		$\frac{19}{8}$			$\frac{20}{8}$				$\frac{21}{8}$		$\frac{\mathbf{8}}{\mathbf{3}}$				$\frac{25}{9}$				$\frac{26}{9}$			$\mathbf{3}$	…
3^{rd}:	4		5		7			8		15			16			17		19		20			21				22		25				26				27			40	…
μ:	$\mathbf{1}$	$\frac{5}{4}$	$\frac{\mathbf{4}}{\mathbf{3}}$	$\frac{7}{5}$	$\frac{\mathbf{3}}{\mathbf{2}}$	$\frac{11}{7}$	$\frac{12}{7}$	$\frac{\mathbf{7}}{\mathbf{4}}$	$\frac{15}{8}$	$\mathbf{2}$	$\frac{31}{15}$	$\frac{32}{15}$	$\frac{\mathbf{15}}{\mathbf{7}}$	$\frac{35}{16}$	$\frac{36}{16}$	$\frac{\mathbf{16}}{\mathbf{7}}$	$\frac{39}{17}$	$\frac{\mathbf{7}}{\mathbf{3}}$	$\frac{45}{19}$	$\frac{\mathbf{19}}{\mathbf{8}}$	$\frac{48}{20}$	$\frac{49}{20}$	$\frac{\mathbf{20}}{\mathbf{8}}$	$\frac{53}{21}$	$\frac{54}{21}$	$\frac{55}{21}$	$\frac{\mathbf{21}}{\mathbf{8}}$	$\frac{58}{22}$	$\frac{\mathbf{8}}{\mathbf{3}}$	$\frac{67}{25}$	$\frac{68}{25}$	$\frac{69}{25}$	$\frac{\mathbf{25}}{\mathbf{9}}$	$\frac{73}{26}$	$\frac{74}{26}$	$\frac{75}{26}$	$\frac{\mathbf{26}}{\mathbf{9}}$	$\frac{79}{27}$	$\frac{80}{27}$	$\mathbf{3}$	…
4^{th}:	5	6	7	8	11	12	13	15	16	31	32	33	35	36	37	39	40	45	46	48	49	50	53	54	55	56	58	59	67	68	69	70	73	74	75	76	79	80	81	121	…
	⋮	⋮	⋮	⋮	⋮	⋮	⋮	⋮	⋮	⋮	⋮	⋮	⋮	⋮	⋮	⋮	⋮	⋮	⋮	⋮	⋮	⋮	⋮	⋮	⋮	⋮	⋮	⋮	⋮	⋮	⋮	⋮	⋮	⋮	⋮	⋮	⋮	⋮	⋮	⋮	⋱

TABLE 49. A “table of branching powers”: The Table gives successive powers of branching function $\lfloor n\mu \rfloor + 1$ for any slope μ, that is, squares, cubes, quartics, etc. of the branching function. Each line beginning with “μ” in the table shows the least μ that yields the integer below it, when applied as the slope of the branching function nested with the power shown at left.

μ:	1	$\frac{3}{2}$					2												$\frac{5}{2}$			
1^{st}:	1	2					3												4			
μ:	$\mathbf{1}$	$\mathbf{\frac{3}{2}}$	$\frac{5}{3}$				$\mathbf{2}$					$\frac{9}{4}$							$\mathbf{\frac{5}{2}}$			
2^{nd}:	1	3	4				7					8							11			
μ:	$\mathbf{1}$	$\mathbf{\frac{3}{2}}$	$\mathbf{\frac{5}{3}}$		$\frac{9}{5}$		$\mathbf{2}$		$\frac{17}{8}$			$\mathbf{\frac{9}{4}}$		$\frac{21}{9}$			$\frac{22}{9}$		$\mathbf{\frac{5}{2}}$			$\frac{31}{12}$
3^{rd}:	1	5	7		8		15		16			19		20			21		29			30
μ:	$\mathbf{1}$	$\mathbf{\frac{3}{2}}$	$\mathbf{\frac{5}{3}}$	$\frac{14}{8}$	$\mathbf{\frac{9}{5}}$	$\frac{17}{9}$	$\mathbf{2}$	$\frac{33}{16}$	$\mathbf{\frac{17}{8}}$	$\frac{37}{17}$	$\frac{38}{17}$	$\mathbf{\frac{9}{4}}$	$\frac{46}{20}$	$\mathbf{\frac{21}{9}}$	$\frac{50}{21}$	$\frac{51}{21}$	$\mathbf{\frac{22}{9}}$	$\frac{54}{22}$	$\mathbf{\frac{5}{2}}$	$\frac{76}{30}$	$\frac{77}{30}$	$\mathbf{\frac{31}{12}}$
4^{th}:	1	8	12	13	15	16	31	32	35	36	37	44	45	48	49	50	52	53	74	75	76	79
	⋮ ⋮	⋮	⋮	⋮	⋮	⋮	⋮	⋮	⋮	⋮	⋮	⋮	⋮	⋮	⋮	⋮	⋮	⋮	⋮	⋮	⋮	⋮

μ:																						3	…
1^{st}:																						5	…
μ:	$\frac{13}{5}$											$\frac{14}{5}$										$\mathbf{3}$	…
2^{nd}:	12											13										17	…
μ:	$\mathbf{\frac{13}{5}}$		$\frac{34}{13}$				$\frac{35}{13}$			$\frac{36}{13}$		$\mathbf{\frac{14}{5}}$			$\frac{40}{14}$				$\frac{41}{14}$			$\mathbf{3}$	…
3^{rd}:	32		33				34			35		38			39				40			53	…
μ:	$\mathbf{\frac{13}{5}}$	$\frac{86}{33}$	$\mathbf{\frac{34}{13}}$	$\frac{89}{34}$	$\frac{90}{34}$	$\frac{91}{34}$	$\mathbf{\frac{35}{13}}$	$\frac{95}{35}$	$\frac{96}{35}$	$\mathbf{\frac{36}{13}}$	$\frac{100}{36}$	$\mathbf{\frac{14}{5}}$	$\frac{110}{39}$	$\frac{111}{39}$	$\mathbf{\frac{40}{14}}$	$\frac{115}{40}$	$\frac{116}{40}$	$\frac{117}{40}$	$\mathbf{\frac{41}{14}}$	$\frac{121}{41}$	$\frac{122}{41}$	$\mathbf{3}$	…
4^{th}:	84	85	87	88	89	90	93	94	95	98	99	108	109	110	113	114	115	116	119	120	121	161	…
	⋮	⋮	⋮	⋮	⋮	⋮	⋮	⋮	⋮	⋮	⋮	⋮	⋮	⋮	⋮	⋮	⋮	⋮	⋮	⋮	⋮	⋮	…

"Branching-function-powerfree" n, passing the sieve (below the line) of 2^{nd} powers, 3^{rd} powers, 4^{th} powers, etc. of branching function $\lfloor (n+1)\mu \rfloor - 1$ for any slope $\mu \geq 1$: 2, 6, 9, 10, 14, 46, 158, 437, 438, 439, 667, 675, 752, 783, 877, 922, 965, 1002, 1004,…

Table 50. A sieve for finding "branching-function-powerfree numbers" by successively sifting out powers greater than or equal to two (those below the line) of branching function $\lfloor (n+1)\mu \rfloor - 1$ for any slope μ, that is, squares, cubes, quartics, etc. of the branching function. Each line beginning with "μ" in the table shows the least μ that yields the integer below it, when applied as the slope of the branching function nested with the power shown at left.

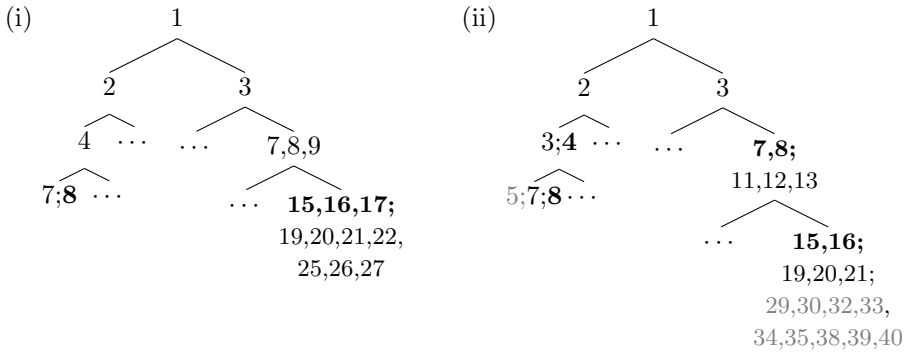

FIGURE 39. Possible values of "outermost" nodes of binary trees arranging the positive integers, using a slope $\frac{3}{2} \leq \mu < 2$ and its Beatty conjugate ν in the branching rule. At left: (i) $n \mapsto (\lfloor n\mu \rfloor + 1, \lfloor n\nu \rfloor + 1)$ (see sieve, Table 49). At right: $n \mapsto (\lfloor (n+1)\mu \rfloor - 1, \lfloor (n+1)\nu \rfloor - 1)$ (see sieve, Table 50).

10. Conclusions

In this second of three parts, the Fibonacci cohort structure proved useful for studying a quilt after Fibonacci (Figure 1). Besides allowing convenient formulas for sequences arising from the quilt, the paper identified Fibonacci cohort structures and more general cohort structures in other sequences of integers, tuples, and functions (Table 8).

In particular, a pair of dual structures, the 2–1- and 1–2-Fibonacci cohort sequence arose repeatedly and dually in the guise of integer sequences, binary trees, Fibonacci numeration, restricted compositions of integers, interspersion arrays, and the free monoids $\{\kappa, \lambda\}^\star$ and $\{\eta, \theta\}^\star$ on pairs of Wythoff, respectively, Wythoff^{-1} functions under composition, and the related $\{\boldsymbol{l}, \boldsymbol{r}\}^\star$, $\{\boldsymbol{L}, \boldsymbol{R}\}^\star$, $\{\bar{\boldsymbol{l}}, \bar{\boldsymbol{r}}\}^\star$, and $\{\bar{\boldsymbol{L}}, \bar{\boldsymbol{R}}\}^\star$. The paper examined these structures and attempted to generalize them with varying degrees of success.

The cohort identities developed in this part of the paper will allow the derivation of interspersion–dispersion properties for the quilt sequences in Part 3 of the paper [40]. Part 3 will also use the quilt to provide a visualization for complementary equations.

11. Longer Proofs

Proof of Lemma 4.5. Lower Bounds First consider a Fibonacci cohort sequence from the 2^{nd} cohort, and suppose that $t \geq 3$ is even and p is even.

$$\begin{aligned}
S_n &= F_{t+p} + S_{n-F_t}, n \in [F_{t+1}, F_{t+2}),\\
&\geq F_{t+p} + S_{F_{t+1}-F_t}\\
&= F_{t+p} + S_{F_{t-1}}\\
&= F_{t+p} + F_{t+p-2} + S_{m-F_{t-2}}, m \in [F_{t-1}, F_t),\\
&\geq F_{t+p} + F_{t+p-2} + S_{F_{t-1}-F_{t-2}}\\
&= F_{t+p} + F_{t+p-2} + S_{F_{t-3}}\\
&= F_{t+p} + F_{t+p-2} + F_{t+p-4} + S_{m-F_{t-4}}, m \in [F_{t-3}, F_{t-2}),\\
&\vdots\\
&\geq F_{t+p} + F_{t+p-2} + F_{t+p-4} + \cdots + F_{p+4} + S_{m-F_4}, m \in [F_5, F_6),\\
&= F_{t+p} + F_{t+p-2} + F_{t+p-4} + \cdots + F_{p+4} + S_{m-3}, m \in \{5, 6, 7\},\\
&\geq F_{t+p} + F_{t+p-2} + F_{t+p-4} + \cdots + F_{p+4} + S_2\\
&= S_2 + \sum_{k=(p+4)/2}^{(t+p)/2} F_{2k}\\
&= S_2 + \sum_{k=0}^{(t+p)/2} F_{2k} - \sum_{k=0}^{(p+4)/2-1} F_{2k}\\
&= S_2 + F_{t+p+1} - F_{p+3}.
\end{aligned}$$

Whereas, for $t \geq 3$ even and p odd,

$$\begin{aligned}
S_n &\geq F_{t+p} + F_{t+p-2} + F_{t+p-4} + \cdots + F_{p+4} + S_{m-F_4}, m \in [F_5, F_6),\\
&= F_{t+p} + F_{t+p-2} + F_{t+p-4} + \cdots + F_{p+4} + S_{m-3}, m \in \{5, 6, 7\},\\
&\geq F_{t+p} + F_{t+p-2} + F_{t+p-4} + \cdots + F_{p+4} + S_2\\
&= S_2 + \sum_{k=(p+4-1)/2}^{(t+p-1)/2} F_{2k+1}\\
&= S_2 + \sum_{k=0}^{(t+p-1)/2} F_{2k} - \sum_{k=0}^{(p+4-1)/2-1} F_{2k}\\
&= S_2 + F_{t+p+1} - F_{p+3}.
\end{aligned}$$

Similarly, for $t \geq 3$ odd and p odd,

$$\begin{aligned}
S_n &\geq F_{t+p} + F_{t+p-2} + F_{t+p-4} + \cdots + F_{p+3} + S_{m-F_3}, m \in [F_4, F_5), \\
&= F_{t+p} + F_{t+p-2} + F_{t+p-4} + \cdots + F_{p+3} + S_{m-2}, m \in \{3, 4\}, \\
&\geq F_{t+p} + F_{t+p-2} + F_{t+p-4} + \cdots + F_{p+3} + S_1 \\
&= S_1 + \sum_{k=(p+3)/2}^{(t+p)/2} F_{2k} \\
&= S_1 + \sum_{k=0}^{(t+p)/2} F_{2k} - \sum_{k=0}^{(p+3)/2-1} F_{2k} \\
&= S_1 + F_{t+p+1} - F_{p+2}.
\end{aligned}$$

Whereas, for $t \geq 3$ odd and p even,

$$\begin{aligned}
S_n &\geq F_{t+p} + F_{t+p-2} + F_{t+p-4} + \cdots + F_{p+3} + S_{m-F_3}, m \in [F_4, F_5), \\
&= F_{t+p} + F_{t+p-2} + F_{t+p-4} + \cdots + F_{p+3} + S_{m-2}, m \in \{3, 4\}, \\
&\geq F_{t+p} + F_{t+p-2} + F_{t+p-4} + \cdots + F_{p+3} + S_1 \\
&= S_1 + \sum_{k=(p+3-1)/2}^{(t+p-1)/2} F_{2k+1} \\
&= S_1 + F_{t+p+1} - F_{p+2}.
\end{aligned}$$

Now for a Fibonacci cohort sequence from the 1st cohort, the foregoing result is identical for $t \geq 2$ odd. For $t \geq 2$ even and p even,

$$\begin{aligned}
S_n &\geq F_{t+p} + F_{t+p-2} + F_{t+p-4} + \cdots + F_{p+2} + S_{m-F_2}, m \in [F_3, F_4), \\
&= F_{t+p} + F_{t+p-2} + F_{t+p-4} + \cdots + F_{p+2} + S_{m-1}, m = 2, \\
&\geq F_{t+p} + F_{t+p-2} + F_{t+p-4} + \cdots + F_{p+2} + S_1 \\
&= S_1 + \sum_{k=(p+2)/2}^{(t+p)/2} F_{2k} \\
&= S_1 + F_{t+p+1} - F_{p+1}.
\end{aligned}$$

Whereas, for $t \geq 2$ even and p odd

$$\begin{aligned}
S_n &\geq F_{t+p} + F_{t+p-2} + F_{t+p-4} + \cdots + F_{p+2} + S_{m-F_2}, m \in [F_3, F_4), \\
&= F_{t+p} + F_{t+p-2} + F_{t+p-4} + \cdots + F_{p+2} + S_{m-1}, m = 2, \\
&\geq F_{t+p} + F_{t+p-2} + F_{t+p-4} + \cdots + F_{p+2} + S_1 \\
&= S_1 + \sum_{k=(p+2-1)/2}^{(t+p-1)/2} F_{2k+1} \\
&= S_1 + F_{t+p+1} - F_{p+1}.
\end{aligned}$$

Upper Bounds

$$\begin{aligned}
S_n &= F_{t+p} + S_{n-F_t}, n \in [F_{t+1}, F_{t+2}),\\
&\leq F_{t+p} + S_{F_{t+2}-F_t-1}\\
&= F_{t+p} + S_{F_{t+1}-1}\\
&= F_{t+p} + F_{t+p-1} + S_{m-F_{t-1}}, m \in [F_t, F_{t+1}),\\
&\leq F_{t+p} + F_{t+p-1} + S_{F_{t+1}-F_{t-1}-1}\\
&= F_{t+p} + F_{t+p-1} + S_{F_t-1}\\
&= F_{t+p} + F_{t+p-1} + F_{t+p-2} + S_{m-F_{t-2}}, m \in [F_{t-1}, F_t),\\
&\vdots\\
&\leq F_{t+p} + F_{t+p-1} + F_{t+p-2} + \cdots + F_{p+3} + S_{m-F_3}, m \in [F_4, F_5),\\
&= F_{t+p} + F_{t+p-1} + F_{t+p-2} + \cdots + F_{p+3} + S_{m-2}, m \in \{3, 4\},\\
&\leq F_{t+p} + F_{t+p-1} + F_{t+p-2} + \cdots + F_{p+3} + S_2,
\end{aligned}$$

from which, for a Fibonacci cohort sequence from the 2nd cohort, continue

$$\begin{aligned}
S_n &\leq S_2 + \sum_{k=p+3}^{t+p} F_k\\
&= S_2 + F_{t+p+2} - F_{p+4},
\end{aligned}$$

whereas, for a Fibonacci cohort sequence from the 1st cohort, continue

$$\begin{aligned}
S_n &\leq S_2 + \sum_{k=p+3}^{t+p} F_k\\
&= S_1 + \sum_{k=p+2}^{t+p} F_k\\
&= S_1 + F_{t+p+2} - F_{p+3}.
\end{aligned}$$

□

Proof of Lemma 4.13(**a**). Base case: First observe that the lemma holds for the initial levels of the two trees.

First Level, **(i)**: $n = 1 = F_2$ in Figure 5, corresponding to $T = \kappa^{2-2} = I$ in Figure 4.

Second Level, **(i)**: $n = 2 = F_3$, corresponding to $T = \kappa^{3-2} = \kappa$. Second Level, **(ii)**: $m = 1$ and $n = 4 = 1 + F_4$, with $F_2 \leq 1 < F_3$ and $F_4 < 4 < F_5$, corresponding to $R = I$ and $T = R\lambda\kappa^{4-2-2} = \lambda$, respectively.

Third Level, **(i)**: $n = 3 = F_4$, corresponding to $T = \kappa^{4-2} = \kappa^2$. Third Level, **(ii)**: $m = 2$ and $n = 7 = 2 + F_5$, with $F_3 \leq 2 < F_4$ and $F_5 < 7 < F_6$, corresponding to $R = \kappa$ and $T = R\lambda\kappa^{5-3-2} = \kappa\lambda$, respectively; $m = 1$ and $n = 6 = 1 + F_5$, with $F_2 \leq 1 < F_3$ and $F_5 < 6 < F_6$, corresponding to $R = I$ and $T = R\lambda\kappa^{5-2-2} = \lambda\kappa$, respectively; and $m = 4$ and $n = 12 = 4 + F_6$, with $F_4 < 4 < F_5$ and $F_6 < 12 < F_7$, corresponding to $R = \lambda$ and $T = R\lambda\kappa^{6-4-2} = \lambda^2$, respectively.

Next, recall that by construction of the trees $n = T(2) - 1$, where T is the corresponding node in Figure 4.

Induction case 1: n is a right child. Suppose $T = R\lambda$, and thus T is a right child of R, and, correspondingly, $n = T(2) - 1$ is a right child of $R(2) - 1$. Then, $n = T(2)-1 = R\lambda(2)-1 = R(5)-1$. Let $m = R(2)-1$. Now, by Proposition 4.7**(b)**, there exists u for which $F_u \leq R(2)-1 < F_{u+1}$, and, moreover, $R(5) = R(2)+F_{u+2}$. Therefore, $n = R(2)-1+F_{u+2}$, and we have $F_{u+2} < F_{u+2}+F_u \leq n < F_{u+2}+F_{u+1} = F_{u+3}$. Thus, n satisfies **(a)(ii)** with $t = u+2$ and $F_{t-2} \leq m < F_{t-1}$, corresponding to $T = R\lambda\kappa^{t-u-2} = R\lambda$, which verifies the formula.

Induction case 2: n is a left child. Suppose $T = S\kappa$, and thus T is a left child of S, and, correspondingly, $n = T(2) - 1 = S\kappa(2) - 1$ is a left child of $S(2) - 1$. Then, $n = T(2) - 1 = S\kappa(2) - 1 = S(3) - 1$.

By Proposition 4.7(b), there exists v for which $F_v \leq S(2) - 1 < F_{v+1}$ and, moreover, $S(3) = S(2)+F_{v-1}$. Therefore, $n = T(2)-1 = S(3)-1 = S(2)+F_{v-1}-1$, and we have $F_{v+1} = F_v + F_{v-1} \leq n < F_{v+1} + F_{v-1} < F_{v+2}$, hence $t = v + 1$.

By induction, either (i) $S(2)-1$ is a Fibonacci number or, (ii) S has an ancestor R satisfying for some u, $F_u \leq R(2)-1 < F_{u+1}$ and $S(2) = R(2)+F_v = R(2)+F_{t-1}$.

Induction subcase 2(i): n is a left child of a Fibonacci number, that is, $S(2) - 1$ is a Fibonacci number. Since $F_v \leq S(2) - 1 < F_{v+1}$, the first inequality must be satisfied with equality, giving $S(2)-1 = F_v$. Thus, $n = S(3)-1 = S(2)+F_{v-1}-1 = F_v + F_{v-1} = F_{v+1}$, and n satisfies **(a)(i)**. Since $S(2) - 1 = F_v$, by induction, we have $S = \kappa^{v-2}$. On the other hand, $n = T(2) - 1 = S\kappa(2) - 1 = \kappa^{v-2}\kappa(2) - 1 = \kappa^{v-1}(2) - 1 = \kappa^{t-2}(2) - 1$, which verifies the formula.

Induction subcase 2(ii): n is a left child whose parent is not a Fibonacci number, that is, $S(2) - 1$ is not a Fibonacci number. Now, $F_v < S(2) - 1 < F_{v+1}$, (with both inequalities strict), and also, by hypothesis, $S(2) - 1$ has an ancestor m with $m = S(2) - 1 - F_v$. Thus, for $n = T(2) - 1 = S\kappa(2) - 1 = S(2) - 1 + F_{v-1} = m+F_v+F_{v-1} = m+F_{v+1} = m+F_t$, as desired. Also, by hypothesis, $m = R(2)-1$ and $S(2) - 1$ correspond to R, respectively, $S = R\lambda\kappa^{v-u-2}$, where $F_u \leq m < F_{u+1}$. Thus, $T = S\kappa = R\lambda\kappa^{v-u-2}\kappa = R\lambda\kappa^{v-u-1} = R\lambda\kappa^{t-u-2}$, which verifies the formula. □

*Proof of Lemma 4.13***(b)**. The result follows as a consequence of the radix algorithm in Proposition 4.10 (see Remark 4.13), but can also be argued by induction using Proposition 4.7(b):

Base Case: Observe that **(b)** holds for the root of the tree, in as much as 1 satisfying $F_2 \leq 1 < F_3$ has left child $2 = 1 + F_1$, and right child $4 = 1 + F_4$.

Induction Case: Since $n = S(2) - 1$, and $F_t \leq n < F_{t+1}$, Proposition 4.7(b) gives for a left child $S\kappa(2) - 1 = S(3) - 1 = S(2) - 1 + F_{t-1} = n + F_{t-1}$, as claimed, and for a right child, $S\lambda(2) - 1 = S(5) - 1 = S(2) - 1 + F_{t+2} = n + F_{t+2}$, as claimed. □

*Proof of Proposition 4.16***(a)***:* Recall Proposition 4.10 and Corollary 4.11.

Case (i): S in the first column of Table 9, first argument

Observe that $S_{n,1}(2) - 1 = S_{n,1}\lambda(1) - 1$, where the algorithm of Proposition 4.10 produces the latter values. Consider $S_{n,1}$ in the first column of Table 9 and observe that by construction, it is either $S_{0,1} = I$ or $S_{n,1}$ ends in the suffix λ, and thus $S_{n,1}\lambda$ ends in λ^2. By Proposition 4.10, therefore, the minimal Fibonacci representation of $S_{n,1}\lambda(1) - 1$ for $n \geq 1$ must terminate in $\cdots 101$.

Now, in the minimal representation of m, the largest Fibonacci index is $F^{-1}(m)$, thus the representation always includes $F_{F^{-1}(m)}$ and never includes $F_{F^{-1}(m)-1}$ (Remark 6.8). The algorithm shows that the representation of $m = S_{n,1}\lambda(1) - 1$ for

$n \geq 1$ also includes $F_{F^{-1}(m)-2}$. The first column of Table 12 includes all such values in increasing order, by construction; thus, the $\mathsf{F}_{n,1}$ are precisely the numbers of the form $n + F_{F^{-1}(n)+2}$, where $n = m - F_{F^{-1}(m)}$. Whereas $\mathsf{F}_{0,1}\lambda(1) - 1 = 1$, the same formula also gives the top element of the column, which begins $\mathsf{F}_{0,1} \equiv S_{0,1}(2) - 1 = I\lambda(1) - 1 = 0 + F_{F^{-1}(0)+2} = 1$ and continues to $\mathsf{F}_{1,1} \equiv S_{1,1}(2) - 1 = \lambda^2(1) - 1 = 1 + F_{F^{-1}(1)+2} = 1 + F_4 = 4$, etc. It suffices to note that $\mathsf{F}_{n,1} \equiv S_{n,1}(2) - 1 = n + F_{F^{-1}(n)+k+1} = n + F_{F^{-1}(n)+2}$.

Case (i): S in the first column of Table 9, second argument Consider $S_{n,1}$ in the first column of Table 9 and observe that since $S_{n,1}(1) - 1 = n$ by construction of the table, Proposition 4.7(a) becomes

$$p_\star(S_{n,1}) = F^{-1}(S_{n,1}(1)-1) = F^{-1}(n). \tag{110}$$

Next, by Proposition 4.10 (see Remark 4.13),

$$S\kappa\lambda(1) - S\lambda(1) = F_{p_\star(S\lambda)-1}; \tag{111}$$

$$S\lambda^2(1) - S\lambda(1) = F_{p_\star(S\lambda)+2}. \tag{112}$$

First note that $S_{0,1} = I$ satisfies the claim trivially:

$$\begin{aligned} S_{0,1}(2) - 1 &= 1 \\ &= 0 + F_{F^{-1}(0)+2}. \end{aligned} \tag{113}$$

Next, for $n \geq 1$, $S_{n,1}$ terminates in λ by construction, so that

$$\begin{aligned} S_{n,1}(2) - 1 &= S_{n,1}\lambda(1) - 1 \\ &= S_{n,1}(1) - 1 + F_{p_\star(S_{n,1})+2} \\ &= S_{n,1}(1) - 1 + F_{F^{-1}(S_{n,1}-1)+2} \\ &= n + F_{F^{-1}(n)+2}, \end{aligned} \tag{114}$$

matching the formula claimed, and where the equalities follow from, respectively, $\lambda(1) = 2$, (112), (110), and construction of the table.

Case (ii): S in column $k \geq 2$ of Table 9

For $k \geq 1$, $S_{n,k} = S_{n,1}\kappa^{k-1}$ by construction, so that

$$\begin{array}{llll} S_{n,2}(2)-S_{n,1}(2) & = S_{n,1}\kappa\lambda(1)-S_{n,1}\lambda(1) & = F_{p_\star(S_{n,1}\lambda)-1} & = F_{p_\star(S_{n,1})+1}, \\ S_{n,3}(2)-S_{n,2}(2) & = S_{n,1}\kappa^2\lambda(1)-S_{n,1}\kappa\lambda(1) & = F_{p_\star(S_{n,1}\kappa\lambda)-1} & = F_{p_\star(S_{n,1})+2}, \\ \vdots & & \vdots & \vdots \\ S_{n,k}(2)-S_{n,k-1}(2) & = S_{n,1}\kappa^{k-1}\lambda(1)-S_{n,1}\kappa^{k-2}\lambda(1) & = F_{p_\star(S_{n,1}\kappa^{k-2}\lambda)-1} & = F_{p_\star(S_{n,1})+k-1}. \end{array}$$

The telescoping sum in the left-hand sides collapses when summed to give

$$\begin{aligned} S_{n,k}(2)-S_{n,1}(2) &= S_{n,1}\kappa^{k-1}\lambda(1)-S_{n,1}\lambda(1) \\ &= \sum_{h=1}^{k-1} F_{p_\star(S_{n,1})+h} \\ &= \sum_{h=1}^{p_\star(S_{n,1})+k-1} F_h - \sum_{h=1}^{p_\star(S_{n,1})} F_h \\ &= F_{p_\star(S_{n,1})+k+1} - F_{p_\star(S_{n,1})+2} \\ &= F_{F^{-1}(n)+k+1} - F_{F^{-1}(n)+2}, \end{aligned}$$

which combined with (113) or (114) yields the desired result,

$$\begin{aligned} S_{n,k}(2) - 1 &= S_{n,1}(2) - 1 + F_{F^{-1}(n)+k+1} - F_{F^{-1}(n)+2} \\ &= n + F_{F^{-1}(n)+2} + F_{F^{-1}(n)+k+1} - F_{F^{-1}(n)+2} \\ &= n + F_{F^{-1}(n)+k+1}. \end{aligned}$$

□

Proof of Proposition 4.16(**b**)*:* Follows from Corollary 4.11, which provides a bijection between equivalence classes $\{\kappa, \lambda\}^\star / \circ \kappa^\star$ and $\mathbb{Z}_+$. First, remove from the domain the kernel of the equivalence relation, that is, the 0^{th} equivalence class $\kappa^\star$, thus considering only the classes on $\{\kappa, \lambda\}^\star \setminus \{\kappa\}^\star$. The value $S(1)$ still provides a bijection between this set and the integers $2, 3, 4, \ldots$. Next consider the standard representatives of these classes, which are tabulated in the first column of Table 9, omitting only the entry on the top row. It suffices to observe that the standard class representatives take the form $S\lambda$, where S ranges through all compositions in $\{\kappa, \lambda\}^\star$, including the identity. Thus $S\lambda(1) - 1$ provides a bijection between $\mathbb{Z}_+$ and all compositions of the form $S\lambda$. Finally consider that $S\lambda(1) - 1 = S(2) - 1$, which therefore provides a bijection between $\{\kappa, \lambda\}^\star$ and $\mathbb{Z}_+$. □

Proof of Lemma 4.27(**a**). Analogous to the proof of Lemma 4.13, use the correspondence between the maximal Fibonacci tree (Figure 8) and the tree of compositions in $\{\theta, \eta\}^\star$ (Figure 7).

Proof of **(a)**, Base case: First observe that the lemma holds for the initial levels of the two trees.

First Level, **(i)**: $n = 1 = F_2$ in Figure 8, corresponds to $T = \eta^{2/2-1} = I$ in Figure 7.

Second Level, **(i)**: $n = 3 = F_4$, corresponds to $T = \eta^{4/2-1} = \eta$. Second Level, **(ii)**: For $F_3 \leq n = 2 < F_4$ with $t = 3$, consider $u = 2$ and observe that $F_2 \leq m = 1 < F_3$ and $n = m + F_t - F_{u-1} = 1 + F_3 - F_1 = 1 + 2 - 1 = 2$, correspond to I and $T = \eta^{(3-2-1)/2}\theta I = \theta$, respectively.

Third Level, **(i)**: $n = 8 = F_6$, corresponds to $T = \eta^{6/2-1} = \eta^2$. Third Level, **(ii)**: For $F_4 \leq n = 4 < F_5$ with $t = 4$, consider $u = 3$ and observe that $F_3 \leq m = 2 < F_4$ and $n = m + F_t - F_{u-1} = 2 + F_4 - F_2 = 2 + 3 - 1 = 4$ correspond to θ and $T = \eta^{(4-3-1)/2}\theta\theta = \theta^2$, respectively. For $F_5 \leq n = 5 < F_6$ with $t = 5$, consider $u = 2$ and observe that $F_2 \leq m = 1 < F_3$ and $n = m + F_t - F_{u-1} = 1 + F_5 - F_1 = 1 + 5 - 1 = 5$ correspond to I and $T = \eta^{(5-2-1)/2}\theta I = \eta\theta$, respectively. For $F_5 \leq n = 6 < F_6$ with $t = 5$, consider $u = 4$ and observe that $F_4 \leq m = 3 < F_5$ and $n = m + F_t - F_{u-1} = 3 + F_5 - F_3 = 3 + 5 - 2 = 6$ correspond to η and $T = \eta^{(5-4-1)/2}\theta\eta = \theta\eta$, respectively.

Next, recall that by construction of the trees $n = N_0(T) + 1$, where T is the corresponding node in Figure 7.

Induction case 1: n is a left child. Suppose $T = \theta R$, and thus T is a left child of R, and, correspondingly, $n = N_0(T) + 1 = N_0(\theta R) + 1$ is a left child of $N_0(R) + 1$. By Proposition 4.24, $F_{p+2} \leq N_0(T) + 1 < F_{p+3}$. Since $F_t \leq N_0(T) + 1 < F_{t+1}$, it must be that $t = p + 2$. Thus, $N_0(T) = N_0(\theta R)$ implies that $F_{t-1} = F_{p+1} \leq N_0(R) + 1 < F_{p+2} = F_t$, and, moreover, the zeroes of R are followed by a run of length $F_{t-1} = F_{p+1}$, respectively, $F_{t-2} = F_p$ of each lower Wythoff, respectively, upper Wythoff number. Consequently, we see that the application of θ to R will change ones to zeros, hence T must have $F_{t-1} = F_{p+1}$ more zeroes than R. Now,

with $F_t \le n < F_{t+1}$, consider $u = t-1$ and $m = N_0(R)+1$, then the formula gives $n - m = F_t - F_{u-1} = F_t - F_{t-2} = F_{t-1}$, as desired, m and n corresponding to R and $T = \eta^{(t-u-1)/2}\theta R = \eta^0\theta R = \theta R$, as desired.

Induction case 2: n is a right child. Suppose $T = \eta S$, and thus T is a right child of S, and, correspondingly, $n = N_0(T)+1 = N_0(\eta S)+1$ is a right child of $N_0(S)+1$. Again, by Proposition 4.24, $F_t = F_{p+2} \le N_0(T)+1 < F_{p+3} = F_{t+1}$ and $N_0(T) = N_0(\eta S)$ implies that $F_{t-2} = F_p \le N_0(S)+1 < F_{p+1} = F_{t-1}$, and, moreover, the zeroes of S are followed by a run of length $F_{t-2} = F_p$, respectively, $F_{t-3} = F_{p-1}$ of each lower Wythoff, respectively, upper Wythoff number. Consequently, observe that the application of η to S will change ones and twos to zeros, hence $N_0(T) - N_0(S) = F_{t-2} + F_{t-3} = F_p + F_{p-1} = F_{t-1} = F_{p+1}$, indicating that T has F_{p+1} more zeroes than S.

By induction, either (i) $N_0(S)+1$ is a Fibonacci number of even index or, (ii) S has an ancestor R satisfying, for some u, $S = \eta^{(p-u-1)/2}\theta R$, with $N_0(S) - N_0(R) = F_p - F_{u-1}$, with $p = t-2$, as in the foregoing.

Induction subcase 2(i): n is a right child of a Fibonacci number of even index, that is, $N_0(S)+1 = F_{t-2} = F_p$ is a Fibonacci number with $t-2 = p$ even. By hypothesis, then, $S = \eta^{p/2-1}$. Consequently, $T = \eta S = \eta\eta^{p/2-1} = \eta^{(p+2)/2-1} = \eta^{t/2-1}$, as desired. Further, $n = N_0(S)+1+F_{t-1} = F_{t-2} + F_{t-1} = F_t$, as desired.

Induction subcase 2(ii): n is a right child whose parent is not a Fibonacci number of even index, namely, $N_0(S)+1$ is not a Fibonacci number of even index. Now, by induction, S has an ancestor R such that for some u, $S = \eta^{(p-u-1)/2}\theta R$, with $N_0(S) - N_0(R) = F_p - F_{u-1}$. Consequently, $T = \eta S = \eta\eta^{(p-u-1)/2}\theta R = \eta^{(p+2-u-1)/2}\theta R = \eta^{(t-u-1)/2}\theta R$, as desired. Now, it remains to show $N_0(T) - N_0(R) = F_t - F_{u-1}$. Indeed, $N_0(T) - N_0(R) = [N_0(T) - N_0(S)] + [N_0(S) - N_0(R)] = F_{p+1} + F_p - F_{u-1} = F_{p+2} - F_{u-1} = F_t - F_{u-1}$, which proves that the formula is valid. □

*Proof of Lemma 4.27***(b)**, Base Case: The result follows is a consequence of the algorithm in Proposition 4.25 (see Remark 4.22), but can also be argued by induction using Proposition 4.24:

Observe that **(b)** holds for the root of the tree, in as much as 1 satisfying $F_2 \le 1 < F_3$ has left child $2 = 1 + F_1$, and right child $3 = 1 + F_3$.

Induction Case: Since $n = N_0(S)+1$, and $F_t \le n < F_{t+1}$, Proposition 4.24, gives for a left child $N_0(\theta S)+1 = N_0(T)+1+F_t = n + F_t$, as claimed, and for a right child, $N_0(\eta S)+1 = N_0(T)+1+F_t+F_{t-1} = N_0(T)+1+F_{t+1} = n + F_{t+1}$, as claimed. □

Proof of Lemma 4.41(a). Consider the well-known identity for Lucas numbers:

$$L_t = \phi^t + (-1/\phi)^t. \tag{115}$$

From (115), observe that Lucas numbers of even index satisfy $L_{2t} = \phi^{2t} + 1/\phi^{2t}$. Thus, the Lucas numbers of even index have a phigits representation of the form $10\cdots01$. Whereas no two consecutive phigits equal 1 in this representation, the representation is minimal.

When adding two numbers, the phigit-wise sum of their minimal base-ϕ representations does not generally give the minimal base-ϕ representation of their sum. In general, the sum of two minimal base-ϕ representations must undergo "carry" operations to reduce the representation to minimal base-ϕ, that is, a vector of 0–1 coefficients without consecutive 1s.

Nevertheless, for a Lucas number L_{2t} of even index, its pair of nonzero phigits ε_{-2t} and ε_{2t} occupy positions "far" from the phigit ε_0 (coefficient of $\phi^0 = 1$ in the representation). Moreover, the larger the Lucas number of even index, the farther from ε_0 its nonzero phigits will be. Thus, if a Lucas number of even index is sufficiently large, its base-ϕ representation can be added phigit-wise to that of another integer n without placing ε_{-2t} and ε_{2t} adjacent to some $\varepsilon_i = 1$ in the representation of n, and thus not triggering any carry operations. In particular, if L_{2t} is sufficiently large, ε_0 will be the same in the base-ϕ representations of n and $n + L_{2t}$.

Specifically, consider the Lucas number of odd index L_{2t+1} and represent this number as $(10)^t \underset{\rightarrow}{1} (01)^t$ using phigits, where the 0^{th} phigit ε_0 is written with an arrow underneath it, and the direction of the arrow indicates the convention $\cdots\varepsilon_{-2}\varepsilon_{-1}\underset{\rightarrow}{\varepsilon_0}\varepsilon_1\varepsilon_2\cdots$, that is, the choice of notation where exponents of ϕ increase from left to right in the sum $\cdots + \varepsilon_{-2}\phi^{-2} + \varepsilon_{-1}\phi^{-1} + \underset{\rightarrow}{\varepsilon_0} + \varepsilon_1\phi + \varepsilon_2\phi^2 + \cdots$.

Further, consider the next smallest Lucas number of even index L_{2t+2}, and represent it similarly using phigits as $1(0)^{2t+1}\underset{\rightarrow}{0}(0)^{2t+1}1$. Observe that L_{2t+2} is indeed sufficiently large — and its nonzero phigits sufficiently far from ε_0 — that it can be added to L_{2t+1} digit-wise to obtain the representation $(10)^{t+1}\underset{\rightarrow}{1}(01)^{t+1}$ of L_{2t+3} without effecting the phigit $\varepsilon_0 = 1$ in the minimal base-ϕ representation of L_{2t+1}, nor introducing an "unreduced" string 11 in the resulting representation.

Moreover, since the number of digits in the minimal base-ϕ representation does not decrease (see, *e.g.*, entry for 190796 in [41]), the minimal base-ϕ representation of any positive integer $S \leq L_{2t+1}$ can be added phigit-wise to that of L_{2t+2}; in particular, $S \leq L_{2t+1}$ and L_{2t+2} have the same 0^{th} phigit (ε_0).

Now, the pair of nonzero phigits in the minimal base-ϕ representations of L_{2t+4}, $L_{2t+6}, L_{2t+6}\ldots$ lie even farther from ε_0 than those of L_{2t+2}. Thus for any Lucas number of even index $2t+2$ or greater, its minimal base-ϕ representation can be added phigit-wise to that of any integer $S = L_{2t+1}$ or smaller to give a minimal base-ϕ representation of the sum, and this sum will have the same 0^{th} phigit as in the minimal base-ϕ representation of S. □

Proof of Lemma 4.41(b). For ease of exposition, let $S \overset{\varepsilon_0}{\sim} R$ indicate that non-negative integers S and R have the same 0^{th} phigit (ε_0) in minimal base-ϕ representation, where S and R are integers or intervals of integers. Using this relation, the statement to be proven reads $[0, L_{2t+1}) \overset{\varepsilon_0}{\sim} [L_{2t}, L_{2t+2})$.

The statement follows by induction, using results of Sanchis and Sanchis [31] on recursive patterns in the sequence of minimal base-ϕ representation of the positive integers. These authors consider the recurrence of an entire block of phigits centered around ε_0, though ε_0 itself is the particular focus here.

First observe that $t = 0$ gives the half-open intervals $[0, L_{2t+1}) = [0, L_1) = [0, 1) = [0]$ and $[0, L_{2t+1}) + L_{2t} = [0, L_1) + L_0 = [0, 1) + 2 = [2, 3) = [2]$, and that these singleton intervals satisfy $[0] \overset{\varepsilon_0}{\sim} [2]$, whereas 0 and 2 share the value $\varepsilon_0 = 0$ in their respective minimal phigits representations (refer to [24] for an introduction and online calculator).

Next, $t = 1$ gives $[0, L_{2t+1}) = [0, L_3) = [0, 4) = [0, 3]$ and $[0, L_{2t+1}) + L_{2t} = [0, L_3) + L_2 = [0, 4) + 3 = [3, 7) = [3, 6]$, and $[0, 3] \overset{\varepsilon_0}{\sim} [3, 6]$, whereas the sequences of integers $0, 1, 2, 3$ and $3, 4, 5, 6$ share the sequence of values of $\varepsilon_0 = 0,\ 1, 0, 0$ in their respective minimal phigits representations.

Finally, $t = 2$ gives $[0, L_{2t+1}) = [0, L_5) = [0, 11) = [0, 10]$ and $[0, L_5] + L_4 = [0, 11) + 7 = [7, 18) = [7, 17]$, and $[0, 10] \overset{\varepsilon_0}{\sim} [7, 17]$, whereas the sequences of integers $0, \ldots, 10$ and $7, \ldots, 17$ share the sequence of values of $\varepsilon_0 = 0,\ 1, 0, 0,\ 1, 0, 0, 0, 1, 0, 0$ in their respective minimal phigits representations.

Now, for $t \geq 3$, consider the decomposition of interval $[0, L_{2t+1})$ into seven (7) subintervals, shown on the left-hand sides of congruences (116)–(122):

$$[0, L_{2t-3}] \overset{\varepsilon_0}{\sim} [L_{2t}, L_{2t} + L_{2t-3}] \tag{116}$$

$$(L_{2t-3}, L_{2t-2}) \overset{\varepsilon_0}{\sim} (L_{2t} + L_{2t-3}, L_{2t} + L_{2t-2}) \tag{117}$$

$$[L_{2t-2}, L_{2t-1}] \overset{\varepsilon_0}{\sim} [L_{2t} + L_{2t-2}, L_{2t+1}] \tag{118}$$

$$(L_{2t-1}, L_{2t}) \overset{\varepsilon_0}{\sim} (L_{2t+1}, L_{2t+1} + L_{2t-2}) \tag{119}$$

$$[L_{2t}, L_{2t} + L_{2t-3}] \overset{\varepsilon_0}{\sim} [L_{2t+1} + L_{2t-2}, L_{2t+1} + L_{2t-1}] \tag{120}$$

$$(L_{2t} + L_{2t-3}, L_{2t} + L_{2t-2}) \overset{\varepsilon_0}{\sim} (L_{2t+1} + L_{2t-1}, L_{2t+1} + L_{2t-1} + L_{2t-4}) \tag{121}$$

$$[L_{2t} + L_{2t-2}, L_{2t+1}) \overset{\varepsilon_0}{\sim} (L_{2t+1} + L_{2t-1} + L_{2t-4}, L_{2t+2}). \tag{122}$$

The seven (7) congruences now follow by induction and the results of Sanchis and Sanchis [31]. By the induction hypothesis, $[0, L_{2t-1}) \overset{\varepsilon_0}{\sim} [L_{2t-2}, L_{2t})$, in particular, $[0, L_{2t-3}] \overset{\varepsilon_0}{\sim} [L_{2t-2}, L_{2t-1}]$. By Proposition 3.2(b) of [31], $[L_{2t-2}, L_{2t-1}] \overset{\varepsilon_0}{\sim} [L_{2t}, L_{2t} + L_{2t-3}]$ for $t \geq 3$. This shows (116).

By Proposition 3.1(d) of [31], $(L_{2t-3}, L_{2t-2}) \overset{\varepsilon_0}{\sim} (L_{2t} + L_{2t-3}, L_{2t} + L_{2t-2})$ for $t \geq 3$. This shows (117).

By Proposition 3.2(c) of [31], $[L_{2t-2}, L_{2t-1}] \overset{\varepsilon_0}{\sim} [L_{2t} + L_{2t-2}, L_{2t+1}]$ for $t \geq 3$. This shows (118).

By Proposition 3.1(b) of [31], $(L_{2t-1}, L_{2t}) \overset{\varepsilon_0}{\sim} (L_{2t+1}, L_{2t+1} + L_{2t-2})$ for $t \geq 2$. This shows (119).

By Propositions 3.2(b) and (d) of [31], $[L_{2t}, L_{2t}+L_{2t-3}] \overset{\varepsilon_0}{\sim} [L_{2t+1}+L_{2t-2}, L_{2t+1}+L_{2t-1}]$ for $t \geq 3$. This shows (120).

By Proposition 3.1(d) of [31], $(L_{2t}+L_{2t-3}, L_{2t}+L_{2t-2}) \overset{\varepsilon_0}{\sim} (L_{2t-3}, L_{2t-2})$ for $t \geq 3$. By the induction hypothesis, $[0, L_{2t-1}) \overset{\varepsilon_0}{\sim} [L_{2t-2}, L_{2t})$, in particular, $(L_{2t-3}, L_{2t-2}) \overset{\varepsilon_0}{\sim} (L_{2t-1}, L_{2t-1} + L_{2t-4})$. By Proposition 3.1(c) of [31], $(L_{2t-1}, L_{2t}) \overset{\varepsilon_0}{\sim} (L_{2t+1} + L_{2t-1}, L_{2t+2})$ for $t \geq 2$, in particular, $(L_{2t-1}, L_{2t-1} + L_{2t-4}) \overset{\varepsilon_0}{\sim} (L_{2t+1} + L_{2t-1}, L_{2t+1} + L_{2t-1} + L_{2t-4})$. This shows (121).

Finally, by Proposition 3.2(c) of [31], $[L_{2t} + L_{2t-2}, L_{2t+1}] \overset{\varepsilon_0}{\sim} [L_{2t-2}, L_{2t-1}]$ for $t \geq 3$. By the induction hypothesis, $[0, L_{2t-1}) \overset{\varepsilon_0}{\sim} [L_{2t-2}, L_{2t})$, in particular, $[L_{2t-2}, L_{2t-1}) \overset{\varepsilon_0}{\sim} [L_{2t-1}+L_{2t-4}, L_{2t})$. By Proposition 3.1(c) of [31], $(L_{2t-1}, L_{2t}) \overset{\varepsilon_0}{\sim} (L_{2t+1}+L_{2t-1}, L_{2t+2})$ for $t \geq 2$, in particular, $(L_{2t-1} + L_{2t-4}, L_{2t}) \overset{\varepsilon_0}{\sim} (L_{2t+1} + L_{2t-1} + L_{2t-4}, L_{2t+2})$. This shows (122).

The seven (7) individual congruences thus demonstrate the congruence of $[0, L_{2t+1})$ to $[L_{2t}, L_{2t+2})$, as the seven (7) intervals on the right-hand sides of (116)–(122) decompose $[L_{2t}, L_{2t+2})$. □

*Proof of Proposition 4.45***(a):** Show the 1–2 relations (40) for the 2–1-Fibonacci cohort sequence with S_1 omitted.

Observe that the 2–1 cohort sequence from the 1st cohort begins $S_1, S_1+F_{2+p}, S_1+F_{3+p}, S_1+F_{2+p}+F_{3+p}, S_1+F_{2+p}+F_{4+p}, \ldots$. Thus, the first few cohorts of the 1–2

cohort sequence satisfy (40) with $\langle f_L, f_R\rangle = \langle F_{t+p-1}, F_{t+p+1}\rangle$, since $S_1 + F_{3+p} - (S_1 + F_{2+p}) = F_{2+p-1}$ for the second cohort and $S_1 + F_{2+p} + F_{3+p} - (S_1 + F_{3+p}) = F_{3+p-1}$ and $S_1 + F_{2+p} + F_{4+p} - (S_1 + F_{2+p}) = F_{3+p+1}$ for the third cohort. In the case of a 2–1-Fibonacci cohort sequence from the 2^{nd} cohort $S_3 = S_2 + F_{p+1}$, substitute S_1 by $S_1' = S_2 - F_{2+p} = S_3 - F_{3+p}$ and make the same argument.

Now for the induction step, take the 1–2 relations (40) with $\langle f_L, f_R\rangle = \langle F_{t+p-1}, F_{t+p+1}\rangle$. Shift the indices, rewriting the relations in terms of elements $S_2, S_3, ...$, and consider them in four blocks, (the last of these being a singleton):

$$S_{F_{t+1}+1} = S_{F_t+1} + F_{t+p-1},$$

(123a) $$\vdots$$

$$S_{F_{t+1}+F_{t-2}} = S_{F_t+F_{t-2}} + F_{t+p-1},$$
$$S_{F_{t+1}+F_{t-2}+1} = S_{F_t+F_{t-2}+1} + F_{t+p-1},$$

(123b) $$\vdots$$

$$S_{F_{t+1}+F_{t-1}} = S_{F_{t+1}} + F_{t+p-1},$$
$$S_{F_{t+1}+F_{t-1}+1} = S_{F_{t-1}+1} + F_{t+p+1},$$

(123c) $$\vdots$$

$$S_{F_{t+2}-1} = S_{F_t-1} + F_{t+p+1},$$

(123d) $$S_{F_{t+2}} = S_{F_t} + F_{t+p+1}.$$

Now consider the 2–1 relations (10) with $f(t) = F_{t+p}$.

First, note that the last relation (123d) is identical to the first relation of (10) for cohort $t+1$, and therefore holds.

Next consider the $F_{t-2} - 1$ relations (123c). Relations (10) (for cohort t) give $S_{F_{t+1}+F_{t-1}+1} = S_{F_t+F_{t-3}+1} + F_{t+p}, \ldots, S_{F_{t+2}-1} = S_{F_{t+1}-1} + F_{t+p}$, while for cohort $t-1$, relations (10) give $S_{F_t+F_{t-3}+1} = S_{F_{t-1}+1} + F_{t+p-1}, \ldots, S_{F_{t+1}-1} = S_{F_t-1} + F_{t+p-1}$. Substituting the latter into the former yields (123c).

The identical procedure for the F_{t-3} relations (123b) gives $S_{F_{t+1}+F_{t-2}+1} = S_{F_{t-2}+1} + F_{t+p+1}, \ldots, S_{F_{t+1}+F_{t-1}} = S_{F_{t-1}} + F_{t+p+1}$. By the induction hypothesis, however, the previous cohort already satisfies (123c) and (123d), *i.e.*, $S_{F_{t-2}+1} = S_{F_t+F_{t-2}+1} - F_{t+p}, \ldots, S_{F_{t-1}} = S_{F_{t+1}} - F_{t+p}$. Substituting the latter into the former yields (123b).

Finally, consider the F_{t-2} relations (123a). Relations (10) (for cohort t) give $S_{F_{t+1}+1} = S_{F_{t-1}+1} + F_{t+p}, \ldots, S_{F_{t+1}+F_{t-2}} = S_{F_t} + F_{t+p}$. Relations (123a) and (123b) for the previous cohort give $S_{F_{t-1}+1} = S_{F_t+1} - F_{t+p-2}, \ldots, S_{F_t} = S_{F_t+F_{t-2}} - F_{t+p-2}$. Substituting the latter into the former yields (123a). □

Proof of Proposition 4.45(**b**)**:** For the converse, observe that the 1–2 cohort sequence begins $S_1, S_1 + F_{1+p}, S_1 + F_{3+p}, S_1 + F_{4+p}, \ldots$. Thus, the first few cohorts of the 2–1 cohort sequence satisfy (10) with $f(t) = F_{t+p}$, since $S_1 - (S_1 - F_{2+p}) = F_{2+p}$ for the second cohort and $S_1 + F_{1+p} - (S_1 - F_{2+p}) = F_{3+p}$ and $S_1 + F_{1+p} + F_{2+p} - S_1 = F_{3+p}$ for the third cohort.

Now for the induction step, take the relations (10) with $f(t) = F_{t+p}$. Shift the indices, rewriting the relations in terms of elements $S_1 - F_{p+2}, S_1, S_2, S_3 ...$, and

consider them in four blocks:

$$\begin{aligned} S_{F_{t+1}-1} &= S_{F_{t-1}-1} + F_{t+p}, \\ S_{F_{t+1}} &= S_{F_{t-1}} + F_{t+p}, \end{aligned} \tag{124a}$$

$$\vdots \tag{124b}$$

$$\begin{aligned} S_{F_{t+1}+F_{t-2}-1} &= S_{F_t-1} + F_{t+p}, \\ S_{F_{t+1}+F_{t-2}} &= S_{F_t} + F_{t+p}, \end{aligned}$$

$$\vdots \tag{124c}$$

$$\begin{aligned} S_{F_{t+1}+F_{t-1}-1} &= S_{F_t+F_{t-3}-1} + F_{t+p}, \\ S_{F_{t+1}+F_{t-1}} &= S_{F_t+F_{t-3}} + F_{t+p}, \end{aligned}$$

$$\vdots \tag{124d}$$

$$S_{F_{t+2}-2} = S_{F_{t+1}-2} + F_{t+p}.$$

Now consider the 1–2 relations (40) with $\langle f_L, f_R \rangle = \langle F_{t+p-1}, F_{t+p+1} \rangle$.

Begin by noting that the first relation (124a) is the same as the last relation of (40) for cohort $t-1$.

Next consider the F_{t-2} relations (124b). Relations (40) (for cohort t) give $S_{F_{t+1}} = S_{F_t} + F_{t+p-1}, \ldots, S_{F_{t+1}+F_{t-2}-1} = S_{F_t+F_{t-2}-1} + F_{t+p-1}$, while for cohort $t-1$, relations (39) give $S_{F_t} = S_{F_{t-1}} + F_{t+p-2}, \ldots, S_{F_t+F_{t-2}-1} = S_{F_t-1} + F_{t+p-2}$. Substituting the latter into the former yields (124b).

The identical procedure for the F_{t-3} relations (124c) yields $S_{F_{t+1}+F_{t-2}} = S_{F_{t-2}} + F_{t+p+1}, \ldots, S_{F_{t+1}+F_{t-1}-1} = S_{F_{t-1}-1} + F_{t+p+1}$. By the induction hypothesis, however, the previous cohort already satisfies relations (124b), thus $S_{F_{t-2}} = S_{F_t} - F_{t+p-1}, \ldots, S_{F_{t-1}-1} = S_{F_t+F_{t-3}-1} - F_{t+p-1}$. Substituting the latter into the former yields (124c).

Finally consider the $F_{t-2}-1$ relations (124d). Relations (40) (for cohort t) give $S_{F_{t+1}+F_{t-1}} = S_{F_{t-1}} + F_{t+p+1}, \ldots, S_{F_{t+2}-2} = S_{F_t-2} + F_{t+p+1}$. Relations (124c) and (124d) for the previous cohort give $S_{F_{t-1}} = S_{F_t+F_{t-3}} - F_{t+p-1}, \ldots, S_{F_t-2} = S_{F_{t+1}-2} - F_{t+p-1}$. Substituting the latter into the former yields (124d). □

Proof of Proposition 4.47(**a**)**:** For a 2–1-Fibonacci cohort sequence S, considering only the left subcohorts gives C_{1_L}, C_{2_L}, C_{3_L}, C_{4_L}, $C_{5_L}, \ldots = (S_1)$, (S_3), (S_5), (S_8, S_9), (S_{13}, S_{14}, S_{15}) , …, so that the resulting sequence is $S_{\llcorner n,1} = S_{n+F_{F^{-1}(n)+1}}$, $n = 0, 1, 2, \ldots$.

However, with each left subcohort reversed, the resulting sequence becomes S_1, S_3, S_5, S_9, S_8, $S_{15}, S_{14}, S_{13}, \ldots$. Denote the resulting sequence with a 0^{th} element by L_n, $n = 0, 1, 2, \ldots$. This allows cohort t of L to be written $D_t = (L_{F_{t+1}}, \ldots, L_{F_{t+2}-1}) = (S_{F_{t+2}-1+F_{F^{-1}(F_{t+2}-1)+1}}, \ldots, S_{F_{t+1}+F_{F^{-1}(F_{t+1})+1}}) = (S_{2F_{t+2}-1}, \ldots, S_{F_{t+3}})$.

Now with a change of index, and reversing the order of the equations, the former block of (39) can be written

$$\begin{aligned} S_{2F_{t+2}-1} &= S_{F_{t+2}-1} + f_L(t+2), \\ &\vdots \\ S_{F_{t+3}} &= S_{F_{t+1}} + f_L(t+2), \end{aligned} \tag{125}$$

for $t = 1, 2, 3 \ldots$. In turn, this set can be split into two blocks,

$$\begin{aligned} L_{F_{t+1}} &= S_{2F_{t+2}-1} = S_{F_{t+2}-1} + f_L(t+2), \\ &\vdots \\ L_{F_{t+1}+F_{t-1}-1} &= S_{F_{t+3}+F_{t-2}} = S_{2F_t} + f_L(t+2), \end{aligned} \tag{126}$$

and

$$\begin{aligned} L_{F_{t+1}+F_{t-1}} &= S_{F_{t+3}+F_{t-2}-1} = S_{2F_t-1} + f_L(t+2), \\ &\vdots \\ L_{F_{t+2}-1} &= S_{F_{t+3}} = S_{F_{t+1}} + f_L(t+2) = L_{F_t-1} + f_L(t+2). \end{aligned} \tag{127}$$

Using (126) twice, and the latter block of (39) once gives

$$\begin{aligned} L_{F_{t+1}} - L_{F_t} &= S_{2F_{t+2}-1} - S_{2F_{t+1}-1} \\ &= S_{F_{t+2}-1} + f_L(t+2) - \left[S_{F_{t+1}-1} + f_L(t+1)\right] \\ &= f_L(t+2) - f_L(t+1) + f_R(t), \\ &\vdots \\ L_{F_{t+1}+F_{t-1}-1} - L_{F_{t+1}-1} &= S_{F_{t+3}+F_{t-2}} - S_{F_{t+2}} \\ &= S_{2F_t} + f_L(t+2) - [S_{F_t} + f_L(t+1)] \\ &= f_L(t+2) - f_L(t+1) + f_R(t), \end{aligned} \tag{128}$$

while using (127) twice, and the former block of (39) once gives

$$\begin{aligned} L_{F_{t+1}+F_{t-1}} - L_{F_{t-1}} &= S_{F_{t+3}+F_{t-2}-1} - S_{2F_t-1} \\ &= S_{2F_t-1} + f_L(t+2) - [S_{F_t-1} + f_L(t)] \\ &= f_L(t+2) - f_L(t) + f_L(t), \\ &= f_L(t+2), \\ &\vdots \\ L_{F_{t+2}-1} - L_{F_t-1} &= S_{F_{t+3}} - S_{F_{t+1}}, \\ &= S_{F_{t+1}} + f_L(t+2) - \left[S_{F_{t-1}} + f_L(t)\right] \\ &= f_L(t+2) - f_L(t) + f_L(t), \\ &= f_L(t+2), \end{aligned} \tag{129}$$

for $t = 3, 4, 5 \ldots$. Writing (128) and (129) together gives

$$\begin{aligned} L_{F_{t+1}} &= L_{F_t} + f_L(t+2) - f_L(t+1) + f_R(t), \\ &\vdots \\ L_{F_{t+1}+F_{t-1}-1} &= L_{F_{t+1}-1} + f_L(t+2) - f_L(t+1) + f_R(t), \\ L_{F_{t+1}+F_{t-1}} &= L_{F_{t-1}} + f_L(t+2), \\ &\vdots \\ L_{F_{t+2}-1} &= L_{F_t-1} + f_L(t+2), \end{aligned}$$

for each cohort C_t, $t = 3, 4, 5 \ldots$, a version of (40) with the cohortizer $\langle f_L(t+2) - f_L(t+1) + f_R(t), f_L(t+2)\rangle$, as claimed.

Finally, for the first and second cohorts, consider $t = 3, 4$ in (39). In particular, $t = 3$ gives $S_4 = S_2 + f_R(3)$ as well as $L_1 = S_3 = S_1 + f_L(3) = L_0 + f_L(3)$, while $t = 4$ gives $L_2 = S_5 = S_2 + f_L(4)$. Combining the last two with $S_2 = S_1 + f_R(2)$ gives $L_2 = S_5 = S_3 + f_L(4) - f_L(3) + f_R(2) = L_1 + f_L(4) - f_L(3) + f_R(2)$, as desired. □

*Proof of Proposition 4.47***(b):** For a 1–2-Fibonacci cohort sequence S, concatenating only the right subcohorts gives $S_1, S_4, S_7, S_{11}, S_{12}, S_{18}, S_{19}, S_{20}, \ldots$. Denote the resulting sequence considered with a 0^{th} element by $R_n = S_{\mathbb{F}_{n,1}} = S_{n+F_{F^{-1}(n)+2}}$, $n = 0, 1, 2, \ldots$. Thus, cohort t of R can be written $D_t = (R_{F_{t+1}}, \ldots, R_{F_{t+2}-1})$ $= (S_{F_{t+1}+F_{F^{-1}(F_{t+1})+2}}, \ldots, S_{F_{t+2}-1+F_{F^{-1}(F_{t+2}-1)+2}}) = (S_{F_{t+1}+F_{t+3}}, \ldots, S_{F_{t+4}-1})$.

Now with a change of index, the latter block of (40) can be written

$$\begin{aligned} S_{F_{t+3}+F_{t+1}} &= S_{F_{t+1}} + f_R(t+2), \\ &\vdots \\ S_{F_{t+4}-1} &= S_{F_{t+2}-1} + f_R(t+2), \end{aligned}$$

for $t = 1, 2, 3 \ldots$. In turn, this set can be split into two blocks,

$$\begin{aligned} R_{F_{t+1}} = S_{F_{t+3}+F_{t+1}} &= S_{F_{t+1}} + f_R(t+2), \\ &\vdots \\ R_{F_{t+1}+F_{t-1}-1} = S_{F_{t+3}+F_{t+1}+F_{t-1}-1} &= S_{F_{t+1}+F_{t-1}-1} + f_R(t+2), \end{aligned} \tag{130}$$

and

$$\begin{aligned} R_{F_{t+1}+F_{t-1}} = S_{F_{t+3}+F_{t+1}+F_{t-1}} &= S_{F_{t+1}+F_{t-1}} + f_R(t+2) = R_{F_{t-1}} + f_R(t+2), \\ &\vdots \\ R_{F_{t+2}-1} = S_{F_{t+4}-1} &= S_{F_{t+2}-1} + f_R(t+2) = R_{F_t-1} + f_R(t+2), \end{aligned} \tag{131}$$

for $t = 1, 2, 3 \ldots$. Evidently, the latter block, (131), in R matches that of (40) in S, so it remains to treat the former block, (131). Using (131), and the former block of (40) once, and (131) a second time gives

$$\begin{aligned} R_{F_{t+1}} - R_{F_t} &= S_{F_{t+3}+F_{t+1}} - S_{F_{t+2}+F_t} \\ &= S_{F_{t+1}} + f_R(t+2) - [S_{F_t} + f_R(t+1)] \\ &= f_R(t+2) - f_R(t+1) + f_L(t), \\ &\vdots \\ R_{F_{t+1}+F_{t-1}-1} - R_{F_{t+1}-1} &= S_{F_{t+3}+F_{t+1}+F_{t-1}-1} - S_{F_{t+2}+F_t+F_{t-2}-1} \\ &= S_{F_{t+1}+F_{t-1}-1} + f_R(t+2) - \left[S_{F_t+F_{t-2}-1} + f_R(t+1)\right] \\ &= f_R(t+2) - f_R(t+1) + f_L(t), \end{aligned} \tag{132}$$

for $t = 3, 4, 5 \ldots$. Writing (132) and (131) together gives

$$\begin{aligned}
R_{F_{t+1}} &= R_{F_t} + f_R(t+2) - f_R(t+1) + f_L(t), \\
&\vdots \\
R_{F_{t+1}+F_{t-1}-1} &= R_{F_{t+1}-1} + f_R(t+2) - f_R(t+1) + f_L(t), \\
R_{F_{t+1}+F_{t-1}} &= R_{F_{t-1}} + f_R(t+2), \\
&\vdots \\
R_{F_{t+2}-1} &= R_{F_t-1} + f_R(t+2),
\end{aligned}$$

for each cohort C_t, $t = 3, 4, 5 \ldots$, a version of (40) with the cohortizer $\langle f_R(t+2) - f_R(t+1) + f_L(t), f_R(t+2)\rangle$, as claimed.

Finally, for the first and second cohorts, consider $t = 3, 4$ in (40). In particular, $t = 3$ gives $S_3 = S_2 + f_L(3)$ as well as $R_1 = S_4 = S_1 + f_R(3) = R_0 + f_R(3)$, while $t = 4$ gives $R_2 = S_7 = S_2 + f_R(4)$. Combining the last two with $S_2 = S_1 + f_L(2)$ gives $R_2 = S_7 = S_4 + f_R(4) - f_R(3) + f_L(2) = R_1 + f_R(4) - f_R(3) + f_L(2)$, as desired. □

Proof of Lemma 4.51. For **(i)**, the definition of their respective slopes $\mu_b = \frac{\phi+b}{\phi+b-1}$ and $\nu_b = \phi+b = 1/(1-1/\mu)$ makes $\kappa_b(n)$ and $\lambda_b(n)$ a pair of complementary Beatty sequences for $n = 1, 2, 3, \ldots$, which is to say that their 0–1-indicator functions sum to unity at each point in this domain: $g_{\mu_b}(n)+g_{\nu_b}(n) = 1$ for integers $n \geq 1$. By [17], express these 0–1-indicator functions as $g_{\mu_b}(n) = f_{1/\mu_b}(n) = \theta_b(n+1) - \theta_b(n)$ and $g_{\nu_b}(n) = f_{1/\nu_b}(n) = \eta_b(n+1) - \eta_b(n)$, to reformulate the partition of unity as $\theta_b(n+1) + \eta_b(n+1) = \theta_b(n) + \eta_b(n) + 1$. Since $\theta_b(1) = \eta_b(1) = 0$, the claim follows by induction.

Claims **(ii)** and **(iii)**, follow from arguments analogous to those in Remark 4.19.

Consider $\theta_b(n)$ and $\eta_b(n)$ in the context of Proposition 4.21. Then on the positive integers, the former has $\lfloor \mu_b \rfloor = 1$ leading zero while the latter has $\lfloor \nu_b \rfloor = b + 1$ leading zeroes.

Further, by Proposition 4.21, the number of copies of each positive integer in the two sequences is given by $f_{\mu_b}(n) + 1 = \lfloor (n+1)\mu_b \rfloor - \lfloor n\mu_b \rfloor$ and $f_{\phi+b}(n) + b + 1 = \lfloor (n+1)(\phi+b) \rfloor - \lfloor n(\phi+b) \rfloor$, respectively. Since $f_{\mu_b}(n) = g_{\phi+b-1}(n)$ (this identity shown below), the sequence Θ_b has runs of length one and two of each number in K_{b-1}, respectively, Λ_{b-1}. Since $f_{\phi+b}(n) = g_\phi(n)$ (this identity also shown below), the sequence H_b comprises runs of length $b + 2$ and $b + 1$ of each of each lower Wythoff number (K_1), respectively, upper Wythoff number (Λ_1).

Claim **(iv)** requires the additional fact (see, *e.g.*, [17]) that for $\mu > 1$ irrational, $g_\mu(n) = f_{1/\mu}(n)$. Then, $\kappa_b(n) - n = \sum_{m=1}^{n-1} f_{\mu_b}(m) = \sum_{m=1}^{n-1} g_{\phi+b-1}(m)$ $= \sum_{m=1}^{n-1} f_{1/(\phi+b-1)}(m) = \eta_{b-1}(n)$, and $\lambda_b(n) - n = \sum_{m=1}^{n-1} f_{\nu_b}(m) = \sum_{m=1}^{n-1} g_\phi(m)$ $= \sum_{m=1}^{n-1} f_{1/\phi)}(m) = \theta_1(n)$.

Finally, to show that $f_{\mu_b}(n) = g_{\phi+b-1}(n)$ and $f_{\phi+b}(n) = g_\phi(n)$, first recall the continued fraction expansions $\mu_b = [1, b, \bar{1}]$ and $\phi + b = [b+1, \bar{1}]$, which give, respectively, convergents $\frac{F_t+bF_{t-1}}{F_{t-2}+bF_{t-1}}$ and $\frac{F_{t+1}+bF_t}{F_t}$ for $t = 1, 2, 3, \ldots$.

Consider that in both sequences of convergents, the sequences of numerators greater than one are $b + 1, b + 2, 2b + 3, 3b + 5, 5b + 8, \ldots$. For convergents to $\mu_1 = \phi$ and $\phi + b$ the sequences of denominators greater than one are both

$F_3, F_4, F_5, F_6, F_7, \ldots = 2, 3, 5, 8, 13, \ldots$, while for $b > 1$ the sequence of denominators greater than one in convergents to μ_b is $b, b+1, b+2, 2b+3, 3b+5, \ldots$.

To show $f_{\mu_b}(n) = g_{\phi+b-1}(n)$, the first step is to observe that the sequence of numerators greater than one in convergents to $\phi + b - 1$ is identical to the sequence of denominators greater than one in convergents to μ_b, for $b > 1$, namely $b, b+1, 2b+1, 3b+2, 5b+3, \ldots$. For $b = 1$, after dropping the first element of latter sequence the remaining denominators $b+1, 2b+1, 3b+2, 5b+3, \ldots = 2, 3, 5, 8, \ldots$ match those of $\mu_1 = \phi$.

Next, equivalence under the calculation method given in [17] also requires $(f_{\mu_b}(1), \ldots, f_{\mu_b}(b)) = (g_{\phi+b-1}(1), \ldots, g_{\phi+b-1}(b))$ for $b > 1$ and for $b = 1$, $(f_\phi(1), f_\phi(2)) = (g_\phi(1), g_\phi(2)) = (1, 0)$, where the latter equality was already noted in Remark 4.19. Thus it remains to observe that for $b > 1$, $(f_{\mu_b}(1), \ldots, f_{\mu_b}(b)) = (0, \ldots, 0, 1) = (g_{\phi+b-1}(1), \ldots, g_{\phi+b-1}(b))$. Thus, by Stolarsky's method of shift operators, $f_{\mu_b}(n) = g_{\phi+b-1}(n)$, for $n = 1, 2, 3, \ldots$ and $b = 1, 2, 3, \ldots$.

To show $f_{\phi+b}(n) = g_\phi(n)$, the first step is to observe that the sequence $2, 3, 5, 8, 13 \ldots$ of numerators greater than one in convergents to ϕ is identical to the sequence of denominators greater than one in convergents to $\phi + b$.

Next, to apply the method, it suffices to calculate that $(f_{\phi+b}(1), f_{\phi+b}(2)) = (g_\phi(1), g_\phi(2)) = (1, 0)$. The calculation is straightforward, whereas as noted above $\lfloor \phi + b \rfloor = b + 1$, and further, $\lfloor 2\phi + 2b \rfloor = 2b + 3$ and $\lfloor 3\phi + 3b \rfloor = 3b + 4$, so that $(f_{\phi+b}(1), f_{\phi+b}(2)) = ((2b+3) - (b+1) - (b+1), (3b+4) - (2b+3) - (b+1)) = (1, 0)$, as claimed. Thus, by Stolarsky's method of shift operators, $f_{\phi+b}(n) = g_\phi(n)$, for $n = 1, 2, 3, \ldots$ and $b = 1, 2, 3, \ldots$. □

Proof of Proposition 5.1(**a**)**:** For 2–1-Fibonacci cohort sequence $(f_n)_{n \geq 1}$ of functions, considering only the left subcohorts (and excluding the right subcohorts) gives $C_{1_L}, C_{2_L}, C_{3_L}, C_{4_L}, C_{5_L}, \ldots = (f_1), (f_3), (f_5), (f_8, f_9), (f_{13}, f_{14}, f_{15}), \ldots$, so that the resulting sequence before reordering is $f_{\vdash_{n,1}} = f_{n+F_{F^{-1}(n)+1}}$, $n = 0, 1, 2, \ldots$ (see Proposition 4.30).

However, with each left subcohort reversed, the resulting sequence becomes f_1, f_3, f_5, f_9, f_8, $f_{15}, f_{14}, f_{13}, \ldots$. Denote the resulting sequence with a 0^{th} element by g_n, $n = 0, 1, 2, \ldots$. This allows cohort t of g to be written $D_t = (g_{F_{t+1}}, \ldots, g_{F_{t+2}-1})$ $= (f_{F_{t+2}-1+F_{F^{-1}(F_{t+2}-1)+1}}, \ldots, f_{F_{t+1}+F_{F^{-1}(F_{t+1})+1}}) = (f_{2F_{t+2}-1}, \ldots, f_{F_{t+3}})$.

Now, Definition 5.1 gives for f_n

$$
\begin{aligned}
f_{F_{t+1}} &= f_L \circ f_{F_{t-1}}, \\
&\vdots \\
f_{2F_t-1} &= f_L \circ f_{F_t-1}, \\
f_{2F_t} &= f_R \circ f_{F_t}, \\
&\vdots \\
f_{F_{t+2}-1} &= f_R \circ f_{F_{t+1}-1},
\end{aligned}
\tag{133}
$$

for each cohort C_t, $t = 3, 4, 5 \ldots$, and $f_2 = f_R \circ f_1$.

Now with a change of index, and reversing the order of the equations, the former block of (133) can be written

$$\begin{aligned} f_{2F_{t+2}-1} &= f_L \circ f_{F_{t+2}-1}, \\ &\vdots \\ f_{F_{t+3}} &= f_L \circ f_{F_{t+1}}, \end{aligned} \tag{134}$$

for $t = 1, 2, 3 \ldots$. In turn, this set can be split into two blocks,

$$\begin{aligned} g_{F_{t+1}} = f_{2F_{t+2}-1} &= f_L \circ f_{F_{t+2}-1}, \\ &\vdots \\ g_{F_{t+1}+F_{t-1}-1} = f_{F_{t+3}+F_{t-2}} &= f_L \circ f_{2F_t}, \end{aligned} \tag{135}$$

and

$$\begin{aligned} g_{F_{t+1}+F_{t-1}} = f_{F_{t+3}+F_{t-2}-1} &= f_L \circ f_{2F_t-1}, \\ &\vdots \\ g_{F_{t+2}-1} = f_{F_{t+3}} &= f_L \circ f_{F_{t+1}} = f_L \circ g_{F_t-1}. \end{aligned} \tag{136}$$

Transform (135), first substituting the latter block of (133), then substituting (135) – (136) with a change of index:

$$\begin{aligned} g_{F_{t+1}} &= f_{2F_{t+2}-1} = f_L \circ f_{F_{t+2}-1} \\ &= f_L \circ f_R \circ f_{F_{t+1}-1} \\ &= f_L \circ f_R \circ (g_{F_t} \diagup f_L \circ) = f_L f_R f_L^{-1} g_{F_t}, \\ &\vdots \\ g_{F_{t+1}+F_{t-1}-1} &= f_{F_{t+3}+F_{t-2}} = f_L \circ f_{2F_t} \\ &= f_L \circ f_R \circ f_{F_t} \\ &= f_L \circ f_R \circ (g_{F_{t+1}-1} \diagup f_L \circ) = f_L f_R f_L^{-1} g_{F_{t+1}-1}, \end{aligned} \tag{137}$$

Transform (136), first substituting the former block of (133), then substituting (135) – (136) with a change of index:

$$\begin{aligned} g_{F_{t+1}+F_{t-1}} &= f_{F_{t+3}+F_{t-2}+1} = f_L \circ f_{2F_t-1} \\ &= f_L \circ f_L \circ f_{F_t-1} \\ &= f_L^2 \circ (g_{F_{t-1}} \diagup f_L \circ) = f_L \circ g_{F_{t-1}}, \\ &\vdots \\ g_{F_{t+2}-1} &= f_{F_{t+3}} = f_L \circ f_{F_{t+1}}, \\ &= f_L \circ f_L \circ f_{F_{t-1}} \\ &= f_L^2 \circ (g_{F_t-1} \diagup f_L \circ) = f_L \circ g_{F_t-1}, \end{aligned} \tag{138}$$

for $t = 3, 4, 5 \ldots$, where the last equality throughout is subject to the existence of the left inverse of f_L. Writing (137) and (138) together gives

$$\begin{aligned}
g_{F_{t+1}} &= f_L f_R \circ (g_{F_t} \diagup f_L \circ) \qquad = f_L f_R f_L^{-1} \circ g_{F_t}, \\
&\vdots \\
g_{F_{t+1}+F_{t-1}-1} &= f_L f_R \circ (g_{F_{t+1}-1} \diagup f_L \circ) = f_L f_R f_L^{-1} \circ g_{F_{t+1}-1}, \\
g_{F_{t+1}+F_{t-1}} &= \quad f_L^2 \circ (g_{F_{t-1}} \diagup f_L \circ) \quad = \qquad f_L \quad \circ g_{F_{t-1}}, \\
&\vdots \\
g_{F_{t+2}-1} &= \quad f_L^2 \circ (g_{F_t-1} \diagup f_L \circ) \quad = \qquad f_L \quad \circ g_{F_t-1},
\end{aligned}$$

for each cohort C_t, $t = 3, 4, 5 \ldots$, a 1–2-Fibonacci cohort sequence $(g_n)_{n \geq 0}$ by left infix under cohortizer $\langle f_L f_R \circ, f_L^2 \circ \rangle (g \diagup f_L \circ) = \langle f_L f_R f_L^{-1} \circ, f_L \circ \rangle (g)$, as claimed.

Finally, for the first and second cohorts, consider $t = 3, 4$ in (133). In particular, $t = 3$ gives $f_4 = f_R \circ f_2$ as well as $g_1 = f_3 = f_L \circ f_1 = f_L \circ g_0$, while $t = 4$ gives $g_2 = f_5 = f_L \circ f_2$. Combining the last two with $f_2 = f_R \circ f_1$ gives $g_2 = f_L \circ f_2 = f_L f_R \circ f_1 = f_L f_R \circ (g_1 \diagup f_L \circ) = f_L f_R f_L^{-1} \circ g_1$, as desired. □

Proof of Proposition 5.1(**b**)**:** For a 1–2-Fibonacci cohort sequence $(f_n)_{n \geq 1}$ of functions, considering only the right subcohorts (and excluding the left subcohorts) gives $C_{1_R}, C_{2_R}, C_{3_R}, C_{4_R}, C_{5_R}, \ldots = (f_1), (f_4), (f_7), (f_{11}, f_{12}), (f_{18}, f_{19}, f_{20}), \ldots$, so that the resulting sequence is $f_{\mathbb{F}_{n,1}} = f_{n+F_{F^{-1}(n)+2}}$, $n = 0, 1, 2, \ldots$.

Denote the resulting sequence with a 0^{th} element by h_n, $n = 0, 1, 2, \ldots$. This allows cohort t of h to be written $D_t = (h_{F_{t+1}}, \ldots, h_{F_{t+2}-1}) = (f_{F_{t+1}+F_{F^{-1}(F_{t+1})+2}}, \ldots, f_{F_{t+2}-1+F_{F^{-1}(F_{t+2}-1)+2}}) = (f_{F_{t+1}+F_{t+3}}, \ldots, f_{F_{t+4}-1})$.

Now, Definition 5.1 gives for f_n

$$\begin{aligned}
f_{F_{t+1}} &= f_{F_t} \circ f_L, \\
&\vdots \\
f_{F_{t+1}+F_{t-1}-1} &= f_{F_{t+1}-1} \circ f_L, \\
f_{F_{t+1}+F_{t-1}} &= f_{F_{t-1}} \circ f_R, \\
&\vdots \\
f_{F_{t+2}-1} &= f_{F_t-1} \circ f_R,
\end{aligned} \tag{139}$$

for each cohort C_t, $t = 3, 4, 5 \ldots$, and $f_2 = f_1 \circ f_L$.

Now with a change of index, the latter block of (139) can be written

$$\begin{aligned}
f_{F_{t+3}+F_{t+1}} &= f_{F_{t+1}} \circ f_R, \\
&\vdots \\
f_{F_{t+4}-1} &= f_{F_{t+2}-1} \circ f_R,
\end{aligned}$$

for $t = 1, 2, 3 \ldots$. In turn, this set can be split into two blocks,

$$\begin{aligned}
h_{F_{t+1}} &= f_{F_{t+3}+F_{t+1}} = f_{F_{t+1}} \circ f_R, \\
&\vdots \\
h_{F_{t+1}+F_{t-1}-1} &= f_{4F_{t+1}-1} = f_{F_{t+1}+F_{t-1}-1} \circ f_R,
\end{aligned} \tag{140}$$

and

$$\begin{aligned} h_{F_{t+1}+F_{t-1}} &= f_{4F_{t+1}} = f_{F_{t+1}+F_{t-1}} \circ f_R = h_{F_{t-1}} \circ f_R, \\ &\vdots \\ h_{F_{t+2}-1} &= f_{F_{t+4}-1} = f_{F_{t+2}-1} \circ f_R = h_{F_t-1} \circ f_R, \end{aligned} \tag{141}$$

for $t = 1, 2, 3 \ldots$. Evidently, the latter block, (141), in h matches that of (139) in f, so it remains to treat the former block, (140).

Transform (140), first by substituting the former block of (139), then by substituting (140) – (141) with a change of index:

$$\begin{aligned} h_{F_{t+1}} &= f_{F_{t+3}+F_{t+1}} = f_{F_{t+1}} \circ f_R \\ &= f_{F_t} \circ f_L \circ f_R \\ &= (h_{F_t}\!\diagup \circ f_R) \circ f_L \circ f_R = h_{F_t} \circ f_R^{-1} f_L f_R, \\ &\vdots \\ h_{F_{t+1}+F_{t-1}-1} &= f_{4F_{t+1}-1} = f_{F_{t+1}+F_{t-1}-1} \circ f_R \\ &= f_{F_{t+1}-1} \circ f_L \circ f_R \\ &= (h_{F_{t+1}-1}\!\diagup \circ f_R) \circ f_L \circ f_R = h_{F_{t+1}-1} \circ f_R^{-1} f_L f_R, \end{aligned} \tag{142}$$

for $t = 3, 4, 5 \ldots$, where the last equality is subject to the existence of the right inverse of f_R. Writing (142) together with (141) gives

$$\begin{aligned} h_{F_{t+1}} &= \quad (h_{F_t}\!\diagup \circ f_R) \circ f_L f_R = \quad h_{F_t} \circ f_R^{-1} f_L f_R, \\ &\vdots \\ h_{F_{t+1}+F_{t-1}-1} &= (h_{F_{t+1}-1}\!\diagup \circ f_R) \circ f_L f_R = h_{F_{t+1}-1} \circ f_R^{-1} f_L f_R, \\ h_{F_{t+1}+F_{t-1}} &= \quad (h_{F_{t-1}}\!\diagup \circ f_R) \circ f_R^2 = \quad h_{F_{t-1}} \circ f_R, \\ &\vdots \\ h_{F_{t+2}-1} &= \quad (h_{F_t-1}\!\diagup \circ f_R) \circ f_R^2 = \quad h_{F_t-1} \circ f_R, \end{aligned}$$

for each cohort C_t, $t = 3, 4, 5 \ldots$, a 1–2-Fibonacci cohort sequence $(h_n)_{n \geq 0}$ by right infix under cohortizer $\langle \circ f_L f_R, \circ f_R^2 \rangle (h\!\diagup \circ f_R) = \langle \circ f_R^{-1} f_L f_R, \circ f_R \rangle (h)$, as claimed.

Finally, for the first and second cohorts, consider $t = 3, 4$ in (139). In particular, $t = 3$ gives $f_3 = f_2 \circ f_L$ as well as $h_1 = f_4 = f_1 \circ f_R = h_0 \circ f_R$, while $t = 4$ gives $h_2 = f_7 = f_2 \circ f_R$. Combining the last two with $f_2 = f_1 \circ f_L$ gives $h_2 = f_2 \circ f_R = f_1 \circ f_L f_R = (h_1\!\diagup \circ f_R) \circ f_L f_R = h_1 \circ f_R^{-1} f_L f_R$, as desired. □

Proof of Lemma 6.19. (Proof for $\overline{\boldsymbol{l}}$ (85). The proofs for $\bar{\boldsymbol{r}}$ (86), $\bar{\boldsymbol{L}}$ and $\bar{\boldsymbol{R}}$ are analogous.) First prove the equality, then interpret the first and second terms as a purely vertical and purely horizontal displacement, respectively, within the tableau. Substituting the definitions of $\overline{\boldsymbol{l}}$ and $\boldsymbol{l}$ into (85) gives

$$\kappa(n+1) - 1 = n + F_{F^{-1}(n)-1} + \theta(n + 1 - F_{F^{-1}(n)}),$$

which for $n \in [F_{t+1}, F_{t+2})$, can be written

$$\kappa(n+1) - 1 = n + F_t + \theta(n + 1 - F_{t+1}),$$

and further, considering the identity $\kappa(m) = m + \theta(m)$ with $m = n + 1$, written as

$$\theta(n+1) = F_t + \theta(n + 1 - F_{t+1}).$$

Next, manipulate

$$0 \leq {}^1\!/\!_\phi(n + 1 - F_{t+1}) - \theta(n + 1 - F_{t+1}) < 1,$$

(with the former inequality strict since $n + 1 \neq F_{t+1}$), into

$${}^1\!/\!_\phi(n+1) - {}^1\!/\!_\phi F_{t+1} - 1 < \theta(n + 1 - F_{t+1}) < {}^1\!/\!_\phi(n+1) - {}^1\!/\!_\phi F_{t+1}.$$

Whereas $\theta(n) \equiv \lfloor {}^n\!/\!_\phi \rfloor$, F_t/F_{t+1} gives convergents of ${}^1\!/\!_\phi$ for $t = 1, 2, 3, \ldots$, and F_t/F_{t+1} is the best rational approximation to ${}^1\!/\!_\phi$ of any quotient with denominator less than F_{t+2}. In particular, for $n + 1 \in [1, F_{t+2})$,

$$0 < |{}^1\!/\!_\phi F_{t+1} - F_t| \leq {}^1\!/\!_\phi(n+1) - \theta(n+1) < 1. \tag{143}$$

Similar to the proof of Lemma 2 of [17] (also see Lemma 1 of Bunder & Tognetti [7]), argue separately for t even and t odd. First, for t even, write (143) as

$$0 < {}^1\!/\!_\phi F_{t+1} - F_t \leq {}^1\!/\!_\phi(n+1) - \theta(n+1) < 1,$$

and manipulate this into

$${}^1\!/\!_\phi(n+1) - 1 - F_t < \theta(n+1) - F_t \leq {}^1\!/\!_\phi(n+1) - {}^1\!/\!_\phi F_{t+1} < {}^1\!/\!_\phi(n+1) - F_t.$$

Thus,

$$\begin{aligned}\theta(n+1) - F_t - 1 \\ \leq {}^1\!/\!_\phi(n+1) - {}^1\!/\!_\phi F_{t+1} - 1 < \theta(n+1-F_{t+1}) < {}^1\!/\!_\phi(n+1) - {}^1\!/\!_\phi F_{t+1} \\ < {}^1\!/\!_\phi(n+1) - F_t,\end{aligned}$$

or

$$-1 < \theta(n + 1 - F_{t+1}) - \theta(n+1) + F_t < {}^1\!/\!_\phi(n+1) - \theta(n+1) < 1,$$

and, the strictly bounded integer quantity equals zero, as desired.

For the case t odd, write (143) as

$$0 < F_t - {}^1\!/\!_\phi F_{t+1} \leq 1 + \theta(n+1) - {}^1\!/\!_\phi(n+1) \leq 1,$$

(with the latter inequality strict since $n + 1 \neq 0$), and manipulate it into

$${}^1\!/\!_\phi(n+1) - F_t < {}^1\!/\!_\phi(n+1) - {}^1\!/\!_\phi F_{t+1} \leq 1 + \theta(n+1) - F_t < 1 + {}^1\!/\!_\phi(n+1) - F_t,$$

Thus,

$$\begin{aligned}{}^1\!/\!_\phi(n+1) - F_t - 1 \\ < {}^1\!/\!_\phi(n+1) - {}^1\!/\!_\phi F_{t+1} - 1 < \theta(n+1-F_{t+1}) < {}^1\!/\!_\phi(n+1) - {}^1\!/\!_\phi F_{t+1} \\ \leq 1 + \theta(n+1) - F_t,\end{aligned}$$

or

$$-1 < {}^1\!/\!_\phi(n+1) - \theta(n+1) - 1 < \theta(n+1-F_{t+1}) - \theta(n+1) + F_t < 1,$$

and once again, the strictly bounded integer quantity equals zero, as desired.

Finally, for $n = F_{t+2} - 1$ the expression $\theta(n+1-F_{t+1}) - \theta(n+1) + F_t$ becomes $\theta(F_t) - \theta(F_{t+2}) + F_t$. Using (76), write

$$\theta(F_t) = \left\lfloor F_{t-1} - (-{}^1\!/\!_\phi)^t \right\rfloor = \begin{cases} F_{t-1}, & t \text{ odd}; \\ F_{t-1} - 1, & t \text{ even}; \end{cases}$$

and

$$\theta(F_{t+2}) = \left\lfloor F_{t+1} - (-1/\phi)^{t+2} \right\rfloor = \begin{cases} F_{t+1}, & t \text{ odd;} \\ F_{t+1} - 1, & t \text{ even.} \end{cases}$$

Consequently

$$\theta(F_t) - \theta(F_{t+2}) + F_t = 0.$$

(Fraenkel, Mushkin, and Tassa cite a similar statement from the theory of continued fractions in the form $\lfloor k_n \mu \rfloor = \begin{cases} h_t, & n \text{ even;} \\ h_t - 1, & n \text{ odd;} \end{cases}$ for convergents $\dfrac{h_t}{k_t}$ to slope μ. In the present case for $\mu = 1/\phi$, $h_t = F_t$, $k_t = F_{t+1}$.)

Now to show that the right-hand-side terms of (85) decompose $\bar{\boldsymbol{l}}$ into vertical-only and horizontal-only components, consider Remark 6.14 that, in a 1–2-Fibonacci cohort tableau, $\boldsymbol{l}$ maps an element of cohort C_t to the element directly below it (in cohort C_{t+1} and in the same horizontal position), since for $n \in [F_{t+1}, F_{t+2})$, $\boldsymbol{l}(n) = n + F_{F^{-1}(n)-1} = n + F_t = F_{t+2} + (n - F_{t+1}) \in [F_{t+2}, F_{t+3})$.

Also for $n \in [F_{t+1}, F_{t+2})$, $F^{-1}(n) = t + 1$ and $F_{F^{-1}(n)+1} = F_{t+1}$, hence the argument $n + 1 - F_{F^{-1}(n)}$ of θ is merely the horizontal position $1, \ldots, F_t$ of n in tableau C_t of the positive integers (Table 6(i)). Thus, $n + 1 - F_{F^{-1}(n)} \le F_t$ and $\theta(n + 1 - F_{F^{-1}(n)}) \le \theta(F_t) = \begin{cases} F_{t-1}, & t \text{ odd;} \\ F_{t-1} - 1, & t \text{ even;} \end{cases} \le F_{t-1}$. Therefore, the right-hand side of (85) is less than or equal to $n + \begin{cases} F_{t+1}, & t \text{ odd;} \\ F_{t+1} - 1, & t \text{ even;} \end{cases} \le n + F_{t+1}$. □

Proof of Lemma 8.1(⊦): For $⊦_{n,k}$, it suffices to have *(i)* $⊦_{0,1} = 1$ for row $n = 0$ and the remainder of the first column ($⊦$ starting on row $n = 1$) to be the sequence $(\boldsymbol{r}(n))_{n \ge 1}$ of right children of the integers $1, 2, 3, \ldots$ in the minimal Fibonacci tree, and *(ii)* for successive entries in a row to match branching from a parent to its left child in the minimal Fibonacci tree, that is, $⊦_{n,k} = \boldsymbol{l}^{k-1}(⊦_{n,1})$.

For claim *(i)* about right branching, the entry $⊦_{0,1} = F_2 = 1$ meets the requirement, and for $k = 1$ and $n \ge 1$, the entries $⊦_{n,1} = \boldsymbol{r}(n) = n + F_{F^{-1}(n)+2}$ by definition, thus matching the right branching from parent n in Figure 15(iii).

For the claim about left branching, recall Proposition 6.18, and, for $n \ge 0$, use (83) to obtain:

$$\begin{aligned} F^{-1}(⊦_{n,k}) &= F^{-1}(n) + k + 1 \\ F^{-1}(⊦_{n,k}) - 1 &= F^{-1}(n) + k \\ F_{F^{-1}(⊦_{n,k})-1} &= F_{F^{-1}(n)+k} \\ F_{F^{-1}(⊦_{n,k})-1} &= F_{F^{-1}(n)+k+2} - F_{F^{-1}(n)+k+1} \\ F_{F^{-1}(n)+k+1} + F_{F^{-1}(⊦_{n,k})-1} &= F_{F^{-1}(n)+k+2} \\ n + F_{F^{-1}(n)+k+1} + F_{F^{-1}(⊦_{n,k})-1} &= n + F_{F^{-1}(n)+k+2} \\ ⊦_{n,k} + F_{F^{-1}(⊦_{n,k})-1} &= ⊦_{n,k+1} \\ \boldsymbol{l}(⊦_{n,k}) &= ⊦_{n,k+1}, \end{aligned}$$

so that $⊦_{n,k+1}$ is indeed the left child of $⊦_{n,k}$ in Figure 15(iii). □

Proof for (⊣): For $⊣_{n,k}$, it suffices to have *(i)* $⊣_{0,1} = 1$ for row $n = 0$ and the remainder of the first column ($⊣$ starting on row $n = 1$) to be the sequence $(\boldsymbol{l}(n))_{n \ge 1}$ of left children of the integers $1, 2, 3, \ldots$ in the minimal Fibonacci tree, and *(ii)* for

successive entries in a row to match branching from a parent to its right child in the minimal Fibonacci tree, that is, $\daleth_{n,k} = \boldsymbol{r}^{k-1}(\daleth_{n,1})$.

For claim *(i)* about left branching, the entry $\daleth_{0,1} = F_3 - 1 = 1$ meets the requirement, and for $k = 1$ and $n \geq 1$, the entries $\daleth_{n,1} = \boldsymbol{l}(n) = n + F_{F^{-1}(n)+2} - 2F_{F^{-1}(n)} = n + F_{F^{-1}(n)-1}$ by definition, thus matching the left branching from parent n in Figure 15(iii).

For the claim about right branching, recall Proposition 6.18, and use (84) to obtain: Case $n = 0$:

$$\begin{aligned}
F^{-1}(\daleth_{0,k}) &= 2k \\
F^{-1}(\daleth_{0,k}) + 2 &= 2k + 2 \\
F_{F^{-1}(\daleth_{0,k})+2} &= F_{2k+2} \\
\daleth_{0,k} + F_{F^{-1}(\daleth_{0,k})+2} &= \daleth_{0,k} + F_{2k+2} \\
\daleth_{0,k} + F_{F^{-1}(\daleth_{0,k})+2} &= F_{2k+1} - 1 + F_{2k+2} \\
\daleth_{0,k} + F_{F^{-1}(\daleth_{0,k})+2} &= F_{2(k+1)+1} - 1 \\
\daleth_{0,k} + F_{F^{-1}(\daleth_{0,k})+2} &= \daleth_{0,k+1} \\
\boldsymbol{l}(\daleth_{0,k}) &= \beth_{0,k+1},
\end{aligned}$$

Case $n > 0$:

$$\begin{aligned}
F^{-1}(\daleth_{n,k}) &= F^{-1}(n) + 2k - 1 \\
F^{-1}(\daleth_{n,k}) + 2 &= F^{-1}(n) + 2k + 1 \\
F_{F^{-1}(\daleth_{n,k})+2} &= F_{F^{-1}(n)+2k+1} \\
F_{F^{-1}(\daleth_{n,k})+2} &= F_{F^{-1}(n)+2k+2} - F_{F^{-1}(n)+2k} \\
F_{F^{-1}(n)+2k} + F_{F^{-1}(\daleth_{n,k})+2} &= F_{F^{-1}(n)+2k+2} \\
n + F_{F^{-1}(n)+2k} - 2F_{F^{-1}(n)} + F_{F^{-1}(\daleth_{n,k})+2} &= n + F_{F^{-1}(n)+2(k+1)} - 2F_{F^{-1}(n)} \\
\daleth_{n,k} + F_{F^{-1}(\daleth_{n,k})+2} &= \daleth_{n,k+1} \\
\boldsymbol{r}(\daleth_{n,k}) &= \daleth_{n,k+1},
\end{aligned}$$

so that for $n \geq 0$, $\daleth_{n,k+1}$ is indeed the right child of $\daleth_{n,k}$ in Figure 15(iii). □

Proof of Lemma 8.1(⊨): For $\vDash_{n,k}$, it suffices to have *(i)* $\vDash_{0,1} = 1$ for row $n = 0$ and the remainder of the first column ($\vDash$ starting on row $n = 1$) to be the sequence $(\boldsymbol{R}(n))_{n\geq 1}$ of right children of the integers $1, 2, 3, \ldots$ in the maximal Fibonacci tree, and *(ii)* for successive entries in a row to match branching from a parent to its left child in the maximal Fibonacci tree, that is, $\vDash_{n,k} = \boldsymbol{L}^{k-1}(\vDash_{n,1})$.

For claim *(i)* about right branching, the entry $\vDash_{0,1} = F_3 - F_2 = 1$ meets the requirement, and for $k = 1$ and $n \geq 1$, the entries $\vDash_{n,1} = \boldsymbol{R}(n) = n + F_{F^{-1}(n)+3} - F_{F^{-1}(n)+2} = n + F_{F^{-1}(n)+1}$ by definition, thus matching the right branching from parent n in Figure 15(iv).

For the claim about left branching, recall Proposition 6.18, and, for $n \geq 0$, use (83) to obtain:

$$\begin{aligned}
F^{-1}(\vdash_{n,k}) &= F^{-1}(n) + k + 1 \\
F_{F^{-1}(\vdash_{n,k})} &= F_{F^{-1}(n)+k+1} \\
F_{F^{-1}(\vdash_{n,k})} &= F_{F^{-1}(n)+k+3} - F_{F^{-1}(n)+k+2} \\
F_{F^{-1}(n)+k+2} + F_{F^{-1}(\vdash_{n,k})} &= F_{F^{-1}(n)+k+3} \\
n + F_{F^{-1}(n)+k+2} - F_{F^{-1}(n)+2} + F_{F^{-1}(\vdash_{n,k})} &= n + F_{F^{-1}(n)+(k+1)+2} - F_{F^{-1}(n)+2} \\
\vdash_{n,k} + F_{F^{-1}(\vdash_{n,k})} &= \vdash_{n,k+1} \\
\boldsymbol{L}(\vdash_{n,k}) &= \vdash_{n,k+1},
\end{aligned}$$

ao that $\vdash_{n,k+1}$ is indeed the left child of $\vdash_{n,k}$ in Figure 15(iv). □

Proof of Lemma 8.1(∃): For $\exists_{n,k}$, it suffices to have *(i)* $\exists_{0,1} = 1$ for row $n = 0$ and the remainder of the first column ($\exists$ starting on row $n = 1$) to be the sequence $(\boldsymbol{L}(n))_{n\geq 1}$ of left children of the integers $1, 2, 3, \ldots$ in the maximal Fibonacci tree, and *(ii)* for successive entries in a row to match branching from a parent to its right child in the maximal Fibonacci tree, that is, $\exists_{n,k} = \boldsymbol{R}^{k-1}(\exists_{n,1})$.

For claim *(i)* about left branching, the entry $\exists_{0,1} = F_2 = 1$ meets the requirement, and for $k = 1$ and $n \geq 1$, the entries $\exists_{n,1} = \boldsymbol{L}(n) = n + F_{F^{-1}(n)+1} - F_{F^{-1}(n)-1} = n + F_{F^{-1}(n)}$ by definition, thus matching the left branching from parent n in Figure 15(iv).

For the claim about right branching, recall Proposition 6.18, and use (84) to obtain:

Case $n = 0$:

$$\begin{aligned}
F^{-1}(\exists_{0,k}) &= 2k \\
F^{-1}(\exists_{0,k}) + 1 &= 2k + 1 \\
F_{F^{-1}(\exists_{0,k})+1} &= F_{2k+1} \\
F_{F^{-1}(\exists_{0,k})+1} &= F_{2k+2} - F_{2k} \\
F_{2k} + F_{F^{-1}(\exists_{0,k})+1} &= F_{2k+2} \\
\exists_{0,k} + F_{F^{-1}(\exists_{0,k})+1} &= F_{2(k+1)} \\
\exists_{0,k} + F_{F^{-1}(\exists_{0,k})+1} &= \exists_{0,k+1} \\
\boldsymbol{R}(\exists_{0,k}) &= \exists_{0,k+1},
\end{aligned}$$

Case $n > 0$:

$$\begin{aligned}
F^{-1}(\exists_{n,k}) &= F^{-1}(n) + 2k - 1 \\
F^{-1}(\exists_{n,k}) + 1 &= F^{-1}(n) + 2k \\
F_{F^{-1}(\exists_{n,k})+1} &= F_{F^{-1}(n)+2k} \\
F_{F^{-1}(\exists_{n,k})+1} &= F_{F^{-1}(n)+2k+1} - F_{F^{-1}(n)+2k-1} \\
F_{F^{-1}(n)+2k-1} + F_{F^{-1}(\exists_{n,k})+1} &= F_{F^{-1}(n)+2k+1} \\
n + F_{F^{-1}(n)+2k-1} - F_{F^{-1}(n)-1} + F_{F^{-1}(\exists_{n,k})+1} &= n + F_{F^{-1}(n)+2(k+1)-1} - F_{F^{-1}(n)-1} \\
\exists_{n,k} + F_{F^{-1}(\exists_{n,k})+1} &= \exists_{n,k+1} \\
\boldsymbol{R}(\exists_{n,k}) &= \exists_{n,k+1},
\end{aligned}$$

so that for $n \geq 0$, $\exists_{n,k+1}$ is indeed the right child of $\exists_{n,k}$ in Figure 15(iv). □

Proof of Lemma 8.3: Propositions 3.2 and 4.40 derived formulas for $a_{n,k}$, respectively $w_{n,k}$, using cohort sequences (Example 4.15 treated the latter). The following arguments derive formulas for the clade quartet using branchings in the successor trees. □

Proof of Lemma 8.3(w): For $w_{n,k}$, it suffices to have *(i)* for the first column $w_{0,1} = 1$ for row $n = 0$ and the remainder of the first column ($w_{n,1}$ starting on row $n = 1$) to be the sequence $(\bar{\boldsymbol{r}}(n))_{n\geq 1}$ of right children of the integers $1, 2, 3, \ldots$ in the minimal successor tree, and *(ii)* for successive entries in a row to follow the branching from a parent to its left child in the minimal successor tree, that is, $w_{n,k} = \bar{\boldsymbol{l}}^{k-1}(w_{n,1})$.

For claim *(i)* about right branching, the entry $w_{0,1} = F_2 = 1$ meets the requirement, and for $k = 1$ and $n \geq 1$, the entries $w_{n,1} = \bar{\boldsymbol{r}}(n) = \kappa(n+1) + n = \kappa(n+1) + (n+1) - 1 = \lambda(n+1) - 1$ by definition equal the right child of parent n in the minimal successor tree. This matches the right branching shown in Figure 15(i).

For the claim about left branching in Figure 15(i), use identities (75) and (76).

Substitute $m = F_{k+1}\kappa(n+1) + F_k n + 1$ into (75) to obtain

$$0 \leq \phi F_{k+1}\kappa(n+1) + \phi F_k n + \phi - \kappa(F_{k+1}\kappa(n+1) + F_k n + 1) < 1.$$

Next, using (76), write this as

$$0 \leq (F_{k+2} - (-\tfrac{1}{\phi})^{k+1})\kappa(n+1) + (F_{k+1} - (-\tfrac{1}{\phi})^k)n + \phi \\ - \kappa(F_{k+1}\kappa(n+1) + F_k n + 1) < 1,$$

or

$$\kappa(n+1)(-\tfrac{1}{\phi})^{k+1} + n(-\tfrac{1}{\phi})^k \\ \leq F_{k+2}\kappa(n+1) + F_{k+1}n + \phi - \kappa(F_{k+1}\kappa(n+1) + F_k n + 1) \\ < 1 + \kappa(n+1)(-\tfrac{1}{\phi})^{k+1} + n(-\tfrac{1}{\phi})^k.$$

Simplify the lower bound $\kappa(n+1)(-\frac{1}{\phi})^{k+1} + n(-\frac{1}{\phi})^k = (-\frac{1}{\phi})^k(-\frac{1}{\phi}\kappa(n+1) + n)$, considering that the minima of $n - \frac{1}{\phi}\kappa(n+1)$ occur at $n = F_{2m+1} - 1$, so that

$$\begin{aligned} &\min_{n,k} \kappa(n+1)(-\tfrac{1}{\phi})^{k+1} + n(-\tfrac{1}{\phi})^k \\ =&\min_{m,k}(-\tfrac{1}{\phi})^k(-\tfrac{1}{\phi}\kappa(F_{2m+1}) + F_{2m+1} - 1) \\ =&\min_{m,k}(-\tfrac{1}{\phi})^k(-\tfrac{1}{\phi}F_{2m+2} + F_{2m+1} - 1) \\ =&\min_{m,k}(-\tfrac{1}{\phi})^k((\tfrac{1}{\phi})^{2m+2} - 1) \\ =&\min_{m,k}(-\tfrac{1}{\phi})^{2m+k+2} - (-\tfrac{1}{\phi})^k \\ =&\lim_{m\to\infty}(-\tfrac{1}{\phi})^{2m+k+2} - (-\tfrac{1}{\phi})^k\Big|_{k=2} \\ =&-(\tfrac{1}{\phi})^2 \\ =&-1 + \tfrac{1}{\phi} \end{aligned}$$

Simplify the upper bound $1 + \kappa(n+1)(-\frac{1}{\phi})^{k+1} + n(-\frac{1}{\phi})^k = 1 + (-\frac{1}{\phi})^k(-\frac{1}{\phi}\kappa(n+1) + n)$, considering that the minima of $n - \frac{1}{\phi}\kappa(n+1)$ occur at $n = F_{2m+1} - 1$, so

that

$$\begin{aligned}
&\max_{n,k} 1+\kappa(n+1)(-\tfrac{1}{\phi})^{k+1}+n(-\tfrac{1}{\phi})^k\\
=&\max_{m,k} 1+(-\tfrac{1}{\phi})^k(-\tfrac{1}{\phi}\kappa(F_{2m+1})+F_{2m+1}-1)\\
=&\max_{m,k} 1+(-\tfrac{1}{\phi})^k(-\tfrac{1}{\phi}F_{2m+2}+F_{2m+1}-1)\\
=&\max_{m,k} 1+(-\tfrac{1}{\phi})^k((\tfrac{1}{\phi})^{2m+2}-1)\\
=&\max_{m,k} 1+(-\tfrac{1}{\phi})^{2m+k+2}-(-\tfrac{1}{\phi})^k\\
=&\lim_{m\to\infty} 1+(-\tfrac{1}{\phi})^{2m+k+2}-(-\tfrac{1}{\phi})^k\Big|_{k=1}\\
=&1+\tfrac{1}{\phi}.
\end{aligned}$$

Continue to manipulate the formula until the desired difference is bounded:

$$\begin{aligned}
-1+\tfrac{1}{\phi} <& F_{k+2}\kappa(n+1)+F_{k+1}n+\phi-\kappa(F_{k+1}\kappa(n+1)+F_kn+1) &<&1+\tfrac{1}{\phi},\\
-1 <& F_{k+2}\kappa(n+1)+F_{k+1}n-\kappa(F_{k+1}\kappa(n+1)+F_kn+1)+1 &<&1,\\
-1 <& w_{n,k+1}-(\kappa(w_{n,k}+1)-1) &<&1,\\
-1 <& w_{n,k+1}-\bar{\boldsymbol{l}}(w_{n,k}) &<&1.
\end{aligned}$$

Thus, the two positive integer quantities have a difference of less than one, proving that the formula for $w_{n,k}$ matches the claim that rows $n \geq 1$ of w give sequences of left branchings in the minimal successor tree (Figure 15(i)). □

Proof of Lemma 8.3(ɯ)*:* For $\mathfrak{w}_{n,k}$, it suffices to have *(i)* $\mathfrak{w}_{0,1}=1$ for row $n=0$ and the remainder of the first column ($\mathfrak{w}_{n,1}$ starting on row $n=1$) to be the sequence $(\bar{\boldsymbol{l}}(n))_{n\geq 1}$ of left children of the integers $1,2,3,\ldots$ in the minimal successor tree, and *(ii)* for successive entries in a row to match branching from a parent to its right child in the minimal successor tree, that is, $\mathfrak{w}_{n,k}=\bar{\boldsymbol{r}}^{k-1}(\mathfrak{w}_{n,1})$.

For claim *(i)* about left branching, the entry $\mathfrak{w}_{0,1}=F_3-1=1$ meets the requirement, and for $k=1$ and $n\geq 1$, the entries $\mathfrak{w}_{n,1}=\bar{\boldsymbol{l}}(n)=\kappa(n+1)-1$ by definition, thus matching the left branching from parent n in Figure 15(i).

For the claim about right branching in Figure 15(i), use identities (75) and (76).

Case $n=0$: Substitute $m=F_{2k+1}$ into (75) to obtain $0\leq \phi F_{2k+1}-\kappa(F_{2k+1})<1$. Next, using (76), write this as

$$\begin{aligned}
0 \leq F_{2k+2}-(-\tfrac{1}{\phi})^{2k+1}-\kappa(F_{2k+1})<1, \text{ or}\\
(-\tfrac{1}{\phi})^{2k+1}\leq F_{2k+2}-\kappa(F_{2k+1})<1+(-\tfrac{1}{\phi})^{2k+1}.
\end{aligned}$$

Simplify the bounds, as

$$-1<-\tfrac{1}{\phi^3}\leq(-\tfrac{1}{\phi})^{2k+1}, \text{ and } 1+(-\tfrac{1}{\phi})^{2k+1}<\lim_{k\to\infty}1-(\tfrac{1}{\phi})^{2k+1}<1,$$

and continue to manipulate the formula until the desired difference is bounded:

$$\begin{aligned}
-1 <& F_{2k+2} && -\kappa(F_{2k+1}) && < 1,\\
-1 <& F_{2k+3} && -\ (F_{2k+1}+\kappa(F_{2k+1})) && < 1,\\
-1 <& F_{2k+3} && -\lambda(F_{2k+1}) && < 1,\\
-1 <& \mathfrak{w}_{0,k+1} && -(\lambda(\mathfrak{w}_{0,k}+1)-1) && < 1,\\
-1 <& \mathfrak{w}_{0,k+1} && -\bar{\boldsymbol{r}}(\mathfrak{w}_{0,k}) && < 1.
\end{aligned}$$

The two positive integer quantities having a difference of less than one, shows that the formula for $\mathfrak{w}_{0,k}$ matches the claim that row $n=0$ gives the sequence of right branchings in the minimal successor tree (Figure 15(i)) descending from 1.

Case $n \geq 1$: Substitute $m = F_{2k-1}\kappa(n+1) + F_{2k-2}n$ into (75) to obtain

$$0 \leq \phi F_{2k-1}\kappa(n+1) + \phi F_{2k-2}n - \kappa(F_{2k-1}\kappa(n+1) + F_{2k-2}n) < 1.$$

Next, using (76), write this as

$$0 \leq (F_{2k}-(-\tfrac{1}{\phi})^{2k-1})\kappa(n+1)+(F_{2k-1}-(-\tfrac{1}{\phi})^{2k-2})n-\kappa(F_{2k-1}\kappa(n+1)+F_{2k-2}n) < 1,$$

or

$$\begin{aligned}
\kappa(n+1)(-\tfrac{1}{\phi})^{2k-1} + n(-\tfrac{1}{\phi})^{2k-2}& \\
\leq F_{2k}\kappa(n+1) + F_{2k-1}n - \kappa(F_{2k-1}\kappa(n+1) + F_{2k-2}n)& \\
< 1 + \kappa(n+1)(-\tfrac{1}{\phi})^{2k-1} + n(-\tfrac{1}{\phi})^{2k-2}.&
\end{aligned}$$

Simplify the lower bound $\kappa(n+1)(-\frac{1}{\phi})^{2k-1}+n(-\frac{1}{\phi})^{2k-2} = (\frac{1}{\phi})^{2k-2}(-\frac{1}{\phi}\kappa(n+1)+n)$, considering that the minima of $n - \frac{1}{\phi}\kappa(n+1)$ occur at $n = F_{2m+1}-1$, so that

$$\begin{aligned}
&\min_{n,k} \kappa(n+1)(-\tfrac{1}{\phi})^{2k-1} + n(-\tfrac{1}{\phi})^{2k-2}\\
=&\min_{m,k} (\tfrac{1}{\phi})^{2k-2}(-\tfrac{1}{\phi}\kappa(F_{2m+1}) + F_{2m+1} - 1)\\
=&\min_{m,k} (\tfrac{1}{\phi})^{2k-2}(-\tfrac{1}{\phi}F_{2m+2} + F_{2m+1} - 1)\\
=&\min_{m,k} (\tfrac{1}{\phi})^{2k-2}((\tfrac{1}{\phi})^{2m+2} - 1)\\
=&\min_{m,k} -(\tfrac{1}{\phi})^{2k-2} + (\tfrac{1}{\phi})^{2m+2k}\\
=&\lim_{m\to\infty} -(\tfrac{1}{\phi})^{2k-2} + (\tfrac{1}{\phi})^{2m+2k}\Big|_{k=1}\\
=&-1.
\end{aligned}$$

Simplify the upper bound $1+\kappa(n+1)(-\frac{1}{\phi})^{2k-1}+n(-\frac{1}{\phi})^{2k-2} = 1+(\frac{1}{\phi})^{2k-2}(-\frac{1}{\phi}\kappa(n+1)+n)$, considering that the maxima of $n - \frac{1}{\phi}\kappa(n+1)$ occur at $n = F_{2m+2}-1$, so

that

$$\begin{aligned}
&\max_{n,k} 1+\kappa(n+1)(-\tfrac{1}{\phi})^{2k-1}+n(-\tfrac{1}{\phi})^{2k-2}\\
=&\max_{m,k} 1+(\tfrac{1}{\phi})^{2k-2}(-\tfrac{1}{\phi}\kappa(F_{2m+2})+F_{2m+2}-1)\\
=&\max_{m,k} 1+(\tfrac{1}{\phi})^{2k-2}(-\tfrac{1}{\phi}F_{2m+3}+F_{2m+2}-2)\\
=&\max_{m,k} 1+(\tfrac{1}{\phi})^{2k-2}((\tfrac{1}{\phi})^{2m+3}-2)\\
=&\max_{m,k} 1-2(\tfrac{1}{\phi})^{2k-2}+(\tfrac{1}{\phi})^{2m+2k+1}\\
=&\lim_{m,k\to\infty} 1-2(\tfrac{1}{\phi})^{2k-2}+(\tfrac{1}{\phi})^{2m+2k+1}\\
=&1.
\end{aligned}$$

Continue to manipulate the formula until the desired difference is bounded:

$$\begin{aligned}
-1 <&\quad F_{2k}\kappa(n+1)+F_{2k-1}n\ -\kappa(F_{2k-1}\kappa(n+1)+F_{2k-2}n)\ <1,\\
-1 <&\ F_{2k+1}\kappa(n+1)+F_{2k}n\\
&-[(F_{2k-1}\kappa(n+1)+F_{2k-2}n)+\kappa(F_{2k-1}\kappa(n+1)+F_{2k-2}n)]<1,\\
-1 <&\ F_{2k+1}\kappa(n+1)+F_{2k}n\quad -\lambda(F_{2k-1}\kappa(n+1)+F_{2k-2}n)\ <1,\\
-1 <&\qquad\qquad \mathfrak{w}_{n,k+1}-(\lambda(\mathfrak{w}_{n,k}+1)-1)\qquad\qquad <1,\\
-1 <&\qquad\qquad \mathfrak{w}_{n,k+1}\ -\bar{\boldsymbol{r}}(\mathfrak{w}_{n,k})\qquad\qquad <1.
\end{aligned}$$

Thus, the two positive integer quantities have a difference of less than one, proving that the formula for $\mathfrak{w}_{n,k}$ matches the claim that rows $n \geq 1$ of $\mathfrak{w}$ give sequences of right branchings in the minimal successor tree. □

Proof of Lemma 8.3(a): For $a_{n,k}$, it suffices to have *(i)* $a_{0,1} = 1$ for row $n = 0$ and the remainder of the first column ($a_{n,1}$ starting on row $n = 1$) to be the sequence of right children $(\bar{\boldsymbol{R}}(n))_{n\geq 1}$ of the integers $1, 2, 3, \ldots$ in the maximal successor tree, and *(ii)* for successive entries in a row to match branching from a parent to its left child in the maximal successor tree, that is, $a_{n,k} = \bar{\boldsymbol{L}}^{k-1}(a_{n,1})$.

For claim *(i)* about right branching, the entry $a_{0,1} = F_3 - 1 = 1$ meets the requirement, and for $k = 1$ and $n \geq 1$, the entries $a_{n,1} = \bar{\boldsymbol{R}}(n) = \kappa(n) + n + 1 = \lambda(n) + 1$ by definition, thus matching the right branching from parent n in Figure 15(ii).

For the claim about left branching in Figure 15(ii), use identities (75) and (76).

Substitute $m = F_{k+1}\kappa(n) + F_k n + F_{k+2} - 1$ into (75) to obtain

$$0 \leq \phi F_{k+1}\kappa(n) + \phi F_k n + \phi F_{k+2} - \phi - \kappa(F_{k+1}\kappa(n) + F_k n + F_{k+2} - 1) < 1.$$

Next, using (76), write this as

$$\begin{aligned}
0 \leq (F_{k+2} - (-\tfrac{1}{\phi})^{k+1})\kappa(n) + (F_{k+1} - (-\tfrac{1}{\phi})^k)n + (F_{k+3} - (-\tfrac{1}{\phi})^{k+2}) - \phi\\
- \kappa(F_{k+1}\kappa(n) + F_k n + F_{k+2} - 1) < 1,
\end{aligned}$$

or

$$\begin{aligned}\kappa(n)(-\tfrac{1}{\phi})^{k+1} + n(-\tfrac{1}{\phi})^k + (-\tfrac{1}{\phi})^{k+2} + \phi \\ \leq F_{k+2}\kappa(n) + F_{k+1}n + F_{k+3} - \kappa(F_{k+1}\kappa(n) + F_k n + F_{k+2} - 1) \\ < 1 + \kappa(n)(-\tfrac{1}{\phi})^{k+1} + n(-\tfrac{1}{\phi})^k + (-\tfrac{1}{\phi})^{k+2} + \phi.\end{aligned}$$

Simplify the lower bound $\kappa(n)(-\frac{1}{\phi})^{k+1}+n(-\frac{1}{\phi})^k+(-\frac{1}{\phi})^{k+2}+\phi = (-\frac{1}{\phi})^k(-\frac{1}{\phi}\kappa(n)+ n+(\frac{1}{\phi})^2)+\phi$, considering that the maxima of $n-\frac{1}{\phi}\kappa(n)$ occur at $n = F_{2m}$, so that

$$\begin{aligned}&\min_{n,k} \kappa(n)(-\tfrac{1}{\phi})^{k+1} + n(-\tfrac{1}{\phi})^k + (-\tfrac{1}{\phi})^{k+2} + \phi \\ =&\min_{m,k}(-\tfrac{1}{\phi})^k(-\tfrac{1}{\phi}\kappa(F_{2m}) + F_{2m} + (\tfrac{1}{\phi})^2) + \phi \\ =&\min_{m,k}(-\tfrac{1}{\phi})^k(-\tfrac{1}{\phi}(F_{2m+1} - 1) + F_{2m} + (\tfrac{1}{\phi})^2) + \phi \\ =&\min_{m,k}(-\tfrac{1}{\phi})^k(1 + (-\tfrac{1}{\phi})^{2m+1}) + \phi \\ =&\lim_{m\to\infty} (-\tfrac{1}{\phi})^k + (-\tfrac{1}{\phi})^{2m+k+1}\Big|_{k=1} + \phi \\ =&1.\end{aligned}$$

Simplify the upper bound $1 + \kappa(n)(-\frac{1}{\phi})^{k+1} + n(-\frac{1}{\phi})^k + (-\frac{1}{\phi})^{k+2} + \phi = 1 + (-\frac{1}{\phi})^k(-\frac{1}{\phi}\kappa(n) + n + (\frac{1}{\phi})^2) + \phi$, considering that the maxima of $n - \frac{1}{\phi}\kappa(n)$ occur at $n = F_{2m}$, so that

$$\begin{aligned}&\max_{n,k} 1 + \kappa(n)(-\tfrac{1}{\phi})^{k+1} + n(-\tfrac{1}{\phi})^k + (-\tfrac{1}{\phi})^{k+2} + \phi \\ =&\max_{m,k} 1 + (-\tfrac{1}{\phi})^k(-\tfrac{1}{\phi}\kappa(F_{2m}) + F_{2m} + (\tfrac{1}{\phi})^2) + \phi \\ =&\max_{m,k} 1 + (-\tfrac{1}{\phi})^k(-\tfrac{1}{\phi}(F_{2m+1} - 1) + F_{2m} + (\tfrac{1}{\phi})^2) + \phi \\ =&\max_{m,k} 1 + (-\tfrac{1}{\phi})^k(1 + (-\tfrac{1}{\phi})^{2m+1}) + \phi \\ =&1 + \phi + \lim_{m\to\infty} (-\tfrac{1}{\phi})^k + (-\tfrac{1}{\phi})^{2m+k+1}\Big|_{k=2} \\ =&3.\end{aligned}$$

Continue to manipulate the formula until the desired difference is bounded:

$$\begin{aligned}1 <&\quad F_{k+2}\kappa(n) + F_{k+1}n + F_{k+3} - \kappa(F_{k+1}\kappa(n) + F_k n + F_{k+2} - 1) &<3 \\ 0 <&F_{k+2}\kappa(n) + F_{k+1}n + F_{k+3} - 1 - \kappa(F_{k+1}\kappa(n) + F_k n + F_{k+2} - 1) &<2 \\ -1 <&F_{k+2}\kappa(n) + F_{k+1}n + F_{k+3} - 1 - (\kappa(F_{k+1}\kappa(n) + F_k n + F_{k+2} - 1) + 1) &<1 \\ -1 <&\quad a_{n,k+1} - (\kappa(a_{n,k}) + 1) &<1 \\ -1 <&\quad a_{n,k+1} - \bar{\boldsymbol{L}}(a_{n,k}) &<1\end{aligned}$$

Thus, the two positive integer quantities have a difference of less than one, proving that the formula for $a_{n,k}$ matches the claim that rows $n \geq 1$ of a give sequences of left branchings in the maximal successor tree. □

Proof of Lemma 8.3(𝔬)*:* For $\mathfrak{o}_{n,k}$, it suffices to have *(i)* $\mathfrak{o}_{0,1} = 1$ for row $n = 0$ and the remainder of the first column ($\mathfrak{o}_{n,1}$ starting on row $n = 1$) to be the sequence $(\bar{\boldsymbol{L}}(n))_{n\geq 1}$ of left children of the integers $1, 2, 3, \ldots$ in the maximal successor tree,

and *(ii)* for successive entries in a row to match branching from a parent to its right child in the maximal successor tree, that is, $\mathfrak{o}_{n,k} = \bar{\boldsymbol{R}}^{k-1}(\mathfrak{o}_{n,1})$.

For claim *(i)* about left branching, the entry $\mathfrak{o}_{0,1} = F_2 = 1$ meets the requirement, and for $k = 1$ and $n \geq 1$, the entries $\mathfrak{o}_{n,1} = \bar{\boldsymbol{L}}(n) = \kappa(n) + 1$ by definition, thus matching the left branching from parent n in Figure 15(ii).

For the claim about right branching in Figure 15(ii), use identities (75) and (76). Substitute $m = F_{2k-1}\kappa(n) + F_{2k-2}n + F_{2k}$ into (75) to obtain

$$0 \leq \phi F_{2k-1}\kappa(n) + \phi F_{2k-2}n + \phi F_{2k} - \kappa(F_{2k-1}\kappa(n+1) + F_{2k-2}n + F_{2k}) < 1.$$

Next, using (76), write this as

$$\begin{aligned} 0 \leq (F_{2k} - (-\tfrac{1}{\phi})^{2k-1})\kappa(n) + (F_{2k-1} - (-\tfrac{1}{\phi})^{2k-2})n + (F_{2k+1} - (-\tfrac{1}{\phi})^{2k}) \\ - \kappa(F_{2k-1}\kappa(n) + F_{2k-2}n + F_{2k}) < 1, \end{aligned}$$

or

$$\begin{aligned} &\kappa(n)(-\tfrac{1}{\phi})^{2k-1} + n(-\tfrac{1}{\phi})^{2k-2} + (-\tfrac{1}{\phi})^{2k} \\ &\quad \leq F_{2k}\kappa(n) + F_{2k-1}n + F_{2k+1} - \kappa(F_{2k-1}\kappa(n) + F_{2k-2}n + F_{2k}) \\ &\quad < 1 + \kappa(n)(-\tfrac{1}{\phi})^{2k-1} + n(-\tfrac{1}{\phi})^{2k-2} + (-\tfrac{1}{\phi})^{2k}. \end{aligned}$$

Simplify the lower bound $\kappa(n)(-\frac{1}{\phi})^{2k-1} + n(-\frac{1}{\phi})^{2k-2} + (-\frac{1}{\phi})^{2k} = (-\frac{1}{\phi})^{2k-2}(-\frac{1}{\phi}\kappa(n) + n + (\frac{1}{\phi})^2)$, considering that the maxima of $n - \frac{1}{\phi}\kappa(n)$ occur at $n = F_{2m}$, so that

$$\begin{aligned} &\min_{n,k} \kappa(n)(-\tfrac{1}{\phi})^{2k-1} + n(-\tfrac{1}{\phi})^{2k-2} + (-\tfrac{1}{\phi})^{2k} \\ =&\min_{m,k}(-\tfrac{1}{\phi})^{2k-2}(-\tfrac{1}{\phi}\kappa(F_{2m}) + F_{2m} + (\tfrac{1}{\phi})^2) \\ =&\min_{m,k}(-\tfrac{1}{\phi})^{2k-2}(-\tfrac{1}{\phi}(F_{2m+1} - 1) + F_{2m} + (\tfrac{1}{\phi})^2) \\ =&\min_{m,k}(-\tfrac{1}{\phi})^{2k-2}(1 + (-\tfrac{1}{\phi})^{2m+1}) \\ =&\min_{m,k}(\tfrac{1}{\phi})^{2k-2}(1 - (\tfrac{1}{\phi})^{2m+1}) \\ =&\lim_{m\to\infty, m\to\infty}(\tfrac{1}{\phi})^{2k-2} - (\tfrac{1}{\phi})^{2m+2k-1} \\ =&0. \end{aligned}$$

Simplify the upper bound $1 + \kappa(n)(-\frac{1}{\phi})^{2k-1} + n(-\frac{1}{\phi})^{2k-2} + (-\frac{1}{\phi})^{2k} = 1 + (-\frac{1}{\phi})^{2k-2}(-\frac{1}{\phi}\kappa(n) + n + (\frac{1}{\phi})^2)$, considering that the maxima of $n - \frac{1}{\phi}\kappa(n)$ occur at $n = F_{2m}$,

so that

$$\begin{aligned}
&\max_{n,k} 1+\kappa(n)(-\tfrac{1}{\phi})^{2k-1}+n(-\tfrac{1}{\phi})^{2k-2}+(-\tfrac{1}{\phi})^{2k}\\
=&\max_{m,k} 1+(-\tfrac{1}{\phi})^{2k-2}(-\tfrac{1}{\phi}\kappa(F_{2m})+F_{2m}+(\tfrac{1}{\phi})^2)\\
=&\max_{m,k} 1+(-\tfrac{1}{\phi})^{2k-2}(-\tfrac{1}{\phi}(F_{2m+1}-1)+F_{2m}+(\tfrac{1}{\phi})^2)\\
=&\max_{m,k} 1+(-\tfrac{1}{\phi})^{2k-2}(1+(-\tfrac{1}{\phi})^{2m+1})\\
=&\max_{m,k} 1+(\tfrac{1}{\phi})^{2k-2}(1-(\tfrac{1}{\phi})^{2m+1})\\
=&\lim_{m\to\infty} 1+(\tfrac{1}{\phi})^{2k-2}(1-(\tfrac{1}{\phi})^{2m+1})\Big|_{k=1}\\
=&2.
\end{aligned}$$

Continue to manipulate the formula until the desired difference is bounded:

$$\begin{aligned}
0< &\ F_{2k}\kappa(n)+F_{2k-1}n+F_{2k+1}-\kappa(F_{2k-1}\kappa(n)+F_{2k-2}n+F_{2k}) &<2,\\
-1< &\ F_{2k}\kappa(n)+F_{2k-1}n+F_{2k+1}-[\kappa(F_{2k-1}\kappa(n)+F_{2k-2}n+F_{2k})+1] &<1,\\
-1< &(F_{2k+1}-F_{2k-1})\kappa(n)+(F_{2k}-\ F_{2k-2})n+(\ F_{2k+2}\ -F_{2k})\\
&\qquad -[\kappa(F_{2k-1}\kappa(n)+F_{2k-2}n+F_{2k})+1] &<1,\\
-1< &\ F_{2k+1}\kappa(n)+F_{2k}n+F_{2k+2}-\ [F_{2k-1}\kappa(n)+F_{2k-2}n+F_{2k}\\
&\qquad +\kappa(F_{2k-1}\kappa(n)+F_{2k-2}n+F_{2k})+1] &<1,\\
-1< &\ F_{2k+1}\kappa(n)+F_{2k}n+F_{2k+2}-[\lambda(F_{2k-1}\kappa(n)+F_{2k-2}n+F_{2k})+1] &<1,\\
-1< &\ \mathfrak{o}_{n,k+1}-[\lambda(\mathfrak{o}_{n,k})+1] &<1,\\
-1< &\ \mathfrak{o}_{n,k+1}-\bar{\boldsymbol{R}}(\mathfrak{o}_{n,k}) &<1,
\end{aligned}$$

Thus, the two positive integer quantities have a difference of less than one, proving that the formula for $\mathfrak{o}_{n,k}$ matches the claim that rows $n \geq 1$ of $\mathfrak{o}$ give sequences of right branchings in the maximal successor tree. □

Proof of Proposition 8.5($\mathsf{F}_{n,k}$): From Proposition 4.16 (using cohorts) or Lemma 8.1 (using trees), $\mathsf{F}_{n,k} = n + F_{F^{-1}(n)+k+1}$. Consider the first row $\mathsf{F}_{0,k}$, having $n = 0$. Then, $\mathsf{F}_{0,k} = 0 + F_{F^{-1}(0)+k+1} = F_{k+1}$, so that $\mathbf{f}(\mathsf{F}_{n,k}) = (k+1)$ and $\boldsymbol{\partial}(\mathsf{F}_{n,k}) = (k+1)$, confirming the first case. Next, the case $k = 1$ gives $\mathsf{F}_{n,1} = n + F_{F^{-1}(n)+2}$. Now, $F_{F^{-1}(n)}$ is the largest Fibonacci number not greater than n. Since minimal Fibonacci representation does not use any two adjacent indices, the indices $(\ldots, F^{-1}(n),\ F^{-1}(n)+2)$ cannot be reduced further. Hence, $\mathbf{f}(\mathsf{F}_{n,1}) = \mathbf{f}(n) \oplus (F^{-1}(n)+2)$, and $\boldsymbol{\partial}(\mathsf{F}_{n,1}) = \boldsymbol{\partial}(n)(2)$. Clearly, for $k = 2, 3, 4, \ldots$ the result also holds, since the indices $(\ldots, F^{-1}(n),\ F^{-1}(n)+k+1)$ are already reduced, as well.

Considering Figure 17(iii), moreover, rows (constant n) of F must be sequences of left branchings in of the minimal Fibonacci tree. □

Proof of Proposition 8.5($\mathsf{T}_{n,k}$): Using Lemma 8.1, consider the first row $\mathsf{T}_{0,k} = F_{2k+1} - 1 = \sum_{h=1}^{k} F_{2h}$. Since this series does not use any two adjacent Fibonacci terms, it is indeed a minimal Fibonacci representation of $\mathsf{T}_{0,k}$, that is, $\mathbf{f}(\mathsf{T}_{0,k}) = (2, 4, \ldots, 2k-2, 2k)$, and $\boldsymbol{\partial}(\mathsf{T}_{0,k}) = (2, 4-2, \ldots, 2k-(2k-2)) = (2)^k$, as claimed for $n = 0$.

Now for $n > 0$, $\daleth_{n,k} = n + F_{F^{-1}(n)+2k} - 2F_{F^{-1}(n)} = n + F_{F^{-1}(n)+2} - 2F_{F^{-1}(n)} + \sum_{h=2}^{k} F_{F^{-1}(n)+2h-1} = n + F_{F^{-1}(n)-1} + \sum_{h=2}^{k} F_{F^{-1}(n)+2h-1}$. For example, $k = 1$ gives $\daleth_{n,1} = n + F_{F^{-1}(n)-1}$. Now, $F_{F^{-1}(n)-1}$ is the second largest Fibonacci number not greater than n, and thus, according to (68), this term is absent from the minimal Fibonacci representation of n, though $\mathbf{f}(n)$ does include $F^{-1}(n)$, and $\mathbf{f}(\daleth_{n,1})$ cannot use any two adjacent indices. So, $\mathbf{f}(\daleth_{n,1}) = \mathbf{f}(n + F_{F^{-1}(n)-1}) = \mathbf{f}(n) \setminus F^{-1}(n) \oplus (F^{-1}(n) + 1) = \mathbf{f}(n)\texttt{++}$, and $\boldsymbol{\partial}(\daleth_{n,1}) = \boldsymbol{\partial}(n)\texttt{++}$, for $n > 0$ as claimed.

Now whereas the k indices $(F^{-1}(n) + 1, F^{-1}(n) + 3, \ldots, F^{-1}(n) + 2k - 1)$ do not contain any two adjacent indices, they already suit the minimal Fibonacci representation. Thus, for $n > 0$ and $k \geq 1$, write $\mathbf{f}(\daleth_{n,k}) = \mathbf{f}(n + F_{F^{-1}(n)-1} + \sum_{h=2}^{k} F_{F^{-1}(n)+2h-1}) = \mathbf{f}(n) \setminus F^{-1}(n) \oplus (F^{-1}(n) + 1, F^{-1}(n) + 3, \ldots, F^{-1}(n) + 2k - 1) = [\mathbf{f}(n)\texttt{++}] \oplus (F^{-1}(n) + 3, \ldots, F^{-1}(n) + 2k - 1)$, corresponding to $\boldsymbol{\partial}(\daleth_{n,k}) = [\boldsymbol{\partial}(n)\texttt{++}](2)^{k-1}$, for $n > 0$ as claimed.

Considering Figure 17(iii), moreover, rows (constant n) of $\daleth$ must be sequences of right branchings in of the minimal Fibonacci tree. □

Proof of Proposition 8.5($\vdash_{n,k}$): From Proposition 4.30 (using cohorts) or Lemma 8.1 (using trees), $\vdash_{n,k} = n + F_{F^{-1}(n)+k+2} - F_{F^{-1}(n)+2}$. Consider the first row $\vdash_{0,k}$, having $n = 0$. Then, $\vdash_{0,k} = 0 + F_{F^{-1}(0)+k+2} - F_{F^{-1}(0)+2} = F_{k+2} - F_2 = F_1 + F_2 + \cdots + F_k$, so that $\mathbf{F}_\star(\vdash_{n,k}) = (1, 2, \ldots, k)$ and $\boldsymbol{\nabla}_\star(\vdash_{n,k}) = (1)^{k-1}$, confirming the first case. Next, the case $k = 1$ gives $\vdash_{n,1} = n + F_{F^{-1}(n)+3} - F_{F^{-1}(n)+2} = n + F_{F^{-1}(n)+1}$. Now, $F_{F^{-1}(n)}$ is the largest Fibonacci number not greater than n. From Proposition 6.8, $F^{-1}(n) \notin \mathbf{F}_\star(N)$ and $F^{-1}(n) - 1 \in \mathbf{F}_\star(N)$. Since maximal Fibonacci expansion does not skip any two adjacent indices, the indices $(\ldots, F^{-1}(n) - 1, F^{-1}(n) + 1)$ cannot be reduced further. Hence, $\mathbf{F}_\star(\vdash_{n,1}) = \mathbf{F}_\star(n) \oplus (F^{-1}(n) + 1)$, and $\boldsymbol{\nabla}_\star(\vdash_{n,1}) = \boldsymbol{\nabla}_\star(n)(2)$. Similarly, for $k = 2, 3, 4, \ldots$ the result also holds, since the indices $(\ldots, F^{-1}(n) - 1, F^{-1}(n) + 1, F^{-1}(n) + 2, \ldots, F^{-1}(n) + k)$ are already reduced.

Considering Figure 17(iv), moreover, rows (constant n) of $\vdash$ must be sequences of left branchings in of the maximal Fibonacci tree.

□

Proof of Proposition 8.5($\dashv_{n,k}$): Using Lemma 8.1, consider the first row $\dashv_{0,k} = F_{2k} = \sum_{h=1}^{k} F_{2h-1}$. Since this series does not skip any two adjacent Fibonacci terms, it is indeed a maximal Fibonacci expansion of $\daleth_{0,k}$, that is, $\mathbf{F}_\star(\daleth_{0,k}) = (1, 3, \ldots, 2k-3, 2k-1)$, and $\boldsymbol{\nabla}_\star(\daleth_{0,k}) = (3 - 1, 5 - 3, \ldots, 2k - 1 - (2k - 3)) = (2)^{k-1}$, as claimed for $n = 0$.

Now for $n > 0$, $\dashv_{n,k} = n + F_{F^{-1}(n)+2k-1} - F_{F^{-1}(n)-1} = n + F_{F^{-1}(n)+1} - F_{F^{-1}(n)-1} + \sum_{h=1}^{k-1} F_{F^{-1}(n)+2h} = n + \sum_{h=0}^{k-1} F_{F^{-1}(n)+2h}$. Now, $F_{F^{-1}(n)-1}$ is the second largest Fibonacci number not greater than n, and thus, according to (65), this term is present in the maximal Fibonacci representation of n, though $\mathbf{F}_\star(n)$ does not include $F^{-1}(n)$. Thus, $\mathbf{F}_\star(\dashv_{n,k}) = \mathbf{F}_\star(n) \oplus (F^{-1}(n), F^{-1}(n) + 2, \ldots, F^{-1}(n) + 2k - 4, F^{-1}(n) + 2k - 2)$, and $\boldsymbol{\nabla}_\star(\daleth_{n,k}) = \boldsymbol{\nabla}_\star(n) \oplus (F^{-1}(n) - (F^{-1}(n) - 1), F^{-1}(n) +$

$2-F^{-1}(n),\ldots,F^{-1}(n)+2k-2-(F^{-1}(n)+2k-4))=\boldsymbol{\nabla}_\star(n)(1)(2)^{k-1}$, for $n>0$, as claimed.

Considering Figure 17(iv), then, rows (constant n) of $\beth$ must be sequences of right branchings in of the maximal Fibonacci tree. □

Proof of Proposition 8.6(w): Proposition 4.40 (using cohorts, see Example 4.15) and Lemma 8.3 (using trees) showed that $w_{n,k}=F_{k+1}\kappa(n+1)+F_kn$ for $n\geq 0$ (also see entry 035513 in [41]).

In particular, for $n=0$, $w_{0,k}=F_{k+1}$. Consequently, $\boldsymbol{\partial}(w_{0,k})=\boldsymbol{\partial}(F_{k+1})=(k+1)$, proving the claim for $n=0$.

Next examine the gaps of $w_{n,k}$ for $n>0$. Now (52) gives $\sigma^k(n)=F_{k-1}n+\sigma(n)F_k$ for $n\geq 1$. Thus, $\sigma^{k+1}(n)=F_kn+\sigma(n)F_{k+1}$. Further, since (51) gives $\sigma(n)=\kappa(n+1)-1$, we have $\sigma^{k+1}(n)=F_kn+(\kappa(n+1)-1)F_{k+1}=F_kn+F_{k+1}\kappa(n+1)-F_{k+1}=w_{n,k}-F_{k+1}$. Consequently, $w_{n,k}\overset{n>0}{=\!=}F_{k+1}+\sigma^{k+1}(n)=w_{0,k}+\sigma^{k+1}(n)$.

Here, writing $\mathbf{f}(n)=(t_1,\ldots,t_s)$, with $t_1>1$, implies that $\boldsymbol{\partial}(n)=(t_1,t_2-t_1,\ldots,t_s-t_{s-1})$. Further, $\mathbf{f}(\sigma^{k+1}(n))=(t_1+k+1,\ldots,t_s+k+1)$, so that $\mathbf{f}(F_{k+1}+\sigma^{k+1}(n))=(k+1,t_1+k+1,\ldots,t_s+k+1)$. Thus, $\boldsymbol{\partial}(F_{k+1}+\sigma^{k+1}(n))=(k+1,t_1,t_2-t_1,\ldots,t_s-t_{s-1})=(k+1)\boldsymbol{\partial}(n)$. So, $\boldsymbol{\partial}(w_{n,k})\overset{n>0}{=\!=}\boldsymbol{\partial}(F_{k+1}+\sigma^{k+1}(n))=\boldsymbol{\partial}(w_{0,k}+\sigma^{k+1}(n))=(k+1)\boldsymbol{\partial}(n)$, as claimed for $n>0$.

Considering Figure 17(i), moreover, rows (constant n) of w must be sequences of left branchings in of the minimal successor tree. □

Proof of Proposition 8.6(ɯ): Using Lemma 8.3, consider the first row $\text{ɯ}_{0,k}=F_{2k+1}-1=\sum_{h=1}^{k}F_{2h}$. Since this series does not use any two adjacent Fibonacci terms, it is indeed a minimal Fibonacci representation of $\text{ɯ}_{0,k}$, that is, $\mathbf{f}(\text{ɯ}_{0,k})=(2,4,\ldots,2k-2,2k)$, and $\boldsymbol{\partial}(\text{ɯ}_{0,k})=(2,4-2,\ldots,2k-(2k-2))=(2)^k$, as claimed for $n=0$.

Now for $n>0$, $\text{ɯ}_{n,k}=F_{2k-1}\kappa(n+1)+F_{2k-2}n-1$. For example, $k=1$ gives $\text{ɯ}_{n,1}=\kappa(n+1)-1$, so that the result $\boldsymbol{\partial}(\text{ɯ}_{n,1})=\boldsymbol{\partial}(\kappa(n+1)-1)$ is trivial. Further, using (51) gives $\text{ɯ}_{n,1}=\sigma(n)$, so that $\mathbf{f}(\text{ɯ}_{n,1})=\mathbf{f}(n)+1$. Whereas if $(\partial_1,\ldots,\partial_r)(n)=(t_1,t_2-t_1,t_3-t_2,\ldots,t_s-t_{s-1})$, then $(\partial_1,\ldots,\partial_r)(\sigma(n))=(t_1+1,t_2-t_1,t_3-t_2,\ldots,t_s-t_{s-1})$, observe that $\boldsymbol{\partial}(\sigma(n))\equiv\texttt{++}\boldsymbol{\partial}(n)=\boldsymbol{\partial}(\text{ɯ}_{n,1})$, as claimed.

More generally, consider $\text{ɯ}_{n,k}=F_{2k-1}\kappa(n+1)+F_{2k-2}n-1$ for $n>0$. Whereas by (51), $\sigma(n)=\kappa(n+1)-1$ and by (52), for $n\geq 1$, $\sigma^k(n)=F_k\sigma(n)+F_{k-1}n=F_k\kappa(n+1)-F_k+F_{k-1}n$, observe that $\sigma^{2k-1}(n)=F_{2k-1}\kappa(n+1)-F_{2k-1}+F_{2k-2}n$, so that $\text{ɯ}_{n,k}\overset{n>0}{=\!=}\sigma^{2k-1}(n)+F_{2k-1}-1$. Whereas if $\mathbf{f}(n)=(t_1,\ldots,t_s)$, then $\sigma^{2k-1}(n)=(t_1+2k-1,\ldots,t_s+2k-1)$, where $t_1\geq 2$. Meanwhile, $F_{2k-1}-1=\sum_{h=1}^{k-1}F_{2h}$, so that $\mathbf{f}(F_{2k-1}-1)=(2,4,\ldots,2k-4,2k-2)$. So, $\mathbf{f}(\text{ɯ}_{n,k})=(2,4,\ldots,2k-4,2k-2,2k-1+t_1,\ldots,2k-1+t_s)$, and $\boldsymbol{\partial}(\text{ɯ}_{n,k})=(2,4-2,\ldots,2k-2-(2k-4),t_1+2k-1-(2k-2),t_2-t_1,\ldots,t_s-t_{s-1})=(2,\ldots,2,t_1+1,t_2-t_1,\ldots,t_s-t_{s-1})=(2)^{k-1}[\texttt{++}\boldsymbol{\partial}(n)]=(2)^{k-1}\boldsymbol{\partial}(\text{ɯ}_{n,1})=(2)^{k-1}\boldsymbol{\partial}(\kappa(n+1)-1)$, as claimed.

Considering Figure 17(i), moreover, rows (constant n) of ɯ must be sequences of right branchings in of the minimal successor tree. □

Proof of Proposition 8.6(a): See Proposition 7.3, noting, moreover, that rows (constant n) of a must be sequences of left branchings in of the maximal successor tree (Figure 17(ii)) □

Proof of Proposition 8.6(𝔰)*:* The proof, like that of (*a*) will use the definition (50) to rely on the independence of the Fibonacci successor from the choice of representation, whereas the successor may differ when computed from the maximal expansion (Remark 6.5). First take $n = 0$ in Lemma 8.3(𝔰) to formulate the first row as $\mathfrak{s}_{0,k} = F_{2k} = \sum_{h=1}^{k} F_{2h-1}$. Since this series includes F_1 and does not skip any two adjacent Fibonacci terms, it is indeed a maximal Fibonacci expansion of $\mathfrak{s}_{0,k}$, that is, $\mathbf{F}_\star(\mathfrak{s}_{0,k}) = (1, 3, \ldots, 2k-3, 2k-1)$, and $\boldsymbol{\nabla}_\star(\mathfrak{s}_{0,k}) = (3-1, 5-3, \ldots, 2k-1-(2k-3))$ $= (2)^{k-1}$, as claimed for $n = 0$.

Now for $n > 0$, consider $\mathfrak{s}_{n,k} = F_{2k-1}\kappa(n) + F_{2k-2}n + F_{2k}$. By Lemma 6.1 and Proposition 6.3, respectively, write the equalities $\mathfrak{s}_{n,k} \overset{n>0}{=\!=} \sigma^{2k-1}(n-1) + 2F_{2k} = \sigma_\star^{2k-1}(n) - 1 + 2F_{2k}$.

For example, consider the case $n = 1$. Since $\mathfrak{s}_{1,k} = 2F_{2k} = F_{2k}+1+\sum_{h=1}^{k-1} F_{2h+1}$, it gives $\mathbf{F}_\star(\mathfrak{s}_{1,k}) = (1, 3, 5, \ldots, 2k-3, 2k-1, 2k)$, which is indeed a maximal Fibonacci expansion since it includes F_1 and does not skip any two adjacent Fibonacci terms. Thus $\boldsymbol{\nabla}_\star(\mathfrak{s}_{1,k}) = (2, \ldots, 2, 1) = (2)^{k-1}(1) = (2)^{k-1}(1)\boldsymbol{\nabla}_\star(1)$, as claimed, where the latter equality corresponds to the first case in Definition 6.3.

Returning to the general case of $n > 0$, note that $\mathfrak{s}_{n,k} = \sigma^{2k-1}(n-1) + \mathfrak{s}_{1,k} = \sigma_\star^{2k-1}(n) + \mathfrak{s}_{1,k} - 1$. Again writing $\mathbf{F}_\star(n) = (1, t_2 \ldots, t_s)$ means that $\boldsymbol{\nabla}_\star(n) = (t_2 - 1, t_3 - t_2, \ldots, t_s - t_{s-1})$, where either $t_2 = 2$ or $t_2 = 3$, and further, $t_r - t_{r-1} \leq 2$, $r = 2, \ldots, s$. Then, since σ is invariant with respect to the choice of representation, write $n - 1 = F_{t_2} + \cdots + F_{t_s}$ so that $\sigma^{2k-1}(n-1) = \sigma_\star^{2k-1}(n) - 1$ $= F_{t_2+2k-1} + \cdots + F_{t_s+2k-1}$. Since the index $t_2 + 2k - 1$ of the least term is equal to either $2k + 1$ or $2k + 2$ and the remaining indices do not skip any two adjacent integers, this Fibonacci representation has no bits in common with that of $\mathfrak{s}_{1,k}$ derived in the above example. Subtracting the greatest index of the latter from the least index of the former its least index gives $t_2 - 2 \leq 2$.

Therefore, merging the indices gives the maximal representation $\mathbf{F}_\star(\mathfrak{s}_{n,k}) \overset{n>0}{=\!=}$ $\mathbf{F}_\star(\mathfrak{s}_{1,k}) \oplus [\mathbf{F}_\star(n) \setminus (1) + 2k - 1] = (1, 3, 5, \ldots, 2k-3, 2k-1, 2k, t_2+2k-1, \ldots, t_s+2k-1)$, and thus $\boldsymbol{\nabla}_\star(\mathfrak{s}_{n,k}) \overset{n>0}{=\!=} (2, \ldots, 2, 1, t_2-1, t_3-t_2, \ldots, t_s-t_{s-1}) = (2)^{k-1}(1)\boldsymbol{\nabla}_\star(n)$, as claimed.

Now, from Proposition 6.3, observe that $\kappa(n) = \sigma_\star(n)$, the maximal Fibonacci successor of n. So, if $\mathbf{F}_\star(n) = (1, t_2 \ldots, t_s)$, then $\mathbf{F}_\star(\kappa(n)+1) = (1, 2, t_2+1 \ldots, t_s+1)$, and $\boldsymbol{\nabla}_\star(\kappa(n) + 1) = (1, t_2 - 1, t_3 - t_2, \ldots, t_s - t_{s-1}) = (1)\boldsymbol{\nabla}_\star(n)$, demonstrating the latter equality of the claim.

Considering Figure 17(ii), moreover, rows (constant n) of 𝔰 must be sequences of right branchings in of the maximal successor tree. □

Proof of Proposition 8.20(**i**). With reference to Tables 33(i) and (ii), let C_t and D_t be cohorts of the respective tableau. Equivalence for the first cohort follows trivially, whereas $C_1\kappa = (S_1\kappa) = (I\kappa) = (T_1\kappa) = D_1\kappa$. For the second cohort, $C_2\kappa = (S_2\kappa) = (\bar{\boldsymbol{l}}\kappa) = (\bar{\boldsymbol{L}}\kappa) = (T_2\kappa) = D_2\kappa$ follows from Proposition 6.9. For the third cohort, $C_3\kappa = (S_3\kappa, S_4\kappa) = (\vec{\boldsymbol{l}}^2\kappa, \bar{\boldsymbol{r}}\kappa,) = (\bar{\boldsymbol{R}}\kappa, \bar{\boldsymbol{L}}^2\kappa) = (T_3\kappa, T_4\kappa) = D_3\kappa$ follows from (87) and (88). To show $C_4\kappa = D_4\kappa$ for the fourth cohort, consider the three elements one at a time, composing each with κ: Firstly, $S_5\kappa = \vec{\boldsymbol{l}}^3\kappa = \bar{\boldsymbol{l}} \circ \vec{\boldsymbol{l}}^2\kappa = S_2\vec{\boldsymbol{l}}^2\kappa = T_2\bar{\boldsymbol{R}}\kappa = \bar{\boldsymbol{L}}\bar{\boldsymbol{R}}\kappa = T_5\kappa$, using the equivalence previously shown for

the second cohort, together with the observation (87) that $\bar{\boldsymbol{l}}^2\kappa = \bar{\boldsymbol{R}} \subset K$. Secondly, $S_6\kappa = \bar{\boldsymbol{r}}\bar{\boldsymbol{l}}\kappa = \bar{\boldsymbol{R}}\bar{\boldsymbol{L}}\kappa = T_6\kappa$, using (89). Finally, $S_7\kappa = \bar{\boldsymbol{l}}\bar{\boldsymbol{r}}\kappa = S_2\bar{\boldsymbol{r}}\kappa = T_2\bar{\boldsymbol{L}}^2\kappa = \bar{\boldsymbol{L}}^3\kappa = T_7\kappa$, using the equivalence previously shown for the second cohort, together with the observation (88) that $\bar{\boldsymbol{r}}\kappa = \bar{\boldsymbol{L}}^2\kappa \subset K$.

For the induction step, expand the definition $C_t = C_{t-1} \circ \bar{\boldsymbol{l}} \oplus C_{t-2} \circ \bar{\boldsymbol{r}}$ into the recursion $C_t = C_{t-2} \circ \bar{\boldsymbol{l}}^2 \oplus C_{t-3} \circ \bar{\boldsymbol{r}}\bar{\boldsymbol{l}} \oplus C_{t-2} \circ \bar{\boldsymbol{r}}$. Similarly, expand the definition $D_t = D_{t-2} \circ \bar{\boldsymbol{R}} \oplus D_{t-1}\bar{\boldsymbol{L}}$ into the recursion $D_t = D_{t-2} \circ \bar{\boldsymbol{R}} \oplus D_{t-3} \circ \bar{\boldsymbol{R}}\bar{\boldsymbol{L}} \oplus C_{t-2} \circ \bar{\boldsymbol{L}}^2$. By the induction hypothesis, $C_{t-3}\kappa = D_{t-3}\kappa$ and $C_{t-2}\kappa = D_{t-2}\kappa$. By (87), (89), and (88), the recursions merely compose C_{t-3} and C_{t-2}, respectively D_{t-3} and D_{t-2} with subsets of K. Thus, the result $C_t\kappa = D_t\kappa$ follows by induction. □

Proof of Proposition 8.20(**ii**). Similar to the proof of **(i)** observe that the sequence of Wythoff signatures begins $1, 0, 1, 1, 0, 1, 0, \ldots$, whereas $S_1\kappa = T_1\kappa \subset K$, $S_2\kappa = T_2\kappa \subset \Lambda$, $S_3\kappa = T_3\kappa \subset K$, $S_4\kappa = T_4\kappa \subset K$, $S_5\kappa = T_5\kappa \subset \Lambda$, $S_6\kappa = T_6\kappa \subset K$, and $S_7\kappa = T_7\kappa \subset \Lambda$.

Using the recursions written in the proof of **(i)**, observe that the Wythoff signatures for compositions in C_t or D_t are the same as the signatures for compositions in the corresponding concatenations $C_{t-2} \oplus C_{t-3} \oplus C_{t-2}$ or $D_{t-2} \oplus D_{t-3} \oplus D_{t-2}$. By induction, a sequence that follows the recursion $C_t = C_{t-2} \oplus C_{t-3} \oplus C_{t-2}$ must also follow one of the recursions $C_t = C_{t-1} \oplus C_{t-2}$ or $C_t = C_{t-2} \oplus C_{t-1}$, thus matching the recursive definition of the Fibonacci word 005614. □

Proof of Proposition 8.20(**iii**),(**iv**),(**v**),(**vi**),(**vii**) *and* (**viii**) *for* $\vdash$. To derive **(iii)** from **(i)**, consider that, in particular, $1 \in K$, and thus by (91), $\vdash_{0,k} = \bar{\boldsymbol{L}}^{k-1}(1) = \begin{cases} 1, & k = 1; \\ \bar{\boldsymbol{l}}\bar{\boldsymbol{r}}^{(k-2)/2}(1), & k \geq 2 \text{ even}; \\ \bar{\boldsymbol{r}}^{(k-1)/2}(1), & k \geq 3 \text{ odd}; \end{cases}$

Consequently, $\vdash_{0,k} = \begin{cases} \bar{\boldsymbol{r}}^{(k-1)/2}(1) = \ \dashv_{0,(k+1)/2}, & k \geq 1 \text{ odd}; \\ \bar{\boldsymbol{l}}\bar{\boldsymbol{r}}^{(k-2)/2}(1) = \ \dashv_{1,k/2}, & k \geq 2 \text{ even}. \end{cases}$ and further that

for $n \geq 1$, $\vdash_{n,k} = T_n\bar{\boldsymbol{R}}\bar{\boldsymbol{L}}^{k-1}(1) = \begin{cases} S_n\bar{\boldsymbol{l}}^2(1), & k = 1; \\ S_n\bar{\boldsymbol{r}}\bar{\boldsymbol{l}}\bar{\boldsymbol{r}}^{(k-2)/2}(1), & k \geq 2 \text{ even}; \\ S_n\bar{\boldsymbol{l}}^2\bar{\boldsymbol{r}}^{(k-1)/2}(1), & k \geq 3 \text{ odd}; \end{cases}$ and thus

$\vdash_{n,k} = \begin{cases} S_n\bar{\boldsymbol{l}}^2\bar{\boldsymbol{r}}^{(k-1)/2}(1) = \ S_n\bar{\boldsymbol{l}}\dashv_{1,(k+1)/2}, & k \geq 1 \text{ odd}; \\ S_n\bar{\boldsymbol{r}}\bar{\boldsymbol{l}}\bar{\boldsymbol{r}}^{(k-2)/2}(1) = \ S_n\bar{\boldsymbol{r}}\dashv_{1,k/2}, & k \geq 2 \text{ even}; \end{cases}$

Here $S_n\bar{\boldsymbol{l}}\dashv_{1,(k+1)/2}$ gives the sequence of elements in the left subcohorts of the 1–2-Fibonacci cohorts of column $(k+1)/2$ of $\dashv$ and $S_n\bar{\boldsymbol{r}}\dashv_{1,k/2}$ gives the sequence of elements in the right subcohorts of the 1–2-Fibonacci cohorts of column $k/2$ of $\dashv$. Conversely, each column $k' = 1, 2, 3, \ldots$ of $\dashv$ splits into two consecutive columns $2k' - 1$ and $2k'$ of $\vdash$.

To reformulate the row indices, it remains to note that $\dashv_{n,1}$ for $n \geq 1$ and $\vdash_{n,1}$ for $n \geq 0$ index the elements in the left, respectively, right subcohorts of a 1–2-Fibonacci cohort tableau from the 1st cohort. □

Proof of Proposition 8.20(**iii**),(**iv**),(**v**),(**vi**),(**vii**) *and* (**viii**) *for* $\vdash$. Analogous to the proofs of the corresponding statements for $\vdash$, noting that $\dashv_{n,1}$ for $n \geq 1$ and $\vdash_{n,1}$ for $n \geq 0$ index the elements in the right, respectively, left subcohorts of a 2–1-Fibonacci cohort tableau from the 1st cohort. □

References

[1] U. Alfred, Exploring the Fibonacci representation of integers, *Fibonacci Quarterly* **1**(4) (1963), 72.

[2] K. Alladi and V. E. Hoggatt, Compositions with ones and twos, *Fibonacci Quarterly* **13**(3) (1975), 233–239.

[3] J.-P. Allouche, J. Shallit, and G. Skordev, Self-generating sets, integers with missing blocks, and substitutions, *Discrete Mathematics* **292** (2005), 1–15.

[4] S. Artstein-Avidan, A. S. Fraenkel, and V. T. Sós, A two-parameter family of an extension of Beatty sequences, *Discrete Mathematics* **308** (2008), 4578–4588.

[5] G. Bergman, A number system with an irrational base, *Mathematics Magazine* **31**(2) (1957), 98–110.

[6] L. Brown Jr., A new characterization of the Fibonacci numbers, *Fibonacci Quarterly* **3**(1) (1965), 1–8.

[7] M. Bunder and K. Tognetti, On the self matching properties of $\lfloor j\tau \rfloor$, *Discrete Mathematics* **241**(1–3) (2001), 139–151.

[8] P. J. Cameron and D. G. Fon-Der-Flaass, Fibonacci notes, (2008), (electronic), `http://www.maths.qmul.ac.uk/~pjc/comb/fibo.pdf`

[9] L. Carlitz, Fibonacci representations, *Fibonacci Quarterly* **6**(4) (1968), 193–220.

[10] A. Cobham, Uniform tag sequences, *Mathematical systems theory* **6**(1–2) (1972), 164–192.

[11] F. M. Dekking, Base phi representations and golden mean beta-expansions, (2019), 1906.08437v1 (electronic), `http://arxiv.org/abs/1906.08437v1`

[12] A. Dubickas, On integer sequences generated by linear maps, *Glasgow Math. Journal* (51) (2009), 243–252.

[13] P. Erdős and I. Joó, On the expansion $1 = \sum q^{-n_i}$, *Periodica Mathematica Hungarica* **23**(1) (1991), 25–28.

[14] H. H. Ferns, On the representation of integers as sums of distinct Fibonacci numbers, *Fibonacci Quarterly* **3**(1) (1965), 21–30.

[15] A. S. Fraenkel, The bracket function and complementary sets of integers, *Canadian J. Mathematics* **21** (1969), 6–27.

[16] A. S. Fraenkel, Iterated floor function, algebraic numbers, discrete chaos, Beatty subsequences, semigroups, *Transactions of the American Mathematical Society* **341**(2) (1994), 639–664.

[17] A.-S. Fraenkel, M. Mushkin, and U. Tassa, Determination of $\lfloor n\theta \rfloor$ by its sequence of differences, *Canadian Mathematical Bulletin* **21**(4) (1978), 441–446.

[18] A.S. Fraenkel, J. Levitt, and M. Shimshoni, Characterization of the set of values $f(n) = [n\alpha], n = 1, 2, \ldots$, *Discrete Mathematics* (2) (1972), 335–345.

[19] R. P. Grimaldi, Compositions without the summand 1, *Congressus Numerantium* **152** (2001), 33–43.

[20] C. Kimberling, Interspersions and dispersions, *Proceedings of the American Mathematical Society* **117**(2) (1993), 313–321.

[21] C. Kimberling, A self-generating set and the golden mean, *Journal of Integer Sequences* **3**(2) (2000), 00.2.8.

[22] C. Kimberling, Complementary equations and Wythoff sequences, *Journal of Integer Sequences* **11**(3) (2008), 08.3.3.

[23] C. Kimberling and K. B. Stolarsky, Slow Beatty sequences, devious convergence, and partitional divergence, *American Mathematical Monthly* **123**(3) (2016), 267–273.

[24] R. Knott, Using powers of phi to represent integers (base phi), (1996-2015), (electronic), `http://www.maths.surrey.ac.uk/hosted-sites/R.Knott/Fibonacci/phigits.html`

[25] D. E. Knuth, Fibonacci multiplication, *Applied Mathematics Letters* **1**(1) (1988), 57–60.

[26] Lafer, Exploring the Fibonacci representation of integers, *Fibonacci Quarterly* **2**(2) (1964), 114,134.

[27] W. Lang, The Wythoff and the Zeckendorf representations of numbers are equivalent, *Applications of Fibonacci Numbers* **6** (1996), 321–337.

[28] Lehmer, On Stern's diatomic series, *American Mathematical Monthly* **2**(36) (1929), 59,67.

[29] C. D. Olds, *Continued Fractions*, Random House, 1963.

[30] G. Rozenberg and A. Lindenmayer, Developmental systems with locally catenative formulas, *Acta Informatica* **2**(3) (1973), 214–248.

[31] G. R. Sanchis and L. A. Sanchis, On the frequency of occurrence of α^i in the α-expansions of the positive integers, *Fibonacci Quarterly* **39** (2001), 123–137.
[32] K. Schmidt, On periodic expansions of Pisot numbers and Salem numbers, *Bull. London Math. Soc.* (12) (1980), 269–278.
[33] J. Shallit, A generalization of automatic sequences, *Theoretical Computer Science* **61**(1) (1988), 1–16.
[34] J. Parker Shectman, A 1–parameter family of binary tree pairs of the integers based on modified Fibonacci numeration and associated I–D arrays. In Preparation.
[35] J. Parker Shectman, Floor composites: Positive integers not expressible as a nested floor function with a single slope. In Preparation.
[36] J. Parker Shectman, The free monoid generated by the four Wythoff and inverse Wythoff functions. In Preparation.
[37] J. Parker Shectman, The Pell quilt and Pell cohort sequences. In Preparation.
[38] J. Parker Shectman, A quilt after Fibonacci, part 1 of 3: Construction of the quilt, (2021), (electronic), `https://arxiv.org/archive/math`
[39] J. Parker Shectman, A quilt after Fibonacci, part 2 of 3: Cohorts, free monoids, and numeration, (2021), (electronic), `https://arxiv.org/archive/math`
[40] J. Parker Shectman, A quilt after Fibonacci, part 3 of 3: Interspersoid–dispersoid arrays and graphical complementarity, (2021), (electronic), `https://arxiv.org/archive/math`
[41] N. J. A. Sloane, On-line encyclopedia of integer sequences, (1964-), (electronic), `http://oeis.org/`
[42] W. Steiner, The joint distribution of greedy and lazy Fibonacci expansions, *Fibonacci Quarterly* **43**(1) (2005), 60–69.
[43] K. B. Stolarsky, Beatty sequences, continued fractions, and certain shift operators, *Canadian Mathematical Bulletin* **19**(4) (1976), 473–482.

São Paulo, Brazil
Email address: `parkershectman@ootlinc.com`